



GEOSCIENCE BC SUMMARY OF ACTIVITIES 2008

Geoscience BC Report 2009-1



GEOSCIENCE BC SUMMARY OF ACTIVITIES 2008



© 2009 by Geoscience BC

All rights reserved. Electronic edition published 2009.

This publication is also available, free of charge, as colour digital files in Adobe Acrobat® PDF format from the Geoscience BC website: <http://www.geosciencebc.com/s/DataReleases.asp>.

Every reasonable effort is made to ensure the accuracy of the information contained in this report, but Geoscience BC does not assume any liability for errors that may occur. Source references are included in the report and users should verify critical information.

When using information from this publication in other publications or presentations, due acknowledgment should be given to Geoscience BC. The recommended reference is included on the title page of each paper. The complete volume should be referenced as follows:

Geoscience BC (2009): Geoscience BC Summary of Activities 2008; Geoscience BC, Report 2009-1, 200 p.

ISSN 1916-2960 Summary of Activities (Geoscience BC)

Cover photo: View from Sander Geophysics Ltd. helicopter while collecting QUEST-West airborne gravity data.
Photo credit: Owen Peterson, Sander Geophysics Ltd.

Foreword

Geoscience BC Overview

Geoscience BC (GBC) is a unique, industry-led, industry-focused, not-for-profit geoscience organization. Since its inception in April 2005 with a \$25 million start-up grant from the Government of British Columbia, GBC has pursued its mandate of attracting new exploration investment to British Columbia through a combination of GBC-led initiatives and funding of partnership projects. The majority of GBC's partnership projects are identified through an annual Request for Proposals (RFP) process, which takes place each fall. Geoscience BC-led geophysical and geochemical surveys have been developed by GBC's Technical Advisory Committees, staff and Project Team, and undertaken by means of contracts awarded through a call for bids, or sole-sourced where specific technical expertise was required.

Geoscience BC obtains industry input into project planning through our Project Team of industry consultants and our two Technical Advisory Committees (Minerals and Oil & Gas) of dedicated industry volunteers and government geoscientists, who advise GBC's Board of Directors on project priorities and review proposals received in response to the RFPs.

As of December 2008, GBC has supported 47 partnership projects with an investment of \$6.6 million, which has been matched by over \$5.6 million in partners' funds. These projects include airborne geophysical surveys, geochemical surveys, mineral deposit studies, mapping projects, data compilations and numerous oil and gas-related projects in the intermontane basins. Projects funded through Geoscience BC's Fall 2008 RFP will be announced in early 2009.

Geoscience BC has also funded three major GBC-led projects: QUEST, QUEST-West and Nechako Seismic. The QUEST and QUEST-West projects focus on highlighting the mineral potential in BC's interior using regional geophysical and geochemical surveys, with QUEST focusing on the Quesnel Terrane between Williams Lake and Mackenzie, and QUEST-West focusing on the Stikine Terrane between Vanderhoof and Terrace. Together, these projects represent over \$10 million in public geoscience investment in BC. Funding partners for QUEST and QUEST-West include the Northern Development Initiative Trust, the Province of British Columbia and the Regional Districts of Bulkley-Nechako and Kitimat-Stikine. All QUEST and some QUEST-West geophysical data are now available through Geoscience BC's website, with the remaining QUEST-West geophysics and geochemistry scheduled for release in early 2009.

The third GBC-led project, Nechako Seismic, is Geoscience BC's first major oil and gas project. The 330 line-kilometres of Vibroseis[®] seismic data collected this past summer in the northern Nechako Basin will aid in determining hydrocarbon potential in the basin. This \$2.5 million project was funded by Geoscience BC and a grant from the Northern Development Initiative Trust, and was made possible through the support of the Nazko First Nation, BC Ministry of Energy, Mines and Petroleum Resources, BC Oil and Gas Commission and Bighorn Land & Field Service Ltd.

In addition to the original start-up grant of \$25 M, the Province of British Columbia has generously supported Geoscience BC with an additional \$11.7 M grant in the 2008 provincial budget.

Geoscience BC Summary of Activities 2008

Geoscience BC is pleased to present the results of ongoing and recently completed geoscience projects and surveys in this, our second edition of the *Geoscience BC Summary of Activities*. The volume is divided into three sections, and contains a total of 21 papers, prepared by industry consultants and contractors, university-based researchers and government geoscientists.

The first section contains two papers on the QUEST-West Project in central British Columbia, highlighting the geophysical and geochemical surveys that make up this \$5.4 million project. The second section contains eleven papers on mineral exploration-related partnership projects supported by Geoscience BC, including geochemical, surficial geology, mapping, mineral deposit and rock property data compilations. The third section contains eight papers highlighting Geoscience BC's Nechako Seismic Project, and complementary partnership projects focused in BC's interior basins. All papers are also available on Geoscience BC's website (www.geosciencebc.com), and we encourage readers to visit website for additional information on all the projects, including project abstracts, posters and presentations, and final datasets for all GBC-funded projects.



Acknowledgments

Geoscience BC would like to thank all the authors of the *Summary of Activities* papers, including project proponents, graduate students and GBC Project Team members, for their contributions to this volume. Geoscience BC would also like to thank RnD Technical for their work in editing and assembling the volume.

Christa Sluggett, M.Sc.
Project Geologist and Communications Co-ordinator
Geoscience BC
www.geosciencebc.com

Contents

QUEST Projects

- Kowalczyk, P.L.:** QUEST-West Geophysics in central British Columbia: new regional gravity and helicopter-borne time-domain electromagnetic data 1
- Jackaman, W., Balfour, J.S. and Reichheld, S.A.:** QUEST-West Project geochemistry: field survey and data reanalysis, central British Columbia (parts of NTS 093E, F, J, K, L, M, N) 7

Minerals Projects

- Jackaman, W.:** Stream geochemical survey sample reanalysis, Terrace and Prince Rupert map areas, western British Columbia (NTS 103I, part of 103J)..... 15
- Ferbey, T.:** Trace-element analysis of clay-sized fraction of archived till samples, Babine porphyry copper district, west-central British Columbia (NTS 093L/09, /16, 093M/01, /02, /07, /08) 19
- Ward, B., Maynard, D., Geertsema, M. and Rabb, T.:** Ice-flow history, drift thickness and drift prospecting for a portion of the QUEST Project area, central British Columbia (NTS 093G, H [west half], J) 25
- Jago, C.J. and Tosdal, R.M.:** Distribution of alteration in an alkalic porphyry copper-gold deposit at Mount Milligan, central British Columbia (NTS 094N/01) 33
- Rhys, D.A., Mortensen, J.K. and Ross, K.:** Investigations of orogenic gold deposits in the Cariboo gold district, east-central British Columbia (parts of NTS 093A, H): progress report. 49
- Hollis, L., Kennedy, L.A. and Hickey, K.A.:** Mineralization and alteration of Cretaceous rocks of the Taseko Lakes region, southwestern British Columbia (NTS 092O/04) 75
- Moore, L.H., Hart, C.J.R. and Marsh, E.E.:** Sulphur sources for gold deposits in the Bridge River–Bralorne mineral district, southwestern British Columbia (part of NTS 092J) 91
- Ruks, T., Mortensen, J.K. and Cordey, F.:** Preliminary results of geological mapping, uranium-lead zircon dating, and micropaleontological and lead isotopic studies of volcanogenic massive sulphide–hosting stratigraphy of the Middle and Late Paleozoic Sicker and Lower Buttle Lake groups on Vancouver Island, British Columbia (NTS 092B/13, 092C/16, 092E/09, /16, 092F/02, /07) 103
- Hartlaub, R.P.:** Sediment-hosted stratabound copper-silver-cobalt potential of the Creston Formation, Purcell Supergroup, southeastern British Columbia (parts of NTS 082G/03, /04, /05, /06, /12)..... 123

- Kirkham, G.D., Miles, W.F., Paradis, S., Finley, B. and Troop, A.:** Time-domain electromagnetic and magnetic survey over the Kootenay Arc, southeastern British Columbia (NTS 082F/03, /04, /06) 133

- Parsons, S., McGaughey, J., Mitchinson, D., Phillips, N. and Lane, T.:** Development and application of a rock property database for British Columbia. 137

Oil and Gas Projects

- Calvert, A.J., Hayward, N., Smithyman, B.R. and Takam Takougang, E.M.:** Vibroseis survey acquisition in the central Nechako Basin, south-central British Columbia (parts of NTS 093B, C, F, G) 145
- Hayward, N. and Calvert, A.J.:** Preliminary first-arrival modelling constraints on the character, thickness and distribution of Neogene and Eocene volcanic rocks in the southeastern Nechako Basin, south-central British Columbia (NTS 092N, O, 093B, C) 151
- Clowes, R.M. and Smithyman, B.R.:** Enhanced velocity structure from waveform tomography of seismic first-arrival data: application to the Nechako Basin, south-central British Columbia (parts of NTS 093B, C, F, G) 157
- Kim, H.S., Cassidy, J.F., Dosso, S.E., and Kao, H.:** Mapping the sedimentary rocks and crustal structure of the Nechako Basin, south-central British Columbia (NTS 092N, O, 093B, C, F, G) using teleseismic receiver functions 163
- Idowu, O., Frederiksen, A. and Cassidy, J.F.:** Seismic tomography of the Nechako Basin, south-central British Columbia (NTS 092N, O, 093B, C, F, G) using ambient seismic noise 171
- Spratt J.E., and Craven, J.A.:** Preliminary images of the conductivity structure of the Nechako Basin, south-central British Columbia (NTS 092N, O, 093B, C, F, G) from the magnetotelluric method. 175
- Mahoney, J.B., Haggart, J.W., MacLaurin, C.I., Forgette, M.M., Goodin, J.R., Balgord, E.A. and Mustard, P.S.:** Regional facies patterns in the northern Jackass Mountain Group, northern Methow Basin, southwestern British Columbia (NTS 092O) 183
- Gagnon, J-F. and Waldron, J.W.F.:** Sedimentation patterns and reservoir distribution in a siliciclastic, tectonically active slope environment, Bowser Basin, northwestern British Columbia (NTS 104B/01) 193

QUEST-West Geophysics in Central British Columbia (NTS 093E, F, G, K, L, M, N, 103I): New Regional Gravity and Helicopter-Borne Time-Domain Electromagnetic Data

P.L. Kowalczyk, Geoscience BC, Vancouver, BC, kowalczyk@geosciencebc.com

Kowalczyk, P.K (2009): QUEST-West geophysics in central British Columbia (NTS 093E, F, G, K, L, M, N, 103I): new regional gravity and helicopter time-domain electromagnetic data; *in* Geoscience BC Summary of Activities 2008, Geoscience BC, Report 2009-1, p. 1–6.

Introduction

Geoscience BC's 2008 QUEST-West Project continues the successful 2007 QUEST program. The survey area adjoins the QUEST area, and extends westward past Terrace and Kitimat (Figure 1). Similar to the QUEST Project, the QUEST-West Project combines airborne geophysical surveys with new regional geochemical data, providing new geoscience datasets that will help uncover the significant mineral potential of central British Columbia. This paper describes the new regional geophysical data acquired in the QUEST-West Project, comprising an airborne gravity survey and a helicopter-borne time-domain electromagnetic survey (Figure 2). The QUEST-West geochemical survey and other projects in the QUEST-West project area are described in other papers in this volume, particularly Jackaman et al. (2008). Funding partners on this project include Geoscience BC, Northern Development Initiative Trust, Regional District of Bulkley-Nechako, Regional District of Kitimat-Stikine and BC Ministry of Energy, Mines and Petroleum Resources.

The QUEST-West airborne gravity survey was released in November 2008 as Geoscience BC Report 2008-10 (for technical details, *see* Sander Geophysics Limited, 2008b), extending westward from the QUEST project area (Figure 3; Barnett and Kowalczyk, 2008). This new gravity dataset joins seamlessly with the 2007 QUEST gravity data (Geoscience BC Report 2008-8; for technical details, *see* Sander Geophysics Limited, 2008a) and the 2008 Natural Resources Canada Nechako Basin gravity data releases (Dumont, 2008a–d). It provides new high-quality data to assist in the identification of regional mineralizing controls and help the mapping of geology beneath cover, and complements the existing aeromagnetic data, geological mapping and new geochemical data (Jackaman et al, 2008). As the dataset crosses two UTM zones, the grids and point data are currently available from the Geoscience BC website in

UTM zone 9 WGS84, UTM zone 10 WGS84, and in the BC Albers projection to accommodate usage in different projections. The survey was flown by Sanders Geophysics Limited using their Airborne Inertially Referenced Gravitometer (AIRGrav™; Sander et al., 2004) and comprises 25 500 line-kilometres (line-km) of new airborne gravity data.

New helicopter-borne time-domain electromagnetic (TEM) data were also acquired over the QUEST-West area (Sattel, 2006). The survey was flown by Aeroquest Limited, using their Aerotem™ III system, with more than 12 900 line-km of helicopter TEM data acquired at a 4 km line spacing (Figure 4). These data complement the airborne gravity data and the existing regional aeromagnetic data. The survey was not intended to prospect for new mineral deposits, but rather to map the regional geological response (i.e., depth of overburden, regional geological bedrock features and throughgoing regional structures). The survey results will assist geological mapping and provide context for exploration projects in the area. Geoscience BC also commissioned detailed helicopter TEM surveys over six known deposits in the QUEST-West area: Morrison, Bell, Granisle, Equity Silver, Endako and Huckleberry (MINFILE 093M 007, 093M 001, 093L 146, 093L 001, 093K 006 and 093E 037; MINFILE, 2008). These case studies will provide useful information to companies planning exploration projects in the QUEST-West and surrounding areas. The QUEST-West helicopter TEM data are expected to be released at Roundup 2009.

Both the airborne gravity data and the helicopter-borne TEM survey were acquired with state-of-the-art, fully calibrated digital systems. The data are of high quality and are amenable to, and intended for, digital processing using inversion methods to produce maps of inferred depth of bedrock, overburden thickness and conductivity, and basement conductivity. The new case-history TEM surveys carried out over particular deposits in the QUEST-West project area add to the orientation survey acquired over the Mount Milligan deposit and the detailed airborne gravity data acquired over the Mount Milligan, Gibraltar and Mount Polley deposits in 2007. This catalogue of deposit re-

Keywords: *QUEST-West, geophysics, gravity, electromagnetic, AIRGrav™, AeroTEM™*

This publication is also available, free of charge, as colour digital files in Adobe Acrobat® PDF format from the Geoscience BC website: <http://www.geosciencebc.com/s/DataReleases.asp>.

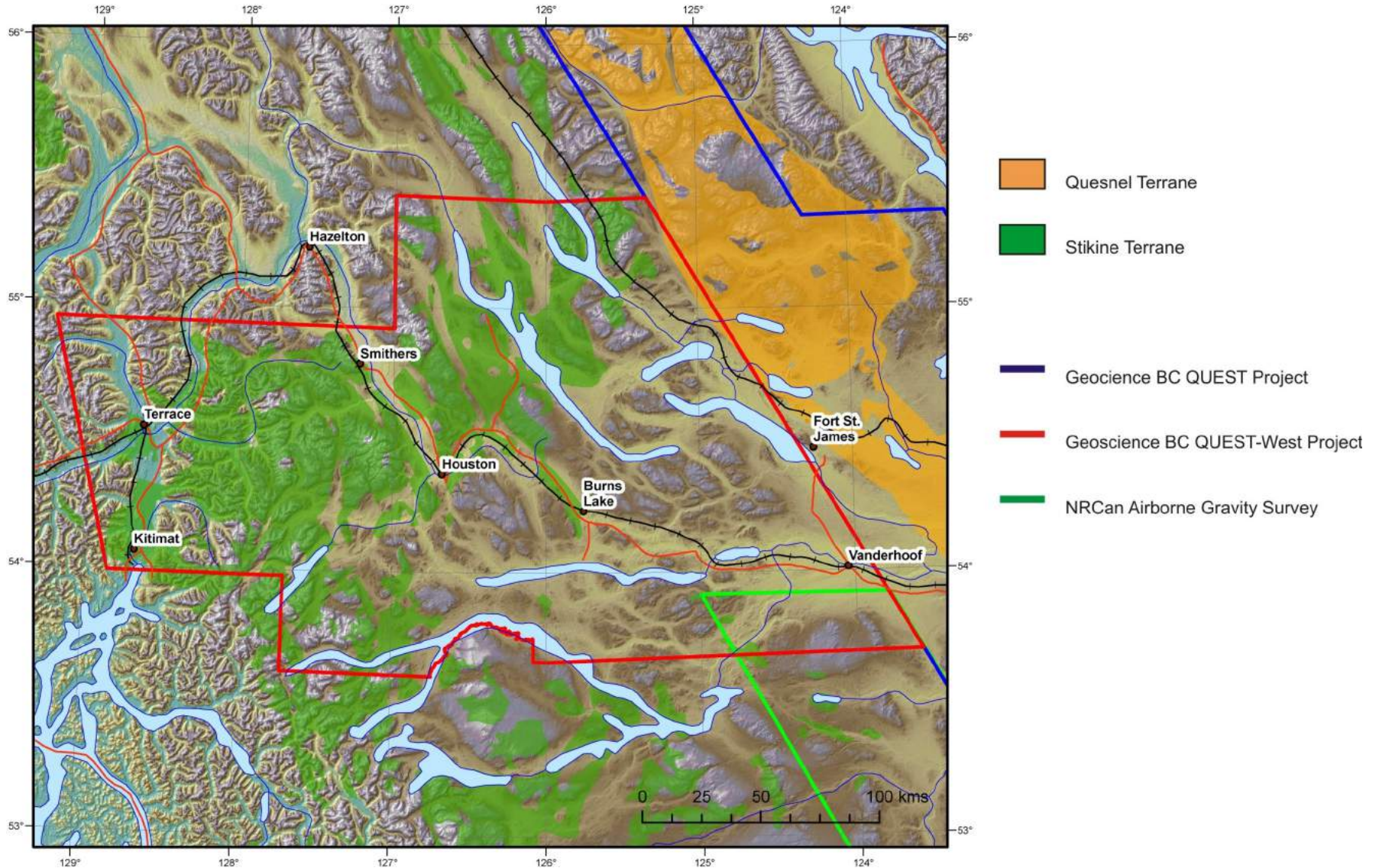


Figure 1. Outline of the Geoscience BC QUEST-West survey areas. The red line shows the limits of the airborne gravity survey, flown at a 2 km line spacing. The blue outline to the east shows the area of the adjoining QUEST survey. The red line shows the limits of the helicopter-borne electromagnetic survey flown at 4 km line spacing. The small parallelogram in the southeast corner represents the area covered by the Natural Resources Canada (NRCan) airborne gravity survey flown in 2007; the area within QUEST-West covered by this survey was excluded from the QUEST-West airborne gravity survey. The QUEST, QUEST-West and NRCan Nechako airborne gravity surveys were all flown to the same specifications and form a seamless, contiguous block of data. Digital elevation model prepared by K. Shimamura, Geological Survey of Canada–Vancouver.

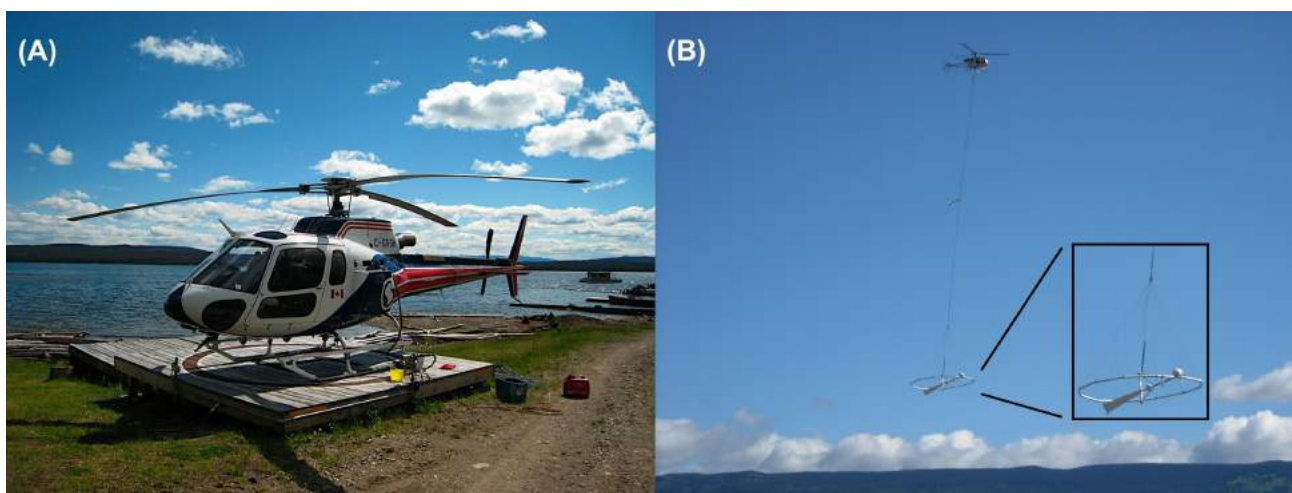


Figure 2. Flying operations during the gravity and electromagnetic surveys: A) helicopter used by Sander Geophysics Limited to acquire the airborne gravity data; Sander elected to fly the gravity survey using a helicopter instead of a fixed-wing aircraft to allow slower flight speeds and better adherence to a preprogrammed 'drape' surface; photo courtesy of O. Peterson, Sander Geophysics Limited; B) helicopter used by Aeroquest Limited, with the AeroTEM™ III system and magnetometer seen beneath the aircraft; inset shows the AeroTEM III transmitter and receiver coils in more detail; a Llama helicopter suitable for mountain flying was used by Aeroquest in the western parts of the survey area to allow better control of the system ground clearance; photo courtesy of Aeroquest Limited. These choices of aircraft improved the quality of the survey, particularly in the more rugged western part of the survey area.

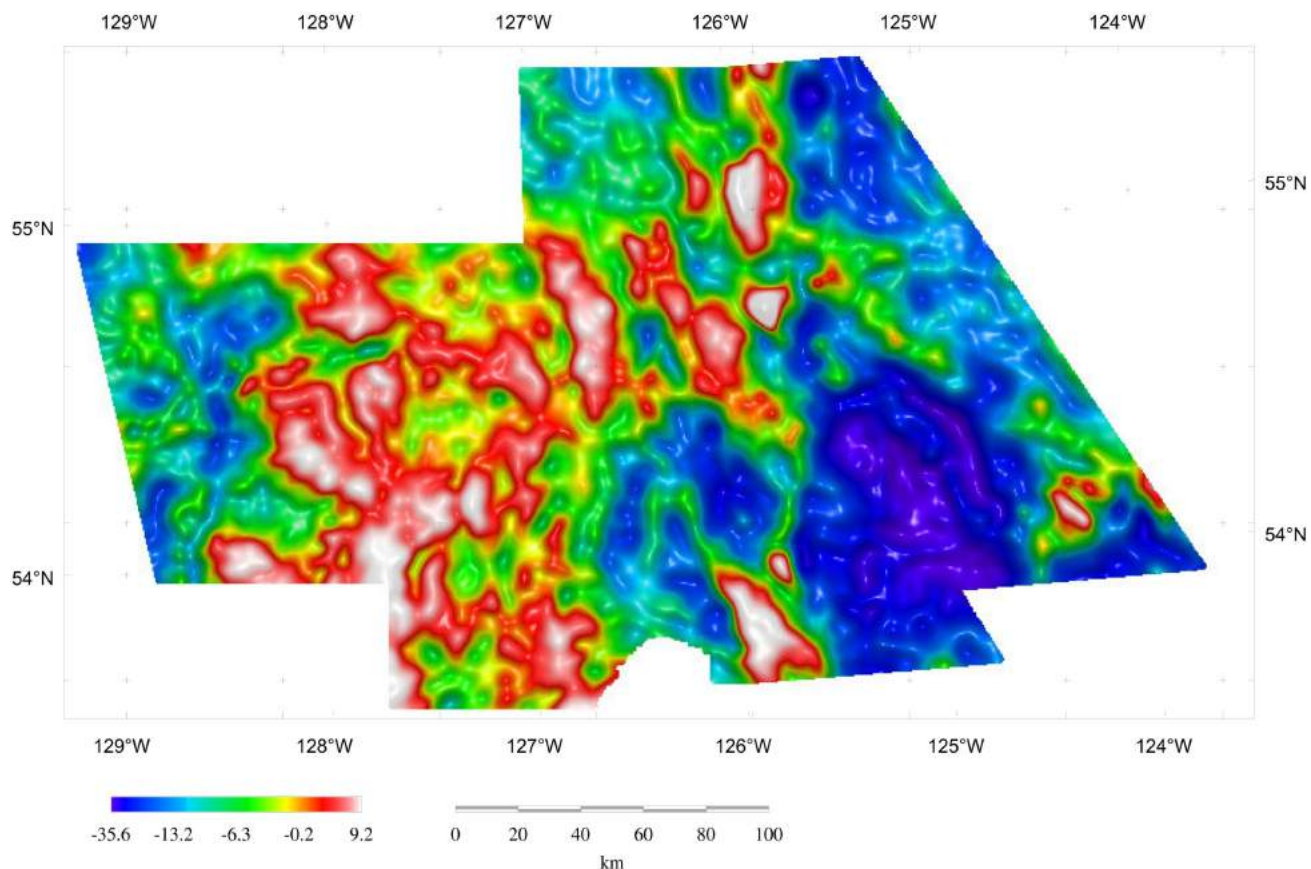


Figure 3. Sun-shadowed image of the 2008 QUEST-West airborne gravity results. Shown is the isostatically corrected Bouguer gravity image, smoothed with a 3 km filter. The flight lines are spaced 2 km apart and are aligned east-west in the UTM zone system. North-south tie lines were flown at 20 km spacing.

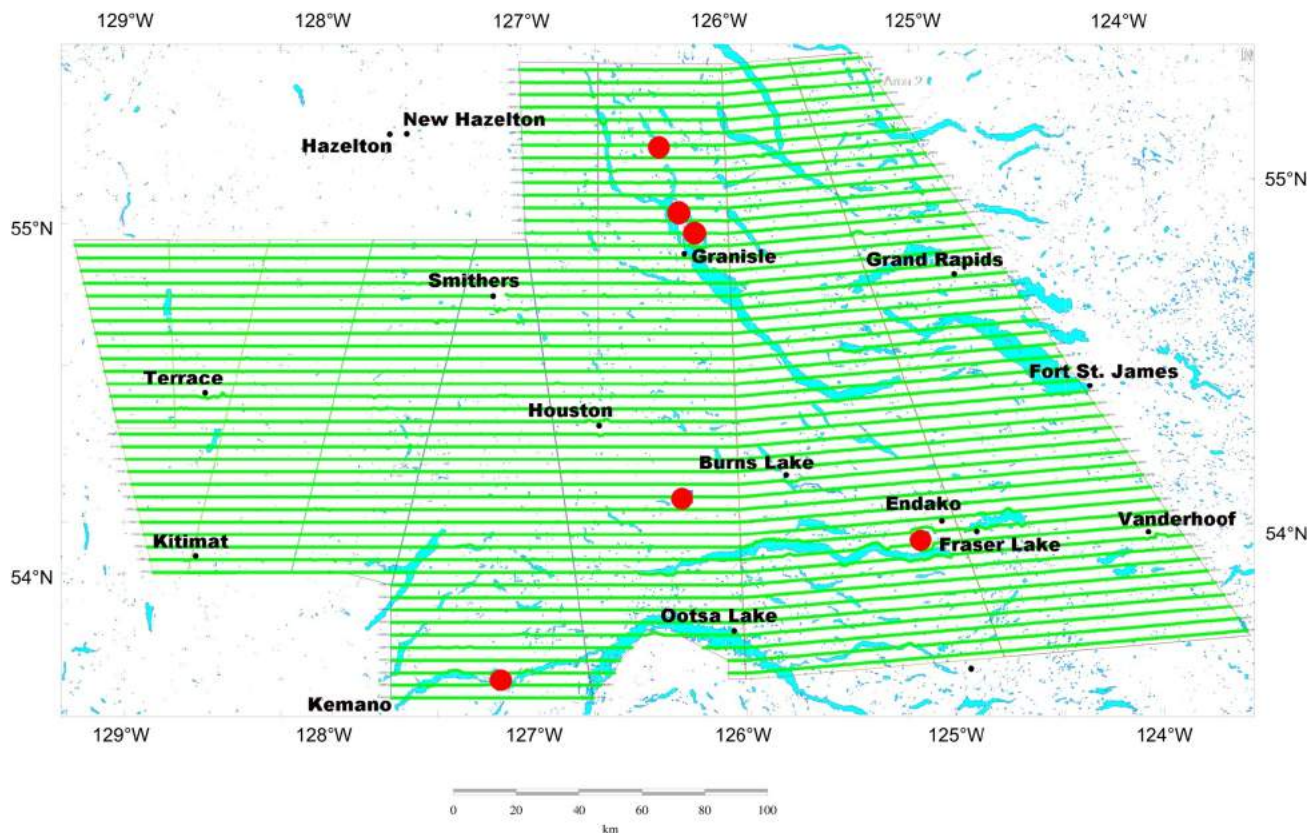


Figure 4. Helicopter-borne TEM survey lines in the QUEST-West project area. The six detailed surveys, marked with red dots, are (from north to south) the Morrison, Bell, Granisle, Equity, Endako and Huckleberry deposits. The regional flight lines are oriented east-west in the UTM co-ordinate system at 4 km spacing. The survey area crosses the boundary between UTM Zones 9 and 10 at latitude 126° W and the lines turn to accommodate the change in orientation of the UTM grid.

sponses will retain its value into the future as reference data sets for the exploration community.

The gravity and TEM flight lines have been selected so that the TEM data are acquired along alternate gravity flight lines. The lines follow even UTM northings, so their location is well defined and they can be used as reference lines for future infilling.

All QUEST-West data will be released through Geoscience BC's website at <http://www.geosciencebc.com/s/DataReleases.asp>.

References

Barnett, C.T. and Kowalczyk, P.L. (2008): Airborne electromagnetics and airborne gravity in the QUEST Project area, Williams Lake to Mackenzie, British Columbia (parts of NTS 093A, B, G, H, J, K, N, O; 094C, D); in Geoscience BC, Summary of Activities 2007, Geoscience BC, Report 2008-1, p. 1–6. , URL <<http://www.geosciencebc.com/s/DataReleases.asp>> [November 27, 2008].

Dumont, R. (2008a): Bouguer anomaly, Nechako Basin airborne gravity survey, Prince George / Nechako River (NTS 93 G and part of 93 F), British Columbia; Geological Survey of Canada, Open File 5883, 1 map at 1:250 000 scale, URL

<http://apps1.gdr.nrcan.gc.ca/mirage/mirage_list_e.php?id=225540> [November 27, 2008].

Dumont, R. (2008b): Bouguer anomaly, Nechako Basin airborne gravity survey, Quesnel / Anahim Lake (NTS 93B and part of 93C), British Columbia; Geological Survey of Canada, Open File 5884, 1 map at 1:250 000 scale, URL <http://apps1.gdr.nrcan.gc.ca/mirage/mirage_list_e.php?id=225541> [November 27, 2008].

Dumont, R. (2008c): First vertical derivative of the Bouguer anomaly, Nechako Basin airborne gravity survey, Prince George / Nechako River (NTS 93 G and part of 93 F), British Columbia; Geological Survey of Canada, Open File 5881, 1 map at 1:250 000 scale, URL <http://apps1.gdr.nrcan.gc.ca/mirage/mirage_list_e.php?id=225538> [November 27, 2008].

Dumont, R. (2008d): First vertical derivative of the Bouguer anomaly, Nechako Basin airborne gravity survey, Quesnel / Anahim Lake (NTS 93 B and part of 93 C), British Columbia; Geological Survey of Canada, Open File 5882, 1 map at 1:250 000 scale, URL <http://apps1.gdr.nrcan.gc.ca/mirage/mirage_list_e.php?id=225539> [November 27, 2008].

Jackaman, W., Balfour, J.S. and Reichheld, S.A. (2009): QUEST-West Project geochemistry: field survey and data reanalysis (parts of NTS 093E, F, J, K, L, M, N), central British Columbia; in Geoscience BC Summary of Activities 2008, Geoscience BC, Report 2009-1, p. 7–14, URL <<http://>

- www.geosciencebc.com/s/DataReleases.asp> [November 27, 2008].
- Sander, S., Argyle, M., Elieff, S. Ferguson, S., Lavoie, V. and Sander, L. (2004): The AIRGrav airborne gravity system (abstract); ASEG-PESA Airborne Gravity 2004 Workshop, Abstracts <http://www.sgl.com/technicalpapers/AIRGrav_airborne_grav_sys.pdf> [November 24, 2008].
- Sander Geophysics Limited (2008a): Airborne gravity survey, Quesnellia Region, British Columbia; Geoscience BC, Report 2008-08, 121 p., URL <<http://www.geosciencebc.com/s/DataReleases.asp>> [November 27, 2008].
- Sander Geophysics Limited (2008b): Airborne gravity survey, QUEST-West, British Columbia; Geoscience BC, Report 2008-10, 129 p. , URL <<http://www.geosciencebc.com/s/DataReleases.asp>> [November 27, 2008].
- Sattel, D. (2006): A brief discussion of helicopter time-domain electromagnetic systems; Society of Exploration Geophysicists, Technical Program Expanded Abstracts, v. 25, p. 1268–1272.

QUEST-West Project Geochemistry: Field Survey and Data Reanalysis, Central British Columbia (parts of NTS 093E, F, J, K, L, M, N)

W. Jackaman, Noble Exploration Services Ltd., Sooke, BC, wjackaman@shaw.ca

J.S. Balfour, Consultant, Cranbrook, BC

S.A. Reichheld, Consultant, Sooke, BC

Jackaman, W., Balfour, J.S. and Reichheld, S.A. (2009): QUEST-West Project geochemistry: field survey and data reanalysis, central British Columbia (parts of NTS 093E, F, J, K, L, M, N); in Geoscience BC Summary of Activities 2008, Geoscience BC, Report 2009-1, p. 7–14.

Introduction

As recently as the early 1990s, large portions of central British Columbia have had limited to no regional geochemical coverage. Although a number of provincial and federal government-funded, reconnaissance-scale stream sediment and water surveys had been completed in the area prior to 1990, the regional coverage was sparse and original analytical results are now considered inadequate. Recognizing these deficiencies, efforts were initiated in 1993 by the BC Geological Survey (BCGS) and Geological Survey of Canada (GSC) to improve the geochemical database of the region. The primary objective of those efforts was to provide high quality data that could be used to better assess the mineral potential and increase the opportunity for new discoveries (Cook, 1997). The subsequent mountain pine beetle infestation further supported the importance of acquiring and developing up-to-date information for this area. From 1993 to 2002, a total of 2122 drainage sediment and water samples were collected as well as samples from other geochemical sampling methods, such as till and biogeochemical surveys (Kerr and Levson, 1997; Jackaman, 2007b). Starting in 2005, Geoscience BC-funded initiatives have added another 6822 new samples to the database and have also supported the reanalysis of 7769 previously collected stream sample pulps using modern analytical methods (Jackaman, 2006a; Jackaman and Balfour, 2007, 2008). In 2009, the collection will be further augmented with the release of data from over 950 new sites and the reanalysis of 3629 samples compiled as part of the 2008 QUEST-West Project (Figure 1).

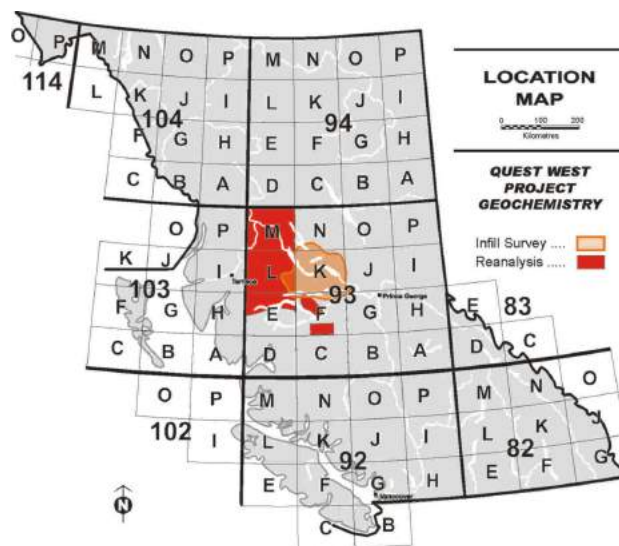


Figure 1. Location of the 2008 QUEST-West drainage sediment survey and sample reanalysis study areas, British Columbia.

QUEST-West 2008 Geochemistry Programs

Although a number of reconnaissance-scale stream surveys have been completed within the more mountainous regions of central BC, much of the flat-lying plateau areas had not been sampled until relatively recently. Characterized by a subdued landscape that includes a large number of potential lake sites (Figure 2), it was determined that lake bottom sediments could be considered an appropriate sample media (Cook, 1993). Used sparingly in other parts of BC but more routinely in central and eastern Canada, the technique has been shown to be effective in identifying regional geochemical patterns as well as anomalous metal concentrations related to mineral deposits (Hoffman, 1976; Coker et al., 1979; Friske, 1991). Supported by the results of this research, lake-based geochemical sampling of BC's central interior proceeded in 1993. The initial phase consisted of several detailed lake sediment surveys in parts of the Nechako River map area (Cook and Jackaman, 1994), the northeast corner of the Fort Fraser map area (Cook et al., 1997) and the Babine porphyry belt (Cook et al., 1998).

Keywords: Nechako Plateau, Fraser Plateau, mineral exploration, geochemistry, multi-element, reanalysis, stream sediment, lake sediment

This publication is also available, free of charge, as colour digital files in Adobe Acrobat® PDF format from the Geoscience BC website: <http://www.geosciencebc.com/s/DataReleases.asp>.



Figure 2. Typical lake sample site found in the flat topography of the Nechako Plateau, central British Columbia.

More recently, Geoscience BC has funded several large-scale surveys (Jackaman, 2006b, 2007a) covering parts of the Nechako and Fraser plateaus as well as the reanalysis of archived stream and lake sediment samples (Geoscience BC, 2008). In 2008, the QUEST-West Project included a 955 site infill survey in the northern Nechako Plateau (Figure 3) and 3629 archived samples were selected for reanalysis (Figure 4). Table 1 provides a complete list of drainage sediment geochemical survey work completed in central BC since 1993.

Infill Drainage Sediment Survey

The 2008 QUEST-West Project geochemical survey covers parts of the northern portion of the Nechako Plateau. Although much of the area was the site of previous stream and lake sediment projects, the target area included a large

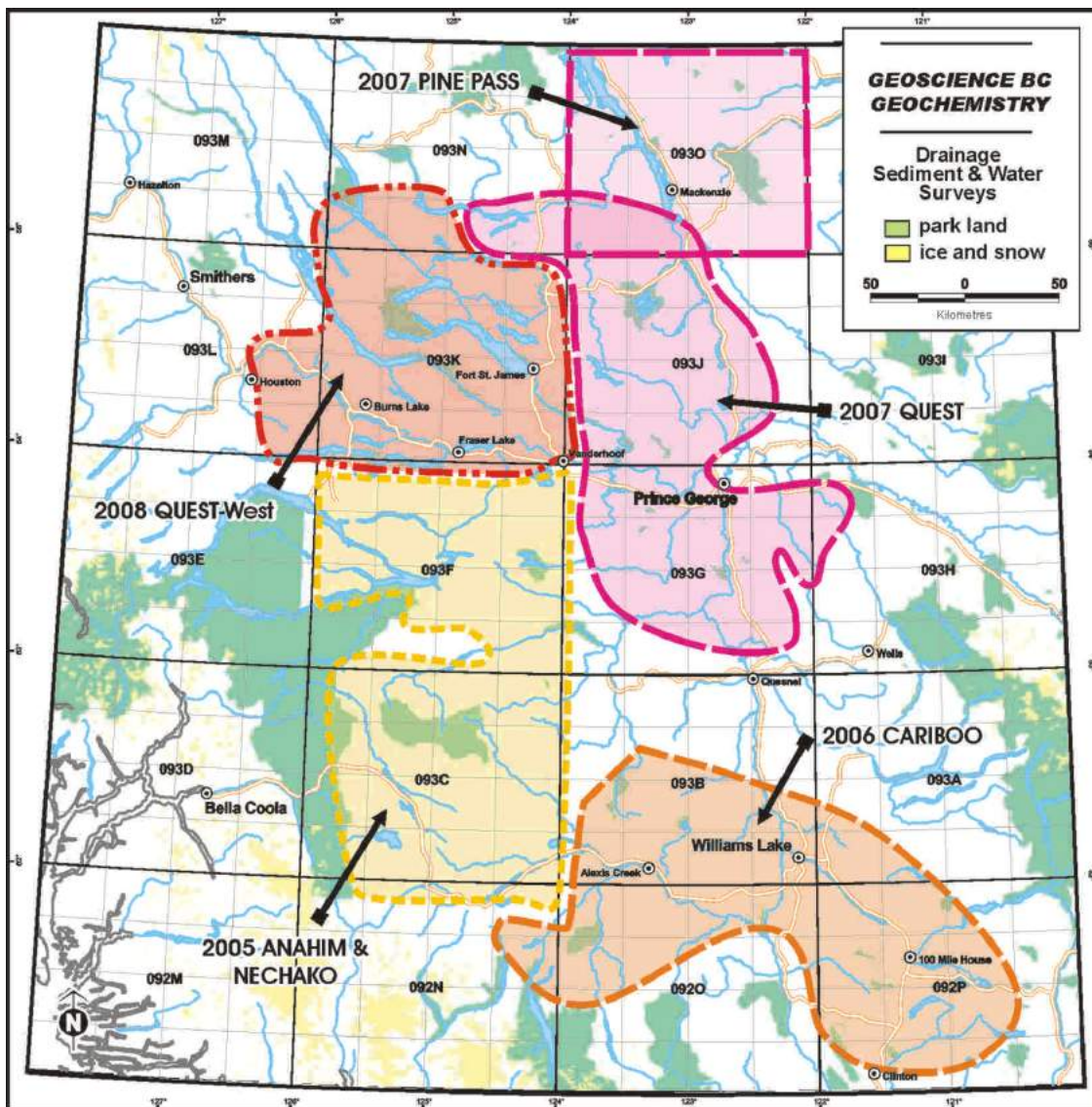


Figure 3. Detailed location map showing the areas where drainage sediment and water surveys have been completed by Geoscience BC in central British Columbia since 2005.

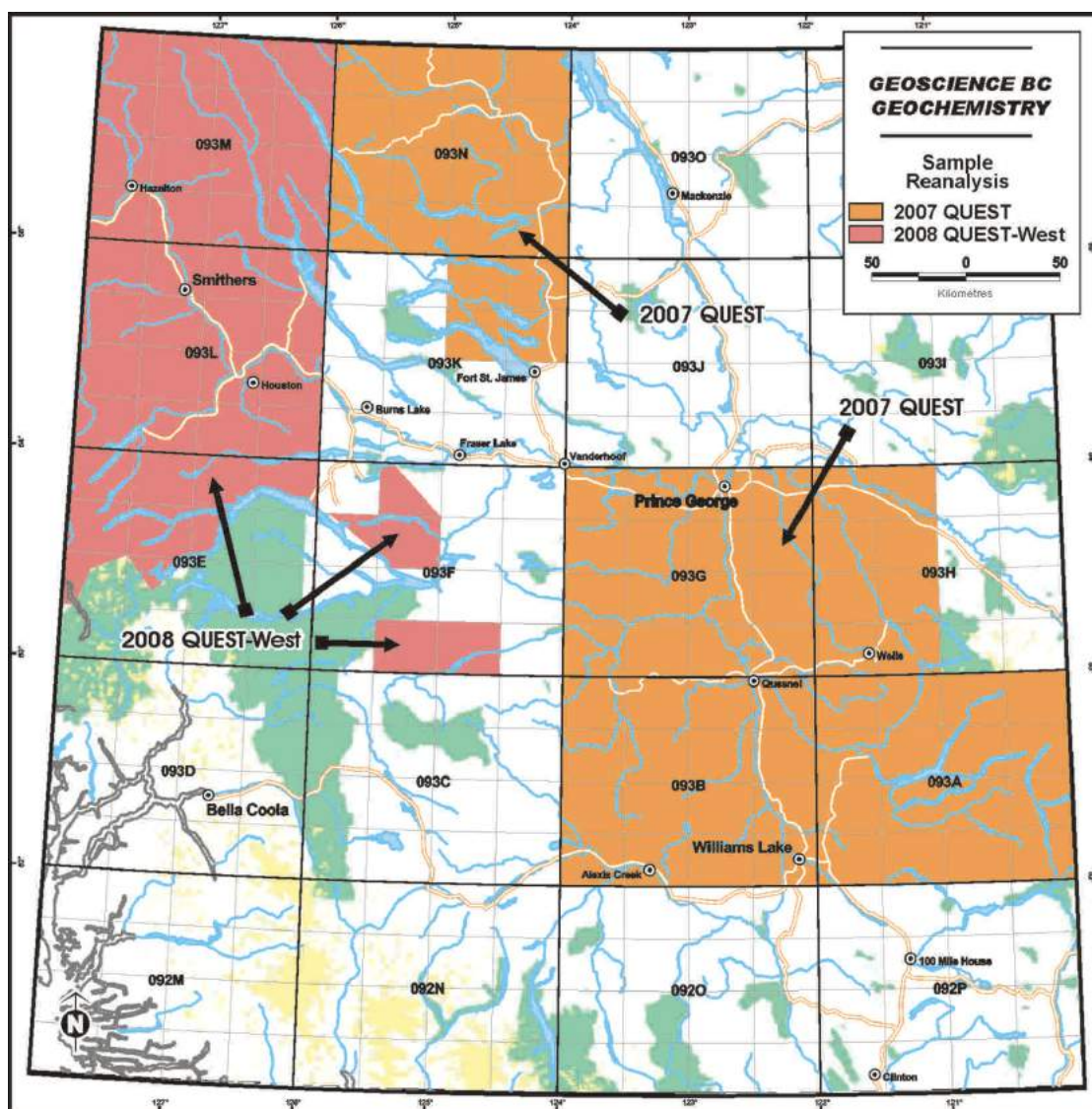


Figure 4. Detailed location map showing the areas of survey sample reanalysis completed by Geoscience BC in central British Columbia since 2005.

Table 1. Drainage sediment geochemical survey areas for work completed in central British Columbia since 1993.

Year	Name	Type	NTS map sheet	Agency	Sites	Samples
1993	Fawnie/Ootsa	Lake survey	093F	BCGS	461	489
1995	Pinchi	Lake survey	093K	BCGS/GSC	413	438
1996	Babine	Lake survey	093L, M	BCGS	332	352
2002	Fort Fraser	Stream survey	093K	BCGS/GSC	795	843
2005	McLeod Lake	Sample reanalysis	093J	BCGS/GSC	1088	1152
2005	Anahim/Nechako	Lake/stream survey	092N, 093C, F	Geoscience BC	1953	2068
2006	Cariboo	Lake survey	092N, O, P, 093A, B	Geoscience BC	1370	1451
2007	QUEST	Lake survey	093G, H, J, N, O	Geoscience BC	2264	2397
2007	Pine Pass	Stream survey	093O	Geoscience BC	854	906
2007	QUEST	Sample reanalysis	093A, B, G, H, K, N	Geoscience BC	5208	5516
2008	Terrace/Prince Rupert	Sample reanalysis	103I, J	Geoscience BC	2128	2253
2008	QUEST-West	Lake/stream survey	093K, L, N	Geoscience BC	952	988
2008	QUEST-West	Sample reanalysis	093E, F, L, M	Geoscience BC	3428	3629

Abbreviations: BCGS, British Columbia Geological Survey; GSC, Geological Survey of Canada

number of new sample sites. In addition, the lake-based work will link a number of lake surveys previously completed in surrounding areas.

Based on standards set by the National Geochemical Reconnaissance (NGR) and BC Regional Geochemical Survey (RGS) programs, helicopter- and truck-supported sample collection was carried out in August and September 2008. A total of 905 lake sediment and water samples and 100 stream sediment and water samples were systematically acquired. Field duplicate sediment and water samples were routinely collected in each analytical block of 20 samples. Combined with the previous survey work, the resulting average sample site density is one site per 7 km² over the 14 500 km² survey area.

Lake sites were accessed using a float-equipped Bell Jet Ranger helicopter (Figure 5) from Interior Helicopter Ltd. (Fort St. James). The sampling crews collected sediment material with a torpedo-style sampler and water samples were saved in 250 mL bottles. Samples were successfully collected from most of the lakes targeted in the survey area. However, some of the smaller ponds and very large, deep lakes were not sampled due to poor sampling conditions. Stream sampling was supported by both truck and helicopter. Approximately 2 kg of fine-grained sediment and 250 mL of clean flowing water was collected at each site. Field observations and site locations were recorded for all sample sites.

At Eco Tech Laboratory Ltd. (Kamloops), dried lake sediment samples were pulverized in a ceramic ring mill to approximately -150 mesh (100 μm) and stream sediment samples were sieved to -80 mesh (177 μm). To monitor and assess accuracy and precision of analytical results, control reference material and analytical duplicate samples were inserted into each block of 20 sediment samples. The sediment samples will be analyzed for base and precious met-

als, pathfinder elements and rare earth elements by inductively coupled plasma mass spectrometry (ICP-MS) and instrumental neutron activation analysis (INAA). Loss-on-ignition and fluorine content will also be determined for sediment material. Fluoride content, conductivity and pH will be determined for the water samples.

Sample Reanalysis

The reanalysis of archived drainage sediment samples by ICP-MS has been found to be a cost-effective means of obtaining new and improved regional geochemical information. The technique provides a significant upgrade from the atomic absorption spectrometry (AAS) method, routinely used for older federal and provincial government-funded geochemical surveys, by making available a wide range of new analytical information at improved detection limits. The work also offers greater data compatibility with laboratory methods currently being employed as well as with other reanalysis initiatives.

Similar to work completed as part of the 2007 QUEST Project, the QUEST-West Project identified a total of 3629 archived survey samples. The samples originated from previous federal government NGR and BC RGS projects. Conducted prior to 1996, the stream- and lake-based surveys covered areas in NTS map sheets 093E, F, L and M (2008 QUEST-West, Figure 4).

Access to government storage facilities located in both Ottawa and Victoria was arranged by GSC and BCGS collection custodians. At the sites, a portion of 1 to 2 g of each archived stream sediment sample was carefully extracted from storage containers (Figure 6). Material from each vial was independently split and transferred to a Ziploc® bag labelled with the sample's original unique identification number. Once secured for shipping, the recovered material was delivered to Acme Analytical Laboratories Ltd. (Van-



Figure 5. Interior Helicopter Ltd.'s helicopter equipped with floats, northern Nechako Plateau, central British Columbia.



Figure 6. Sample recovery at the Geological Survey of Canada sample storage facility in Ottawa.

cover). At the lab, each sample was tested for 37 elements by ICP-MS analysis using an aqua regia digestion.

Project Summary

For the past 30 years, developing and maintaining the provincial drainage sediment geochemical database has been an ongoing task for the GSC and the BCGS. These programs have successfully compiled data for over 65 000 sample sites covering 70% of BC (Lett, 2005). The results of the work are considered an important mineral exploration tool. Surveys have helped stimulate follow-up mineral exploration that is valued in the millions of dollars and has been credited with the discovery of numerous mineral prospects. Recent contributions associated with a number of

Geoscience BC initiatives have also been significant in adding value to this important exploration resource. This is particularly true in BC's central interior where new geochemical data has been collected for close to 17 000 samples at an average sample density of one sample every 8 km². Figures 7 and 8 illustrate the significant improvement made to overall sample coverage since 2005. As a result of these efforts, central BC now has one of the country's most comprehensive collections of drainage sediment geochemical information. Compiled to established standards, released in a timely fashion and presented in usable formats, data from the Geoscience BC projects will make an important contribution in stimulating mineral exploration as well as complement other geoscience research and data mining activities for an area that is considered to have a

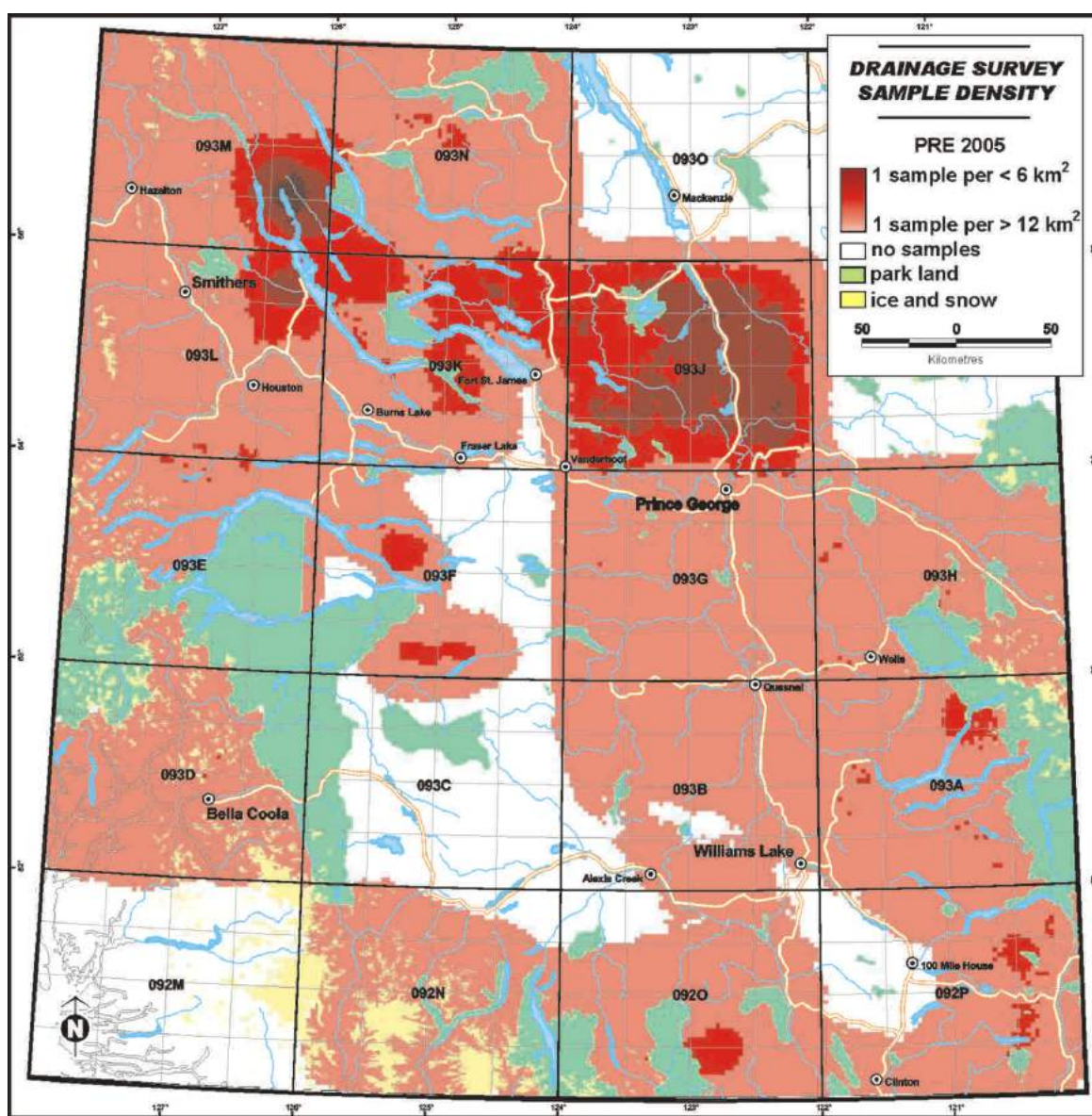


Figure 7. The contour image map shows the overall drainage sediment sample density for central British Columbia prior to 2005.

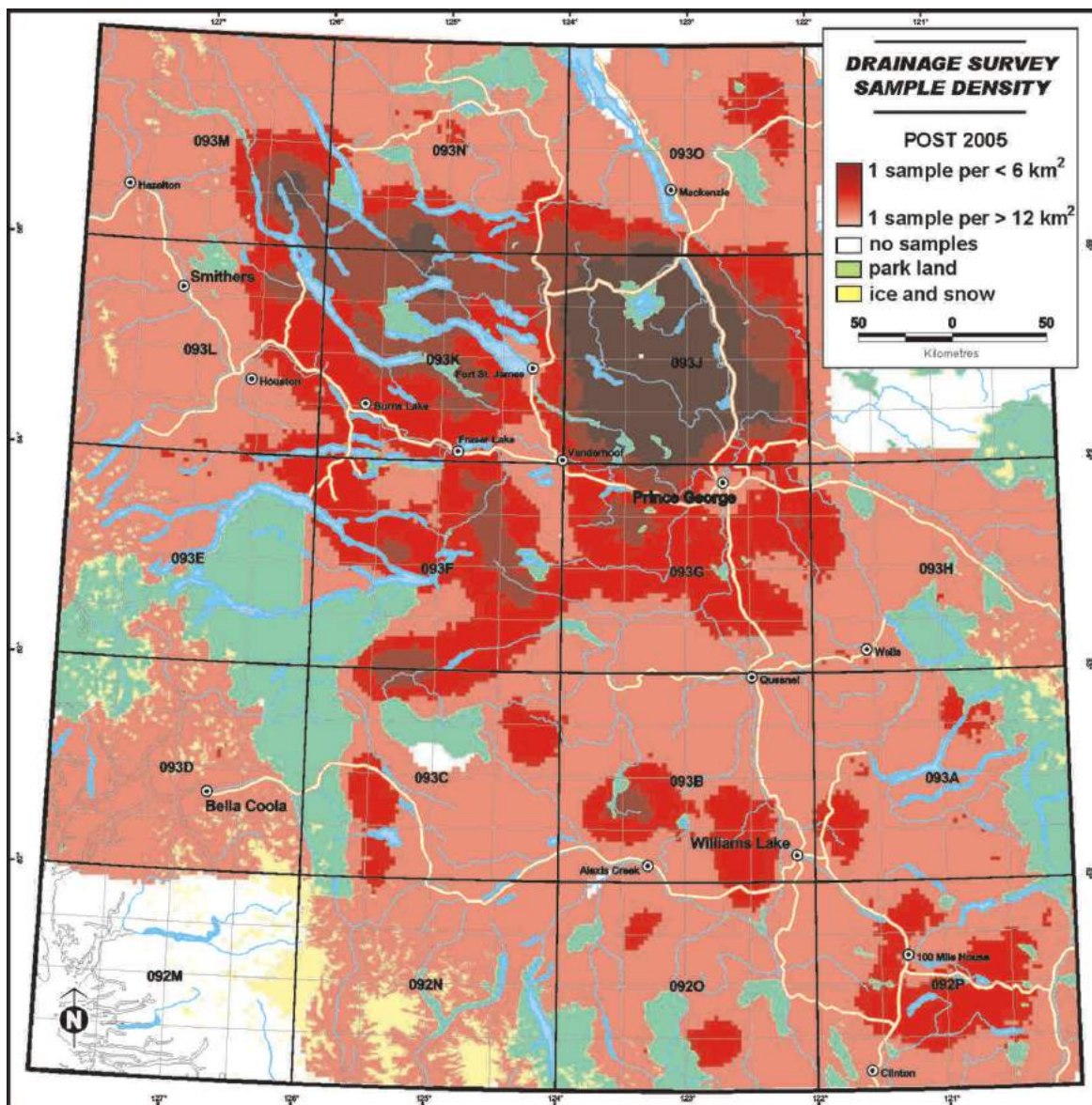


Figure 8. The contour image map shows the significant improvement to overall drainage sediment sample density as a result of new field surveys completed from 2005 to 2008, central British Columbia.

great potential for future discoveries of base- and precious-metal deposits, such as those found at the Endako, Equity Silver, Gibraltar, Huckleberry, Mount Polley, QR and Mount Milligan mining properties.

Acknowledgments

The authors acknowledge P. Friske and M. McCurdy of NRCan and D. Lefebure and R. Lett of the BCGS for their assistance with the reanalysis work; Interior Helicopters Ltd. for their air support; J. Faulkner for his excellent helicopter flying abilities; S. Webb, E.M. Jackaman and E.S. Jackaman for their contributions both on the ground and in the air; the many services located in the communities of Burns Lake, Fraser Lake and Fort St. James. This project was funded by Geoscience BC in partnership with the

Northern Development Initiative Trust and the Regional District of Bulkley-Nechako.

References

- Coker, W.B., Hornbrook, E.H.W. and Cameron, E.M. (1979): Lake sediment geochemistry applied to mineral exploration; *in* Geophysics and Geochemistry in the Search for Metallic Ores, P.J. Hood (ed.), Geological Survey of Canada, Economic Geology Report 31, p. 435–478.
- Cook, S.J. (1993): Preliminary report on lake sediment studies in the Northern Interior Plateau, central British Columbia (093C, E, F, K, L); *in* Geological Fieldwork 1992, BC Ministry of Energy, Mines and Petroleum Resources, Paper 1993-1, p. 475–481.
- Cook, S.J. (1997): Regional and property-scale application of lake sediment geochemistry in the search for buried mineral de-

- posits in the southern Nechako Plateau area, British Columbia (093C, E, F, K, L); *in* Interior Plateau Geoscience Project: Summary of Geological, Geochemical and Geophysical Studies, L.J. Diakow and J.M. Newell (ed.), BC Ministry of Energy, Mines and Petroleum Resources, Paper 1997-2, p. 175–203.
- Cook, S.J. and Jackaman, W. (1994): Regional lake sediment and water geochemistry of part of the Nechako River map area (093F/2, 3; parts of 093F/6, 11, 12, 13, 14); BC Ministry of Energy, Mines and Petroleum Resources, Open File 1994-19, 31 p.
- Cook, S.J., Jackaman, W., McCurdy, M.W., Day, S.J. and Friske, P.W.B. (1997): Regional lake sediment and water geochemistry of part of the Fort Fraser map area, British Columbia (093K/9, 10, 15, 16); BC Ministry of Energy, Mines and Petroleum Resources, Open File 1996-15, 33 p.
- Cook, S.J., Lett, R.E.W., Levson, V.M., Jackaman, W., Coneys, A.M. and Wyatt, G.J. (1998): Regional lake sediment and water geochemistry of the Babine porphyry belt, central British Columbia (093L/9, 16; 093M/1, 2, 7, 8); BC Ministry of Energy, Mines and Petroleum Resources, Open File 1997-17, 33 p.
- Friske, P.W.B. (1991): The application of lake sediment geochemistry in mineral exploration; *in* Exploration Geochemistry Workshop, Geological Survey of Canada, Open File 2390, p. 4.1–4.2.
- Geoscience BC (2008): Geoscience BC's QUEST Project, geochemical sample reanalysis; Geoscience BC, Report 2008-3, URL <<http://www.geosciencebc.com/s/DataReleases.asp#d>> [November 2008].
- Hoffman, S.J. (1976): Mineral exploration of the Nechako Plateau, central British Columbia, using lake sediment geochemistry; Ph.D. thesis, University of British Columbia, 346 p.
- Jackaman, W. (2006a): Drainage sediment and water geochemical surveys in the Anahim Lake and Nechako River map areas (NTS 093C & 93F), central British Columbia; *in* Geological Fieldwork 2005, BC Ministry of Energy, Mines and Petroleum Resources, Paper 2006-1 and Geoscience BC, Report 2006-1, p. 295–302.
- Jackaman, W. (2006b): Regional drainage sediment and water geochemical data, Anahim Lake and Nechako River, central British Columbia (NTS 93C & 93F); Geoscience BC, Report 2006-4, 463 p.
- Jackaman, W. (2007a): Regional drainage sediment and water geochemical data, South Nechako Basin and Cariboo Basin, central British Columbia (parts of NTS 92N, O, P, 93A, B); Geoscience BC, Report 2007-6, 332 p.
- Jackaman, W. (2007b): Geoscience BC mountain pine beetle data repository, version 1.0; Geoscience BC, Report 2007-9, URL <<http://www.geosciencebc.com/s/2006-012.asp#dat>> [November 2008].
- Jackaman, W. and Balfour, J.S. (2007): South Nechako Basin and Cariboo Basin lake sediment geochemical survey (parts of NTS 092N, O, P; 093A, B), central British Columbia; *in* Geological Fieldwork 2006, BC Ministry of Energy, Mines and Petroleum Resources, Paper 2007-1 and Geoscience BC, Report 2007-1, p. 311–314.
- Jackaman, W. and Balfour, J.S. (2008): QUEST Project geochemistry: field surveys and data reanalysis (parts of NTS 093A, B, G, H, J, K, N, O), central British Columbia; *in* Geoscience BC Summary of Activities 2007, Geoscience BC, Report 2008-1, p. 7–10.
- Kerr, D.E. and Levson, V.M. (1997): Drift prospecting activities in British Columbia: an overview with emphasis on the Interior Plateau; *in* Interior Plateau Geoscience Project: Summary of Geological, Geochemical and Geophysical Studies, L.J. Diakow and J.M. Newell (ed.), BC Ministry of Energy, Mines and Petroleum Resources, Paper 1997-2, p. 159–173.
- Lett, R.E.W. (2005): Regional geochemical survey database on CD; BC Ministry of Energy, Mines and Petroleum Resources, GeoFile 2005-17, CD-ROM.

Stream Geochemical Survey Sample Reanalysis, Terrace and Prince Rupert Map Areas, Western British Columbia (NTS 103I, part of 103J)

W. Jackaman, Noble Exploration Services Ltd., Sooke, BC, wjackaman@shaw.ca

Jackaman, W. (2009): Stream geochemical survey sample reanalysis, Terrace and Prince Rupert map areas, western British Columbia (NTS 103I, part of 103J); in Geoscience BC Summary of Activities 2008, Geoscience BC, Report 2009-1, p. 15–18.

Introduction

The reanalysis of archived stream sediment samples by inductively coupled plasma mass spectrometry (ICP-MS) is accepted as a cost-effective means of obtaining new and improved regional geochemical information. This technique provides a significant upgrade from the atomic absorption spectroscopy (AAS) method routinely used for federal and provincial government-funded, reconnaissance-scale drainage sediment surveys conducted before 1999. The use of ICP-MS not only provides a wide range of new analytical information at improved detection limits but also offers greater data compatibility with laboratory methods currently being employed.

Recognizing the advantages associated with this type of initiative, Geoscience BC in partnership with the Terrace Economic Development Authority (TEDA), the Regional District of Kitimat Stikine through the Northern Development Initiative Trust (NDIT) and the KT Industrial Development Society (KTIDS) provided funding for the recovery and analyses of 2382 stream sediment pulps. This material originated from a 1978 geochemical survey conducted in the Terrace and Prince Rupert areas (NTS map sheets 103I and part of 103J; Figure 1).

Results of the Terrace and Prince Rupert Geochemical Survey Sample Reanalysis Project is expected to stimulate mineral exploration by presenting new high-quality geochemical information for an area that is considered to have good potential for future discoveries of precious- and base-metal deposits. The region has an active mining and exploration background with several past-producing mines, such as the Edye Pass mine (MINFILE 103J 015; MINFILE, 2008) and the M&K mine (MINFILE 103I 062). Historical metal recovery for the entire region is estimated to include 680 kg of gold, 550 kg of silver, 71 000 kg of copper, 42 000 kg of lead and 4000 kg of zinc (MINFILE, 2008). Project results will also significantly enhance existing geochemical data and other available geoscience information

Keywords: Terrace, Prince Rupert, mineral exploration, geochemistry, multi-element, reanalysis, stream sediment

This publication is also available, free of charge, as colour digital files in Adobe Acrobat® PDF format from the Geoscience BC website: <http://www.geosciencebc.com/s/DataReleases.asp>.

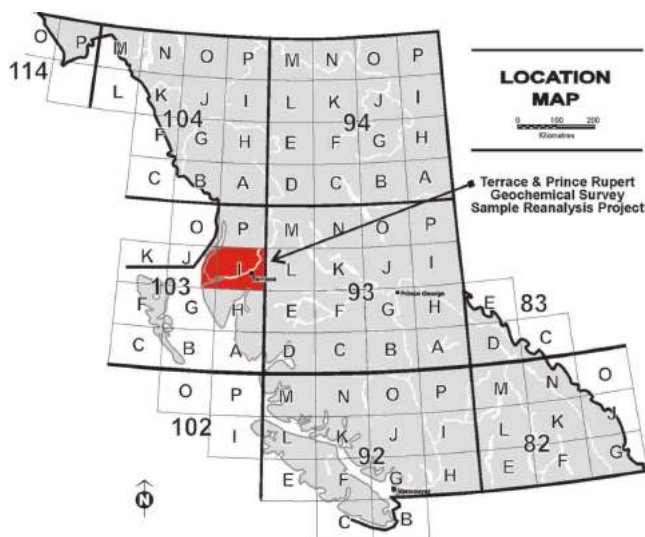


Figure 1. Location of the study area in western British Columbia.

as well as complement new exploration initiatives. Potential long-term economic benefits could also be generated from increased mineral exploration and deposit discoveries.

Project History

Originally conducted in 1978 by the Geological Survey of Canada (GSC) as part of their National Geochemical Reconnaissance (NGR) program, the Terrace and Prince Rupert survey included the collection of stream sediment and water samples from 2128 sites covering an area of 17 500 km² (Figure 2). The results of the survey were released in 1981 (Ballantyne et al., 1981) and included analytical data for only 13 metals (Table 1) in the stream sediment samples. By design, portions of samples from these government-funded regional geochemical surveys were saved on the understanding that advances in laboratory methods would provide opportunities to further develop the federal and provincial geochemical databases.

In the early 1990s, as part of the BC Regional Geochemical Survey (RGS) program and in co-operation with the GSC, over 24 000 archived sample pulps were reanalyzed by instrumental neutron activation analysis (INAA) for gold and a range of pathfinder metals and rare earth elements

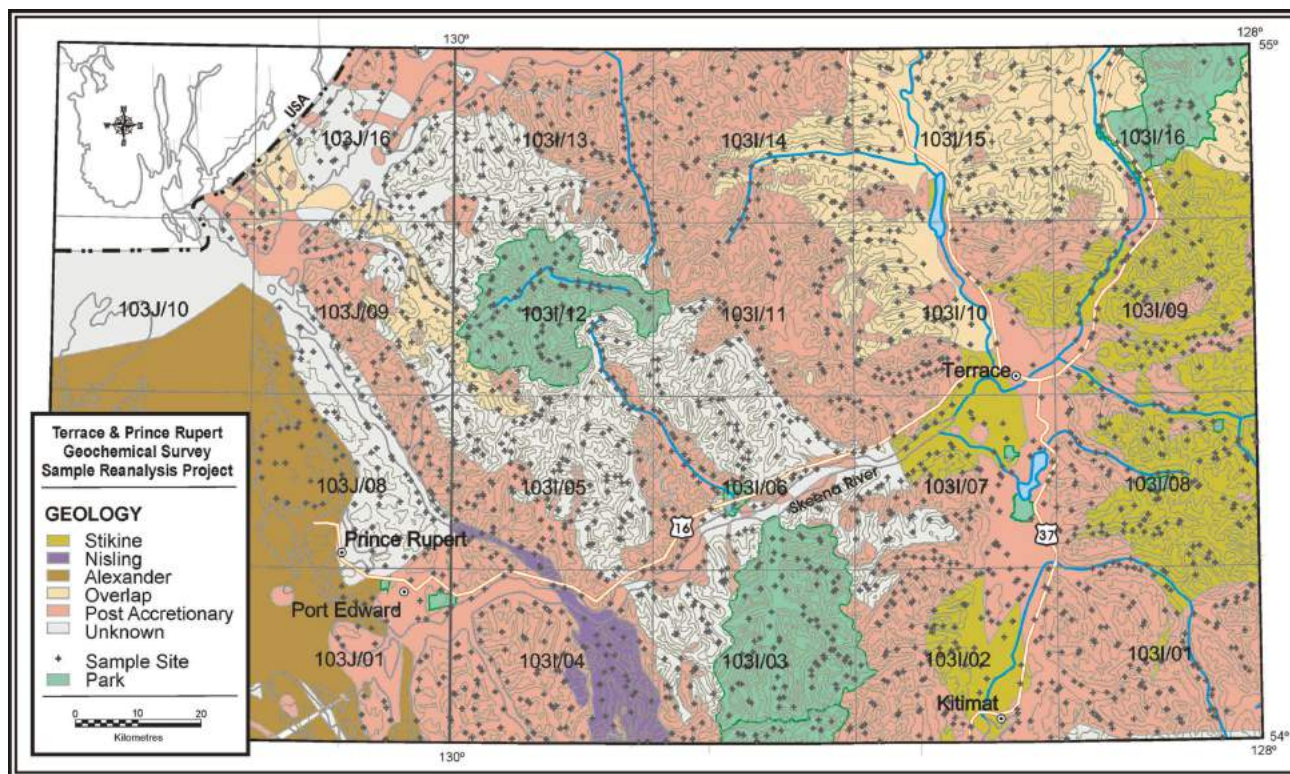


Figure 2. Geology of the Terrace and Prince Rupert map areas with the distribution of sample sites (after Massey et al., 2005; Ballantyne et al., 1981).

(Table 2). This province-wide initiative provided access to important new analytical information at improved detection limits and has significantly enhanced the utility of the provincial geochemical database (Jackaman et al., 1992). INAA results for the Terrace and Prince Rupert samples were released in 1995 (BC Ministry of Energy, Mines and Petroleum Resources, 1995). The work generated renewed interest in the areas surveyed and stimulated increased exploration activity.

More recently, saved NGR and RGS sample pulps are being reanalyzed by ICP-MS. The BC Geological Survey

(BCGS), in co-operation with the GSC, funded the reanalysis of 1152 stream sediment samples from the McLeod Lake map sheet (Lett and Bluemel, 2006). As part of Geoscience BC's QUEST initiative, reanalysis results for a total of 3976 drainage sediment pulps, from around the Prince George area, were released to the public in January 2008 (Jackaman and Balfour, 2008; Geoscience BC, 2008). A total of 4160 stream and lake samples, from the White Sail Lake and Smithers area, have been reanalyzed as part of the QUEST-West project (Jackaman et al., 2009). The current Terrace and Prince Rupert reanalysis work will also contribute to this effort of providing up-to-date analytical information for previously surveyed areas within the province.

Project Methodology

Drainage sediment pulps from previous NGR and RGS programs are currently stored at facilities in Ottawa and Victoria. The collections are maintained by Natural Resources Canada (NRCan) and the BCGS, respectively. Samples are stored in plastic containers organized by NTS map sheet designation and in order of sample identification numbers. Opportunely, the archive also includes original analytical duplicate and control reference samples that can be used to monitor and assess the accuracy and precision of any subsequent analytical work. On average, up to 30 g of the -80 mesh (180 µm) sediment fraction is available but, in

Table 1. List of elements and associated detection limits from published atomic absorption spectroscopy (AAS) analysis (Ballantyne et al., 1981).

Element	Detection limit	Units
Arsenic	0.5	ppm
Cobalt	2	ppm
Copper	2	ppm
Iron	0.02	%
Lead	2	ppm
Manganese	5	ppm
Mercury	10	ppb
Molybdenum	1	ppm
Nickel	2	ppm
Silver	0.2	ppm
Tungsten	1	ppm
Uranium	0.5	ppm
Zinc	2	ppm

Table 2. List of elements and associated detection limits from published instrumental neutron activation analysis (INAA; BC Ministry of Energy, Mines and Petroleum Resources, 1995).

Element	Detection limit	Units
Antimony	0.1	ppm
Arsenic	0.5	ppm
Barium	100	ppm
Bromine	0.5	ppm
Cerium	5	ppm
Cesium	10	ppm
Chromium	5	ppm
Cobalt	5	ppm
Gold	2	ppb
Hafnium	1	ppm
Iron	0.2	%
Lanthanum	5	ppm
Lutetium	0.2	ppm
Molybdenum	1	ppm
Nickel	10	ppm
Rubidium	5	ppm
Samarium	0.5	ppm
Scandium	0.5	ppm
Sodium	0.1	%
Tantalum	0.5	ppm
Terbium	0.5	ppm
Thorium	0.5	ppm
Tungsten	2	ppm
Uranium	0.2	ppm
Ytterbium	2	ppm
Zirconium	200	ppm

some cases, samples may be missing or there is insufficient material remaining in the storage vials.

Geoscience BC, with support from NRCan and the BCGS, was provided access to the Terrace and Prince Rupert samples stored in Ottawa. A 1 to 2 g portion of archived stream sediment sample was carefully extracted from storage containers. Material from each vial was independently split and transferred to a Ziploc® bag labelled with the sample's original unique identification number. Once secured for shipping, the recovered material was delivered to Acme Analytical Laboratories Ltd. (Vancouver). At the lab, each sample was analyzed for 53 elements by ICP-MS analysis using an aqua regia digestion. A complete list of the elements and associated detection limits are provided in Table 3.

The resulting data was carefully checked for analytical quality using inserted blind duplicate and control reference samples. When the information was determined to be complete and accurate, the data was digitally merged with original sample site location information, AAS and INAA analytical results and field observations. This data compilation was prepared for public distribution in digital and hard copy formats and is scheduled to be released by Geoscience BC in December 2008.

Table 3. List of elements and associated detection limits from inductively coupled plasma mass spectrometry (ICP-MS) analysis using an aqua regia digestion, Terrace and Prince Rupert map areas.

Element	Detection limit	Units
Aluminum	0.01	%
Antimony	0.02	ppm
Arsenic	0.1	ppm
Barium	0.5	ppm
Beryllium	0.1	ppm
Bismuth	0.02	ppm
Boron	20	ppm
Cadmium	0.01	ppm
Calcium	0.01	%
Cerium	0.1	ppm
Cesium	0.02	ppm
Chromium	0.5	ppm
Cobalt	0.1	ppm
Copper	0.01	ppm
Gallium	0.1	ppm
Germanium	0.1	ppm
Gold	0.2	ppb
Hafnium	0.02	ppm
Indium	0.02	ppm
Iron	0.01	%
Lanthanum	0.5	ppm
Lead	0.01	ppm
Lithium	0.1	ppm
Magnesium	0.01	%
Manganese	1	ppm
Mercury	5	ppb
Molybdenum	0.01	ppm
Nickel	0.1	ppm
Niobium	0.02	ppm
Palladium	10	ppb
Phosphorus	0.001	%
Platinum	2	ppb
Potassium	0.01	%
Rhenium	1	ppb
Rubidium	0.1	ppm
Scandium	0.1	ppm
Selenium	0.1	ppm
Silver	2	ppb
Sodium	0.001	%
Strontium	0.5	ppm
Sulphur	0.02	%
Tantalum	0.05	ppm
Tellurium	0.02	ppm
Thallium	0.02	ppm
Thorium	0.1	ppm
Tin	0.1	ppm
Titanium	0.001	%
Tungsten	0.1	ppm
Uranium	0.1	ppm
Vanadium	2	ppm
Yttrium	0.01	ppm
Zinc	0.1	ppm
Zirconium	0.1	ppm

Project Summary

The primary objective of the Terrace and Prince Rupert Geochemical Survey Sample Reanalysis Project is to stimulate mineral exploration interest in the region by providing the mining and exploration community with new, high-quality analytical information. To accomplish this, a total of 2380 archived sample pulps from a regional geochemical survey completed in the region almost 30 years ago have been reanalyzed by ICP-MS. The resulting geochemical data compilation will provide local miners and prospectors with over 90 elements in stream sediments for each of the 2128 sample sites at an average density of one site every 8 km². In addition, the work will complement ongoing efforts by the BCGS and GSC to develop a comprehensive collection of geochemical information for the province. The provincial geochemical database includes analytical information for approximately 65 000 sample sites and covers over 70% of BC (Lett, 2005).

Acknowledgments

The author acknowledges L. McKeown (Progressive Ventures Ltd., Terrace) for her contributions to the development and support of this project; Geoscience BC, TEDA, NDIT and KTIDS for funding the initiative; P. Friske and M. McCurdy of NRCan and D. Lefebure and R. Lett of the BCGS for their assistance; and the support received from other mining and exploration groups currently working in the survey area.

References

Ballantyne, S.B., Hornbrook, E.H.W. and Johnson, W.M. (1981): National Geochemical Reconnaissance, Prince Rupert-Terrace, British Columbia (NTS 1031 and part of 103J); Geological Survey of Canada, Open File 772, 93 p.

BC Ministry of Energy, Mines and Petroleum Resources (1995): Regional Geochemical Survey, Terrace and Prince Rupert (NTS 1031, J); BC Ministry of Energy, Mines and Petroleum Resources, BC RGS 1/42, URL <<http://www.empr.gov.bc.ca/Mining/Geoscience/Geochemistry/RegionalGeochemistry/Pages/1031J.aspx>> [November 2008].

Geoscience BC (2008): Geoscience BC's QUEST Project, geochemical sample reanalysis; Geoscience BC, Report 2008-3, URL <<http://www.geosciencebc.com/s/DataReleases.asp#d>> [November 2008].

Jackaman, W. and Balfour, J.S. (2008): QUEST Project geochemistry: field surveys and data reanalysis (parts of NTS 093A, B, G, H, J, K, N, O), central British Columbia; *in* Geoscience BC Summary of Activities 2007, Geoscience BC, Report 2008-1, p. 7–10.

Jackaman, W., Balfour, J.S. and Reichheld, S.A. (2009): QUEST-West Project geochemistry: field survey and data reanalysis (parts of NTS 093E, F, J, K, L, M), central British Columbia; *in* Geoscience BC Summary of Activities 2008, Geoscience BC, Report 2009-1, p. 7–14.

Jackaman, W., Matysek, P.F. and Cook, S.J. (1992): The regional geochemical survey program: summary of activities; *in* Geological Fieldwork 1991, BC Ministry of Energy, Mines and Petroleum Resources, Paper 1992-1, p. 307–318.

Lett, R.E.W. (2005): Regional geochemical survey database on CD; BC Ministry of Energy, Mines and Petroleum Resources, GeoFile 2005-17, CD-ROM.

Lett, R.E.W. and Bluemel, B. (2006): Re-analysis of regional geochemical survey stream sediment samples from the McLeod Lake area (NTS map sheet 093J); BC Ministry of Energy, Mines and Petroleum Resources, GeoFile 2006-09, 220 p.

Massey, N.W.D., MacIntyre, D.G., Desjardins, P.J. and Cooney, R.T. (2005): Digital map of British Columbia: whole province; BC Ministry of Energy, Mines and Petroleum Resources, GeoFile 2005-1.

MINFILE (2008): MINFILE BC mineral deposits database; BC Ministry of Energy, Mines and Petroleum Resources, URL <<http://www.empr.gov.bc.ca/Mining/Geoscience/MINFILE/>> [November 2008].

Trace-Element Analysis of Clay-Sized Fraction of Archived Till Samples, Babine Porphyry Copper District, West-Central British Columbia (NTS 093L/09, /16, 093M/01, /02, /07, /08)

T. Ferbey, British Columbia Geological Survey, Victoria, BC, travis.ferbey@gov.bc.ca

Ferbey, T. (2009): Trace-element analysis of clay-sized fraction of archived till samples, Babine porphyry copper district, west-central British Columbia (NTS 093L/09, /16, 093M/01, /02, /07, /08); in Geoscience BC Summary of Activities 2008, Geoscience BC, Report 2009-1, p. 19–24.

Introduction

The Babine porphyry copper district has high potential to host porphyry copper deposits. Situated north of Houston, British Columbia, the district has a rich mineral exploration history and has hosted two producing porphyry copper mines (Bell and Granisle; Figures 1, 2). There are numerous mineral showings in the district, including four developed prospects (Morrison, Dorothy, Hearne Hill, Fireweed; Figure 2). There is unstaked ground within the Babine porphyry copper district and, relative to districts to the east and northwest, it remains underexplored.

Levson (2001a, 2002) mapped the surficial geology of the Babine porphyry copper district and collected 937 basal till samples for trace-element geochemical analyses on the silt-plus clay-sized fraction (<0.063 mm). As a result of this work, 66 multisite, multi-element geochemical exploration targets were identified, over 13 of which are situated within unstaked ground (Levson, 2002). An additional 18 multisite, single-element geochemical exploration targets are situated within unstaked ground. These targets were identified by assessing the magnitude of elevated metal concentrations in till within the context of glacial dispersal patterns and transport direction, other geochemical datasets, and surficial and bedrock geology data (Levson, 2002).

The objectives of this study are to

- conduct trace-element geochemical analyses on the clay-sized fraction of archived till samples collected in the Babine porphyry copper district; and
- use these new geochemical data to further constrain and better define previously identified geochemical targets within the Babine porphyry copper district and possibly identify new targets.

Keywords: Babine porphyry copper district, till geochemistry, clay-sized fraction

This publication is also available, free of charge, as colour digital files in Adobe Acrobat® PDF format from the Geoscience BC website: <http://www.geosciencebc.com/s/DataReleases.asp>.

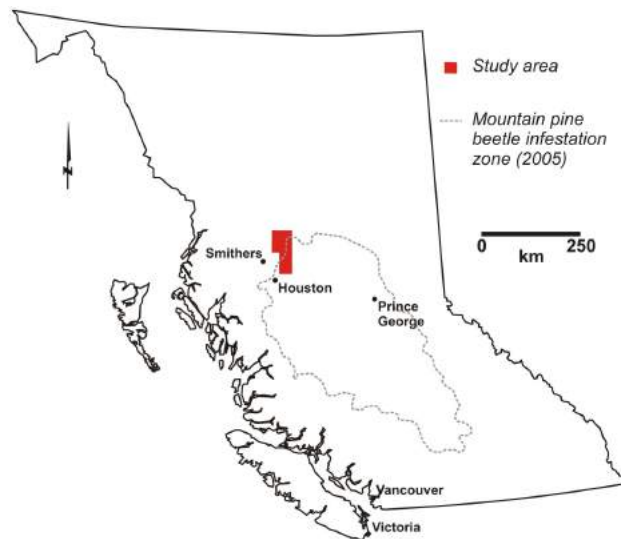


Figure 1. Location of study area in west-central British Columbia.

The goal of this study is to provide to the mineral exploration community a new, high quality, regional-scale, geochemical dataset that will help guide exploration efforts in the Babine porphyry copper district. This study will also serve as a reintroduction to the original surficial geology and till geochemistry work completed by Levson (2001a, 2002), and the other geological and geochemical data collected as part of the Nechako NATMAP project (Struik and MacIntyre, 2000). It is hoped that the new geochemical data generated as part of this study will contribute toward longer-term benefits from increased mineral exploration activity in an area adversely affected by the mountain pine beetle infestation.

Study Area

The Babine porphyry copper district is situated in west-central BC, in NTS map areas 093L/09, /16, 093M/01, /02, /07, /08 (Figure 2), and falls within the Nechako Plateau physiographic region. This region can be characterized as having low relief and gently rolling topography (Holland, 1976). Large, elongate, southwest-trending lakes are common in lower valley settings (e.g., Babine, Takla, Morrison,

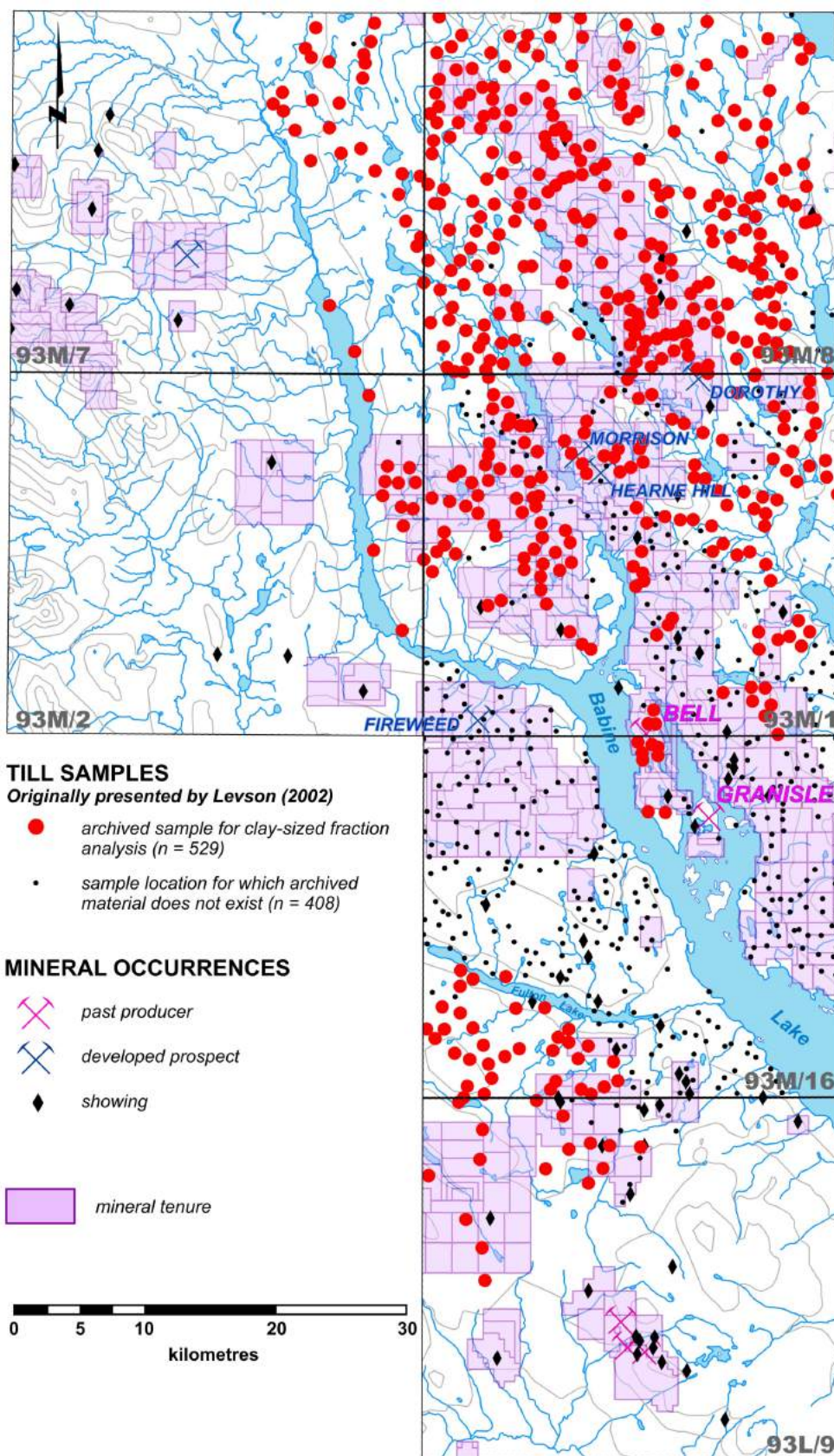


Figure 2. Location of till samples collected within the Babine porphyry copper district, west-central British Columbia. Locations of past-producing mines, developed prospects and showings are also shown.

Nakinilerak and Fulton lakes). Although the study area does become more mountainous in the north, as the Skeena Mountains are approached, bedrock outcrop in this region is limited as a ubiquitous cover of Late Wisconsinan drift dominates the landscape. These sediments have at least partially covered the Eocene Babine intrusive rocks which, along with neighbouring country rocks, host the copper-gold mineralization that occurs within the Babine porphyry copper district.

Till is the dominant surficial deposit in the study area. These deposits vary in thickness from less than one to several metres and can be ridged or rolling, hummocky or a subdued representation of underlying bedrock topography. On steeper slopes, in the northern part of the study area in particular, the till begins to thin and is closely associated with colluvial deposits and discontinuous bedrock outcrop. Continuous bedrock outcrop is limited to some of the higher peaks in the study area, such as Frypan and Trail (Levson, 2002). Streamlined glacial features, produced by moving ice (e.g., flutes and drumlins) can be found in the study area and are typically oriented subparallel to major valleys (Levson, 2002). Hindering mineral exploration are thick glaciolacustrine units that can be associated with the larger lakes, in particular Babine Lake. Glaciofluvial deposits also occur in the study area and are typically interpreted to be associated with areas of stagnant ice along with ice-proximal and subglacial fluvial systems.

Previous Work

Levson (2002) presents high quality, regional-scale, till geochemical data for the Babine porphyry copper district. Included in these regional till geochemical data are property-scale, orientation till surveys conducted in the vicinity and down-ice of past-producing porphyry copper mines (Bell and Granisle) and developed prospects. In his study, till samples collected down-ice of nearly all existing mineral properties (0.5 km or more) have >95th percentile metal concentrations, commonly of more than one metal. For example, till samples in the vicinity of the developed prospects of Morrison and Hearne Hill (porphyry copper, molybdenum, gold) have >98th percentile concentrations of copper, lead, gold, silver and antimony.

The utility of till-based surveys in the region is proven by a study south of the study area, in the Fawnie Creek map area (NTS 093F/03). Cook et al. (1995) conducted a comparative study on the ability of regional lake sediment and till geochemistry surveys to identify known mineral occurrences. In this study, tills identified all seven known prospects in the study area with >95th percentile element concentrations. Nine of eleven potential new prospects presented in this study were also identified with till samples, which had >95th percentile concentrations of multiple elements.

Other work has been conducted in areas adjacent to the Babine porphyry copper district. Tipper (1994) describes the ice-flow history of the Smithers map area (NTS 093L). Tipper (1971) also describes glacial features and glacial histories of areas south of the study area. Plouffe and Ballantyne (1993) and Plouffe (1997, 2000) have also mapped Quaternary deposits and conducted till geochemistry surveys for areas south and west of the study area. Ferbey (2008) provides a geographically referenced list of drift prospecting surveys that have been conducted in BC.

Methodology

Till geochemical surveys can detect known sources of mineralization and identify new geochemical exploration targets (e.g., Sibbick and Kerr, 1995; Plouffe, 1997; Ferbey and Levson, 2007). Till geochemical surveys are well suited to assessing the mineral potential of ground covered by glacial drift. Basal till, a specific type of drift and the sample medium used in these surveys, is ideal for these assessments as it has a relatively simple transport history, is deposited directly down-ice of its source, and produces a geochemical signature that is aerially more extensive than its bedrock source and therefore at a regional-scale can be more easily detected (Levson, 2001b).

To date, regional till geochemical surveys conducted by the British Columbia Geological Survey (BCGS) have only used the silt- plus clay-sized fraction of tills (i.e., <0.063 mm fraction). Trace-element geochemical analyses on clay separations, or heavy mineral analyses, have not been conducted. Producing a clay-sized fraction from tills has in the past been cost prohibitive. With an increase in interest in this size fraction by clients, however, preparation labs now offer clay separations at reasonable and competitive prices.

Clay separations have been routinely used for geochemical interpretations by the Geological Survey of Canada (GSC) since 1973 (Shilts, 1995). Analysis of the clay-sized fraction in basal tills is ideal for exploration targets such as porphyry copper deposits as it has been shown that base metals (more specifically, some chalcophile elements) tend to concentrate in this fraction due to clay-sized particles' (dominated by phyllosilicate) high cation exchange capacity (Nikkarinen et al., 1984; Shilts, 1984, 1995; DiLabio, 1995). In the context of base-metal exploration, trace-element analyses of the clay-sized fraction of tills (<0.002 mm) can increase the contrast between elevated and background element concentrations, as compared to the same analyses using silt- plus clay-sized fraction (<0.063 mm). This is due to the fact that minerals such as quartz and feldspar are reduced in clay-sized fraction and therefore do not dilute the geochemical signature of the sample. As a result, elevated geochemical values can be identified with more certainty. It is hoped that this increase

in geochemical contrast will further constrain and better define the geochemical targets previously identified by Levson (2002) within the Babine porphyry copper district, and possibly identify new ones.

Sample Preparation and Analysis

Analytical determinations by inductively coupled plasma emission spectrometry (ICP-ES) and instrumental neutron activation analysis (INAA) have already been carried out on the silt- plus clay-sized fraction (<0.063 mm) of 937 basal till samples collected within the Babine porphyry copper district, and are presented in detail by Levson (2002). Of the original 937 samples, material from 529 samples remains in BCGS archives (Figure 2).

As part of this study, the clay-sized fraction of the 529 archived till samples will be separated following the procedures outlined by Girard et al. (2004). It is imperative that a regimented procedure be followed, in particular the length of time samples are spun in a centrifuge and the velocity at which the centrifuge operates, in order for a clay-sized separation (<0.002 mm) to be consistently produced. For this study, de-ionized water will be used throughout the centrifuge and decanting process, instead of the sodium hexametaphosphate solution suggested by Girard et al. (2004).

For each reprocessed sample, a 0.5 g split will be analyzed for a total of 37 elements by inductively coupled plasma mass spectrometry (ICP-MS) following an aqua regia digestion. These analyses will be conducted at Acme Analytical Laboratories Ltd. (Vancouver).

Quality Control

Quality control measures were implemented during the initial collection of the archived samples. For each block of 20 samples submitted for analysis, one field duplicate (taken at a randomly selected sample site) was included. As part of this study, one analytical duplicate (a sample split after sample preparation but before analysis) and one reference standard will be included for each block of 20 samples. Reference standards will either be certified Canada Centre for Mineral and Energy Technology (CANMET) standards or one of several BCGS geochemical reference materials. Field duplicate samples will be used to measure the combined sampling and analytical variability, whereas analytical duplicates will provide a measure of analytical variability only. Certified reference standards will be used to measure the accuracy of each analytical method and BCGS geochemical reference materials will be used to measure analytical precision.

Summary and Future Data Release

At present, clay separations are being produced for 529 archived till samples from the Babine porphyry copper dis-

trict. Upon completion of separations, these samples will be analyzed by ICP-MS following an aqua regia digestion. Analytical determinations on the clay-sized fraction (<0.002 mm) can increase the contrast between elevated and background element concentrations, as compared to the same analyses using the silt- plus clay-sized fraction (<0.063 mm). These new, high quality, geochemical data will be used to further constrain and better define geochemical targets within the Babine porphyry copper district and targets previously identified by Levson (2002) using determinations on the silt- plus clay-sized fraction of these till samples, and to potentially identify additional geochemical exploration targets.

An update on this study will be given at the Mineral Exploration Roundup 2009 poster session. The new geochemical data generated from this study will be released in the spring of 2009. This release will include interpretations of these data and an integration of them with work presented by Levson (2002), including the region's ice-flow history and inferred detrital transport direction(s) in basal till.

Acknowledgments

Geoscience BC is gratefully acknowledged for funding the analytical portion of this study. R. Lett (BCGS) is thanked for assisting with pulling archived till samples. K. Vickers and S. Nicholson are also thanked for cataloguing and packing samples for shipment. B. Ward (Simon Fraser University) is thanked for his review of this manuscript.

References

- Cook, S.J., Levson, V.M., Giles, T.R. and Jackaman, W. (1995): A comparison of regional lake sediment and till geochemistry surveys: a case study from the Fawnie Creek area, central British Columbia; *Exploration Mining Geology*, v. 4, p. 93–101.
- DiLabio, R.N.W. (1995): Residence sites of trace elements in oxidized till; *in* Drift Exploration in the Canadian Cordillera, P.T. Bobrowsky, S.J. Sibbick, J.M. Newell and P. Matysek (ed.), BC Ministry of Energy, Mines and Petroleum Resources, Paper 1995-2, p. 139–148.
- Ferbey, T. (2008): Regional to property-scale drift prospecting surveys in British Columbia; BC Ministry of Energy, Mines and Petroleum Resources, GeoFile 2008-12, one map sheet.
- Ferbey, T. and Levson, V.M. (2007): The influence of ice-flow reversals on the vertical and horizontal distribution of trace elements in tills, Huckleberry mine area, west-central British Columbia; *in* Application of Till and Stream Sediment Heavy Mineral and Geochemical Methods to Mineral Exploration in Western and Northern Canada, R.C. Paulen and I. McMartin (ed.), Geological Association of Canada, Short Course Notes 18, p. 145–151.
- Girard, I., Klassen, R.A. and Laframboise, R.R. (2004): Sedimentology laboratory manual, Terrain Sciences Division; Geological Survey of Canada, Open File 4823, 137 p.
- Holland, S.S. (1976): Landforms of British Columbia: a physiographic outline; BC Ministry of Energy, Mines and Petroleum Resources, Bulletin 48, 138 p.

- Levson, V.M. (2001a): Quaternary geology of the Babine porphyry copper district: implications for geochemical exploration; *Canadian Journal of Earth Sciences*, v. 38, p. 733–749.
- Levson, V.M. (2001b): Regional till geochemical surveys in the Canadian Cordillera: sample media, methods, and anomaly evaluation; *in* *Drift Exploration in Glaciated Terrain*, M.B. McClenaghan, P.T. Bobrowsky, G.E.M. Hall and S.J. Cook (ed.), Geological Society, Special Publication 185, p. 45–68.
- Levson, V.M. (2002): Quaternary geology and till geochemistry of the Babine porphyry copper belt, British Columbia (NTS 93 L/9, 16, M/1, 2, 7, 8); BC Ministry of Energy, Mines and Petroleum Resources, Bulletin 110, 278 p.
- Nikkarinen, M., Kallio, E., Lestinen, P. and Äyräs, M. (1984): Mode of occurrence of copper and zinc in till over three mineralized areas in Finland; *Journal of Geochemical Exploration*, v. 21, p. 239–247.
- Plouffe, A. (1997): Reconnaissance till geochemistry on the Chilcotin Plateau (92O/5 and 12); *in* Interior Plateau Geoscience Project: Summary of Geological, Geochemical and Geophysical Studies (092N, 092O, 093B, 093C, 093F, 093G, 093G), L.J. Diakow, P. Metcalfe and J. Newell (ed.), BC Ministry of Energy, Mines and Petroleum Resources, Paper 1997-2, p. 145–157.
- Plouffe, A. (2000): Quaternary geology of the Fort Fraser and Manson River map areas, central British Columbia; Geological Survey of Canada, Bulletin 554, 62 p.
- Plouffe, A. and Ballantyne, S.B. (1993): Regional till geochemistry, Manson River and Fort Fraser area, British Columbia (93K, 93N), silt plus clay and clay size fractions; Geological Survey of Canada, Open File 2593, 210 p.
- Shilts, W.W. (1984): Till geochemistry in Finland and Canada; *Journal of Geochemical Exploration*, v. 21, p. 95–117.
- Shilts, W.W. (1995): Geochemical partitioning in till; *in* *Drift Exploration in the Canadian Cordillera*, P.T. Bobrowsky, S.J. Sibbick, J.M. Newell and P. Matysek (ed.), BC Ministry of Energy, Mines and Petroleum Resources, Paper 1995-2, p. 149–163.
- Sibbick, S.J. and Kerr, D.E. (1995): Till geochemistry of the Mount Milligan area, north-central British Columbia; recommendations for drift exploration for porphyry copper-gold mineralization; *in* *Drift Exploration in the Canadian Cordillera*, P.T. Bobrowsky, S.J. Sibbick, J.M. Newell and P. Matysek (ed.), BC Ministry of Energy, Mines and Petroleum Resources, Paper 1995-2, p. 167–180.
- Struik, L.G. and MacIntyre, D.G. (2000): Nechako NATMAP project overview, central British Columbia, year five; Geological Survey of Canada, Current Research 2000-A10, 10 p.
- Tipper, H.W. (1971): Glacial geomorphology and Pleistocene history of central British Columbia; Geological Survey of Canada, Bulletin 196, 89 p.
- Tipper, H.W. (1994): Preliminary interpretations of glacial and geomorphic features of Smithers map area (93L), British Columbia; Geological Survey of Canada, Open File 2837, 7 p.

Ice-Flow History, Drift Thickness and Drift Prospecting for a Portion of the QUEST Project Area, Central British Columbia (NTS 093G, H [west half], J)

B. Ward, Department of Earth Sciences, Simon Fraser University, Burnaby, BC, bcward@sfu.ca

D. Maynard, Denny Maynard & Associates Ltd., North Vancouver, BC

M. Geertsema, British Columbia Ministry of Forests, Northern Interior Forest Region, Prince George, BC

T. Rabb, Department of Earth Sciences, Simon Fraser University, Burnaby, BC

Ward, B., Maynard, D., Geertsema, M. and Rabb, T. (2009): Ice-flow history, drift thickness and drift prospecting for a portion of the QUEST Project area, central British Columbia (NTS 093G, H [west half], J); *in* Geoscience BC Summary of Activities 2008, Geoscience BC, Report 2009-1, p. 25–32.

Introduction

Central British Columbia has areas of highly prospective bedrock geology but mineral exploration has been limited due to the thick cover of surficial deposits. To help spur economic growth in this region, which has been severely affected by the mountain pine beetle, the federal and provincial governments are funding geological projects such as QUEST. Significant knowledge gaps exist in the glacial history of the QUEST Project area and thus pose a significant hindrance to mineral exploration. Knowledge of the glacial history, specifically the ice-flow history and dominant transport direction, is vital to interpret data from geochemical surveys of the area. This project is designed to address this knowledge gap by providing a Quaternary framework along with both regional and detailed till geochemical surveys. The study area comprises NTS map sheets 093G, H (west half) and J (Figure 1).

This ambitious project will occur over three years and provide

- 1) the regional glacial geological framework for map areas NTS 093G, H (west half) and J (i.e., the central portion of the QUEST area);
- 2) a map of approximate drift cover for areas within NTS 093 G, H (west half) and J based on existing surficial geology, soils and landform mapping augmented with reconnaissance field observations;
- 3) terrain mapping of six 1:50 000 scale sheets (NTS 093J/05, /06, /11, /12, /13, /14);
- 4) till geochemical data (inductively coupled plasma mass spectrometry [ICP-MS] with aqua regia digestion and instrumental neutron activation analysis [INAA] for

trace, minor and major elements), gold grain counts and heavy mineral separates for samples collected within these new sheets; and

- 5) detailed geochemical surveys down-ice of two geophysical anomalies (interpreted from geophysical data [Barnett and Kowalczyk, 2008]).

This work will help to stimulate mineral exploration in beetle-kill-affected areas by releasing new surficial geology and geochemical survey data and providing a framework for companies to interpret their own datasets. This project will also provide invaluable training for at least two graduate students and numerous undergraduate students.

Fieldwork occurred in late June and early July 2008. The initial two weeks concentrated on collecting striation data for the ice-flow history and checking the validity of existing soil and landform and surficial geology mapping to be used for drift thickness mapping. The second half of the fieldwork season concentrated on till geochemistry sampling in areas down-ice from two geophysical anomalies. The results of the first field season are given below.

Study Area and Physiography

The study area occurs in the heart of the QUEST project area (Figure 1). The majority of this area lies in the relatively low relief area of the Interior Plateau (Mathews, 1986), including its subdivisions, the Fraser Basin and Nechako Plateau. It is characterized by glacial lake deposits, drumlinized drift and glaciofluvial outwash and esker deposits (Holland, 1976).

Regional Quaternary History

The Cordilleran Ice Sheet has repeatedly covered BC and portions of Yukon, Alaska and Washington over the last two million years (Armstrong et al., 1965; Clague, 1989). Growth of the Cordilleran Ice Sheet is thought to have followed four phases as defined by Davis and Mathews (1944): alpine phase, intense alpine phase, mountain ice

Keywords: *ice-flow history, drift prospecting, geochemical survey, terrain mapping, drift thickness, striations, heavy minerals*

This publication is also available, free of charge, as colour digital files in Adobe Acrobat® PDF format from the Geoscience BC website: <http://www.geosciencebc.com/s/DataReleases.asp>.

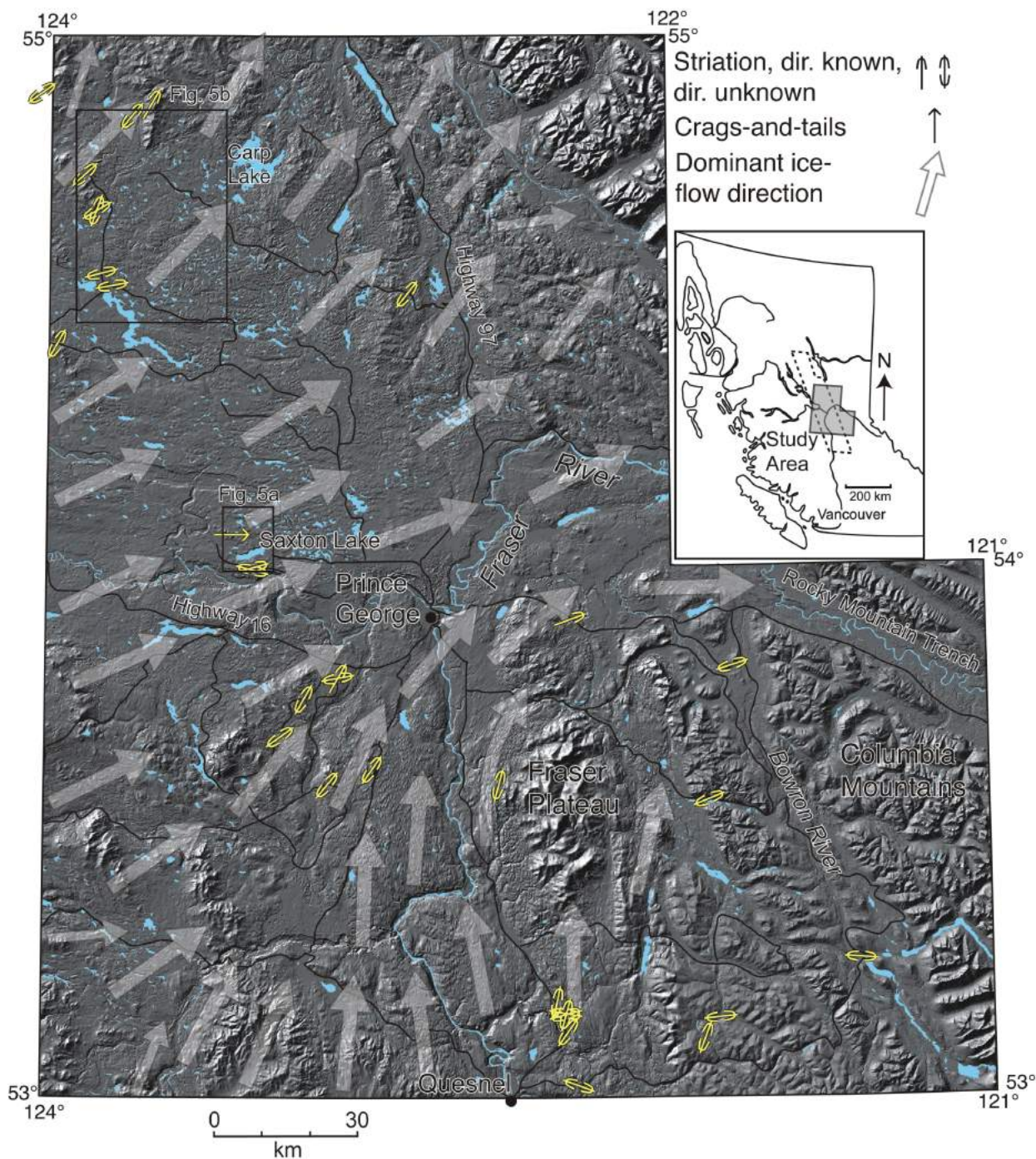


Figure 1. Digital elevation model of the study area with ice flow information. Drumlinized drift is evident throughout most of the study area. Striation data is from field observations in summer 2008. Some striation sites were simplified to avoid cluttering. Inset map indicates the location of the study area (shaded area) in relation to British Columbia and the QUEST Project geophysical survey area (dashed line). D. Turner (Simon Fraser University) compiled the digital elevation model. Abbreviation: dir, direction.

sheet phase and continental ice sheet phase (Fulton, 1991; Figure 2). In short, ice originated in alpine areas as valley glaciers. Over time, these valley glaciers extended out from mountain fronts as piedmont glaciers and eventually grew into mountain ice sheets. Eventually, the ice sheet would have grown into a continental ice sheet. Throughout this sequence, topography has less and less control over ice flow, until the continental ice sheet phase when ice flows inde-

pendent of topography. At its maximum extent, the Cordilleran Ice Sheet was up to 900 km wide and up to 2000–3000 m thick over much of the Interior Plateau, closely resembling the present-day Greenland Ice Sheet.

During the Late Wisconsinan, the last glaciation to affect BC, ice was advancing out of the Coast Mountains by 28 000 BP. In the study area, it is unclear how extensive the

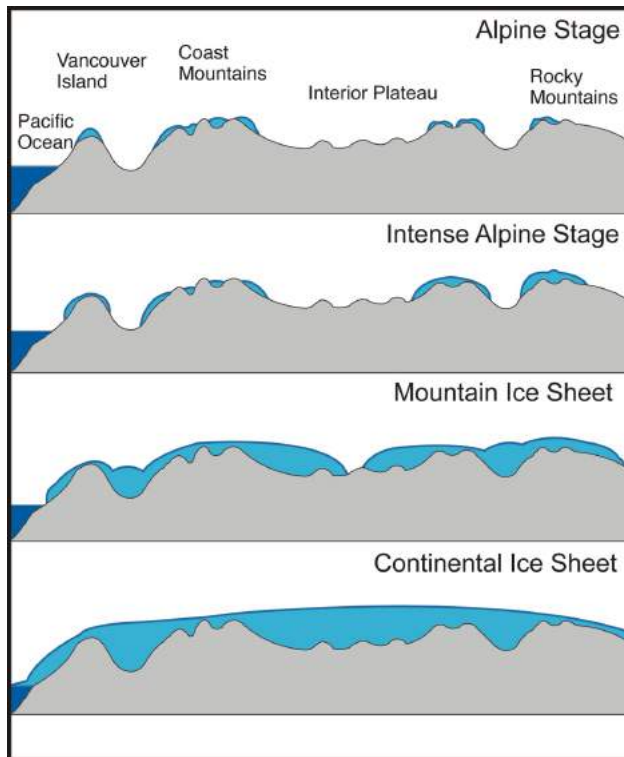


Figure 2. Hypothesized sequence of ice growth for the Cordilleran Ice Sheet (*modified after* Fulton, 1991).

glaciers in the cirques of the Caribou Mountains were. Paleoenvironmental reconstructions from this time indicate conditions were very arid, not conducive to growing large local glaciers (Ward et al., 2005). However, it is clear that a large glacial lake existed in the Bowron Valley indicating that ice in the Rocky Mountain Trench blocked the mouth before local ice extended out of the valley. Radiocarbon ages indicate that ice covered the Bowron Valley sometime after 20 000 BP. Maximum extent also occurred after this but there is no chronological control. Evidence that the Cordilleran Ice Sheet attained continental ice sheet status is provided in a study by Stumpf et al. (2000), which shows that the ice divide shifted eastward from the Coast Mountains to over the Interior Plateau, just to the west of the study area.

In contrast, deglaciation was characterized by downwasting, followed by widespread stagnation throughout much of the interior (Fulton, 1967); the ice sheet melted from the top down. It appears that the equilibrium line either rose very close to or above the top of the glacier. Initially, regional ice flow continued but was less vigorous. As uplands became exposed, significant flow was restricted to valleys. Eventually, as the ice sheet continued to thin, ice tongues in the valleys became stagnant and ceased to move. This style of deglaciation is characterized by flights of lake levels starting in the highest valleys and ending in the lowest valleys. This is caused by the highest elevations becoming ice-free first and lakes being ponded by ice in the lower

valleys. It is also characterized by extensive ice stagnation topography (e.g., hummocky or kame-and-kettle topography and the presence of eskers). Deglacial lakes dammed by ice in the larger valleys are common in the Bowron Valley and on the east side of the Rocky Mountain Trench. The last lake in the area, Glacial Lake Fraser, occupied the Fraser River valley.

Results

Ice Flow

The ice-flow history of the study area was determined by compiling ice-flow information from existing maps (Tipper, 1971; Clague, 1998a, b; Blais-Stevens and Clague, 2007) and combining it with observations made in the field. The ice-flow indicators on the pre-existing maps generally consist of macroforms such as drumlins, flutings, crags-and-tails and streamlined bedrock ridges. Drumlins generally comprise thick (>3 m), ridged till (Figure 3a) that is commonly described as an inverted teaspoon shape. These ridges are oriented parallel to ice flow and are asymmetric in long profile, with a steeper up-ice side and a gentler down-ice side. Flutings are more elongate till ridges, without the asymmetric long profile. Crags-and-tails have an up-ice outcrop of glacially smoothed, resistant bedrock and a down-ice tail of till (Figure 3b). Streamlined bedrock ridges are similar in shape to flutings. Drumlins are common throughout the study area and were not measured in the field as they are evident on digital elevation models (DEM; Figure 1), topographic maps and Google™ Earth images.

Ice-flow indicators measured in the field were mainly microflow indicators, such as grooves, striations and rat tails. Striations and grooves are glacial erosion features that form by debris in the base of the ice being dragged along the bedrock surface (Figure 3c, e, f). They are usually considered to be bidirectional, meaning that a flow direction is not evident from examination of the striation or groove itself, however, examination of the outcrop upon which the striations are measured can give a sense of direction by the presence of a plucked surface on one of the outcrop edges. Plucked surfaces are evidenced by a steep vertical edge caused by the overriding ice freezing onto the bedrock and removing blocks, usually along joints. Rat tails form where there are more resistant portions with a rock unit (i.e., clasts in a conglomerate, porphyroblasts, phenocrysts, etc). These resistant portions also protect the rock immediately down-ice, forming a small protuberance that has a tail pointing down-ice (Figure 3d, f). These features are considered to be unidirectional, giving flow direction. The Telkwa volcanic rocks have more resistant clasts that commonly form rat tails (Figure 3f).

Striations were measured at a total of 33 sites. At some of these sites, numerous directions were recorded (Figure 3d–

f), at others only one dominant direction was recorded. Finding striations was challenging due to the lack of bedrock exposures in parts of the field area, and the weathered nature of some of the outcrops present. In most cases, ex-

cept for some fresh roadcuts, striations were only found after sediment, usually till, was scraped, brushed or washed off bedrock surfaces. Where more than one orientation was observed, it was sometimes possible to determine a relative



Figure 3. a) Roadcut through a drumlin, central portion of NTS 093J. A till sample was taken for geochemical analysis. b) Crag-and-tail, Saxton Lake area. The glacially smoothed crag and tail are indicated. c) Example of a glacially smoothed striated outcrop, along Highway 16 east of Prince George. d) Rat tails on a glacially smoothed outcrop, along Highway 16 east of Prince George. Two ages of ice flow are indicated, the older flow (1) formed the rat tails and the younger flow (2) truncated the tails. e) Two striation directions are present on this outcrop near Saxton Lake but no age relationship could be determined. f) Striated faceted surface (1) is older than the striations and rat tails (2), along Highway 16 west of Prince George.

age or timing by looking for crosscutting relationships or the relative location of the different striated surfaces. For example, if large grooves are present and there are striations in the groove, the groove must be older than the striations. Similarly, by noting the dominant direction of ice movement on an outcrop, striations found on protected surfaces in the lee (down-ice) of this direction are likely older (Figure 3f). Relative age control was only possible at a few sites, and most of these were within 20° of each other. These slight differences likely reflect minor changes during deglaciation.

The dominant ice-flow direction in the area is relatively easy to demonstrate using the orientations of numerous drumlins (Figure 1), except for portions of NTS 093H where drumlins are rare. These data were supplemented by observations on the striations, rat tails and grooves. The drumlin data indicate the dominant ice divides, to the south and west of the study area, controlled the drumlin-forming ice flow. These two flow sources interacted, with ice flow from the west appearing to be dominant, causing ice flow to be deflected eastward. This deflection is evident on the DEM to the southeast of Prince George along the margin of the uplands of the Fraser Plateau. This ice continued to flow to the east along the Rocky Mountain Trench. In the north part of the study area, the dominant flow changes from east-northeast to northeast.

Striation data in general correspond with ice flow indicated by the drumlins, however, some exceptions occur. For example, in the vicinity of Saxton Lake (Figure 1) striations and a crag-and-tail indicate ice flow to the east. This likely represents a readvance over the area during deglaciation, something confirmed by examination of sections in the area. There are several sites in the southeast part of the study area where valley-parallel striations were recorded. These likely reflect valley-parallel flow during deglaciation, when ice had thinned enough that topography exerted more of an influence.

Drift Thickness

A relative drift thickness map is currently being constructed. This map will prove useful to companies planning till-sampling programs and locating areas where bedrock outcrop or near surface subcrop are most likely to occur. This map is being constructed from a mix of existing Geological Survey of Canada (GSC) surficial geology mapping, soil and landform mapping and some airphoto interpretation. Surficial geology maps at a scale of 1:100 000 exist in the northwest, southwest and southeast portions of NTS 093G. Soil and landform mapping at a scale of 1:50 000 exists for the west half of NTS 093H, all of NTS 093G but only the south half of NTS 093J. As terrain mapping will occur in the northwest portion of NTS 093J, reconnaissance mapping will be undertaken to provide drift

thickness information. Unfortunately, there is no terrain mapping for the Quest area. The limited, existing, mainly reconnaissance-scale, terrain stability mapping is inappropriate for this map. Reconnaissance field observations carried out in the summer of 2008 will be incorporated. This and existing map information will be merged to the generalized map units outlined below:

- 1) Shallow to bedrock terrain. Rock outcrops are common and/or at shallow depth (usually at <1 m). Surficial deposits are dominantly derived from local bedrock (e.g., colluvium and weathered rock) but thin mantles of till can also occur.
- 2) Variable thickness of till, usually <3 m thick. Some discontinuous bedrock outcrops occur and bedrock can be expected in relatively shallow excavations such as roadcuts. Isolated areas of low-lying and depressional terrain may have second- and third-order derivative sediments at the surface, covering the till.
- 3) Mainly a continuous cover of thick till, usually 3 to >10 m thick. Bedrock outcrops are rare and usually the underlying rock surface will only be exposed in deep excavations (e.g., pits). Surface mantles of second- and third-order derivative sediments are probable in isolated areas of low-lying and depressional terrain.
- 4) Thicker and continuous surface cover of second- and third-order derivative sediments, including glaciofluvial, glaciolacustrine, fluvial, lacustrine, organic and anthropogenic (e.g., mine waste). Surface exposures of till and/or bedrock are rare and may only be encountered in deep excavations.

Isolated bedrock outcrops in units of thicker drift will be identified with an onsite symbol. Generalized ice-flow information will be included on these maps to assist with the planning of drift prospecting programs. Because of the generalized and simplified nature of the units, however, training of samplers on the identification of till is essential to ensure a consistent sample medium.

Till Geochemistry

Till samples were collected in the vicinity of two geophysical anomalies, which were identified by the authors in collaboration with P.L. Kowalczyk, PK Geophysics Inc. (personal communication, 2008). Both sites occur on NTS 093J, one in the south around Saxton Lake and one in the central-west area of the map sheet (site locations [labelled as Figure 5a, b] are shown on Figure 1). Initially, a total of four anomalies were identified by the integration of existing geophysical data and recently acquired geophysical data, released by Geoscience BC (Sander Geophysics Limited, 2008), with regional lake- and stream-sediment geochemical data. Based on the lack of till occurring at the surface and their proximity to populated areas (sampling is difficult on private land), two of these areas were found to be unsuitable.



Figure 4. Typical dense, massive basal till found throughout the study area.

Basal till in the study area is a dense, dark grey, matrix-supported diamicton. This basal till is composed of 25–40% gravel-sized material (clasts) and the matrix is usually sandy silt (Figure 4). Sampling proved difficult because of access problems and lack of suitable sample media. For both anomalies, many of the mapped roads had been deactivated and were undrivable with a four-wheel-drive truck. The Saxton Lake geophysical anomaly occurs in the transition between glaciolacustrine deposits associated with Glacial Lake Fraser and areas of till. Thus, glaciolacustrine deposits covering till deposits limited sampling. In the

vicinity of the northern geophysical anomaly, there were extensive areas of sand, which are likely postglacial eolian deposits, and some areas of glaciofluvial deposits.

Basal till samples were collected at a total of 123 sites within and adjacent to the two study areas (Figure 5). At each sample site, three separate samples were collected for 1) clay separation at Saskatchewan Research Council followed by ICP-MS (Package 1-DX) at Acme Analytical Laboratories Ltd.; 2) silt plus clay separation and INAA (Package 1D EnH) at Activation Laboratories Ltd.; and 3) archiving at the BC Geological Survey (BCGS). As well, at 30 of these sites >10 kg till samples were collected for heavy mineral separation and gold grain counts, which are to be carried out at Overburden Drilling Management Services. The <0.25 mm fraction of the heavy mineral concentration will be sent for INAA. These analytical data will be used to identify anomalous samples which will then have the heavy minerals picked and identified. Initial results will be released at Roundup 2009. Funding obtained from the federal government’s Mountain Pine Beetle (MPB) Program, under the direction of C. Hutton (GSC, NRCan), will cover the costs for the majority of these analyses, allowing more Geoscience BC funds to be used for analysis of samples next year. This funding will also allow for additional analysis by ICP-MS of the silt- plus clay-sized fraction samples already analyzed by INAA. Analytical variability

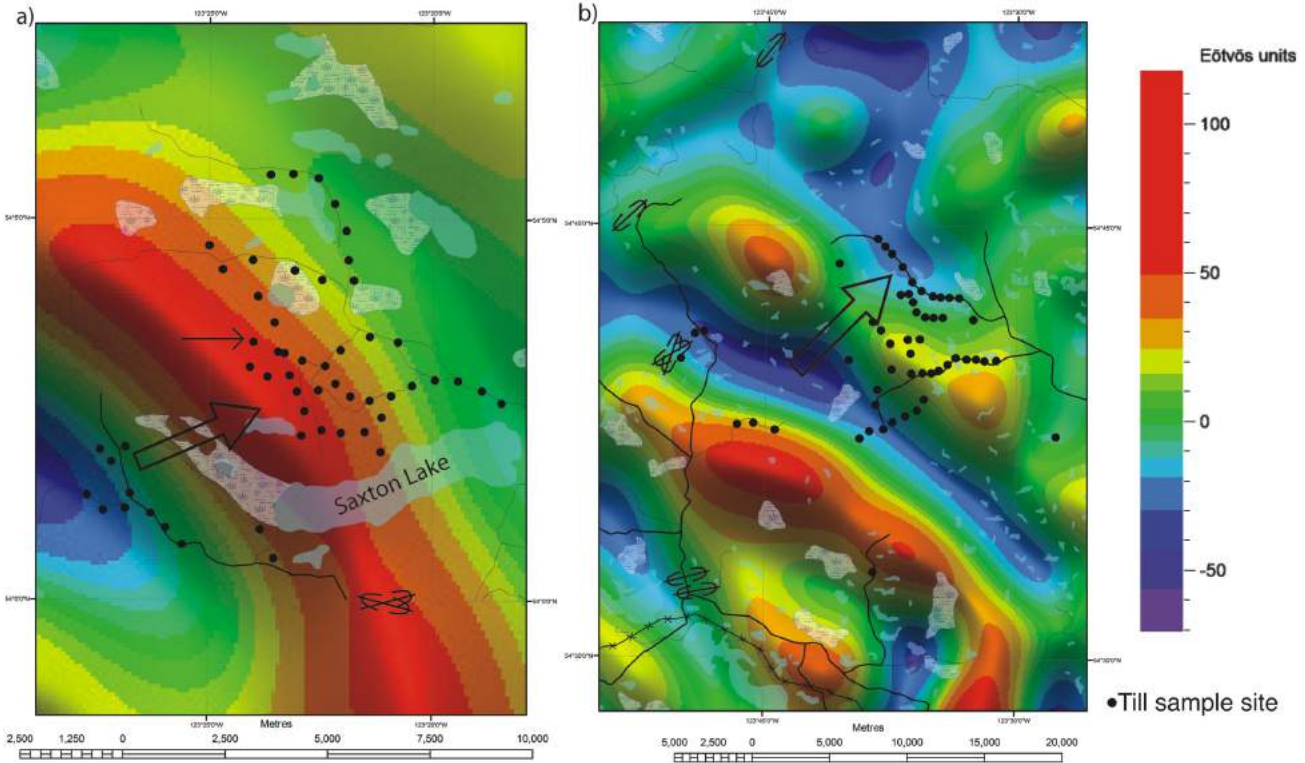


Figure 5. Sample locations for the detailed till geochemical surveys associated with linear magnetic geophysical anomalies (*modified after Sander Geophysics Limited, 2008*). Striations and dominant ice flow indicated with same symbols from Figure 1. Note the difference in scale between the two images: **a)** Saxton Lake; and **b)** North 200 road. Location of images shown on Figure 1.

between the ICP-MS datasets for the two size fractions will be assessed. If results warrant, this type of analysis may be continued for samples collected next summer.

To quantify the accuracy and precision of these analytical data a combination of field duplicates, analytical duplicates and standards are being utilized. For the 143 samples submitted for analysis, six were field duplicates, seven were analytical duplicates and six were standards obtained from R. Lett at the BCGS for use in this study.

Depending on these initial results, areas sampled in the summer of 2008 may be revisited in the summer of 2009 to collect more samples and therefore increase sample density. Next summer, all-terrain vehicles will be rented to allow further access and more foot traverses will be planned.

Future Work

Terrain Mapping and Associated Till Geochemistry

In the summer of 2009, two graduate students will carry out terrain mapping on four to five 1:50 000 scale sheets in the northwest portion of NTS 093J. The senior authors will map another one to two map sheets in the same vicinity. Terrain mapping will utilize the BC classification system (Howes and Kenk, 1997). Associated with this mapping, till samples will be taken for geochemical analysis. The same sampling strategy and analytical control used in the detailed surveys described above will be utilized.

Conclusion

Progress has been made on the glacial geological framework and drift prospecting for a portion of the QUEST Project area. Ice-flow history and drift thickness data has been collected. Till samples associated with two geophysical anomalies have been collected and will be analyzed. These studies will continue next year with the addition of two graduate students who will undertake terrain mapping and more till sampling.

Acknowledgments

The majority of funding for this project was provided by Geoscience BC and many thanks to C. Anglin and C. Slugget for helping to make this project happen. Funding for the majority of the geochemical analysis was provided by the Mountain Pine Beetle (MPB) Program under the direction of C. Hutton (GSC, NRCan). M. Dinsdale, W. Grafton, M. van Hees, D. Vis, K. Kennedy and I. Sellers provided able assistance in the field. The manuscript benefited from review by T. Ferbey.

References

Armstrong, J.E., Crandell, D.R., Easterbrook, D.J. and Nobel, J.B. (1965): Late Pleistocene stratigraphy and chronology in

southwestern British Columbia and northwestern Washington; Geological Society of America Bulletin, v. 76, p. 321–330.

Barnett, C.T. and Kowalczyk, P.L. (2008): Airborne electromagnetic and airborne gravity in the QUEST Project area, Williams Lake to Mackenzie, British Columbia (parts of NTS 093A, B, G, H, J, K, N, O; 094C, D); *in* Geoscience BC Summary of Activities 2007, Geoscience BC, Report 2008-1, p. 1–6.

Blais-Stevens, A. and Clague, J.J. (2007): Surficial geology, southeastern portion of the Prince George map area, British Columbia; Geological Survey of Canada, Open File 5274, scale 1:100 000.

Clague, J.J. (1989): Chapter 1: Quaternary geology of the Canadian Cordillera; *in* Quaternary Geology of Canada and Greenland, R.J. Fulton (ed.), Geological Survey of Canada, Geology of Canada Series No. 1. p. 17–96.

Clague, J.J. (1998a): Surficial geology, Cluculz Lake, British Columbia; Geological Survey of Canada, Open File 3638, scale 1:100 000.

Clague, J.J. (1998b): Surficial geology, West Road (Blackwater) River, British Columbia; Geological Survey of Canada, Open File 3639, scale 1:100 000.

Davis, N.F.G. and Mathews, W.H. (1944): Four phases of glaciation with illustrations from southwestern British Columbia; *Journal of Geology*, v. 52, p. 403–413.

Fulton, R.J. (1967): Deglaciation studies in Kamloops region, an area of moderate relief, British Columbia; Geological Survey of Canada, Bulletin 154, p. 1–36.

Fulton, R.J. (1991): A conceptual model for growth and decay of the Cordilleran Ice Sheet; *Geographie physique et Quaternaire*, v. 45, p. 281–286.

Holland, S.S. (1976): Landforms of British Columbia – a physiographic outline; BC Ministry of Energy, Mines and Petroleum Resources, Bulletin 48, 138 p.

Howes, D.E. and Kenk, E., editors (1997): Terrain classification system for British Columbia (revised edition); BC Ministry of Environment and Ministry Crown Lands, Ministry of Environment Manual 10.

Mathews, W.H. (1986): Physiographic map of the Canadian Cordillera; Geological Survey of Canada, “A” Series Map 1701A, scale 1:5 000 000.

Sander Geophysics Limited (2008): Airborne gravity survey, Quesnellia Region, British Columbia; Geoscience BC, Report 2008-08, 121 p.

Stumpf, A.J., Broster, B.E. and Levson, V.M. (2000): Multiphase flow of the late Wisconsinan Cordilleran ice sheet in Western Canada; Geological Society of America, Bulletin, v. 112, p. 1850–1863.

Tipper, H.W. (1971): Glacial geomorphology and Pleistocene history of central British Columbia; Geological Survey of Canada, Bulletin 196, 89 p.

Ward, B.C., Telka, A.M., Mathewes, R.W. and Geertsema, M. (2005): A paleoecological record of climatic deterioration from Middle to Late Wisconsinan time on the Interior Plateau of British Columbia, Canada; *in* Water, Ice, Land, and Life: The Quaternary Interface, Canadian Quaternary Association, Conference, June 5–8, 2005, Winnipeg, Manitoba, Program with Abstracts, p. A101.

Distribution of Alteration in an Alkalic Porphyry Copper-Gold Deposit at Mount Milligan, Central British Columbia (NTS 094N/01)

C.J. Jago, Mineral Deposit Research Unit, University of British Columbia, Vancouver, BC

R.M. Tosdal, Mineral Deposit Research Unit, University of British Columbia, Vancouver, BC,
rtosdal@eos.ubc.ca

Jago, C.J. and Tosdal, R.M. (2009): Distribution of alteration in an alkalic porphyry copper-gold deposit at Mount Milligan, central British Columbia (NTS 094N/01); *in* Geoscience BC Summary of Activities 2008, Geoscience BC, Report 2009-1, p. 33–48.

Introduction

The Mount Milligan alkalic porphyry Cu-Au deposit provides an excellent example of sulphide and alteration-mineral zonation for alkalic porphyry systems in British Columbia (BC), as it is moderately tilted ~30–50°, based on the geometry of the intrusive stock and the interpreted dip of the host supracrustal rocks (Rebagliatti 1988; Delong et al., 1991; Sketchley et al., 1995; Delong, 1996; Jago et al., 2007; Jago, 2008). This geometry makes the magmatic-hydrothermal system amenable to the study of vertical and lateral changes over a range of paleodepths, based on examination of a fence of vertical drillholes that crosses the deposit. Moreover, an important fault, the Rainbow fault, separates a lower Cu-Au-rich core zone from the upper Au-rich, Cu-poor zone that is inferred to be the shallower Au-enriched segment of the deposit, thereby increasing the total vertical exposure.

The Mount Milligan site is located 155 km northwest of Prince George (Figure 1). It is the youngest dated (183–182 Ma) of the known major mineralized alkalic porphyry systems in BC (Afton-Ajax, Copper Mountain–Ingerbelle, Galore Creek, Lorraine, Mount Polley and Red Chris; Barr et al., 1976; Mortensen et al., 1995), and represents one of the silica-saturated deposits (Lang et al., 1995). The deposit is located in central Quesnellia, at the terminus of an ~45 km east-southeast structural trend that extends from the southern edge of the Hogem batholith along Chuchi Lake. The deposit (including the Main and Southern Star monzonitic stocks, and hydrothermally affected hostrock) is hosted in mildly shoshonitic volcanic rocks of the Triassic and Early Jurassic Takla Group. It has a measured and indicated resource of 417.1 million tonnes at 0.41 g/t Au and 0.21% Cu (Terrane Metals Corp., 2007), containing 5.5 million ounces Au and 1.9 billion pounds Cu. Mount

Milligan is Au enriched compared to other porphyry Cu deposits in BC.

Geological Setting

Alkalic intrusions of the Paleozoic–Mesozoic Stikinia and Quesnellia terranes are associated with regionally extensive successions of calcalkaline to mildly alkaline rocks of shoshonitic affinity (K-enriched mafic to intermediate composition) that were produced by complex subduction processes during amalgamation of the late oceanic-arc superterrane to ancestral North America (Mortimer, 1987; Nelson and Bellefontaine, 1996). The rocks in the vicinity of Mount Milligan were emplaced onto and intruded into the Mississippian volcano-sedimentary Lay Range arc and the Pennsylvanian–Permian Slide Mountain marginal basin, a likely back-arc basin between Quesnellia and ancestral North America.

Quesnellia had a two-phase development. The Upper Triassic Nicola and Takla groups (Carnian to Norian, ~227–210 Ma) in southwestern and northeastern BC, respectively, record the evolution of the first phase. These groups consist of basal sedimentary rocks overlain by volcanic and volcanoclastic successions dominated by marine augite-phyric basalt and andesite of calcalkaline to shoshonitic affinity. Coeval intrusions are also present. The high-K and mildly shoshonitic rocks crop out intermittently over a 1000 km strike length in northern Quesnellia (Mortimer, 1987; Nelson et al., 1992). These rocks host and are genetically associated with Late Triassic alkalic porphyry Cu-Au deposits (Barr et al., 1976; Lang et al., 1995). The second stage consists of Early Jurassic carbonate and clastic sedimentary sequences unconformably overlying the Triassic volcanic rocks. In the Mount Milligan area, however, volcanism continued after a Late Triassic to Early Jurassic hiatus, resulting in the paraconformably overlying Early Jurassic Chuchi Lake and Twin Creek successions (Pliensbachian to Toarcian, ~196–180 Ma). These rocks exhibit greater compositional heterogeneity than the Upper Triassic sequence and are composed mainly of plagioclase-augite-phyric, subalkaline to shoshonitic igneous rocks (Nelson and Bellefontaine, 1996). The Mount Milligan Cu-

Keywords: *alkalic porphyry Cu-Au, alteration assemblages, zonation*

This publication is also available, free of charge, as colour digital files in Adobe Acrobat® PDF format from the Geoscience BC website: <http://www.geosciencebc.com/s/DataReleases.asp>.

Au porphyry and related plutons are part of the second stage, and hosted by the Witch Lake succession. Igneous rocks in the Mount Milligan deposit area have U-Pb ages (zircon, titanite, rutile) ranging from 186.9 ± 3.3 to 182.5 ± 4 Ma (Mortensen et al., 1995; Nelson and Bellefontaine,

1996; R. Friedman, pers. comm., 2008). Regionally, subduction had ceased by ~ 186 – 181 Ma with the accretion of Quesnellia to ancestral North America (Mihalynuk et al., 1994). The Mount Milligan porphyry stocks thus formed during the final plutonic activity of the Quesnellia

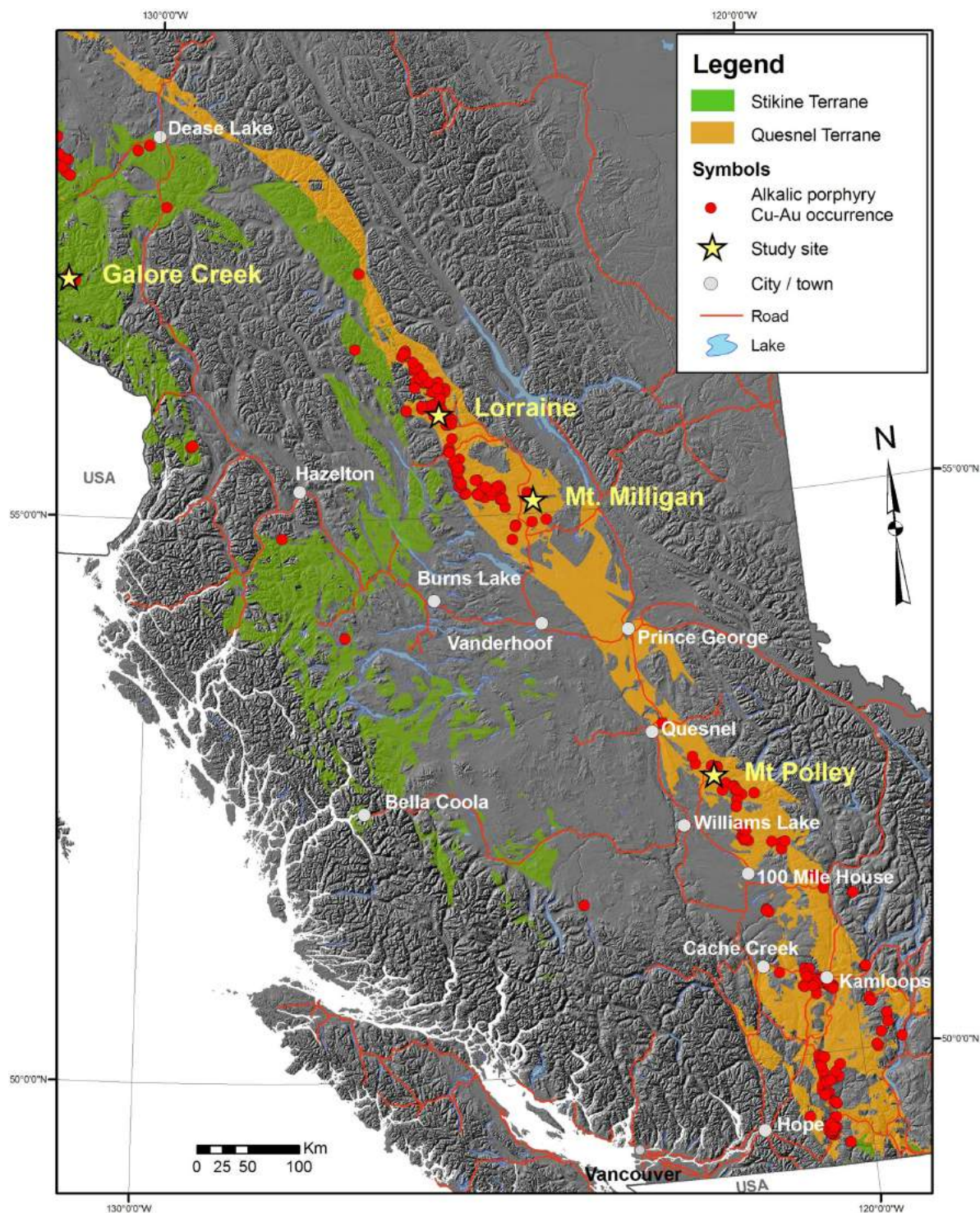


Figure 1: Location of alkaalic porphyry Cu deposits in British Columbia, showing location of Mount Milligan with respect to the other deposits and to the Triassic and Early Jurassic Quesnel and Stikine terranes. The Hogem batholith underlies the area around Lorraine and extends southward on the eastern margin of the Pinchi fault toward Mount Milligan.

magmatic-arc system, and were broadly contemporaneous with amalgamation of the marine arc to the margin of North America.

The Hogem batholith has a linear northwesterly trend parallel to the Pinchi fault system, separating the Quesnellia and Cache Creek terranes and suggesting a structural control over batholith emplacement (Nelson and Bellefontaine, 1996). A break in the regional structural trend beneath Chuchi Lake, suggesting a pre-Triassic fault, extends east-southeast from the southern edge of the batholith, transverse to the arc. The inferred fault lies along trend with an east-southeast shift in the Hogem regional magnetic high, indicating deflection by this basement structure. The magnetic anomaly continues ~25 km eastward to the Mount Milligan intrusive suite, a monzonite-diorite-granite pluton located ~7 km north of the porphyry deposit (Nelson and Bellefontaine, 1996). Compositions and textures suggest the pluton is an extension of the Hogem batholith, which implies that the monzonitic porphyry stocks of the Mount Milligan deposit to the south also emanate from a buried extension of the Hogem batholith.

Supracrustal Rocks

The Witch Lake succession, the host supracrustal sequence at Mount Milligan (Figures 2, 3), consists of a moderately northeast-dipping, alternating coherent and clastic sequence that includes porphyritic clinopyroxene basaltic trachyandesite (Lang, 1992; Barrie, 1993; Sketchley et al., 1995). Coherent rocks are lavas and (or) shallow intrusions (Figure 4). Outside the area of intense alteration toward the 66 zone, beyond ~250 m from the MBX stock, the hostrocks contain ~25% clinopyroxene (lesser hornblende) and 3–5% subhedral plagioclase phenocrysts. Plagioclase constitutes 25–50% of the trachytic-textured feldspar groundmass, and cryptocrystalline K-feldspar forms the remainder. Plagioclase is oligoclase-andesine, which is slightly more calcic than the oligoclase in the basaltic trachyandesite and in the Rainbow dike of the MBX zone but comparable to the plagioclase in the MBX stock and Lower monzonite dike in the 66 zone. Apparent- and/or pseudobreccia textures, composed of rounded gravel- to cobble-sized clasts of basaltic trachyandesite in a compositionally similar matrix, are common throughout the hostrocks; some of these textures result from alteration processes, but others are primary volcaniclastic rocks.

Three rock units are critical to the structural interpretation of the hostrock sequence (Figure 3). The Lower Trachyte is an ~70 m thick conformable unit of intensely altered rock situated ~180 m below the Rainbow dike. At depth in drillhole 90-652, the rock has thin mafic laminations that resemble shear bands but could also represent bedding planes in fine epiclastic material (Nelson and Bellefontaine, 1996). These laminations, oriented at ~30° to the horizontal axis of the vertical drillcore, in conjunction with the interpreted orientations of the MBX stock and Rainbow dike, provide the basis for concluding a moderate tilt to the deposit (Sketchley et al., 1995). Compositionally, the Lower Trachyte unit is more silica deficient than is implied in the term ‘trachyte’, and would be more accurately described as tephriphonolite (after Lang, 1992; Barrie, 1993). The use of ‘trachyte’ in the name of this unit refers to trachytic microtexture rather than composition. The very fine grained trachytic-textured rocks are characterized by abundant acicular feldspar microlites. Ghosts of former augite phenocrysts are composed of biotite-chlor-

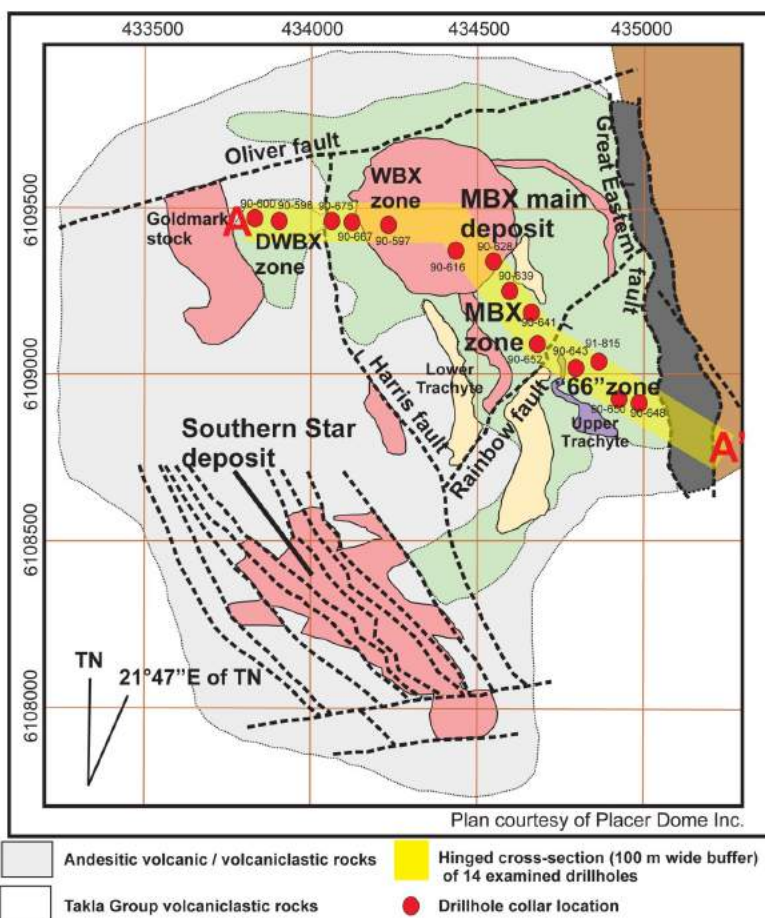


Figure 2: Plan view of the Mount Milligan alkalic porphyry Cu-Au deposit, showing interpreted geology (including the MBX Main deposit, Southern Star deposit and Goldmark stock), major faults, four ore-zone divisions within the MBX Main deposit (DWBX, WBX, MBX and 66), orientation of the hinged cross-section, and locations of the drillholes investigated. Original lithology provided by Placer Dome Inc.

ite±actinolite. Pyrite has replaced some augite phenocrysts and has precipitated in partings, where it is typically mantled by chlorite.

In the 66 zone, the Upper Trachyte unit is an ~20 m thick sequence of weakly vesicular, trachytic-textured rock that forms recrystallized fine granular lenses, and gravel-sized clasts in faults. Compositionally, the unit plots as tephriphonolite (Lang, 1992; Barrie, 1993), but it may be potassically altered trachyandesite, based on the presence of relict mafic phenocrysts. As with the Lower Trachyte unit, hairline fractures filled with sulphide resemble shear bands dipping at 35° to the horizontal axis of drillcore. Similarly oriented layering is defined by granular lenses of K-feldspar (~0.1 mm grains), quartz (5–10 modal %) and minor fragmental plagioclase. These lenses may also reflect relict bedding.

In contrast to the rest of the deposit, the hangingwall of the DWBX zone comprises faulted, polymict fragmental units, which are possibly resedimented hyaloclastite. Juvenile clasts with nondeformed cusped and tabular shards, and vesicles filled by hydrous microminerals constitute the western fringe of the system in drillhole 90-600.

Intrusive Rocks

The MBX stock is a northwest-striking, elliptical intrusive body with a principal axis ratio of ~2:1 and a diameter of ~400 m. It has a circular near-surface expression due to tilting (Figure 2). The composite stock has at least three plagioclase-phyric phases. Compositions range from normative quartz monzonite to monzodiorite and plot within the alkaline and shoshonitic fields (Lang, 1992; Barrie, 1993). Textural variations include (Figure 5) 1) plagioclase phyric, 2) crowded plagioclase phyric, 3) flow-aligned plagioclase, 4) medium-grained equigranular, 5) xenolithic monzonite containing monzonitic and biotite-magnetite hornfels xenoliths, 6) magmatic-hydrothermal breccia with pink K-feldspar cement, and 7) apparent-breccia resulting from pervasive K-feldspar alteration. Separate intrusive phases have been identified using textural changes and the ratio of modal plagioclase to mafic minerals. Contacts between the phases are typically gradational or obscured by pervasive K-feldspar alteration.

In the WBX zone (drillhole 90-667), the intrusive sequence includes an early monzonite phase with crowded, sericitized plagioclase phenocrysts in a K-feldspar-rich

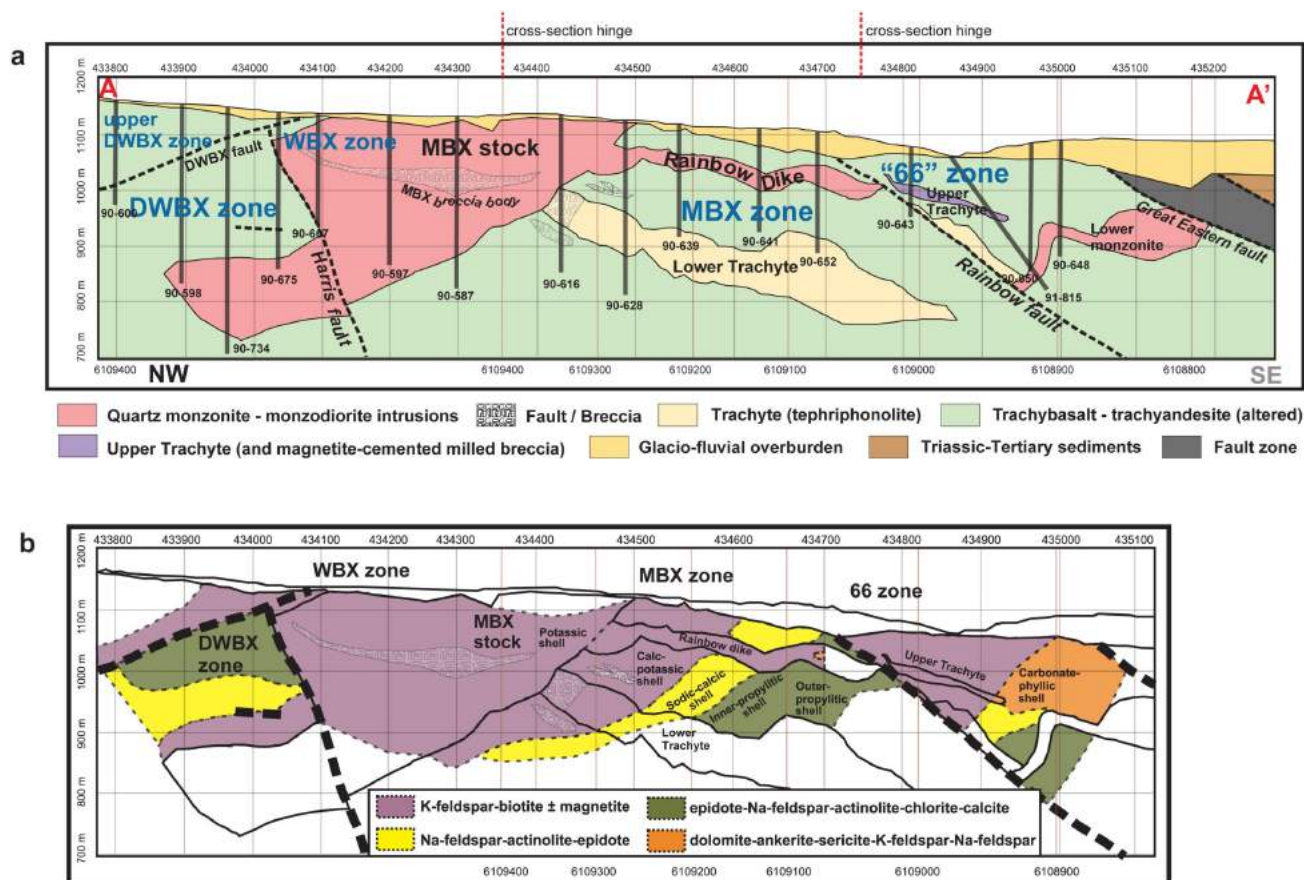


Figure 3: Profile view of the Mount Milligan alkalic porphyry Cu-Au deposit along the hinged cross-section showing **a)** interpreted geology, major structures, four ore-zone divisions of the MBX Main deposit (DWBX, WBX, MBX, and 66), and locations of the drillholes investigated (original lithology provided by Placer Dome Inc.); **b)** distribution of alteration assemblages superposed on the geology.

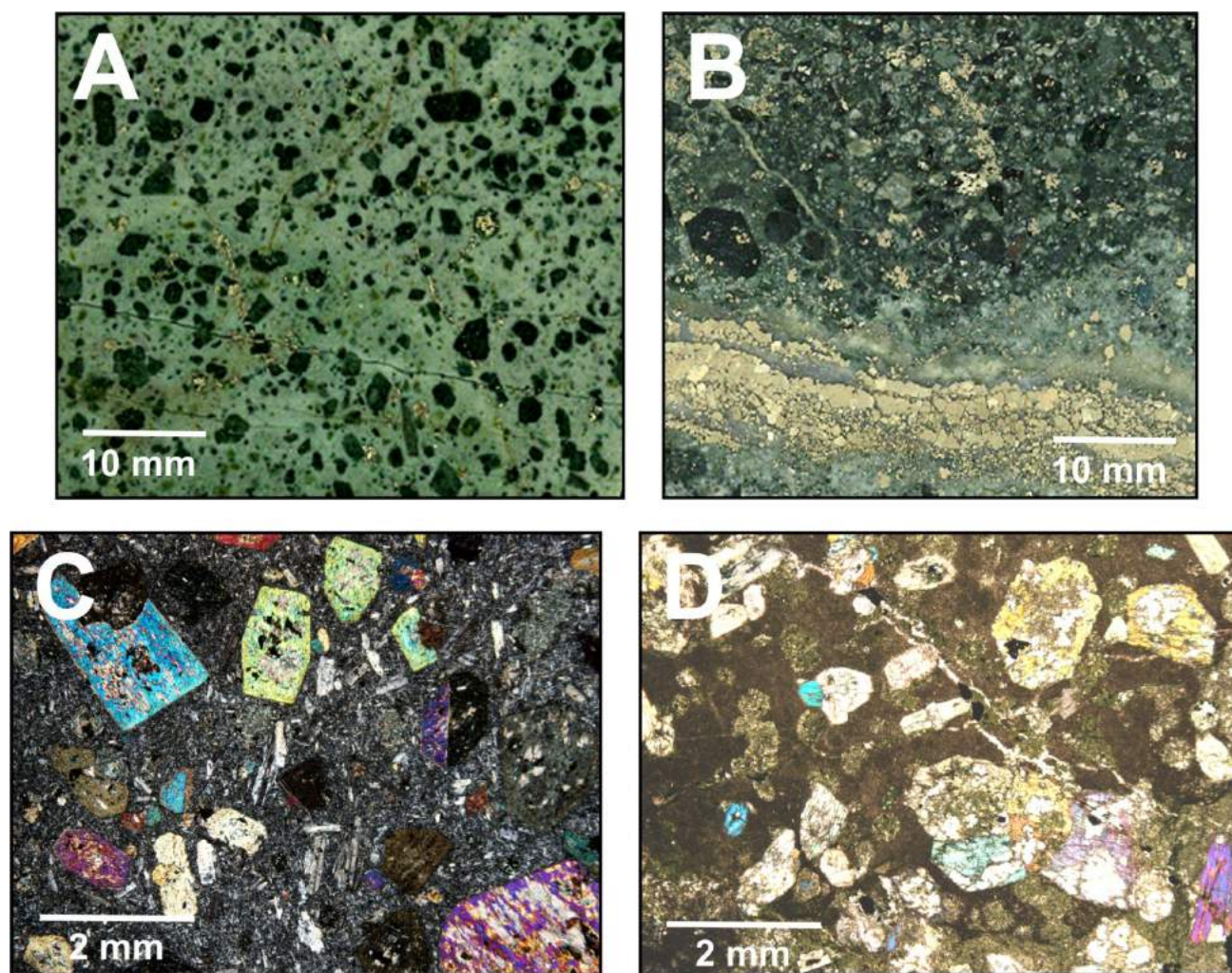


Figure 4: Examples of hostrocks of the Witch Creek succession: **A)** hornblende-augite-phyric trachyandesite altered to K-feldspar-Na-feldspar-actinolite (drillhole 90-598 at 123.3 m); **B)** coarse augite phenocrysts (4–15 mm) in chlorite-altered basaltic trachyandesite with ribboned pyrite-carbonate L3 vein and Na-feldspar-epidote halo (drillhole 90-675 at 174.2 m); **C)** photomicrograph of weakly chloritized trachyandesite with oligoclase-andesine fragments (1 mm) and augite phenocrysts (drillhole 90-648 at 176.5 m); **D)** photomicrograph of basaltic trachyandesite with chlorite-altered devitrified groundmass and glomeroporphyritic augite (drillhole 90-641 at 118 m).

groundmass. This phase forms the outer ~40 m rim of the stock. Inside the stock, the early phase is cut by crowded plagioclase-phyric monzodiorite with a more biotitic groundmass. Both phases are locally mineralized. Weakly sericitized plagioclase-phyric diorite is the youngest phase. In general, the rocks are composed of >60% crowded plagioclase (oligoclase-andesine) with thin albite rims. Primary K-feldspar phenocrysts (~2.5 mm) are also present. Plagioclase is commonly zoned and replaced by a fine-grained sericite. The monzonite groundmass is composed of K-feldspar (~80%) with minor Na-plagioclase (10%), hydrothermal biotite (5%) after primary biotite, and magnetite (1–5%).

A variably jigsaw-brecciated to clast-rotated breccia body extends the length of the MBX stock. It ranges in thickness from 2 m in the WBX zone to 50 m beneath the poorly mineralized centre of the stock, and to 5 m near the MBX zone.

The overall geometry is poorly constrained. Where observed in drillcore, it varies from a hematitic, pink, K-feldspar-cemented crackle-breccia to a milled breccia with rounded monzonite pebbles in a magnetite-altered matrix. Chalcopyrite veinlets cut clasts and cement.

The monzodioritic Rainbow dike extends outward from the southeastern to southern margin of the MBX stock. It is an ~50 m thick, east-dipping conformable body for ~250 m, and would be better described as a sill. Approximately 200 m due east of the stock, it has a bowl shape where the sill-like body changes to a vertical, curvilinear dike-like body. Geochemical data (Barrie, 1992) suggest that the Rainbow dike is more silica undersaturated than the MBX stock.

Where least altered, the Rainbow dike is a crowded plagioclase-phyric monzodiorite (Lang, 1992; Barrie,

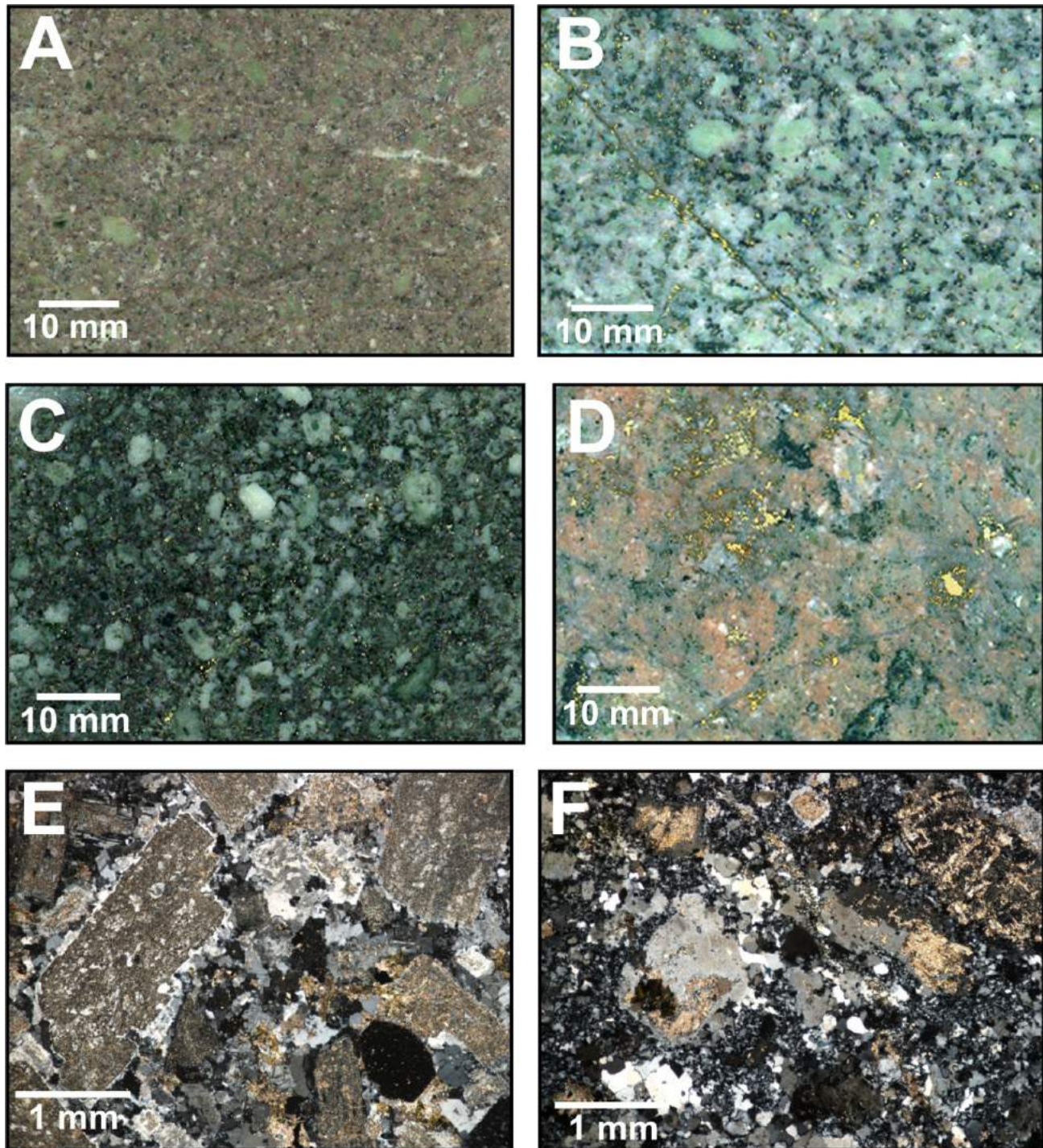


Figure 5: Drillcore sections showing the variety of composition, texture, alteration and sulphide mineralization of monzonitic to monzodioritic rocks in the MBX stock: **A)** sericitized plagioclase-phyric monzonite with K-feldspar-rich matrix, and minor disseminated magnetite (drillhole 90-616 at 126.0 m); **B)** weakly sericitized, crowded plagioclase-phyric monzonite with K-feldspar-altered rims, and interstitial biotite; disseminated sulphide replaces biotite surrounding chalcopyrite veinlet (drillhole 90-597 at 223 m); **C)** plagioclase-phyric monzodiorite with ~10% magnetite-bearing matrix (drillhole 90-667 at 133.0 m); **D)** intense K-feldspar-quartz alteration with clotted biotite replaced by sulphide (drillhole 90-597 at 223 m); **E)** photomicrograph of weakly altered monzonite; sericitized phenocrysts have Na-plagioclase rims; apatite (opaque) at lower right (drillhole 90-597 at 123 m); **F)** photomicrograph of strong potassic alteration converting monzonite to a granular K-feldspar-quartz assemblage; K-feldspar replaces sericitized plagioclase laths (drillhole 90-597 at 223 m).

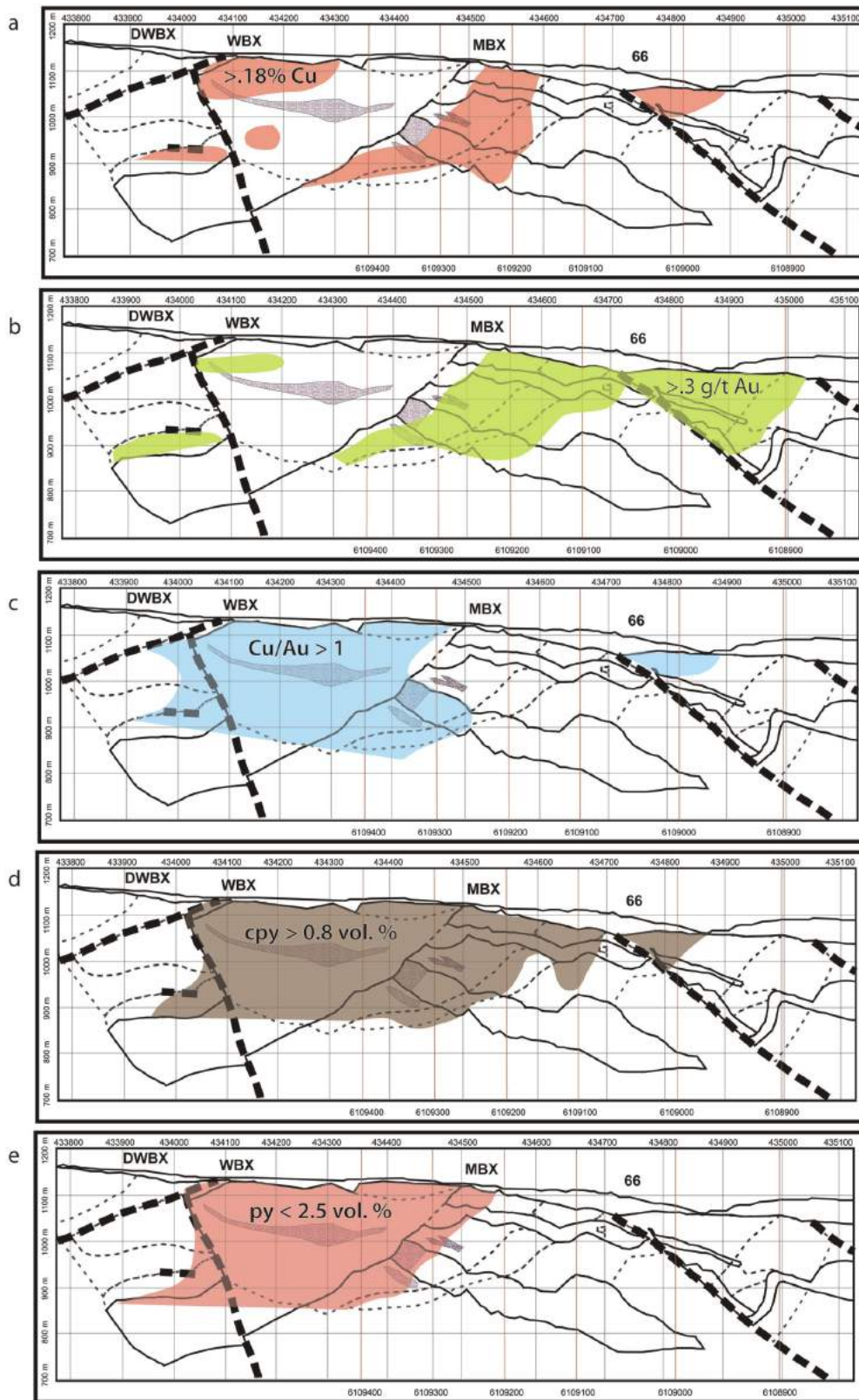


Figure 6: a) Copper grade, b) Au grade, c) Cu/Au ratio, d) chalcopyrite mode estimated in the field, and e) pyrite mode estimated in the field, superposed on alteration shells (dotted lines on cross-sections) along the hinged cross-section through the Mount Milligan alkalic porphyry Cu-Au deposit (see Figure 3b). Data are binned into five ranges using the Jenks Natural Breaks classing method, which is based on identifying groupings that exist naturally in the data (Jenks and Caspall, 1971). Fire-assay data were provided by Placer Dome Inc. (now part of Barrick Gold Corp.).

1993) with smaller phenocrysts (~2 mm) than those common to the MBX stock. Plagioclase is albite-oligoclase. The groundmass is pale grey K-feldspar with disseminated biotite, trace carbonate and sericite. Within 25 m of the stock (drillhole 90-628), the dike contains gravel-sized monzonitic xenoliths that are probably derived from the stock. The dike is typically in fault contact with host supracrustal rock. Dike contacts, particularly within ~50 m of the stock, are locally obscured due to intense alteration (Sketchley et al., 1995).

Late-mineral dikes in the MBX Main deposit include northeast-trending, moderately northwest-dipping trachyte and monzonite dikes. Northwest-trending, steeply northeast-dipping porphyritic hornblende-plagioclase diorite dikes are the youngest intrusive rock to occur (Sketchley et al., 1995).

Alteration and Mineralization

The deposit is divided into four zones based on location of ore and interpreted structural architecture (Rebagliati, 1988; Sketchley et al., 1995). These are, from west to east (Figures 2, 3)

the DWBX zone (downdropped WBX), which lies west of the stock and west of the steeply east-dipping Harris fault that separates the DWBX on the west from the WBX zone to the east;

the WBX zone, which includes the western portion of the MBX stock, the deepest continuous portion, plus an ~40 m wide, biotite-altered envelope of MBX monzonite and host rock that is cut by the DWBX fault;

the MBX (magnetite breccia) zone, which represents the main Cu-Au orebody and is located immediately southeast of the MBX stock along strike from the Rainbow dike and Lower Trachyte unit; and

the downthrown 66 zone, which lies in the hanging wall of the Rainbow fault, an east-northeast-trending, moderately southeast-dipping crossfault that truncates the Rainbow dike and MBX zone to the south.

The north-striking, shallowly east-dipping Great Eastern fault has truncated the hydrothermal features immediately east of the bowl-like portion of the Rainbow dike. The fault separates the Mount Milligan system from early Tertiary volcanic and sedimentary rocks. A second crossfault, the east-northeast trending subvertical Oliver fault, lies immediately north of the MBX stock.

MBX Zone

In the MBX zone (Figure 3), chalcopyrite and minor bornite are associated with potassic (biotite-K-feldspar) alteration and magnetite (Figure 6) within the biotite alteration shell along the brecciated margin of the MBX stock and in the stratiform Lower Trachyte unit and Rainbow dike. Sul-

phide-bearing quartz veins (Figure 7) are also concentrated at the margins of the MBX stock within monzonite and biotite hornfels. Sodic-calcic alteration (Na-feldspar-actinolite-epidote; (Figure 8) overprints the outer margin of the potassic shell and passes outward to inner- (Figure 9) and outer-propylitic alteration (epidote-Na-feldspar-calcite-actinolite-chlorite), and regional chloritic alteration (Figure 3). The grades of Cu and Au are maximized where albitization of the potassic zone is strongest (Figure 6a-b). Moderate Au grade continues outward within the pyrite halo associated with the peripheral assemblages. A carbonate-phyllitic (dolomite-ankerite-sericite-pyrite) vein within the distal Rainbow dike has elevated Au and Cu grades (Figure 10D). Late-stage epidote-chlorite-pyrite has exploited permeable stratigraphic horizons within the biotite shell (Figure 3).

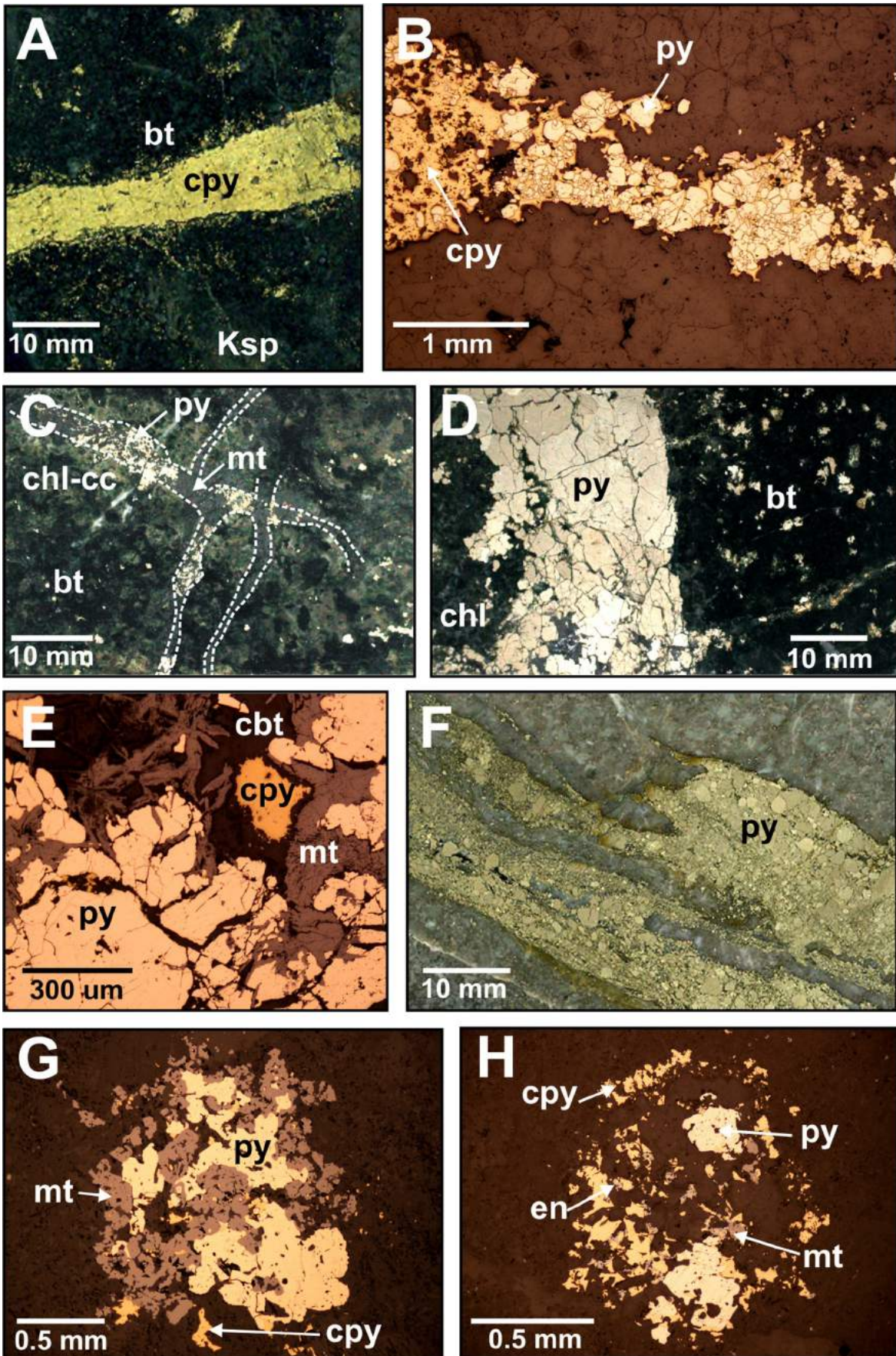
66 Zone

In the 66 zone (Figure 3) above the Rainbow fault, the potassic assemblage reappears and is marked by pervasive K-feldspar alteration and Cu-Fe sulphides in the Upper Trachyte unit, and biotite alteration of surrounding trachyandesite (Figures 3b, 11). Sheeted magnetite veins are concentrated at the lower contact of the Upper Trachyte. The unit terminates in a magnetite breccia, which transitions into a zone of intense carbonate-phyllitic alteration. Elevated Au grade is present within minor faults and along late-mineral dike contacts within the carbonate-phyllitic assemblage, but decreases with distance from the Upper Trachyte. Gold grade sharply decreases in the outer-propylitic and chloritic alteration zones that surround the carbonate-phyllitic-altered shell (Figure 6a-c).

DWBX Zone

In the lower DWBX zone (Figure 3), an ~30 m envelope of Cu-Au associated with potassic alteration and magnetite is nested along the upper contact of a monzonite, potentially the down-dropped MBX stock, where it is cut off by the Harris fault (Figure 6a-c). Pervasive outer-propylitic alteration of volcaniclastic conglomerate bordering the biotite

Figure 7: Early- to transitional-stage veins and replacement sulphide minerals, Mount Milligan alkalic porphyry Cu-Au deposit: **A)** chalcopyrite vein with biotite halo (drillhole 90-675 at 254 m); **B)** photomicrograph of chalcopyrite-pyrite vein with pyrite grains entrained in chalcopyrite (drillhole 90-628 at 38 m); **C)** magnetite-chalcopyrite±pyrite veins in dendritic array with carbonate-chamosite halos (drillhole 90-639 at 116.2 m); **D)** pyrite-magnetite±chalcopyrite veins (drillhole 90-639 at 50.6 m); **E)** photomicrograph of vein, showing magnetite surrounding coarse pyrite and interstitial carbonate replacing trace chalcopyrite (drillhole 90-639 at 50.6 m); **F)** vein cutting monzonite in fault zone between the MBX stock and biotite hornfels (drillhole 90-616 at 194.5 m). **G)** and **H)** photomicrographs of chalcopyrite-pyrite-magnetite±enargite replacement of clinopyroxene phenocrysts (drillhole 90-639 at 34.5 and 50.6 m). Abbreviations: py, pyrite; cpy, chalcopyrite; en, enargite; mt, magnetite; bt, biotite; chl, chlorite; cbt, carbonate; cc, calcite.



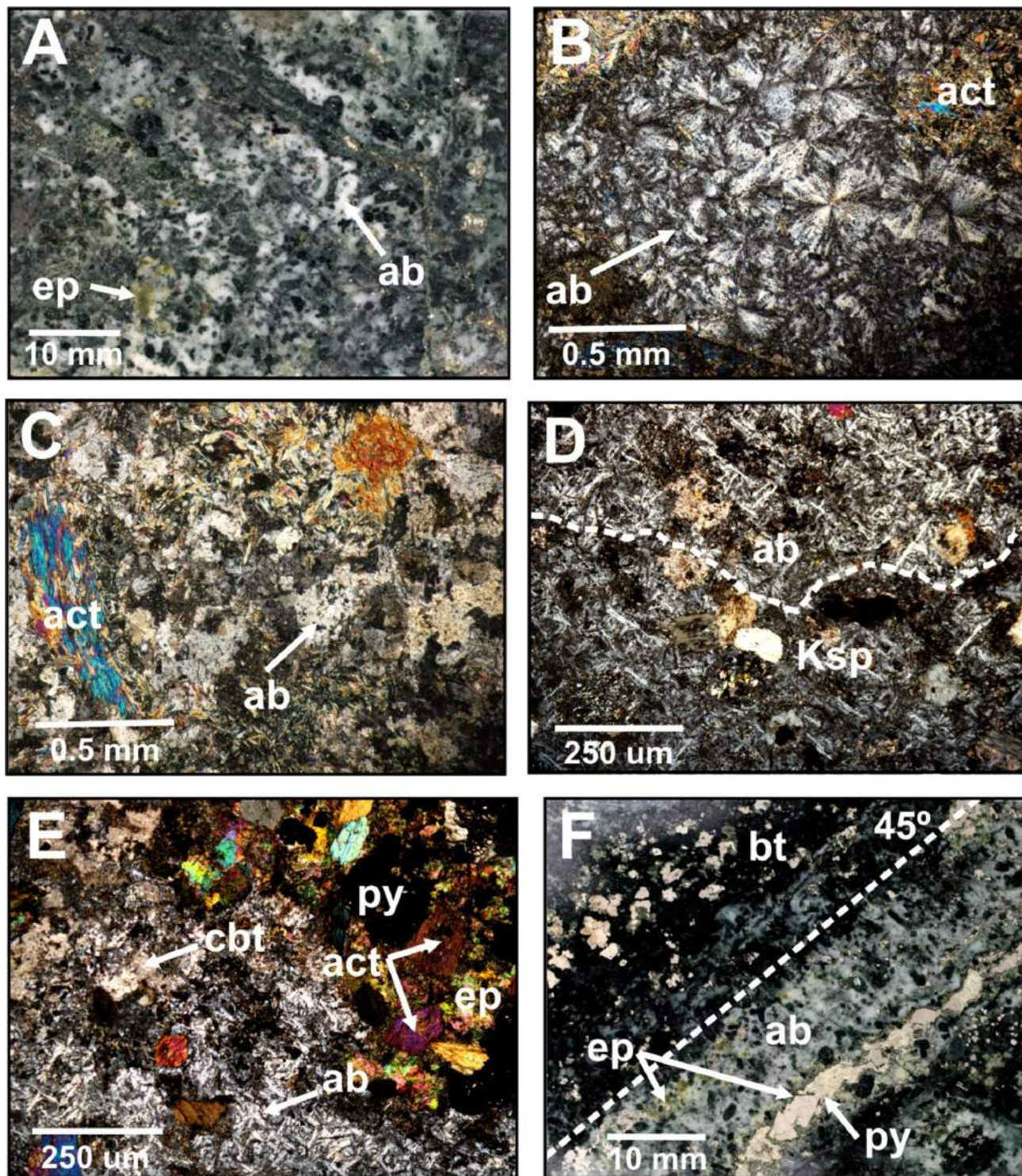


Figure 8: Sodic-calcic (outer-calcipotassic) alteration, Mount Milligan alkalic porphyry Cu-Au deposit: **A)** selective-pervasive albization of basaltic trachyandesite and weak epidote after Na-plagioclase (drillhole 90-639 at 135 m); **B)** photomicrograph of bow-tie texture of Na-plagioclase groundmass with scattered actinolite needles (drillhole 90-639 at 166 m); **C)** photomicrograph of disintegration of actinolitized phenocrysts within albitized groundmass (drillhole 90-639 at 127.6 m); **D)** photomicrograph of reaction front between Na-plagioclase and K-feldspar alteration (drillhole 90-639 at 193.8 m); **E)** photomicrograph of pyrite-epidote-carbonate replacing Na-plagioclase groundmass (drillhole 90-639 at 193.8 m); **F)** pyrite-chalcopyrite vein with epidote selvage and Na-plagioclase halo overprinting biotite along coarse layering (flow-banding?) at 45° to the horizontal axis of the drillcore (drillhole 90-639 at 182 m). Abbreviations: Ksp, K-feldspar; bt, biotite; ab, Na-plagioclase; act, actinolite; ep, epidote; cbt, carbonate; py, pyrite.

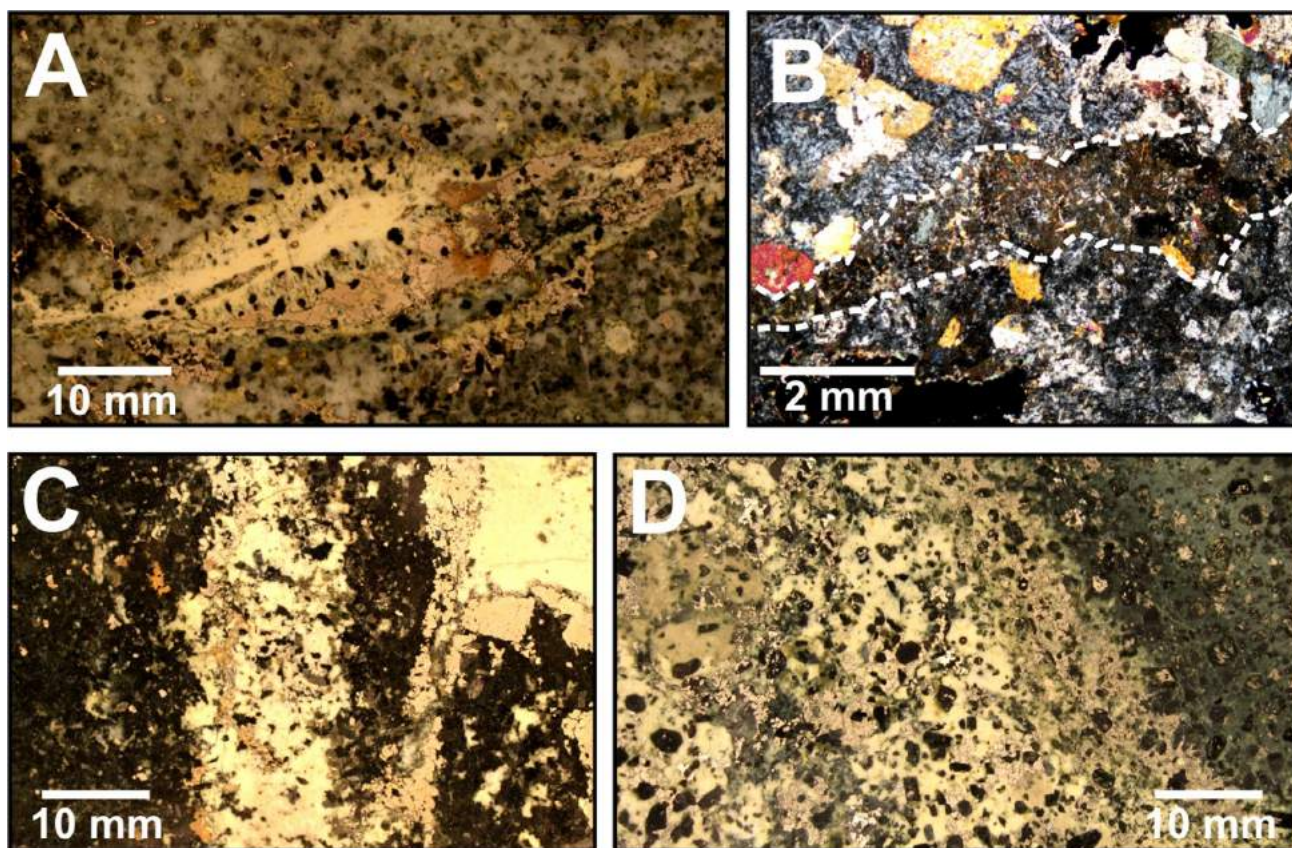


Figure 9: Inner-propylitic alteration, Mount Milligan alkalic porphyry Cu-Au deposit: **A)** Microcrystalline epidote–Na-plagioclase–actinolite–calcite vein with associated pyrite, and cloudy K-feldspar halo (drillhole 90-641 at 112.2 m). **B)** in thin section, the vein is composed of actinolite needles, fine-grained epidote and Na-plagioclase after K-feldspar; scanning electron microscope analysis indicates the prismatic blue mineral in the upper right corner is epidote, although it resembles zoisite (drillhole 90-641 at 112.2 m); **C)** very fine grained epidote–Na-feldspar alteration with coarse pyrite and chlorite halo after biotite (drillhole 90-641 at 132.1 m); **D)** pyrite-rich P1-stage alteration band overprinting chloritized trachyandesite (drillhole 90-815 at 127 m).

hornfels becomes more chloritic towards the Harris fault. Late pyrite veins that cut the potassic zone may be genetically linked with the outer-propylitic assemblage.

Paragenesis

The alteration and metal zoning at the Mount Milligan deposit is divided into vertical and lateral components (Figure 3). Laterally, alteration progresses from potassic and local calcpotassic to sodic-calcic to inner- and outer-propylitic assemblages, spanning ~350 m in the MBX zone. Vertically, alteration progresses from potassic to carbonate-phyllitic assemblages, spanning ~300 m in the MBX and 66 zones. The intimate association of metal and alteration zonation with ore grade at the Mount Milligan MBX Main deposit is discernible when comparing alteration shells to fire-assay data (Figure 6a, b).

The potassic and calcpotassic shell is most extensive in the MBX zone, extending ~260 m from the MBX stock, but is largely overprinted by younger alteration stages beyond ~130 m. Copper and Au have a greater than 1:1 relationship (wt %/[g/t]) in the deepest levels (lower DWBX zone,

WBX zone), a subequal relationship at intermediate levels (deep MBX zone, Lower Trachyte unit), and less than unity surrounding the Rainbow dike (Figure 6c). The Cu/Au ratio generally decreases upward and outward with increasing Cu and Au grade, although an ~75 m wide interval of highest grade occurs within the Lower Trachyte unit in drillhole 90-628.

Potassic alteration is present in the down-dropped 66 zone (Figure 3), where it is centred on the fault-bounded Upper Trachyte unit. Copper and Au grades are slightly lower than in the upper MBX zone (Figure 6a–c). However, Au grade increases by 100% where the potassic assemblage terminates in a magnetite-altered milled breccia (drillhole 91-815; Figure 11C), and carbonate-phyllitic alteration intensifies.

Sodic-calcic alteration defines an intermediate zone between calcpotassic- and propylitic-stage assemblages (Figure 3). It is strongest along the upper margin of the Lower Trachyte unit, but extends below the Lower Trachyte as close as ~50 m to the MBX stock. From the deepest known extent upward to the footwall of the Rainbow dike

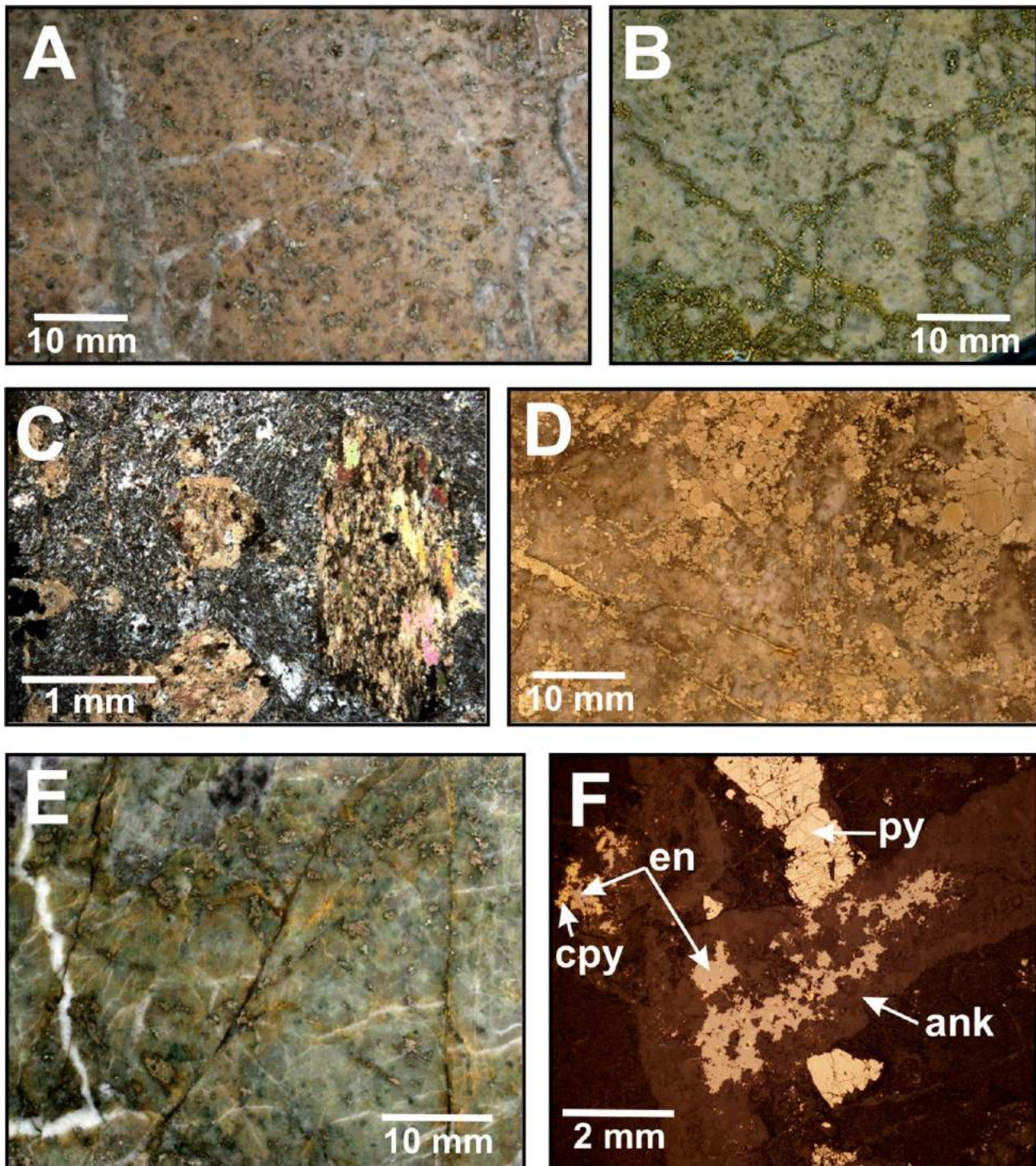


Figure 10: Carbonate-phyllitic alteration, Mount Milligan alkalic porphyry Cu-Au deposit: **A)** salmon pink phengite-dolomite-illite±brucite-arfvedsonite alteration with pyrite pseudomorphs and dolomite veinlet stockwork (drillhole 90-650 at 60.5 m); **B)** stockwork of pyrite veinlets in carbonate-phyllitic alteration (drillhole 90-648 at 123 m); **C)** photomicrograph of dolomite pseudomorphs in trachytic-textured groundmass; alteration is muscovite-illite-chlorite-biotite; pyrite also replaces phenocrysts and is finely disseminated in the groundmass (drillhole 90-648 at 59.9 m); **D)** carbonate-phyllitic vein in distal Rainbow dike with Au-bearing sulphide (5.11 g/t Au); alteration is dolomite-ankerite-sericite-illite (drillhole 90-652 at 81.1 m); **E)** carbonate-phyllitic alteration at the upper margin of the Rainbow dike, ~15 m from the MBX stock; alteration is quartz-ankerite-adularia-muscovite-biotite-Na-feldspar-pyrite (90-628 at 31 m); **F)** photomicrograph of ankerite veinlet cutting pyrite veinlet in Lower Trachyte unit; remobilized chalcopyrite is replaced by Cu-sulphosalt; alteration is muscovite-ankerite-brucite-illite (drillhole 90-628 at 201.1 m). Abbreviations: ank, ankerite; cp, chalcopyrite; py, pyrite; en, enargite (Cu-sulphosalt).

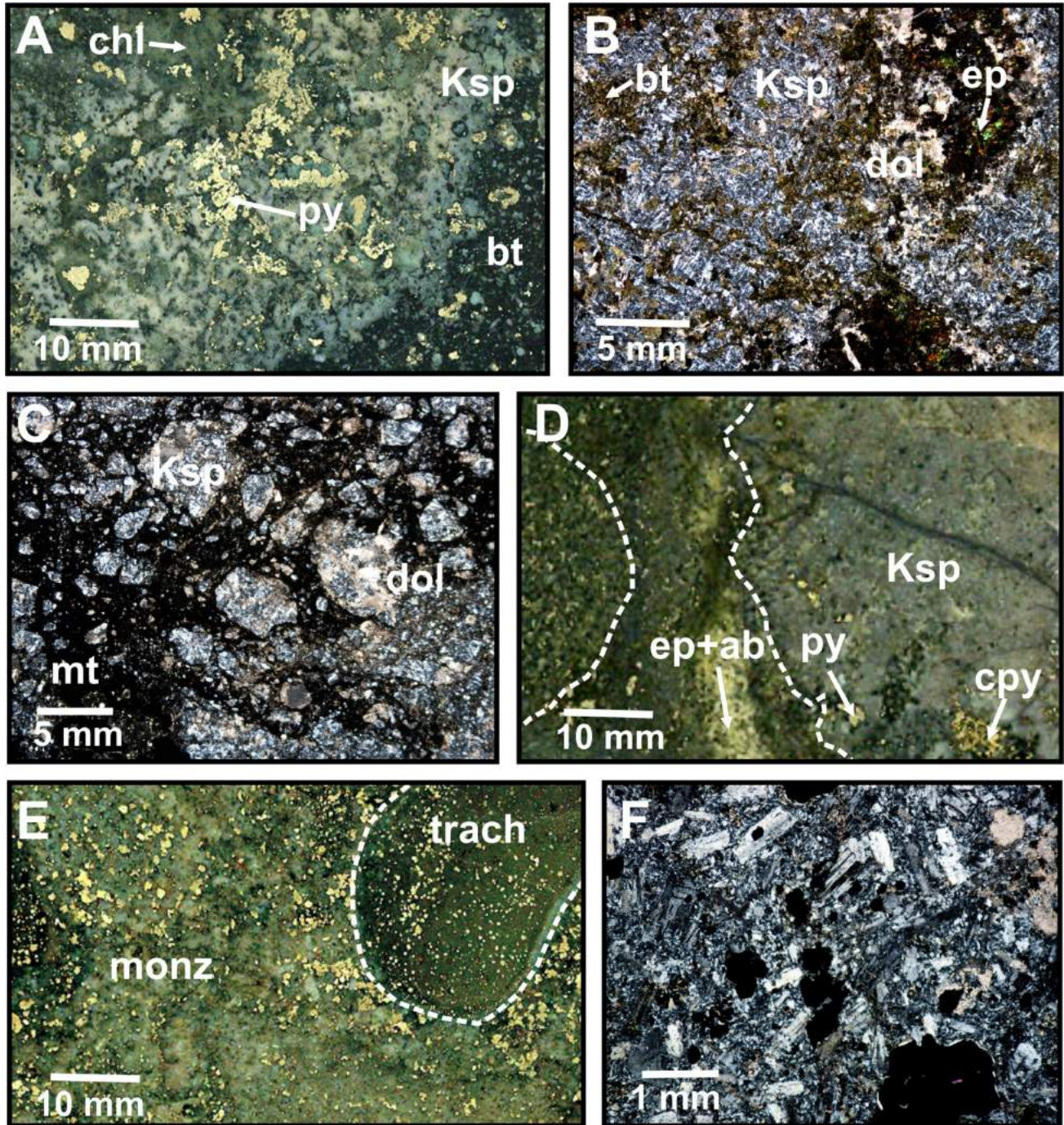


Figure 11: Intermediate-stage potassic alteration in the 66 zone, Mount Milligan alkalic porphyry Cu-Au deposit: **A)** auriferous K-feldspar–pyrite overprinting biotite-altered trachyandesite, footwall of the Upper Trachyte (drillhole 91-815 at 103 m); **B)** photomicrograph of the Upper Trachyte unit, with biotite-filled microfracture network overprinted by pyrite-epidote-dolomite clots (drillhole 91-815 at 86 m); **C)** photomicrograph of magnetite-cemented milled breccia with trachytic clasts altered to K-feldspar–dolomite, southeastern terminus of Upper Trachyte (drillhole 91-815 at 81.1 m); **D)** intensely K-feldspar–altered clasts in breccia at the upper contact of the Rainbow fault (bedded trachyte unit, Placer Dome Inc.), with clotted biotite replaced by sulphide; epidote-albite-chlorite alteration is present between clasts (drillhole 90-643 at 102.5 m); **E)** xenolithic monzonite with trachyte xenolith (drillhole 91-815 at 183 m); **F)** photomicrograph of xenolithic monzonite, with oligoclase-andesine phenocrysts in K-feldspar groundmass; mafic minerals are replaced by pyrite and minor carbonate. Abbreviations: Ksp, K-feldspar; bt, biotite; chl, chlorite; dol, dolomite; ep, epidote; ab, albite; cpy, chalcopyrite; py, pyrite; trach, trachyte; monz, monzonite.

(drillhole 90-639), the Au grade of the sodic-calcic shell increases by ~70%. This represents the best Cu-Au grade of the deposit apart from that within the Lower Trachyte (drillhole 90-628), which may be a deeper portion of the same assemblage.

Inner-propylitic alteration (Na-feldspar-epidote-pyrite) lies outboard of the sodic-calcic shell in the MBX zone at ~150 m from the MBX stock, and also overprints the calcopotassic assemblage (Figure 3). Chalcopyrite-magnetite is destroyed where overprinted by epidote, which is reflected in the low Cu grade, whereas Au grade can remain moderately high.

Late-stage carbonate-phyllitic alteration (Figure 3) in the 66 zone develops outward from potassic alteration centred on the Upper Trachyte, and also occurs in a 1.7 m wide vein at the lower margin of the Rainbow dike (drillhole 90-652). Gold grade reaches peak values where the carbonate-phyllitic assemblage commences (~4–5 g/t; Figure 6b). It decreases outward to modest levels (0.1–0.6 g/t) except along minor faults and dike contacts, which remain at elevated grade (~1–3 g/t). Chalcopyrite is present in trace amounts within the dominant pyrite, where it hosts gold. In the MBX zone, carbonate-phyllitic alteration overprints the upper margin of the Rainbow dike beyond ~230 m from the stock. It follows the Lower Trachyte for at least 90 m, where Cu-sulphosalt replacement of chalcopyrite is observed in ankerite veins.

Outer-propylitic alteration (epidote-chlorite-pyrite) is peripheral to all other alteration stages in the MBX and 66 zones (Figure 3b) but also cuts across the earlier assemblages along permeable horizons. Much of the lower DWBX zone is overprinted by the outer-propylitic stage, reflecting an abundance of permeable volcanic-conglomerate as hostrock. Gold grade is moderate to weak and Cu is insignificant (Figure 6a–c).

A deposit-wide pyrite halo (Sketchley et al., 1995; Oldenberg et al., 1997) is associated with peripheral sodic-calcic, inner- and outer-propylitic, and carbonate-phyllitic assemblages where pyrite abundance is typically 1–5 modal % (Figure 6d, e).

Lateral and Vertical Zonation

The Cu-Au ore zone coincides with chalcopyrite-pyrite- and magnetite-bearing potassic alteration in the MBX stock and basaltic trachyandesite hostrock. The magnetite-associated inner calcopotassic shell extends ~130 m outward from the stock margin and abruptly terminates within the sodic-calcic zone. Biotite alteration continues another ~150 m into the hostrock but is overprinted by the sodic-calcic (~100–150 m from the stock margin), inner-propylitic (~150–220 m) and outer-propylitic assemblages

(>220 m). Biotite also shows little compositional variation within the deposit (DeLong, 1996).

In the 66 zone, the Upper Trachyte hosts a magnetite-bearing Cu-mineralized calcopotassic assemblage, which is surrounded by sodic-calcic and inner- and outer-propylitic assemblages with increasing depth (Figure 2b). Dolomite-ankerite replacement of mafic phases characterizes the Upper Trachyte but increases in intensity to the southeast, forming a funnel-shaped body of carbonate-phyllitic alteration in the hostrock.

Conclusions

The highly faulted, Early Jurassic Mount Milligan alkalic porphyry Cu-Au deposit is tilted, providing an oblique cross-section through an alkalic porphyry system. Potassic alteration defines the core and appears to pass upward into a carbonate-phyllitic alteration assemblage. Laterally, the magmatic plume marked by the potassic and calcopotassic alteration is fringed by sodic-calcic and finally the inner- and outer-propylitic assemblages. The critical element enabling the reconstruction of the vertical alteration was the recognition of the repetition of potassic alteration immediately above the Rainbow fault in the lower levels of the 66 zone.

Acknowledgments

Support for the porphyry component of the project derives from the following companies and organizations, and their financial and logistical support is gratefully acknowledged: Geoscience BC, Natural Sciences and Engineering Research Council of Canada, AngloGold Ashanti Ltd., Amarc Resources Ltd., Barrick Gold Corporation, Imperial Metals Corporation, Lysander Resources Ltd., Newcrest Mining Limited, Newmont Mining Corporation, NovaGold Resources Inc. and Teck Cominco Limited. The authors are particularly indebted to Terrane Metals Corp. for their logistical support and scientific collaboration.

Mineral Deposit Research Unit (MDRU) contribution 229.

References

- Barr, D.A., Fox, P.E., Northcote, K.E. and Preto, V.A. (1976): The alkaline suite of porphyry copper deposits—a summary; in *Porphyry Deposits of the Canadian Cordillera*, A. Sutherland Brown (ed.), Canadian Institute of Mining and Metallurgy, Special Volume 25, p. 359–367.
- Barrie, C.T. (1993): Petrochemistry of shoshonitic rocks associated with porphyry copper-gold deposits of central Quesnellia, British Columbia, Canada; *Journal of Geochemical Exploration*, v. 48, p. 225–258.
- DeLong, R.C. (1996): Geology, alteration, mineralization and metal zonation of the Mt. Milligan porphyry copper-gold deposits; M.Sc. thesis, University of British Columbia, 121 p.

- Delong, R.C., Godwin, C.I., Harris, M.W., Cairn, N.M. and Rebagliati, C.M. (1991): Geology and alteration at the Mount Milligan gold-copper porphyry deposit, central British Columbia; in *Geological Fieldwork 1990*, BC Ministry of Energy, Mines and Petroleum Resources, Paper 1991-1, p. 199–206.
- Jago, C.P. (2008): Metal- and alteration-zoning, and hydrothermal flow paths at the moderately-tilted, silica-saturated Mt. Milligan Cu-Au alkalic porphyry deposit; M.Sc. thesis, University of British Columbia, Vancouver, BC, 210 p.
- Jago, P., Tosdal, R. and Chamberlain, C. (2007): Mt. Milligan—an exemplary Cu-Au alkalic porphyry system; Arizona Geological Society meeting, *Ores & Orogenesis*, Program with Abstracts, p. 166–167.
- Jenks, G.F. and Caspall, F.C. (1971): Error on choroplethic maps: definition, measurement, reduction; *Annals of the Association of American Geographers*, v. 61, p. 217–244.
- Lang, J.R. (1992): Mount Milligan geochemistry; Mineral Deposit Research Unit (MDRU), Porphyry Cu-Au Project, Year 1, Section 7, p. 2–49.
- Lang, J.R., Lueck, B., Mortensen, J.K., Russell, J.K., Stanley, C.R. and Thompson, J.F.H. (1995): Triassic–Jurassic silica-undersaturated and silica-saturated alkalic intrusions in the Cordillera of British Columbia: implications for arc magmatism; *Geology*, v. 23, p. 451–454.
- Mihalynuk, M.G., Nelson, J. and Diakow, L.J. (1994): Cache Creek terrane entrapment: oroclinal paradox within the Canadian Cordillera; *Tectonics*, v. 13, p. 575–595.
- Mortensen, J.K., Ghosh, D.K. and Ferri, F. (1995): U-Pb geochronology of intrusive rocks associated with copper-gold porphyry deposits in the Canadian Cordillera; in *Porphyry Deposits of the Northwestern Cordillera of North America*, T.G. Schroeter (ed.), Canadian Institute of Mining and Metallurgy, Special Volume 46, p. 142–158.
- Mortimer, N. (1987): The Nicola Group: Late Triassic and Early Jurassic subduction-related volcanism in British Columbia; *Canadian Journal of Earth Sciences*, v. 24, p. 2521–2536.
- Nelson, J.L. and Bellefontaine, K.A. (1996): The geology and mineral deposits of north-central Quesnellia: Tezzeron Lake to Discovery Creek, Central British Columbia; BC Ministry of Energy, Mines, and Petroleum Resources, Bulletin 99, p. 100.
- Nelson, J.L., Bellefontaine, K., Rees, C. and MacLean, M. (1992): Regional geological mapping in the Nation Lakes area; in *Geological Fieldwork 1991*, BC Ministry of Energy, Mines, and Petroleum Resources, Paper 1992-1, p. 103–118.
- Oldenberg, D.W., Li, Y. and Ellis, R.G. (1997): Inversion of geophysical data over a copper gold porphyry deposit: a case history for Mt. Milligan; *Geophysics*, v. 62, p. 1419–1431.
- Rebagliati, C.M. (1988): Mt. Milligan property assessment report, Omineca Mining Division NTS 93/1, latitude 55°08' N, longitude 124°04' W; unpublished report prepared for United Lincoln Resources Inc.
- Sketchley, D.A., Rebagliati, C.M. and Delong, C. (1995): Geology, alteration and zoning patterns of the Mt. Milligan copper-gold deposit; in *Porphyry Deposits of the Northwestern Cordillera of North America*, T.G. Schroeter (ed.), Canadian Institute of Mining and Metallurgy, Special Volume 46, p. 650–665.
- Terrane Metals Corp. (2007): New Mt. Milligan resource estimate 1.9 billion lb. copper and 5.5 million oz. gold; Terrane Metals Corp., press release, August 21, 2007, URL <<http://www.terrane.com/s/NewsReleases.asp>> [November 10, 2008].

Investigations of Orogenic Gold Deposits in the Cariboo Gold District, East-Central British Columbia (Parts of NTS 093A, H): Progress Report

D.A. Rhys, Panterra Geoservices Inc., Surrey, BC

J.K. Mortensen, University of British Columbia, Vancouver, BC, jmortensen@eos.ubc.ca

K. Ross, Panterra Geoservices Inc., Surrey, BC

Rhys, D.A., Mortensen, J.K. and Ross, K. (2009): Investigations of orogenic gold deposits in the Cariboo gold district, east-central British Columbia (parts of NTS 093A, H): progress report; *in* Geoscience BC Summary of Activities 2008, Geoscience BC, Report 2009-1, p. 49–74.

Introduction

The famous Cariboo Au rush in east-central BC was triggered by the discovery of rich placer-Au deposits on several creeks in the Likely and Wells-Barkerville areas (Figure 1) between 1859 and 1862. This area has subsequently yielded an estimated 2.5 to 3 million ounces (80–96 tonnes) of placer Au (e.g., Levson and Giles, 1993), roughly half of BC's total historic placer-Au production. Gold-bearing orogenic gold-quartz veins and associated pyritic replacement deposits in metamorphic rocks of the Barkerville terrane were discovered soon after placer mining began and have produced approximately 1.2 million ounces (38.3 tonnes) of Au since that time. Lode-Au exploration continues in both the Wells-Barkerville area and structurally higher rock units of the Quesnel terrane farther to the south and west, where the Spanish Mountain and Frasersgold deposits occur (Figure 1). Together with the Wells-Barkerville area, the Spanish Mountain and Frasersgold deposits, and several other areas of Au prospects along and adjacent to placer-Au-bearing creeks in both the Barkerville and Quesnel terranes define the Cariboo Au district (CGD), which includes much of the central and northwestern parts of the 093A map sheet, as well as the southwestern part of the 093H map sheet (Figure 1).

Although individual deposits of the Quesnel terrane differ in character from those in the Barkerville terrane, much of the Au in each of these terranes is contained within quartz-carbonate veins of broadly 'orogenic' vein type (Goldfarb et al., 2005) that are comparable in style and structural timing. In several deposits in these areas, however, older styles of pyritic and quartz-pyrite mineralization that predate

these late orogenic veins are developed in close association with the later veins, suggesting mineralization was a protracted or multiphase process. Despite exciting new discoveries that have been made throughout the Cariboo Au district over the past two decades, very limited recent research has been done directly on the deposits in the area.

This report documents the initial results of a one-year, reconnaissance-level study of lode-Au mineralization and potential of the CGD (Figure 1), which began in 2008. The main goals of the study are to provide constraints on the age(s) and structural controls on mineralization in different parts of the CGD. This is being achieved through a synthesis of previous work in the region combined with focused structural, geochronological and Pb isotopic studies of some of the main lode-Au occurrences in the belt. The objective of this work is to improve the understanding of some key aspects of the geology and Au metallogeny of the CGD, providing guidelines to the future exploration of the district and enabling comparisons to other similar Au districts globally.

Regional Geological Framework

The CGD is underlain by parts of four main terranes (Figure 1). Bedrock in most of the northern and eastern parts of the area comprises middle-greenschist- to lower-amphibolite-grade, polydeformed metamorphic rocks of the Barkerville terrane (the northern extension of the Kootenay terrane) and the structurally overlying Cariboo terrane, which are juxtaposed along the northeast-dipping Pleasant Valley thrust fault (Struik, 1987, 1988). The Barkerville and Cariboo terranes are 'pericratonic' in character, comprising mainly metamorphosed equivalents of continent-derived siliciclastic protoliths with interlayered marble units and granitic orthogneiss, and are thought to have formed in close proximity to the western margin of Laurentia. Structurally overlying both the Barkerville and Cariboo terranes in the northern part of the area are mafic volcanic rocks and associated pelagic sedimentary units of the oceanic Antler allochthon, which forms part of the Slide

Keywords: Cariboo gold district, Barkerville terrane, orogenic Au, vein, replacement, intrusion, Ar/Ar geochronology, Pb isotopes

This publication is also available, free of charge, as colour digital files in Adobe Acrobat® PDF format from the Geoscience BC website: <http://www.geosciencebc.com/s/DataReleases.asp>.

Mountain terrane. The southwestern margin of the Barkerville terrane is structurally overlain along the Eureka thrust by much less deformed and less metamorphosed volcanic and sedimentary strata of the Quesnel terrane, which in this area consists of mainly Middle–Late Triassic volcanic rocks and phyllitic siliciclastic units. The Crooked amphibolite (Figure 1) occurs as a discontinuous, strongly deformed and metamorphosed lens of mafic metavolcanic rocks and minor serpentinite along the Eureka thrust between the Quesnel terrane and the underlying Barkerville terrane. The nature and terrane affiliation of the Crooked amphibolite is uncertain, with some workers interpreting it to be either a basal unit of the Quesnel terrane (e.g., Bloodgood, 1992; Panteleyev et al., 1996), whereas others consider it to be a thrust-bounded slice of the Slide Mountain terrane that is sandwiched between the underlying Barkerville terrane and the base of the Quesnel terrane (e.g., Ash, 2001; Ray et al., 2001; Ferri and Schiarizza, 2006). Other isolated klippe of mafic metavolcanic rocks of uncertain terrane affiliation overlie Barkerville terrane metamorphic rocks on Hardscrabble Mountain and Island Mountain (Struik, 1988; Ferri and Schiarizza, 2006).

The Quesnel terrane in this area mainly comprises a package of weakly deformed, variably phyllitic, carbonaceous siliciclastic rocks (locally termed the ‘black phyllite’ by Rees, 1987; equivalent to the ‘black pelite succession’ of Logan, 2008) with minor mafic volcanic and volcanoclastic interlayers. This lower, dominantly metaclastic package is overlain along the Spanish thrust (Struik, 1988; Logan, 2008) by mafic to intermediate volcanic rocks assigned to the Late Triassic Nicola Group. The sedimentary package has yielded Middle–Late Triassic fossil ages (Bloodgood, 1992; Panteleyev et al., 1996).

Several suites and ages of intrusive rocks are present in the Wells-Barkerville area and adjoining portions of the Barkerville terrane. Strongly deformed granitic to granodioritic orthogneiss bodies occur in several localities, particularly in the vicinity of Quesnel Lake and east of Eureka Peak (Figure 1). Several of these intrusions have yielded early Mississippian U-Pb zircon crystallization ages (Mortensen et al., 1987; Ferri et al., 1999). Variably

foliated metadiorite occurs as small, widespread but volumetrically minor sills, dikes and irregular bodies within the Snowshoe Group of the Barkerville terrane (Struik, 1988; Schiarizza and Ferri, 2003). In rare instances, the metadiorite forms sills up to several hundred metres in thickness. Pickett (2001) and Ray et al. (2001) describe dioritic intrusive rocks in drillcore in the Island Mountain and Mosquito Creek areas, respectively, that may belong to this intrusive suite. Samples of diorite from two localities near Barkerville and one in the Keithley Creek area approximately 30 km to the southeast have given Early Permian U-Pb zircon crystallization ages of 277–281 Ma (Ferri and Friedman, 2002). In the Wells-Barkerville area, several small, strongly altered, foliated felsic bodies termed the Proserpine intrusions have been documented, which appear to have been emplaced prior to the D₂ folding (Struik, 1988; Schiarizza and Ferri, 2003). Younger, rare, locally quartz-phyric rhyolite dikes that appear to be post-tectonic

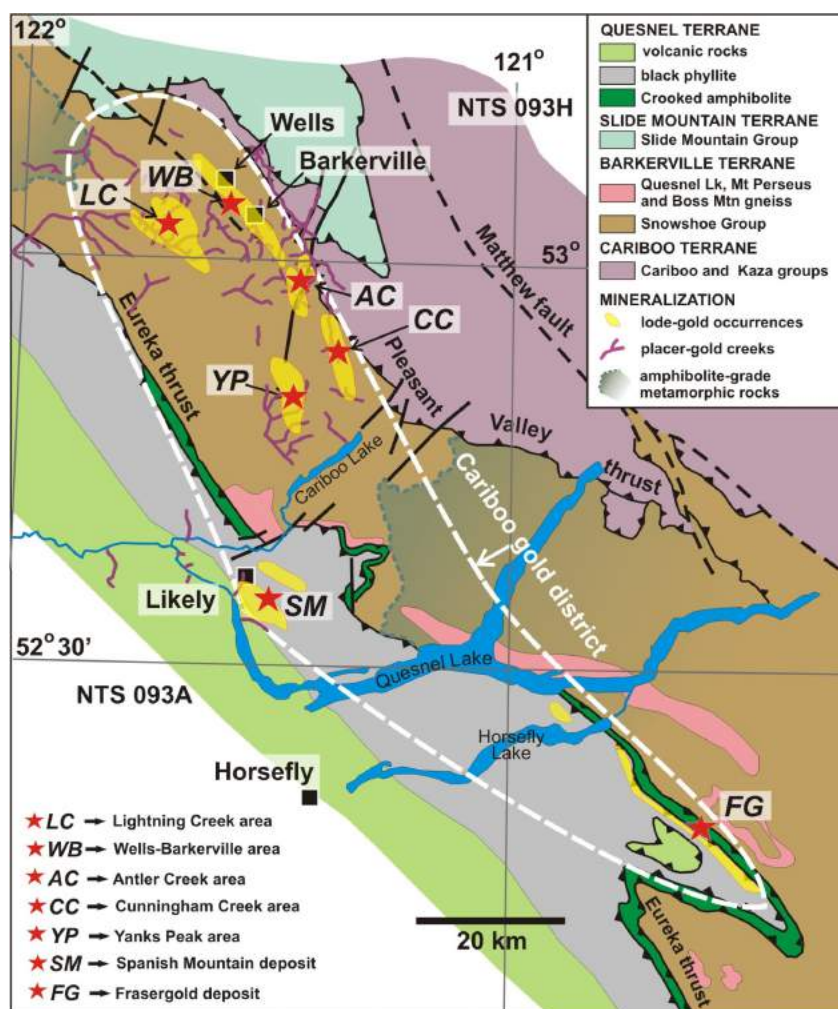


Figure 1: Regional geological setting of the Cariboo Au district, showing principal terranes and major lithological packages. Areas of known lode-Au occurrences are shaded in yellow, and placer-Au-producing creeks are indicated by thick purple lines. Principal known Au-producing areas in the Barkerville terrane are in areas of greenschist-grade metamorphism and do not extend into amphibolite-grade domains.

(Holland, 1954; Struik, 1988) and relatively fresh lamprophyre dikes have also been mapped in several localities in the eastern Barkerville terrane area by Struik (1988) and Termuende (1990). No isotopic age constraints are currently available for the Proserpine intrusions or for the rhyolite or lamprophyre dikes.

Within the black phyllite succession of the Quesnel terrane, several small intrusions that have been mapped southeast of Quesnel Lake range from diorite, monzonite and syenite in composition and are probably Late Triassic to Early Jurassic in age (Panteleyev et al., 1996).

Metamorphic rocks in the CGD record several distinct phases of deformation and metamorphism. Regionally, most workers recognize two dominant syn- to postaccretionary phases of deformation that affect rocks in both the Quesnel and Barkerville terranes, broadly termed phase 1 and phase 2 by previous workers (e.g., Panteleyev et al., 1996; Schiarizza and Ferri, 2003; Ferri and Schiarizza, 2006). Pre-accretionary older fabrics have also been recognized locally in the Barkerville terrane, but are overprinted by the later phase 1 and phase 2 events. Phase 1 structures (generally the earliest recognizable fabrics, termed D_1 here) produced a penetrative slaty to phyllitic cleavage (S_1) that is axial planar to generally east- to northeast-verging, tight to isoclinal, generally northwest-trending F_1 folds and shear zones. The phase 1 (D_1) event is generally thought to be associated with the emplacement of the Nicola Group rocks in the Quesnel terrane onto the Barkerville terrane along the Eureka thrust (Rees, 1987; Bloodgood, 1987, 1992; Panteleyev et al., 1996; Ferri and Schiarizza, 2006). The phase 1 event was accompanied by, and was locally outlasted by peak regional metamorphism. Phase 2 structures (D_2) regionally include the Eureka Peak syncline (Figure 1), which openly refolds both the earlier S_1 foliation and associated folds and the D_1 Eureka thrust (Bloodgood, 1992). The D_2 structures are associated with development of a secondary, locally dominant crenulation cleavage (S_2), which is axial planar to the Eureka syncline and other phase 2 folds (F_2 ; Bloodgood, 1987, 1992). An intense, shallowly northwest-plunging composite intersection and elongation lineation (L_2) occurs at the intersection of S_2 and older S_1 foliation, and is parallel to F_2 fold axes. The long axes of many Au-bearing zones in the area are parallel to L_2 , and extensional veins related to many Au deposits in the area are approximately orthogonal to L_2 . Late north- to northeast-trending crenulation cleavage and kink bands form later, retrograde low-strain events regionally.

In the Barkerville terrane, second-phase (F_2) folds form extensive, recumbent and southwest-verging nappe structures that have amplitudes of approximately 25 km (Ferri and Schiarizza, 2006). These result in the overturning of large portions of the Barkerville terrane stratigraphy. They, in turn, are affected by the Lightning Creek anticline and an

open, northwest-trending upright fold that runs through central portions of the Barkerville terrane, and to which late (S_3) crenulation cleavage is axial planar.

Structurally late northerly to north-northeasterly trending, right-lateral (dextral) faults occur throughout the CGD, extending across and offsetting lithological contacts including major thrust surfaces associated with terrane boundaries. These faults have a protracted structural history, locally displaying early semibrittle fabrics, with widespread later brittle displacements along clay gouge seams. These structures are often spatially associated with late gold-quartz veins that are widespread throughout the district.

Absolute age constraints on the timing of the various metamorphic and structural events that have affected the Barkerville and Quesnel terranes prior to this study were very limited. Peak metamorphism is thought to have occurred at approximately 174 ± 4 Ma, based on a U-Pb age for metamorphic titanite from near Quesnel Lake (Mortensen et al., 1987). Andrew et al. (1983) reported a similar K-Ar whole-rock age of 179 ± 8 Ma for phyllite at the Cariboo Gold Quartz mine. Potassium-argon ages of 141 ± 5 Ma (Andrew et al., 1983) and 139 ± 5 Ma (Alldrick, 1983) have been reported for sericite associated with mineralized quartz veins at the Cariboo Gold Quartz and Mosquito Creek mines, respectively. An essential aspect of understanding the relative timing and controls on Au mineralization throughout the CGD district is whether the different-phased fabrics associated with the principal deformation events and metamorphism summarized above are correlative throughout the region, especially across terrane boundaries. Since the principal fabrics across the region are syn- to postaccretionary in timing, and foliations and associated folds can be traced continuously across the region with similar relative ages, styles and orientations, the sequence of regional deformation is considered here to be correlative between the Quesnel and Barkerville terranes, although absolute ages of each event could vary locally both between and within individual terranes if deformation was transgressive across the area. Ongoing geochronology associated with this study should help to provide further constraints.

Field and Analytical Studies from 2008

Our fieldwork in the CGD included detailed field examination of lode-Au occurrences and collection of an extensive suite of samples for petrographic, dating and geochemical studies. Systematic surface mapping of the Spanish Mountain deposit area in conjunction with drillcore review was also undertaken during the fieldwork program to further understand the setting and controls on mineralization there. A substantial amount of $^{40}\text{Ar}/^{39}\text{Ar}$ dating has now been completed from the Wells-Barkerville area as part of this

study, and four U-Pb zircon ages have also been determined for samples from the Spanish Mountain area. In addition, a number of sulphide samples from the Wells-Barkerville area have been analyzed for Pb isotopic compositions. Results of field studies in the principal field areas that were examined are summarized below in the context of previously published and unpublished work, together with a preliminary interpretation of the results of the new dating and isotopic studies. Additional geochronological, isotopic and petrographic work is currently underway and will be synthesized in future publications.

Lode-Au Deposits in the Barkerville Terrane

The Barkerville terrane hosts the highest frequency of lode-Au occurrences in, and records most of the historical lode Au and placer production from, the CGD. Known lode-Au occurrences are most abundant over an approximately 50 km strike length from Cariboo Lake in the northwest to several kilometres northwest of Wells (Figure 1). Within this area, mineralization occurs in two parallel north-northwest-oriented trends:

The first trend is located along the northeastern margin of the Barkerville terrane, extending from the Wells-Barkerville area southeastwards through prospects on Antler and then Cunningham creeks (Figure 1).

The second trend lies approximately 10 km to the west-southwest of the above trend in central portions of the Barkerville terrane, and comprises two clusters of lode-Au deposits: the Lightning Creek area in the north and Yanks Peak area to the southeast (Figure 1). Although few Au occurrences are reported between these two areas, numerous quartz veins and vein systems are visible on ridgetops between them.

Principal placer-producing creeks are spatially associated with, or drain the ridges in these trends (Figure 1), suggesting that much of the placer Au is locally sourced. The termination of these mineralized trends before the intersection of the biotite isograd to the southeast of Cariboo Lake and to the west-northwest of Wells (Figure 1) suggests that the associated vein systems may be preferentially localized in lower-greenschist-grade rocks (Struik, 1988). These trends may correspond to structural corridors formed by high-strain zones or faults in the region, within which additional local lithological and structural controls may have focused mineralization.

Wells-Barkerville Area, Barkerville Terrane

The Wells-Barkerville area is by far the most important Au-producing camp within the CGD, having been the source of virtually all historical lode-Au production and much of the placer production from the district (Hall, 1999). Lode-Au production in the camp has come from the Cariboo Gold Quartz (093H 019), Island Mountain (093H 019) and Mosquito Creek (093H 025) mines, which collectively de-

fine a single, shallow northwest-plunging mineralizing system that is developed over a 4.5 km strike length, from which 1.23 million ounces of Au have been produced (Hall, 1999). Gold mineralization exhibits both strong structural and stratigraphic control, and is developed mainly within 150 m of the northeast-dipping contact between interbedded quartzite, sericite, phyllite and limestone of the Downey succession to the northeast ('Baker' unit in mine terminology), and carbonaceous metaturbiditic rocks of the Hardscrabble succession to the southwest ('Rainbow' unit). Showings and deposits continue for another 10 km to the southeast from the Cariboo Gold Quartz mine in the same stratigraphic position (e.g., Warspite, Hard Cash, Antler Mountain; Figure 1; Sutherland Brown, 1957). Mineralization is of two varieties, replacement and vein mineralization, which occur together within a broad zone of diffuse iron-carbonate-sericite alteration and high D₂ strain (Skerl, 1948; Sutherland Brown, 1957; Hall, 1999; Rhys and Ross, 2001).

Replacement Mineralization

Replacement mineralization comprises multiple small (500–40 000 tonnes), manto-like, folded, northwest-plunging, rod-shaped bodies of massive, fine-grained pyrite+iron-carbonate+quartz that replace limestone bands within 25 m of the structural base of the Downey (Baker unit) succession in the Island Mountain and Mosquito Creek mines in northwestern portions of the camp (Benedict, 1945; Alldrick, 1983; Robert and Taylor, 1989). Approximately 32% of lode production from the camp was from this mineralization type (Hall, 1999). Ore shoots plunge parallel to the axes of, and are spatially associated with the hinge zones of mesoscopic D₂ folds, at least locally where they are intersected by northeast-dipping S₂-parallel thrust surfaces in zones of higher strain. The pyrite bodies contain coarse-grained dolomite, pyrite and arsenopyrite on their margins (Figure 2a), and are often enveloped by sericite±iron-carbonate/dolomite±fuchsite alteration or silicification, both of which replace the host limestone outward from the pyrite mineralization. Mineralization is commonly banded, with alternating pyrite and carbonate-dominant bands (Figure 2b). Highest Au grades are associated with fine-grained pyrite within which Au occurs as grains along crystal boundaries and fractures.

Replacement mineralization of similar character at the Bonanza Ledge zone (093H 140) occurs 2.25 km to the southeast of the Cariboo Gold Quartz–Mosquito system (Rhys and Ross, 2001; Yin and Daignault, 2007). However, the Bonanza Ledge zone is hosted by, and replaces thinly bedded metaturbidites of the Hardscrabble succession that are approximately 500 m structurally lower than the Rainbow-Baker contact area, which hosts replacement mineralization in the Mosquito and Island Mountain mines. This suggests the potential for stratabound mineralization in other

parts of the local stratigraphy. Mineralization in the Bonanza Ledge zone occurs in discrete areas of massive, banded and veinlet pyrite within a 20–100 m wide zone of intense sericite–iron–magnesium–carbonate–pyrite alteration. High-grade mineralization (5–80 g/t Au) occurs in areas locally more than 30 m thick comprising 10–70% pyrite (Figure 2c) in a gangue of muscovite, dolomite–ankerite and quartz, forming at least two crudely shallowly-plunging zones. Gold occurs as 2.5–60 µm native grains on fractures or grain boundaries in pyrite with galena and chalcopyrite, or encapsulated in pyrite. Sheeted pale grey veins and silicification occur peripheral to the alteration zone. Gold-bearing zones grade laterally and vertically into sets of non-gold-bearing pyrite–pyrrhotite–chlorite–iron–carbonate veinlets in mauve sericite±albite±chlorite alteration (Figure 2d).

Quartz Vein Mineralization

At least two stages of quartz veining occur in the district, comprising an early, poorly mineralized and deformed set

of veins that are cut by later Au-bearing, late-tectonic quartz–carbonate–pyrite veins. The early veins are moderately northeast-dipping, variably deformed quartz±gold–carbonate±muscovite veins that are commonly developed in all three of the principal Wells area mines (Rhys and Ross, 2001). They are characterized by silvery to white muscovite as aggregates and networks in the quartz, as well as blebby, coarse iron–carbonate aggregates, and often have green to silver muscovite alteration envelopes. They are generally low in pyrite content, but pyrite clots occur in some larger veins. The veins range up to 1 m thick, are boudinaged and folded, laterally discontinuous along strike and affected by most or all D₂ strain (Figure 3). These veins contain only background or low (<2 g/t) Au concentrations. In some locations, veins of this type form several generations, which display a gradation in strain state and mineralogy. Although lacking significant Au and predating main-stage quartz veining, they are localized along the same corridor as the later Au-bearing veins and also extend into basal portions of the Baker unit to the northeast. These dif-

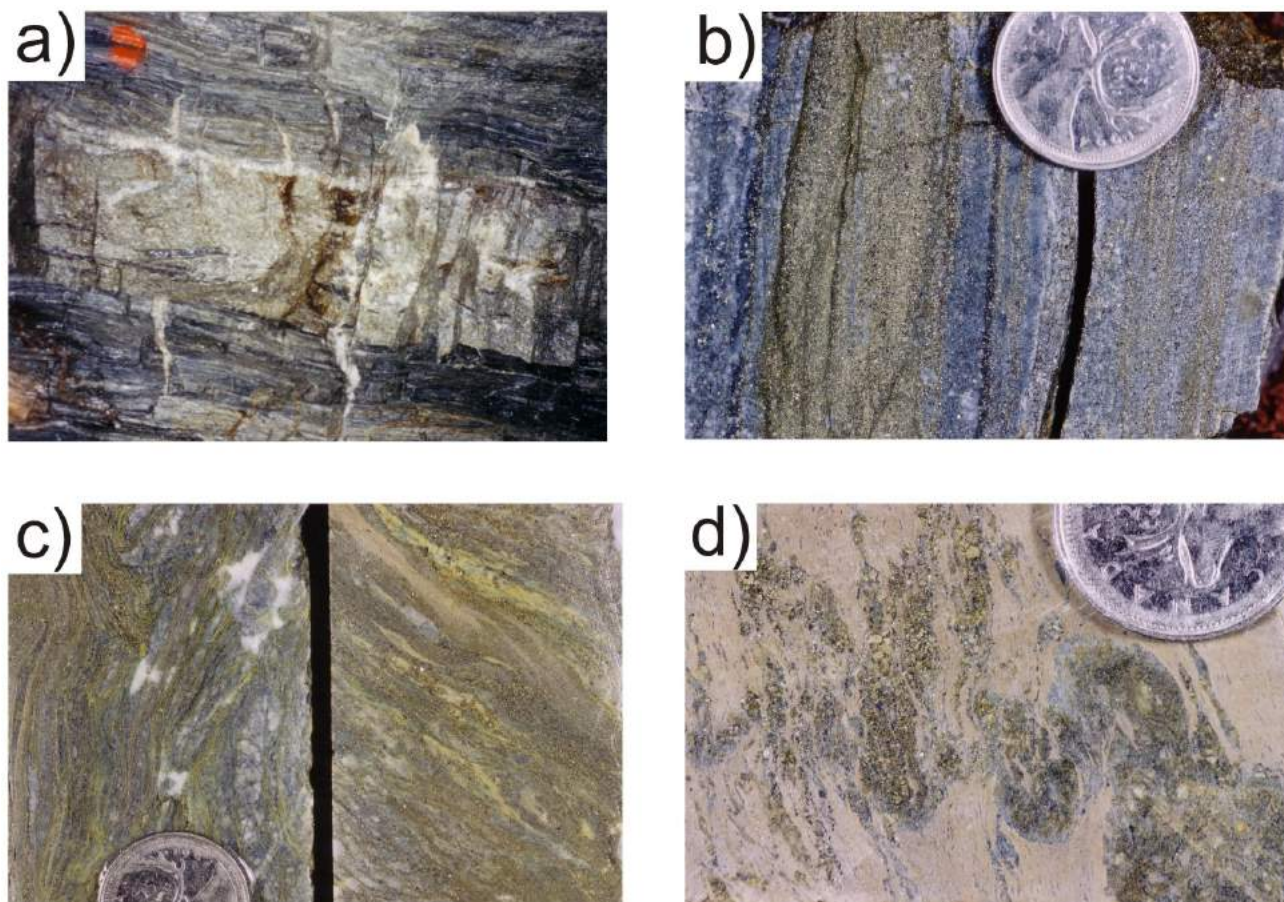


Figure 2: Style of replacement mineralization in the Wells-Barkerville area: **a)** band of pyrite replacement mineralization in the foliated limestone of the Baker unit, 4400 level, Mosquito Creek mine; field of view 2 m; note pale peripheral quartz–carbonate margins to the pyrite and the steeply dipping, northeast-trending quartz extensional veinlets that emanate off the replacement zone; **b)** detail of fine-grained, banded pyritic replacement mineralization in blue-grey dolomitized limestone from the Mosquito mine, 4400 level; **c)** typical replacement-style pyritic mineralization from the Bonanza Ledge zone, showing fine-grained pervasively disseminated pyrite lamina and bands that alternate with dolomitic (left) and tan sericite altered (right) matrix; the protolith was calcareous siltstone (left) and mudstone (right); **d)** Purple-grey peripheral sericite alteration to the Bonanza Ledge zone containing ptymatically folded pyrite-pyrrhotite veinlets.

fer from the younger, northwest-trending Au-bearing ‘strike’ veins such as the BC vein, although previous workers have often included them in that set. Relative timing relationships between these older deformed quartz veins and replacement mineralization was not established in the field.

In contrast, main-stage quartz veins associated with Au mineralization are structurally late and postdate all D_1 and much or all D_2 strain in the region. They have been the source of approximately 68% of the lode-Au production in the Wells-Barkerville area (Hall, 1999), comprising almost all of the Au production from the Cariboo Gold Quartz mine and a significant amount from the other two mines. Although individual veins are discordant to stratigraphy, the vein systems as a whole are stratabound and generally confined to 150–250 m of stratigraphy within grey pelitic to psammitic phyllite of the Rainbow unit over the entire >4 km length of the system. The favourable portions of the Rainbow unit lie immediately adjacent to, and to the southwest of the Rainbow-Baker contact area where replacement mineralization is developed, and veins frequently extend up to or into the same horizons as the replacement mineralization (Skerl, 1948).

The Au-bearing veins comprise east-trending, steeply dipping, low displacement sinistral shear veins (‘diagonal’ veins; Figures 4a, b, 5b) with strike lengths of 20–150 m and coeval, sheeted sets of northeast-trending extensional veins (‘orthogonal’ or ‘transverse’ veins; Figures 4c, 5a) that together form complex vein arrays (Skerl, 1948; Sutherland Brown, 1957). Veins consist of white quartz+pyrite with iron-carbonate±muscovite selvages and pyritic cores that often display a two-stage paragenesis from early fibrous carbonate-quartz to younger massive quartz-pyrite in vein cores (Figure 4d). Scheelite and fuchsite are local accessory minerals, and native gold occurs in association with pyrite and locally cosalite and bismuthinite (Skerl, 1948). Extensional transverse veins commonly



Figure 3: Folded early quartz-carbonate vein with muscovite envelopes, Mosquito mine, 4400 level. The vein is within the lower portions of the Baker limestone. Field of view is 1.2 m, and view is southwest of drift wall.

contain quartz-carbonate fibres aligned perpendicular to vein walls, consistent with dominantly or nearly pure extensional opening (Figure 4d). Adjacent to replacement mineralization, the veins typically cut across it, although in some locations extensional veins may emanate off the margins of pyrite replacement zones (Figure 2a).

The diagonal veins are commonly distributed en échelon along the favourable Rainbow stratigraphic horizons, and may be linked by, or terminate in horsetail-like arrays of extensional veins. The structural style of veins is dominantly brittle, but local stylolitic pressure-solution seams, sinistral shear bands and sigmoidal shapes to extensional veins support local semibrittle behaviour during vein formation (Figure 4a, b). The most concentrated zones of veining are developed mainly in the Rainbow 1 unit (grey, fine-grained metaturbidite) where north-trending, east-dipping, late- D_2 dextral faults cross the stratigraphy, defining individual mineralized zones of multiple veins that are named after the corresponding faults. Although the veins postdate most D_2 strain and cut across F_2 fold closures, they are kinematically consistent with formation in response to northeast-directed D_2 shortening, and extensional (diagonal) veins in this set are generally oriented orthogonal to the L_2 lineation (Figure 4c), suggesting that they formed in response to extensional opening parallel to L_2 , collectively suggesting a late- D_2 timing. Associated north-trending dextral faults may also contain veining and Au mineralization (Richards, 1948), although the faults have typically seen much later brittle displacement that disrupts the veining and has formed significant clay gouge.

A third type of Au-bearing quartz vein is the ‘strike’ or ‘A’ vein type, which are more continuous, fault-hosted, northwest-trending and steeply northeast-dipping shear veins (Johnston and Uglow, 1926; Sutherland Brown, 1957). Although not common in the main mine trend, the best examples of this style of veining occur to the southeast of the Cariboo Gold Quartz mine near the Bonanza Ledge zone. The largest vein of this type is the BC vein, which has been traced in outcrop and drilling for 800 m, is locally >30 m thick (Figure 6) and is localized in a carbonaceous phyllite termed the BC unit, which lies approximately 500 m southwest of the Rainbow-Baker contact. Several shallowly northwest-plunging pyritic ore shoots were historically mined from the vein from underground workings connected to the Cariboo Gold Quartz mine. Timing relationships are similar to other Au-bearing veins in the district, with a late timing indicated by its planar nature, and the presence of brecciated wallrock fragments within it that contain rotated S_1 and S_2 foliations, indicating that vein formation continued to late during or after D_2 , since D_2 fabrics are affected. The BC vein, like other Au-bearing veins in the district, is spatially associated with older, folded replacement mineralization. The Bonanza Ledge zone occurs

between, immediately within, and for up to 50 m into its footwall.

Relationships between Mineralization Types and their Potential Controls

A block model illustrating vein relationships and kinematics of principal Au-bearing veins in the Wells-Barkerville area is illustrated in Figure 5b. Diagonal, sinistral shear veins may be conjugate to the north-trending faults. Transverse extensional veins are developed at a high angle to the northwest-plunging L_2 elongation lineation and probably

formed due to extension parallel to L_2 . Together, the kinematics, orientations and strain states of the veins and faults suggest that all of these structures formed during inclined northeast-directed shortening, potentially late during D_2 . The common occurrence of older deformed quartz veins along the same structural northwest-trending corridors as the Au-bearing veins suggest that the Au-bearing veins represent the culmination of a sequence of quartz veining that may have occurred sporadically during regional D_2 deformation, but until the latter stages was not significantly Au bearing.

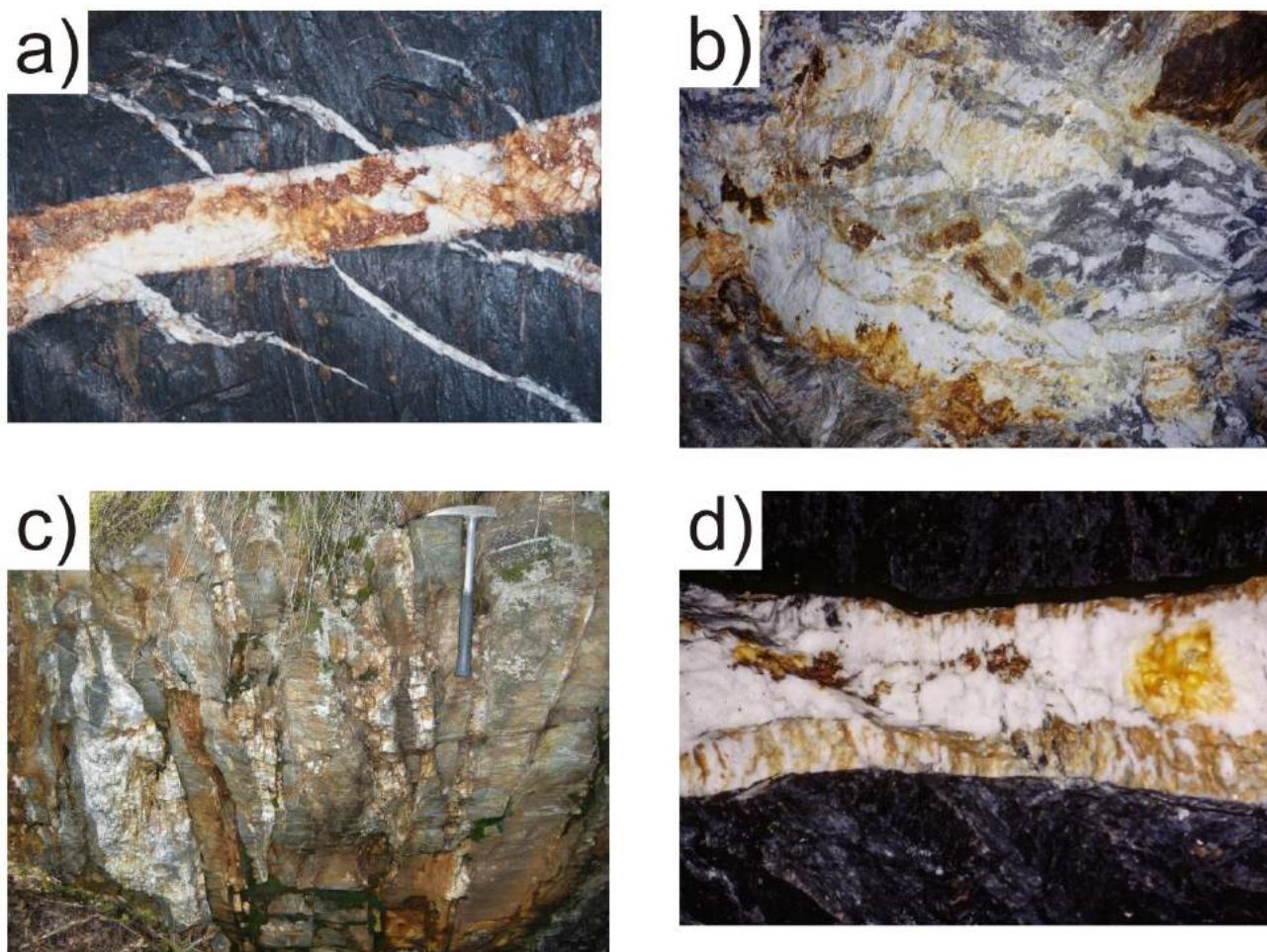


Figure 4: Main-stage Au-bearing quartz vein systems in the Wells-Barkerville area: **a)** east-northeast-trending quartz vein in intermediate orientation between diagonal and transverse vein orientation contains clots of coarse, partially oxidized pyrite, and is obliquely joined by north-northeast-trending extensional veins; angular relationships between the two vein types suggest that the extensional veinlets formed in response to a minor component of sinistral displacement on the principal vein; note that since this is a view up at the back, the apparent shear sense is reversed; field of view = 2 m, Cariboo Gold Quartz mine 1200 level; **b)** mineralized quartz-pyrite fault-fill, east-trending diagonal vein, Mosquito Creek mine, 4400 level; the vein is approximately 0.8 m thick; discrete slip surfaces with pyritic pressure-solution seams disrupt vein surfaces internally and synthetic shear bands oblique to the shear vein walls record an apparent sinistral shear sense; note that the view is up at the back so apparent shear-sense indicators are reversed; the grey banding in the vein is pyrite; **c)** sheeted north-east-trending quartz+pyrite+iron-carbonate extensional veins on the southeast side of Williams Creek at the Blackjack prospect near Barkerville; view is to the northeast; note the shallowly northwest-plunging L_2 lineation on the foliation surfaces (dips shallowly to left) to which the veins are nearly orthogonal; rusty carbonate-pyrite alteration affects the phyllitic wallrocks; hammer for scale; **d)** northeast-trending extensional ('transverse') vein in the Cariboo Gold Quartz mine; two stages of vein filling are apparent: fibrous quartz-carbonate intergrowths aligned at high angles to vein walls form the first, non-Au-bearing veining phase on vein margins, while the central vein fill comprises massive quartz with pyrite clots; view up at the back, Cariboo Gold Quartz mine, 1200 level, Rainbow zone; the vein is 0.3 m thick.

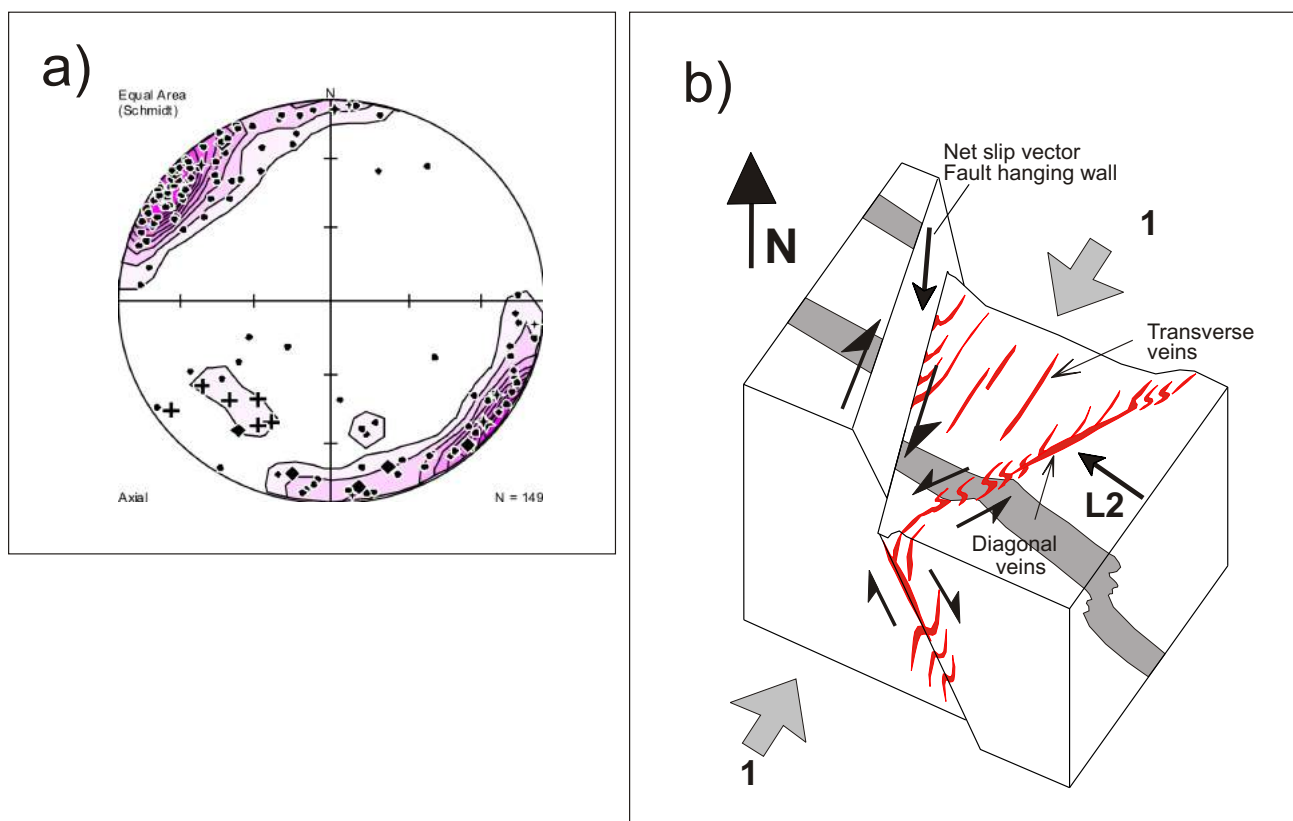


Figure 5: Geometries of Au-bearing veins in the Wells-Barkerville area: **a)** equal-area projection of poles to quartz veins in the central Wells-Barkerville area Au system; data are from underground workings and surface exposures in the Cariboo Gold Quartz and Mosquito mines, and at the surface along Lowhee Creek; symbols are as follows: small dots, extensional veins; diamonds, diagonal veins; large crosses, BC vein; note the dominant steep northeast trends to extensional veins; data are from Rhys and Ross (2001) with additional data collected in 2008; **b)** block model illustrating interpreted relationships between the principal Au-bearing vein sets and north-trending dextral >east-side-down faults in response to inclined northeast-directed shortening.



Figure 6: Surface exposure of the BC vein, a major 'strike' vein, looking southeast. This thick, northwest-trending fault-fill vein hosts several ore shoots and lies directly adjacent to the Bonanza Ledge zone. Note person for scale (right).

There has been much speculation regarding the relationships between the replacement and vein styles of mineralization in the Wells-Barkerville area (e.g., Benedict, 1945; Robert and Taylor, 1989). The replacement mineralization is clearly strained, but in the absence of definite strain markers it is uncertain whether it is affected by both D₁ and D₂ strains, or only by the latter event. The occurrence of the replacement mineralization in F₂ fold hinges and the overall plunge of the mineralization parallel to those folds may imply syn-D₂ timing, although the tectonic focus of earlier mineralization into the fold hinges is also possible.

The close spatial association of the replacement and later vein mineralization in a single, northwest-plunging mineralizing system could imply 1) a genetic link, representing different products of a single, long-lived, synmetamorphic and syn-Jurassic deformational and mineralizing event; 2) a two-stage mineralizing process whereby vein-hosted mineralization was remobilized from older Au-enriched replacement ores late in the structural history or 3) the replacement and Au-bearing veining episodes represent independent and temporally separate mineralizing events that both introduced Au into respective areas but were controlled by common structural and fluid channels that were

subject to later remobilization. Pure *in situ* or short-distance remobilization of Au into the later veins from replacement mineralization is unlikely, since the quartz veins are significantly greater producers, and are far more geographically extensive, both within the Wells-Barkerville area and in other lode-Au-bearing areas throughout the Barkerville terrane. In addition, remobilization does not explain the preferential development of the quartz veins themselves, which rapidly diminish in abundance outside the northwest-plunging zones of replacement mineralization. The spatial association instead implies a common control on fluid flow in the mineralizing system. Further work will attempt to evaluate the relationship between these mineralization types, but initial geochronological results outlined below support a sufficiently short time frame to allow a genetic link between the mineralization types.

Although the principal Au-bearing vein systems in the Wells-Barkerville area are commonly concentrated near, and are kinematically compatible with formation during dextral displacement along north-trending faults, this relationship does not explain the stratabound nature of the vein systems, which instead also suggests a significant element of control by northwest-trending structures. Northeast-dipping S_2 foliation-parallel slip surfaces and high-strain zones are common in the underground workings, often attenuating fold limbs, and may have been active up until late

during D_2 . If so, as a northwest-trending corridor of higher strain, these could represent the principal fluid channels to the Au-bearing veins, which if still active into waning stages of D_2 when northerly trending faults formed, then intersecting thrust surfaces with the faults may have created structurally permeable sites for fluid focus and vein deposition. If northeast-dipping, late- D_2 thrust corridors control vein mineralization, then this may explain the association with earlier replacement mineralization if it too formed earlier along the same D_2 high-strain corridors.

Wells-Barkerville Area: Dating and Isotopic Studies

Field studies in the Wells-Barkerville area during 2008 included the re-examination of key rock units and styles of mineralization in outcrop and drillcore, and extensive sampling for $^{40}\text{Ar}/^{39}\text{Ar}$ and U-Pb zircon dating and sulphide Pb isotope studies. A total of thirteen $^{40}\text{Ar}/^{39}\text{Ar}$ ages for micas have been determined from throughout the Wells-Barkerville area, using samples previously collected by Rhys and Ross (2001) when underground workings were still accessible, allowing access to areas of historic mining. New dating results are presented in Table 1.

The better-constrained $^{40}\text{Ar}/^{39}\text{Ar}$ results define a relatively narrow age range, from 138.2 to 155.2 Ma, for samples of country rock schist, micaceous alteration zones around known Au deposits and mica samples in and adjacent to

Table 1. Summary of new $^{40}\text{Ar}/^{39}\text{Ar}$ dating results from Wells-Barkerville area.

Sample No.	Rock Type and Location	Interpreted $^{40}\text{Ar}/^{39}\text{Ar}$ Age
BL-073	Baker unit, sericitic quartzite, Lowhee Creek	Rising spectrum to ca. 153 Ma (re-run rising spectrum to ca. 150 Ma)
BL-135	Rainbow 2 unit (upper) 1500 Level Cariboo Gold Quartz mine; muscovite-quartz-carbonate phyllite	146.6 ± 1.1 Ma (poor plateau)
BL-122A	Deformed pre-mineral vein, 1200 Level Cariboo Gold Quartz mine; muscovite coating fractures and in vein envelopes	153.7 ± 0.9 Ma (good plateau)
BL-130	Deformed pre-mineral vein, from Myrtle prospect trenches	155.2 ± 1.0 Ma (excellent plateau)
BL-086	Baker unit, north Lowhee Creek, muscovite-quartz phyllite in hanging wall of Bonanza Ledge zone	151.5 ± 0.8 Ma (good plateau)
BL-043	Fuchsite bearing Fe-carbonate, muscovite alteration of calcareous mudstone along Lowhee Creek	151.5 ± 0.8 Ma (excellent plateau)
BL-133-4	4400 Level Mosquito Creek Mine; banded fine grained ankerite pyrite replacement ore	148.5 ± 1.0 Ma (excellent plateau)
2K-31, 211-1	Replacement ore, Bonanza Ledge zone; banded muscovite-pyrite phyllite with coarse pyrite-Fe-carbonate bands	138.2 ± 0.8 Ma (good plateau)
BL-134-1	Replacement ore, Bonanza Ledge zone; muscovite phyllite with disseminated pyrite	Rising spectra to ca. 142 Ma (re-run 135.5 ± 0.8 Ma; partial plateau)
BL-002	Muscovite phyllite with oxidized pyrite porphyroblasts in hangingwall of Bonanza Ledge zone	142.8 ± 0.8 Ma (good plateau)
BL-125-1	Diagonal quartz vein, 1200 Level Cariboo Gold Quartz mine; clots of coarse randomly oriented muscovite within vein	147.6 ± 0.8 Ma (good plateau)
BL-129-1	Extensional quartz vein, 4400 Level northwest of Mosquito Creek mine; coarse muscovite on envelope to vein	141.4 ± 0.8 Ma (excellent plateau)
BL-128-1	Extensional quartz vein, 4400 Level southwest of Mosquito Creek mine; randomly oriented coarse muscovite	142.6 ± 0.8 Ma (excellent plateau)

both early (deformed) and late quartz veins. Muscovite in hostrock schist and associated with early, deformed quartz veins tend to give slightly older ages (>146.6 Ma), whereas muscovite from within replacement style and extensional-vein style Au ore gives largely overlapping ages in the range of 138.5–147.6 Ma. The Wells-Barkerville area has only experienced metamorphism up to lower-greenschist facies (sub-biotite isograd) and peak metamorphic temperatures (and growth or recrystallization of muscovite) were associated with the earlier stages of deformation (D₁ and D₂; Struik, 1988; Schiarizza and Ferri, 2003; Ferri and Schiarizza, 2006). Peak temperatures of metamorphism in the area, therefore, did not exceed 400–430°C and may have been somewhat lower. Since the closure temperature of the Ar isotopic system in muscovite is ~350°C, it is suggested that the ⁴⁰Ar/³⁹Ar muscovite ages listed above are probably close to the age of formation and do not reflect slow cooling of the Barkerville terrane as a whole. If correct, this would suggest that the last significant metamorphic event that affected the region associated with the D₂ event occurred in Late Jurassic to earliest Cretaceous time, and most or all of the Au mineralization in the Wells-Barkerville area formed at approximately the same time or very slightly later. Such timing is feasible, given the field relationships described above. Four additional muscovite samples from occurrences within the Wells-Barkerville area are currently being dated using ⁴⁰Ar/³⁹Ar methods, along with biotite from a late lamprophyre dike.

Andrew et al. (1983) reported Pb isotopic analyses for galena from four Au-bearing quartz veins and one replacement-style sulphide occurrence in the Wells-Barkerville area and areas farther to the south. An additional three galena and six pyrite samples from veins and two pyrite samples from replacement-style mineralization have been analyzed from the Wells-Barkerville area (mainly Mosquito Creek and Bonanza Ledge zones). The combined datasets are shown in Figure 7, along with the ‘shale curve’ of Godwin and Sinclair (1982) for reference.

All of the sulphide Pb isotopic analyses for the Wells-Barkerville area and vicinity fall on or above the ‘shale curve’, which is an approximation of the evolution of Pb isotopes within both the North American miogeocline in the northern Cordillera and the pericratonic terranes that lie immediately to the west (including the Barkerville terrane). This indicates that the Pb and presumably all other contained metals in the deposits and occurrences in the Wells-Barkerville area are entirely of crustal derivation, and could potentially have been derived from local bedrock units. In

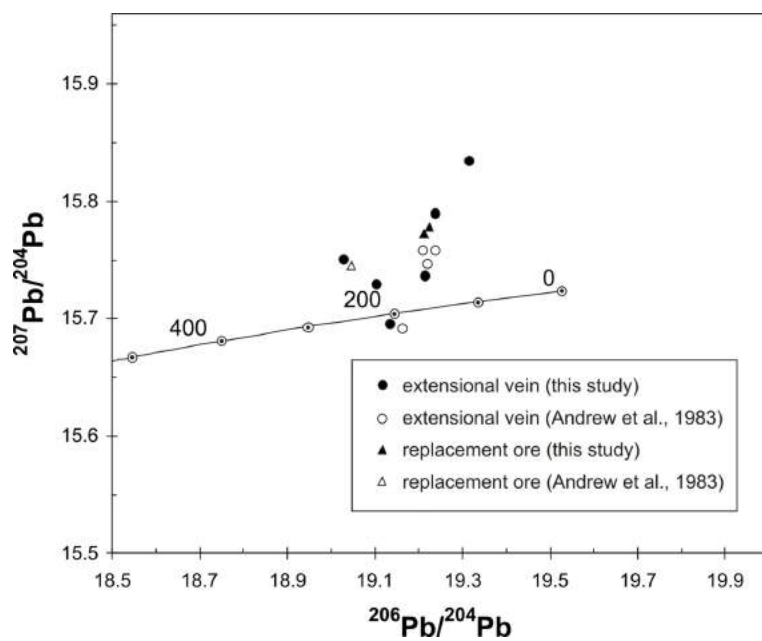


Figure 7. Sulphide Pb isotopic compositions from replacement- and vein-style Au mineralization in the Wells-Barkerville area. The ‘shale curve’ of Godwin and Sinclair (1982) is shown for reference.

addition, analyses of sulphide minerals from replacement-style mineralization completely overlap with those from crosscutting quartz veins, suggesting that the metals in these two distinct styles of mineralization had very similar sources and the veins and replacements are very similar in age (as also suggested by the ⁴⁰Ar/³⁹Ar dating results discussed above). A total of 23 additional sulphide samples, representative of the complete range of styles and geographic location of Au occurrences within the Wells-Barkerville area and vicinity, are currently being analyzed.

Cunningham Creek Area

Southeast of the Wells-Barkerville area, vein showings extend discontinuously over a 40 km strike length to Cariboo Lake, and are associated with significant placer-Au-producing drainages such as Cunningham, Keithley, Antler and Grouse creeks (Schiarizza, 2004). These collectively define the southern portion of the eastern mineralizing trend in the Barkerville terrane illustrated in Figure 1. This area, and the Yanks Peak area to the west, were both visited during the fieldwork program to assess mineralization controls and collect geochronological and isotopic samples. Initial observations from the Cunningham Creek work are summarized here for comparative purposes to the nearby Wells-Barkerville area. Geochronological and isotopic analyses are underway.

Gold prospects along Cunningham Creek (Figure 1) include the Craze Creek, Hibernian, B zone, Jewelry Shop, Silver Vein and Cariboo Hudson (093A 071) prospects. Within these areas, lode-Au mineralization occurs mainly

in sets of structurally late quartz-sulphide veins of comparable style to those at the Wells-Barkerville area, although the controls by north-trending faults are more apparent, and veins more frequently display a semibrittle style. The hostrock type is a northwest-trending grey phyllite of the Downey succession (Schiarizza and Ferri, 2003).

In the vicinity of Craze Creek, three prospects (Hibernian, Jewelry Shop and the B zone) comprise at least three north-trending, mineralized fault zones in which fringing arrays of Au-bearing quartz-sulphide veins are developed. The faults comprise narrow, semibrittle shear zones that trend north with steep dips, and cut across the northwest-trending, moderately northeast-dipping phyllite sequence. Primary compositional layering, dominant foliations (S_1 and S_2) and deformed quartz veins locally deflect into parallelism with more northerly trends as they approach the shear zone slip surfaces (Figure 8a), which with offset lithological contacts and synthetic shear bands record dominantly dextral displacement on the fault-slip surfaces. Gold-bearing quartz veins, often with coarse-grained pyrite-arsenopyrite and minor galena and sphalerite fill are abundant within several metres of, and between closely spaced slip surfaces (Termuende, 1990). The larger veins, which are up to 1 m thick, trend northwest, exploiting S_1 foliation surfaces, but rapidly thin within a few metres of the shear-zone slip surfaces. Extensional veins and veinlets rotate from east-west to west-northwest trends as they approach slip surfaces, defining sigmoidal geometries both consistent with the shear sense, and with vein formation simultaneous with dextral displacement on the shear zones. Minor sigmoidal dextral extensional vein arrays are present adjacent to the shear zones, recording similar kinematics (Figure 8b).

To the south of the Craze Creek prospects, prospects including Skarn (Silver mine), Penny Creek and Cariboo Hudson comprise northerly to north-northwesterly trending, discordant and steeply dipping fault-fill veins (Delancey, 1988; Termuende, 1990). Deflections of rock units and foliations, as well as offsets of lithological contacts by a few metres to tens of metres, record dextral displacement across the veins, consistent in shear sense to the shear zones at Craze Creek. These veins contain abundant galena, sphalerite, pyrite, tetrahedrite and arsenopyrite, which may be banded parallel to vein walls (Figure 8c). The veins are much more Ag-rich than those in the Craze Creek area to the northwest. Collectively, these define a corridor of mineralized faults and veins that is approximately 600 m wide along the east side of Cunningham Creek.



Figure 8: Vein systems in the Cunningham Creek area: **a)** plan view of north-trending, quartz-vein-filled shear-zone slip surface (at centre, runs from left to right) that truncates the adjacent grey pyrite-arsenopyrite-quartz veins at the Jewelry Box showing; the veins emanate off the slip surface and are parallel to northwest-trending S_1 foliation; note deflection of the deformed quartz veins and S_1 foliation into the shear plane at the centre, compatible with dextral displacement along the structure; hammer for scale; **b)** northeast-trending sigmoidal en échelon array of extensional veins adjacent to the Jewelry Box shear zone records dextral shear; hammer for scale; **c)** view northward of the Silver Vein occurrence; this is a north-trending, steeply east-dipping banded shear vein that is fault hosted and contains quartz, pyrite, galena and tetrahedrite; deflection of S_1 foliation and juxtaposition of quartzite (right) against carbonaceous phyllite (left) across the fault and vein suggest dextral displacement; person for scale.

The Cunningham Creek area veins display similar timing relationships to regional fabrics such as main-stage, Au-bearing quartz veins in the Wells-Barkerville area. The veins postdate all D₁ and most or all D₂ strain, and are associated with northerly trending dextral faults. The style of associated shear zones at Craze Creek is more semibrittle in character than is generally seen in the Wells-Barkerville area or other areas, potentially suggesting slightly higher temperatures or lower strain rates during vein formation. The veins are also kinematically consistent with formation in response to northeast-directed shortening, potentially late during D₂. As in the Wells-Barkerville area, despite being hosted by discordant northerly trending fault and shear zones, mineralization is generally stratabound and is localized principally in the northwest-trending package of the Downey phyllite within several hundred metres of the contact with black siltite and phyllite of the Hardscrabble succession (Scharizza and Ferri, 2003).

Geological Setting and Au Mineralization in Quesnellia Metasedimentary Units

Two significant Au deposits have been discovered within lower-greenschist-grade metasedimentary and metavolcanic units in the lower part of Quesnellia: these are the Spanish Mountain (CPW) deposit, which is held by Skygold Ventures Ltd., and the Frasergold deposit, which is currently being evaluated by Hawthorne Gold Corp. (Figure 1).

Spanish Mountain (093A 043)

The Spanish Mountain deposit occurs within the black phyllite package of the Quesnel terrane, approximately 3 km east of its probable thrust contact with overlying mafic volcanic rocks of the Nicola Group to the southwest (Spanish thrust, Figure 1; Logan, 2008). The deposit is hosted by interbedded slaty to phyllitic, dark grey to black siltstone, carbonaceous mudstone, greywacke and minor conglomerate that are locally intruded by plagioclase±quartz-phyric dikes and sills.

Rocks in the vicinity of the Spanish Mountain deposit are folded, but generally trend northwest with overall northeasterly dips. Graded bedding in drillholes observed suggests that the sequence is in an overturned, megascopic F₁ fold limb (Singh, 2008). Previous work by Skygold Ventures (Singh, 2008) and surface mapping and drillcore review conducted during this study have estab-

lished that the stratigraphy in the deposit area comprises two main lithological packages:

An extensive lower package of siltstone and fine-grained greywacke that underlies southwestern portions of the ridge crest of Spanish Mountain southwest of the main zones of the deposit and forms the structurally lowest, but stratigraphically highest part of the immediate lithological sequence of the deposit.

A sequence of carbonaceous phyllite and interbedded siltstone that structurally overlays the siltstone-greywacke sequence to the northeast and contains two prominent marker units: a fine-grained, pale-grey greywacke unit (typically 40–100 m thick) that contains a heterolithic and mud-chip conglomerate marker (<1–10 m thick) at its base, and a siltstone unit (70–130 m in thickness) that is often silicified and carbonate-sericite-altered, and contains altered, thin sills of probable mafic protolith. This sequence of dominantly carbonaceous phyllite is the principal host to mineralization at the deposit. It has been further subdivided into three units based on their stratigraphic position with respect to the markers termed from structurally lowest (in the southwest) to highest (in the northeast): the Lower, Main zone and North zone argillites (Singh, 2008). Volumetrically

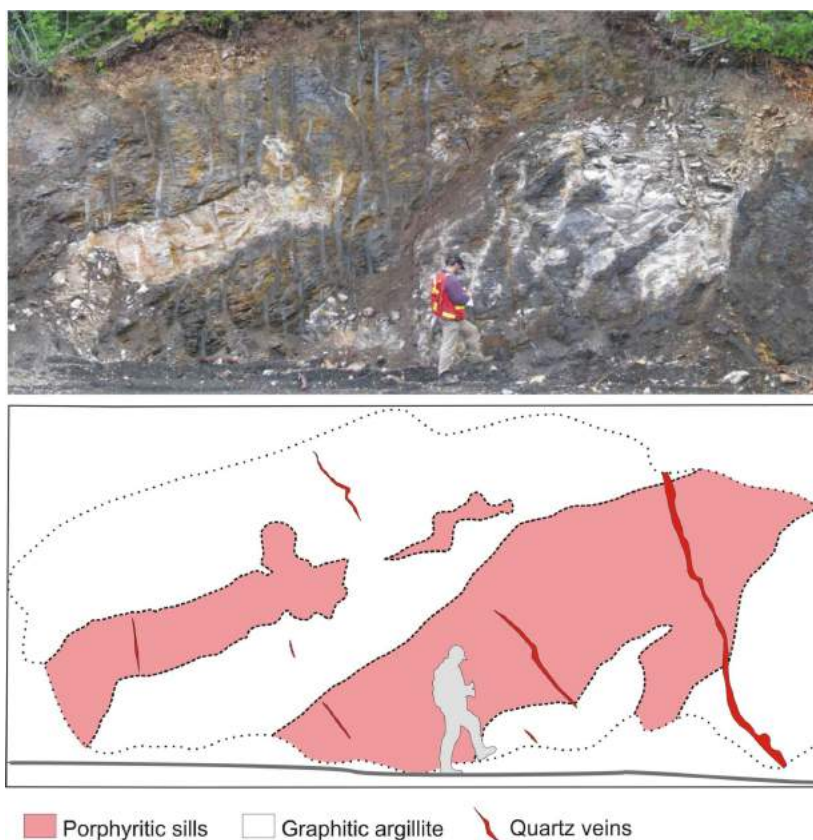


Figure 9: View to the southwest of a drill cut-out in lower portions of the carbonaceous phyllite sequence on Spanish Mountain. The photo illustrates two concordant, deformed and S₁-parallel porphyritic sills (in pink in the schematic diagram) that are cut by northwest-trending, steeply northwest-dipping quartz extensional veins (shown in red). These intrusions have yielded U-Pb zircon ages of 185.6 ±1.5 to 187 ±0.8 Ma.

minor amounts of interlayered mafic tuff and amygdaloidal basalt also occur within the sequence outside of the immediate deposit area (Singh, 2008).

The Spanish Mountain sequence is also characterized by the presence of plagioclase±quartz±hornblende sills and locally dikes, which commonly occur in the Lower argillite at the structural base of the carbonaceous phyllite sequence (Figure 9). They are also present in the siltstone-greywacke sequence to the southwest on the top of the ridge. The sills range in thickness from a few tens of centimetres to locally up to 100 m thick, the latter in one lenticular sill at the contact between the carbonaceous phyllite and underlying siltstone and greywacke sequences southwest of the deposit. These sills are affected by all phases of folding, alteration and quartz-vein mineralization (Figure 9). Locally irregular outlines to the contacts of these sills and brecciation on their finer-grained margins that may represent peperitic textures suggest that they may have been intruded into unconsolidated sediments. Variable proportions of quartz, feldspar and porphyritic textures suggest a suite of different intrusions. Probable mafic sills that are present within the altered siltstone marker unit are generally narrow and may be laterally discontinuous, locally becoming discordant to S_0 .

Alteration

Widespread alteration affects rock types on Spanish Mountain. The most extensive alteration consists of iron-magnesium-carbonate+muscovite (sericite)±pyrite with accessory rutile that varies in style between different rock types. Two generations of carbonate occur as discrete porphyroblasts in the finer-grained carbonaceous phyllite and silty units; an early phase with rounded porphyroblasts up to 0.8 cm in diameter, which is wrapped by the dominant foliation, displaying a ‘knotted’ texture and a younger phase of rhombic porphyroblasts that overgrows at least the S_1 foliation. In the greywacke and the feldspar-porphyr sills, carbonate-sericite alteration is finer grained, more pervasive and commonly texturally destructive, which in some cases hinders distinction between the two rock types. The alteration does not affect carbonaceous material in the carbonaceous phyllite, which remains dark in colour. Altered greywacke and feldspar-pyritic intrusions are pale tan to nearly white. Locally, in the greywacke marker of the upper sequence and in quartz-bearing intrusive phases, fuchsite occurs as mantles around isolated, probable xenocrysts of chromite and small angular mafic or ultramafic xenoliths. The most intense alteration affects the siltstone marker that lies between the Main and Upper argillite units in the upper carbonaceous phyllite sequence, and the structurally lower portions of the greywacke marker unit. The siltstone marker package is intensely carbonate-sericite-altered, bleached and silicified, and textural evidence suggests that siltstone may have been hornfelsed (quartz-bio-

tite altered), possibly related to the intrusion of mafic sills, prior to the bleaching, which is related to the carbonate-muscovite alteration. In this unit, bright green chrome mica (fuchsite), intergrown with intense carbonate alteration assemblages, replaces the mafic sills that cut the silicified siltstone package. Pervasive alteration of the types described above predate at least S_2 foliation, since muscovite is aligned within foliation planes, fuchsite may occur as S_2 -parallel stylolitic pressure-solution seams, and carbonate porphyroblasts are often wrapped by dominant foliation.

Structural History

The sequence of deformation in the Spanish Mountain area is consistent with the general phase 1–phase 2 events defined by Bloodgood (1992) and Panteleyev et al. (1996) for the region, although local differences in fold geometry and an additional folding event that differ from these previous interpretations are also evident. First-phase (S_1) foliation is generally layer parallel and penetrative. Isoclinal F_1 fold hinges were locally observed in the greywacke marker unit, where they are likely intrafolial and may result in local tectonic thickening of some units. Presence of dominantly overturned bedding facing directions in drillholes in the deposit area suggest that the hosting lithological sequence is inverted (Singh, 2008). This implies that the deposit may lie on the overturned limb of an F_1 fold nappe, a geometry that has not been previously documented in this part of the Quesnel terrane.

Second-phase foliation development at Spanish Mountain comprises moderate to shallow southwest-dipping spaced foliation that is axial planar to the folds, crenulates and locally transposes S_1 , and is axial planar to dominant, northeasterly verging phase 2 folds. Fold axes plunge shallowly southeast. Map patterns and cross-sectional interpretation suggest that a megascopic, recumbent phase 2 fold hinge with a broad hinge zone lies in the northeast portions of the deposit area, separating the sequence into moderately northeast dipping and subvertical limbs to the southwest and northeast, respectively, on the northern flanks of Spanish Mountain in the vicinity of the North zone. At a property scale, phase 2 fold hinges may be noncylindrical and vary in plunge direction (B. Singh, pers. comm., 2008), potentially due to interaction with previous phases of folding.

A significant observation from the current study is that an additional phase of folding is evident in the Spanish Mountain area between the regional phase 1 and phase 2 events of Panteleyev et al. (1996). These open to tight folds affect S_1 foliation but are obliquely crossed and overprinted by the spaced, second-phase foliation. Folds of this type plunge moderately to the southeast, and have steeply dipping axial planes; axial-planar cleavage is weakly developed or absent. These folds are best developed and widespread in the siltstone-sandstone unit southwest of the main deposit area, but also occur locally in the higher carbonaceous phyllite

sequence where they were observed to affect portions of the silicified siltstone unit. For the purposes of this paper, they are coded F_{2a} folds, whereas the folds and foliation associated with the widespread second-phase foliation are coded F_{2b} and S_2 , respectively, for consistency with the defined regional nomenclature. The megascopic phase 2 fold (F_{2b}) mentioned above is likely accentuated by, and may tighten earlier folds associated with this additional F_{2a} event. The presence of these folds suggests that the regional structural history may be more complex than has been previously de-

termined, although telescoping of subsequent events may obscure such patterns.

As in other parts of the district, latest prominent structural features in the Spanish Mountain area comprise north- to northeast-trending brittle faults. Faults measured during this study most frequently have moderate to steep west-northwest dips and north-northeast trends. Significant northwest-trending faults were also observed locally. The faults are typically defined by zones of clay gouge, which

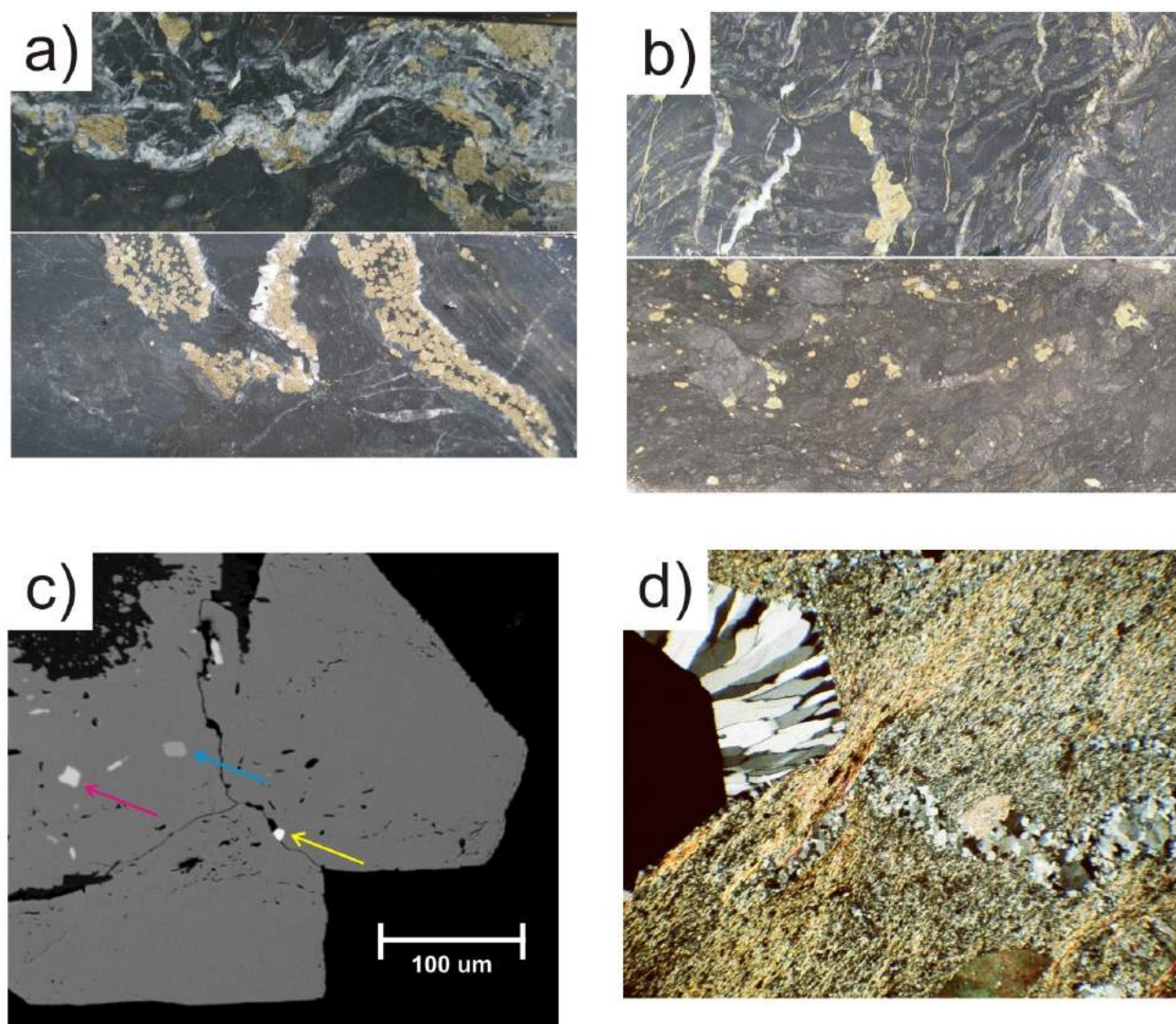


Figure 10: Early pyrite-quartz veinlets and disseminated pyrite in carbonaceous phyllite, Spanish Mountain deposit: **a)** folded quartz-pyrite veinlets; note fine- to medium-grained habit of pyrite and euhedral nature of the pyrite grains in the lower sample; (top) DDH515, 102.9 m; (bottom) DDH697, 155.5 m; both of these samples contained <1 g/t Au; **b)** (top) pyrite-quartz stringers at high angle to S_0 in thinly laminated phyllite are affected by incipient ptgmatic folding; pyrite is euhedral; DDH259, 57.0 m, from interval grading 2.22 g/t Au; (bottom) disseminated pyrite±quartz aggregates in tectonically disrupted carbonaceous mudstone; DDH289, 21.0 m, 3.13 g/t Au; **c)** scanning electron microscope (SEM) backscatter image of euhedral pyrite aggregate from sample in **b)** (bottom); note mica trails inside the pyrite that defines S_1 foliation, indicating pyrite formation after D_1 ; a grain of electrum (yellow arrow) occurs on a fracture between pyrite grains, while chalcocopyrite (red arrow) and sphalerite (blue arrow) are encapsulated in the pyrite; 'um' = microns; **d)** photomicrography illustrating a quartz pressure shadow on a euhedral pyrite grain (opaque, at left); fibres in the pressure shadow are aligned parallel to the S_2 foliation defined by sericite in the surrounding phyllite; note folded quartz veinlet at right; DDH252, 116.7 m, in an interval grading 3.46 g/t Au; plane-polarized light, field of view 3 mm.

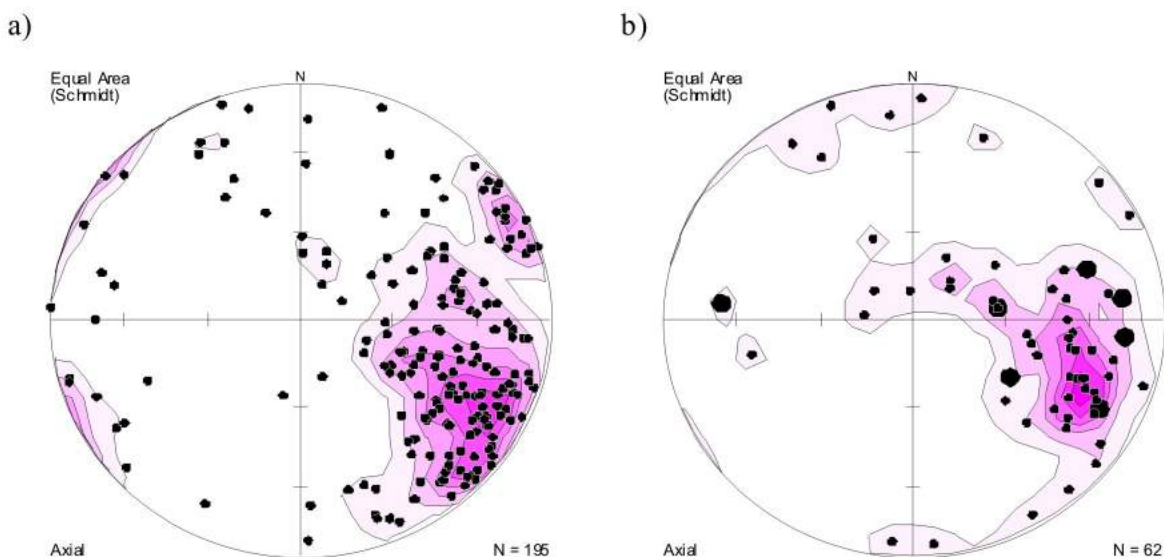


Figure 11: Equal-area projections of poles to orientations of quartz veins in the Spanish Mountain deposit. All data were collected by the authors in 2008: **a)** quartz veins <5 cm thick; these are dominantly extensional veins; steep northwest dips predominate, but veins also range to more northerly and northwesterly trends with west to southwest dips; **b)** quartz veins >5 cm thick, including fault-hosted and shear veins; note the dominant northerly trends and steep westerly dips, which include several significant faults containing cataclastically deformed vein material; large dots represent ribboned shear veins, mainly from the North zone.

commonly include cataclastically deformed quartz-vein material. These, however, may in part be localized along earlier, probably more semibrittle shear zones since it was noted, particularly in drillcore, that foliated chloritic or more intensely foliated shear zones and foliated cataclasite were commonly present, and localized some quartz veining. Fault thickness is highly variable, with thicker faults containing up to several metres of gouge and broad damage zones. Carbonaceous material has in some cases been remobilized along fractures and veinlets into carbon-poor greywacke and intrusions, locally forming black crackle breccia adjacent to faults and larger associated quartz veins.

Gold Mineralization

The Spanish Mountain deposit is a bulk tonnage Au system that also includes local higher-grade Au-bearing quartz veins. The most economically significant Au mineralization (>1 g/t Au) occurs in wide zones (10–135 m) hosted dominantly within the black argillite and siltstone, and to a lesser extent in greywacke, often straddling the contact (Singh, 2008). These zones may occur as a set of stacked, roughly lensoidal zones, which at a local scale are stratabound and spread most widely along carbonaceous phyllite ('argillite') units, but at a deposit scale are stacked and linked, defining an overall northerly elongate mineralizing system that is developed discordantly across several stratigraphic horizons. The largest zone identified to date is the 'Main zone', which has been traced by drilling over a strike length of approximately 1.3 km and width of 500 m (Singh, 2008). The 'Lower zone' occurs beneath the Main zone, in the structurally lower, carbonaceous argillite unit

of the same name. The smaller, less well-defined North zone occurs in the structurally highest carbonaceous unit (Singh, 2008).

Within these mineralized zones, there are at least two periods of mineralization: an earlier phase of disseminated pyrite and pyrite-quartz veinlets, and a later phase of fault-related quartz veining. The early pyrite mineralization comprises stringers and up to 2 cm wide veinlets of pyrite+quartz+iron-magnesium-carbonate and spatially associated disseminated pyrite that are preferentially developed within carbonaceous phyllite in mineralized zones (Figure 10a, b). The disseminated pyrite often occurs in aggregates with quartz. Pyrite in both the veinlets and disseminations varies from fine to medium grained and is often euhedral. Carbonaceous phyllite may be tectonically disrupted, with destruction of S_1 foliation and incipient cataclastic brecciation in areas of pyrite development (Figure 10b), and veinlets and pyrite may occur on or adjacent to slip surfaces that define narrow shear zones, suggesting potential control by faulting, possibly thrust faults, along the carbonaceous (graphitic) argillite units. Pyrite-quartz veinlets are often ptlygmatically folded and are affected by at least D_2 strain (Figure 10a). The euhedral disseminated pyrite grains and aggregates overgrow S_1 foliation and early folds, which may be preserved as micaceous trails within the grains (Figure 10c), but in turn are wrapped by S_2 foliation and have fibrous quartz pressure shadows aligned parallel to S_2 surfaces (Figure 10d), collectively suggesting that they formed late during or after D_1 , and prior to most D_{2b} strain. Electrum and native gold have been observed as <5–20 m grains encapsulated in and along fractures in this

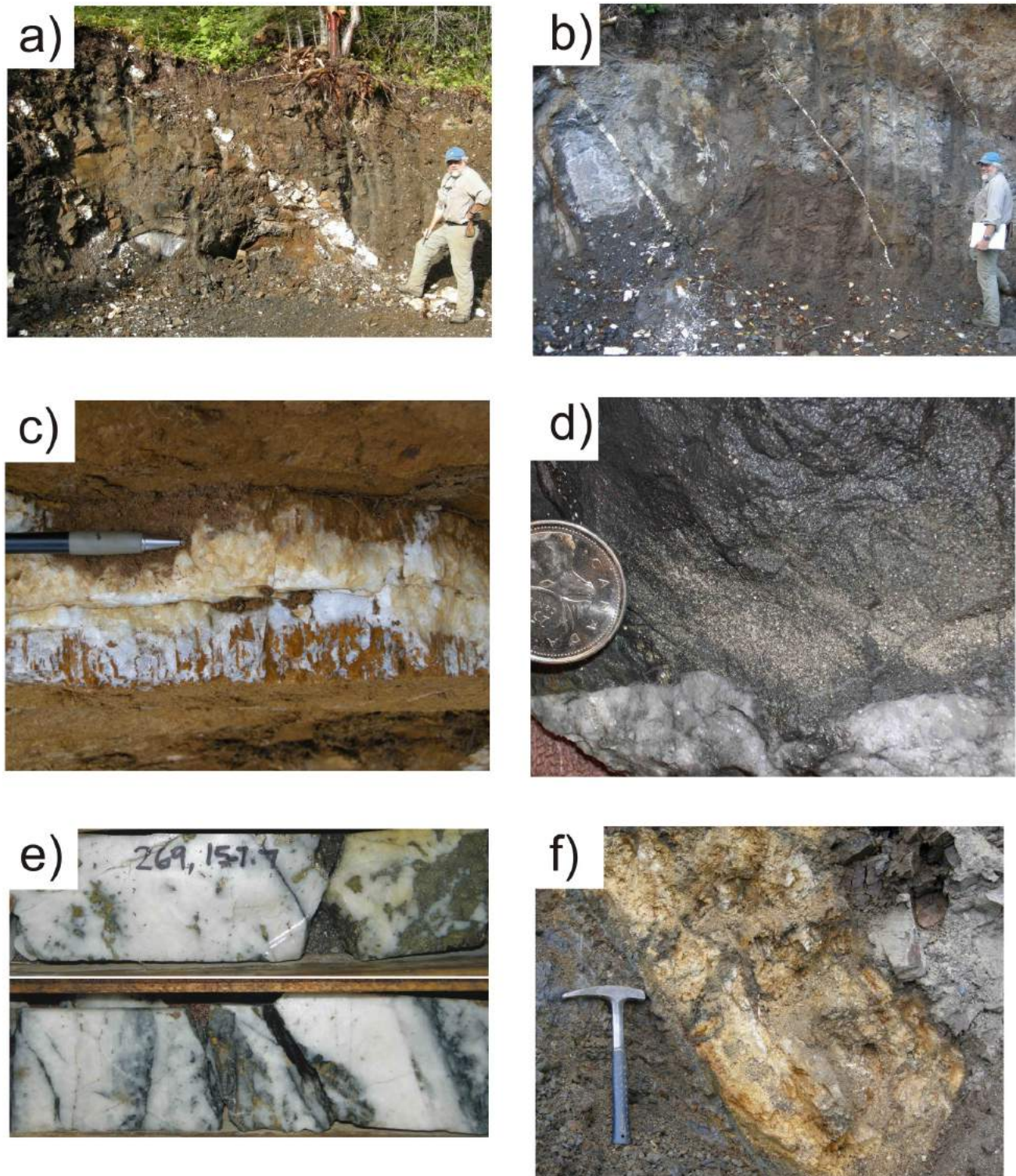


Figure 12: Spanish Mountain Au-bearing quartz veins: **a)** sheeted northwest-dipping quartz extensional veins hosted by carbonaceous phyllite in the North zone surface exposures, view southwest, person for scale; **b)** sheeted northwest-dipping quartz extensional veins hosted by carbonaceous phyllite in the Main zone surface exposures, view southwest, person for scale; **c)** extensional vein in sill hosted by the southern siltstone sequence shows paragenesis from early fibrous quartz-carbonate on margins, to more massive quartz-pyrite in core, pencil for scale; **d)** M1 pit, quartz extensional vein (below) with pyrite envelope (centre) in carbonaceous phyllite, quarter for scale; **e)** brecciated, friable rusty quartz vein in northerly trending, west-dipping fault; view south, Main zone exposures; core is approximately 5 cm wide; **f)** high-grade (23.9 g/t Au) ribboned quartz shear vein with pyrite clots (above) and carbonaceous-pyritic black slip surfaces and breccia bands (below) in a fault zone; hole 269, 157.7 m; hammer for scale.

style of pyrite and free in the quartz carbonate within the veinlets (Ross, 2006), indicating that this early pyrite-quartz episode introduced Au into the system, where it may contain a significant amount of low-grade mineralization in the deposit (Singh, 2008). Although it is possible that some of the euhedral pyrite could have formed from recrystallization or remobilization of an earlier, potentially Au-bearing diagenetic or synsedimentary pyrite phase (that has locally been identified at Spanish Mountain; R. Large, pers. comm., 2007), the common association of the euhedral pyrite with quartz veinlets, occurrence of pyritic zones as multiple stacked zones that occur across different stratigraphic horizons, lateral decreases in pyrite abundance in stratigraphic units away from mineralized zones, and local cataclastic brecciation of carbonaceous phyllite in pyritic areas suggests that the pyrite is dominantly hydrothermally and tectonically controlled. Although this style of mineralization is clearly auriferous in many areas, no direct correlation between Au grade and pyrite content has been established (Singh, 2008).

The second mineralizing event at Spanish Mountain is associated with tectonically late quartz veins and faults that share similarities with the dominant, late vein-related Au mineralization episode in the Barkerville terrane. They cut the folded, early quartz-pyrite veins described above and are most often manifested by sets of sheeted, northeast-trending and steeply northwest-dipping (Figures 11a, 12a, b) quartz±iron-carbonate extensional veins <5 cm thick that may contain minor pyrite, galena, sphalerite and tetrahedrite. In surface exposures, base metals were noted most abundantly in veins within the North zone. Sheeted extensional veins are typically spaced from a metre to several metres apart in mineralized carbonaceous phyllite (Figure 12a, b). Vein densities are often much higher in sandstone and in feldspar- or quartz-phyric sills. While usually having blocky quartz fill, prismatic quartz and fibrous quartz-carbonate aligned at high angles to vein walls are also often present, consistent with an extensional origin. A paragenesis of early quartz-carbonate on vein margins and central blocky quartz vein fill is locally apparent, and similar to vein paragenesis observed in the Wells-Barkerville area (Figures 4b, 12c). Locally, more than one generation of veining is developed, with successive generations becoming less carbonate rich and more quartz rich, consistent with the paragenesis described above (B. Singh, pers. comm., 2008). The extensional veins may have disseminated pyrite envelopes that extend for several centimetres into the surrounding wallrock (Figure 12d).

In drillcore, areas of highest Au grade and most occurrences of visible Au were associated with quartz veins. Gold grades typically increase in areas of quartz veining, particularly in association with mineralized faults (*see below*), although a direct association between quartz vein density and grade has not been established (Singh, 2008). It

was noted, however, that quartz-vein distribution in outcrop mimics that of the distribution of mineralized zones. To the south in the lower siltstone package, Au prospects (e.g., Ropes of Gold) occur principally in folded plagioclase-phyric sills where they are cut by sets of quartz extensional veins, which often have pyrite envelopes.

Extensional veins are also associated with shear veins and fault-hosted veins. North-northeast-trending, west-northwest-dipping (Figure 11b) clay gouge-filled faults, commonly containing unconsolidated, cataclastically deformed vein material (Figure 12e), are present within many outcrop exposures, and are often intersected in drillcore in mineralized zones. These may be surrounded by more concentrated sets of extensional veins, which were in several cases noted to join the fault-hosted veins suggesting a coeval timing. Several fault-hosted shear veins up to 2 m thick were also noted in core and outcrop, comprising ribboned quartz-pyrite veins with carbonaceous or pyritic stylolitic slip surfaces and banding (Figure 12f), and which have been variably brecciated by later, postmineralization brittle displacement. These locally contain high Au grades.

Since significant postmineralization faulting has occurred along the faults hosting vein mineralization and has brecciated the quartz and obscured any primary kinematic indicators that may have been present, it is not possible to determine the syn-vein kinematics of faults. However, the association of steeply dipping, northeast-trending quartz extensional veins with the faults, and junction of some extensional veins with fault-fill veins, are geometrically compatible with the vein orientations in most portions of the Barkerville terrane, suggesting syn-vein dextral oblique slip (northwest side down) faulting in response to northeast-directed shortening. The structurally late timing of extensional veins at Spanish Mountain, which cut across all fabrics and folds without deflection, and the occurrence of extensional veining at high angles to the shallow southeast-plunging L₂ intersection lineation are also compatible with a late D₂ timing of vein formation.

Discussion

The proposed two-stage history of Au mineralization at the Spanish Mountain property may be analogous to the mineralizing history in the Wells-Barkerville area. As with that area, the later vein mineralization is spatially coincident with earlier forms of more deformed sulphide-bearing mineralization. It is unclear what the relative proportions of Au the early pyrite and later fault-related quartz-veining events each contribute at Spanish Mountain, but the later quartz-vein-associated mineralization is more widespread and often higher grade than the early pyritic mineralization. To explain the coincidence of the two forms of mineralization, simple remobilization of early mineralization during later events into the later quartz veins is considered unlikely here, as this process does not explain why vein quartz den-

sities are highest in the mineralized zones. As with the Wells-Barkerville area, if remobilization was the main mechanism by which Au was localized into the later veins, the later veins themselves would be expected to be developed regionally, and not coincidentally focused in the older areas of mineralization. The occurrence of both the early mineralization and quartz veining in a series of stacked zones that collectively cross stratigraphic boundaries in a crudely northerly elongate zone with evidence for cataclasis and faulting associated with both the early and later mineralizing episodes suggest that the Spanish Mountain deposit may be developed in a zone of longer-lived tectonic activity. Widespread early alteration of the Spanish Mountain sequence near mineralized zones in the form of carbonate porphyroblast development, sericite-carbonate alteration of feldspathic rock types, and fuchsite-carbonate alteration of mafic sills in the silicified siltstone marker may be coincident with the earlier pyrite-quartz event, as these styles of alteration are affected by D_{2b} fabric. Early, local silicification of the siltstone marker, potentially associated with the mafic sills, may have also aided in fluid focus and vein development during the later quartz-veining events, by forming an impermeably and rheologically competent buttress to fluid flow.

Ongoing Dating, Petrographic and Isotopic Studies at Spanish Mountain

During the fieldwork at Spanish Mountain, an extensive suite of samples for $^{40}\text{Ar}/^{39}\text{Ar}$ mica and U-Pb zircon dating, as well as for detailed petrographic, lithogeochemical and Pb isotopic studies were collected, and analyses are currently underway. A lithogeochemical study of the intrusive rocks is also currently in progress.

Zircon grains have been separated from four separate intrusive bodies that intrude the contact area between the lower siltstone and upper carbonaceous phyllite sequence at Spanish Mountain. These have recently been dated at the University of British Columbia (UBC) using laser ablation inductively coupled plasma-mass spectrometry (ICP-MS) U-Pb methods. The four samples give similar ages of 185.6 ± 1.5 Ma to 187.3 ± 0.8 Ma. These intrusions have been affected by D_1 deformation and later events, having been boudinaged and wrapped by S_1 foliation. Consequently, these ages place a maximum age on both the D_1 deformation that has affected the phyllite in this area and the Au mineralization and associated alteration. These intrusions may be related to the suite of Jurassic-aged intrusions (unit 7 of Panteleyev et al., 1996), which are mapped as isolated stocks in the same sedimentary package of rocks to the south of Quesnel and Horsefly lakes, and to the west where they intrude the Triassic–Early Jurassic basaltic rocks and related volcanoclastic rocks. The only dated bodies in the unit 7 suite, however, have given somewhat older ages (>193 Ma) and compositionally, these bodies most closely resemble those in the Mt. Polley area, all of which have

been dated at ca. 200 Ma using U-Pb methods (Mortensen et al., 1995). The only intrusions within Quesnellia that have given reliable (U-Pb) crystallization ages similar to those in the Spanish Mountain area are those that are associated with the Mt. Milligan Cu-Au porphyry system north of Prince George.

Frasergold (093A 150)

The Frasergold property, located approximately 60 km southeast of Spanish Mountain, covers an ~10 km long, northwest-trending area of mineralized prospects, defined by drilling and anomalous Au in soils along the northeast limb of the Eureka Peak syncline (Figure 1). Mineralization at Frasergold is hosted by the same general sequence of Middle–Upper Triassic metasedimentary rocks that occurs at Spanish Mountain, comprising a fine-grained turbidite sequence that is dominated by black carbonaceous phyllite with local thin interbeds of metasiltstone, and more rarely, fine-grained metasandstone. Unlike Spanish Mountain, however, intrusive rocks appear to be absent from the section at Frasergold. Stratigraphy in the Frasergold deposit area dips moderately to shallowly to the southwest in the deposit area. Regional mapping suggests that the overall sequence is upright and occurs on the northeast limb of the regional Eureka syncline (Bloodgood, 1987, 1992).

Alteration

The carbonaceous phyllite in the Frasergold deposit area, like portions of the Spanish Mountain sequence, is characterized by the presence of coarse iron-carbonate porphyroblasts. Foliation (both S_1 and S_2 , see below) wraps around the porphyroblasts, creating a bumpy to dimpled ‘knotted’ texture to foliation surfaces. The porphyroblasts may represent a broad alteration envelope to the mineralizing system, as in other sediment-hosted districts globally. Although the carbonate porphyroblasts are wrapped by, and therefore predate S_2 foliation, they overgrow S_1 foliation surfaces and folds, indicating their formation during or after D_1 , but prior to D_2 (Figure 13), and consistent with a secondary origin that could be alteration related. If they are related to mineralization, then this relationship helps constrain mineralization timing.

Gold Mineralization

Gold mineralization on the Frasergold property occurs within, or is spatially associated with stratabound sets of white quartz+iron-carbonate+muscovite+pyrite veins that are developed in the ‘knotted’ iron-carbonate porphyroblastic carbonaceous phyllite unit. The veins form complex sets that are developed in concentrated zones several metres to tens of metres wide that dip collectively to the southwest and form a bulk tonnage low-grade Au deposit. An inferred historical resource (not compliant with NI43-101) of 6.6 million tonnes grading 0.055 oz/t Au to depths

of 100 m and over a 3 km strike length has been reported (Goodall and Campbell, 2007).

Structural History

Quartz veins within mineralized zones at Frasergold comprise mainly subparallel, approximately S_0/S_1 parallel (concordant) quartz veins and veinlets (Figure 14a) that are composed of blocky, recrystallized white quartz with minor iron-carbonate, and common silvery muscovite selvages. These veins are affected by both D_1 and D_2 strain and are often transposed and boudinaged in the plane of S_1 , locally with the development of internal S_1 -parallel sericite stylolite. The veins are affected by F_2 folds (Figure 14b) and vary in orientation across F_2 fold limbs, although are generally within or almost parallel with S_0/S_1 . Yellow-brown, coarse, blocky iron-carbonate typically occurs as clots, bands and selvages on veins, and contains disseminated pyrite \pm pyrrhotite with local trace amounts of chalcopyrite, sphalerite and galena.

The concordant S_0/S_1 and thicker, discordant veins join one another without crosscutting relationships (Figure 14c), have the same mineralogy, and are equally as deformed, suggesting that they are all part of a single vein generation, or several very closely timed but now indistinguishable vein generations that form part of a single veining episode. Although primary geometries and morphologies of the veins have now been obscured by deformation, the narrower concordant veins frequently form arrays with local en échelon patterns that splay off the larger discordant veins in a relationship that could represent a shear vein or extensional vein relationship, with the larger veins forming minor reverse oblique slip or shear veins (Figure 14c). The vein systems may have originally formed networks of widely spaced, reverse shear veins that were joined by sets of abundant extensional veins that could have been broadly localized along with, or adjacent to a thrust within the phyllite sequence. Collectively the vein networks, and potential stringer or disseminated pyrite mineralization in the vein wallrock, define a bulk-tonnage, low-grade deposit.

The Frasergold vein system could represent a semibrittle shear vein or extensional vein array that formed along with, or adjacent to a concordant or semiconcordant D_1 shear zone. Similar sets of veins associated with D_1 thrusts are reported throughout the region by Bloodgood (1992). An early to syn- D_1 timing of mineralization is suggested based on the strain state and relations of the veins to fabrics, since the veins are affected by a significant amount of D_1 strain, but predate all D_2 deformation. This is consistent with the late- D_1 to pre- D_2 implied timing of the carbonate porphyroblasts based on textural relationships. Apart from a few isolated stringers, structurally late, steeply dipping and northeast-trending quartz extensional veins and shear veins seen in the Barkerville lode-Au deposits and at Spanish Mountain are absent at Frasergold.

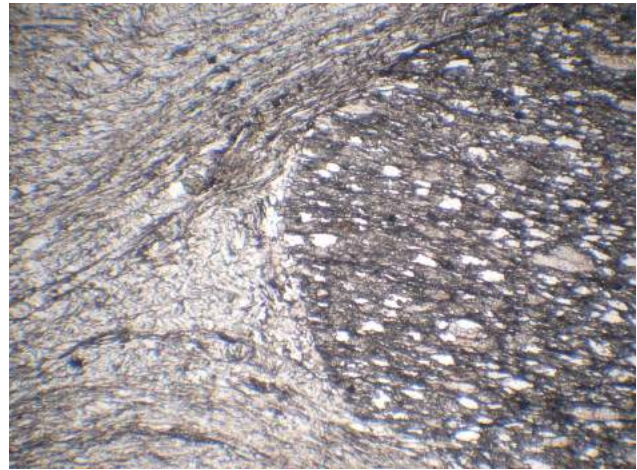


Figure 13: Photomicrograph of a carbonate porphyroblast (right side of image) in carbonaceous phyllite at the Frasergold deposit. Note the porphyroblast overgrows S_1 foliation, which is preserved as muscovite and quartz alignment internally within it. The S_2 foliation wraps around the porphyroblast at left and crenulates the older S_1 foliation outside the porphyroblast. Frasergold drillhole 07-295, 124.2 m. Plane-polarized light, field of view 3 mm.

Other Au occurrences of a similar style occur along strike to the southeast and northwest of the Frasergold deposit in the same belt of Triassic phyllite. The Kusk occurrence (093A 061; Belik, 1988) is located approximately 4 km south-southeast of Frasergold, and the Forks occurrence (093A 092; Howard, 1989) is just south of the east end of Horsefly Lake, approximately 20 km northwest of Frasergold. At both the Forks and Kusk occurrences, like the Frasergold deposit, Au occurs in variably deformed and boudinaged quartz veins within grey carbonaceous phyllite with iron-carbonate porphyroblasts. Collectively, these occurrences and the Frasergold deposit define a mineralized corridor that is nearly 35 km long.

Discussion

If the S_1 and S_2 fabrics at Frasergold can be convincingly demonstrated to be related across the CGD, then the Frasergold veins could be comparable to the early, deformed sets of pyrite-quartz veins observed at Spanish Mountain and the quartz-carbonate-muscovite veins that predate main phases of Au veining in the Wells-Barkerville area, which are also widespread in other lode-Au trends in the Barkerville terrane. Alternatively, if D_1 and D_2 deformation events and associated fabrics (S_1 , S_2 , L_2) that are recorded across the CGD are not coeval and instead are progressively transgressive across the area, the Frasergold mineralization may be coeval with other generations of veining, or potentially may represent a separate mineralizing event that is not manifested in other parts of the district. The former is considered most likely, since the Eureka Peak syncline and its associated fabrics can be traced continuously to the northwest to the Spanish Mountain area by



Bloodgood (1987, 1992), and the existing K-Ar age is similar to the ages of earliest mineralization in the Wells-Barkerville area.

Ongoing Dating, Petrographic and Isotopic Studies at Frasergold

A K-Ar age of 151 ± 5 Ma was reported by Panteleyev et al. (1996) for sericite from a mineralized quartz vein at the Frasergold occurrence. This is similar to $^{40}\text{Ar}/^{39}\text{Ar}$ ages obtained for mica grains from metamorphic rocks and early deformed quartz veins in the Wells-Barkerville area (discussed above), which would be consistent with the mineralized veins at Frasergold being older than most of the Au-bearing veins in the Wells-Barkerville area. This age remains to be corroborated by $^{40}\text{Ar}/^{39}\text{Ar}$ dating. During the fieldwork, a representative suite of samples for $^{40}\text{Ar}/^{39}\text{Ar}$ dating ($n = 5$) was collection from both underground and surface exposures and from drillcore, which included muscovite from veins, in vein selvages and from surrounding wallrock. Mineralized samples for the sulphide Pb isotope and detailed petrographic studies were also collected and will be analyzed as the project progresses.

Discussion: Initial Conclusions and Outstanding Questions

Our new $^{40}\text{Ar}/^{39}\text{Ar}$ ages from the Wells-Barkerville area indicate that early, deformed quartz veins were emplaced some time between 146.6 and 155.2 Ma, whereas both Au-bearing pyritic replacement deposits and extensional veins formed in the range of 138.5–147.6 Ma in latest Jurassic to earliest Cretaceous time. If these vein systems formed during, and in the waning stages of D_2 deformation as is interpreted, then these ages not only date the formation of the Au deposits and occurrences in the region but also constrain the timing of the D_2 event in the Barkerville terrane.

We recognize a separate deformation event in the Spanish Mountain area that occurred between the regionally defined D_1 (phase 1) and D_2 (phase 2) foliation forming events. Although an additional phase of folding between D_1 and D_2 has not been recognized in the Wells-Barkerville area, the intensity of the D_2 event in that area is sufficiently

high that evidence for it may be obscured by overprinting deformation.

Although isotopic age data has not yet been obtained for Au-bearing veins in the Spanish Mountain area, the Au-bearing veins there exhibit similar geometries and timing relationships as vein systems in the Barkerville terrane. Based on similarities in vein style, orientations and suggested kinematics, and timing with respect to the dominant foliations, it is speculated that the Au-bearing extensional veins in the Wells-Barkerville area and the Spanish Mountain area occurred at the same time, probably in waning stages of D_2 , and in response to shortening to the northeast, during initial formation of the north-trending dextral faults. Gold-bearing veins in the Frasergold area are clearly older than those at Spanish Mountain, but it is permissible that they formed at the same time as the early, deformed and locally Au-bearing quartz veins in the Wells-Barkerville area, and the early pyrite-quartz mineralization at Spanish Mountain. Although clearly related to discordant late faults in many parts of the Barkerville terrane, the commonly stratabound nature to these quartz veins also suggests a form of combined structural-stratigraphic control, where waning activity on D_2 thrusts could have contributed to the distribution of mineralized corridors within which discordant faults may have localized vein mineralization early in their history during a change in tectonic conditions.

Throughout most of the CGD, Au mineralization occurs dominantly in or associated with quartz veins, but the Wells-Barkerville area and Spanish Mountain deposit demonstrate their potential association with earlier, more sulphide-rich types of mineralization. If these early styles of mineralization are genetically related to the younger quartz-vein sets, they suggest that these deposits define zones of long-lived hydrothermal fluid flow that exploited common, but evolving fluid channelways. If so, the different styles of mineralization may reflect temporal changes in fluid composition, strain state, paleodepth and temperature spanning regional D_2 deformation. The spatial association also suggests the potential for early sulphide-rich styles of mineralization in areas where only quartz-vein deposits have been explored for thus far. It might be expected that

Figure 14: Style of deformed vein systems in the Frasergold deposit: **a)** stratabound nature of deformed quartz veins in outcrop near Grouse Creek; the S_2 foliation is parallel to the rock hammer, and axial planar to folds of the veins; view northwest; **b)** folded, concordant extensional veins; view southeast in underground workings, field of view 2 m; **c)** a banded, southwest-dipping discordant vein, at the lower right, is joined in its hangingwall by folded, narrower semiconcordant quartz extensional veins; although folded by F_2 folds, the veins in the hangingwall of the larger vein display geometries compatible with development as sigmoidal extensional-vein arrays in the hangingwall of a larger shear vein; view northwest in underground workings; **d)** larger, steeply dipping 0.5 m wide white quartz veins with Au-bearing orange-brown iron-carbonate+pyrite bands; view southeast in underground workings; larger, 15–50 cm thick quartz-carbonate veins (Figure 14c) that are developed at moderate to high angles to S_0/S_1 are also associated with the concordant veins; these generally have higher iron-carbonate content than the smaller concordant veins, but contain the same blocky recrystallized white quartz fill; although thicker than the other veins, these veins are also discontinuous and may terminate laterally or vertically. These thicker veins are openly folded by folds with axial-planar S_2 foliation; highest grades (>3 g/t Au) commonly occur associated with the larger veins where they contain most abundant clots of iron-carbonate+pyrite, which may be aligned in discontinuous lenses of bands parallel to vein walls (Figure 14c); Au occurs both as relatively coarse, free grains associated with masses of iron-carbonate, pyrite and/or pyrrhotite within the veins and also as fine grains within quartz near vein margins.

these earlier pyritic forms of mineralization could vary in style depending on the hostrock, as is demonstrated by the variation from pervasive replacement of limestone seen at the Island Mountain and Mosquito deposits, to the coalescing series of pyritic veinlets with disseminated pyrite that comprises the siltstone-hosted Bonanza Ledge zone. If so, if more calcareous units are present in the Spanish Mountain stratigraphy, it is possible that these might also be preferentially replaced by pyrite associated with the early mineralizing event there.

Regional Indicators for Au Mineralization in the CGD

Carbonate alteration is widespread in all three Au-bearing areas that have been examined in the CGD. At Frasersgold and Spanish Mountain, mineralized zones are characterized by the presence of distinctive 'knotted' schist textures caused by the presence of abundant iron-carbonate porphyroblasts. These porphyroblasts formed relatively early in the structural evolution of each area (syn-D₁ or early D₂). At Spanish Mountain, the carbonate porphyroblasts are widespread and extend well beyond mineralization, but they may reflect a broad peripheral effect to the alteration associated with the early pyrite-quartz mineralization. The porphyroblasts at Frasersgold, however, could potentially represent an alteration effect related to the emplacement of the Au-bearing veins, since both the veins and the porphyroblasts formed early. It is interesting to note that very similar iron-carbonate porphyroblasts are closely associated with deformed Au-bearing quartz veins at both the Kusk Au occurrence 4 km to the south of Frasersgold and the Forks occurrence 20 km to the northwest. 'Knotted' schist fabrics have not been reported thus far from any other localities within the Triassic black phyllite; thus this could represent a useful field criterion for identifying potentially Au-bearing zones in the region.

Rusty brown iron-carbonate alteration, commonly associated with disseminated pyrite, is also commonly associated with Au-bearing veins in the Wells-Barkerville area, where it occurs pervasively, often affecting feldspar in sandstone and siltstone beds and laminations over broad portions of the sequence surrounding the areas of veining in the Cariboo Gold Quartz and Island Mountain mines. Much of the fine-grained carbonaceous grey phyllite in the Wells area have no visible alteration if coarser beds are not present, except for local areas of carbonate and/or pyrite porphyroblast development.

In most of the lode-bearing portions of the Barkerville terrane, mineralization in late quartz veins and replacement mineralization are spatially associated with sets of early, deformed and boudinaged quartz-carbonate-muscovite veins. These are also abundant between Yanks Peak and Lightning Creek, where thick, blocky early quartz vein rub-

ble is commonly exposed on ridgetops and in alpine areas, linking the Au-bearing domains at Yanks Peak and Lightning Creek. These associations suggest that quartz vein generations of all types, even if not significantly Au bearing, may be indicators of nearby, or along-strike areas of Au mineralization associated with later generations of quartz-vein mineralization.

Possible Role of Intrusions in Au Mineralization

Although all of the mineralization in the CGD is considered to be orogenic in style, intrusive rocks are present in the vicinity of Au mineralization in both the Spanish Mountain area and the Wells-Barkerville area. At Spanish Mountain, mafic (?) to felsic sill complexes dated at 185–187 Ma are spatially associated with the main mineralized area. The intrusions predate all deformation phases in the area and have been overprinted by the late carbonate-fuchsite alteration that appears to be associated with the mineralization. It is interesting, however, to note that the intrusions also coincide spatially with iron-carbonate porphyroblast development, raising the possibility that porphyroblast development, and possibly an early introduction of Au into the sedimentary sequence in this area, may have been associated with the emplacement of Early Jurassic intrusions. However, there is no evidence at this point for intrusions of this age in any of the other areas of iron-carbonate porphyroblast development and Au mineralization elsewhere in the Triassic black phyllite package (e.g., Frasersgold).

Although both predeformation (Proserpine intrusions) and postdeformation (rhyolite and lamprophyre dikes) intrusions have been recognized in the Wells-Barkerville area, it seems unlikely that either of these intrusive events is related to the Au mineralization, although isotopic dating of the younger set of intrusions is now underway to test this.

Some of the problems that the authors are tackling in the CGD also bear directly on the origin of orogenic Au deposits globally. Work that is currently underway in two of the other main Phanerozoic orogenic Au districts in the world (Klondike Au belt, Yukon and Otago schist belt, New Zealand) by Mortensen and collaborators from the University of Otago (MacKenzie et al., 2007; Mortensen et al., unpublished data) has clearly demonstrated that at least two distinct end-members of orogenic Au deposits can be recognized on the basis of the source of metals and fluids involved. In the Otago schist belt in New Zealand, it has been shown convincingly that metals and fluids that formed orogenic Au veins were derived by metamorphic dehydration reactions across the greenschist-amphibolite facies transition at considerable depth beneath the mineralized region (e.g., Pitcairn et al., 2007). This is the most common genetic model for orogenic Au deposits espoused in the re-

cent literature (e.g., Goldfarb et al., 2005). In the Klondike Au district in western Yukon, however, MacKenzie et al. (2008) and Mortensen (unpublished data) have shown that the metals contained within orogenic veins in that area are locally derived from a distinctive package of submarine felsic metavolcanic rocks that contain small, precious-metal-enriched VMS occurrences, and host or immediately underlie the vein systems. Vein-hosted Au mineralization in the Wells-Barkerville area closely resembles that in the Klondike Au district, and the intimate association between clusters of Au-bearing quartz veins and Au-rich hostrocks in different parts of the CGD (Au-bearing pyritic mantos in the Wells-Barkerville area and disseminated Au in altered metaclastic rocks at Spanish Mountain) argues that the CGD likely has more in common with the Klondike Au district than with the Otago schist belt.

Dunne et al. (2001) carried out a reconnaissance level fluid inclusion study of Au-bearing quartz veins in the Wells-Barkerville area. An extensive suite of samples of vein quartz for fluid inclusion analysis was collected from throughout the CGD during the course of the 2008 fieldwork program. These samples will form the basis for a fluid chemistry study that is currently planned of Au-bearing veins in the Barkerville terrane and lower portions of the Quesnel terrane by Mortensen and colleagues from the University of Leeds. In addition, compositional data for placer- and lode-Au samples from throughout the CGD that were reported by McTaggart and Knight (1993) are currently being reinterpreted and additional compositional work on the McTaggart and Knight sample suite is underway. This will include work on additional lode-Au samples that were collected during 2008.

There are some outstanding questions regarding lode-Au deposits and potential in the CGD:

What are the absolute ages of, and relationships between, Au-bearing veins and earlier pyrite mineralization in the CGD?

If related, are they part of a coeval or temporally transgressive mineralizing event across the district now exposed at different structural levels?

What are the ages of Au-bearing veins at the Frasersgold deposit, and are they related to older forms of mineralization that are observed elsewhere in the district?

What are the specific structural controls on mineralization in each of these areas, and is there evidence for interaction between late D₂ thrust activity and younger faults that localized mineralization?

What is the nature and source of the metals and mineralizing fluids in each camp?

The authors' ongoing research in the CGD is directed at these and other key questions. It is believed that resolving these questions will provide valuable new insights into the nature and origin of Au in the CGD, and will result in new

exploration criteria that can be applied to ongoing exploration efforts not only within the CGD, but also elsewhere in BC.

Acknowledgments

This project is funded by Geoscience BC with matching support from Hawthorne Gold Corporation, Skygold Ventures Ltd. and International Wayside Gold Mines Ltd. The authors are extremely grateful for the hospitality, logistical support and access provided by all three of these companies during the fieldwork component of this study that was conducted in August. F. Callaghan of International Wayside Gold Mines Ltd. is particularly thanked for funding the use of a helicopter, which allowed the authors to access areas within the Barkerville terrane that would otherwise have been inaccessible during the duration of the fieldwork program. Rhys and Ross also would like to acknowledge the companies' permission to draw from the results of previous consulting work they conducted in the region. The manuscript has benefited from editorial reviews by J. Logan and B. Singh.

References

- Alldrick, D.J. (1983): The Mosquito Creek mine, Cariboo gold belt (93H/4); *in* Geological Fieldwork 1982, BC Ministry of Energy, Mines and Petroleum Resources, Paper 1983-1, p. 99–112.
- Andrew, A., Godwin, C.I. and Sinclair, A.J. (1983): Age and genesis of Cariboo gold mineralization determined by isotope methods (93H); *in* Geological Fieldwork 1982, BC Ministry of Energy, Mines and Petroleum Resources, Paper 1983-1, p. 305–313.
- Ash, C.H. (2001): Relationship between ophiolites and gold-quartz veins in the North American Cordillera; BC Ministry of Energy, Mines and Petroleum Resources, Bulletin 108, 140 p.
- Belik, G.D. (1988): Percussion drilling report on the Kusk 5 and Kusk A mineral claims, Cariboo Mining Division, British Columbia; BC Ministry of Energy, Mines and Petroleum Resources, Assessment Report 18 025, 12 p.
- Benedict, P.C. (1945): Structure at the Island Mountain mine, Wells, British Columbia; Transactions, Canadian Institute of Mining and Metallurgy, v. 48, p. 755–770.
- Bloodgood, M.A. (1987): Deformational history, stratigraphic correlations and geochemistry of eastern Quesnel Terrane rocks in the Crooked Lake area, central British Columbia, Canada; M.Sc. thesis, University of British Columbia, 165 p.
- Bloodgood, M.A. (1992): Geology of the Eureka Peak and Spanish Lake map areas, British Columbia; BC Ministry of Energy, Mines and Petroleum Resources, Paper 1990-3, 36 p.
- Delancey, P. (1988): 1987 Cunningham Creek property report; British Columbia; BC Ministry of Energy, Mines and Petroleum Resources, Assessment Report 17 114, 26 p.
- Dunne, K.P.E., Ray, G.E. and Webster, I.C.L. (2001): Preliminary fluid inclusion study of quartz vein and massive banded stringer pyrite mineralization in the Barkerville gold camp, east-central British Columbia; *in* Geological Fieldwork

- 2000, BC Ministry of Energy, Mines and Petroleum Resources, Paper 2001-1, p. 169–190.
- Ferri, F. and Friedman, R.M. (2002): New U-Pb and geochemical data from the Barkerville subterrane; *in* Slave-northern Cordillera Lithospheric Evolution (SNORCLE) Transect and Cordilleran Tectonics Workshop meeting, LITHOPROBE Report 82, p. 75–76.
- Ferri, F. and Schiarizza, P. (2006): Reinterpretation of the Snowshoe Group stratigraphy across a southwest-verging nappe structure and its implications for regional correlations within the Kootenai Terrane; *in* Paleozoic Evolution and Metallogeny of Pericratonic Terranes at the Ancient Pacific Margin of North America, M. Colpron and J.L. Nelson (ed.), Canadian and Alaskan Cordillera: Geological Association of Canada, Special Paper 45, p. 415–432.
- Ferri, F., Höy, T. and Friedman, R.M. (1999): Description, U-Pb age and tectonic setting of the Quesnel Lake gneiss, east-central British Columbia; *in* Geological Fieldwork 1998, BC Ministry of Energy, Mines and Petroleum Resources, Paper 1999-1, p. 69–80.
- Godwin, C.I. and Sinclair, A.J. (1982): Average lead isotope growth curves for shale-hosted zinc-lead deposits, Canadian Cordillera; *Economic Geology*, v. 77, p. 675–690.
- Goldfarb, R.J., Baker, T., Dube, B., Groves, D.I., Hart, C.J.R. and Gosselin, P. (2005): Distribution, character, and genesis of gold deposits in metamorphic terranes; *in* Economic Geology 100th Anniversary Volume, J.W. Hedenquist, J.F.H. Thompson, R.J. Goldfarb and J.P. Richards (ed.), Society of Economic Geologists, Inc., p. 407–450.
- Goodall, G. and Campbell, K. (2007): Summary report and exploration potential on the Frasergold Project; NI43-101 Report for Hawthorne Gold Corporation, 51 p.
- Hall, R. D. (1999): Cariboo gold project at Wells, British Columbia; International Wayside Gold Mines Limited, URL <http://www.wayside-gold.com/i/pdf/RHall_report.pdf> [November 2008], 52 p.
- Holland, S.S. (1954): Geology of the Yanks Peak–Roundtop Mountain area, Cariboo District, British Columbia; BC Ministry of Energy, Mines and Petroleum Resources, Bulletin 34, 102 p.
- Howard, D.A. (1989): Geological, diamond drilling and trenching results from the 1988 exploration program on the Forks 1-4, AR 1-2, TEP 1-3 claims, Cariboo Mining Division, MacKay River District, British Columbia; BC Ministry of Energy, Mines and Petroleum Resources, Assessment Report 18 471, 45 p.
- Johnston, W.A. and Uglow, W.L. (1926): Placer and vein deposits of Barkerville, Cariboo District, British Columbia; Geological Survey of Canada, Memoir 149, 246 p.
- Levson, V.M. and Giles, T.R. (1993): Geology of Tertiary and Quaternary gold-bearing placers in the Cariboo region, British Columbia (93A, B, G, H); BC Ministry of Energy, Mines and Petroleum Resources, Bulletin 89, 202 p.
- Logan, J., (2008): Geology and mineral occurrences of the Quesnel Terrane, Cottonwood map sheet, central British Columbia (NTS 093G/01); *in* Geological Fieldwork 2007, BC Ministry of Energy, Mines and Petroleum Resources, Paper 2008-1, p. 69–86.
- MacKenzie, D., Craw, D. and Mortensen, J.K. (2007): Structural controls on orogenic gold mineralisation in the Klondike goldfield, Canada; *Mineralium Deposita*, doi:10.1007/s00126-007-0173-z.
- MacKenzie, D., Craw, D., Mortensen J.K. and Liverton, T. (2008): Disseminated gold mineralization associated with orogenic veins in the Klondike schist, Yukon; *in* Yukon Exploration and Geology 2007, D.S. Emond, L.R. Blackburn, R.P. Hill and L.H. Weston (ed.), Yukon Geological Survey, p. 215–224.
- McTaggart, K.C. and Knight, J. (1993): Geochemistry of lode and placer gold of the Cariboo District, B.C.; BC Ministry of Energy, Mines and Petroleum Resources, Open File 1993-30, 24 p.
- Mortensen, J.K., Ghosh, D. and Ferri, F., 1995, U-Pb age constraints of intrusive rocks associated with Copper-Gold porphyry deposits in the Canadian Cordillera; *in* Porphyry Deposits of the Northwestern Cordillera of North America, T.G. Schroeter (ed.), CIM Special Volume 46, p. 142–158.
- Mortensen, J.K., Montgomery, J.R. and Phillipone, J. (1987): U-Pb zircon, monazite and sphene ages for granitic orthogneiss of the Barkerville Terrane, east-central British Columbia; *Canadian Journal of Earth Sciences*, v. 24, p. 1261–1266.
- Panteleyev, A., Bailey, D.G., Bloodgood, M.A. and Hancock, K.D. (1996): Geology and mineral deposits of the Quesnel River–Horsefly map area, central Quesnel Trough, British Columbia (NTS map sheets 93A/5, 6, 7, 11, 12, 13; 93B/9, 16; 93G/1; 93H/4); BC Ministry of Energy, Mines and Petroleum Resources, Bulletin 97, 156 p.
- Pickett, J.W. (2001): Diamond drilling and geochemical soil sampling report on a portion of the IGM Group of mineral claims; BC Ministry of Energy, Mines and Petroleum Resources, Assessment Report 26 492, 57 p.
- Pitcairn, I.K., Teagle, D.A.H., Craw, D., Olivo, G.R., Kerrich, R.T. and Brewer, T.S. (2007): Sources of metals and fluids in orogenic gold deposits: insights from the Otago and Alpine schists, New Zealand; *Economic Geology*, v. 101, p. 1525–1546.
- Ray, G.E., Webster, I.C.L., Ross, K. and Hall, R. (2001): Geochemistry of auriferous pyrite mineralization at the Bonanza Ledge, Mosquito Creek mine and other properties in the Wells-Barkerville area, British Columbia; *in* Geological Fieldwork 2000, BC Ministry of Energy and Mines, Paper 2001-1, p. 135–167.
- Rees, C.J. (1987): The Intermontane-Omineca Belt boundary in the Quesnel Lake area, east-central British Columbia: tectonic implications based on geology, structure and paleomagnetism; Ph.D. thesis, Carleton University, 421 p.
- Rhys, D.A. and Ross, K.V. (2001): Evaluation of the geology and exploration potential of the Bonanza Ledge zone, and adjacent areas between Wells and Barkerville, east-central British Columbia; internal company report prepared for International Wayside Gold Mines Ltd., URL <<http://www.wayside-gold.com/i/pdf/Rhys-Ross-2001.pdf>> [November 2008], 110 p.
- Richards, F. (1948): Cariboo Gold Quartz mine; *in* Structural Geology of Canadian Ore Deposits, Canadian Institute of Mining and Metallurgy, p. 162–168.
- Robert, F. and Taylor, B.E. (1989): Structure and mineralization at the Mosquito Creek gold mine, Cariboo District, B.C.; *in* Structural Environment and Gold in the Canadian Cordillera, Geological Association of Canada, Cordilleran Section, Short Course no. 14, p. 25–41.
- Ross, K.V. (2006): Petrographic study of the Spanish Mountain project, Cariboo Mining District; internal company report prepared for Skygold Ventures Ltd., 64 p.

- Schiarizza, P. (2004): Bedrock geology and lode gold occurrences, Cariboo Lake to Wells, British Columbia, parts of NTS 93A/13, 14; 93H/3, 4; BC Ministry of Energy, Mines and Petroleum Resources, Open File 2004-12, 1:100 000 scale.
- Schiarizza, P. and Ferri, F. (2003): Barkerville Terrane, Cariboo Lake to Wells: a new look at stratigraphy, structure and regional correlations of the Snowshoe Group; *in* Geological Fieldwork 2002, BC Ministry of Energy, Mines and Petroleum Resources, Paper 2003-1, p. 79–96.
- Skerl, A.C. (1948): Geology of the Cariboo Gold Quartz mine; *Economic Geology*, v. 43, p. 571–597.
- Singh, B. (2008): Technical report on the Spanish Mountain property for Skygold Ventures Ltd.; NI43-101 report filed on SEDAR, 92 p.
- Struik, L.C. (1987): The ancient western North American margin: an Alpine rift model for the east-central Canadian Cordillera; Geological Survey of Canada, Paper 87-15, 19 p.
- Struik, L.C. (1988): Structural geology of the Cariboo Gold Mining District, east-central British Columbia; Geological Survey of Canada, Memoir 421, 100 p.
- Sutherland Brown, A. (1957): Geology of the Antler Creek area, Cariboo District, British Columbia; BC Ministry of Energy, Mines and Petroleum Resources, Bulletin 38, 105 p.
- Termuende, T. (1990): Geological report on the Craze Creek (Cunningham) property for Loki Gold Corporation; BC Ministry of Energy, Mines and Petroleum Resources, Assessment Report 19 793, 21 p. plus maps.
- Yin, J. and Daignault, P. (2007): Report on the 2006 exploration program on the Golden Cariboo project, Wells, B.C.; BC Ministry of Energy, Mines and Petroleum Resources, Assessment Report 28 990, 44 p.

Mineralization and Alteration of Cretaceous Rocks of the Taseko Lakes Region, Southwestern British Columbia (NTS 092O/04)

L. Hollis, Department of Earth and Ocean Sciences, University of British Columbia, Vancouver, BC, lhollis@eos.ubc.ca

L.A. Kennedy, Department of Earth and Ocean Sciences, University of British Columbia, Vancouver, BC

K.A. Hickey, Department of Earth and Ocean Sciences, University of British Columbia, Vancouver, BC

Hollis, L., Kennedy, L.A. and Hickey, K.A. (2009): Mineralization and alteration of Cretaceous rocks of the Taseko Lakes region, southwestern British Columbia (NTS 092O/04); in Geoscience BC Summary of Activities 2008, Geoscience BC, Report 2009-1, p. 71–86.

Introduction

Porphyry copper deposits are the major source of copper in the world today (Titley et al., 1981). They are large hydrothermal systems intimately related to the exsolution of fluids from high in the crust. Tectonic environments, magma composition and crustal environment of emplacement all play a role in determining the metal endowment of these deposits (Richards, 2003). From the distribution of porphyry deposits around the world, it is clear that the magmatic-hydrothermal systems responsible for their genesis occur in pulses restricted in time and space. The western Cordillera of Canada has several large porphyry deposits (e.g., Highland Valley, Galore Creek, Island Copper and Gibraltar), the majority of which are associated with alkaline magmatism and are of Mesozoic age (Lowell and Guilbert, 1970). There are less well-known occurrences of large copper porphyry deposits in other terranes of British Columbia (BC) that are spatially associated with the Coast Plutonic Complex (CPC); the largest of these is the Prosperity deposit (Figure 1). With estimated resources of 9.4 million ounces of gold and 3.5 billion pounds of copper (MINFILE 092O 041; MINFILE, 2008), Prosperity could become BC's largest producing porphyry deposit. The Prosperity deposit is a calcalkaline porphyry characterized by the intrusion of quartz diorite and plagioclase porphyry into surrounding Lower Cretaceous marine shale and marine to nonmarine Lower to Upper Cretaceous andesitic pyroclastic rocks with intercalated massive to porphyritic flows (MINFILE 092O 041; MINFILE, 2008). Occurrences of hydrothermal alteration and mineralization have been found within 25 km of the Prosperity deposit in rocks of a similar age and paleogeographic-tectonic setting. These occurrences lie in the Taseko Lakes area and may represent a tectono-temporal suite of porphyry copper deposits in BC. Acquiring a better understanding of their age,

their tectonic setting and the degree to which they represent magmatic-hydrothermal systems, will make it easier to access these deposits.

This report is a summary of the results of the main author's Geoscience BC-funded M.Sc. study on a porphyry copper deposit and spatially associated hydrothermal showings that lie in rocks of similar age, composition and tectonic setting to those of the Prosperity deposit. The study area is located in southwestern BC, approximately 50 km south of the town of Williams Lake and 25 km south of the well-defined Prosperity copper-gold porphyry deposit (Figure 1).

The main goals of the project are to

- characterize mineralogical and chemical alteration and their paragenetic relationships;
- understand the physicochemical evolution of the hydrothermal systems;
- determine the age of intrusion, alteration and mineralization;
- define the tectonic and geological framework of hydrothermal activity;
- consider the hydrothermal showings' association to other hydrothermal activity in the same belt of rocks; and
- assess the potential for finding another belt of porphyry copper deposits within BC.

The current paper presents results of geological mapping, petrography, $^{206}\text{Pb}/^{238}\text{U}$ and $^{40}\text{Ar}/^{39}\text{Ar}$ geochronology, thermochronology, fluid inclusion analysis and a preliminary stable isotope study. These results indicate that a period of porphyry-related intrusion and mineralization occurred during the Late Cretaceous, around the same time that similar events were taking place in the nearby Prosperity deposit.

Regional Geological Setting

British Columbia is composed of various orogenic belts that are part of a larger geographic area known as the Canadian Cordillera. The Coast Belt forms the core of the lon-

Keywords: porphyry, copper, hydrothermal, Taseko Lakes

This publication is also available, free of charge, as colour digital files in Adobe Acrobat® PDF format from the Geoscience BC website: <http://www.geosciencebc.com/s/DataReleases.asp>.

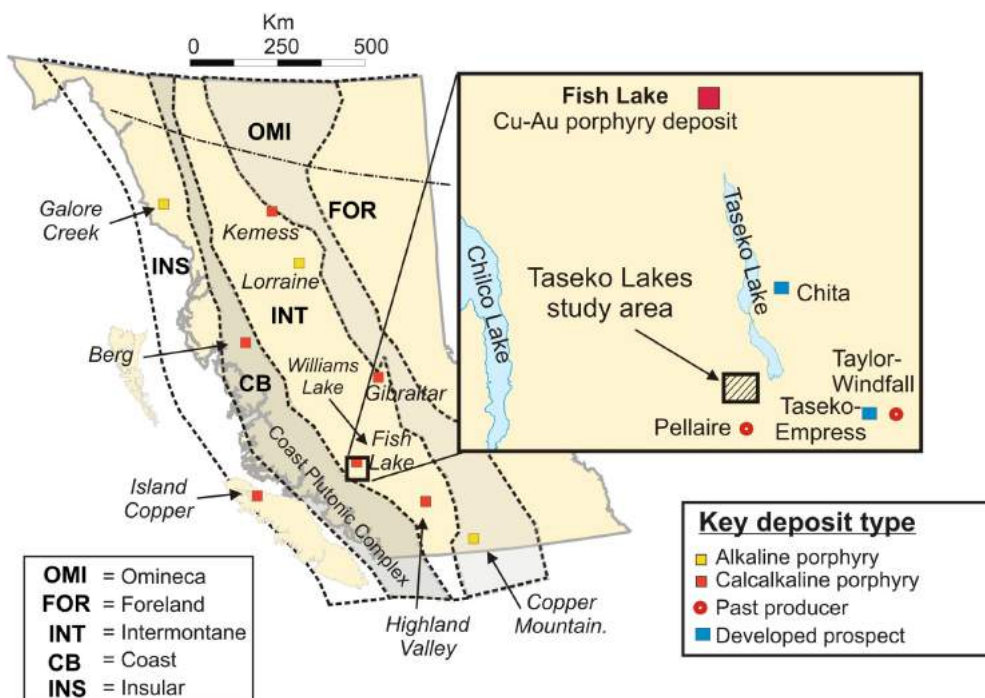


Figure 1. Location of major alkaline and calcalkaline copper porphyry deposits in BC. The inset map shows the location of the Prosperity deposit, past producers Pellaire (gold mine), Taseko-Empress (copper-gold developed prospect) and Taylor Windfall (gold mine), and the Taseko Lakes study area.

gest mountain belt in the western Cordillera (Rusmore and Woodsworth, 1991) and is the suture zone between the Intermontane Belt (to the east) and the Insular Belt (to the west). The Taseko Lakes region of southwest BC is located near the eastern limit of the CPC. It is along this boundary that the Prosperity deposit is located (Figure 1). The batholith is thought to have been produced, from the Jurassic to the Eocene, by the subduction of the Insular Superterrane along the continental margin of North America.

In southwest BC, the Coast Belt is divided into the southwest and southeast Coast belts. The southwest Coast Belt consists of Middle Jurassic to mid-Cretaceous plutonic rocks and Early Cretaceous volcanic rocks. The southeast Coast Belt includes Early Cretaceous arc rocks and clastic rocks. The study area is located within the southeast Coast Belt, and includes rocks that belong to the Cretaceous Tchaikazan River succession and the Powell Creek Formation (Tipper, 1969, 1978; McLaren, 1990; Monger et al., 1994; Schiarizza et al., 1997; Israel, 2001).

Israel (2001) concluded that the study area straddles the boundary between the Gambier arc and the Tyaughton Basin, and suggested that the uplift of Early Cretaceous rocks provided a source of material for the Tyaughton Basin. By mid-Cretaceous time, the plate configuration had changed, leading to dominantly contractional deformation. Dextral strike-slip and contractional fault movements occurred in

the area from the mid-Cretaceous to the Tertiary (Journey and Friedman, 1993; Schiarizza et al., 1997; Israel et al., 2006). During the later Paleocene to Eocene epochs, contractional movement was superseded by dominantly dextral strike-slip movement, forming large-scale faults (e.g., Tchaikazan and Yalakom faults).

Evidence for hydrothermal activity and mineralization is widespread throughout the southeast Coast Belt, highlighted by numerous small metallic showings, developed prospects and altered hostrocks. These are largely associated with, and located proximal to, the intrusions contained within Lower to Upper Cretaceous marine and nonmarine sedimentary and andesitic volcanic rocks, which are particularly well-developed in the Tchaikazan River succession and the Powell Creek Formation.

Local Geology

Rocks in the study area range from Permian to Early Cretaceous in age. The two main units recognized are the Early Cretaceous volcano-sedimentary Tchaikazan River succession and the Late Cretaceous Powell Creek Formation (Figure 2a; McLaren, 1990; Israel, 2001). Several large, north-dipping normal faults are exposed and a large, east-striking thrust sheet, which placed the Tchaikazan River succession on top of the Powell Creek Formation, divides the area. These units host several copper showings, the three largest of which are referred to as Hub, Charlie and Northwest Copper (Figure 2a).

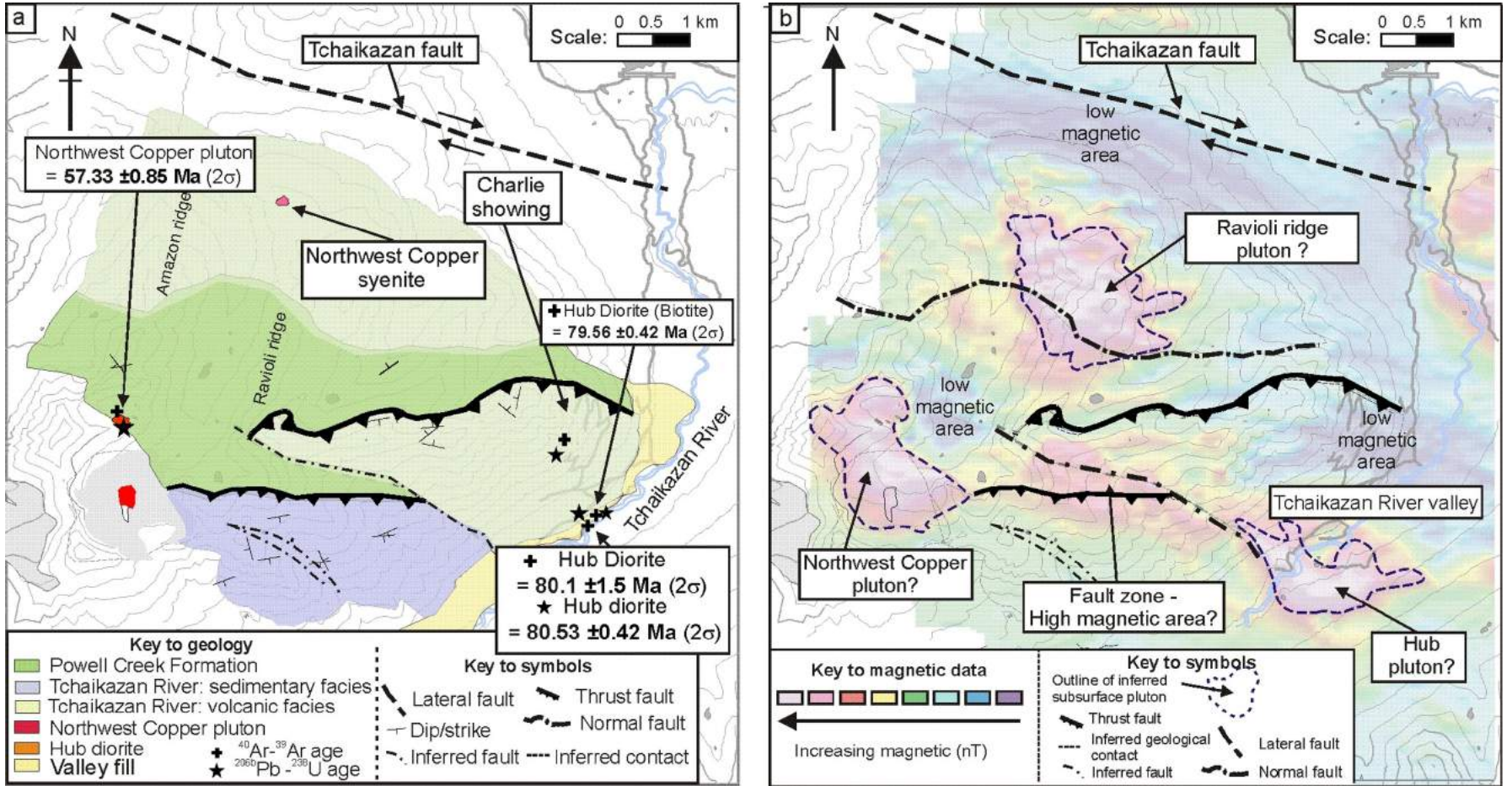


Figure 2. Maps of the Taseko Lakes study area highlighting: **a)** the three mineral showings (Hub, Charlie and Northwest Copper) and the major structural and geological boundaries; **b)** magnetic anomalies that reveal the inferred subsurface extents of igneous bodies.

Lithological Units

Tchaikazan River Succession

The oldest packages of rocks located in the study area are the approximately 1 km thick (Israel, 2001) volcano-sedimentary packages of the Tchaikazan River succession (Figure 2a), which is split into volcanic- and sedimentary-dominated facies. The volcanic facies is characterized by intercalated subaqueous to subaerial volcanic rocks, typically andesitic in composition, and massive andesite flows dominate its upper parts. The sedimentary facies is characterized by marine sedimentary rocks that are highly variable in terms of grain size, bed thickness, structure and rock type (Hollis et al., 2008), including medium to coarse-grained, well-sorted sandstone, conglomerate, siltstone, and mudstone.

Israel (2001) suggested that the Tchaikazan River succession could be as old as 136 Ma, maybe even 146 Ma, and a minimum depositional age is constrained by the Mt. Pilkington intrusion that crosscuts the succession and yields a Pb/U zircon age of 102 ± 2 Ma. The Pb/U dating of zircons for this study yielded ages of 80.7 ± 0.8 Ma and 76.6 ± 0.7 Ma for two feldspar porphyry dikes that crosscut the volcanic facies of the Tchaikazan River succession.

The rocks of the Tchaikazan River succession can be subdivided into three lithological associations: 1) primary volcanic, 2) sedimentary (either volcanic or sedimentary derived) and 3) hypabyssal. Primary volcanic facies are generally the product of effusive volcanic eruption, while hypabyssal intrusions include dikes that are mostly discordant to stratigraphy and sedimentary facies include those formed where volcanic processes have had no influence upon deposition, but can nevertheless comprise volcanic-derived material.

The Tchaikazan River succession likely represents a marine rock sequence deposited near an active arc region. The increase in volcanic material towards the stratigraphic top of the succession suggests a progressive increase in arc-related volcanism. The calcalkaline signatures of the volcanic rocks place them into volcanic arc related and marginal-basin settings.

Powell Creek Formation

The youngest formation in the study area is the Powell Creek Formation, characterized by an extensive package of interbedded, nonmarine, subaerial volcanic and volcanoclastic rocks. Massive volcanic flow units, breccia flows and resedimented volcanoclastic rocks dominate the formation. The Powell Creek Formation is inferred to be at least 93.5 ± 0.8 to 89.3 ± 1 Ma in age (Schiarizza et al., 1997).

The nonhomogeneous facies of the Powell Creek Formation are highly variable, consisting of massive, poorly sor-

ted, matrix-supported volcanoclastic units of sandstone, siltstone and breccia. The predominantly rounded or angular clasts lack chilled margins, vesicle zonation or radial jointing patterns and are internally massive. Differential weathering of clasts to the surrounding matrix material is frequently observed, causing clasts to protrude from the host matrix (Hollis et al., 2006). The andesite clasts are often plagioclase phyric and hosted within an aphanitic, dark maroon andesite.

The Powell Creek Formation shows aspects of mass flow, traction and suspension, yielding resedimented (syneruptive) volcanoclastic deposits. Sand-sized particles likely dominated sedimentation processes during aggradation, as indicated by the presence of large volumes of coarse crystalline material (particularly feldspar and quartz) shed from the surrounding volcanic environment. The weathering, erosion and reworking of volcanic material produced a widespread volcanogenic sedimentary deposit.

Intrusive Rocks

The study area is host to a variety of intrusive rocks, ranging from dikes to larger plutonic bodies, the largest of which is located within the Tchaikazan River valley and is known as the Hub diorite (Figures 2, 3). It is this diorite that hosts much of the porphyry-style mineralization observed at the Hub porphyry deposit (see below).

Hub Intrusive Centre

A suite of several igneous rocks characterizes the Hub porphyry deposit; outcrops are dominated by coarsely crystalline, massive, porphyritic diorite composed of plagioclase (~50%), biotite (10–25%) and hornblende (25%) phenocrysts in an aphanitic, plagioclase-dominated groundmass. The $^{40}\text{Ar}/^{39}\text{Ar}$ (biotite and hornblende) and $^{206}\text{Pb}/^{238}\text{U}$ (zircon) geochronology constrained the age of the Hub diorite to ca. 80 Ma (Figures 3, 4a–c). The Hub diorite is cut by an unmineralized plug of equigranular monzonite as well as by a 5 m wide feldspar-hornblende porphyry dike which, though unmineralized, contains up to 7% pyrite. Samples from this single feldspar-hornblende dike from the intrusive centre yielded an age of ca. 70 Ma. Feldspar porphyry dikes considered to be part of this intrusive centre were also sampled from the Charlie showing area, where they crosscut the Early Cretaceous rocks of the Tchaikazan River succession (see above); these yielded ages of 80.7 ± 0.8 Ma, 77.49 ± 0.97 Ma and 76.6 ± 0.7 Ma (Figure 4–f).

Northwest Copper Intrusive Centre

The youngest intrusive rock in the study area is the Northwest Copper pluton, which is exposed in the western portion of the study area (Figure 2). It is felsic in composition, containing approximately 40% quartz, 30% plagioclase and 30% other minerals, including biotite and hornblende.

This complex intrusion, characterized by several compositional variations, contains numerous round xenoliths of the Powell Creek Formation and crosscutting aplite dikes. The Northwest Copper pluton yielded a Pb/U zircon age of 57.33 ± 0.85 Ma (Figure 4g), while a diorite dike proximal to the Northwest Copper pluton gave a $^{40}\text{Ar}/^{39}\text{Ar}$ hornblende cooling age of 60.01 ± 0.46 Ma (Figure 4h). A small plug of equigranular syenite that occurs on the northern part of Ravioli ridge (Figure 2) comprises >60% anhedral nepheline crystals, 30% quartz and 10% hornblende.

Other Intrusive Rocks

Throughout the study area, numerous feldspar-hornblende dikes of unknown age crosscut the Cretaceous volcanic rocks. These dikes are highly altered and do not appear to be related to the igneous centres, but could be related to the Tchaikazan Rapids pluton (ca. 6 Ma; Israel, 2001), which is found to the north of the study area. Subsurface intrusions are inferred from the aeromagnetic data (Figure 2b). Some magnetic highs correspond well to known intrusive bodies even though they are sitting in volcanic rocks; others are interpreted as representing subsurface intrusions (Figure 2b) that are presumably similar in age to the Hub or Northwest Copper intrusive rocks.

Structure

Thrusts

Large, contractional, north-verging thrust faults placing andesite rocks of the Tchaikazan River succession atop the younger Powell Creek Formation are a dominant feature in the study area. These faults, dipping moderately to the southwest and generally striking east (Figure 2), are characterized by gouge-rich zones that are up to several metres thick. Timing of thrusting is not well constrained, but a sample of fine-grained illite collected from one of these large thrust zones yielded a $^{40}\text{Ar}/^{39}\text{Ar}$ cooling age of 60.53 ± 0.33 Ma (Blevings, 2008).

The northwestern part of the mapped area is dissected by a large normal fault (Figure 2) that juxtaposes the early Tchaikazan River succession next to the Powell Creek Formation; it is inferred to dip steeply to the north and to have a normal offset. The Tchaikazan fault, observed to the north of Ravioli ridge, is a southeast-striking, high-angle, right lateral fault (Figure 2; Israel, 2001). It is the largest structure observed in the area, with a strike length of nearly 200 km and suggested dextral offset of 8 km (Israel, 2001).

Mesoscale striated fault surfaces are common in many parts of the study area, but the lack of good marking units prevents determining the extent of displacement. These fault surfaces are particularly well-developed in the Charlie showing area and around the thrust area, where faults typically dip $>50^\circ$, strike northwest and have unknown ki-

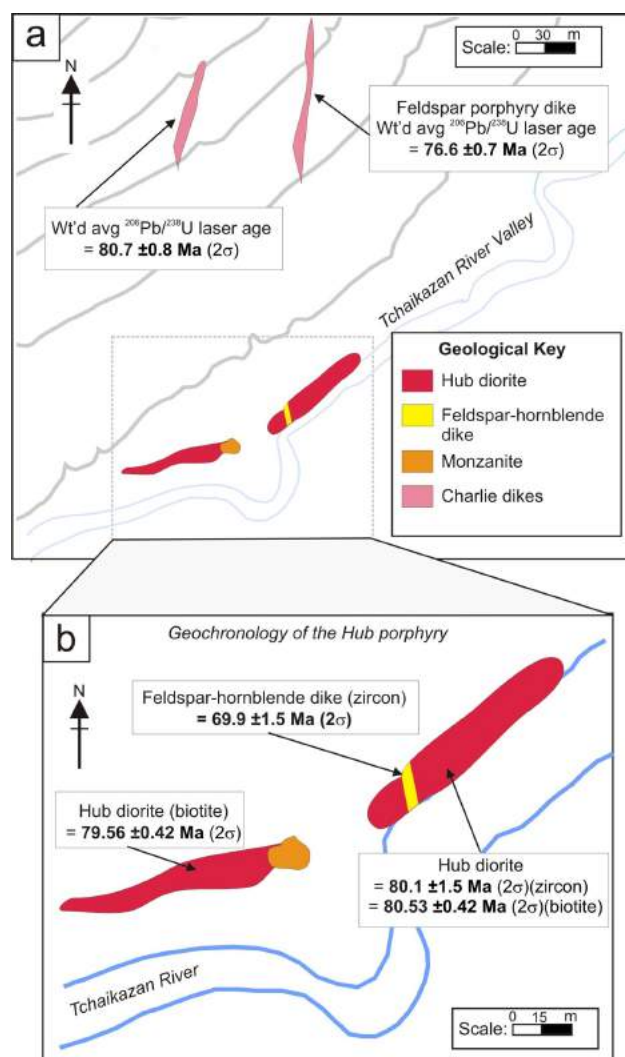


Figure 3. Maps of the Hub porphyry deposit and surrounding Charlie dikes showing: **a)** geological and **b)** geochronological data.

nematics. The fault zones are relatively narrow, steeply dipping to the south ($>60^\circ$) and visible over several tens of metres. Shear zones, brittle fracturing and vein density increase to the northwest of the Tchaikazan River valley.

Character of Alteration and Mineralization

The study area can be divided into three domains showing evidence for hydrothermal alteration referred to as the Hub porphyry, the Charlie showing (where gold-bearing veins were previously reported) and the Northwest Copper showing (where native copper and chalcopyrite-bearing veins have been observed).

Hub Porphyry

The Hub porphyry, hosted in the Hub diorite, is located within the Tchaikazan River valley and exposed along the Tchaikazan River itself (Figures 2, 3). Exposure is generally poor and limited to a few hundred metres along man-

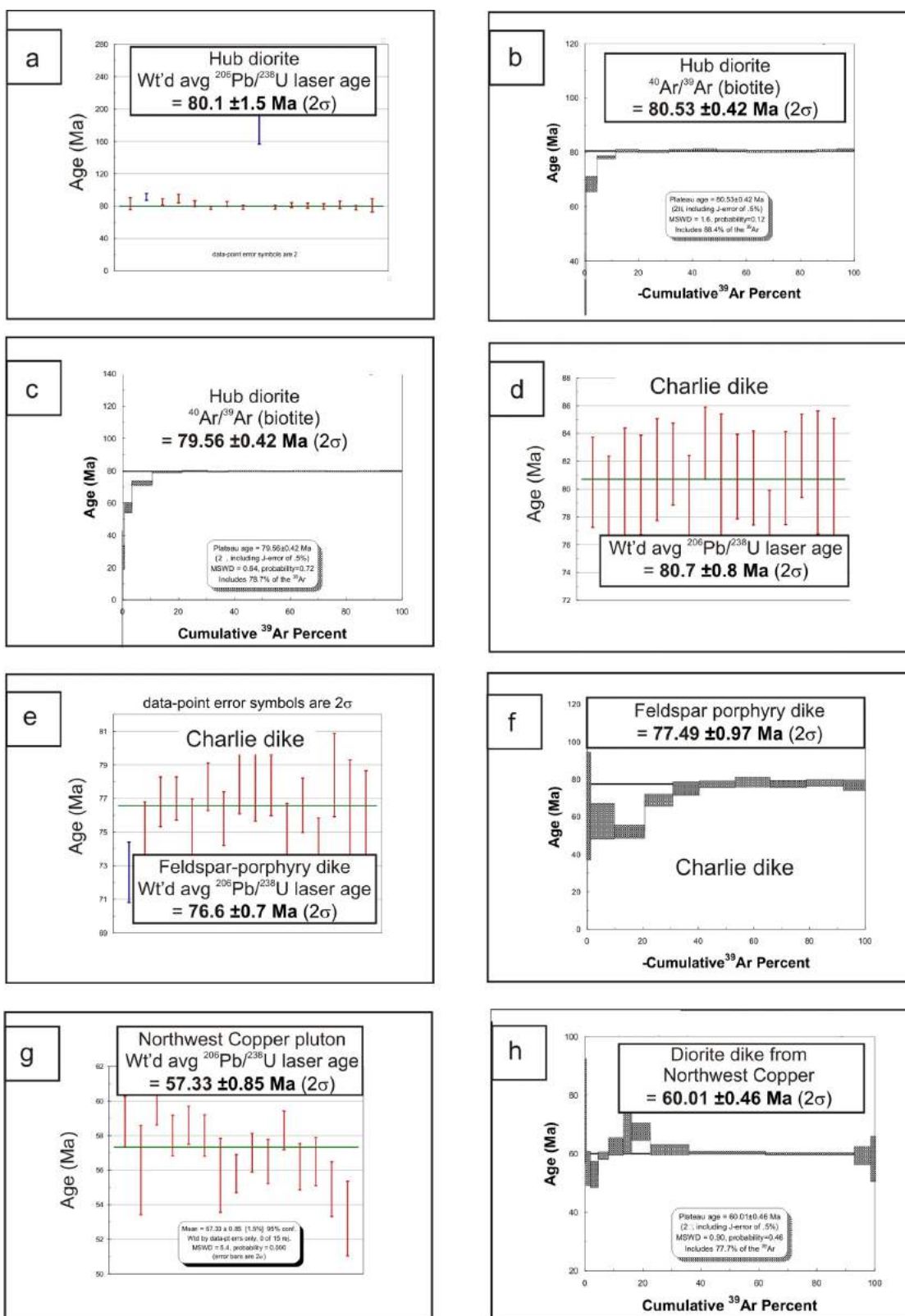


Figure 4. Plots showing geochronological data: **a)** $^{206}\text{Pb}/^{238}\text{U}$ age determination for the Hub diorite; **b)** $^{40}\text{Ar}/^{39}\text{Ar}$ (biotite) age determination for Hub diorite; **c)** $^{40}\text{Ar}/^{39}\text{Ar}$ (biotite) age determination for the diorite phase at the Hub showing; **d)** $^{206}\text{Pb}/^{238}\text{U}$ age determination for the crosscutting dike at Charlie showing; **e)** $^{206}\text{Pb}/^{238}\text{U}$ (zircon) age determination for a similar feldspar porphyry dike at the Charlie showing; **f)** $^{40}\text{Ar}/^{39}\text{Ar}$ (hornblende) cooling age determination for the same dike as in **e)**; **g)** $^{206}\text{Pb}/^{238}\text{U}$ (zircon) age determination for the Northwest Copper pluton; and **h)** $^{40}\text{Ar}/^{39}\text{Ar}$ hornblende cooling age determination for the diorite dike at the Northwest Copper showing.

made geological trenches and to drillcore from four drillholes. Hydrothermal activity is preserved by a phase of hydrothermal breccia and biotite-magnetite alteration, locally intense sericite and propylitic alteration, and chalcopyrite±bornite±molybdenite mineralization.

Alteration

Hydrothermal Breccia

A magnetite-biotite-altered hydrothermal breccia (Figures 5, 6a, b) is volumetrically the second-most prominent rock type observed at the Hub showing, after the dominant diorite phase (see above). Recent drilling has shown the breccia extends to a depth of at least 260 m (Figure 5). The hydrothermal breccia typically consists of ~60% matrix/cement, 30% clast material and 0–10% open space. Fragments are dominated by compositions reflecting the immediate wallrocks, including fine-grained andesite, diorite, quartz-vein fragments (Figure 6c, d) and rare monzonite. Most of the fragments, especially those of diorite and monzonite, are subangular to subrounded and typically measure a few centimetres in diameter; however, it appears that blocks of andesite (metres in size), likely representing

pieces of the host wallrocks, are present within the stratigraphy. The breccia is most common in the upper parts of drillholes, where it forms along the margin of a gently southeasterly (?) dipping sheet of Hub diorite.

Biotite-Magnetite Alteration

Brown, fine-grained biotite is the dominant alteration mineral in the hydrothermal breccia, but it also contains variable amounts of magnetite and quartz (Figure 6). The biotite-magnetite assemblage is confined to the Hub showing. Hydrothermal biotite typically replaces magmatic biotite and hornblende, and is often pseudomorphed by later chlorite.

Sericite Alteration

Sericite partially replaces plagioclase phenocrysts locally within the Hub diorite. Intense sericite alteration is observed within the youngest feldspar-hornblende dike at the Hub showing. Weak to moderate sericite alteration is observed throughout the Hub diorite, where fine-grained sericite selectively replaces plagioclase phenocrysts.

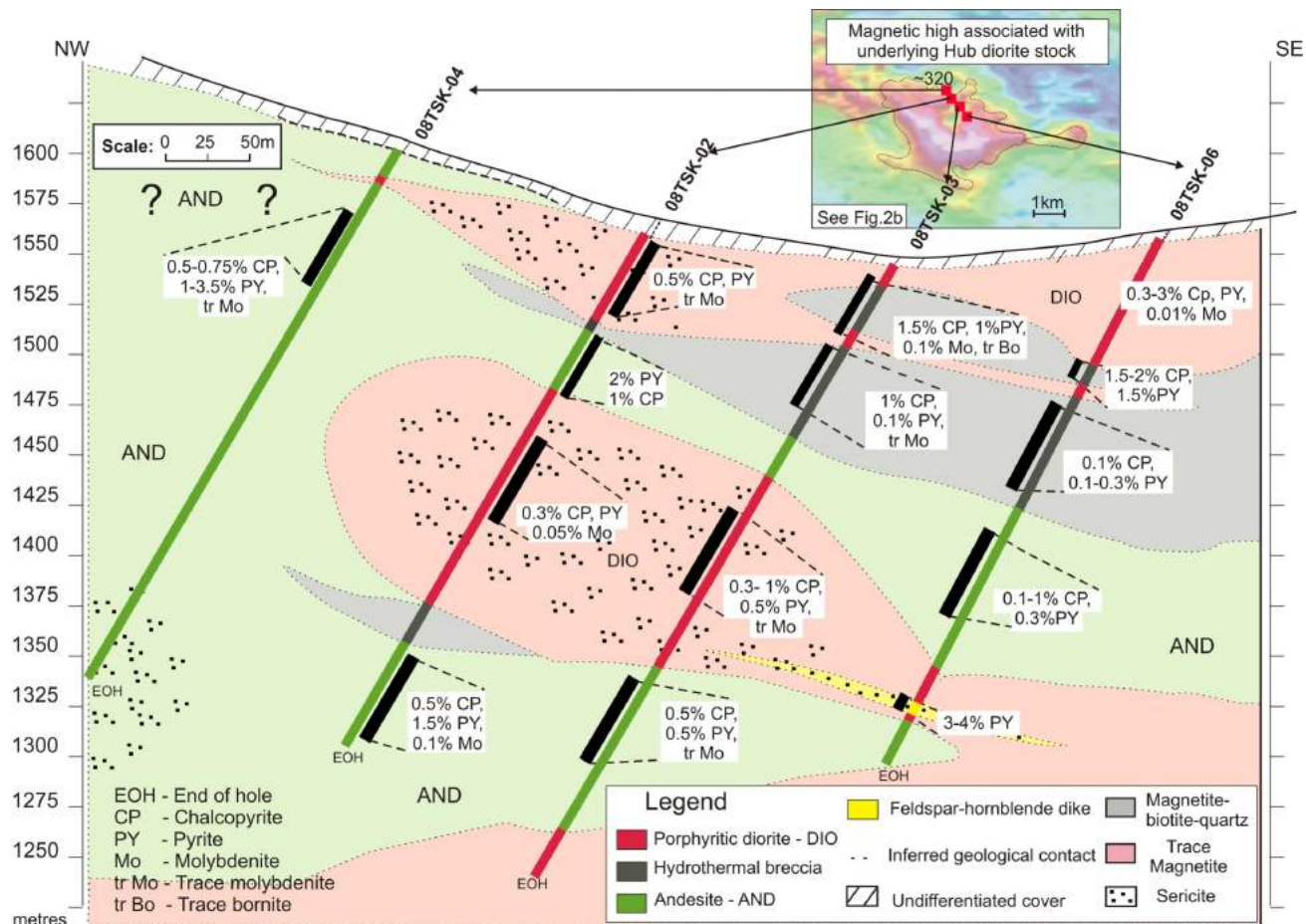
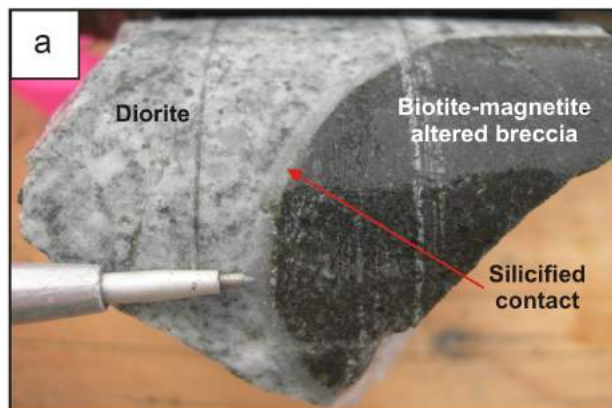


Figure 5. Cross-section of four drillholes from the Hub porphyry looking northeast showing rock types, alteration and mineralization. Inset map shows the inferred magnetic anomaly.

Drillcore



Outcrop

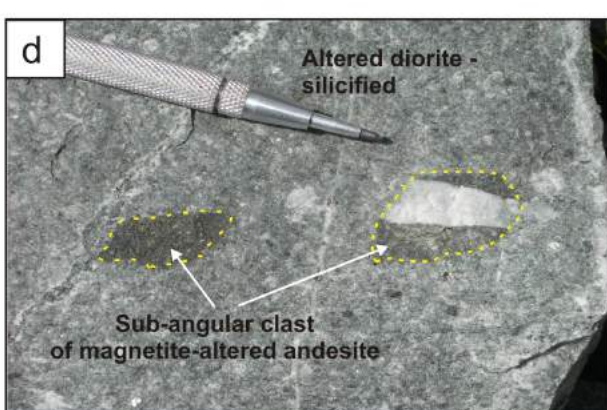
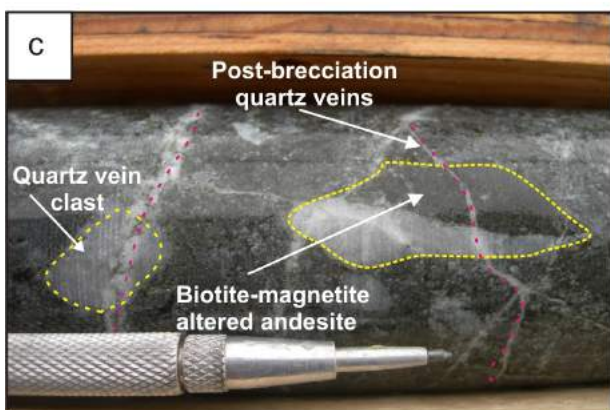


Figure 6. Comparison of features observed from drillcore and outcrop within the magnetite-biotite-altered hydrothermal breccia: **a)** hole 08TSK-02 sample (depth of 100.2 m) showing the contact between the Hub diorite and the hydrothermal breccia; **b)** same relationship as observed in (a) for sample taken from trenches at the Hub showing; **c)** hole 08TSK-06 (depth of 89 m), showing clastic breccia with andesite and quartz vein clasts; and **d)** same textural and compositional relationship as observed in (c).

Chlorite-Epidote (Propylitic) Alteration

Chlorite replaces primary biotite, plagioclase and hornblende locally in the Hub diorite; secondary biotite of the magnetite-biotite alteration is also pseudomorphed by chlorite (see above). Fine-grained epidote alteration is rare. Later chlorite alteration has affected the magmatic, disseminated and vein replacement biotite in the potassic alteration zone.

Mineralization

The Hub porphyry contains copper and molybdenite mineralization. The mineralization takes several forms, including those of sulphide-bearing quartz stockwork veining, disseminated sulphides in the Hub diorite and sulphide phases as cement in the hydrothermal breccia. Chalcopyrite, bornite, molybdenite and galena are among the common sulphide mineral assemblages observed. Disseminated chalcopyrite, pyrite and rare bornite and galena were observed within rocks of the Hub diorite and the hydrothermal breccia. Disseminated sulphides are typically <1 mm in size and located within the groundmass of the rock.

Massive quartz veins containing sulphide minerals, consisting of pyrite, chalcopyrite, molybdenite and rare bornite and galena, are common. The sulphides are often massive in form, with the most commonly observed sulphide assemblage consisting of pyrite and chalcopyrite. Molybdenite is rarely seen in close association with chalcopyrite, but stringers of molybdenite are found locally in association with large quartz veins (>5 cm thick) throughout the drillcore. Fracture-coats of fine-grained molybdenite were observed in the Hub diorite. In the hydrothermal breccia, chalcopyrite and pyrite exhibit void-filling or interstitial textures.

Stable Isotope Results

A total of four quartz veins and one magnetite vein were sampled using standard mean ocean water (SMOW) analysis. The quartz veins typically hosted chalcopyrite mineralization and measured up to 1 cm in thickness. The suite of quartz veins from the Hub diorite displayed $\delta^{18}\text{O}$ (SMOW) rock values ranging from 8.7 to 10.3, while the magnetite vein yielded a $\delta^{18}\text{O}$ rock value of 3.4. These values corre-

late with typical values for hydrothermal fluids derived from a magmatic source.

Depth of Emplacement

The evolution of porphyry copper deposits is strongly affected by the depth of emplacement and the effect this has on the solubility of volatiles and metals in the hydrothermal fluid. Fluid inclusion samples were prepared from several veins from the Hub diorite, but yielded no independent evidence of pressure and, hence, depth. Instead, low-temperature fission-track thermochronology was used in an attempt to reconstruct the depth at which mineralization occurred, as this technique can provide estimates of exhumation.

A sample of the Hub diorite was collected from the valley base for zircon (ZFT) and apatite (AFT) fission track analysis (Figure 7a, b). A sample from the Hub intrusive complex yielded a ZFT date of 85.6 ± 1.8 Ma, which corresponds to the time of emplacement of the Hub diorite determined from Ar/Ar and Pb/U dating (Figure 3). In the case of geologically realistic exhumation rates, the closure temperature for ZFT is 200–240°C (Reiners and Brandon, 2006). The correspondence between Pb/U, Ar/Ar and ZFT determinations implies that the Hub diorite cooled to below 200–240 °C immediately after emplacement which; for geothermal gradients of 25–30°C/km, would imply an emplacement depth of <6–9 km. The AFT sample yielded a date of 31.4 ± 1.8 Ma, a result significantly younger than the Hub diorite; this sample is therefore thought to be a product of exhumation rather than cooling of the pluton. A closure temperature of ~90–120°C and a geothermal gradient of 25°C/km would correspond to a depth of 3–4 km at 31 Ma.

Five additional samples of Cretaceous intrusive rocks from differing elevations were also collected for AFT analysis to assess age-elevation relationships (Figure 7a, b). All six samples produced a near-linear age-elevation relationship corresponding to an average exhumation rate of 40 m/Ma over a period of 55–30 Ma (Figure 7a). This average exhumation rate would imply that the present exposure of the Hub porphyry was at an approximate depth of 5 km at 55 Ma; if the same exhumation rate continued back to the time of emplacement, it would imply an approximate depth of 6 km (Figure 7c). Comparatively, the estimated stratigraphic thickness of the units above the emplacement depth of the Hub porphyry into the Tchaikazan River succession is estimated as ~5 km, an estimate consistent with the AFT result.

Charlie and Northwest Copper Showings Area

This area is located to the northwest of the Hub porphyry (Figure 2). Hydrothermal alteration is variably developed across this area, as are several small polymetallic showings (the range of alteration types is discussed below). Most of the andesite rocks of the area display primary assemblages of plagioclase and hornblende.

Alteration

‘Propylitic’ Alteration

A chlorite-epidote±calcite–alteration assemblage is widespread throughout the andesitic units of the Charlie and Northwest Copper showings (Figure 8). Typically, these alteration minerals replace primary igneous phases, such as hornblende, biotite and plagioclase (Figure 9a–c). It is difficult to know whether this replacement is related to a regional, low-temperature metamorphic event, or whether it is a distal, lower temperature ‘propylitic’ component of the magmatic-hydrothermal porphyry system.

Intense Epidote (Ca) Alteration

Strong epidote alteration and vein epidote is most commonly found proximal to large-scale faults, particularly in the area of the Northwest Copper showing (Figure 8). Epidote typically replaces mafic phenocrysts of the andesite rocks assigned to the Tchaikazan River succession and Powell Creek Formation. Fine-grained, massive epidote pods and vein epidote are located near the Northwest Copper pluton (see above). Interestingly, garnet was found in an isolated sample within this alteration assemblage, which suggests the presence of higher temperature calcic alteration components.

Sericite Alteration

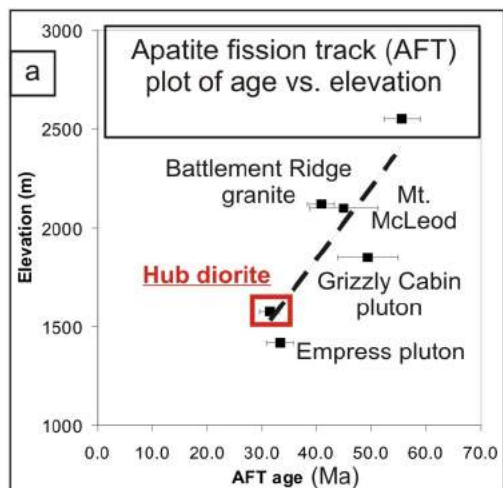
Sericite alteration in the area of the Charlie and Northwest Copper showings is typically expressed as sericite replacement of plagioclase and mafic minerals in andesite and feldspar porphyry dikes, and as quartz-pyrite-sericite alteration in parts of the Tchaikazan River succession sedimentary facies (Figure 9d, e). Sericite also forms selvages to quartz-sulphide veins throughout the area.

‘Advanced Argillic’ Alteration

Argillic alteration is locally developed on the western flank of the Northwest Copper showing (Ravioli ridge; Figure 8), a zone proximal to a large east-striking normal fault (Figure 2a). The Powell Creek rocks in the hangingwall appear to have undergone significant silicification. Hydrous clay minerals, such as kaolinite, dickite, montmorillonite and halloysite, were identified using shortwave infrared (SWIR) analysis and characterize this alteration zone (Figure 9f). The clay imparts a distinctive colour and texture to the rock resulting in a white/yellow earthy rock that contrasts with the surrounding maroon-coloured Powell Creek Formation.

Mineralization

Mineralization is varied throughout the two areas: The Charlie showing area hosts comb-texture quartz veins, which contain polymetallic sulphide assemblages, and the Northwest Copper showing, as its name implies, hosts milky-coloured, massive quartz veins, which contain native copper, tetrahedrite, digenite, and chalcocite. The main



b

Name	Easting	Northing	Elevation	Igneous rock
Hub diorite	453430	5668870	1572 m	Porphyritic diorite
Empress	471890	5661590	1420 m	Porphyritic granite
Grizzly Cabin	457161	5663835	1850 m	Quartz monzodiorite
Mt. McLeod	473567	5660789	2120m	Granodiorite
Mt. McLeod	473633	5658101	2550 m	Coarse granite
Battlement Ridge	456935	5675682	2100 m	Equigranular granite

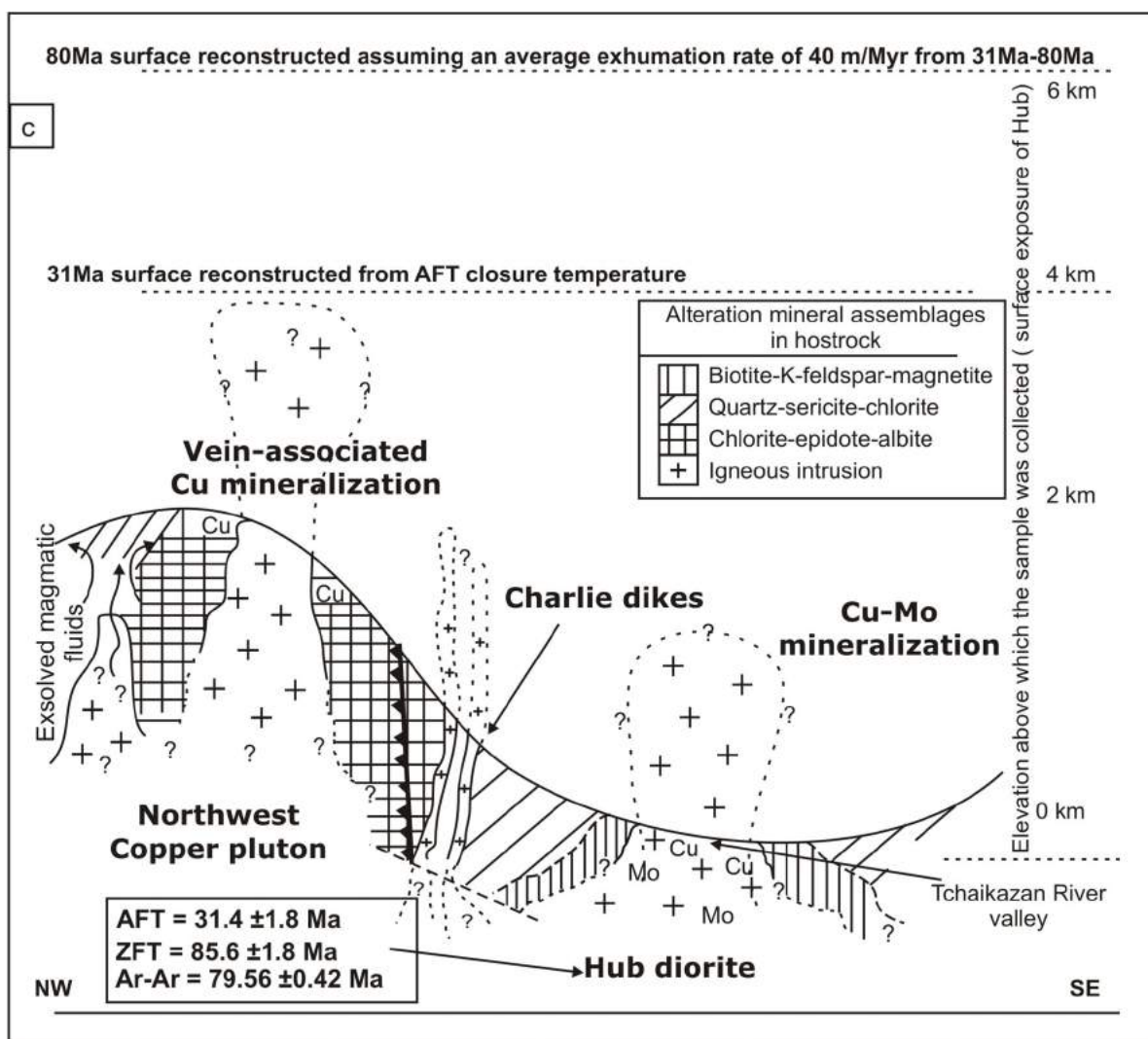


Figure 7. Thermochronology results and related cross-section showing **a**) apatite fission track age vs. elevation plot (m) for five samples of Cretaceous intrusive rocks collected within the Taseko Lakes study area and best-fit line through the data that yields an average exhumation rate of 55 to 30 Ma; **b**) table of the collected thermochronology samples' character, location and elevation; and **c**) schematic cross-section of the study area from northwest to southeast, reconstructing the surface expression at 6 km (80 Ma), 4 km (30 Ma) and present-day.

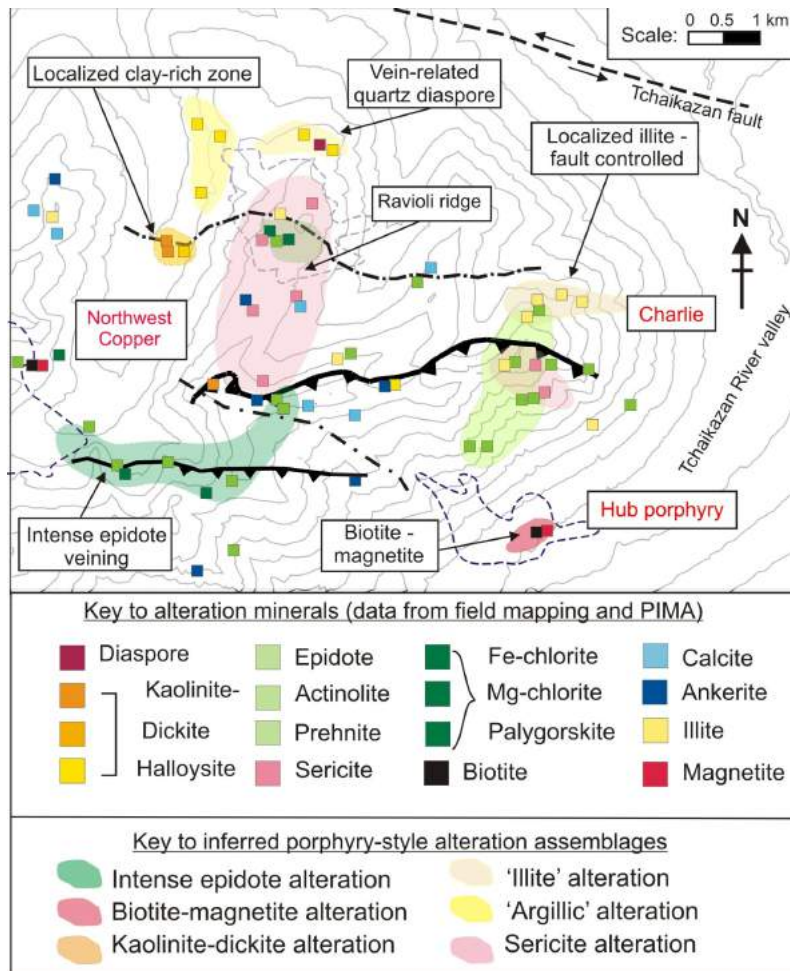


Figure 8. Location of alteration zones in the Taseko Lakes study area showing alteration minerals and alteration assemblages, including the 'propylitic' chlorite-epidote, 'advanced argillic' clay-dominated and 'potassic' biotite-magnetite alteration zones.

styles of mineralization are described in greater detail below:

Comb-texture, sulphide-bearing quartz veins are a style of vein characterized by massive, comb tooth quartz with a centre-fill of chalcopyrite or pyrite, and rare galena. Veins are on average 2 cm thick, reaching a maximum thickness of 5 cm.

Coarse tetrahedrite, malachite, and azurite. Tetrahedrite was located in numerous samples from a subcrop of quartz-diaspore vein material; it is typically coarse-grained and accounts for up to 5% of the vein material. Malachite and azurite were developed in the silicified material surrounding the tetrahedrite-bearing zone.

Stringers of, and disseminated native copper were located in two locations near the Northwest Copper thrust fault. The native copper was associated with milky white, massive quartz veinlets. Malachite and chrysocolla alteration around the veins was an indicator to their copper content. Native copper veins are also reported from the southern part of Ravioli ridge.

Epidote-chalcopyrite-pyrite-magnetite veins occur only within the area of the Northwest Copper showing, proximal to the Northwest Copper pluton. Chalcopyrite is typically coarse grained and associated with pyrite and minor coarse magnetite. Magnetite forms thin, discontinuous stringers associated with the epidote and chalcopyrite. Pyrite forms massive aggregates in centimetre-thick veins. The veins typically exhibit 1–5 cm wide alteration selvages of illite and chlorite.

Fluid Inclusion Analysis

A total of ten doubly polished thin sections of quartz vein material were chosen after petrographic analysis using plane polarized light. Many of the typically coarse-grained and massive veins were host to sulphide mineralization. The fluid inclusions within were variable in type, distribution pattern, homogenization temperature, phase content and volume-percent vapour, a pattern commonly found in other porphyry copper deposits.

Primary fluid inclusions (P) were rarely sufficiently developed, or too small, to be readily analyzed (Figure 10). This is not uncommon in samples from the porphyry environment and is the reason behind the need to analyze larger inclusions. Growth zones in quartz crystals are the usual host to these P inclusions (Figure 10a); however, these were too small for analysis ($<5 \mu\text{m}$). The inclusions are liquid-rich, two-phased (liquid to vapour ratio), subspherical and lack secondary daughter minerals. A single, small vapour bubble accounts for less than 15% of the inclusion (maximum

of 40%). Abundant secondary and fluid inclusions (Figure 10b) are typically small and crosscut crystal boundaries. Measurements of the melting temperature of ice [$T_m(\text{ice})$] for the liquid-rich, halite-undersaturated inclusions range between -0.8 and -3.4°C and homogenize at temperatures between 169 and 193°C . Melting data provides a sensitive measure of bulk salinities, which range between 1.7 and 5.1 wt. \% NaCl equivalents. The inclusions are a record of low-salinity dilute fluids trapped under conditions ranging from 190 to 230°C . Fluid inclusion analysis

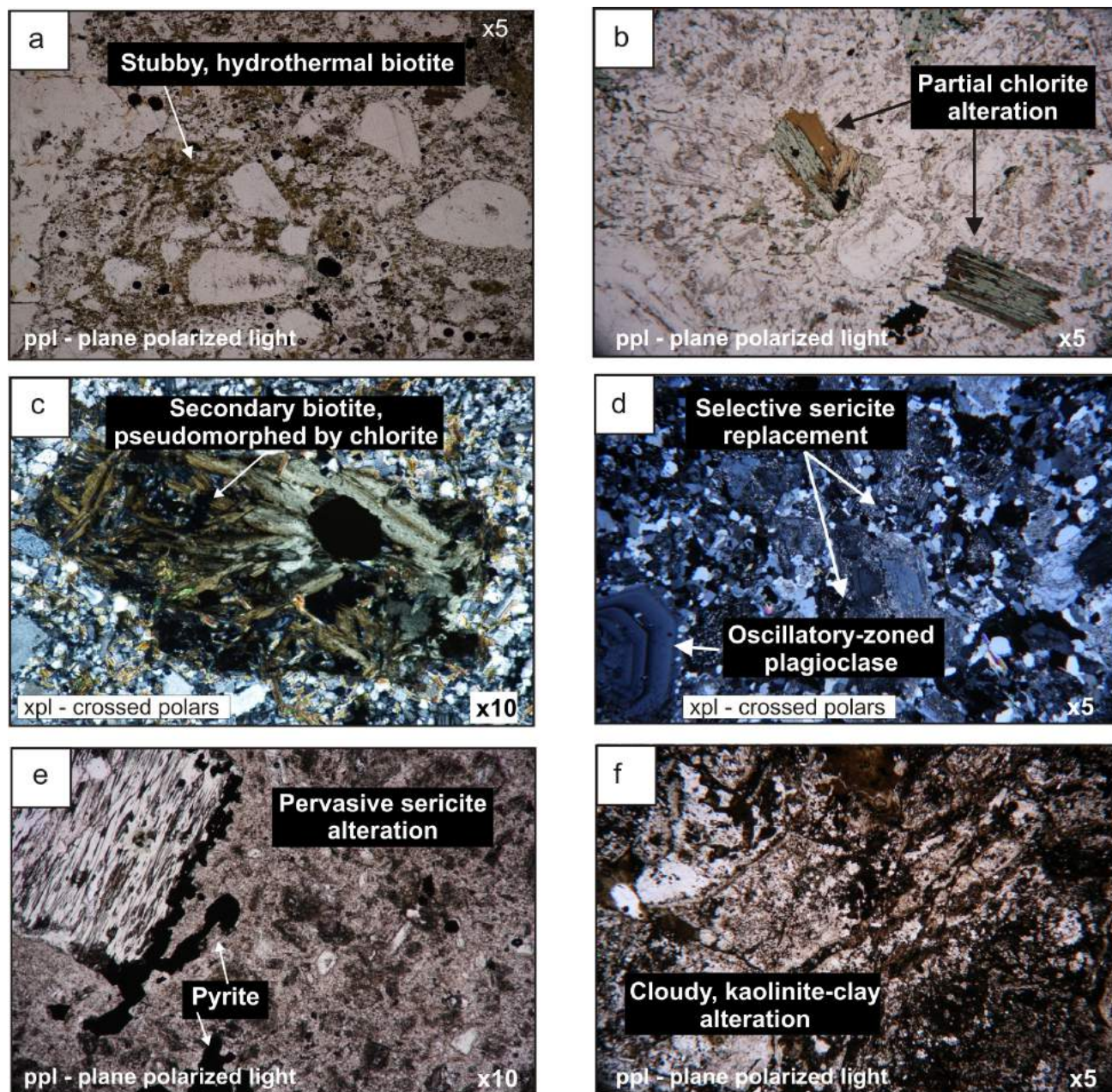


Figure 9. Photomicrographs of the Charlie and Northwest Copper andesite samples showing **a**) stubby, hydrothermal biotite infill (ppl); **b**) partial chlorite alteration of biotite (xpl); **c**) replacement of hornblende by secondary biotite, which is then replaced by subsequent chlorite; **d**) partial, patchy sericite alteration of plagioclase phenocrysts (xpl); **e**) pervasive sericite alteration (ppl); and **f**) pervasive kaolinite alteration (xpl).

proved inconclusive in generating a paleodepth or realistic temperature for the magmatic-hydrothermal system.

Stable Isotope Results

A total of nine samples of vein calcite were taken from areas of the Charlie and Northwest Copper showings (results shown in Figure 11a–c). These veins were typically massive calcite-only veins or quartz veins with a calcite centre-fill. The samples display $\delta^{13}\text{C}$ fluid values ranging from -9.853 to -3.265 , and $\delta^{18}\text{O}$ fluid values, from 5.891 to 11.088 (Figure 11c). These values are within the range of values suggested as corresponding to a deep-seated or magmatic source for the CO_2 carbon which is characterized by $\delta^{13}\text{C}$ fluid values ranging from -3 to -8 , with a mean at -6 per mil (Ford and Green, 1977; Dreher et al., 2008). However, Kerrich and Wyman (1990) stated that the same signature could be created by leaching of carbonate hostrocks or oxidation of free carbon, and does not necessarily indicate that the CO_2 is of mantle or magmatic origin. Therefore the C and O isotope data presented in this report do not clearly discriminate between the possible fluid sources.

The suite of quartz veins from the Hub showing displayed $\delta^{18}\text{O}$ (SMOW) rock values ranging from 8.7 to 10.3 (Figure 11a). These veins display typical igneous values (Taylor, 1968), whereas samples taken from the Charlie and Northwest Copper showings revealed $\delta^{18}\text{O}$ values progressing outward from the Hub porphyry (Figure 11b). Samples from quartz-magnetite veins near the Northwest Copper pluton yielded formation temperatures of 490°C for $\delta^{18}\text{O}$ from coprecipitating quartz and magnetite (Figure 11b), calculated using isotope fractionation data to gain an appropriate temperature of formation. A kaolinite mineral sample from the Northwest Copper ‘advanced argillic’ alteration zone yielded a $\delta^{18}\text{O}$ rock value of 6.6 , and a δH rock value of -113 (Figure 11a).

Interpretation

The Hub porphyry system displays the igneous, alteration and metallogenic signatures of a calcalkaline copper porphyry deposit. Mineralization is hosted in the 80 Ma Hub diorite and cut by 69 Ma feldspar-hornblende dikes, constraining the age of mineralization to between ca. 80 and 70 Ma. The Hub diorite appears to have been emplaced at a depth of 5 – 6 km at this time. Thrusting at approximately 60 Ma led to the placement of the Tchaikazan River succession over the Powell Creek Formation. Subsequent exhumation at a rate of 40 m/Ma from 80 to 31 Ma and of >100 m/Ma from 31 Ma to the present day gives a depth of 3 – 4 km.

The dominance of the potassic mineral assemblage (higher temperature hydrothermal alteration) at the Hub porphyry is inferred to be proximal to the centre of the porphyry system. Weak sericite alteration occurs as a lower temperature overprint. There is no physical evidence of a fault located between the Hub and Charlie showings, nor would the reconstructed stratigraphic relationships require that one have occurred. Therefore, the ‘propylitic’ and ‘illite’ alterations in the Charlie showing area appear to be placed a true 800 m above the core zone of potassic alteration at the Hub showing and are thought to be a distal expression of the magmatic-hydrothermal system. The strong vein-associated epidote alteration of hostrocks and vein epidote located near thrust faults may well reflect hydrothermal activity associated with the development of these structures post-porphyry activity, around 60 Ma ago. Sericite alteration, which is most developed on Ravioli ridge, may lie above the inferred subsurface intrusion and therefore be a result of the distal effects of magmatic-derived fluids. The ‘advanced argillic’ alteration zone represents a near-surface alteration and its acidic nature was likely a product of acidic magmatic vapour condensation. The epidote alteration appears related to fluid flow around faults, and the Northwest Copper pluton, suggesting a probable hydrothermal alteration age of ca. 60 Ma.

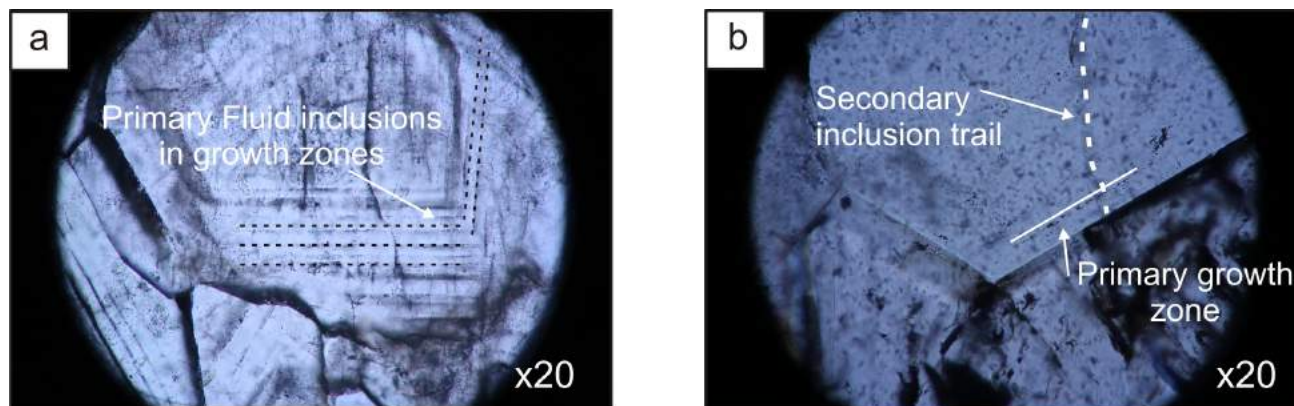


Figure 10. Photomicrographs of fluid inclusions as seen in plane-polarized light: **a)** primary fluid inclusions in growth zones in quartz crystals; and **b)** secondary fluid-inclusion trail crosscutting earlier primary assemblage.

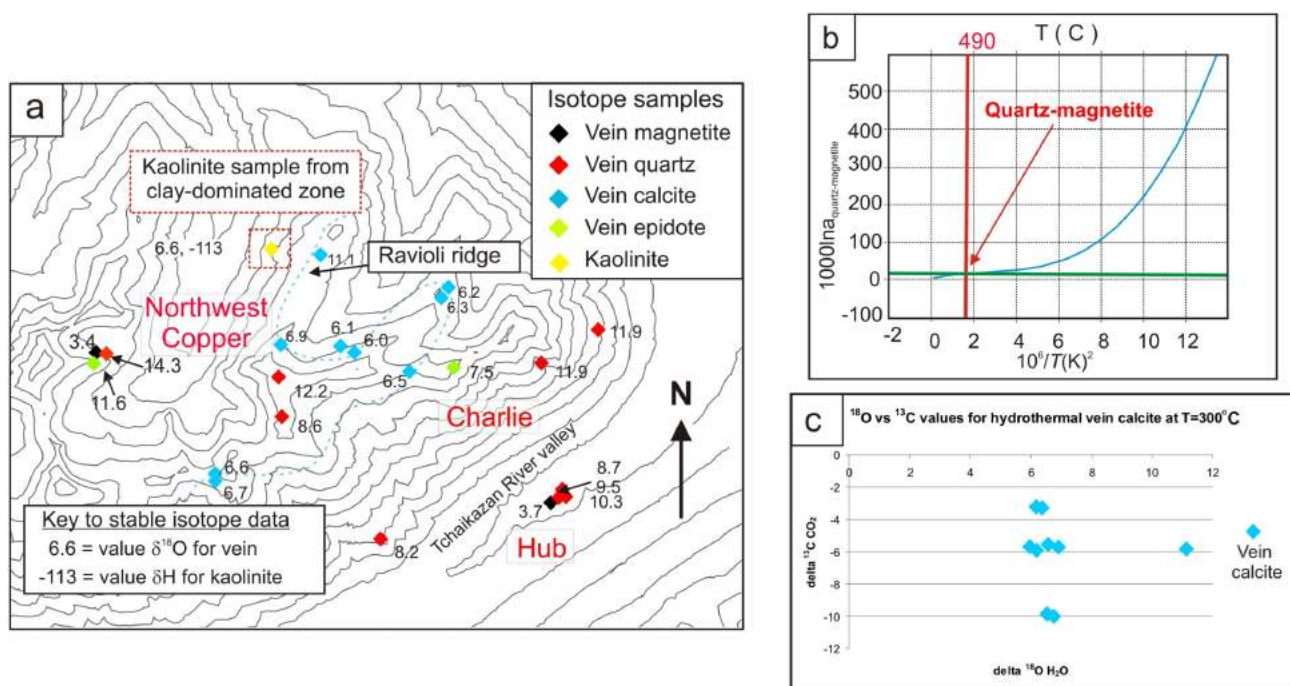


Figure 11. Stable isotope analysis results and hydrothermal fluid temperature plots: **a)** topographic map of the location of stable isotope samples taken from vein material and kaolinite rock sample highlighting the Hub, Charlie and Northwest Copper showings; **b)** $\delta^{18}\text{O}$ plot for the mineral pair quartz-magnetite showing that the quartz and magnetite veins at the Northwest Copper showing formed at $\sim 490^\circ\text{C}$, as determined using equations from Zhang et al. (1989) and Chacko et al. (2004) for $\Delta(A-B) = 10.8\text{‰}$ (just within the limits of normal igneous rocks); and **c)** plot of $\delta^{18}\text{O}$ vs. $\delta^{13}\text{C}$ values for hydrothermal vein calcite samples (see blue squares in (a)) for a hypothesized temperature of 300°C .

Discussion and Implications

The similarity of the ages and geological composition of the intrusive rocks of the Hub porphyry to those observed in the Charlie showing area suggests that the mineralization at both localities may be linked to the same period of magmatism responsible for the 77 Ma Prosperity deposit. The Northwest Copper showing is different in terms of mineralogy, alteration and age, and is probably linked to separate magmatic activity, perhaps a younger hydrothermal event related to the thrusting at around 60–55 Ma.

The Hub porphyry deposit is the same age as other deposits in the region, in particular the 80 Ma Taseko-Empress showing (Figure 1; see Blevings, 2008) and the larger Prosperity deposit. The same age and similar depth of the Hub porphyry, Taseko-Empress and Prosperity deposits may point to an 80 Ma suite of porphyry deposits formed by subduction-related magmatism that was capable of producing porphyry-style mineralization. The porphyry system at Taseko Lakes formed at the deep end of the spectrum of known porphyry deposits (Sillitoe, 1972, 1973). Given the calculated AFT and ZFT depth of the Hub porphyry, two possibilities arise: Either much of the overlying deposit has been lost, or the porphyry deposit was inherently smaller or perhaps truncated (by thrusting of the late Cretaceous crunch?) porphyry deposit. While these Cretaceous rocks

do present evidence of magmatic hydrothermal alteration, the evidence supporting their ability to host Prosperity-style mineralization is limited.

Conclusions

The Cretaceous igneous rocks of the Tchaikazan River succession and Powell Creek Formation are host to copper mineralization which occurred between ca. 80 and 70 Ma (Figure 12). Mineralized centres in this area include the Hub diorite, proximal to the Northwest Copper pluton, and the small, vein-related Charlie showing. The character of the mineralization and the hydrothermal alteration is typical of that attributed to porphyry deposits. High temperature potassic alteration is confined to the core of the Hub porphyry and is characterized by biotite-magnetite alteration of the hydrothermal breccia. Distal regions are altered to a chlorite-epidote-calcite alteration that can, and should, be differentiated from an intense epidote-only alteration assemblage proximal to fault zones. Sericite alteration is locally restricted and is pervasive in late crosscutting feldspar-hornblende dikes associated with the Hub porphyry.

The ages for the structures in the study area are not well-constrained, but an illite (Ar/Ar) age for a thrust fault at the Northwest Copper showing yielded an age of 60.53 ± 0.33 Ma, which indicates that mineralization likely occurred post-deformation or during the same period of

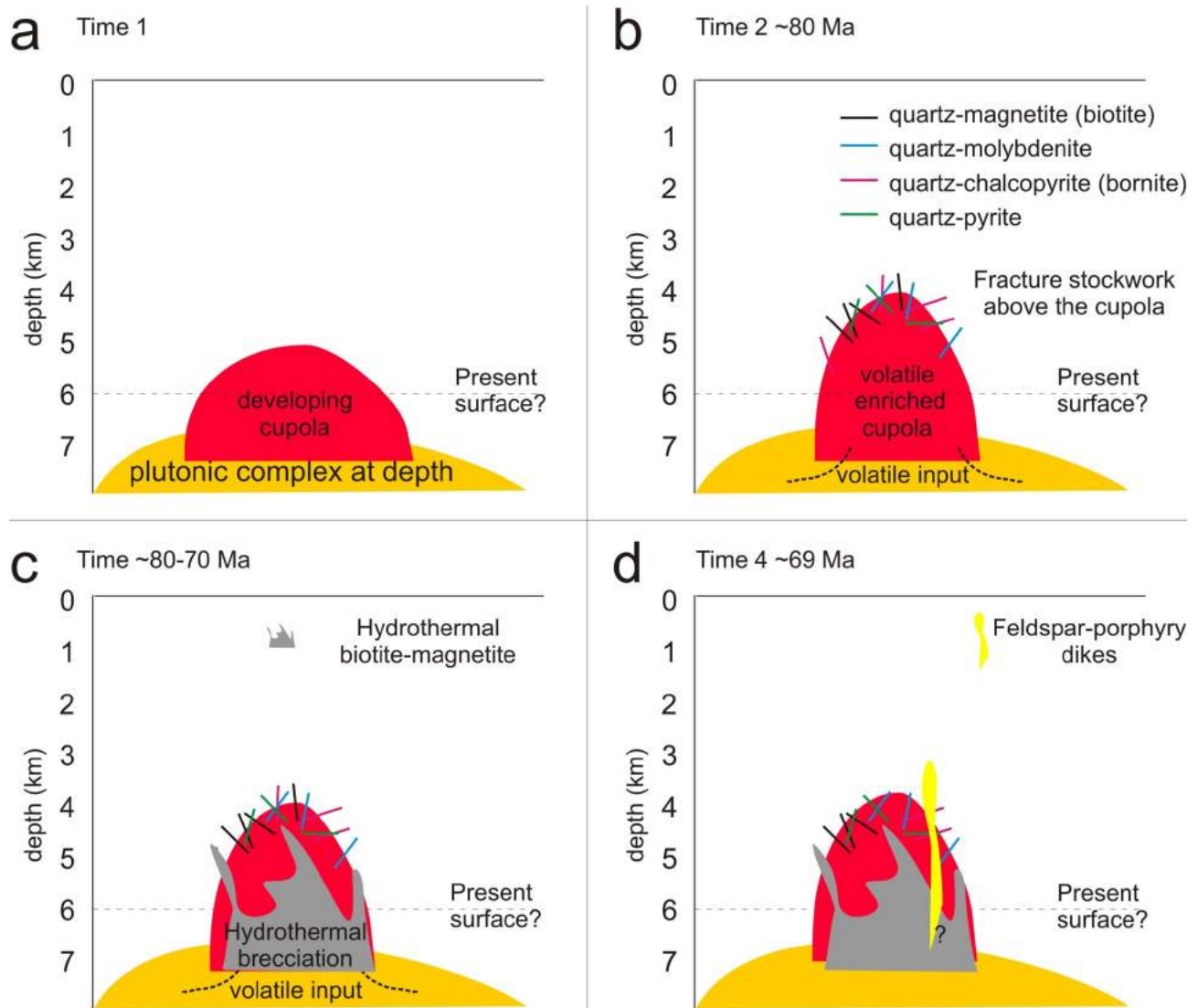


Figure 12. Schematic diagram depicting the evolution of the Hub showing's hydrothermal system in the Taseko Lakes study area: **a)** a large granodiorite pluton at depth develops a cupola at its top; **b)** quartz-magnetite and quartz-sulphide veins form, after volatile input from depth; **c)** brecciation of the granodiorite and surrounding andesite wallrocks occurs, infill of magnetite, biotite and quartz occurs as cement; and **d)** cooling of the magmatic system and intrusion of feldspar porphyry dikes at ca. 70 Ma.

magmatism as the 57 Ma Northwest Copper pluton. This age is consistent with that of the Poison Mountain (Cu±Mo±Au) porphyry prospect, where K-Ar dating (hornblende and biotite) has yielded an age of 59–56 Ma (MINFILE 0920 046; MINFILE, 2008) for the intrusion, potassic alteration and mineralization.

Both stable isotope studies and microthermometric data from fluid inclusion analysis on the Taseko Lakes area proved uncertain. However, low-temperature thermochronology using AFT and ZFT provided an estimated average erosion rate of 40 m/Ma, which indicates that the porphyry system was emplaced at a depth of 5–6 km. The similarity in age, composition, mineralogy and geological setting of the Hub porphyry to that of the neighbouring Prosperity deposit is encouraging, and indicates

that Late Cretaceous conditions were conducive to producing large porphyry copper deposits.

The results gathered over three field seasons of work indicate that the Taseko Lakes area displays evidence of porphyry-style intrusion, alteration and mineralization. The relationships derived from field mapping and laboratory work provide a useful background for the effective continued exploration of the study area.

Acknowledgments

The authors would like to thank J. Mortensen for reviewing this paper prior to submission and Galore Resources Inc. for their logistical support. Thanks also go to Equity Exploration Consultants for providing invaluable field experi-

ence during the 2008 field season and access to drilling information. Galore Resources Inc. and Geoscience BC are thanked for their financial contribution to the project.

References

- Blevings, S.K. (2008): Geologic framework for Late Cretaceous magmatic-hydrothermal mineralization in the Taseko Lakes region, southwestern B.C.; M.Sc. thesis, University of British Columbia, 244 p.
- Chacko, T., Cole, D.R. and Horita, J. (2001): Equilibrium oxygen, hydrogen and carbon isotope fractionation factors applicable to geologic systems; *Reviews in Mineralogy and Geochemistry*, v. 43, no. 1, p. 1–81.
- Dreher, A.M., Xavier, R.P., Taylor, B.E. and Martini, S.L. (2008): New geologic, fluid inclusion and stable isotope studies on the Controversial Igarapé Bahia Cu-Au deposit, Carajá Province, Brazil; *Mineralium Deposita*, v. 43, no. 2, p. 161–184.
- Ford, J. H. and Green, D. C. (1977): An oxygen- and hydrogen-isotope study of the Panguna porphyry-copper deposit, Bougainville; *Australian Journal of Earth Sciences*, v. 24, no. 1-2, p. 63–80, doi: 10.1080/00167617708728967.
- Hollis, L., Blevings, S.K., Chamberlain, C.M., Hickey, K.A. and Kennedy, L.A. (2006): Mineralization, alteration, and structure of the Taseko Lakes region, southwestern British Columbia: preliminary analysis; *in* Geoscience BC Summary of Activities, Geoscience BC, Report 2007-1, p. 297–306.
- Hollis, L., Hickey, K. and Kennedy, L.A. (2008): Mineralization and alteration associated with an hypothesized copper (molybdenum) porphyry system in the Taseko Lakes area, southwestern British Columbia (NTS 0920/04); *in* Geoscience BC Summary of Activities, Geoscience BC, Report 2008-1, p. 55–66.
- Israel, S. (2001): Structural and stratigraphic relationships within the Tchaikazan River area, southwestern British Columbia: implications for the tectonic evolution of the southern Coast Belt; M.Sc. thesis, University of British Columbia, 129 p.
- Israel, S., Kennedy, L.A., Schiarizza, P., Friedman, R.M. and Villeneuve, M. (2006): Evidence for Early to Late Cretaceous, sinistral deformation in the Tchaikazan River area, southwestern British Columbia: implications for the tectonic evolution of the southern Coast Belt; *in* Paleogeography of the western North American Cordillera, J. Haggart, R.J. Enkin and J.W.H. Monger (ed.), Geological Association of Canada, Special Paper 46, p. 331–350.
- Journeay, J. M. and Friedman, R.M. (1993): The Coast Belt Thrust System: evidence of Late Cretaceous shortening in southwest British Columbia; *Tectonics*, v. 12, no. 3, p. 756–775.
- Kerrick, R. and Wyman, D. (1990): Geodynamic setting of mesothermal gold deposits: an association with accretionary tectonic regimes; *Geology*, v. 18, no. 9, p. 882–885.
- Lowell, D.J. and Guilbert, J.M. (1970): Lateral and vertical alteration-mineralization zoning in porphyry ore deposits; *Economic Geology*, v. 65, no. 4, p. 373–408.
- McLaren, G. P. (1990): A mineral resource assessment of the Chilko Lake planning area; BC Ministry of Energy, Mines and Petroleum Resources, Bulletin 81, 117 p.
- MINFILE (2008): MINFILE BC mineral deposits database; BC Ministry of Energy, Mines and Petroleum Resources, URL <<http://www.empr.gov.bc.ca/Mining/Geoscience/MINFILE/Pages/default.aspx>> [October 2008].
- Monger, J. W. H., van der Heyden, P. J., Journeay, M., Evenchick, C. A. and Mahoney, J. B. (1994): Jurassic-Cretaceous basins along the Canadian Coast Belt; their bearing on pre-Mid-Cretaceous sinistral displacements; *Geology*, v. 22, p. 175–178.
- Reiners, P.W. and Brandon, M.T. (2006): Using thermochronology to understand orogenic erosion; *Annual Review of Earth and Planetary Sciences*, v. 34, p. 419–466.
- Richards, J.P. (2003): Tectono-magmatic precursors for porphyry Cu-(Mo-Au) deposit formation; *Economic Geology*, v. 98, no. 8, p. 1515–1533.
- Rusmore, M. E. and G. J. Woodsworth (1991): Coast Plutonic Complex: a mid-Cretaceous contractional orogen; *Geology*, v. 19, no. 9, p. 941–944.
- Schiarizza, P., Gaba, R.G., Glover, J.K., Garver, J.I. and Umhoefer, P.J. (1997): Geology and mineral occurrences of the Taseko-Bridge River area; BC Ministry of Energy, Mines and Petroleum Resources, Bulletin 100, 291 p.
- Sillitoe, R.H. (1972): A plate tectonic model for the origin of porphyry copper deposits; *Economic Geology*, v. 67, no. 2, p. 184–197.
- Sillitoe, R.H. (1973): The tops and bottoms of porphyry copper deposits; *Economic Geology*, v. 68, no. 6, p. 799–815.
- Taylor, H.P. (1968): The oxygen isotope geochemistry of igneous rocks; *Contributions to Mineralogy and Petrology*, v. 19, no. 1, p. 1–70.
- Tipper, H.W. (1969): Mesozoic and Cenozoic geology of the northeast part of the Mount Waddington map-area (92N), Coast district, British Columbia. Geological Survey of Canada, Paper 68-33.
- Tipper, H.W. (1978): Geology of Taseko Lakes map-area (92 O), British Columbia; Geological Survey of Canada, Open File 534.
- Titley, S.R. and Beane, R.E. (1981): Porphyry copper deposits; part I, geologic settings, petrology, and tectonogenesis; *Economic Geology and the Bulletin of the Society of Economic Geologists*, v. 75, 214 p.
- Umhoefer, P.J. and Schiarizza, P. (1996): Latest Cretaceous to early Tertiary dextral strike-slip faulting on the southeastern Yalakom fault system, southeastern Coast Belt, British Columbia; *Geological Society of America Bulletin*, v. 108, no. 7, p. 768–785.
- Zhang, X., Nesbitt, B. E. and Muehlenbachs, K. (1989): Gold mineralization in the Okanagan Valley, southern British Columbia: fluid inclusion and stable isotope studies; *Economic Geology*, v. 84, no. 2, p. 410–424.

Sulphur Sources for Gold Deposits in the Bridge River–Bralorne Mineral District, Southwestern British Columbia (Part of NTS 092J)

L.H. Moore, University of Western Australia, Crawley, WA, Australia, jazzadelic@hotmail.com

C.J.R. Hart, Centre for Exploration Targeting, University of Western Australia, Crawley, WA, Australia

E.E. Marsh, United States Geological Survey, Denver, CO

Moore, L.H., Hart, C.J.R. and Marsh, E.E. (2009): Sulphur sources for gold deposits in the Bridge River–Bralorne mineral district, southwestern British Columbia (part of NTS 092J); in Geoscience BC Summary of Activities 2008, Geoscience BC, Report 2009-1, p. 91–102.

Introduction

The Bridge River–Bralorne mineral district is the largest historical lode-Au producer in British Columbia, collectively producing over 4 million oz of Au between 1897 and 1971 (Church, 1996). The district covers an area of approximately 1700 km² and is located 180 km north of Vancouver, on the eastern side of the Coast Belt, in southwestern BC (Figure 1).

Although dominated by Au occurrences, the camp is characterized by three main metal associations: Au dominant, Sb dominant and Hg dominant. The numerous deposits and mineral occurrences that make up this district form a spatial zonation, with Au in the west, Sb in the centre and Hg in the east (Pearson, 1975). There is no definitive explanation for this distribution, but a number of geological models have been suggested. Leitch et al. (1991a) conducted a detailed geochronological analysis on the Bralorne Au deposits, and concluded that the source of the fluids was from the intrusive rocks that form the Coast Plutonic Complex to the west, and as they cooled, they sent out pulses of heat and fluid toward the east, resulting in the current metal zonation. After this analysis, Leitch et al. (1991b) performed a geochemical and isotopic analysis on the Au deposits from the Bralorne-Pioneer camp and construed that the fluids actually had a mix of metamorphic and magmatic origins, with an increase in mixing with meteoric fluids as the depth decreased. Church (1996) concluded that the close proximity of the Bendor batholith and Coast Plutonic Complex provided the structural controls and heat source for the circulation of connate and young fluids that formed the orogenic Au deposits at Bridge River–Bralorne

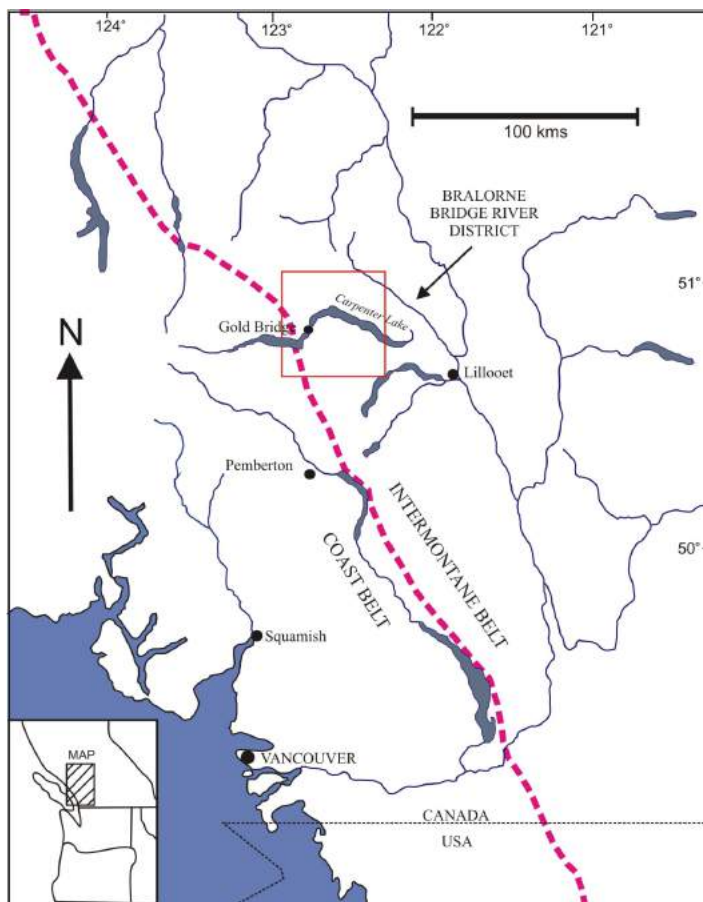


Figure 1. Location of the Bridge River–Bralorne mineral district in BC. The pink dotted line represents the boundary between the Coast Belt and the Intermontane Belt.

mineral district. However, Ash (2001) suggested an ophiolitic association for the Au deposits, and that mineralization occurred during their obduction in the mid-Cretaceous. Maheux (1989) conducted a stable-isotope and fluid-inclusion study on the larger Sb deposits and on the basis of the data, deduced that a meteoric-derived hydrothermal fluid was the source for the district metal zonation. Schiarizza et al. (1997), on the basis of regional mapping, decided that episodic reactivation of strike-slip faults gave rise to metallogenic events that resulted in the metal

Keywords: sulphur isotopes, sulphur source, orogenic gold, fluids

This publication is also available, free of charge, as colour digital files in Adobe Acrobat® PDF format from the Geoscience BC website: <http://www.geosciencebc.com/s/DataReleases.asp>.

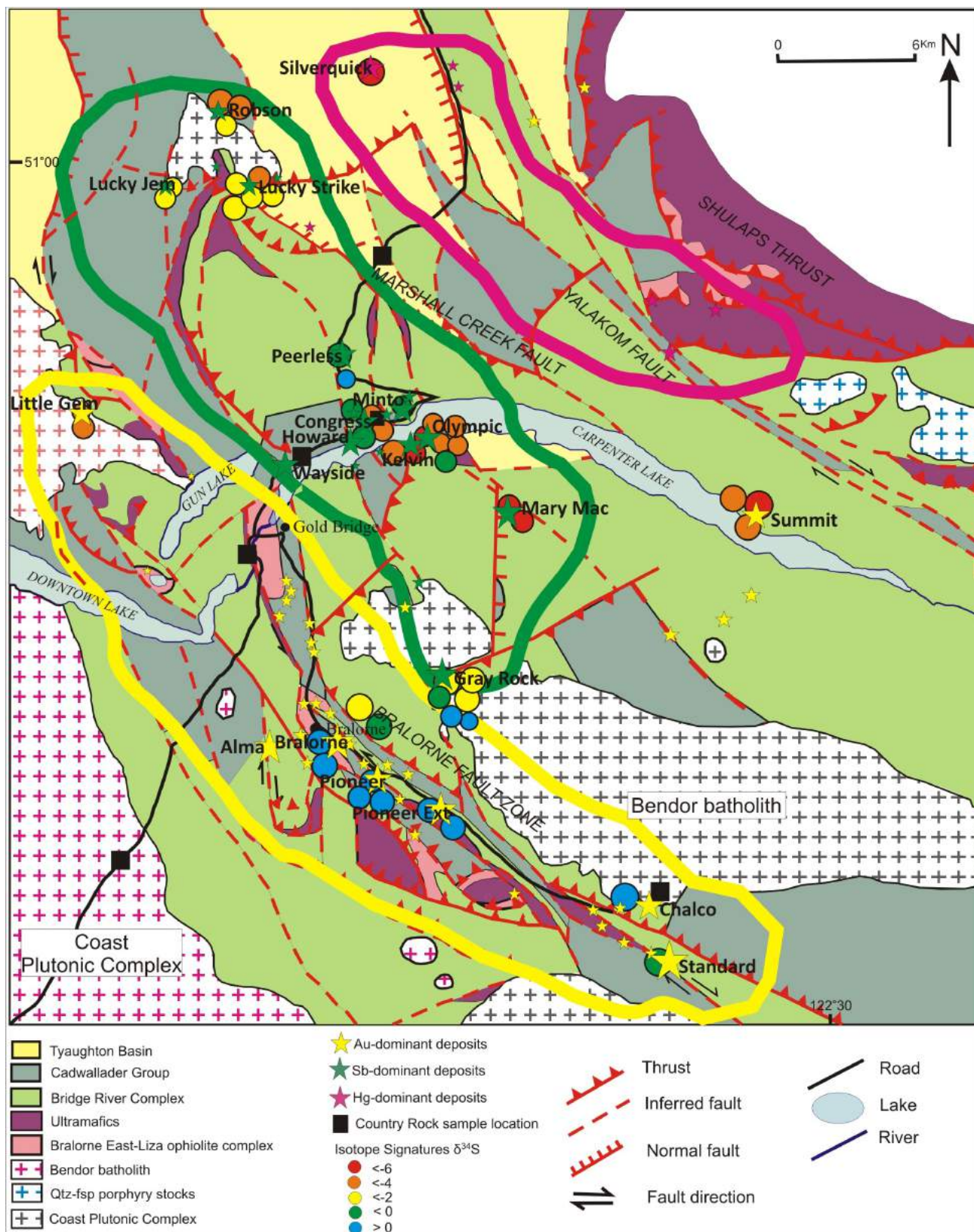


Figure 2. Regional geology of the Bridge River–Bralorne mineral district, showing deposit type and distribution. Distribution pattern is represented by circular coloured lines; green, Sb type; pink, Hg type; yellow, Au type. Larger stars are sampled deposits and occurrences. *Modified after Church (1996), Maheux (1989) and Scharizza et al. (1997).*

zonation in the district. Specifically, the three main faults (Bralorne-Eldorado, Castle Pass, Marshall Creek–Yalakom) were active at different times, producing three mineralizing events. Determining the correct source for the S and fluids is important because it can be used to generate more effective exploration models.

Various isotopic methods can be applied to hydrothermal deposits to provide constraints on their formation models. Sulphur isotopes, in particular, can be a powerful tool to identify the source(s) of S in hydrothermal mineral systems. Although the Bridge River–Bralorne mineral district benefits from a significant amount of geochemical data (Leitch et al., 1989, 1991b; Maheux, 1989), the S source(s) responsible for the mineralization, and likely for Au transport, have not been identified. Therefore, verifying the S isotopic compositions of the mineralization and potential source rocks can assist in eliminating some confusion and will help define an exploration model and provide a strong foundation to evaluate the overall Au prospectivity of the district.

A detailed S isotope study was conducted, with samples taken from all three metal zones, as well as from the numerous rock units that form the country rocks and are considered to be potential S sources.

Regional Geology

The Bridge River–Bralorne mineral district straddles the boundary between the Middle Jurassic–Late Cretaceous Coast Belt and the Late Paleozoic–Mesozoic Intermontane Belt that together comprise this part of the southwestern Canadian Cordillera (Schiarizza et al., 1997). This complex region resulted from episodic deformational, depositional and magmatic events from the Late Paleozoic to Middle Tertiary. In the Middle–Late Jurassic, two main tectonic assemblages collided: the oceanic backarc basin Bridge River Complex (Figure 2) comprising basalt, gabbro, chert, shale, argillite and ultramafic rocks was juxtaposed with the island arc Cadwallader Group, which consists of volcanic rocks and marine and arc-marginal clastic strata (Schiarizza et al., 1997). During and after terrane collision, the Late Jurassic–Cretaceous Tyaughton Basin, which consists of mostly clastic sedimentary rocks and shale, was deposited on top of these two terranes (Church, 1996).

Contractional deformation during the mid-Cretaceous resulted in a series of major structural systems. In the Bridge River district, these are the Bralorne fault zone (Cadwallader break), the Yalakom fault system, the Shulaps thrust and a network of northwest-trending faults (Figure 2; Leitch, 1990; Schiarizza et al., 1997). Deformation above the Cadwallader Group occurred along the Shulaps thrust, the Bralorne fault zone and Bralorne–East Liza ophiolite assemblages, respectively, resulting in wedges of ophiolite and ultramafic rocks along these zones,

marking the region of crustal shortening. The ophiolite rocks include greenstone, diorite, gabbro, tonalite and serpentinite (Schiarizza et al., 1997).

Regional plutonic and volcanic events were episodic during the Cretaceous and Tertiary. The Coast Plutonic Complex (CPC) is the main component of the southwestern Coast Belt, as well as the main granitic intrusion of this region, and marks the southwest corner of the mineral district (Schiarizza et al., 1997). The Bendor batholith is a younger constituent east of the CPC, in the form of an outlier pluton, which runs for 20 km in a northwest-trending direction between the Bralorne fault zone and the Marshall Creek fault (Figure 2). These intrusions comprise granodiorite to quartz diorite, characterized by massive hornblende>biotite>pyroxene and magnetite-titanite, and generally have sharp contacts with a 1 km contact metamorphism halo. A mass of mafic to felsic dikes intrude all of the units. These dikes include 85.7 Ma hornblende porphyry, 86–91 Ma albitite dikes, plagioclase porphyry and lamprophyre. These are all considered to be hypabyssal equivalents of the CPC (Church, 1996).

Dextral strike-slip movement reactivated many of the older northwest-trending faults, especially along the Yalakom fault system, which includes the Marshall Creek, Shulaps thrust, Castle Pass, Bralorne fault zone and Relay Creek faults (Umhoefer and Schiarizza, 1996). These structures postdate the accretionary contractional structures at 67 Ma, but continued to be active through to 40 Ma (Schiarizza et al., 1997).

Metallogeny and Deposit Geology

The previously operating mines in the district are Bralorne, Pioneer, Wayside, Minto, Congress and Silverquick, and surrounding these there are more than 60 mineral occurrences. The variety of mineral occurrences includes Au dominant, Sb dominant, Hg dominant and the occasional Cu-Mo prospect (Woodsworth et al., 1977).

Gold Association

The Au-dominant deposits and occurrences occupy the area along the Bralorne fault zone (Figure 2) between the Bendor batholith and Coast Plutonic Complex. The zone is underlain by both the Bridge River Complex and Cadwallader terrane sedimentary and volcanic units, as well as wedges of ultramafic rocks and ophiolite (Figure 2; Church, 1996). Gold-quartz veins are hosted in the diorite and gabbro of the Bralorne–East Liza ophiolite complex, which is bordered by serpentinite on one side and is within close proximity to the Bendor batholith on the other. The average thickness of the veins is 1 m and they are ribboned with septa of sulphide minerals, sericite and native Au (Leitch et al., 1989). Veins often follow the older albitite dike contacts and the extensive network of faults that are

part of the Bralorne zone (Leitch, 1990). Fuchsite alteration is a prominent feature of this mineralization type, being directly associated with the hydrothermal veins, but found a fair distance from the deposits. The dominant sulphide minerals are arsenopyrite and pyrite, with a lesser amount of sphalerite, galena, chalcopyrite, pyrrhotite and stibnite. There is a high Au/Ag ratio, with Au occurring as free Au, often in association with massive arsenopyrite, which is found next to the veins (Church, 1996). The paragenesis of the Au mineralization begins with deposition in the veins of lean quartz with minor pyrite and fuchsite. The veins are then refractured and refilled with Au- and arsenopyrite-bearing quartz with minor sphalerite, galena, chalcopyrite and tetrahedrite (Figure 3).

Antimony Association

The Sb deposits and occurrences, characterized by the Congress and Minto mines, are found distributed through the central northwest-trending region in Figure 2. Veins are generally smaller than the Au deposits and are discontinuous in the shear zones, have a low Au-Ag ratio, and a larger amount of mixed sulphide minerals (Church, 1996). Cairnes (1937) and Maheux (1989) identified two main styles of mineralization for the Sb deposits; one (Sb-Au-Ag±Hg) with a dominant stibnite phase that is associated with some Au mineralization and a lesser amount of other sulphide phases, while the other (Ag-Au±Sb) is base-metal enriched and has a wider variety of sulphide phases. Examples of the stibnite-dominant mineralization include the Congress and Howard mines, while the base-metal mineralization is seen at the Minto and Olympic mines. The greenstone and sedimentary rocks of the Cadwallader Group host the base-metal-enriched mineralization with veins following the contact between cherty sedimentary

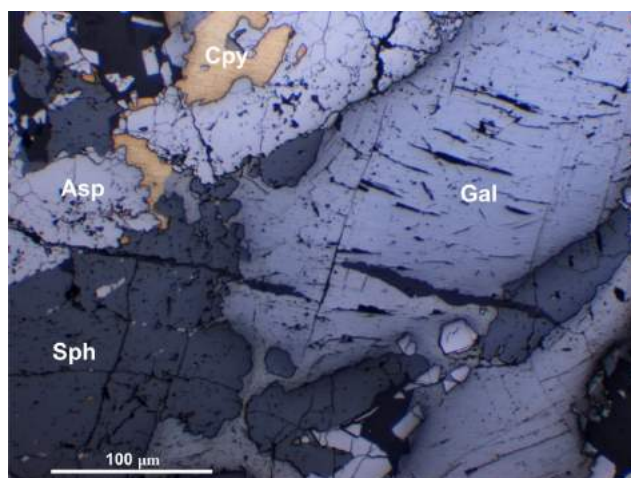


Figure 3. Reflected light photograph at 5× magnification of the Peter vein, showing sulphide mineral equilibria. Notice that all sulphide minerals in this photo are in equilibrium. Late-stage refracturing of the veins by quartz-carbonate has occurred. Abbreviations: Asp, arsenopyrite; Cpy, chalcopyrite; Gal, galena; Sph, sphalerite.

rocks and the diorite dike. The principal sulphide minerals include arsenopyrite, pyrite, sphalerite and jamesonite with minor phases of galena, chalcopyrite, pyrrhotite and stibnite. The paragenetic sequence of the base-metal-type mineralization begins with quartz-ankerite lodes dominated by early- to main-stage pyrite, arsenopyrite, chalcopyrite and sphalerite; the minor sulphide minerals were also deposited during this main stage while quartz, Au and minor base-metal sulphide minerals came in late in the process. The Congress- and Howard-type mineralization is found in shear zones that follow the contact between sedimentary rocks and volcanic units of the Cadwallader Group. Mineralization is made up of fissure fillings and replacement bodies and is discontinuous along the shear zone (Figure 4). Principal sulphide minerals for this mineralization include stibnite, which occurs in sulphide clumps with arsenopyrite, pyrite (Figure 5) and sphalerite, and minor sulphide minerals are galena, tetrahedrite, chalcopyrite, jamesonite, pyrrhotite, cinnabar and native Au (Maheux,

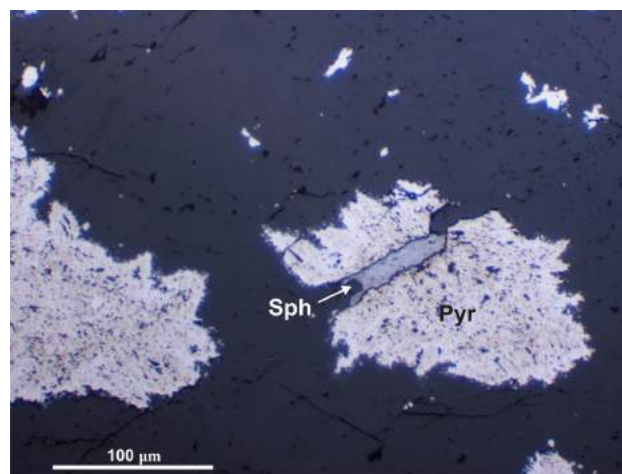


Figure 4. Reflected-light photograph at 5× magnification of the Howard Sb deposit, showing sphalerite in equilibrium with pyrite. Abbreviations: Pyr, pyrite; Sph, sphalerite.

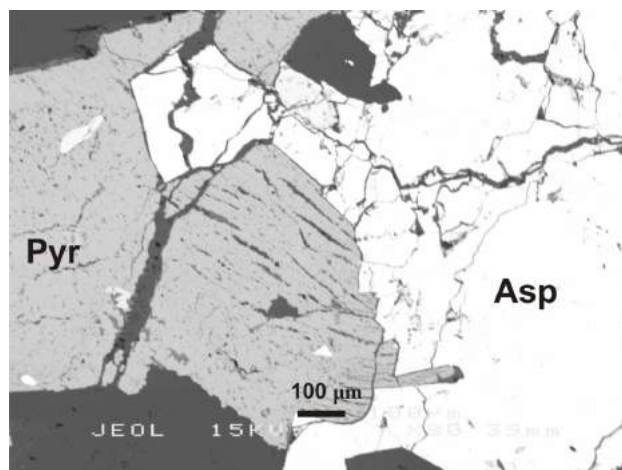


Figure 5. Scanning electron microscope (SEM) image of the Summit deposit, showing arsenopyrite and pyrite in equilibrium. Abbreviations: Asp, arsenopyrite; Pyr, Pyrite.

1989). The mineral paragenesis can be summarized into first-stage quartz-ankerite±calcite with pyrite and arsenopyrite, deposition of quartz and massive stibnite, open space filling by quartz-carbonate with minor tetrahedrite, sphalerite, jamesonite and cinnabar, and late-phase Au associated with stibnite as fracture filling and inclusions.

Mercury Association

Mercury mineralization, characterized by cinnabar, occurs along the Yalakom and Relay Creek fault systems in the north-northeast region of the district. The sedimentary rocks of the Tyaughton Basin and greenstone of the Bridge River Complex underlie these deposits. Cinnabar mineralization in the brecciated conglomerate (Figure 6) is associated with quartz, calcite, limonite and clay minerals. Smear flakes of cinnabar are also present on the walls and gouges of faults (Silverquick deposit; Church, 1996). Stibnite is also associated with cinnabar, and together they occur in quartz veinlets and as disseminated grains (Manitou deposit; Schiarizza et al., 1997).

Previous Models for Sulphur and Fluid Sources

Possible sources for the mineralizing fluids and S that formed the deposits and occurrences of the Bridge River–Bralorne mineral district included the Coast Plutonic Complex (Leitch et al., 1991a), ophiolite from the Bralorne–East Liza ophiolite complex (Ash, 2001), the Bendor batholith (Church, 1996) and reactivated faults (Schiarizza et al., 1997). Geochronology values from the Bralorne–Pioneer Au veins indicate that the age of mineralization is 67 Ma (Hart et al., 2008). Since the majority of pluton emplacement of the Coast Plutonic Complex occurred around 90 Ma (Leitch et al., 1991a), it is evidently too old to provide heat and fluid sources for mineralization. Additionally, the albitite dikes are also 90–85 Ma (Leitch et al., 1991a), so they are >20 Ma older than mineralization and the Bralorne–East Liza ophiolite, which was thrust into the zone during the mid-Cretaceous deformation (Leitch et al., 1989). As a result, mineralization cannot be directly or genetically related to these features. The Bendor batholith, with an age of 65 Ma, is apparently 2 Ma younger than the mineralization at 67 Ma (Hart et al., 2008), and is therefore unrelated. The only geological event with the same age (67 Ma) as the mineralization is the reactivated dextral strike-slip faults, which are part of the Yalakom fault system (Schiarizza et al., 1997).

Sulphur Isotopes

A S isotopic study was conducted to determine the isotopic signature of S in sulphide minerals, from a wide range of deposits and mineral occurrences throughout the district. Analyses from 25 different mineral occurrences and deposits are presented, encompassing all three mineralization

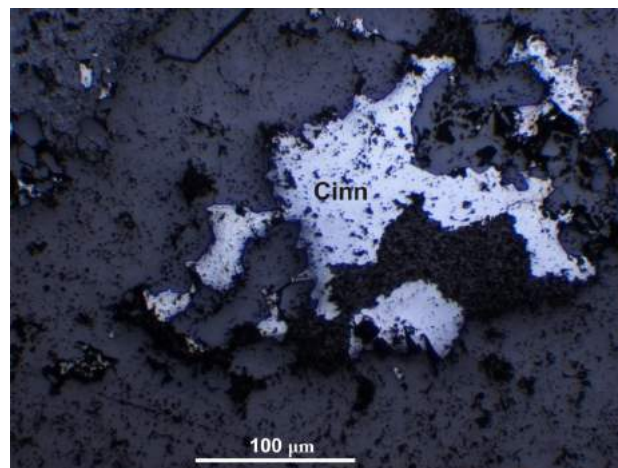


Figure 6. Reflected light photograph at 10× magnification of the Silverquick Hg deposit. Cinnabar is intergrown with specks of wallrock. Cinn: Cinnabar.

types (Figure 2). Most samples had more than one sulphide mineral, and therefore provided an opportunity to obtain more than one isotope analysis from a single deposit. Fifty-four S isotopic analyses are presented in Table 1.

In addition, country rock samples of the main representative units were analyzed for their S isotopic composition in order to provide a comparison point for the mineral isotope data. Nine samples of country rock were taken during fieldwork in June 2008. Samples include CPC; Bendor batholith; biotite schist, basalt, gabbro and greywacke from the Bridge River Complex; basalt and albitite from the Cadwallader Group; serpentinite from the Bralorne ophiolite complex; and the Silverquick Formation shaly sedimentary rocks from the Tyaughton Basin.

Samples were analyzed by the mass spectrometer at the United States Geological Survey (USGS) in Denver, Colorado, and included sulphide minerals from each deposit type and the surrounding country rock (Figure 2). The selected sulphide grains from the deposits include pyrite, sphalerite, arsenopyrite, galena, pyrrhotite, stibnite and cinnabar. Two S extraction methods for whole-rock samples by Tuttle et al. (1986) and Sasaki et al. (1979) were conducted on the country rocks. The analytical process involved a few steps of acid digestion, using a combination of different acids, of the very finely crushed country rocks in order to convert any S present in the rock to Ag₂S and BaSO₄, which was then analyzed by the mass spectrometer.

The range of the S isotopic signatures for sulphide minerals of all three deposit types collectively is from +4.3 to –9‰ (per mil; Table 1). The Au deposits and occurrences range from +4.3 to –2.7‰ with a mean of +1, Sb-associated mineral occurrences from +0.2 to –9‰ with a mean of –3.8‰ and Hg at –6.2‰ (Figure 7). The Sb deposits and occurrences had the most samples from a wide sampling area, which could explain the wider range in values, whereas the

Table 1. Sulphur isotopes (listed as ‰ relative to Canon Diablo Troilite (CDT)) of deposits in the Bridge River–Bralorne mineral district.

Sample ID	Deposit	Mineral	$\delta^{34}\text{S}$	Sample ID	Deposit	Mineral	$\delta^{34}\text{S}$	Sample ID	Deposit	Mineral	$\delta^{34}\text{S}$
Au-dominant deposits											
PIEBITER	Piebiter	py	0.0	PLS	Peerless	py	0.1	MINTO	Minto	sph	-1.1
PNE3	Pioneer	py	3.5	MINTO	Minto	py	-0.8	OLY COR 7	Olympic Core	sph	-4.1
BRALORNE	Bralorne	py	3.2	RBS	Robson	py	-3.1	LS3	Lucky Strike	pyrr	-3.7
PNEX2	Pioneer Extension	py	2.9	KV2	Kelvin	py	-5.9	KV2	Kelvin	gal	-8.6
PETER	Peter Vein	py	-1.7	LS1	Lucky Strike	py	-2.7	GR2	Grey Rock	gal	-2.5
LGM1	Little Gem	py	-4.5	GR8	Grey Rock	py	0.0	GR8	Grey Rock	gal	-2.5
STD2	Standard	stib	-1.7	GR2	Grey Rock	py	-0.6	LYJ11	Lucky Jem	asp	-2.7
PETER	Peter Vein	sph	-3.2	LYJ1	Lucky Jem	py	-2.2	MINTO	Minto	asp	-0.7
BRALORNE	Bralorne	asp	1.4	OLYM2	Olympic	py	-0.8	LS2	Lucky Strike	asp	-3.9
PNE2	Pioneer	asp	4.3	99-8	99-8	py	-3.5	LS3	Lucky Strike	asp	-4.0
PNE3	Pioneer	asp	3.5	MM3	Mary Mac	stib	-8.6	RBS	Robson	asp	-4.9
PNE4	Pioneer	asp	2.5	CONG2	Congress	stib	-4.8	99-8	99-8	asp	-2.8
LGM1	Little Gem	asp	-5.5	MM5	Mary Mac	stib	-9.0	LOVE OIL	Love Oil	asp	-1.5
Sb-dominant deposits											
SMT1	Summit	py	-5.9	LS1	Lucky Strike	stib	-7.5	Hg-dominant deposit			
SMT2	Summit	py	-6.0	CONG2	Congress	stib	-4.7	SQ2	Silverquick	cinn	-6.2
OLYCOR6	Olympic Core	py	-6.3	SMT2	Summit	sph	-4.3				
OLYCOR7	Olympic Core	py	-4.9	RBS	Robson	sph	-4.2				
OLYCOR7	Olympic Core	py	-5.1	LS1	Lucky Strike	sph	-3.4				
OLYCOR6	Olympic Core	py	-5.8	PLS	Peerless	sph	-0.6				

Abbreviations: py, pyrite; stib, stibnite; asp, arsenopyrite; sph, sphalerite; pyrr, pyrrhotite; gal, galena; cinn, cinnabar

Hg deposit only had one sample and one value. The majority of the isotopic values from the Au deposits occur above 0‰, while the Sb values exhibit a few different cluster points, one occurring around -6‰, one at -2.3 to -4.5‰ and one around -1‰. There are also outliers at -8.8 and -9‰ for Sb mineralization and -2 and +4.1‰ for Au mineralization. When separated according to deposit type, the data show a clear pattern of a decrease in the heavier isotope, which is movement toward lighter ratios, from Au, through Sb, to Hg deposits (Figure 7). The distribution of the isotope patterns correlates with the deposit-type distribution, thus showing a spatial zonation from west to east of a decrease in the heavier isotope.

The whole-rock signatures of the nine country-rock units yield a large range, from -21.7‰ for the Silverquick Formation, to +14.1‰ for the Congress basalt (Table 2; Figure 8). The sedimentary units (Silverquick Formation, Bridge River schist and Bridge River greywacke) display highly negative ^{34}S values at -21.7‰, an average of 17.65‰ and an average of -17.53‰, respectively. The two intrusions, the Coast Plutonic Complex and the Bendor batholith, yielded values of -0.4‰ and -1.7‰, respectively. The serpentinite yielded four measurements, with an average of +4.45‰, exhibiting a slight enrichment in ^{34}S , but still within the magmatic range (Ohmoto and Rye, 1979). The two basalt units, Cadwallader basalt and Bridge River basalt, do not show the same similarity in S isotope values that the other country rock groups (intrusions and sedimentary rocks) do. The Cadwallader basalt produced values with an average of +13.45‰,

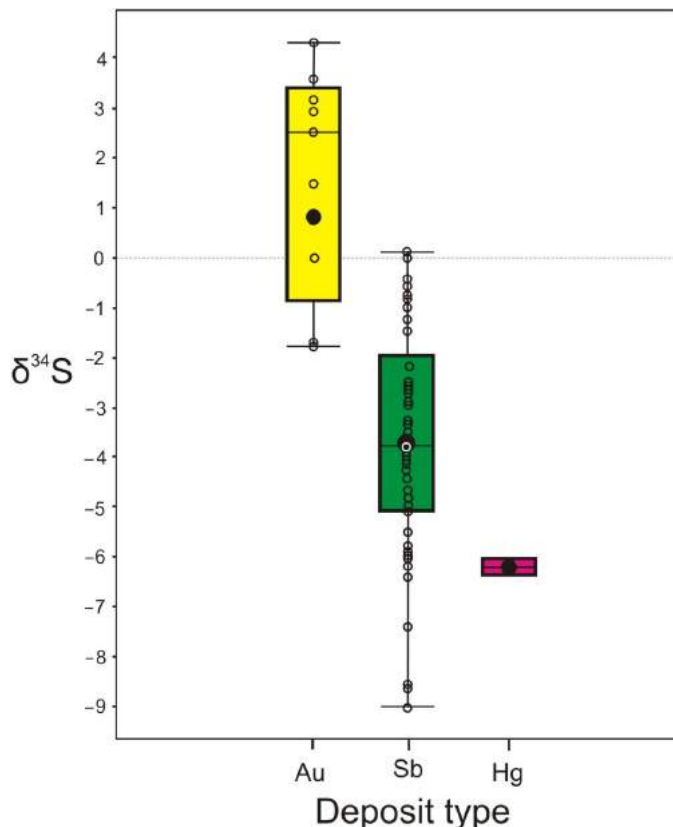


Figure 7. Box-and-whisker plot of deposit S isotope signatures showing dispersal of data throughout ranges. Mineralization type presented from west to east, showing the decrease in ^{34}S spatial zonation pattern.

while the Bridge River basalt has values with an average of +3.4‰.

The isotopic signatures for the country rock are overall consistent with previous studies (Ohmoto and Rye, 1979) on S isotope reservoirs, and have the typical signatures one would expect. The one exception is the Cadwallader basalt, which has a more positive ³⁴S than the archetypal basalt (usually closer to 0‰).

Geothermometry

Sulphur geothermometry is the measurement of the temperature of equilibration, and is based on the fractionation of S isotopes between two compounds, such as PbS and ZnS (Seal, 2006). For this calculation to be accurate, the compounds must be in equilibrium with each other, and must also not have undergone re-equilibration or alteration.

The temperature dependence of the fractionation factors must be known and pure minerals must be separated for isotopic analysis (Seal, 2006). The temperature is calculated by measuring the difference in the ³⁴S values of two sulphide minerals in equilibrium and plotting the result on a graph showing the equilibrium constant and isotope fractionation factor as a function of temperature. Pyrite is gen-

erally not as reliable as it tends to be in equilibrium across a range of temperatures (Ohmoto and Rye, 1979; Rye and Ohmoto, 1974; Seal, 2006). For this exercise, pyrite-galena and pyrite-sphalerite will be used as there are no sphalerite-galena pairs.

The data are presented in Table 3. It shows that there are no consistencies in temperatures between the mineralization

Table 2. Sulphur isotopes (listed as ‰ relative to CDT) of country rock in the Bridge River–Bralorne mineral district.

Sample ID	Country Rock Member	Sulphide type	δ ³⁴ S
WAYW3 SEDS	Bridge River Complex greywacke	mono	-19.9
WAYW3 SEDS	Bridge River Complex greywacke	di	-12.7
WAYW3 SEDS	Bridge River Complex greywacke	total	-20.0
WAYW2 BASALT	Bridge River Complex basalt	mono	2.3
WAYW2 BASALT	Bridge River Complex basalt	total	4.5
WAYW1 GABBRO	Bridge River Complex gabbro	mono	1.5
SERP1	Bralorne–East Liza ophiolite complex serpentinite	mono	4.3
SERP1	Bralorne–East Liza ophiolite complex serpentinite	di	4.6
SERP2	Bralorne–East Liza ophiolite complex serpentinite	mono	4.2
SERP2	Bralorne–East Liza ophiolite complex serpentinite	total	4.7
CONG BASALT	Cadwallader Group basalt	mono	13.4
CONG BASALT	Cadwallader Group basalt	mono	14.1
CONG BASALT	Cadwallader Group basalt	total	12.9
COAST	Coast Plutonic Complex	mono	-0.4
SQF1-W	Silverquick Formation shale	di	-21.7
BENDOR	Bendor batholith	total	-1.7
CHALCO SCHIST	Bridge River Complex schist	mono	-17.8
CHALCO SCHIST	Bridge River Complex schist	di	-16.2
CHALCO SCHIST	Bridge River Complex schist	total	-17.5
CHALCO SCHIST	Bridge River Complex schist	total	-17.7
CHALCO SCHIST	Bridge River Complex schist	total	-19.2

Abbreviations: mono, monosulphide; di, disulphide; total, total sulphur

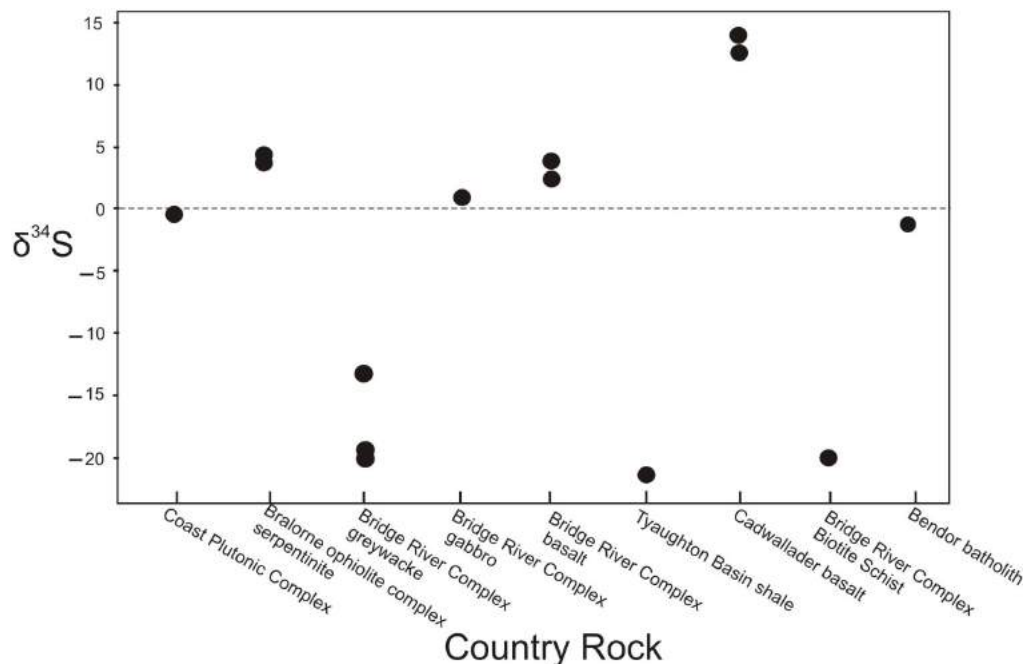


Figure 8. Plot of country rock isotope signatures. Samples organized from west to east.

Table 3. Temperature estimates using the sulphide-pair method from Seal (2006).

Sample ID	Deposit	Mineral Pairs $\delta^{34}\text{S}$		$\text{min}_1\text{-min}_2$	$\text{Inamin-H}_2\text{S}$	$\times 10^5$	$\times 10^6/\text{min}_1\text{-min}_2$	SQRT	TEMP
		Gal	Py						
KV2	Kelvin	-8.6	-5.9	2.7	1.03	1030000	381481.4815	617.6419	344.4919
GR8	Grey Rock	-2.5	0	2.5	1.03	1030000	412000	641.8723	368.7223
GR2	Grey Rock	-2.5	-0.6	1.9	1.03	1030000	542105.2632	736.278	463.128
		Py	Sph						
PLS	Peerless	0.1	-0.6	0.70709	0.3	300000	424274.3777	651.3635	378.2135
SMT2	Summit	-6.0	-4.3	1.70000	0.3	300000	176470.5882	420.084	146.934
MINTO	Minto	-0.8	-1.1	0.37016	0.3	300000	810453.8825	900.2521	627.1021
LS1	Lucky Strike	-2.7	-3.4	0.65468	0.3	300000	458240.633	676.9347	403.7847
OLYC0R7	Olympic Core	-5	-4.1	0.91423	0.3	300000	328145.7142	572.84	299.69
PETER	Peter Vein	-1.7	-3.2	1.52718	0.3	300000	196440.3296	443.2159	170.0659
RBS	Robson	-3.1	-4.2	1.2	0.3	300000	254698.3533	504.6765	231.5265
		Py	Stib						
LS1	Lucky Strike	-2.7	-7.5	4.8	1.15	1150000	240830.6404	490.745	217.595

Abbreviations: Gal, galena; Py, pyrite; Stib, stibnite; Sph, sphalerite; SQRT, square root

types. The one value for Au is extremely low at 170°C. Antimony mineralization types display a very large range, from 146 to 627°C, without clustering around any one temperature. The calculated temperature values for these deposits and occurrences are inconsistent with the known models for not only this district (Maheux 1989; Leitch et al. 1991b), but for orogenic Au deposits in general (Groves et al., 2003).

Figure 9 shows previously calculated fluid-inclusion temperature data for the mineralization types in the district. The Au deposits are hot, ranging from 280 to 365°C, the Sb deposits are cooler with a range of 220 to 300°C and Hg deposits are the coolest with mineralizing fluid temperatures around 190°C. These temperatures are more within the expected range for this type of hydrothermal system. There are many inconsistencies between the data in Figure 9 and Table 3. The Au temperature in Table 3 (using sulphide pairs) is 200°C cooler than the temperatures in Figure 9 (using fluid inclusions). The Sb mineralization displays a much smaller range in Figure 9 than in Table 3, but there is a small overlap between the two ranges; Robson (RBS) in Table 3 has a calculated temperature of 231°C, which is on the lower end of the Figure 9 range. The main problem with the data in Table 3 is that it was calculated using sulphide pairs that are not the recommended pairs (sphalerite and galena), and all pairs involved pyrite, which is the least reliable of the sulphide minerals used for that method of calculation. Unfortunately, the pairs used were the best possible pairs out of the analyzed sulphide minerals.

Discussion

Sulphur isotopes can be extremely useful for establishing the genesis of an ore deposit, and can additionally provide information on the temperature of mineralization, chemical conditions and mechanisms of ore deposition and the source of the S in the ore-forming fluid (Ohmoto and Rye, 1979). A previous S isotope study on the Bralorne–Pioneer Au deposit by Leitch et al. (1991b) was interpreted to show that the fluids were primarily magmatic and metamorphic, but had a component of late-stage meteoric mixing.

The S isotopic signatures of the mineralization types and their distributions from west to east across metal zones that characterize the district can result from an increasing reaction of the mineralizing fluids with the S in the country rock. As there are a variety of country rocks surrounding the mineralization types, there are also a variety of S

Fluid inclusion temperatures of deposit types

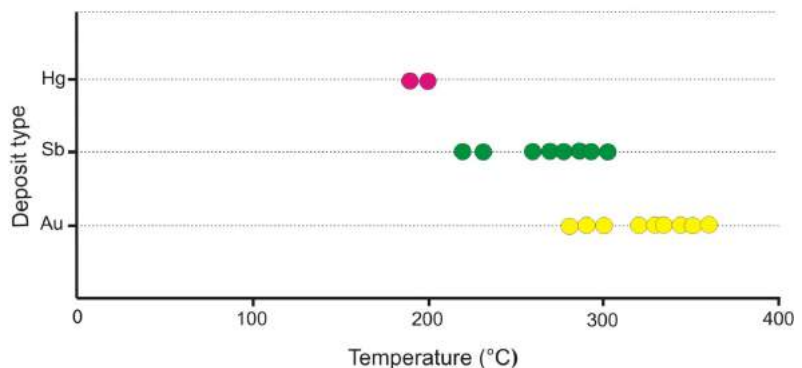


Figure 9. Temperatures of deposits calculated from fluid-inclusion studies by Maheux (1989) and Leitch et al (1991b).

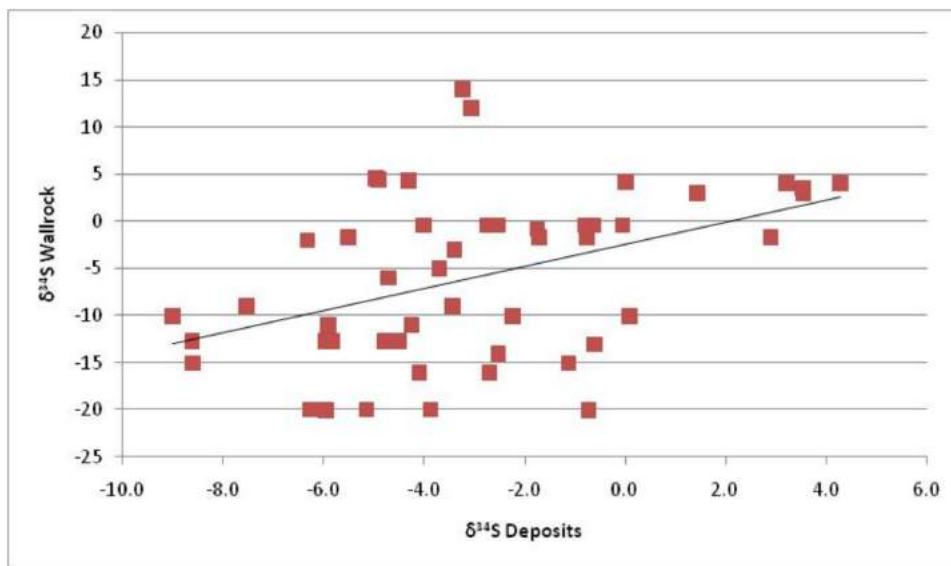


Figure 10. Graph showing the correlation between country rock and deposit S isotope signatures.

sources. The assumption was made that there would be mixing of S from different sources, combining to produce a unique S isotope value. It seems unlikely that as fluid travels along a pathway, it only scavenges S from one source, unless one rock type is enriched in S or that S is more accessible/soluble. Mixing of the S between two very different isotopic sources, for example, serpentinite (+4.4‰) of the Bralorne ophiolite complex and greywacke of the Bridge River Complex (−19‰), would result in a ^{34}S somewhere in between those two values, depending on the fluid chemistry at the time.

To establish the contributions that country rock S makes toward the S in the sulphide minerals of the deposits, deposit isotope values were assigned to its country rock host value. In the case where there was more than one country rock, a combined value was calculated. This was done using geological information from Maheux (1989), Leitch et al. (1991b), Church (1996), Schiarizza et al. (1997) and Ash (2001), and is displayed in Figure 10. The result generates a positive slope, showing a correlation between the country rocks and the mineralizing fluids, emphasizing that the country rock S isotope signature affects the deposit isotope signature. The decreasing ^{34}S pattern in Figure 7 can be interpreted to suggest that there is an increase in a reduced S source, which is enriched in ^{33}S over ^{34}S . Since reduced S sources are generally sedimentary in origin (Ohmoto and Rye, 1979), this means an increase in sedimentary rock interaction from west to east is likely. The temperature data in Figure 9 also shows a distribution from west to east, with fluids hotter in the west and cooler in the east. Therefore, the trend from west to east from Au deposits through to Hg deposits is a general trend that results from higher amounts of fluid–country rock interactions and indicates that the

mineral occurrences get the majority of their S from the adjacent country rocks.

A similar study was performed on analogous Au deposits in southeastern Alaska on the west side of the Coast Plutonic Complex, which also found a correlation between the S isotopic ratios of the country rock and the Au mineralization (Goldfarb et al., 1997). Gold veins dated at 55–66 Ma postdate the initial period of collision by 100 Ma, and were emplaced at depths of 3–10 km with vein formation temperatures of 225–375°C. Depos-

its that were hosted in diorite had values that clustered around 0‰, while veins hosted in argillite showed ranges of −6 to −12‰. The conclusion of this study was that the nearby sedimentary rocks provided the source for the majority of the S in the ore-bearing fluids, with possible igneous rock-hosted contributions. While Goldfarb et al. (1997) stated that there was a possibility of a small fluid contribution from the proximal calcalkaline intrusions, it was also concluded that on a broader scale, this hydrothermal activity could be related to rising crustal temperatures associated with ongoing collision, metamorphism and crustal dehydration. Considering the Bridge River–Bralorne mineral district is located on the eastern edge of the Coast Plutonic Complex, which was a magmatic arc that continues up into southern Alaska, it is likely that the metamorphism that generated crustal dehydration occurring in southeastern Alaska also took place in southwestern BC, thus providing metamorphogenic crustal hydrothermal fluids.

A metamorphic origin of ore-forming fluids has been proposed at a number of large-scale orogenic lode-Au deposits around the world, including the Mother Lode district in the North American Cordillera and Macraes Flat in the Otago Province, New Zealand. Nitrogen, hydrogen and oxygen isotope studies indicated that metamorphic dehydration reactions of subduction-accretion complexes along the North America Cordillera resulted in dilute-aqueous, carbonic fluids (Jia et al., 2003). A S isotope study on the Macraes Flat Au deposit in the Otago Province found that the ^{34}S of the sulphide minerals from the deposit had a narrow range of −3 to −1‰, while the Otago schist had a range of −6 to +6‰, suggesting that the S was derived from the schist (Craw et al., 1995). A later study discovered a depletion in ore-forming elements between the greenschist and amphibolite facies

rocks in the Otago schist, and an enrichment in the same elements in the orogenic Au deposits in Otago (Pitcairn et al., 2006), suggesting that the metamorphically derived ore-forming fluids scavenged the elements from those rocks, depositing them further along the fluid pathway.

From the geological and S isotope information in the Bridge River–Bralorne mineral district, it can be assumed that there is one fluid source for all three deposits, with the Au deposits the closest to this source, in relation to the other mineralization types, the Sb an intermediate distance and the Hg the farthest away. The reactivated dextral strike-slip faults were active at the time of mineralization (67 Ma). Therefore, they would provide the perfect fluid conduits for a deeper crustal, metamorphic source of fluids, which according to the correlation between the country rock S and deposit S, was closest to the Au deposits and occurrences, then travelled up and outwards, toward the Sb and Hg occurrences. The temperature data (Figure 9) also supports this conclusion, as it shows the Au mineralization formed from the hottest fluids, Sb from the intermediate and the Hg from the coolest.

The initial ^{34}S of the fluids may have started out at +4‰, and as this fluid travelled up the fluid conduits, it interacted with the country rock S, and evolved its ^{34}S . Since the S in the fluids forming the Au mineralization have had the least opportunity to react with the S in the country rock, and the dominant rock type along the Bralorne fault zone is gabbro, the ^{34}S is closest to +4‰, only deviating a small amount from this value, which is to be expected as reactions will occur between the fluid and the country rock when a fluid travels along its path. The Sb mineralization has a more negative ^{34}S than the Au, which is a result of a higher amount of S sourced from the basalt and sedimentary-dominant country rocks along the Hg fault zones. The Hg mineralization has the overall most negative ^{34}S out of the three mineralization types; consequently, the fluids have purloined the most S from the country rocks, which are sedimentary rocks from the Tyaughton Basin.

Conclusions

The Bralorne–Bridge River mineral district is one of the most significant historical lode-Au producers in BC, and regionally displays a characteristic metal zonation from west to east of Au through Sb- to Hg-associated mineralization. Each mineralization has a characteristic range of ^{34}S values, from +4.3 to –2.7‰ for Au, from +0.2 to –9‰ for Sb and –6.2‰ for Hg that display a decreasing ^{34}S pattern from west to east. When the deposit sulphide mineral ^{34}S values are compared with their respective hostrocks, a correlation was found that demonstrates an increasing reaction of the country rock S with the S in the fluids and reflects the different types of hostrocks. When the S isotope patterns are combined with the cooling temperature trend of miner-

alizing fluids from west to east, it provides evidence of one fluid source for the three dominant types of mineralization in the district.

The deduction of a fluid source for this region is similar to the crustal continuum model (Groves et al., 1998), which states that Sb and Hg mineralization are higher crustal, epizonal equivalents to the mesozonal orogenic Au deposits that all formed from one fluid source that travelled along the same fluid pathway. Assuming this model is true to this district, there is a possibility that there are hypozonal Au deposits somewhere in the region underneath Sb and Hg deposits in the Bralorne–Bridge River mineral district.

In conclusion, a single, deep-crustal fluid source for all three types of deposits flowed up along reactivated strike-slip faults, scavenging S from the country rock as it went. Therefore, there are different S sources for each deposit type, but each type has its own distinctive ^{34}S range, making it identifiable. This impacts the approaches to regional exploration strategies as the most prospective Au deposits will have a more positive ^{34}S , which can easily be determined.

Acknowledgments

Funding for this project comes from Geoscience BC with the support from the University of Western Australia and the USGS. Support from C. A. Gulbransen, C. Johnson, R.S. Thurston, R. Rye and the USGS Denver is also appreciated. Members of the staff at the Gold Bridge Hotel are thanked for their hospitality. R. Goldfarb is thanked for his support of this project and his hospitality.

References

- Cairnes, C. E. (1937): Geology and mineral deposits of the Bridge River Mineral Camp, British Columbia; Geological Survey of Canada, Memoir 213, 140 p.
- Church, B.N. (1996): Bridge River mining camp geology and mineral deposits; BC Ministry of Energy, Mines and Petroleum Resources, Paper 1995-3, 160 p.
- Craw, D., Hall, A.J., Fallick, A.E. and Boyce, A.J. (1995): Sulphur isotopes in a metamorphogenic gold deposit, Macraes mine, Otago schist, New Zealand; *New Zealand Journal of Geology and Geophysics*, v. 38, p. 131–136.
- Goldfarb, R.J., Miller, L.D., Leach, D.L. and Snee, L.W. (1997): Gold deposits in metamorphic rocks of Alaska; *Economic Geology*, Monograph 9, p. 151–190.
- Groves, D.I., Goldfarb, R.J., Gebre-Mariam, M., Hagemann, S.G. and Robert, F. (1998): Orogenic gold deposits: a proposed classification in the context of their crustal distribution and relationship to other gold deposit types; *Ore Geology Reviews*, v. 13, p. 7–27.
- Groves, D.I., Goldfarb, R.J., Robert, F. and Hart, C.J.R. (2003): Gold deposits in metamorphic belts: overview of current understanding, outstanding problems, future research, and exploration significance; *Economic Geology*, v. 98, p. 1–29.

- Hart, C.J.R., Goldfarb, R.J., Ullrich, T.D. and Friedman, R. (2008): Gold, granites and geochronology: timing of formation of the Bralorne–Pioneer gold orebodies and the Bendor batholith, southwestern British Columbia (NTS 092J/15); *in* Geoscience BC Summary of Activities 2007, Geoscience BC, Paper 2008-1, p. 47–54.
- Jia, Y., Kerrich, R. and Goldfarb, R.J. (2003): Metamorphic origin of ore-forming fluids for orogenic gold-bearing quartz vein systems in the North American Cordillera: constraints from a reconnaissance study of ^{15}N , D, and ^{18}O ; *Economic Geology*, v. 98, p. 109–123.
- Leitch, C.H.B. (1990): Bralorne: a mesothermal, shield-type vein gold deposit of Cretaceous age in southwestern British Columbia; *Economic Geology: CIM Bulletin*, v. 83, p. 53–80.
- Leitch, C.H.B., Dawson, K.M. and Godwin, C.I. (1989): Early Late Cretaceous–Early Tertiary gold mineralization: a galena lead isotope study of the Bridge River mining camp, southwestern British Columbia, Canada; *Economic Geology*, v. 84, p. 2226–2236.
- Leitch, C.H.B., Godwin, C.I., Brown, T.H. and Taylor, B.E. (1991b): Geochemistry of mineralizing fluids in the Bralorne–Pioneer mesothermal gold vein deposit, British Columbia, Canada; *Economic Geology*, v. 86, p. 318–353.
- Leitch, C.H.B., van der Heyden, P., Godwin, C.I., Armstrong, R.L. and Harakal, J.E. (1991a): Geochronometry of the Bridge River camp, southwestern British Columbia; *Canadian Journal of Earth Sciences*, v. 28, p. 195–208.
- Maheux, P.J. (1989): A fluid inclusion and light stable isotope study of antimony-associated gold mineralisation in the Bridge River District, British Columbia, Canada; M.Sc. thesis, University of Alberta, 160 p.
- Ohmoto, H. and Rye, R.O. (1979): Isotopes of sulfur and carbon; *in* *Geochemistry of Hydrothermal Ore Deposits*, v. 2, H. L. Barnes (ed.), John Wiley & Sons, p. 509–567.
- Pearson, D.E. (1975): Bridge River map-area (92J/15); *in* *Geological Fieldwork 1974*; BC Ministry of Energy, Mines and Petroleum Resources, Paper 1975-2, p. 35–39.
- Pitcairn, I.K., Teagle, D.A.H., Craw, D., Olivo, G.R., Kerrich, R. and Brewer, T.S. (2006): Sources of metals and fluids in orogenic gold deposits: insights from the Otago and Alpine schists, New Zealand; *Economic Geology*, v. 101, p. 1525–1546.
- Rye, R.O. and Ohmoto, H. (1974): Sulfur and carbon isotopes and ore genesis: a review; *Economic Geology*, v. 69, p. 826–842.
- Sasaki, A., Arikawa, Y. and Folinsbee, R.E. (1979): Kiba reagent method of sulfur extraction applied to isotopic work; *Geological Survey of Japan Bulletin*, v. 30, p. 241–245.
- Schiarizza, P., Gaba, R.G., Glover, J.K., Garver, J.I. and Umhoefer, P.J. (1997): Geology and mineral occurrences of the Taseko–Bridge River area; BC Ministry of Energy, Mines and Petroleum Resources, Bulletin 100, 291 p.
- Seal, R.R. (2006): Sulfur isotope geochemistry of sulfide minerals; *in* *Reviews in Mineralogy and Geochemistry: Sulfide Mineralogy and Geochemistry*, v. 61, D.J. Vaughan (ed.), Mineralogical Society of America, p. 633–677.
- Tuttle, M.L., Goldhaber, M.B. and Williamson, D.L. (1986): An analytical scheme for determining forms of sulphur in oil shales and associated rocks; *Talanta*, v. 33, no. 12, p. 953–961.
- Umhoefer, P.J. and Schiarizza, P. (1996): Latest Cretaceous to early Tertiary dextral strike-slip faulting on the southeastern Yalakom fault system, southeastern Coast Belt, British Columbia; *GSA Bulletin*, v. 108, no. 7, p. 768–785.
- Woodsworth, G.J., Pearson, D.E. and Sinclair, A.J. (1977): Metal distribution patterns across the eastern flank of the Coast Plutonic Complex, south-central British Columbia; *Economic Geology*, v. 72, no. 2, p. 170–183.

Preliminary Results of Geological Mapping, Uranium-Lead Zircon Dating, and Micropaleontological and Lead Isotopic Studies of Volcanogenic Massive Sulphide–Hosting Stratigraphy of the Middle and Late Paleozoic Sicker and Lower Buttle Lake Groups on Vancouver Island, British Columbia (NTS 092B/13, 092C/16, 092E/09, /16, 092F/02, /07)

T. Ruks, Mineral Deposit Research Unit, Department of Earth and Ocean Sciences, University of British Columbia, Vancouver, BC, tyler_ruks@hotmail.com

J.K. Mortensen, Mineral Deposit Research Unit, Department of Earth and Ocean Sciences, University of British Columbia, Vancouver, BC

F. Cordey, CNRS UMR 5125, Université Claude Bernard Lyon 1, 69622, Villeurbanne Cedex, France

Ruks, T., Mortensen, J.K. and Cordey, F. (2008): Preliminary results of geological mapping, uranium-lead zircon dating, and micropaleontological and lead isotopic studies of volcanogenic massive sulphide–hosting stratigraphy of the Middle and Late Paleozoic Sicker and Lower Buttle Lake groups on Vancouver Island, British Columbia (NTS 092B/13, 092C/16, 092E/09, /16, 092F/02, /07); in Geoscience BC Summary of Activities 2008, Geoscience BC, Report 2009-1, p. 103–122.

Introduction

Volcanogenic strata of the mid-Paleozoic Sicker Group on Vancouver Island (Figure 1) occur in several distinct basement highs (referred to herein as ‘uplifts’). These rocks host the world-class Myra Falls volcanogenic massive sulphide (VMS) deposit (combined production and proven and probable reserves in excess of 40 million tonnes of Zn-Cu-Au-Ag sulphides), as well as numerous other VMS deposits and occurrences, including those in the Big Sicker Mountain area in the southeastern part of the Cowichan Lake uplift (Figure 1). Three of these deposits in the Cowichan Lake uplift, the Lenora, Tye and Richard III (MINFILE occurrences 092B 001, 092B 002, 092B 003; MINFILE, 2008) have seen limited historical production. The Lara deposit (MINFILE occurrence 092B 129), farther to the northwest, also contains a significant drill-indicated resource of 1 146 700 tonnes grading 3.01% Zn, 1.05% Cu, 0.58% Pb, 32.97 g/t Ag and 1.97 g/t Au (Kelso et al., 2007). Geological mapping (Massey and Friday, 1987; Mortensen, 2005; Ruks and Mortensen, 2006) suggests that the the Big Sicker Mountain area consists mainly of deformed mafic to felsic volcanic and volcanoclastic rocks of the Nitinat and McLaughlin Ridge formations, and high-level intrusions of the Saltspring intrusive suite, as well as abundant gabbroic dikes and sills of the Triassic Mount Hall gabbro (Figure 2). Recent geological mapping in the Cowichan Lake uplift (this study) has been a continuation

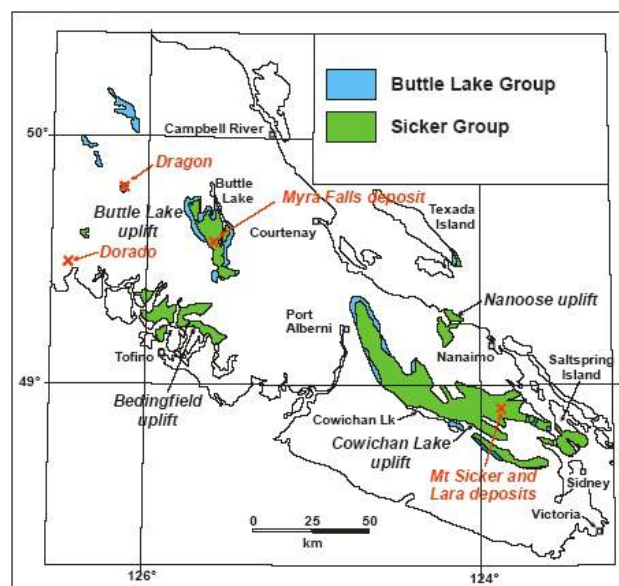


Figure 1. Distribution of Paleozoic strata of the Sicker and Buttle Lake groups on Vancouver Island and the Gulf Islands.

of our efforts to develop a stratigraphic framework for Sicker arc development and VMS mineralization in the Sicker Group. Work conducted on Cowichan Lake uplift mineral tenure owned by project sponsors Treasury Metals Inc. and Westridge Resources Inc. concentrated on resolving the geological setting and age of the Lara VMS deposit and other VMS occurrences in the area, as well as examining new bedrock exposure created by recent logging activity. Reconnaissance fieldwork on new bedrock exposure owned by Westridge Resources Inc. culminated in the discovery of a new, polymetallic VMS occurrence. Mapping in the Mount Brenton area by Treasury Metals Inc. has identified a prospective zone where intensely sericite-al-

Keywords: Sicker Group, Paleozoic, Vancouver Island, Cowichan Lake uplift, volcanogenic massive sulphide, stratigraphy, uranium-lead zircon geochronology, lithogeochemistry

This publication is also available, free of charge, as colour digital files in Adobe Acrobat® PDF format from the Geoscience BC website: <http://www.geosciencebc.com/s/DataReleases.asp>.

tered and pyrite-mineralized felsic ash tuff is overlain, in turn, by silicified argillite and a chlorite-altered ash tuff of intermediate composition. A similar geological setting is associated with massive sulphide mineralization at the Lenora deposit (Ruks and Mortensen, 2006). Geological mapping and sampling were also focused in the vicinity of the Lady A iron formation (Treasury Metals Inc.; MINFILE 092B 033). The Lady A is similar to other iron formations occurring in rocks that are stratigraphically above VMS mineralization at the Lenora, Tyee and Richard III occurrences, and is believed to represent oxide-facies iron mineralization related to hydrothermal mineralizing systems similar to those that formed the underlying VMS deposits. Resolving the timing of iron formation mineralization in the Sicker Group is critical for establishing the duration of VMS-related hydrothermal activity.

Geological mapping in the Cowichan Lake uplift of the Port Alberni area (Massey and Friday, 1989) indicates that this area is largely underlain by basalt to basaltic andesite volcanic rocks of the Duck Lake and Nitinat formations, respectively, in addition to felsic tuffaceous volcanoclastic rocks belonging to the McLaughlin Ridge Formation. McLaughlin Ridge Formation rocks in the Port Alberni area are interpreted to represent deposition distal from a volcanic centre, which is thought to be represented in the Saltspring Island–Cowichan Lake area by felsic intrusive rocks of the Saltspring intrusive suite (Massey and Friday, 1989). However, geological mapping of new exposures in the Port Alberni area (this study) indicates that felsic volcanic rocks of potential McLaughlin Ridge Formation age are present in significant quantities, necessitating a reinterpretation of the nature of the Sicker Group and its VMS potential in the Port Alberni area.

Sedimentary, mafic volcanic and carbonate rocks of the Nanoose uplift have been tentatively correlated with both the Sicker and Buttle Lake groups (Yorath et al., 1999). However, no geochronological or biostratigraphic sampling has demonstrated an age that facilitates comparisons with the Sicker Group. To resolve outstanding stratigraphic problems in the Nanoose uplift, reconnaissance fieldwork in the area this summer focused on sampling prospective rock types for geochronology and biostratigraphy. Of particular importance is resolving the age of mafic volcanic rocks in the area.

Mapping in the Hesquiat and Gold River areas, on the Dorado and Dragon properties (Paget Resources Corporation; Figure 1), has identified several new VMS occurrences hosted in potential Sicker Group rocks. Geological mapping and sampling on the Dragon property by previous workers indicates the presence of several polymetallic massive sulphide lenses with grades up to 7.33% Zn, 1.34% Pb, 173 ppm Cu, 680 ppb Au and 19.2 g/t Ag over a 2 m thickness (Jones, 1997). Geological mapping of the Dorado and

	Muller, 1977 (Vancouver Island)	Juras, 1987 (Buttle Lake Uplift)	Yorath et al., 1999 (Alberni area)
Sicker Gp		Buttle Lake Gp	Henshaw Fm
	Buttle Lk Fm		St. Mary Lk Fm
	Sediment Sill Unit	Mt Mark Fm	
	Myra Fm		
	Nitinat Fm	Sicker Gp	Flower Ridge Fm
	Thelwood Fm		
	Myra Fm		Nitinat Fm
	Price Fm		Duck Lk Fm

Figure 2. Stratigraphic nomenclature for the Sicker and Buttle Lake groups on Vancouver Island (Yorath et al., 1999).

Dragon properties indicates that mafic and felsic volcanic rocks and contained VMS mineralization are overlain by volcano-sedimentary and carbonate rocks, including calcareous tuffaceous sedimentary rocks and fossiliferous limestone, respectively. Nowhere else in the Sicker Group are carbonate rocks observed to directly, and apparently conformably, overlie felsic volcanic rocks and VMS mineralization. This relationship indicates that radical stratigraphic differences exist between rocks of the Dragon property and better studied exposures of the Sicker Group in the Cowichan Lake and Myra Falls areas. These stratigraphic differences may be explained by large changes in volcanic and sedimentological facies or the presence of an unrecognized cycle of arc magmatism and VMS mineralization on Vancouver Island.

The 2008 fieldwork in the Sicker Group commenced in early August and finished in mid-October 2008. Information pertaining to the Dorado property of Paget Resources Corporation is based on fieldwork conducted in 2007. Both reconnaissance and detailed geological mapping, together with sampling for litho-geochemistry, U-Pb zircon dating, and Nd, Hf and Pb isotopic studies, were conducted in the Cowichan Lake, Port Alberni, Nanoose, Gold River and Hesquiat areas over this period. This report presents a summary of this fieldwork, with emphasis on key stratigraphic relationships and areas of economic importance.

Regional Geology of the Sicker Group

The mid-Paleozoic Sicker Group on southern and central Vancouver Island represents the oldest rocks in the Wrangellia Terrane. Equivalents of the Sicker Group are not present in Wrangellia in northwestern British Columbia, southwestern Yukon and southern Alaska, where the oldest rock units are the Skolai Group, which is no older than Pennsylvanian (e.g., Katvala, 2006). This, and other differences between the Wrangellian stratigraphy on Vancouver Island and that in more northerly exposures, empha-

size the lack of understanding regarding much of Wrangellia (e.g., Katvala, 2006) and the need for further studies. The Cowichan Lake uplift on Vancouver Island and adjacent portions of the Gulf Islands is the largest of four uplifts that expose the Sicker and overlying late Paleozoic Buttle Lake groups (Figure 1).

Previous detailed studies of the Sicker Group have focused mainly on the stratigraphic setting of VMS mineralization at the Myra Falls deposits in the Buttle Lake uplift (Figure 1; e.g., Juras, 1987; Barrett and Sherlock, 1996). Regional mapping of the Cowichan Lake uplift by Massey and Friday (1987, 1989) and Yorath et al. (1999) led to a stratigraphic framework that may be applicable to the entire Sicker Group (Figure 2). This framework, however, is based on mapping in only one of the four main uplifts of Sicker Group rocks, and is supported by a limited amount of biostratigraphic and isotopic age data (e.g., Brandon et al., 1986). Major along- and across-strike facies changes and geochemical variations are to be expected in submarine volcanic sequences such as the one that forms the Sicker Group; hence, the regional applicability of the stratigraphic framework of Yorath et al. (1999) must be tested with detailed mapping and subsequent lithogeochemical and U-Pb dating studies. This is critical for regional exploration for VMS deposits within the Sicker Group. For example, the questions of whether VMS deposits and occurrences in the Cowichan Lake uplift are all of the same age, and whether their hostrocks are directly correlative with those that host the Myra Falls deposit, are of obvious importance.

The Sicker Group within the Cowichan Lake uplift is presently interpreted to represent three distinct volcanic and volcanoclastic assemblages that together are thought to record the evolution of an oceanic magmatic arc (Massey, 1995; Yorath et al., 1999). The lowermost Duck Lake Formation yields mainly normal mid-ocean-ridge basalt (N-MORB) geochemical signatures (Massey, 1995) and is interpreted to represent the oceanic-crust basement on which the Sicker arc was built. The upper portions of the Duck Lake Formation yield tholeiitic to calcalkaline compositions and may represent primitive arc rocks. The Duck Lake Formation is overlain by the Nitinat Formation, which comprises mafic, submarine volcanic and volcanoclastic rocks with dominantly calcalkaline compositions and trace-element signatures typical of volcanic arc settings. These rocks are interpreted as an early stage of arc development. The andesitic to mainly dacitic and rhyolitic McLaughlin Ridge Formation overlies the Nitinat and is believed to be correlative with the Myra Formation, the hostrocks for the Myra Falls deposits (Figure 2). Rocks of the McLaughlin Ridge and Myra formations reflect a more evolved stage of arc activity. Eruption of Nitinat volcanic and volcanoclastic rocks appears to have occurred from several widely scattered centres, whereas the McLaughlin Ridge Formation within the Cowichan Lake uplift is

thought to represent eruption from one or more major volcanic edifices. The abundance of proximal felsic volcanoclastic rocks and the presence of voluminous comagmatic felsic intrusions in the Saltspring Island and Duncan areas (Figure 1) indicate that one of these major volcanic centres was located in this area. Plant fossils indicate that at least a minor amount of the McLaughlin Ridge volcanism occurred in a subaerial setting. In the Port Alberni area, the McLaughlin Ridge Formation has previously been interpreted to comprise felsic, fine-grained tuffaceous volcanoclastic and epiclastic rocks, suggesting deposition distal from a volcanic centre. The identification of significant quantities of proximal felsic volcanic rocks in the Alberni area this year suggests that an additional felsic volcanic centre may be located in the Port Alberni area. Deposition of sedimentary and volcano-sedimentary rocks of the overlying Fourth Lake Formation of the Buttle Lake Group followed the cessation of Sicker arc magmatism, and scarce mafic volcanic rocks contained within the Fourth Lake Formation yield enriched tholeiitic rather than the calcalkaline compositions that characterize the McLaughlin Ridge. Massey (1995) speculated that the Buttle Lake Group may represent a marginal-basin assemblage that developed on top of the Sicker arc.

Studies of the Sicker and Buttle Lake groups on southern Saltspring Island by Sluggett (2003) and Sluggett and Mortensen (2003) provided new U-Pb zircon age constraints on both felsic volcanic rocks of the McLaughlin Ridge Formation and several bodies of Saltspring intrusions. This work demonstrates that two distinct episodes of felsic magmatism occurred in this portion of the Cowichan Lake uplift. One sample of felsic volcanic rocks from the McLaughlin Ridge Formation and three samples of Saltspring intrusions yielded U-Pb ages in the range 356.5–359.1 Ma. A somewhat older U-Pb age of 369.7 Ma was obtained from a separate body of the Saltspring intrusions at Burgoyne Bay on the southwest side of Saltspring Island, indicating that magmatism represented by the McLaughlin Ridge Formation and associated Saltspring intrusions occurred over a time span of at least 15 Ma. There is insufficient age control available at this point to determine whether the magmatism was continuous or episodic during this time period.

Rocks in the Nanoose uplift (Figure 1) have been tentatively correlated with both the Sicker Group and the Buttle Lake Group, and comprise fine clastic rocks, chert, diabasic to andesitic volcanic rocks and limestone (Yorath et al., 1999). A fossil sample from crinoidal limestone in the Nanoose uplift provided brachiopods that yielded a Permian age and fusulinids that yielded a Middle Pennsylvanian age (Muller, 1980). However, diabasic and andesitic pillow lavas in the area have unknown stratigraphic affinities. On the Ballenas Islands, however, these pillow lavas are associated with green and grey chert, and are interbedded with a

red tuff breccia which contains both scoriaceous mafic volcanic clasts and crinoidal limestone clasts. The association between mafic flows, chert and a conspicuous breccia unit containing crinoidal limestone clasts is strikingly similar to geological relationships observed in the Lacy Lake–Horne Lake region (Ruks and Mortensen, 2007), suggesting a potential correlation between the two areas.

The age and stratigraphy of rocks underlying the Dragon and Dorado properties, in the vicinity of Gold River and Hesquiat, respectively, is poorly constrained. The Dragon property is located approximately 80 km west of Campbell River, 20 km northwest of Gold River and 65 km northwest of the Myra Falls mine of Breakwater Resources Ltd. (Figure 1). Regional mapping of the Dragon property area by Muller (1977) interpreted the rocks underlying the Dragon property as amphibolite-grade metamorphic rocks belonging to the Westcoast Crystalline Complex. Muller described the Westcoast Crystalline Complex as amphibolite-facies metamorphic rocks belonging to the Middle Paleozoic Sicker Group, the Late Paleozoic Buttle Lake Group and the Triassic Karmutsen Formation. After the discovery of massive sulphides in float on the Dragon property by prospector E. Specogna, work by Noranda geologists culminated in the discovery of the Falls and North VMS occurrences (Kemp and Gill, 1993). Further geological mapping and diamond-drilling by Noranda and Westmin geologists indicated that these showings, with grades up to 7.33% Zn, 1.34% Pb, 173 ppm Cu, 680 ppb Au and 19.2 g/t Ag over a 2 m thickness, are associated with the contact zone between underlying bimodal volcanic rocks and overlying sedimentary rocks and limestone (Jones, 1997). Volcanic rocks of the Dragon property that underlie massive sulphide mineralization consist of massive, flow-banded rhyolite, andesite and tuffaceous felsic and intermediate volcanic rocks. Sedimentary and carbonate rocks overlying and interlayered with massive sulphide mineralization on the Dragon property consist of chert, mudstone, calcareous mudstone, fossiliferous felsic tuff, fossiliferous wackestone and marble.

The Dorado property is located approximately 17 km north of the village of Hesquiat, on the west coast of Vancouver Island. Like the Dragon property, rocks underlying the Dorado property were originally interpreted by Muller (1977) as amphibolite-facies metamorphic rocks assigned to the Westcoast Crystalline Complex. However, geological mapping of the area by Marshall et al. (2006) has shown the region to be underlain by abundant mafic volcanic rocks of potential Sicker Group affinity, and by sedimentary and carbonate rocks of potential Buttle Lake Group affinity. Following up on reports by Marshall et al. (2006) of polymetallic VMS-style stockwork mineralization in the area, Paget Resources Corporation staked the Dorado property and soon after discovered several polymetallic massive sulphide occurrences. Massive sulphide mineralization on

the Dorado property is associated with the contact between massive, variably silica-altered, clinopyroxene- and feldspar-phyric andesite and overlying tuffaceous, volcano-sedimentary rocks.

Results of New Fieldwork in the Cowichan Lake Area

Mapping for 2008 fieldwork was conducted using ESRI's ArcPad™ 7 on a Hewlett-Packard IPaq HX4700 Pocket PC wirelessly connected to a GlobalSat® BT-359W Bluetooth GPS receiver. The BC Geological Survey's regional geology compilation for UTM Zone 10, southwestern BC, as well as numerous geological maps derived from mineral exploration assessment reports, were used for reference (Massey et al., 2005).

Westridge Resources Inc.

Due to fire-season access restrictions during this field season, only 1 day has been spent on Westridge Resources Inc. ground thus far. As a result, additional work on the Westridge Resources mineral tenure is planned for late November of 2008. Work carried out thus far has concentrated on resolving the geological setting of the Breen Lake massive sulphide occurrences (MINFILE 092B 090; Figure 3).

The Breen Lake area is underlain by east-striking, steeply dipping, andesitic and rhyolitic volcanic rocks that have been intruded by gabbro. The most prospective massive sulphide mineralization discovered to date in the Breen Lake area is the Jane showing. This showing consists of two adits reported to intersect several massive sulphide lenses (pyrrhotite-sphalerite-chalcopyrite) up to 0.46 m wide and 1.52 m long, of which a 0.91 m sample assayed 16.1% Zn (Fyles, 1950; Pattison and Money, 1988). The adits of the Jane showing were located during the 2008 site visit, but no sulphide mineralization could be found due to infill of the adits with overburden. The adits are collared in a zone of strongly foliated felsic ash tuff, which is presumed to be the host to the mineralization. Approximately 500 m to the east of the Jane adit, a new massive sulphide showing was discovered in new exposure created by recent logging-road construction at the north end of Breen Lake. This showing consists of a 10–20 cm wide band of massive pyrite, chalcopyrite and trace sphalerite mineralization hosted in a sericite- and chlorite-altered, intermediate to dacitic ash tuff (Figure 4). Much of the showing is covered by road-building material and overburden, so the true size of the mineralization remains to be established. Additional work to be conducted on Westridge Resources ground this winter will focus on evaluating the geological setting of this new discovery, as well as that of other mineral occurrences in the vicinity. Particular attention will be given to mapping new exposures of Sicker Group stratigraphy created by recent logging-road construction in the area.

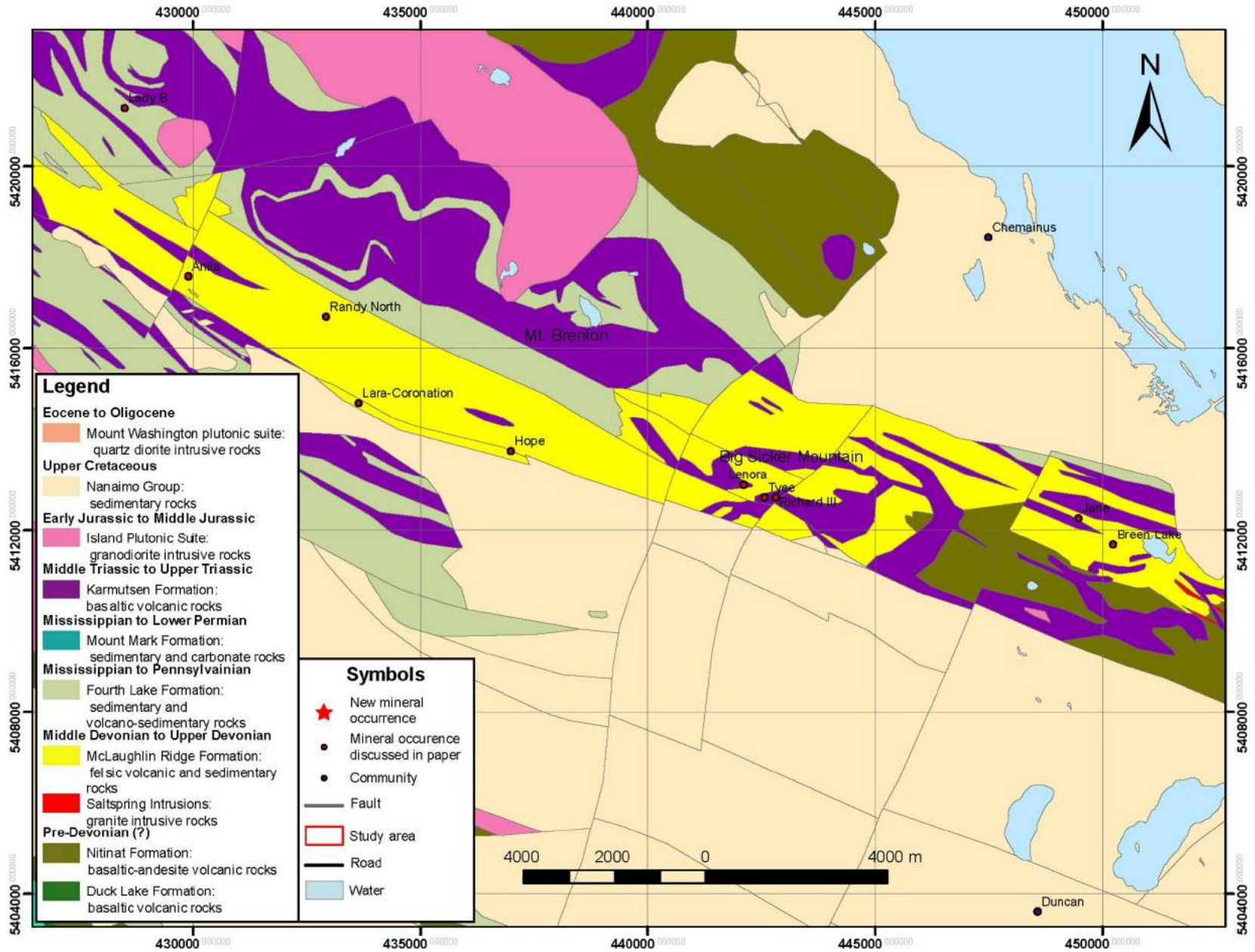


Figure 3. Regional geology, selected mineral occurrences and areas of study for 2008 fieldwork in the Cowichan Lake area (modified from Massey et al., 2005).

Treasury Metals Inc.

Work conducted on Treasury Metals Inc. ground this field season (the 'Lara property') focused on visiting known mineral occurrences with the goal of establishing their geological setting and age, as well as on conducting fieldwork in areas of new exposure created by logging-road construction. Unfortunately, due to a depressed forestry market during the past few years, very limited logging has been conducted on the Lara property and, as a result, there has been little new exposure created since the last main phase of exploration on the property in the 1980s by Laramide Resources Inc., Abermin Resources Corp. and Minnova Inc. However, forestry companies have recently marked much of the Lara property for logging, so there is a good chance that new bedrock exposures will be created there in the near future.

The Lara property hosts many VMS occurrences, the most notable of which is the Lara VMS deposit or Coronation trend (Figure 3). It consists of two main zones, the Corona-

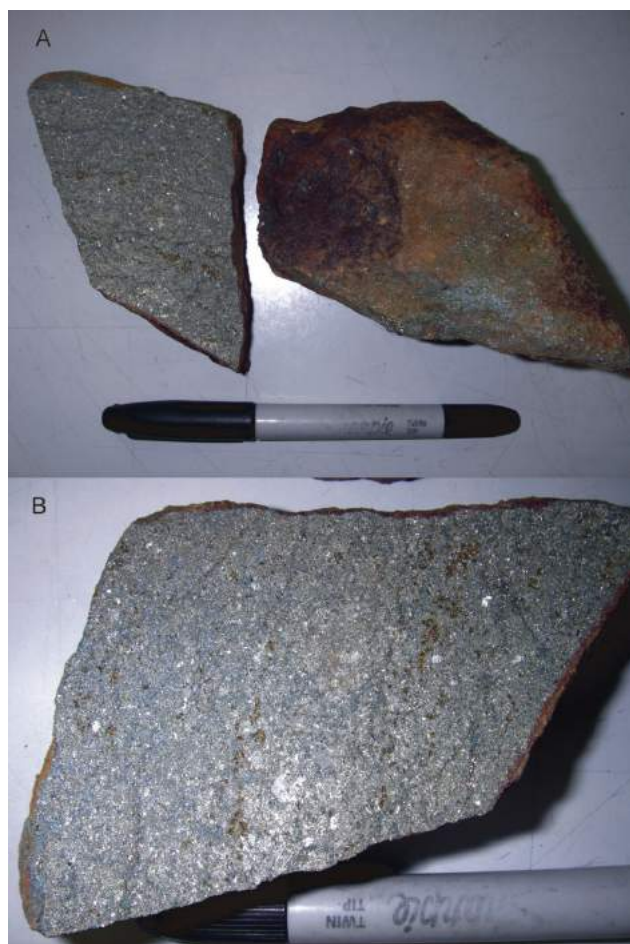


Figure 4. New massive sulphide mineralization discovered on the Westridge Resources Inc. mineral tenure in the Breen Lake area: **A)** medium- to coarse-grained massive pyrite with interstitial chalcopyrite and trace sphalerite; **B)** close-up of massive sulphide mineralization.

tion and Coronation Extension zones, collectively referred to as the Coronation trend, that combine for an indicated resource at a 1% Zn cut-off of 1 146 700 tonnes at 3.01% Zn, 1.05% Cu, 0.58% Pb, 32.97 g/t Ag and 1.97 g/t Au (Kelso et al., 2007). Sulphide mineralization of the Coronation and Coronation Extension zones is hosted by strongly silicified, coarse-grained rhyolite crystal tuff and ash tuff (Kelso et al., 2007). Surface mapping and sampling of two Coronation zone trenches was conducted during this study. The westernmost trench mapped in the Coronation zone (UTM Zone 10, 433489E, 5414841N, NAD83) is a flooded pit with sparse bedrock exposure at its north end (Figure 5a). Here, dark grey to black, medium-grained massive sulphides, consisting of 95% black sphalerite and 5% chalcopyrite, are in sharp contact with an intensely silica- and sericite-altered felsic ash tuff containing trace to 0.5% quartz and feldspar crystals up to 3 mm in size (Figure 5a). Bedding in this altered tuff dips steeply to the north. Massive sulphide mineralization in this pit contains elongated blebs of carbonate up to 2 cm wide and 10 cm long. The easternmost trench mapped in the Coronation zone (UTM Zone 10, 433558E, 5414824N) contains similar, medium-grained, massive sulphide mineralization comprising abundant black sphalerite with lesser chalcopyrite and pyrite (Figure 5b). This mineralization is hosted within a strongly silicified felsic crystal tuff with 2% quartz crystals up to 2 mm in size and abundant bull-quartz veining (up to 30 cm in width). Significant structural complexity is exposed in this trench, with felsic tuff on the east side of the massive sulphides being observed to fold into the plane of the mineralization (Figure 5b). No folding was observed in areas of the trench west of the massive sulphide mineralization, suggesting the potential for sinistral drag folding along the plane of massive sulphide mineralization. The absence of fault gouge associated with potential fault motion in this area may be explained by strain accommodation via massive sulphide recrystallization. Abundant concordant bull-quartz veining in felsic crystal tuff immediately east of the massive sulphide mineralization is probably the result of space filling during folding (Figure 5b).

The Randy North showing (MINFILE 092B 128), located approximately 2 km to the north of the Coronation zone (Figure 3), consists of several zones of anomalous polymetallic mineralization hosted in strongly sericite-altered felsic volcanoclastic rocks (Kelso et al., 2007). Exposures in the vicinity of the Randy North showing are often covered by thick moss, making geological mapping of the area problematic. In this area, moderately to strongly sericite-altered and highly foliated felsic crystal tuff, with 1–3% quartz crystals up to 5 mm size, hosts zones of intense pyrite stockwork mineralization. A small outcrop of medium-grained, sandy intermediate tuff was observed approximately 400 m to the southwest of this area (downsection?). Moderately sericite-altered, quartz-

potassic-feldspar porphyry becomes dominant to the west of the area, extending for at least 400 m along strike. This unit contains up to 20% potassic feldspar and quartz phenocrysts up to 5 mm in size, and may represent the subvolcanic heat source for the Randy North mineralizing system.

The Hope showing (MINFILE 092B 110) is situated along the southern flanks of Mount Brenton and approximately 3.5 km southeast of the Coronation zone (Figure 3). The showing comprises a small roadside outcrop of silicified felsic crystal tuff with 1% quartz crystals up to 2 mm in size. This tuff is intruded by gabbro, with intense silicification at the contact. Mineralization observed at the showing consists largely of disseminated pyrite with trace chalcopyrite veinlets and malachite staining. Sampling of the Hope showing by previous workers has yielded results up to 0.2% Cu, 0.85% Pb, 2.95 g/t Au and 25.03 g/t Ag, with barium contents averaging about 2% (Belik, 1983). Sampling of Hope showing mineralization for Pb isotope analysis has been conducted in order to determine if it is syngenetic with felsic volcanic rocks in the area.

Approximately 1.7 km north of the Hope showing, a potentially new prospective zone for VMS mineralization has been identified (Figure 3). Although much of this zone is poorly exposed in roadbed outcrop, key stratigraphic relationships are still visible. Here, an intensely sericite-altered felsic ash tuff, with 1–2% disseminated pyrite and trace quartz crystals, is overlain by a silicified argillite. Overlying the silicified argillite is a chlorite schist with 15–20% ankerite augen up to 5 mm in size. Collectively, this package dips steeply to the northeast. Massive sulphide mineralization at the Lenora adit, located approximately 6 km to the southeast (Figure 3), is associated with the contact between a similar, intensely sericite-altered felsic ash tuff and silicified argillite (Ruks and Mortensen, 2006). The stratigraphic package that hosts anomalous polymetallic mineralization of the Randy North zone is also capped by argillite (Kelso et al., 2007).

The Anita zone (MINFILE 092B 037), located approximately 4.7 km northwest of the Coronation zone (Figure 3), consists of polymetallic sulphide mineralization situated close to the contact between mafic tuffaceous rocks and felsic volcanoclastic rocks. The best drill intersection of the Anita horizon to date is diamond-drill hole 87-37, which intersected 2.5 m of 2.37% Cu, 0.73% Pb, 2.73% Zn, 46 g/t Ag and 0.72 g/t Au hosted in a pyritic felsic tuff. Another hole, 88-49, included a 4.9 m interval of 2.3% Cu, 0.49% Pb, 3.66% Zn, 73.9 g/t Ag and 1.9 g/t Au. The lithology that hosts the mineralization in the Anita zone is not known, as this information is not available in assessment reports. Mapping in the Anita zone (this study) has located several exposures of moderately to intensely sericite-altered felsic ash and crystal tuff, with up to 1% quartz crystals up to

4 mm in size. Sampling of felsic volcanic rocks associated with the Anita zone for U-Pb (zircon) geochronology was conducted in order to determine if it is part of the same

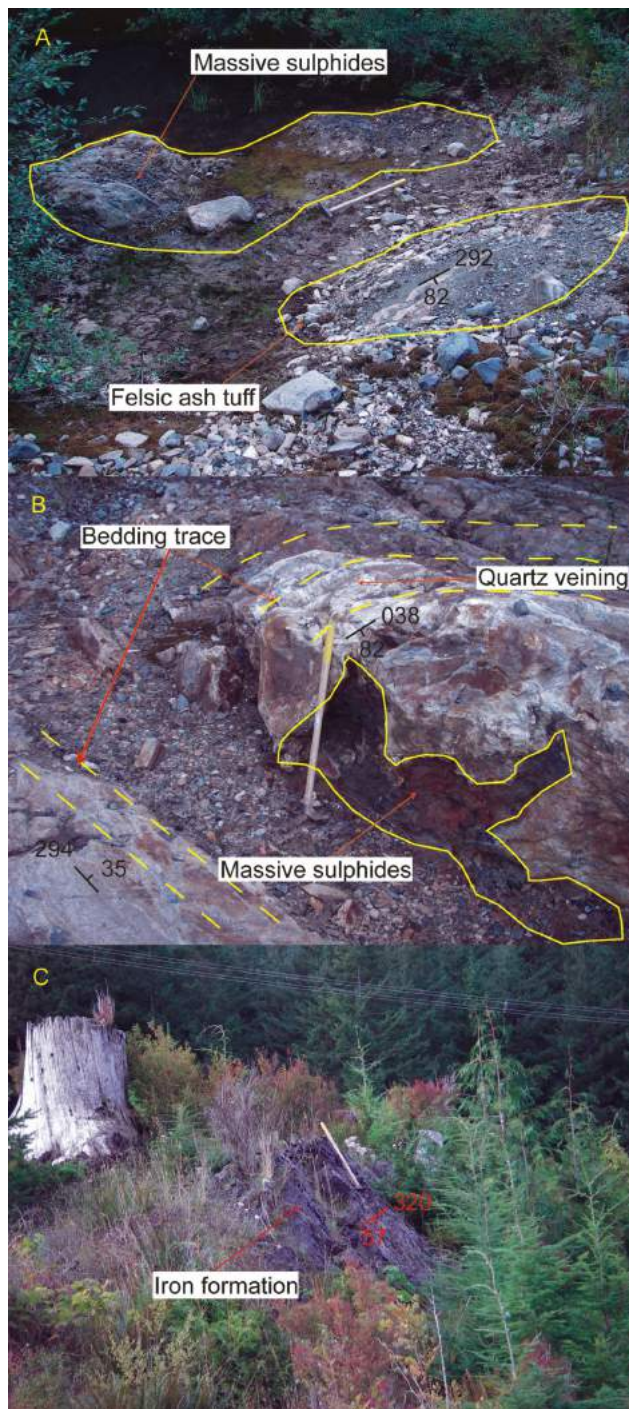


Figure 5. A) Massive sulphide mineralization in contact with silicified felsic ash tuff at the northwest pit, Coronation zone, Lara property of Treasury Metals Inc. **B)** Massive sulphide mineralization hosted by silica- and sericite-altered felsic ash and crystal tuff, northeast pit, Coronation zone; rocks on the east side of the massive sulphide mineralization are folded into the mineralization, suggesting the presence of drag folding. **C)** Fine- to medium-grained massive magnetite of the Lady B iron formation of Treasury Metals Inc. (MINFILE 092B 33).

stratigraphic package that hosts the Coronation trend or the Big Sicker Mountain VMS deposits. Fieldwork this summer also indicated that the MINFILE location for the Anita showing is incorrect, with the Anita shaft located at UTM co-ordinates Zone 10, 429862E, 5417127N (NAD83), approximately 450 m south of the MINFILE position.

The Lady B iron formation (MINFILE 092B 033) is similar to other iron formations occurring in rocks that are stratigraphically above VMS mineralization at the Myra Falls, Lenora, Tye and Richard III occurrences, and is believed to represent oxide-facies iron mineralization related to hydrothermal mineralizing systems similar to those that formed the underlying VMS deposits. Resolving the timing of iron formation mineralization in the Sicker Group is critical for establishing the duration of VMS-related hydrothermal activity. The Lady B iron formation is located beneath a major power line, and is accessible from the south via a deactivated logging road in the vicinity of the Anita zone (Figure 3). The showing consists of a 15 m by 3 m outcrop of fine- to medium-grained, massive black magnetite (Figure 5c). The massive magnetite contains rusty pyritic zones up to 30–40 cm in size and trace blebs of chalcopyrite up to 2 mm in size. Abundant dacitic to intermediate volcanic rocks are located to the south of showing. These volcanic rocks are less felsic than those associated with VMS occurrences to the south (downsection?), and comprise light grey-green, dacitic to intermediate tuff with abundant feldspar crystals and weakly sericite-altered, flattened pumice clasts. Crystal-poor, ash-rich layers of similar colour are also abundant, many of which contain chlorite-altered, flattened pumice clasts. In certain locations, ash-rich zones pick up a strong fabric, becoming phyllitic in texture and potentially representing zones of shearing. Volcanic rocks most proximal to the Lady B iron formation were sampled for U-Pb (zircon) geochronology in order to resolve the age of iron formation mineralization and constrain a minimum age for VMS-related hydrothermal activity in Sicker Group rocks of the Cowichan Lake area.

Results of New Mapping in the Port Alberni Area

Mapping of Sicker Group bedrock geology and sampling for litho geochemistry, U-Pb zircon and Ar/Ar hornblende geochronology, and Pb, Nd and Hf isotope tracer studies was conducted in the Port Alberni area. This work was concentrated 1) in the vicinity of recent logging activity southeast of Horne Lake; 2) on mineral tenure owned by Bitterroot Resources Ltd. and Mineral Creek Ventures Inc.; and 3), in the McLaughlin Ridge area, in the vicinity of Kammat and Peak lakes (Figures 1, 6). Bedrock exposure in all areas is moderate, with the best exposures occurring in logging-road cuts. Off-road exposures are typically covered with thick layers of moss and organic detritus, often in forested, low-light conditions.

Horne Lake Area

The oldest rocks encountered in recent mapping southeast of Horne Lake (Figure 6, region A) are assigned to the Nitinat Formation (Massey and Friday, 1989). These consist largely of dark green, often clinopyroxene-phyric andesitic sandy tuff, lapilli tuff, tuff breccia and agglomerate. Andesite clasts are dominantly subangular to subrounded, variably hematite or silica altered, variably clinopyroxene phyric, and attain sizes up to 15 cm. Clinopyroxene crystals reach sizes up to 1 cm and are typically euhedral. Chlorite and epidote amygdules are often present, reaching sizes up to 5 mm.

Andesitic volcanic rocks pass upwards into a package of low-energy marine sedimentary rocks, consisting of argillite, radiolarian chert and silty to sandy intermediate tuff. This relationship is strikingly similar to that observed in the Lacy Lake–Horne Lake area, where chert, argillite and intermediate tuff also overlie mafic volcanic rocks (Ruks and Mortensen, 2007).

Felsic volcanic rocks predominate farther upsection. These consist primarily of dacite and rhyodacite lapilli tuff, tuff breccia and dacite intrusions. Felsic volcanoclastic rocks in this area contain potassic feldspar and biotite, as well as quartz-phyric dacite and rhyodacite clasts ranging from <1 to 30 cm in size and from subrounded to subangular in shape (Figure 7a). Matrix material in felsic volcanoclastic rocks of this area consists largely of feldspar, with more rare examples containing a mixture of feldspar and euhedral clinopyroxene. The presence of euhedral clinopyroxene crystals in the matrix of dacite-rhyodacite lapilli tuff and tuff breccia is significant, as it indicates the coexistence of mafic and felsic volcanism, or the reworking of underlying mafic volcanic material. In one locality, a feldspar- and biotite-phyric dacite plug is observed to intrude felsic sandy tuff (Figure 7b). Feldspar and biotite phenocrysts reach sizes of 5–7 mm. Trace quartz phenocrysts were also observed. Potential peritectic interaction zones were observed along the margin of the intrusion. In these zones, margins of the dacitic plug were brecciating in sandy tuff, with subangular to angular clasts of dacite porphyry ranging from <1 to 10 cm in size.

Bitterroot Resources Ltd. and Mineral Creek Ventures Inc.

Work continued on the Bitterroot Resources Ltd. mineral tenure in the Port Alberni area this year (the ‘Debbie property’), with the focus of resolving the age of Sicker Group stratigraphy and contained mineral occurrences in the area (Figure 6, regions B and C). Much of the bedrock underlying the Bitterroot Resources and Mineral Creek Ventures mineral tenure is interpreted to comprise rocks of the Duck Lake and Nitinat Formations (Massey and Friday, 1989). The Duck Lake Formation consists of pillow basalt, pillow

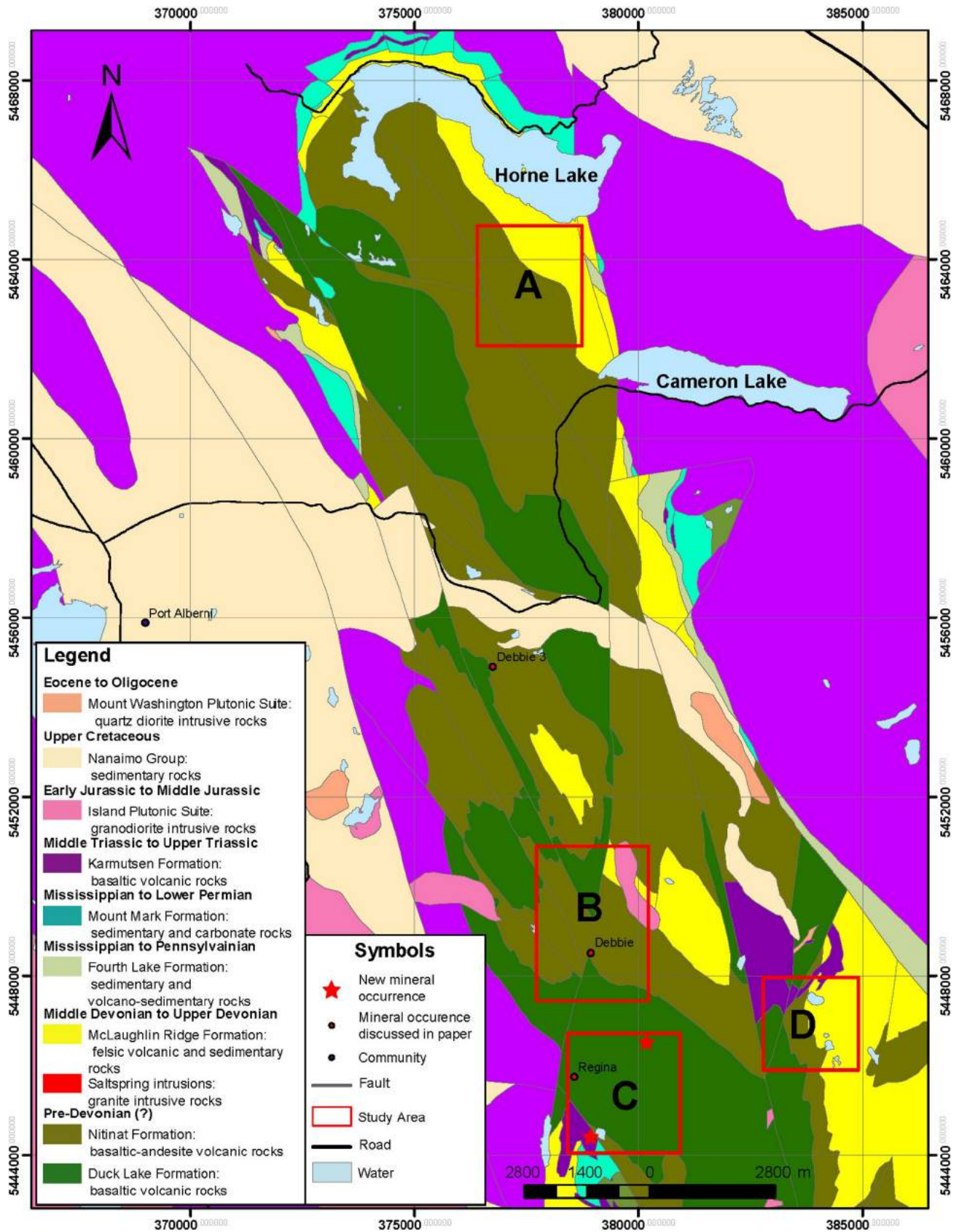


Figure 6. Regional geology (modified from Massey, 2005), selected mineral occurrences and areas of study for 2008 fieldwork in the Port Alberni area.

breccia and interflow mafic tuffaceous sedimentary rocks, and is believed to represent the oceanic crust upon which the Sicker arc was built (Massey and Friday, 1989). As such, Duck Lake Formation rocks are interpreted as the oldest in the Sicker Group and, by default, the oldest in Wrangellia (Massey and Friday, 1989). The VMS mineralization of the Debbie 3 occurrence (MINFILE 092F 445), owned by Bitterroot Resources and Mineral Creek Ventures, consists of four stratiform lenses of banded massive sphalerite with minor chalcopyrite and galena, each band ranging between 5 and 20 cm in thickness. The best grade obtained from sampling of this mineralization by previous workers includes 14.1% Zn, 0.87% Pb and 0.12% Cu over a 20 cm thickness. The mineralization is hosted in fine-grained chloritic schist with variable carbonate, sericite and silica alteration (Ruks and Mortensen, 2007). The chloritic schist hosting Debbie 3 mineralization is spatially associated with clinopyroxene-phyric andesitic volcanic rocks assigned to the Nitinat Formation. The Debbie 3 VMS occurrence is therefore believed to represent the oldest VMS

mineralization in the Sicker Group. Since most exploration for VMS mineralization in the Sicker Group has focused on bimodal volcanic rocks belonging to the McLaughlin Ridge and Myra formations, the relatively unexplored Duck Lake and Nitinat formations represent attractive targets for this style of mineralization.

Due to the absence of rocks in the Nitinat and Duck Lake formations that are amenable to radiometric dating, much of the work conducted on the Bitterroot Resources and Mineral Creek Ventures mineral tenure this season focused on locating and sampling radiolarian chert for biochronology. Samples of chert associated with mafic to intermediate tuff assigned to the Nitinat Formation were collected from various locations on the property, most notably from chert interbedded with intermediate tuff in the vicinity of the Debbie exploration tunnel (Figure 6) and workings in the immediate vicinity.

In the Duck Lake area (Figure 6, region C), mapping and sampling were conducted on the Duck Lake Formation type section (Massey and Friday, 1989), as well as in the vicinity of the Regina Cu-Au vein occurrence. Along the Duck Lake Formation type section, massive pillow-basalt flows alternate with interflow sandy to silty mafic tuff containing rare chert beds. Several samples of sandy mafic to intermediate tuff were collected for U-Pb (zircon) geochronology. Pillow-basalt flows were sampled for geochemical and isotope-tracer studies. Where recrystallization was not too strong, chert was collected for radiolarians.

A new mineral occurrence was discovered on the Bitterroot Resources and Mineral Creek Ventures mineral tenure during this fieldwork. This new mineral occurrence is located approximately 130 m southwest of Duck Lake (Figure 6, region C). Here, a unit of massive diabase assigned to the Triassic Karmutsen Formation is crosscut by several gossanous zones up to 30 cm in width (Figure 8b). These zones are filled with 3–4% coarse pyrite and up to 0.5% coarse-grained to blebby chalcopyrite. Intense silicification of the diabase is associated with these gossanous zones. A bed of fine-grained massive sulphide (dominantly pyrite) was discovered in a new exposure along China Creek Main (Figure 6, region C). The bed is approximately 20 cm wide and interbedded with siliceous argillite (Figure 8a). Mafic sandy tuff and scoriaceous mafic volcanic rocks are also found in the immediate vicinity of the mineralization. Siliceous interbeds within the massive sulphide mineralization were sampled for radiolarian biostratigraphy.

McLaughlin Ridge: Peak and Kammat Lakes Area

The type section for the McLaughlin Ridge Formation (Yorath et al., 1999) is located on McLaughlin Ridge, approximately 18 km southeast of Port Alberni and 1 km

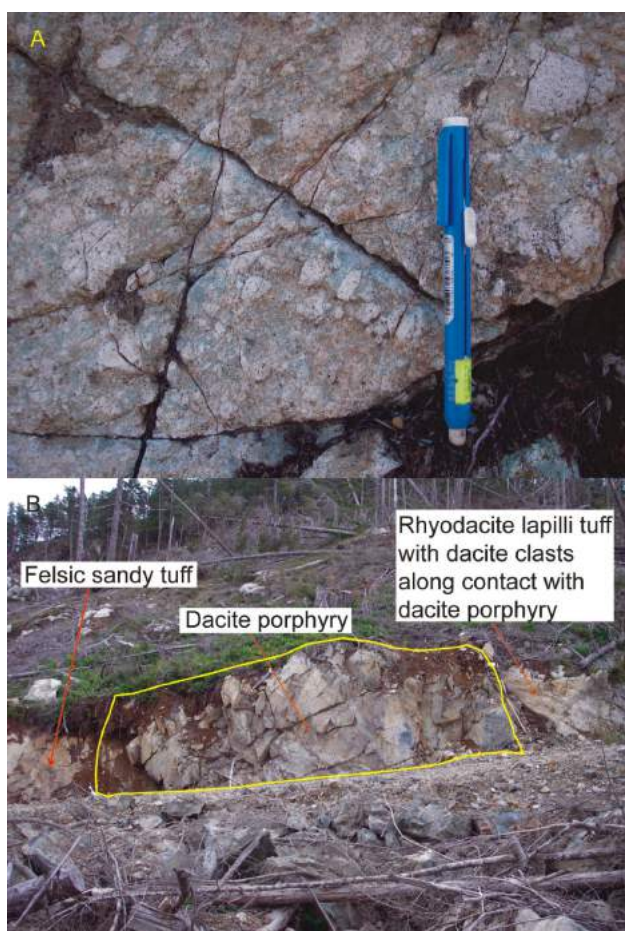


Figure 7. Newly discovered felsic volcanic rocks in the Horne Lake area: **A)** rhyodacite lapilli tuff; **B)** feldspar-quartz-phyric dacite porphyry intruding felsic lapilli and sandy tuff; clasts of dacite porphyry are found in the tuff near the contact zone with the intrusion, suggesting potential periperitic interaction.

southwest of Peak Lake (Figure 6, region D). The McLaughlin Ridge Formation in this area consists of volcanoclastic strata, lesser greenstone and minor chert. Volcanoclastic rocks in the McLaughlin Ridge Formation type-section area are believed to represent andesitic volcanic rocks that have been reworked from the underlying Nitinat Formation. Yorath et al. (1999) correlated rocks of the McLaughlin Ridge Formation type-section area with felsic volcanic rocks and contained VMS mineralization found in the Cowichan Lake and Buttle Lake uplifts (e.g., the Big Sicker Mountain/Lara and Myra Falls deposits, respectively). However, there are no radiometric or biostratigraphic ages to support any of these correlations.

Reconnaissance fieldwork this summer was conducted in the Peak and Kammat Lakes area (Figure 6, region D), in the immediate vicinity of the McLaughlin Ridge Formation type section (Yorath et al, 1999). Here, abundant buff-weathering, often chevron-folded, red and green

radiolarian chert is interbedded with green, intermediate, silty to sandy tuff. The tuff is well sorted, with coarser fractions containing abundant feldspar crystals. Radiolarian chert was sampled in several localities. In one locality, laminated radiolarian chert was observed to have its bedding deflected by an aphyric clast of unknown lithology (Figure 9). This clast might be a coarse clast transported via turbidite flow, or it may be a volcanic bomb. The latter possibility is significant as it would indicate the coexistence of volcanism during chert deposition and would aid in correlations between stratigraphy in the McLaughlin Ridge area and that of other Sicker Group localities.

Rocks encountered in the Peak and Kammat Lakes area are dominated by radiolarian chert interbedded with intermediate tuff, but the chert becomes interlayered with basaltic sills to the southwest. Basaltic sills intruding the chert package often contain abundant spherulites and quartz amygdules up to 4 mm in size; acicular feldspar phenocrysts up to 1 mm in size; and subhedral, chlorite-altered mafic phenocrysts up to 1.5 mm in size. Chert layers ap-



Figure 8. Newly discovered mineralization in the Port Alberni area: **A)** stratiform massive pyrite in a new exposure along Duck Lake Main; the mineralization is interbedded with siliceous argillite, chert and mafic sandy to lapilli tuff; **B)** gossanous and silica-altered zones within a massive diabase are associated with quartz-vein-hosted pyrite and chalcopyrite mineralization; the dashed yellow line is the trace of the mineralized zone.

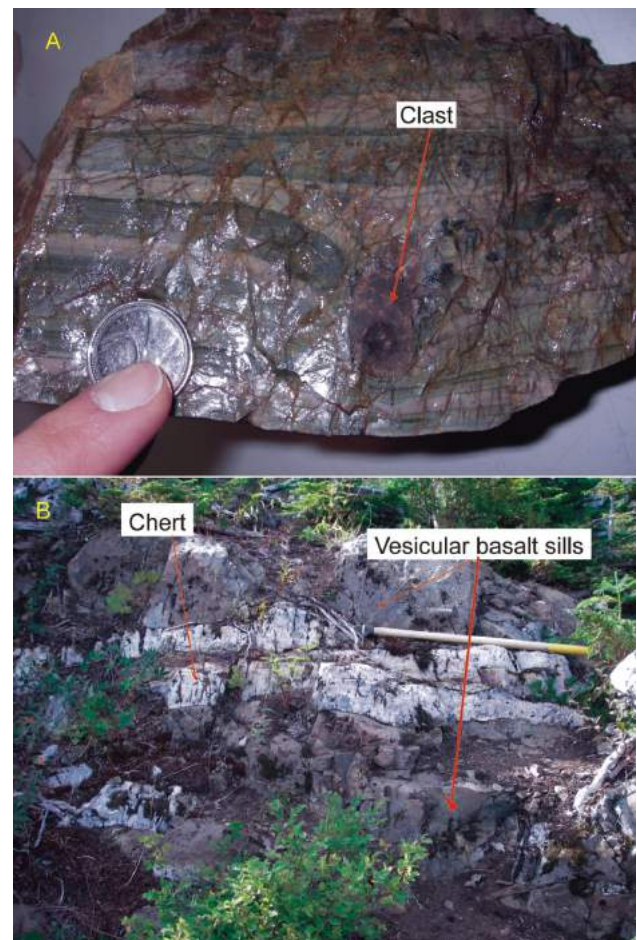


Figure 9. **A)** Bedding in radiolarian chert is deflected by a fine-grained, purple, rounded clast of unknown lithology. **B)** Highly quartz-vesicular and often spherulitic basalt sills intrude radiolarian chert; recrystallization of radiolarian chert is often observed in areas where basalt sills are abundant.

pear, in places, to have been mildly brecciated and recrystallized by the sills. A large gabbroic intrusion has been mapped to the southwest of these sills, and there is a high probability that these basaltic sills may be apophyses derived from this larger intrusion. Geochemical sampling of these sills has been conducted in order to determine their affinities. A localized chlorite- and serpentine-altered zone within the gabbro was observed to contain trace malachite staining. Malachite staining in this zone is associated with a small pyrite-bearing pod approximately 20 cm in size.

The abundant chert, intermediate tuff and gabbro observed in new bedrock exposures in the Peak and Kammat lakes area during this study all occur in areas previously mapped as McLaughlin Ridge, Nitinat and Duck Lake formations (Yorath et al., 1999). Since these new exposures of interbedded chert and intermediate tuff are not typical units observed in the Nitinat and Duck Lake formations, this suggests that there are significant problems with existing geological maps for the area that can only be resolved with additional mapping.

Results of Reconnaissance Geological Fieldwork in the Nanoose Uplift Area

One day of reconnaissance geological fieldwork was conducted in the Nanoose uplift area (Figure 1). This work focused on sampling for U-Pb (zircon) geochronology and radiolarian biostratigraphy. Sedimentary rocks were most common and comprise interbedded argillite, grey-black siltstone, fine to coarse sandstone and green chert. Sandstone in the area ranges from moderately to poorly sorted arenite and lithic arenite. This sandstone contains an abundant feldspathic component and, in places, abundant subrounded chert clasts. Samples for U-Pb (zircon) detrital geochronology were taken from several localities. Substantial outcrops of green chert were also observed, especially in the immediate vicinity of the Department of National Defence naval base. This chert is typically highly fractured and, in places, was observed to contain potential radiolarian fossils. A large body of granodiorite of unknown age was also observed and sampled for geochronology.

Results of Geological Mapping on the Dorado and Dragon Properties (Paget Resources Corporation), Hesquiat–Gold River Area

Dorado Property

Geological mapping at 1:5000 scale of a portion of the property (Paget Resources Corporation; Figures 1, 10) was conducted over six days in 2007. The first visit was designed to follow up on the discovery by Marshall et al. (2006) of polymetallic VMS-style stockwork mineralization hosted in mafic volcanic rocks. Reconnaissance geo-

logical mapping in the vicinity of Marshall's showing by Paget Resources Corporation geologists led to the discovery of polymetallic massive sulphide mineralization (Figure 10, regions A and B). Massive sulphide mineralization has so far been discovered in two locations on the Dorado property, and is associated with the contact between mafic volcanic rocks and overlying tuffaceous sedimentary rocks.

The first massive sulphide mineralization discovered on the Dorado property is located in a shot-rock blast pit, near the contact between a variably silica-altered, chlorite amygdule-bearing, feldspar-phyric basaltic flow and overlying intermediate tuffaceous sandstone (Figure 10, region A). Here, a massive sulphide pod, measuring 1.5 m by 3 m and consisting of fine-grained pyrrhotite with trace chalcopyrite, is hosted within the basalt. Sulphide stringers up to 1 cm wide are abundant near the massive sulphide mineralization. Numerous massive sulphide boulders of similar composition are found in close proximity to the showing; some of them appear to have been used as substrate for a bridge crossing a creek that drains immediately to the east of the pit. The most silicified zones within the host basalt are associated with abundant quartz and epidote veinlets. Some zones of autobreccia are present in the basalt host. These zones contain abundant grey, glassy, angular silicified clasts up to 2 cm in size. Approximately 430 m southwest of this zone is a second zone of massive sulphide mineralization (Figure 10, region B). Here, boulders of fine- to medium-grained massive pyrrhotite+chalcopyrite, up to 50 cm in size, occur as float beneath a large, gossanous outcrop of highly silica-altered, feldspar-clinopyroxene-phyric andesite porphyry (Figure 11). Pyrrhotite mineralization is abundant, as both stringers and disseminations. Euhedral feldspar and clinopyroxene phenocrysts form approximately 25% of the rock. Plagioclase feldspar constitutes approximately 85% of the phenocryst assemblage and reaches sizes up to 3 mm. Clinopyroxene phenocrysts are variably chlorite altered, form 15% of the phenocryst assemblage and reach sizes up to 1 cm. This altered and mineralized porphyry was traced in the map area for approximately 350 m to the southwest along an overgrown logging skidder road. Less altered, variably sulphide-mineralized examples of feldspar- and clinopyroxene-phyric andesite are abundant in the map area (Figure 10, region C) and are most likely representative of massive intermediate flows. These mafic volcanic rocks are massive and less porphyritic to nearly aphyric in nature. They often contain abundant epidote alteration in the form of ovoid patches up to 10 cm in width. Fine-grained sulphide minerals are often found in the cores of these patches. In places, pyrrhotite and chalcopyrite stringers are present, typically with strong silica alteration along their margins.

Overlying altered and mineralized mafic volcanic rocks are intercalated tuff and massive intermediate volcanic rocks

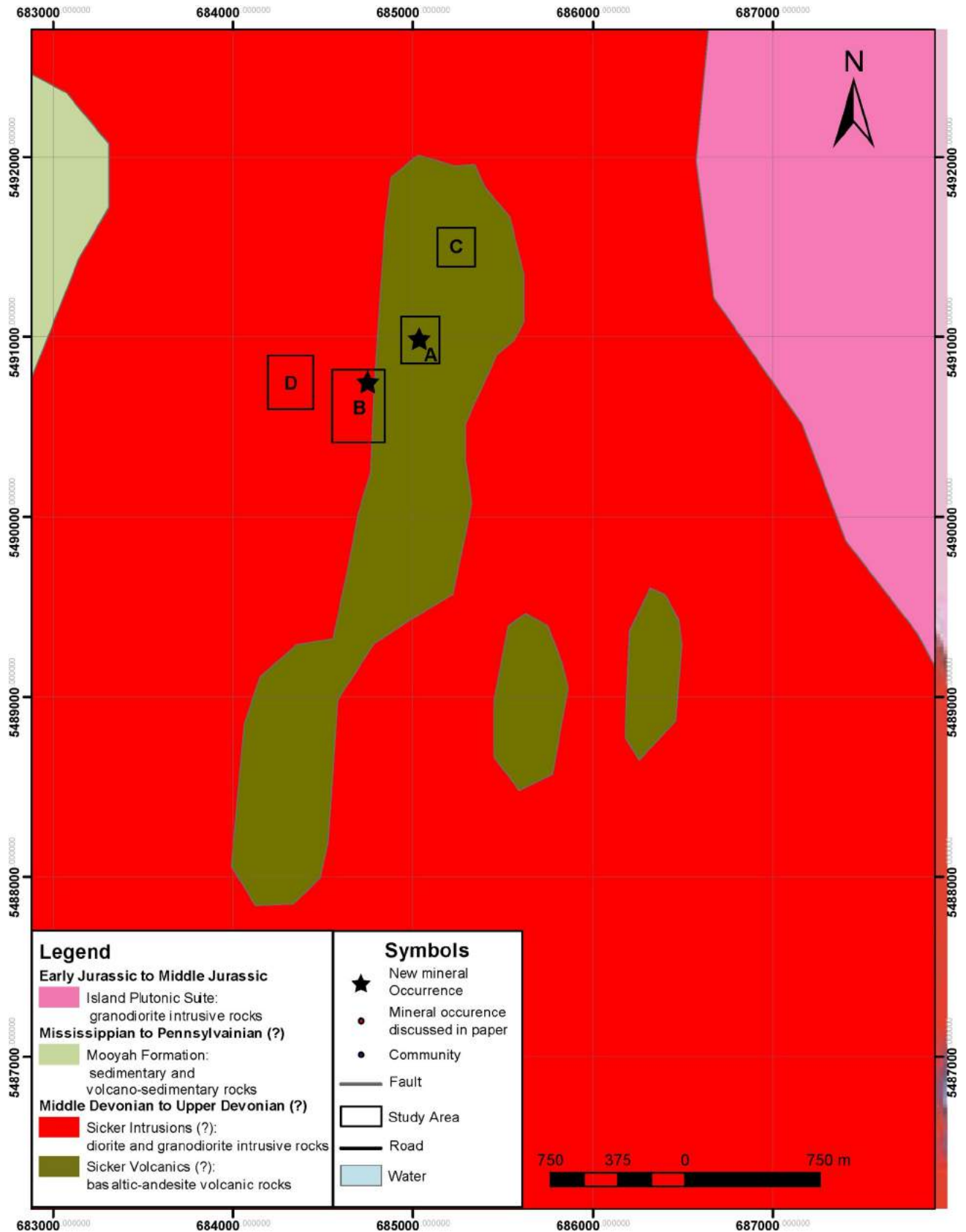


Figure 10. Regional geology, selected mineral occurrences and areas of study for 2007 fieldwork on the Dorado property of Paget Resources Corporation (modified from Marshall et al., 2006).

(Figure 10, region D). Volcaniclastic rocks comprise heterolithic lapilli tuff with mafic volcanic and chert clasts in a feldspar-crystal matrix. Sandy intermediate tuff, containing abundant feldspar crystals and variable concentrations clinopyroxene crystals, is also abundant. Massive feldspar-phyric porphyry of intermediate composition is associated with tuffaceous zones, but whether it represents intrusions or flows is undetermined.

Dragon Property

The Dragon property is located approximately 80 km west of Campbell River, 20 km northwest of Gold River and 65 km northwest of the Myra Falls mine of Breakwater Resources Ltd. (Figure 1). A combination of reconnaissance and 1:5000 scale mapping was conducted on the Dragon property over 10 days. This work focused on establishing the geological setting for known mineral occurrences on the property, and for understanding the stratigraphy of the property geology in general. The work was successful in identifying several prospective new zones of mineralization, including a new polymetallic massive sulphide discovery (Figure 12).

Massive sulphide mineralization of the Dragon property typically consists of varying proportions of fine- to medium-grained massive pyrrhotite, chalcopyrite and sphalerite at the contact between felsic volcanic rocks and overlying volcano-sedimentary and carbonate rocks. This prospective horizon has been traced over a strike length of 4.4 km, and shows signs of VMS-style alteration and mineralization throughout (Figure 12).

The original massive sulphide discoveries on the Dragon property include the Falls and North showings, which comprise three massive sulphide lenses with grades up to 7.33% Zn, 1.34% Pb, 173 ppm Cu, 680 ppb Au and 19.2 g/t Ag over 2 m (Jones, 1997; Figure 12). This massive sulphide mineralization is interlayered with laminated chert, mudstone and calcareous mudstone that strikes southwesterly and dips steeply to the northwest. Bivalve (?) fossils have been observed in cherty tuff overlying the Falls and North showings.

During the course of this summer's fieldwork on the Dragon property, a new massive sulphide showing was discovered approximately 1 km south of the Falls and North showings (Figure 12, region A). This showing consists of several fine- to medium-grained, pyrrhotite+chalcopyrite-bearing massive sulphide boulders, up to 1.5 m by 1 m in size, found in float (Figure 13a). One of the boulders contains massive sulphide mineralization in contact with strongly silica-altered aphyric rhyolite, indicating a rhyolitic host for the mineralization. These boulders were discovered at the top of a large set of cliffs consisting of aphyric, flow-banded massive rhyolite, and are located proximal to the contact zone between felsic volcanic rocks

and overlying sedimentary and carbonate rocks. This contact zone is exposed in outcrop approximately 50 m to the west. Here, strongly silica-altered and stockwork-sulphide-mineralized rhyolite with localized zones of flow breccia is overlain by argillite, chert, siltstone, calcareous argillite and limestone. Rhyolite breccia in this area contains angular, jigsaw-fit clasts, up to 6 cm in size, in a dark-coloured matrix of fine-grained disseminated garnet and biotite clots up to 1 cm in size. Chert beds in this contact zone often contain 0.5–1% disseminated pyrrhotite, and argillite beds contain abundant pyrrhotite veinlets. Calcareous wackestone beds contain abundant coral fossils.

Another new zone of mineralization was discovered approximately 1 km north of the Falls and North showings (Figure 12, region B). Here, similar to the geological setting of the new massive sulphide discovery south of the Falls and North showings, intensely silica-altered and stockwork-sulphide (pyrrhotite and chalcopyrite)-mineralized aphyric rhyolite is conformably overlain by felsic tuff, chert, argillite and carbonate, which dip steeply to the west-northwest (Figure 13b). Intensely silica-altered rhyo-



Figure 11. A) Massive pyrrhotite and chalcopyrite mineralization from region B of the Dorado property of Paget Resources Corporation; **B)** Strongly silica-altered and stockwork-sulphide-mineralized, clinopyroxene- and feldspar-phyric andesite porphyry from region B of the Dorado property.

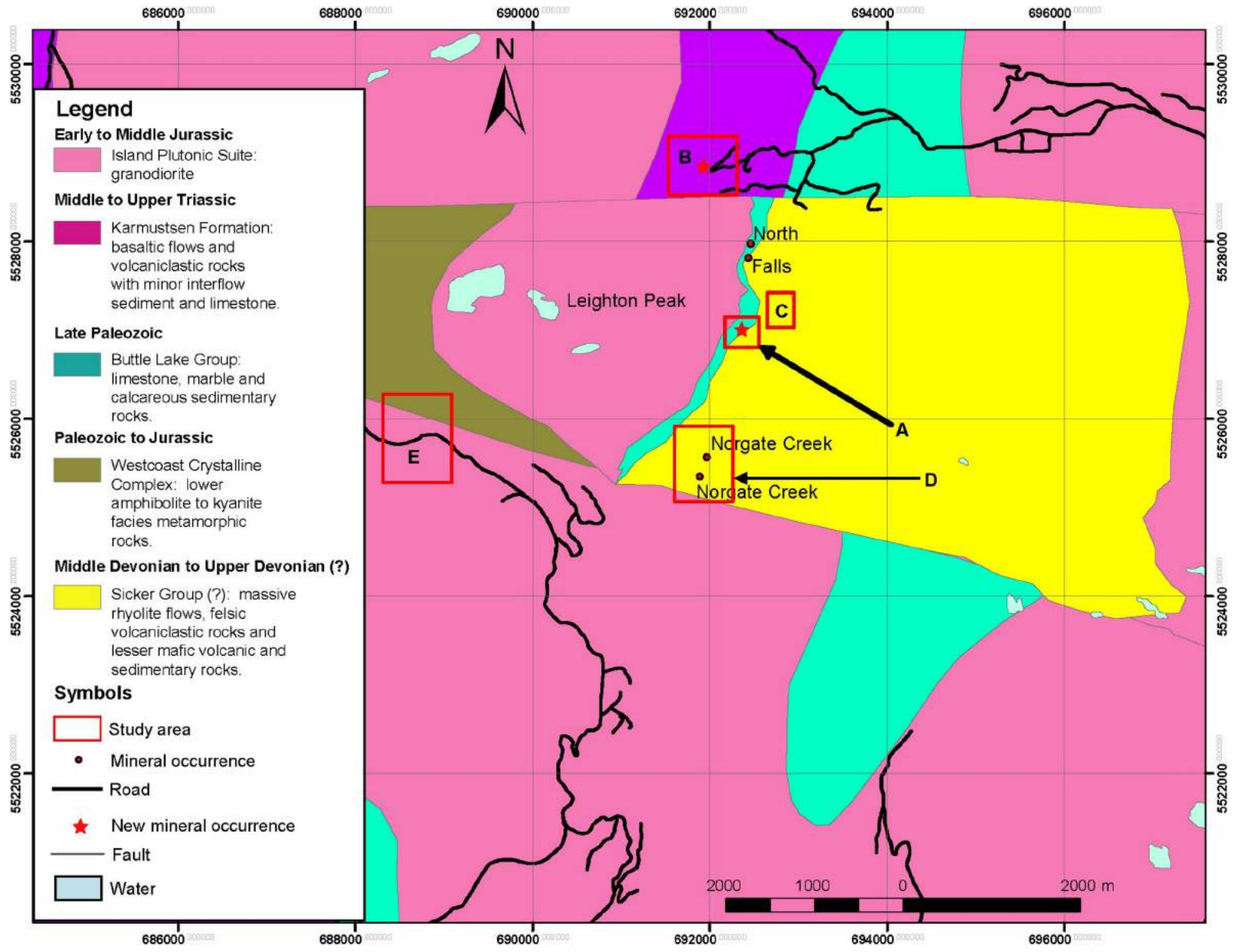


Figure 12. Regional geology (*modified from Massey, 2005; Jones, 1997*), selected mineral occurrences and areas of study for 2008 fieldwork on the Dragon property of Paget Resources Corporation.

lite in this area is highly gossanous and hosts abundant pyrrhotite and chalcopyrite stringers up to 2 cm thick. Disseminated sulphides consist largely of pyrrhotite and reach concentrations up to 2%. Greater concentrations of disseminated sulphides are associated with areas of strong silica alteration. Green chert containing bands of fine-grained garnet immediately overlie altered and mineralized rhyolite. Fossiliferous felsic ash tuff overlies the chert and contains crinoid and coral fossils. Carbonate increases in concentration upsection and consists of calcareous mudstone, and medium- to coarse-grained marble that is interbedded with chert and silicified argillite (Figure 13b). Chert contains up to 1% pyrrhotite blebs up to 2 mm in size.

The ridge east of Leighton Peak hosts substantial thicknesses of massive, flow-banded, largely aphyric rhyolite (Figure 12, region C). Flow banding is very abundant in felsic volcanic rocks, and its orientation generally mimics that of regional fabrics, which dip moderately to steeply to the west-northwest. Folding in the flow banding is abundant, and tends to occur as outcrop-scale isoclines (Figure 13c). Since no prominent foliations were observed in the vicinity of these tight folds or in the field area, it is probable that the folding is not tectonic but rather related to folding of the rhyolite due to viscous drag during eruption. In places, thin sedimentary horizons can be observed between flows. These are typically black graphitic argillite, often containing angular clasts of aphyric rhyolite up to 1 cm in size. Felsic volcanic rocks are also very abundant in the Norgate Creek area, located approximately 2 km south-southwest of the Falls and North showings (Figure 12, region D). These rocks typically comprise massive, weakly quartz-phyric rhyolite that is variably silica altered and mineralized with sulphide stringers (pyrrhotite, sphalerite and chalcopyrite). Near the top of a recent logging slash in the Norgate area, a strongly metamorphosed heterolithic tuff breccia was observed proximal to the contact with overlying sedimentary and carbonate rocks. Here, metamorphosed volcanic clasts up to 10 cm in size are variably stretched, angular and often jigsaw fit. Eighty percent of the clasts contain abundant white sugary muscovite, and may represent metamorphosed felsic volcanic clasts. Fifteen percent of clasts are represented by a light grey variety containing 3% biotite porphyroblasts, and might represent metamorphosed intermediate volcanic rocks. Five percent of the clasts contain nearly 100% medium- to coarse-grained biotite, and may represent metamorphosed mafic volcanic rocks. The matrix of this breccia contains abundant biotite porphyroblasts up to 3 mm in size. In places, this breccia acquires a fabric reflected in strongly stretched metavolcanic clasts in a biotite-rich matrix. Mineralization in the Norgate Creek area consists of pyrrhotite and sphalerite stringers in felsic volcanic rocks, and occurs both at the contact zone with overlying carbonate sedimentary rocks and nearly 1 km east of this contact, within the felsic volcanic pile.

In the Conuma River area, approximately 4 km to the southwest of the Falls and North showings, felsic volcanic rocks consist of heterolithic tuff breccia, graded beds of tuffaceous sedimentary rocks and quartz-feldspar porphyry



Figure 13. A) New massive sulphide mineralization discovered this summer on the Dragon property of Paget Resources Corporation. B) Contact zone between massive, silica-altered and stockwork-sulphide-mineralized rhyolite and overlying chert, felsic tuff and carbonate rock; this contact hosts all known massive sulphide occurrences on the Dragon property. C) Folded, flow-banded rhyolite on the ridge to the east of Leighton Peak.

sills (Figure 12, region E). In one outcrop, a heterolithic lapilli tuff with white, aphyric, felsic volcanic clasts and grey siltstone clasts up to 2 cm in size normally grades into sandy tuff, silty tuff and mudstone. These rocks are interpreted to represent turbidites. In the same outcrop, these volcano-sedimentary rocks are intruded by a quartz-feldspar-phyric rhyodacite sill. This sill has irregular contacts with the volcano-sedimentary rocks and, in many places, is observed to contain engulfed clasts of volcano-sedimentary rocks. Fine-grained garnets are present as disseminations within all rock types in the outcrop but are found in larger concentrations within grey siltstone clasts. In the immediate vicinity of this outcrop is a heterolithic tuff breccia containing large, subrounded clasts of quartz-feldspar porphyry and grey siltstone up to 10 cm in size. These clasts are set in a matrix consisting largely of feldspar crystals. Garnet and biotite porphyroblasts are present in both the matrix and the siltstone clasts. Stratified rocks in the Conuma River area have been observed to dip both moderately and steeply to the southwest and northeast, respectively, which is significantly different from the prominent west-northwest dip observed in stratified rocks to the north of Norgate Creek and east of Leighton Peak. More bedrock mapping is required in this area to constrain the location of the contact between felsic volcanic rocks and overlying sedimentary and carbonate rocks. Not only is this contact highly prospective for VMS mineralization, but it also serves as a stratigraphic marker horizon that can help resolve differences in structural style throughout the property.

Mapping on the Dragon property this summer has shown that potential Sicker Group felsic volcanic rocks are much more extensive than is shown on existing geological maps of the area (e.g., Figure 12, regions B and E). More mapping needs to be conducted in the area to further constrain the extent of potential Sicker Group bedrock geology.

Summary

Fieldwork in 2008 has continued with the focus of resolving the stratigraphy and tectonic history of the Sicker Group and its contained mineral occurrences via a combination of bedrock mapping and sampling for geochronology (U-Pb, Ar/Ar), biostratigraphy (macrofossils, radiolarians and conodonts), geochemistry (major and trace elements) and isotopic analyses (Nd and Pb; whole rock and sulphides, respectively). In the Cowichan Lake uplift, the goal of the fieldwork has been to resolve the geological and stratigraphic setting of VMS mineralization, particularly for those VMS deposits and occurrences on mineral tenure owned by Treasury Metals Inc. and Westridge Resources Inc. During this summer, a new polymetallic massive sulphide showing was found on Westridge Resources ground, and a prospective zone for VMS mineralization was identified on Treasury Metals ground. Sampling for U-Pb (zircon) geochronology in the immediate vicinity of the

Lady B iron formation (Treasury Metals Inc.) was conducted to constrain the longevity of the VMS mineralizing hydrothermal system in the Cowichan Lake area.

Fieldwork in the Port Alberni area focused on examining new bedrock exposures southeast of Horne Lake, as well as continuing examinations of bedrock and mineralization hosted by rocks of the Nitinat and Duck Lake formations on ground owned by Bitterroot Resources Ltd. Examinations of new exposures in the Kammat and Peak lakes area were also conducted. Southeast of Horne Lake, recent logging activity has resulted in the discovery of a large area underlain by proximal felsic volcanic rocks. This finding is highly significant, as Sicker Group rocks of the Port Alberni area have previously been interpreted to represent a depositional area distal from felsic magmatic centres (Yorath et al., 1999). Not only does this new discovery indicate the presence of a new centre of felsic magmatism in the Sicker Group, but it has large positive implications for the VMS potential of Sicker Group rocks in the Port Alberni area. Reconnaissance fieldwork in new exposures of Sicker Group rocks of the Peak-Kammat lakes area has shown that significant revisions are necessary to the existing geological map for the area. Sampling of abundant radiolarian chert in this area was conducted to determine an age for rocks of the McLaughlin Ridge Formation type section (Yorath et al., 1999). Abundant sampling for geochronology and radiolarian biostratigraphy was conducted on ground owned by Bitterroot Resources Ltd., to determine the age of mafic volcanic rocks of the Nitinat and Duck Lake formations. Resolving the ages of these units is critical for understanding the temporal evolution of the Sicker arc, and the earliest history of the Wrangellia Terrane. Two new mineral occurrences were discovered on the Bitterroot Resources mineral tenure: stratiform massive sulphide mineralization interlayered with mafic volcanic rocks and silicified argillite; and pyrite-chalcopyrite mineralization associated with strongly silica-altered zones in massive diabase.

Reconnaissance fieldwork in the Nanoose area focused on resolving the age of sedimentary, carbonate and volcanic rocks that have previously been interpreted as potential correlatives to the Buttle Lake and Sicker groups. Abundant sampling for U-Pb (zircon) detrital geochronology and radiolarian biostratigraphy was conducted.

In the Gold River and Hesquiat areas, geological fieldwork was carried out on potential Sicker Group rocks underlying the Dragon and Dorado properties, respectively (Paget Resources Corp.), where new polymetallic massive sulphide occurrences were discovered. On the Dorado property, massive sulphide mineralization was discovered by Paget Resources Corporation geologists in several localities, both proximal to the contact zone between clinopyroxene-phyric, variably silica-altered and stockwork sulphide-

mineralized mafic volcanic rocks and overlying tuffaceous sedimentary rocks. A new polymetallic massive sulphide occurrence and a new highly prospective zone for VMS mineralization were discovered on the Dragon property. Massive sulphide mineralization on the Dragon property is located proximal to the contact between massive, variably silica-altered and stockwork sulphide–mineralized felsic volcanic rocks (dominantly rhyolite flows) and overlying volcano-sedimentary rocks, chert and carbonate rocks. The juxtaposition of fossiliferous carbonate rocks and felsic tuff with underlying VMS mineralization and felsic volcanic rocks is observed nowhere else in the Sicker Group. It raises the possibility that volcanic rocks and mineralization on the Dragon property may represent a cycle of arc magmatism and VMS mineralization not previously recognized on Vancouver Island.

Future Work

Fieldwork in 2009 will be pursued in the Cowichan Lake and Port Alberni areas, with additional work planned in potential outcrops of Sicker Group rocks in the Bedingfield Bay and Muchalat Inlet (Gold River–Hesquiat) areas. In the Cowichan Lake area, work will focus on understanding the stratigraphic and volcanological setting of VMS occurrences hosted by the Sicker Group, particularly those of the Lara/Coronation, Randy and Anita zones, north and west of Big Sicker Mountain (MINFILE occurrences 092B 129, 092B 128 and 092B 037, respectively). Particular emphasis will be placed on understanding the stratigraphic and volcanological setting of other potential VMS occurrences in the immediate vicinity of, and west of, Cowichan Lake. Additional regional work in the Alberni area will focus on identifying stratigraphic marker horizons within the Sicker Group that can be used to constrain the age of lithological units in the area, particularly those belonging to the Duck Lake and Nitinat formations.

In the Bedingfield Bay and Muchalat Inlet areas, similar regional and focused outcrop-scale mapping and sampling will be conducted to better understand the stratigraphy and volcanological setting of potential Sicker Group rocks and VMS occurrences, most notably in the vicinity of the Rant Point occurrence (MINFILE occurrence 092F 494) and the Dorado and Dragon properties (Paget Resources Corporation). In parallel with the geological mapping and synthesis work, the authors will also carry out additional U-Pb dating, lithochemical, and Nd, Hf and Pb isotopic studies to constrain the age and magmatic evolution of Sicker Group volcanic rocks and to develop a framework through which VMS occurrences hosted by the Sicker Group can be distinguished from younger, epigenetic sulphide occurrences.

Acknowledgments

This project is jointly funded by a Geoscience BC grant, Bitterroot Resources Ltd., Paget Resources Corporation, Treasury Metals Ltd., Westridge Resources Inc., a Natural Sciences and Engineering Research Council of Canada (NSERC) Discovery Grant to JKM and an NSERC post-graduate scholarship to TR. The authors thank N. Massey for discussions and insights into the geology of the Sicker Group and S. McKinley for having provided a critical review of this manuscript. The authors thank C. Amy and W. Ruks for assistance in the field and Island Timberlands for land access assistance. They also thank several prospectors, consultants and explorationists working on Vancouver Island, especially M. Becherer of Mineral Creek Ventures Inc., M. Carr of Bitterroot Resources Ltd., J. Bradford of Paget Resources Corporation, E. Specogna of Specogna Minerals Corp., T. Sadlier-Brown of Westridge Resources Inc., S. McKinley of Cambria Geosciences, S. Tresierra, J. Houle, H. McMaster and the late A. Francis, for sharing their time and knowledge of Sicker Group geology and mineralization.

References

- Barrett, T.J. and Sherlock, R.L. (1996): Volcanic stratigraphy, lithochemistry and seafloor setting of the H-W massive sulfide deposit, Myra Falls, Vancouver Island, British Columbia; *Exploration and Mining Geology*, v. 5, p. 421–458.
- Belik, G.D. (1983): Trenching, geophysical and geological report on the Lara property, Victoria Mining Division, British Columbia, 48 53 N, 123 52 W, NTS 92B/13W; BC Ministry of Energy, Mines and Petroleum Resources, Assessment Report 11123, 71 p.
- Brandon, M.T., Orchard, M.J., Parrish, R.R., Sutherland Brown, A. and Yorath, C.J. (1986): Fossil ages and isotopic dates from the Paleozoic Sicker Group and associated intrusive rocks, Vancouver Island, British Columbia; *in* Current Research, Part A, Geological Survey of Canada, Paper 86-1A, p. 683–696.
- Fyles, J.T. (1950): Jane, Sally and Sally No. 2; *in* Minister of Mines Annual Report, 1949, BC Ministry of Energy, Mines and Petroleum Resources, p. A224–A225.
- Jones, M.I. (1997): 1996 assessment report, Dragon property, diamond drilling, Alberni and Nanaimo Mining Divisions, NTS map areas 92E/16E, 92L/1E, 49 55 00 N, 126 20 00 W; BC Ministry of Energy, Mines and Petroleum Resources, Assessment Report 24895, 189 p.
- Juras, S.J. (1987): Geology of the polymetallic volcanogenic Buttle Lake camp, with emphasis on the Price hillside, central Vancouver Island, British Columbia, Canada; unpublished Ph.D. thesis, University of British Columbia, Vancouver, BC, 279 p.
- Katvala, E.C. (2006): Re-examining the stratigraphic and paleontologic definition of Wrangellia; *Geological Society of America, Abstracts with Program*, v. 38, p. 24.
- Kelso, I., Wetherup, S. and Takats, P. (2007): Independent technical report and mineral resource estimation, Lara polymetallic property, British Columbia, Canada; unpub-

- lished company report prepared by Caracle Creek International Consulting for Laramide Resources Ltd.
- Kemp, R. and Gill, G. (1993): Geological, geochemical and diamond drilling report on the Specogna-Muchalat property, NTS 92E/16, Alberni Mining Division; BC Ministry of Energy, Mines and Petroleum Resources, Assessment Report 23125, 48 p.
- Marshall, D., Lesiczka, M., Xue, G., Close, S. and Fecova, K. (2006): Update on the mineral deposit potential of the Nootka Sound region (NTS 092E), west coast of Vancouver Island, British Columbia; *in* Geological Fieldwork 2005, Geoscience BC, Report 2006-1, p. 323–330.
- Massey, N.W.D. (1995): Geology and mineral resources of the Duncan sheet, Vancouver Island, 92B/13; BC Ministry of Energy, Mines and Petroleum Resources, Paper 1992-4.
- Massey, N.W.D. and Friday, S.J. (1987): Geology of the Chemainus River–Duncan area, Vancouver Island (92C/16, 92B/13); BC Ministry of Energy, Mines and Petroleum Resources, Paper 1988-1, p. 81–91.
- Massey, N.W.D. and Friday, S.J. (1989): Geology of the Alberni–Nanaimo Lakes area, Vancouver Island (92F/1W, 92F/2E and part of 92F/7); BC Ministry of Energy, Mines and Petroleum Resources, Open File 1987-2.
- Massey, N.W.D., MacIntyre, D.G., Desjardins, P.J. and Cooney, R.T., (2005): Digital map of British Columbia: Tile NM10 Southwest BC; BC Ministry of Energy, Mines and Petroleum Resources, GeoFile 2005-3.
- MINFILE (2008): MINFILE BC mineral deposits database; BC Ministry of Energy, Mines and Petroleum Resources, URL <<http://www.empr.gov.bc.ca/Mining/Geoscience/MINFIL E/Pages/default.aspx>> [November 2008].
- Mortensen, J.K. (2005): Stratigraphic and paleotectonic studies of the Middle Paleozoic Sicker Group and contained VMS occurrences, Vancouver Island, British Columbia; *in* Geological Fieldwork 2005, BC Ministry of Energy, Mines and Petroleum Resources, Paper 2006-1, p. 331–336.
- Muller, J.E. (1977): Geology of Vancouver Island; Geological Survey of Canada, Open File 463, 1:250 000 scale.
- Muller, J.E. (1980): The Paleozoic Sicker Group of Vancouver Island, British Columbia; Geological Survey of Canada, Paper 79-30, 23 p.
- Pattison, J.M. and Money, D.P. (1988): 1987 drilling report on the West claims; Project # 094/107, situated 1 km west of Crofton, BC in the Victoria Mining Division; BC Ministry of Energy, Mines and Petroleum Resources, Assessment Report 17007, 252 p.
- Ruks, T.R. and Mortensen, J.K. (2006): Geological setting of volcanogenic massive sulphide occurrences in the Middle Paleozoic Sicker Group of the southeastern Cowichan Lake uplift (NTS 092B/13), southern Vancouver Island; *in* Geological Fieldwork 2006, Geoscience BC, Report 2007-1, p. 381–394.
- Ruks, T. and Mortensen, J.K. (2007): Geological setting of volcanogenic massive sulphide occurrences in the Middle Paleozoic Sicker Group of the Cowichan Lake uplift, Port Alberni area, southern Vancouver Island, British Columbia; *in* Geoscience BC Summary of Activities 2007, Geoscience BC, Report 2008-1, p. 77–92.
- Sluggett, C.L. (2003): Uranium-lead age and geochemical constraints on Paleozoic and Early Mesozoic magmatism in Wrangellia Terrane, Saltspring Island, British Columbia; unpublished B.Sc. thesis, University of British Columbia, Vancouver, BC, 56 p.
- Sluggett, C.L. and Mortensen, J.K. (2003): U-Pb age and geochemical constraints on the paleotectonic evolution of the Paleozoic Sicker Group on Saltspring Island, southwestern British Columbia; Geological Association of Canada–Mineralogical Association of Canada, Joint Annual Meeting, Program with Abstracts, v. 28.
- Yorath, C.J., Sutherland Brown, A. and Massey, N.W.D. (1999): LITHOPROBE, southern Vancouver Island, British Columbia; geology; Geological Survey of Canada, Bulletin 498, 145 p.

Sediment-Hosted Stratabound Copper-Silver-Cobalt Potential of the Creston Formation, Purcell Supergroup, Southeastern British Columbia (Parts of NTS 082G/03, /04, /05, /06, /12)

R.P. Hartlaub, Department of Mining and Mineral Exploration, British Columbia Institute of Technology, Burnaby, BC, Russell_Hartlaub@bcit.ca

Hartlaub, R.P. (2009): Sediment-hosted stratabound copper-silver-cobalt potential of the Creston Formation, Purcell Supergroup, south-eastern British Columbia (parts of NTS 082G/03, /04, /05, /06, /12); in Geoscience BC Summary of Activities 2008, Geoscience BC, Report 2009-1, p. 123–132.

Introduction

Siliciclastic sedimentary rocks contain significant Cu (Hitzman, 2000), so large cratonic basins are good source regions for this important resource. Sediment-hosted stratabound Cu deposits are the second most important global source of Cu, after porphyry Cu deposits, in terms of total resource (Singer, 1995). Major stratabound Cu deposits lie within the Kupferschiefer belt of Europe and the Zambian Copperbelt of Africa (Cailteux et al., 2005). The Paleoproterozoic Belt-Purcell Basin has a sediment thickness of at least 19 km within the central part of the basin in British Columbia (Cook and van der Velden, 1995) and up to 18 km in the United States (Winston and Link, 1993). This large thickness of sediment was deposited in a relatively short period of time (Evans et al., 2000), leading to the formation of numerous sediment-hosted stratabound Cu-Ag occurrences in the quartzite-dominated Revett Formation (Hayes and Einaudi, 1986; Boleneus et al., 2005). These deposits, including the Troy, Rock Creek and Montanore, are all located in western Montana (Figure 1).

In Canada, the Mesoproterozoic Purcell Basin hosts the Sullivan mine, one of the world's top SEDEX past-producers of Zn and Pb (Goodfellow and Lydon, 2007). This deposit is hosted in the Aldridge Formation of the lower Purcell Supergroup and, consequently, these strata have seen extensive base metal exploration. Rocks above the Aldridge Formation (middle and upper Purcell Supergroup) have received much less attention in BC, even though they host polymetallic veins (e.g., Paiement et al., 2007) and sediment-hosted Cu (\pm Ag \pm Co) occurrences.

A two-year research project was launched in 2007 to examine the stratabound Cu potential of the Purcell Supergroup. Field studies by the first author were conducted primarily in areas south and east of Cranbrook (NTS 082G/03, /04,

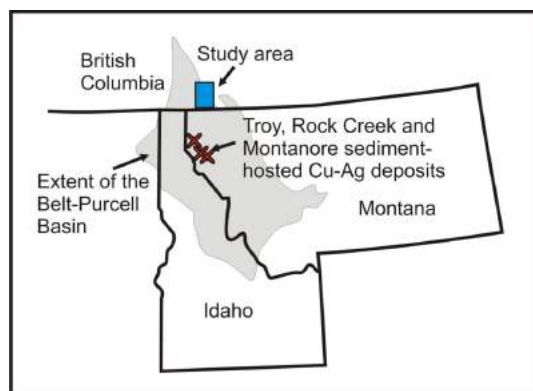


Figure 1. Approximate extent of the exposed Belt-Purcell Basin in British Columbia, Montana, Idaho and Washington (known as the 'Purcell Basin' in Canada and the 'Belt Basin' in the United States). The location of the study area (shown by the rectangle) and known sediment-hosted Cu deposits are also shown.

/05, /06, /12), an area that was previously mapped by Höy and Carter (1988). Approximately 10 weeks of geological mapping, including a focused examination of the Creston Formation around Yahk Mountain in the McGillivray Range, were conducted in 2007 and 2008. Data and samples were collected for magnetic susceptibility measurements, litho-geochemical studies and a pilot biogeochemical survey. The Troy and Montanore stratabound Cu-Ag deposits of Montana were visited in order to better identify exploration strategies for this class of mineral deposit.

Initial results of a regional examination of known sediment-hosted Cu occurrences from the Purcell Supergroup were published by Hartlaub and Paradis (2008). The present paper moves to an examination of the potential for 'Revett style' (Cox et al., 2007) deposits in the Belt-Purcell Basin in Canada.

Geological Setting and Regional Stratigraphy of the Belt-Purcell Basin

The Mesoproterozoic Belt-Purcell Basin is an intracontinental rift system filled by marine and fluvial

Keywords: Purcell Supergroup, sediment-hosted Cu, red bed, Creston Formation, Revett Formation, stratabound, quartzite

This publication is also available, free of charge, as colour digital files in Adobe Acrobat® PDF format from the Geoscience BC website: <http://www.geosciencebc.com/s/DataReleases.asp>.

sediments that extends from southeastern BC into Idaho, western Montana and eastern Washington (Höy, 1993; Elston et al., 2002; Lydon, 2007). It is known as the ‘Belt Basin’ (containing the Belt Supergroup strata) in the United States and the ‘Purcell Basin’ (Purcell Supergroup) in Canada. The basin developed as a branching system of sub-basins along basement structures and was later shortened and folded during several periods of deformation (Höy et al., 2000; Price and Sears, 2000). In southeastern BC, the oldest rocks of the Purcell Supergroup are exposed along the core and western margin of a large-scale anticlinorium (Purcell anticlinorium).

Mesoproterozoic rocks of the Purcell Basin in Canada have been stratigraphically subdivided in different ways by different authors working in different locations. A complete discussion of stratigraphic nomenclature and changes within the basin is available in Höy (1993), Winston and Link (1993) and Gardner and Johnston (2007). The lower 12 km of the basin are ‘rift-fill’ turbidite rocks, the Aldridge Formation in Canada, which are intruded by the mafic Moyie sills, dated at 1468 ± 2 Ma (Anderson and Davis, 1995). The Creston, Kitchener and Van Creek formations overlie the Aldridge Formation, and constitute the middle succession of the Purcell Supergroup (Figures 2, 3). They

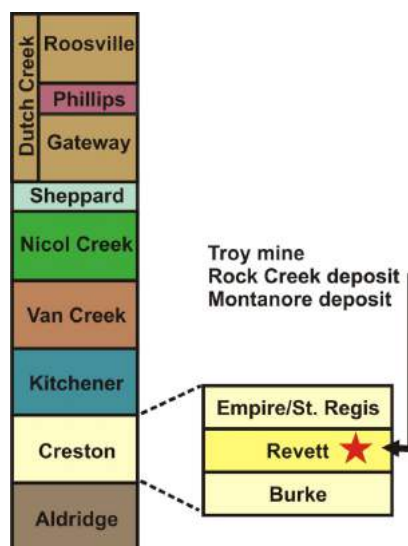


Figure 3. Simplified stratigraphic column for the Purcell Supergroup in the study area (modified from Höy, 1993).

represent the beginning of the ‘rift-cover’ sequence (Lydon, 2007) but predate the eruption of a thick package of flood basalts (the Purcell lavas or the Nicol Creek Formation). A porphyritic rhyolite in the Purcell lavas in Montana yielded an age of 1443 ± 7 Ma (Evans et al., 2000). Directly overlying the flood basalts of the Nicol Creek Formation are coarse clastic and stromatolitic carbonate rocks of the Sheppard Formation. The shallow-water, fine-grained clastic rocks of the upper Purcell Supergroup include the Gateway, Phillips and Roosville formations (Höy, 1993).

In southeastern BC, the Purcell Basin has been folded along a north-northwest-trending axis and has been transported eastwards during regional compression associated with the late Cretaceous Rocky Mountain orogeny (Chandler, 2000; Höy et al., 2000; Price and Sears, 2000). A sub-greenschist grade of metamorphism exists throughout much of the Purcell Supergroup; however, the metamorphic grade is locally higher.

A glacial overburden blanket of variable thickness covers much of the Purcell Mountains south of Cranbrook. This overburden places a severe limitation on mapping and prospecting activities in the region. Outcrops are limited to steep cliff faces, roadcuts and local ridges. Although the lack of exposure may have limited the ability to conduct prospecting and soil sampling, other methods can now be applied to the region in order to identify prospective areas beneath the glacial cover.

Geology and Subdivisions of the Creston Formation

The Creston Formation (Schofield, 1915) has been previously divided into three units based on lithology and envi-

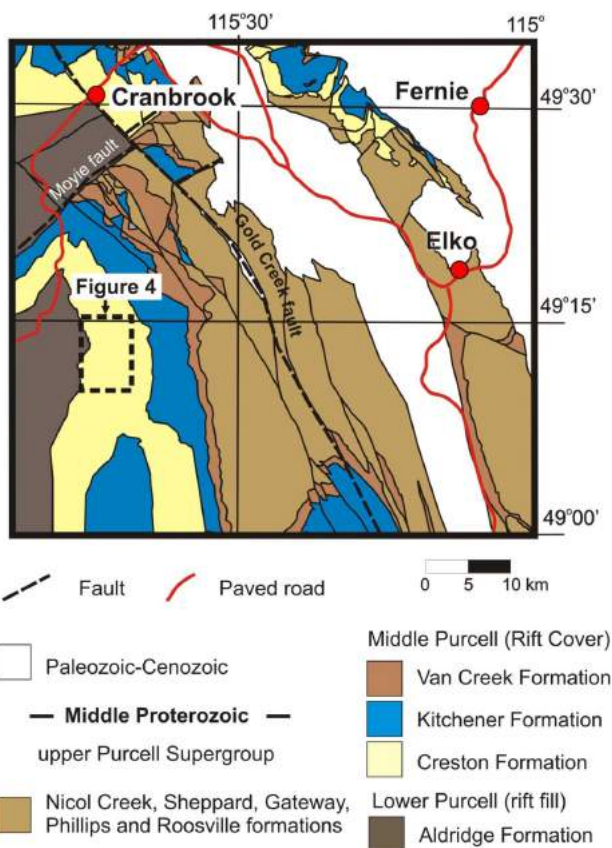


Figure 2. Simplified geology of the Purcell Supergroup (modified from Höy et al., 1995), showing the location of the study area (Figure 4).

ronment of deposition (Höy, 1993). These three subdivisions (C1, C2 and C3) are considered to be roughly equivalent to the Burke, Revett and St. Regis formations in Montana. On the eastern side of the Purcell Basin, McMechan (1981) further subdivided the Creston into five informal units. Both the upper and lower contacts of the Creston are reported to be gradational (Höy, 1993). Study of the Creston Formation has been relatively limited compared to the more than 86 measured sections and numerous logged drillcores reported from the Burke, Revett and St. Regis formations in Montana and Idaho (Mauk and White, 2004; Boleneus et al., 2005).

An area underlain by the Creston Formation south of Cranbrook, near Yahk Mountain, was chosen for more detailed mapping (Figure 4). The area is considered prospective for sediment-hosted Cu because it contains a significant thickness of middle Creston Formation and hosts a small Cu occurrence, discovered in 2007. The Yahk Mountain area lies on the eastern limb of the Purcell anticlinorium, about 15 km north of the border with Montana. The Creston Formation in this area dips 15–20° east-northeast and is best exposed at higher elevations. For comparative purposes, additional sections of Creston Formation were examined on the east side of Moyie Lake and from drillholes west of Cranbrook. More than 50 samples of Creston sedimentary rocks were collected for future detailed petrographic and geochemical analysis.

The Creston Formation is notable for its alternating units of shallow-water siltstone, argillite, quartzite and silty quartzite. Ripple marks and crossbeds are abundant and consistent with sediment deposition in a relatively shallow, high-energy environment (Figure 5A). Flame structures, load casts, scour surfaces, rip-up clasts and desiccation structures occur locally. Hematite and pyrite also occur locally (Figure 5B), but subhedral to euhedral magnetite is widespread. Magnetic susceptibility readings for the Creston range from 0.1×10^{-3} SI units to more than 15×10^{-3} SI, with an average of $\sim 4 \times 10^{-3}$ SI. These readings are much higher than those of the other strata in the Purcell Supergroup, which rarely exceed 0.2×10^{-3} SI. Metamorphic biotite, muscovite and staurolite occur sporadically and indicate that local conditions may have peaked at middle amphibolite facies.

Basal, middle and upper divisions of the Creston Formations occur in the Yahk Mountain map area and are discussed in detail below. These three subdivisions are roughly the same as those of Höy (1993) and appear to be equivalent to the Burke, Revett and St. Regis formations in Montana:

The **basal Creston (C1)** is dominated by green-grey siltstone and argillite with rare thin beds of quartzite. Siltite-argillite couplets are common, and a distinctive

dark grey to black fissile siltstone occurs. The abundance of syneresis cracks and a lack of desiccation cracks have been cited as evidence that this unit was entirely subaqueous (McMechan, 1981). The Burke Formation in Montana is reported as siltite and argillite that has a range of colours including greenish grey, purple, reddish grey and minor black and grey (Winston and Link, 1993). Several Cu occurrences were noted within the uppermost part of C1 and are described below.

The **middle Creston (C2)** contains interbedded sequences of variably bleached, medium- to thick-bedded siltstone, quartzite and silty quartzite. The base of unit C2 is difficult to constrain; however, the first appearance of thick-bedded white quartzite is used to mark the appearance of the Revett Formation in Montana (Hayes, pers. comm., 2008). The abundance of desiccation cracks in the middle Creston is consistent with repeated subaerial exposure during deposition. Siltstone of the middle Creston is commonly light green, grey or purple. The less abundant quartzite beds within the Yahk Mountain area, when compared to the Troy and Montanore areas of Montana, may be due to limited exposure. The grain size in the middle Creston rarely exceeds a medium sand, consistent with what is described from the majority of the Revett Formation (Boleneus et al., 2005). Much of the Revett has been interpreted to have formed via fluvial braided channels and sheet-flood deposits (Winston and Link, 1993)

The **upper Creston (C3)** resembles the lower Creston in that it is dominated by green, lenticular bedded siltstone and argillite with very few quartzite beds. Siltstone-argillite couplets are common. The stratigraphically equivalent unit in Montana is the St. Regis Formation.

Intrusive Rocks

Although there are relatively few intrusive rocks in the region (Figure 2), coarse-grained gabbro dikes and sills are scattered throughout. A single, poorly exposed gabbro dike cuts the middle Creston in the Yahk Mountain area (Figure 4), but other similar dikes locally cut the Kitchener Formation. A U-Pb zircon crystallization age of 1439 ± 2 Ma (Brown and Woodfill, 1998) for a gabbro sill exposed east of Moyie Lake is within error of the U-Pb zircon age of 1443 ± 7 Ma (Evans et al., 2000) for rocks equivalent to the Nicol Creek Formation in Montana. Therefore, the gabbro sill is likely part of a feeder system to the overlying Nicol Creek basalts. Another gabbro dike cutting the Kitchener Formation near Cranbrook contains numerous chalcopyrite-rich veins (Hartlaub and Paradis, 2008); however, ‘Revett style’ Cu deposits have not been linked to any magmatic events.

Stratabound Cu±Ag±Co Potential of the Middle Creston Formation

The mineral potential of an area is commonly related to past discoveries and currently operating mines. By this standard, any Revett-equivalent rocks in the Purcell Basin should be considered to have a high mineral potential despite the lack of significant discoveries in the middle Creston north of the Montana-BC border.

Knowledge of the conditions required to form stratabound copper deposits is important to better understand the min-

eral potential of the middle Creston. The majority of sediment-hosted stratabound Cu deposits are formed within continental-rift basins due to movement of moderately low pH and oxidized fluids within permeable, shallow-water sedimentary and, more rarely, volcanic rocks (Brown, 1992). Copper, silver, cobalt, lead and other metals are leached from minerals within the sedimentary and/or igneous rocks and carried elsewhere and precipitated. Cox et al. (2007) subdivided sediment-hosted Cu deposits into three groups, based primarily on how Cu precipitates from the fluids. In the reduced-facies deposits, oxidized mineralizing brine interacts with some form of reductant and depos-

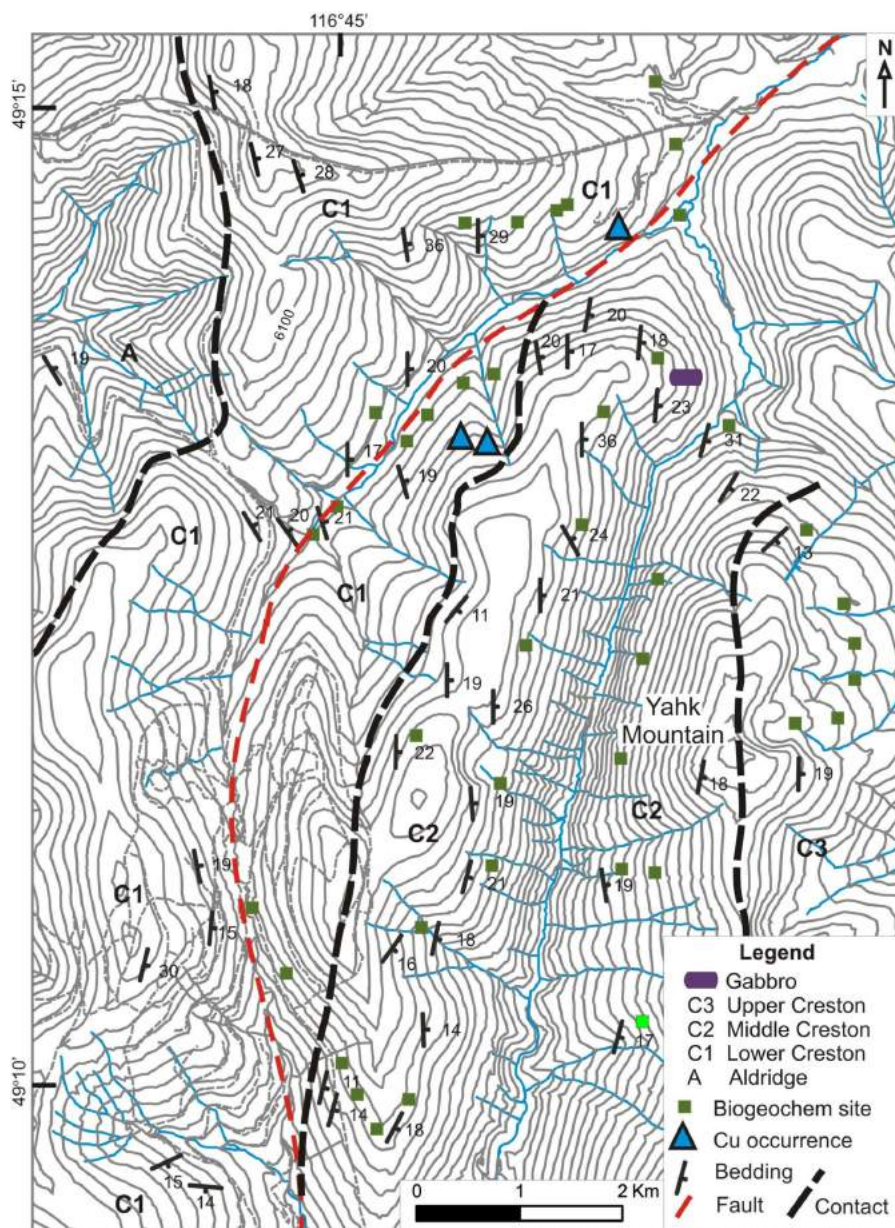


Figure 4. Simplified geology of the Yahk Mountain area south of Cranbrook. Unit descriptions are found in the text. Contour interval is 100 feet. Geological formations in the map area are the Aldridge (A), basal Creston (C1), middle Creston (C2) and upper Creston (C3). See Figure 2 for regional location.

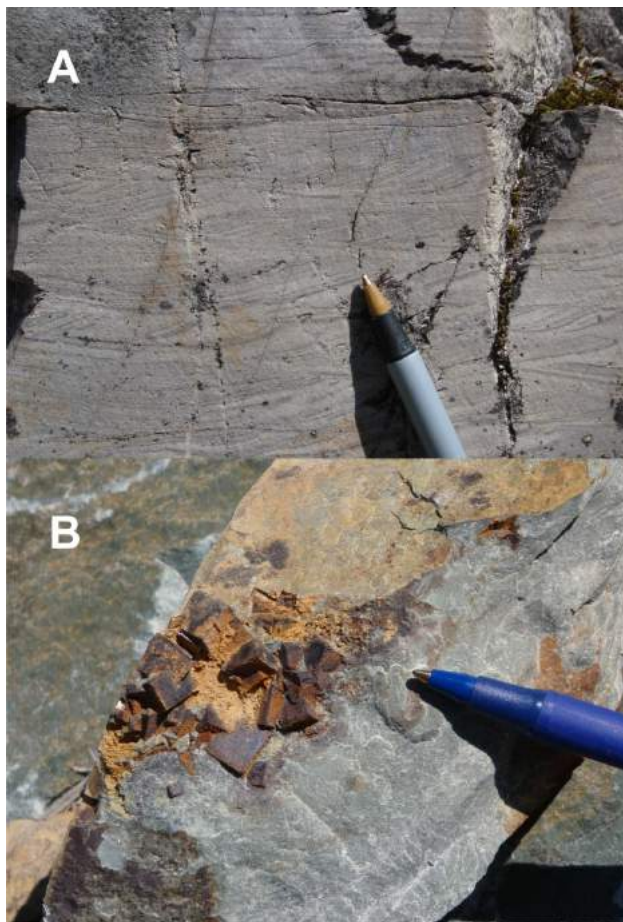


Figure 5. A) Crossbedding in quartzite of the Middle Creston Formation (C2) on Yahk Mountain (UTM Zone 11, 593687E, 5448550N, NAD 83). **B)** Euhedral oxidized pyrite in quartzite of the Creston Formation (UTM 589483, 5465047E).

its $\text{Cu}\pm\text{Ag}\pm\text{Co}$ above or lateral to the red-bed sedimentary rocks (Figure 6). This reductant may be a reduced unit, such as black shale, or sulphur derived by bacterial reduction of seawater sulphates (Cailteux et al., 2005). It is the presence of the reductant that can lead to large, high-grade deposits, such as those in the Kupferschiefer and Central Africa. Red-bed-hosted deposits lack or have limited amounts of reducing hostrocks and are typically low grade and small tonnage (Cox et al., 2007). Deposits in the Revett Formation can be viewed as their own subtype, since the known deposits are hosted in quartz-rich sandstone. Unlike the red-bed deposits, however, a reductant in the form of pyritic sand bodies, or possibly hydrocarbon fluids, is believed to have localized Cu and Ag mineralization (Boleneus et al., 2005; Hayes, pers. com., 2008). The control that sedimentary structures locally provide on the distribution of disseminated sulphides is typically cited (e.g., Garlick, 1988; Cailteux et al., 2005) as evidence that Cu mineralization occurred prior to compaction and lithification of sediments. For example, sulphides may occur within troughs of ripples and ore may show signs of

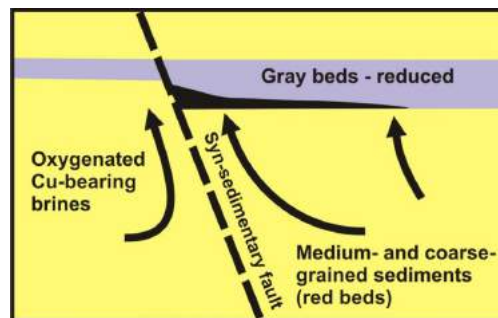


Figure 6. Typical model for the formation of sediment-hosted stratabound Cu deposits. The scale of the mineralizing system can vary from local to district.

sedimentary deformation, such as slumping or compaction (Garlick, 1988).

Several key points from the deposit models indicate the characteristics important to stratabound $\text{Cu}\pm\text{Ag}\pm\text{Co}$ exploration in the Purcell Basin:

- relatively thick units of oxidized, shallow-water sediments
- evidence for movement of brines through these oxidized sediments
- evidence for local precipitation of disseminated sulphides along early sedimentary structures

The Yahk Mountain area (Figure 4) encompasses all three of these important factors. Evidence for large-scale movement of oxidized fluids is noted within the area as scattered exposures of spectacular purple and red hematite mottling along bedding planes and fractures (Figure 7A) that occur immediately south and east of Cu mineralization. A similar style of alteration occurs within the Kupferschiefer sediment-hosted Cu deposits in Poland (Cox et al., 2007) and may mark the location of a localized redox front. Manganese minerals were noted on many fracture and joint surfaces in the same area (Figure 7B). However, this alteration process may be related to a later event. Boleneus et al. (2005) indicated that a lavender shade to the sedimentary rocks is occasionally apparent above and below, but not within, the prospective horizons of the Revett Formation.

In 2007, a new occurrence of disseminated Cu sulphides was discovered within the Creston Formation along the Tepee Creek forestry road (Hartlaub and Paradis, 2008; UTM 593577E, 5454607N). The new showing, named 'Tepee Creek', consists of green argillite containing fine bornite and chalcopyrite disseminated along the bedding planes. Minor amounts of green copper oxidation mark the discovery outcrop, and two grab samples returned assay results with Cu (564 and 2086 ppm) and Ag (2 and 6 ppm) values (Hartlaub and Paradis, 2008). In 2008, a 30 m section of outcrops along a forestry road was discovered to contain trace amounts of disseminated malachite and chalcopyrite in siltstone (UTM 592315E, 5452924N). Assay analyses

for samples from this location are underway. Although these Cu showings do not occur within quartzite, Cu occurrences have been reported from both fine and coarse units of the Burke, Revett and St. Regis formations (Boleneus et al., 2005). Along the east side of Moyie Lake, there are several locations where crosscutting quartz and quartz-carbonate veins and breccias contain copper sulphides (Figure 8A–C). This copper mineralization postdates stratabound mineralization and may indicate later remobilization of metals.

Key Exploration Strategies

Having identified a reasonable potential for sediment-hosted, stratabound Cu±Ag±Co mineralization on the Canadian side of the Belt-Purcell Basin, it is useful to note some of the key strategies that may be utilized for future exploration in the region. These exploration strategies were gleaned by examining the literature and visiting the sediment-hosted stratabound Cu deposits of Montana.

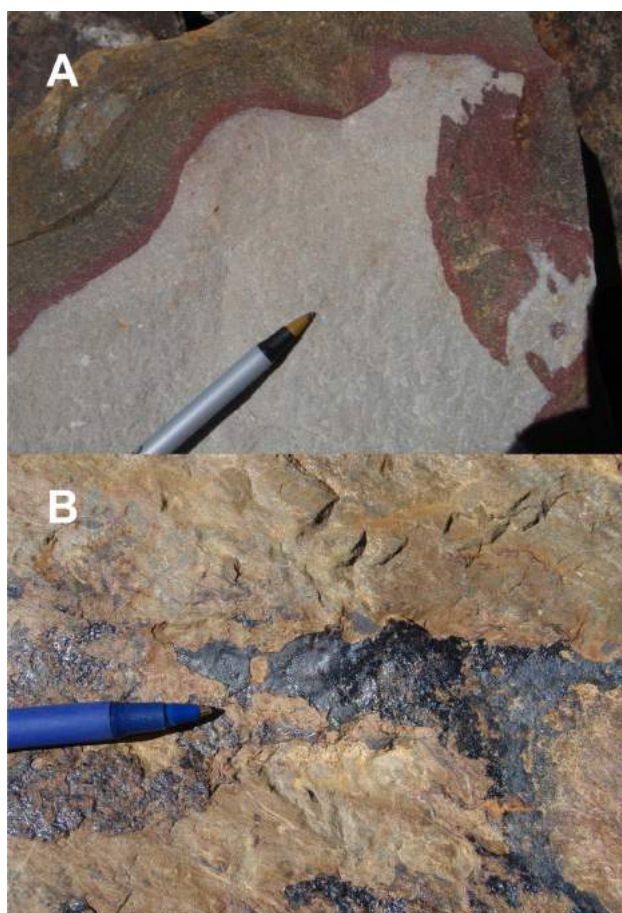


Figure 7. A) Red and purple iron-oxide alteration patterns within sandstone of the middle Creston Formation (UTM Zone 11, 594161E, 5453650N, NAD 83). This alteration is especially striking due to the white bleaching (argillic alteration) of the rock. Bleaching may indicate leaching of Cu and other metals from the rock, as has been seen in the Revett Formation. **B)** Manganese oxide, likely pyrolusite, on a joint surface (UTM 594038E, 5453531N).

Stream and biogeochemical sampling: Prospecting stream geochemical anomalies led to initial discoveries at most of the stratabound Cu deposits in Montana (Hayes, pers. comm., 2008). Although a BC Geological Survey database of regional stream sampling exists, a more detailed study will need to be carried out in selected parts of the Creston Formation outcrop area.

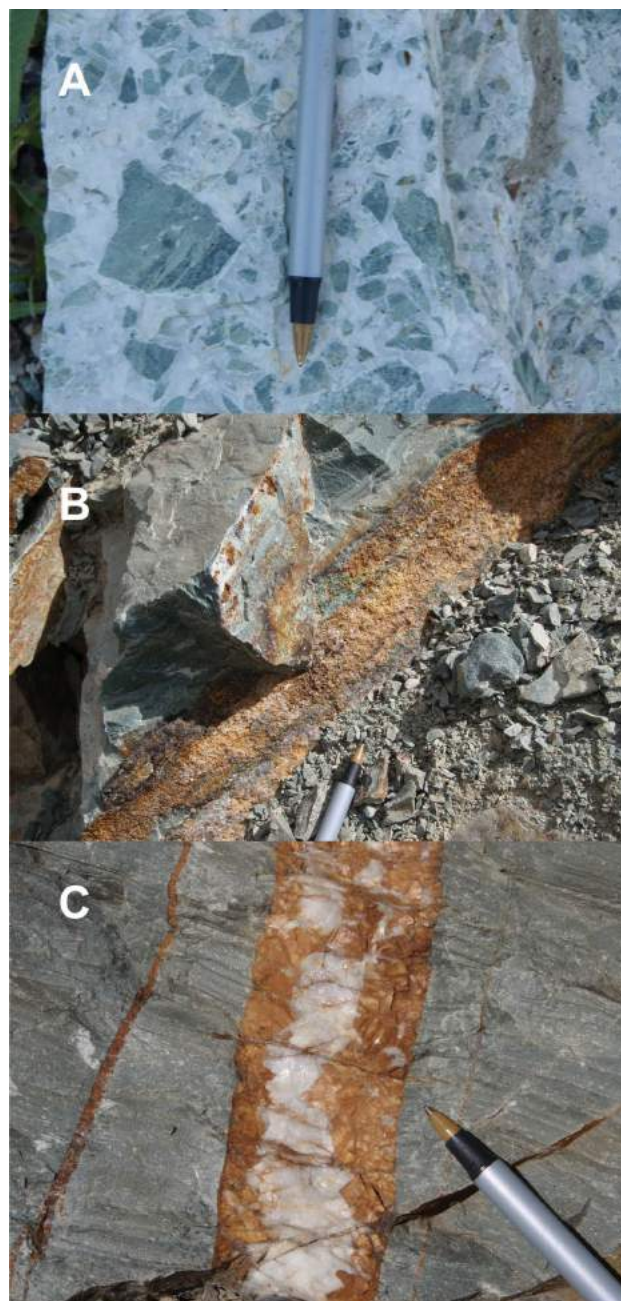


Figure 8. A) Breccia composed of siltstone-argillite clasts in a quartz vein matrix. The breccia locally contains chalcocopyrite and is exposed in a roadcut on the east side of Moyie Lake (UTM Zone 11, 585407E, 5466634N, NAD 83). **B)** Quartz, iron carbonate, chalcocopyrite and malachite cementing joint surfaces in the Creston Formation (UTM 585475E, 5467010N). **C)** Silty quartzite and argillite from the middle Creston Formation cut by a quartz-carbonate vein (UTM 585059E, 5464231N).

Biogeochemical sampling may also help provide targets in areas of poor exposure.

Tracing of prospective strata: Several of the deposits in Montana were discovered by a simple strategy of exploring along prospective stratigraphic horizons after traces of mineralization had been discovered (Hayes, pers. comm., 2008). Thick-bedded quartzite is the typical hostrock for the Revett deposits of Montana (Figure 9A), but the finer grained sedimentary rocks should not be ruled out. The disseminated nature of the mineralization is not always apparent, especially where limonite has partially replaced chalcopyrite (Figure 9B, C).

Induced-polarization surveys: Despite the low of concentration of sulphides, stratabound Cu deposits should produce IP anomalies due to the otherwise restricted presence of sulphides and graphite within the Creston Formation.

Aeromagnetic mapping: The abundance of magnetite within the Creston Formation indicates that detailed aeromagnetic imagery would be useful for tracing contacts in areas of poor exposure. A full evaluation of magnetic susceptibility measurements collected in 2008 has not yet been completed; however, initial results indicate that both mineralized and nonmineralized Creston Formation rocks have similar magnetic susceptibility values.

Future Products and Research Directions

Release of a GIS map dataset including outcrop locations, lithological interpretations, structural measurements, magnetic-susceptibility measurements and georeferenced photos

Publication of measured sections from prospective areas of the middle and upper Purcell Supergroup; lithological descriptions will be further constrained by petrographic analysis of reference samples

Public release of the complete biogeochemical and lithogeochemical database

Publication of new geochronological data

Completion of fluid inclusion studies on mineralized quartz veins from the Creston and Sheppard formations; this study will be completed in order to constrain the temperature and chemistry of mineralizing fluids

Acknowledgments

Research funding for this project was provided by Geoscience BC, and by Targeted Geoscience Initiative 3 (TGI-3) of Natural Resources Canada. C. Kennedy, D. Pighin and D. Grieve are all thanked for their informative discussions on the geology and mineral resources of the Purcell Basin. C. Campbell (2008) and T. Razi (2007) provided excellent assistance in the field. Expertise in biogeochemical sampling and analytical methods was pro-

vided by C. Dunn and R. Scagel. Thanks go to D. Feeback and Revett Minerals Inc. for the insightful tour of surface and underground exposures at the Troy mine. A greater understanding of Belt Basin metallogeny was provided by T. Hayes of the United States Geological Survey during a field visit to the Montanore deposit, Montana. Constructive discussions and comments by S. Paradis and B. Anderson were critical to this work.

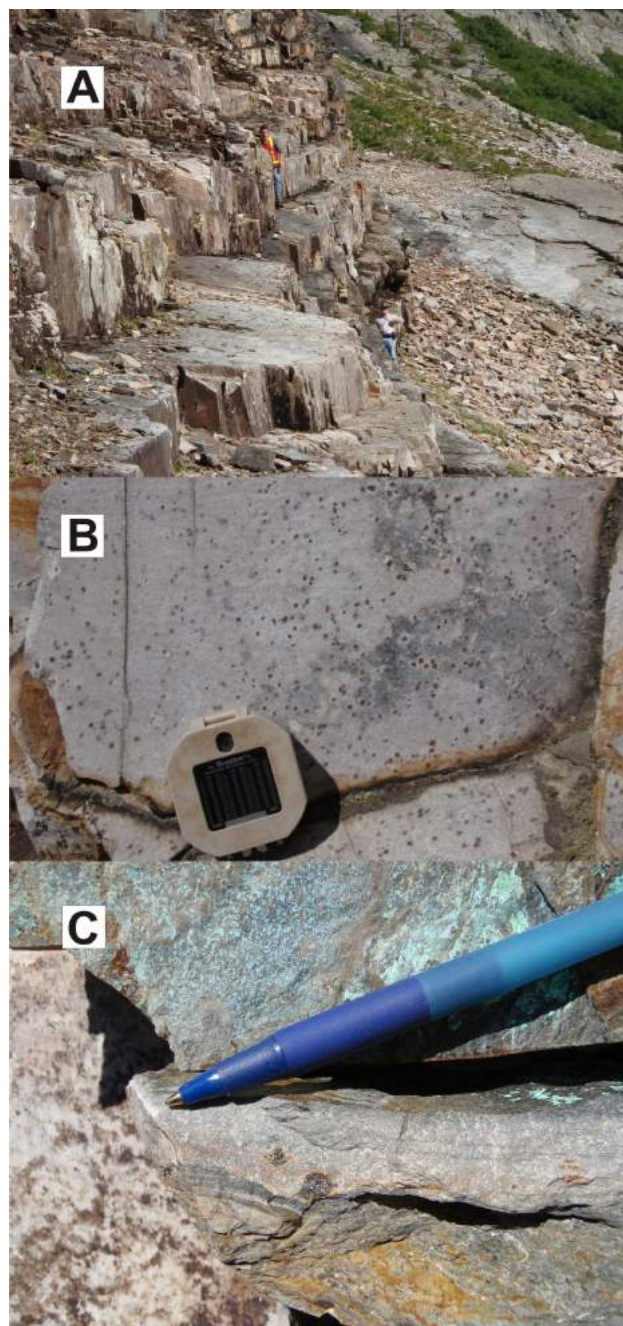


Figure 9. A) Thick-bedded quartzite of the lower Revett Formation. B) Limonite spots replacing chalcopyrite in lower Revett Formation quartzite. C) Detail of limonite spots replacing chalcopyrite and chrysocolla alteration. All three photos were taken at exposures of the Montanore deposit on the north shore of Rock Lake, Montana.

References

- Anderson, H.E. and Davis, D.W. (1995): U-Pb geochronology of the Moyie Sills, Purcell Supergroup, southeastern British Columbia: implications for the Mesoproterozoic geological history of the Purcell (Belt) Basin; *Canadian Journal of Earth Sciences*, v. 32, p. 1180–1193.
- Boleneus, D.E., Appelgate, L.M., Stewart, J.H. and Zientek, M.L. (2005): Stratabound copper-silver deposits of the Mesoproterozoic Revett Formation, Montana and Idaho; United States Geological Survey, Scientific Investigations Report 2005–5231, 66 p.
- Brown, A.C. (1992): Sediment-hosted stratiform copper deposits; *Geoscience Canada*, v. 19, p. 125–141.
- Brown, D.A. and Woodfill, R.D. (1998): The Moyie Industrial Partnership Project: geology and mineralization of the Yahk-Moyie Lake area, southeastern British Columbia (82F/01E, 82G/04W, 82F/08E, 82G/05W); *in Geological Fieldwork, 1997*, BC Ministry of Energy Mines and Petroleum Resources, Paper 1998-1, p. 1–22.
- Cailteux, J.L.H., Kampunzu, A.B., Lerouge, C., Kaputo, A.K. and Milesi, J.P. (2005): Genesis of sediment-hosted stratiform copper-cobalt deposits, central African Copperbelt; *Journal of African Earth Sciences*, v. 42, p. 134–158.
- Chandler, F.W. (2000): The Belt-Purcell Basin as a low latitude passive rift: implications for the geological environment of Sullivan type deposits; Chapter 6 *in The Geological Environment of the Sullivan Deposit*, British Columbia, J.W. Lydon, T. Höy, J.F. Slack, and M.E. Knapp (ed.), Geological Association of Canada, Mineral Deposits Division, Special Publication 1, p. 82–112.
- Cook, F.A. and van der Velden, A.J. (1995): Three-dimensional crustal structure of the Purcell anticlinorium in the Cordillera of southwestern Canada; *Geological Society of America Bulletin*, v. 107, p. 642–664.
- Cox, D.P., Lindsey, D.A., Singer, D.A. and Diggles, M.F. (2007): Sediment-hosted copper deposits of the world: deposit models and database; United States Geological Survey, Open-File Report 03-107 (revised 2007).
- Elston, D.P., Enkin, R.J., Baker, J. and Kisilevsky, D.K. (2002): Tightening the belt: paleomagnetic-stratigraphic constraints on deposition, correlation, and deformation of the middle Proterozoic (ca. 1.4 Ga) Belt-Purcell Supergroup, United States and Canada; *Geological Society of America Bulletin*, v. 114, p. 619–638.
- Evans, K.V., Aleinikoff, J.N., Obradovich, J.D. and Fanning, C.M. (2000): SHRIMP U-Pb geochronology of volcanic rocks, Belt Supergroup, western Montana: evidence for rapid deposition of sedimentary strata; *Canadian Journal of Earth Sciences*, v. 37, p. 1287–1300.
- Gardner, D.W. and Johnston, S.T. (2007): Sedimentology, correlation, and depositional environment of the upper Purcell Supergroup, northern Purcell Basin, southeastern British Columbia; *Geological Survey of Canada, Current Research 2007-A6*, 13 p.
- Garlick, W.G. (1988): Algal mats, load structures, and symsedimentary sulfides in Revett Quartzite of Montana and Idaho; *Economic Geology*, v. 83, p. 1259–1278.
- Goodfellow, W.D. and Lydon, J.W. (2007): Sedimentary exhalative (SEDEX) deposits; *in Mineral Deposits of Canada: A Synthesis of Major Deposit Types, District Metallogeny, the Evolution of Geological Provinces, and Exploration Methods*, W.D. Goodfellow (ed.), Geological Association of Canada, Mineral Deposits Division, Special Publication 5, p. 581–607.
- Hartlaub, R.P. and Paradis, S. (2008): Evaluation of the geology and stratabound base metal potential of the middle and upper Purcell Supergroup, southeastern British Columbia (NTS 082G/03, 04, 05, and 06); *in Geological Fieldwork 2007*, BC Ministry of Energy Mines and Petroleum Resources. Paper 2008-1, p. 9–16.
- Hayes, T.S. and Einaudi, M.T. (1986): Genesis of the Spar Lake strata-bound copper-silver deposit, Montana: part I, controls inherited from sedimentation and pre-ore diagenesis; *Economic Geology*; v. 81, p. 1899–1931.
- Hitzman, M.W. (2000): Source basin for sediment-hosted stratiform Cu deposits: implications for the structure of the Zambian Copperbelt; *Journal of African Earth Sciences*, v. 30, p. 855–863.
- Höy, T. (1993): Geology of the Purcell Supergroup in the Fernie west-half map area, southeastern British Columbia; BC Ministry of Energy, Mines and Petroleum Resources, Bulletin 84, 157 p.
- Höy, T. and Carter, G. (1988): Geology of the Fernie west half map sheet (and part of Nelson east half) (082G/W half, 082F/E half); BC Ministry of Energy, Mines, and Petroleum Resources, Open File 1988-14, scale 1:100 000.
- Höy, T., Anderson, D., Turner, R.J.W. and Leitch, C.H.B. (2000): Tectonic, magmatic, and metallogenic history of the early synrift phase of the Purcell Basin, southeastern British Columbia; Chapter 4 *in The Geological Environment of the Sullivan Deposit*, British Columbia, J.W. Lydon, T. Höy, J.F. Slack, and M.E. Knapp (ed.), Geological Association of Canada, Mineral Deposits Division, Special Publication 1, p. 32–60.
- Höy, T., Price, R.A., Legun, A., Grant, B. and Brown, D. (1995): Purcell Supergroup, southwestern British Columbia, Geological Compilation Map (82G, F, E, 82J/SW, 82K/SE); BC Ministry of Energy, Mines and Petroleum Resources, Geoscience Map 1995-1, scale 1:250 000.
- Lydon, J.W. (2007): Geology and metallogeny of the Belt-Purcell Basin; *in Mineral Deposits of Canada: A Synthesis of Major Deposit Types, District Metallogeny, the Evolution of Geological Provinces, and Exploration Methods*, W.D. Goodfellow (ed.), Geological Association of Canada, Mineral Deposits Division, Special Publication 5, p. 581–607.
- Mauk, J.L. and White, B.G. (2004): Stratigraphy of the Proterozoic Revett Formation and its control on Ag-Pb-Zn vein mineralization in the Coeur d’Alene district, Idaho; *Economic Geology*, v. 99, p. 295–312.
- McMechan, M.E. (1981): The Middle Proterozoic Purcell Supergroup in the southwestern Purcell Mountains, British Columbia and the initiation of the Cordilleran miogeocline, southern Canada and adjacent United States; *Bulletin of Canadian Petroleum Geology*, v. 29, p. 583–621.
- Paiement, J.-P., Beaudoin, G. and Paradis, S. (2007): Geological setting of Ag-Pb-Zn veins in the Purcell Basin, British Columbia; *Geological Survey of Canada, Current Research 2007-A4*, 10 p.
- Price, R.A. and Sears, J.W. (2000): A preliminary palinspastic map of the Mesoproterozoic Belt-Purcell Supergroup, Canada and USA: implications for the tectonic setting and structural evolution of the Purcell anticlinorium and the Sullivan deposit; *in The Geological Environment of the Sullivan Deposit*, British Columbia, J.W. Lydon, T. Höy, J.F. Slack and

- M.E. Knapp, M.E. (ed.), Geological Association of Canada, Mineral Deposits Division, Special Publication 1, p. 61–81.
- Schofield, S.J. (1915): Geology of the Cranbrook map area, BC; Geological Survey of Canada, Memoir 76, 245 p.
- Singer, D.A. (1995): World class base and precious metal deposits—a quantitative analysis; *Economic Geology*, v. 90, p. 88–104.
- Winston, D. and Link, P.K. (1993): Middle Proterozoic rocks of Montana, Idaho and eastern Washington: the Belt Supergroup: *in* Precambrian: Conterminous United States, J.C. Reed, Jr, M.E. Bickford, R.S. Houston, P.K. Link, R.W. Rankin, P.K. Sims and W.R. Van Schmus (ed.), Geological Society of America, *Geology of North America*, v. C-2, p. 487–517.

Time-Domain Electromagnetic and Magnetic Survey over the Kootenay Arc, Southeastern British Columbia (NTS 082F/03, /04, /06)

G. D. Kirkham, Geoscience BC, Vancouver, BC, kirkham@geosciencebc.com

W. F. Miles, Natural Resources Canada, Ottawa, ON

S. Paradis, Geological Survey of Canada, Sidney, BC

B. Finley, Dajin Resources Corp., Vancouver, BC

A. Troop, Sultan Minerals Inc., Vancouver, BC

Kirkham, G.D., Miles, W.F., Paradis, S., Finley, B. and Troop, A. (2009): Time-domain electromagnetic and magnetic survey over the Kootenay Arc, Southeastern British Columbia (NTS 082F/03, /04, /06); in Geoscience BC Summary of Activities 2008, Geoscience BC, Report 2009-1, p. 133–136.

Introduction

The Kootenay Arc is located in southeastern British Columbia (BC), in the Omineca Belt of the Canadian Cordillera. It is defined as a lens-shaped belt of highly deformed rocks that extends approximately 400 km from north of Revelstoke to the Canada–United States border. It is located between the Purcell Mountains to the east and the Monashee metamorphic complex to the west (Figure 1).

The Kootenay Arc contains a number of carbonate-hosted zinc-lead deposits, including important past-producers such as Reeves MacDonald, Jersey and HB in the Salmo camp (MINFILE 082FSW026, 082FSW009 and 082FSW004, respectively; MINFILE, 2008), and Bluebell in the Slocan camp (MINFILE 082FNE043). Figure 1 shows the simplified geology of the Kootenay Arc and the location of some past-producers and prospects (Paradis, 2007).

A 4367 line-kilometre (line-km) time-domain electromagnetic and magnetic survey has been initiated as a partnership between Geoscience BC, Natural Resources Canada (NRCan) and two industry partners, Dajin Resources Corp. and Sultan Minerals Inc. The combination of NRCan (federal government), Dajin and Sultan (industry) and Geoscience BC (industry led and funded by the BC provincial government) is a showcase geoscience partnership for gathering valuable geophysical and geological data. This cost-effective strategy will enable a better understanding of the geology of the Kootenay Arc and develop new mineral exploration targets in BC.

Keywords: Kootenay Arc, geophysics, electromagnetic, magnetic
This publication is also available, free of charge, as colour digital files in Adobe Acrobat® PDF format from the Geoscience BC website: <http://www.geosciencebc.com/s/DataReleases.asp>.

Description of Survey

Prior to launching the survey, work was undertaken by the Geological Survey of Canada (i.e., NRCan) to determine basic rock properties of the geological formations within the proposed survey area, in order to identify which geophysical methods (if any) would be best suited to

- 1) developing an accurate geological map of the survey area, and
- 2) targeting potential base metal deposits within the survey area.

The rock properties study indicated that a time-domain electromagnetic and magnetic survey was best suited to furthering these goals. Potential deposit types anticipated in this region include carbonate-hosted zinc-lead, sedimentary exhalative (SEDEX), molybdenum and tungsten skarns, polymetallic veins and porphyry deposits. The combined electromagnetic-magnetic survey is deemed applicable to exploration for all these deposit types.

Once the survey area was identified, the optimal line spacing for data collection was determined to be 200 m. Potential industry partners were then invited to contribute to the costs of collecting infill data at 100 m spacing. Two companies, Dajin and Sultan, chose to participate in his survey, thereby adding to the total line-kilometres of data to be collected.

In summary, the survey area extends from the United States border east of Salmo to latitude 49 22'N (Figure 2). The survey will acquire time-domain electromagnetic and magnetic data. The electromagnetic system will require a dipole moment with a minimum of 200 000 Am², a dual-axis receiver and a stinger-mounted magnetometer. The traverse flight-line spacing is 200 m with an orientation of 100 , with the addition of the 100 m infill lines as mentioned above. In addition, control lines are to be flown perpendicular to the traverse lines at a spacing of 1000 m, per stan-

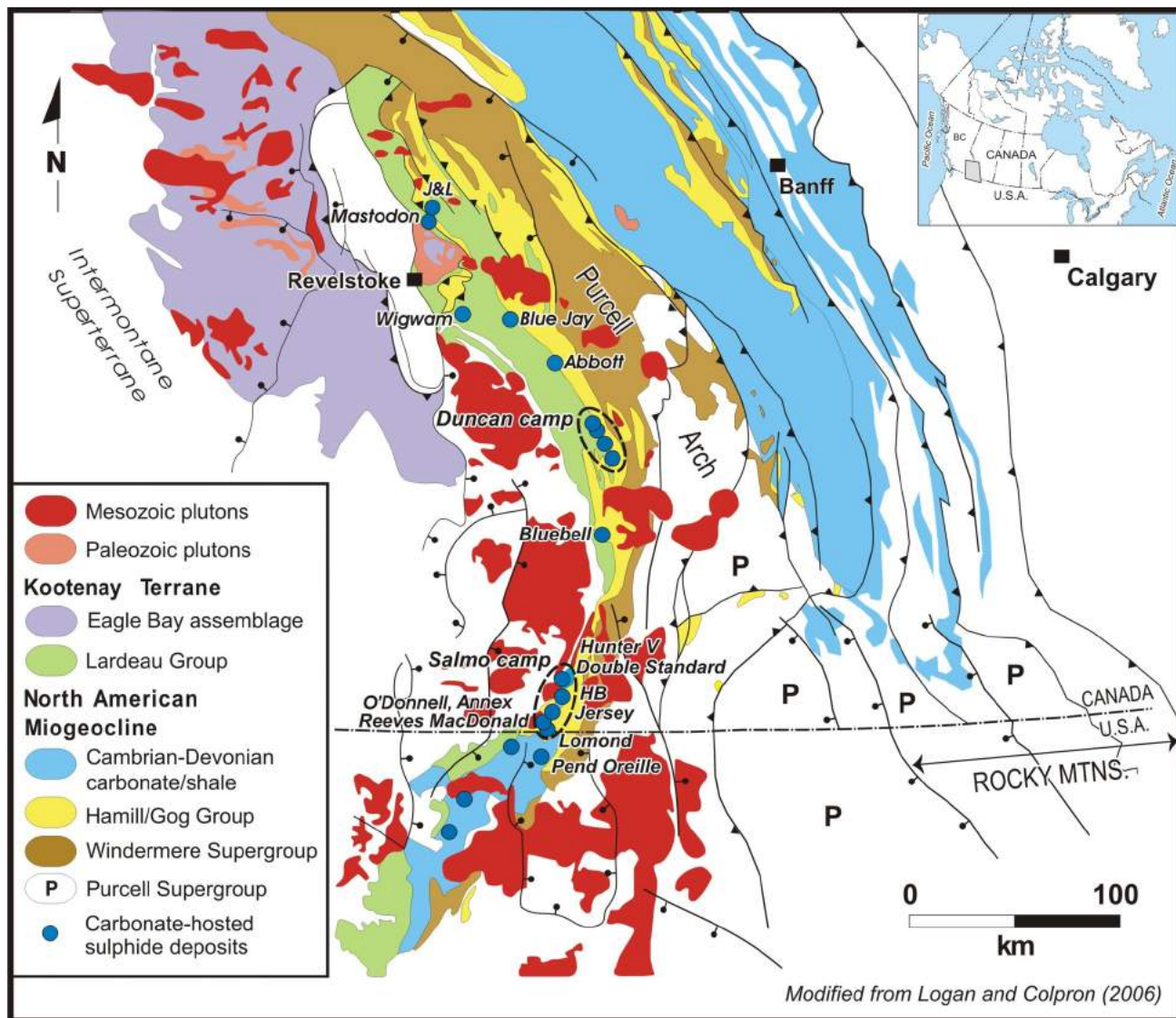


Figure 1. Location and simplified geology of the Kootenay Arc, showing zinc-lead past-producers and prospects (after Paradis, 2007).

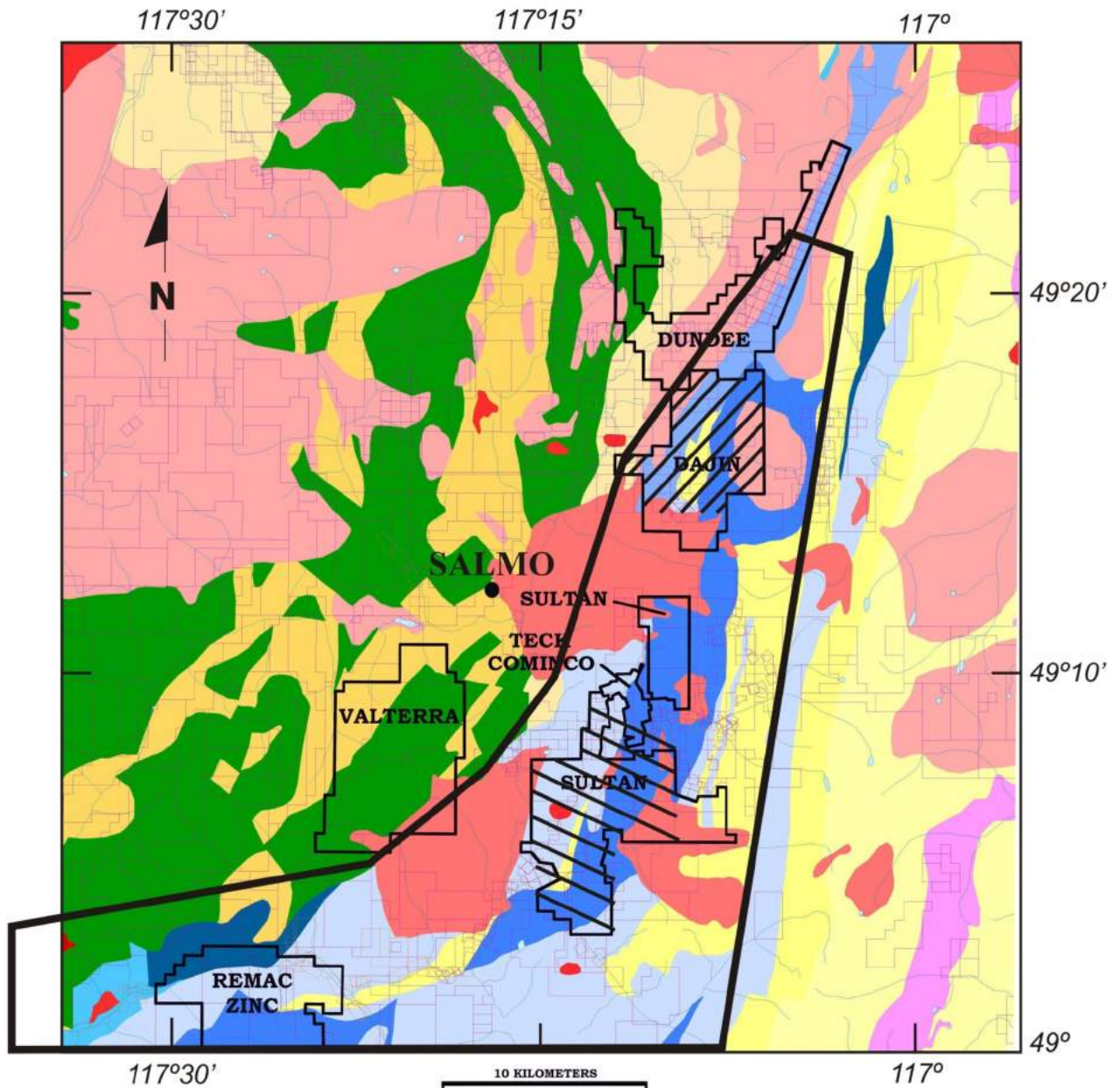


Figure 2. Area to be covered by Kootenay Arc electromagnetic-magnetic survey, with 100 m infill lines over Dajin Resources Corp. and Sultan Minerals Inc. claims.

standard practice. It should be noted that, due to the rugged terrain, the survey will be by helicopter. The survey will consist of 4367 line-km (including industry infill lines) once completed.

References

MINFILE (2008): MINFILE BC mineral deposits database; BC Ministry of Energy, Mines and Petroleum Resources, URL

<http://www.empr.gov.bc.ca/Mining/Geoscience/MINFILE/Pages/default.aspx> [November 2008].

Paradis, S. (2007): Carbonate-hosted Zn-Pb deposits in southern British Columbia—potential for Irish-type deposits; *in* Current Research 2007-A10, Geological Survey of Canada, 9 p., URL <http://geopub.nrcan.gc.ca/moreinfo_e.php?id=224161> [November 2008].

Development and Application of a Rock Property Database for British Columbia

S. Parsons, Mira Geoscience Limited, Westmount, QC, sharonp@mirageoscience.com

J. McGaughey, Mira Geoscience Limited, Westmount, QC

D. Mitchinson, Department of Earth and Ocean Sciences, University of British Columbia, Vancouver, BC

N. Phillips, Centre for Advanced Geophysics, Mira Geoscience, Vancouver, BC

T. Lane, CAMIRO, Toronto, ON

Parsons, S., McGaughey, J., Mitchinson, D., Phillips, N. and Lane, T.E. (2009): Development and application of a rock property database for British Columbia; in Geoscience BC Summary of Activities 2008, Geoscience BC, Report 2009-1, p. 137–144.

Introduction

Physical rock property data, systematically recorded and comparable in standard formats, are integral to successful interpretation of subsurface geology from geophysics. This project represents a beginning in building a useful database for British Columbia (BC). The data release is the result of a significant amount of work by Mira Geoscience Limited and the Geological Survey of Canada (GSC) to produce a standardized, high-quality set of nearly 900 000 data points for the province. A significant amount of work was required to bring all data to Rock Property Database System (RPDS) standards. The result was a significant ‘in-kind’ effort by Mira Geoscience and GSC staff that exceeded the budget of the project. The project would not have been possible without combined funding from Geoscience BC, Mira Geoscience, the Geological Survey of Canada, BHP Billiton, Terrane Metals and Teck Cominco. A significant amount of industry data remains to be added to the database.

Project 2006-015 started in October 2006, when Mira Geoscience was contracted by the Canadian Mining Industry Research Organization (CAMIRO) to assemble and organize physical rock property data for BC. A large amount of rock property data exists for the province but is in various hard-copy and digital formats, and archived at many locations across the country, thus making it difficult to amalgamate. One of the objectives of this project was to bring together all available data for BC into standard digitized formats on a common integration platform. The project focused on rock property data collected by the Geological Survey of Canada from various borehole surveys in the 1980s and 1990s, measurements related to mapping of BC

basins, and the Targeted Geoscience Initiative and other recent surveys in the Nechako Basin.

The strategy was to compile the various rock property data for BC into the Rock Property Database System (RPDS), a database application developed over the last 8 years by a consortium of industry and government agencies, and managed by Mira Geoscience. Data delivered in this project are in two formats: 1) database files on DVD intended to be downloadable from BC Geological Survey’s MapPlace, and 2) files accessible on ‘RPDS’ through the Mira Geoscience website. The database is an Oracle-based relational data management system that brings together geological and geophysical information, and facilitates interpretation of rock properties and corresponding geological description across geographic areas. This permits statistical and spatial characterization of the rock property environment for various ore deposit types in different geological settings. The significance of RPDS is that it provides a single repository for rock property data, as opposed to many disparate sources, thus allowing large-scale aggregation of data and in-depth analysis of rock property relationships. During the term of this project, public access to RPDS data through the Mira Geoscience website was considerably improved through a separate contract with the GSC.

Approximately 881 064 physical rock property measurements from wireline, drillcore and surface samples from across BC have been procured from both government and industry sources. These data have been entered into RPDS at Mira Geoscience, adding to the existing archive of more than 5 million rock property measurements. In addition to data archiving and management capabilities, RPDS also provides value-added summary tables of population statistics for various rock types across geographic areas. The summary tables for BC will be provided with the final project report. In addition, all data in RPDS are currently publicly available through an online Web interface at www.mirageoscience.com/rpds. All data from BC will be made available for the MapPlace website. The final report

Keywords: *geophysics, physical rock property data*

This publication is also available, free of charge, as colour digital files in Adobe Acrobat® PDF format from the Geoscience BC website: <http://www.geosciencebc.com/s/DataReleases.asp>.

will include descriptions of the specific project deliverables and the project datasets; a summary of the RPDS application, including the generation of the statistical output tables; a description of the digital files; and all data on a DVD.

Project Data

Data Distribution

The Rock Property Database System currently houses 881 064 physical rock property records from borehole wireline, drillcore and surface samples within BC. Physical properties measured in boreholes include density, magnetic susceptibility, conductivity, resistivity, density count, gamma-ray count, induced polarization (IP), total field magnetic, spectral gamma-gamma ratio, self potential (SP), SP gradient, single-point resistivity, temperature and temperature gradient. All data have been entered into RPDS and meta-classifications, unit conversions, and coordinate system conversions have been applied, and general data-quality assessment and control completed. The following sections describe the datasets in more detail. Tables 1a–c summarize the BC data in RPDS. The spatial distribution of data collected from BC and entered into RPDS is shown in Figure 1.

Wireline Data

Borehole wireline data (Figure 1, open circles) from 23 holes, consisting of 198 logging runs between 1986 and 1994, were provided by the Borehole Geophysics Group at the Geological Survey of Canada in Ottawa. Mira Geoscience travelled to Ottawa to collect the digital and hard-copy data archived on multiple DVDs and more than 150 hand-written field logging sheets. Multiple DVDs were copied from GSC archives, which contained various ASCII-text files transferred from original logging tapes. These ASCII-text files contained raw and processed data per logging run and, where available, lithology files per borehole. Logging run metadata were photocopied from original hard-copy field logging sheets, which provided critical information pertaining to the logging runs as well as for deciphering raw data file names in order to associate the appropriate raw data with processed data files. Additional metadata were acquired from supplementary hard-copy documents, open file reports and personal communication with GSC contributors. Where available, hole trace and assay files were generated manually from hard-copy core logs, and paper maps were digitized to PDF format. Finally, data and metadata were formatted to RPDS import standards and entered into the system. This formatting involved applying geological and quality indicator classifications, performing unit and co-ordinate conversions, and completing minor data-quality control. Due to the multiple sources of information, a significant amount of work was required to prepare the data for entry into RPDS.

Surface Sample Data

Data on 13 554 new and recent surface samples (Figure 1, red circles) were supplied by GSC-Vancouver. This dataset contains mainly magnetic susceptibility and density measurements, with a small population of conductivity measurements. The data were provided as one large Excel spreadsheet. Prior to entry into RPDS, the data were classified and formatted to fit RPDS import standards. For example, magnetic susceptibility data were converted from 10^{-6} or 10^{-3} SI to SI, and density data were converted from kg/m^3 to g/cm^3 . In some cases, rock codes and rock code descriptions were supplied in separate files. These rock descriptions had to be attributed and then master rock types assigned. Duplicate entries in the provided datasets were removed and unique sample IDs (Location ID) were assigned. Although RPDS uses an Excel spreadsheet for sample entry, each dataset required full reformatting prior to entry into the database system. A large part of the formatting was performed by R. Enkin's group at the GSC in collaboration with Mira Geoscience.

In addition to the surface sample data, 118 density and velocity measurements from the Sullivan deposit already existed in RPDS. These data are included in the output data files that will accompany the final report. The surface sample data are a very important part of the database, particularly because they cover a large areal extent of the province, compared to local borehole data. These data enable characterization of the density and magnetic susceptibility of mappable rock units.

Borehole Drillcore Data

Borehole drillcore data from the Mount Milligan Cu-Au porphyry project (Figure 1, blue circles) were provided courtesy of Terrane Metals Corp. The data were received as one Excel spreadsheet but needed a significant amount of reformatting and data preparation due to the large number of boreholes provided and data storage artifacts from the provider's own database system, which were inconsistent with RPDS standards. For example, the provider's database stored depth as a depth start and depth end range, whereas RPDS stores actual physical property data for samples at one depth value. As with the surface sample data, this dataset was attributed with rock code descriptions, master rock types were assigned, measurements were converted from 10^{-3} SI to SI, negative and zero values were removed, and unique sample IDs (Location ID) were assigned.

RPDS Application

General Overview

The Rock Property Database System (RPDS) is designed as an integration platform for combining geophysical and

Table 1. Summary of physical rock property data from British Columbia, collected and entered in RPDS, by a) data type, b) physical property, and c) location.

a) General data type

General data type	Count		
	Holes	Logging runs	Records
Borehole	23	198	854,851
Borecore Sample	179		12,541
Surface Sample			13,672
Total			881,064

b) Geophysical data summary

Parameter	Sample/borecore record count	Wireline record count		Total records
		Borehole count	Record count	
Density	2,483	12	19,064	21,547
Magnetic Susceptibility	23,644	19	127,516	151,160
Conductivity	27	4	11,956	11,983
Velocity	59			59
Resistivity		21	107,063	107,063
Density Count		8	26,637	26,637
Gamma Ray Count		17	55,101	55,101
Induced Polarization		11	50,122	50,122
Total Field Magnetics		10	55,551	55,551
Spectral Gamma-Gamma Ratio		20	45,856	45,856
Self Potential Gradient		11	55,459	55,459
Self Potential		11	53,979	53,979
Single Point Resistivity		10	55,976	55,976
Temperature Gradient		22	94,918	94,918
Temperature		22	95,653	95,653
Total Records	26,213	198	854,851	881,064

c) Data summary by location

Area of data acquisition	Data provider	Data type	Total records	Physical properties measured
Adams Lake		SS	559	M,D,C
Bowser & Sustut Basins		SS	1203	M,D
Cariboo		SS	1865	M,D
Chilcotin		SS	953	M,D
Coast		SS	81	M
Interior Plateau	GSC-Vancouver	SS	91	M
Kootenay Arc	(R. Enkin, C. Lowe, B. Anderson)	SS	1268	M,D,C
Nechako		SS	6310	D,M
N. Cascades		SS	8	M
Omineca		SS	6	M
Queen Charlotte		SS	850	M,D
Rockies		SS	68	M
Skeena/Bulkley		SS	67	M
Thompson		SS	225	M,D
Sullivan Deposit	Previously in RPDS	SS	118	D,V
Mt. Milligan	Terrane Metals (D. O'Brien)	BC	12,541	M
Chu Chua		BH	43,899	C,DC,IP,M,R,SG,T,TG
Equity Silver		BH	55,495	C,D,IP,M,R,SG,T,TG,GC
Goldstream		BH	80,762	DC,GC,IP,M,R,SG,T,TG
Highland Valley	GSC-Ottawa	BH	77,211	DC,GC,IP,R,SG,SP,SPG,T,TG,M
Lara/Buttle Lake	(J. Mwenifumbo)	BH	170,971	DC,GC,IP,M,R,SG,T,TG
Myra Falls		BH	392,081	D,GC,M,MAG,R,SG, SP,SPG,SPR,T,TG
Sullivan		BH	34,432	C,DC,IP,M,R,SG,T,TG,GC,SPR

Data type abbreviations: SS, surface sample; BC, core borehole sample; BH, wireline borehole data

Physical properties measured' abbreviations: M, magnetic susceptibility; D, density; DC, density count; C, conductivity; R, resistivity; GC, gamma count; SG, spectral gamma-gamma; IP, induced polarization; SP, self potential; SPG, self potential gradient; T, temperature; TG, temperature gradient; V, velocity

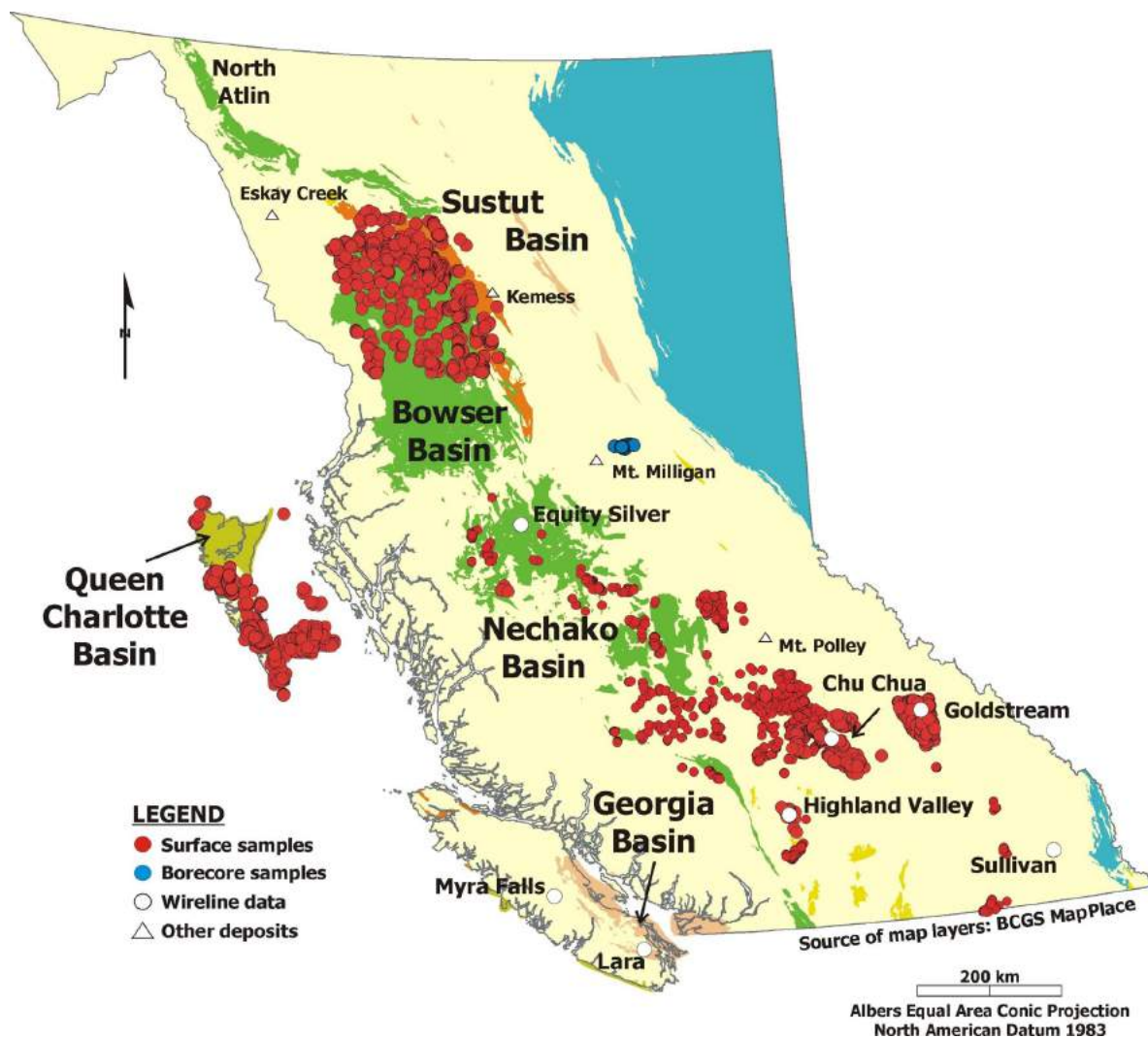


Figure 1. Spatial distribution of data from British Columbia entered in RPDS. The source of base layers is the BC Geological Survey MapPlace Web server. Map co-ordinates are in NAD83 Albers equal area conic projection. Surface samples are denoted by red circles, borehole drillcore samples by blue circles, and borehole wireline locations by white circles.

geological data to effectively query rock property statistics for specific rock types across geographic areas. This allows the user to answer such questions as “What is the average density of basalt in the Chilcotin Group?” or “What is the average resistivity of a rhyolite in a VMS-type deposit?” These types of questions are answered in RPDS by distillation of the large amount of data into manageable, interpretable, queryable data tables. Firstly, RPDS creates ‘geological intervals’ for common occurrences of geological information (a geological signature). This process is repeated at depth along the hole for each change in one of the geological variables. Then, for each interval, the physical property parameters are combined and population statistics calculated for that specific geological signature at that depth. The next phase of data distillation combines each common interval, further summarizing the data. Next, the area classification of each borehole is assessed and physical properties for all common geological intervals across all

holes within the same geographic area are combined. Finally, this information is combined with sample data having the same geological signature for the same area. Therefore, all occurrences in any borehole or sample within the Bowser Basin area in BC are combined, providing, for example, one mean density value for a *Sandstone with Argillic Alteration* from the *Brothers Peak Formation* in the *Bowser Basin* area.

Data Model

Various tables in RPDS store information pertaining to all borehole and sample data entered into the database. This information includes physical property data and metadata related to the entire logging/sampling process (location, equipment, personnel, project descriptions, laboratory methods and processing/calibration history), as well as information related to geological units and associated geochemical and geotechnical data.

The storage of borehole wireline physical property data in RPDS is based on the concept of logging runs. Logging run data are stored in the Process Log Table, which contains the calibrated and processed logging run data for each borehole. These data are considered the ‘live data’ in RPDS and are used for calculating the population statistics. Raw data are stored elsewhere in the database for archival purposes only. The Process Log Table stores the physical property values from various depths as measured along the borehole. Since the depth intervals for each measurement may vary per logging run, it is important to normalize these values to a constant depth interval in order to correlate each of the parameters for different logging runs. This is performed in the Forced Interval Table of RPDS.

The Forced Interval Table interpolates the Process Log data for each physical property to a common reference sampling interval of 10 cm. Physical properties from the Forced Interval Table may be correlated since, as they are interpolated to the same depth, they represent measurements of the same rock sample.

In parallel, a significant amount of available laboratory measurements are stored in the Sample Table. This table accommodates the physical property data and all associated metadata from laboratory measurements of both drillcore samples and surface samples of varying origin.

Geological information for wireline, drillcore and surface sample data is stored separately in the database, in the Geological Property Table. This table includes information on lithology, alteration, formation, geological age and assay analyses, and includes space for storing core photos that are rapidly visible on-the-fly. Lithology is stored as the specific lithological unit name, using the local nomenclature from the data source. However, in addition to this name, a geological ‘Master Lithology Classification’ scheme has been developed to provide a more general hierarchical description of the unit. This allows for consistent and more practical data querying within the RPDS environment. The geological data are combined with the borehole and sample data to produce the comprehensive Physical/Sample Properties Table.

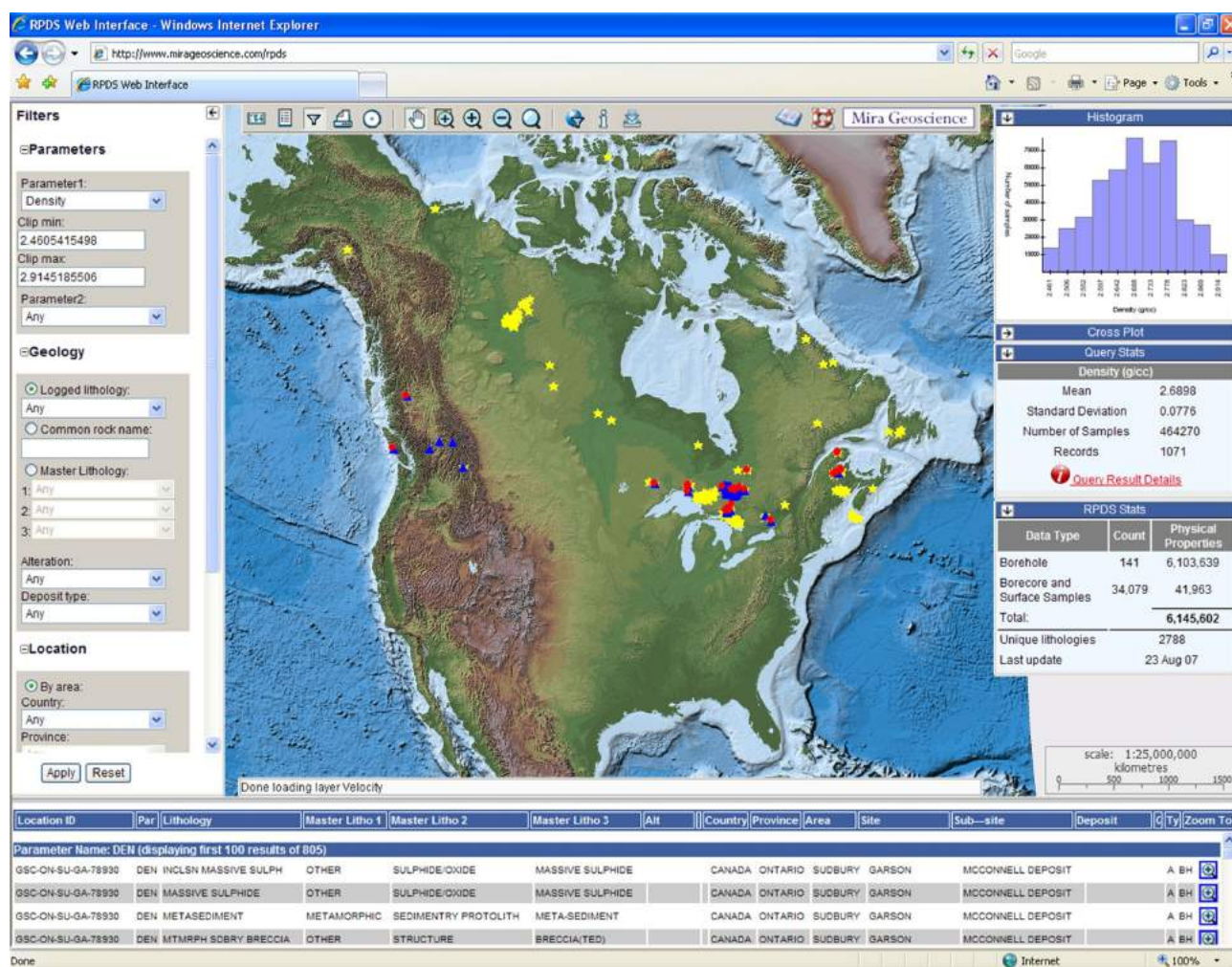


Figure 2. Rock Property Database System (RPDS) Web interface.

The Physical/Sample Properties Table is a composite table where logging-run data taken from the Forced Interval Table and sample data taken from the Sample Table are correlated with geological information. This is also where population statistics of physical properties as a function of geological classification are pre-stored for rapid query. This table lists, for each borehole, the mean values, standard deviations and sample counts for physical properties per unique lithological interval encountered in the borehole. At present, population statistics are calculated on the following 16 parameters, although others can be added to this list: gamma-ray, potassium, uranium, thorium, density, magnetic susceptibility, conductivity, temperature, temperature gradient, induced polarization (IP), resistivity, self potential (SP), SP gradient, velocity, neutron porosity and caliper. This table is further summarized in the Regional Properties Table.

The Regional Properties Table is the final step in the data distillation process, whereby physical property data are summarized and stored by combining mean physical property values from the same regional area that possess a common geological fingerprint (i.e., the same formation/lithology/alteration combination). Therefore, the physical properties of all occurrences of one geological unit in a borehole are averaged and combined with any other occurrences of that geological combination in the same area. As mentioned above, this provides one series of statistical summary values (mean, minimum, maximum, standard deviation, median, number of samples) for each physical property, for each unique geological combination in the same geographic area.

Web Interface

All data within RPDS are publicly accessible through a map-based Web query interface at <http://www.mirageosience.com/rpds>. The Web interface is designed to communicate with the RPDS Oracle database to provide rapid, up-to-date query results on population statistics, including histograms, multiparameter crossplots and metadata. Queries can be refined by physical property parameter, geological parameters, location information, location type (wireline vs. drillcore vs. surface sample measurements) and data quality. The map interface also includes a series of pre-rendered map layers for rapid visualization. These layers include base maps, geological maps and various symbolized layers showing the data distribution per physical property parameter. In addition, all data and selected metadata can be downloaded directly from the website using the data downloading tools, which provide pre-rendered Log View plots for borehole data visualization prior to download and various file-format export options. Finally, complete help documentation and a step-by-step tutorial on interface functionality are available through the interface.

Case Study of Mount Milligan Porphyry

Terrane Metals Corp. contributed 12 541 measurements of magnetic susceptibility from 180 boreholes, along with geological descriptions and corresponding 2-D and 3-D models. Samples were measured every 1–2 m down each borehole. From these data and local geophysical surveys, an analysis was done of the application of magnetic susceptibility. The recommended steps of analysis are summarized below. Illustrations of these steps are included in the final project report.

Step 1: Assemble local and regional magnetic surveys: High-resolution surveys (<200 m line spacing) are preferred.

Step 2: Gather the corresponding surface geology: Locally, intrusions such as the Mt Milligan monzonite can be correlated with magnetic anomalies.

Step 3: Assemble representative cross-section(s) of the deposit geology: Before modelling the geophysics, it is necessary to have a good integration of the geology and an understanding of the deposit model.

Step 4: Assemble corresponding cross-section(s) of mineralization and alteration: As best as possible, there is a need to define the geophysical attributes of the deposit halo. This understanding starts with a 2-D and 3-D characterization of the mineralization and associated alteration zonation.

Step 5: Assemble spreadsheets of magnetic susceptibility data with location and geology of each sample: Each property measurement requires an associated location and rock description, preferably with associated major and accessory minerals.

Step 6: Understand the behaviour of magnetic susceptibility:

- a) Define the ranges and distribution of the susceptibility for different rock types and alteration assemblages.
- b) Identify unique ranges that can be distinguished from a large dataset. Are there unique physical property ranges for mineralized rocks?
- c) Are there any relationships between susceptibility and mineralogy? Can susceptibility act as a proxy for mineral abundance?
- d) Findings: Rock types have bimodal distribution of magnetic susceptibility. There is an absence of systematic patterns.

Step 7: Examine the variation of magnetic susceptibility in borehole logs. They found that the highest magnetic susceptibilities are with magnetite associated with potassic-altered andesite adjacent to the monzonite intrusion. Unaltered andesite has low susceptibility. Potassic alteration in

the monzonite has moderate susceptibility related to biotite and minor magnetite.

Step 8: To examine the spatial relationships of magnetic susceptibility, the physical properties are incorporated into inversion models. Modelling is done in the following three stages:

- 1) Construction of a synthetic model: The exercises by Mitchinson and Phillips (2008) illustrated how synthetic models can be used to show expectations of detectability as target contrast, size and depth are changed. A series of synthetic models was constructed:
 - a) The mineralized stock has magnetic susceptibility of 32.3×10^{-3} SI, compared to a background of 0.68×10^{-3} SI.
 - b) Forward modelling of the distribution of magnetic susceptibility data results in an annular geometry. The model uses a mesh of 2525 m by 2325 m, with cell sizes of 25 m on each side.
 - c) An unconstrained synthetic model inversion generates a cone of anomalous magnetic susceptibility that approximates the location of the intrusive stock. Higher magnetic susceptibility values are at the top of the model and lower values at the bottom. Models indicate magnetic susceptibility values similar to what was measured in boreholes.
 - d) Experimentation with reduced contrast, smaller targets and burial at 150 m illustrate that detection would be more difficult. At depth, a similar target could be detected but the target would be smoother with less definition. Targets of small size could merge into the background. Deposits of similar size but lower contrast could be identified from surface surveys.
- 2) Construction of a constrained inversion: Constrained inversions require significant input by geologists and communication with the geophysicist. The Mount Milligan demonstration provided a model of the deposit geology and the spatial distribution of magnetic susceptibility in boreholes. A series of inversion models was constructed, with each case based on the following specific constraints:

- a) geological reference model for the monzonite stock
- b) geological reference model for the stock margin
- c) geometry of the magnetic body, assuming uniform magnetic susceptibility, that provides significant detail on the shape of the magnetic altered margin of the stock
- d) the geological contact (note that the shape of the magnetic anomaly changes considerably compared to the unconstrained model)
- e) drillhole-controlled boundaries of the magnetic susceptibility (the borehole data significantly change the configuration of magnetic bodies to steep planar zones)
- f) interpolated reference and bounds where values are kriged (this version also shows a steep geometry that corresponds to faults and dikes)

Conclusions from the Demonstration Study

The study has demonstrated that a limited amount of data can be informative. However, the data need to be well correlated and rock types identified. It is essential to examine and understand the relationship between rock physical properties and geology, alteration and mineralization. This demonstration shows that physical properties can be used to refine inversions in many different ways. As well, synthetic models can be used to test whether the geophysical method can be used to detect a deposit. The similarity of the different methods to constrain inversions implies that the data are good and the method robust. The constraint methodology depends on the inversion methodology, the amount and type of data and the exploration goal. The full project report and data are expected to be available on MapPlace by January 2009.

References

- Mitchinson, D. and Phillips, N. (2008): Improving exploration through physical property analysis and modelling: examples from Mount Milligan Cu-Au deposit; *in* Extracting Geology and Geophysics: The Application of Physical Rock Properties to Improve Exploration Targeting, T. Lane (comp.), Association for Mineral Exploration British Columbia, Mineral Exploration Roundup 2008, unpublished short course volume.

Vibroseis Survey Acquisition in the Central Nechako Basin, South-Central British Columbia (Parts of NTS 093B, C, F, G)

A.J. Calvert, Geoscience BC, Vancouver, BC and Department of Earth Sciences, Simon Fraser University, Burnaby, BC, acalvert@sfu.ca

N. Hayward, Department of Earth Sciences, Simon Fraser University, Burnaby, BC

B.R. Smithyman, Department of Earth and Ocean Sciences, University of British Columbia, Vancouver, BC

E.M. Takam Takougang, Department of Earth Sciences, Simon Fraser University, Burnaby, BC

Calvert, A.J., Hayward, N., Smithyman, B.R., and Takam Takougang, E.M. (2009): Vibroseis survey acquisition in the central Nechako Basin, south-central British Columbia (parts of 093B, C, F, G); *in* Geoscience BC Summary of Activities 2008, Geoscience BC, Report 2009-1, p. 145–150.

Introduction

The Nechako Basin, located in the interior plateau of British Columbia between the Coast Mountains and the Rocky Mountains, has seen very little exploration for hydrocarbons, in marked contrast to the Western Canadian Sedimentary Basin. Ferri and Riddell (2006) provided an overview of this exploration history, which is summarized here. Investigation of reports of surface oil and gas in the Kersley area, south of Quesnel, led to the drilling of the first well in 1931, with some further wells drilled in the same area in the 1950s, but no oil and gas shows were identified (Hayes, 2002). In 1960, Honolulu Oil Corp. acquired 44 line-kilometres of seismic data near Nazko, west of Quesnel, and drilled one well, a-4-L (Figure 1), which was dry with a few live oil shows (Ferri and Riddell, 2006). In an attempt to better define the basin stratigraphy, Hudson's Bay Oil and Gas Co. Ltd. drilled well c-75-A near Redstone in the southern part of the basin, also in 1960. In 1972, another well was drilled near Punchaw, southwest of Prince George; although some oil stains were noted at fault contacts, the well intersected 250 m of unconsolidated material above volcanic rocks identified as being from the Cache Creek Terrane (Ferri and Riddell, 2006). The only extensive exploration of the Nechako Basin was carried out by Canadian Hunter Exploration Ltd. between 1979 and 1986. The company acquired approximately 3000 line-kilometres of gravity data and 1300 line-kilometres of seismic data, and drilled two wells in 1980, another two in 1981 and a final well in 1985, before abandoning its exploration of the area. Ten gas shows were reported in three wells, and 26 live oil and 49 dead oil shows were detected during drilling (Hannigan et al., 1994).

The structure and hydrocarbon potential of the basin were most recently reviewed by Hannigan et al. (1994), but remain poorly understood. Some key results of their study are summarized below. Exploration wells have penetrated Early Eocene to Pliocene sedimentary rocks, but no hydrocarbon shows were detected in these rocks. These sedimentary rocks are typically interbedded with volcanic sequences, whose thicknesses can exceed 1000 m. Porosity in sand units averages approximately 8%. The Late Cretaceous oil and gas plays involve open and transitional marine to terrestrial sediments, which filled the Nechako Basin from the east. Structural traps would likely involve compressional folds and drag folds over thrust faults, together with normal fault blocks that formed in the Middle to Late Eocene. Primary porosity in these rocks appears to be very low, but secondary fracture porosity does exist. Carbonaceous and bituminous shale and sandstone, plus some coal, suggest a potential for the generation of gas. The most significant oil and gas plays in the Nechako Basin are in sedimentary rocks of the Taylor Creek (Riddell et al., 2007) and Skeena (Hannigan et al., 1994) groups, which can be as thick as 400–3000 m and were derived mostly from the east by uplift of the Omineca Belt in the Early Cretaceous. Potential reservoir sand units have been suggested within marine and nonmarine sandstone and shale sequences. Five wells have penetrated these Early Cretaceous strata, where all the oil and gas shows in the Canadian Hunter wells were identified. Jurassic rocks in the Nechako Basin are generally metamorphosed and likely to be overmature with regard to hydrocarbon preservation.

The evolution of the Nechako Basin is poorly known because much of the basin is covered by Tertiary and more recent volcanic rocks and glacial deposits. Jurassic–Cretaceous rocks found along the southern and northern margins of the basin probably continue beneath the volcanic/glacial cover, but their subsurface extent has not been defined. Early Cretaceous rocks are exposed along the Nazko River valley and define a north-northwesterly trend at the surface

Keywords: *Nechako Basin, seismic reflection*

This publication is also available, free of charge, as colour digital files in Adobe Acrobat® PDF format from the Geoscience BC website: <http://www.geosciencebc.com/s/DataReleases.asp>.

in the central part of the basin (Figure 1). Rocks of this age are also found farther south in a few limited surface outcrops and the three southern exploration wells. The gravity data recorded by Canadian Hunter exhibit a variation of 50 mGal across the basin (Ferri and Riddell, 2006), and one

interpretation of the distribution of gravity anomalies is that a number of sub-basins are present. However, with the extensive volcanic cover and limited geophysical data, it is not clear whether the Early Cretaceous sedimentary rocks were deposited within separate sub-basins or are the rem-

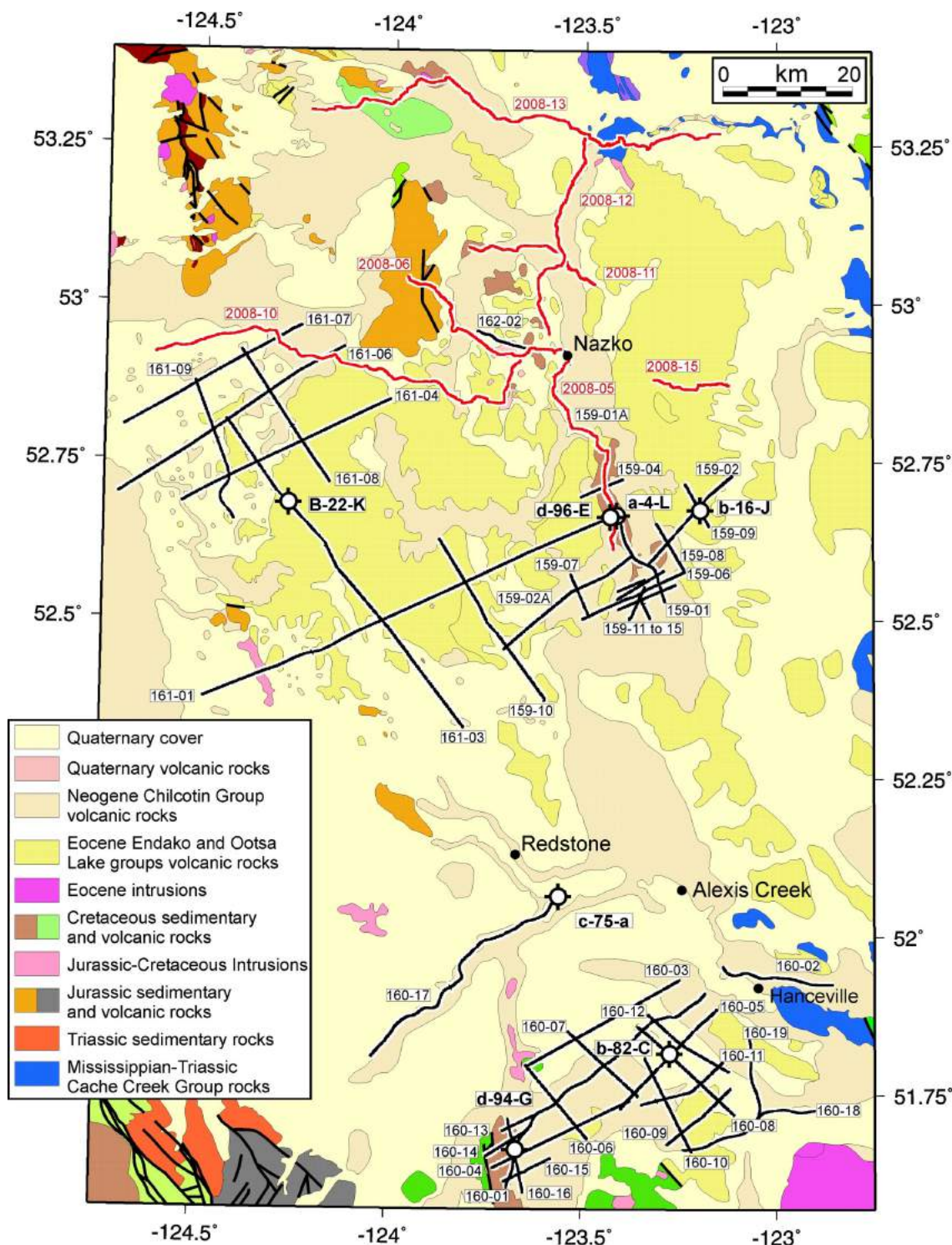


Figure 1. Geology of the Nechako Basin, showing the 1020 line-kilometres of the Canadian Hunter Ltd. seismic lines (black) that were reprocessed by Geoscience BC, and the seismic lines acquired by Geoscience BC in the summer of 2008 (red).

nants of a much larger basin. This fundamental question on the nature of the Nechako Basin was not resolved by the seismic data acquired by Canadian Hunter because the quality of the images was often poor, likely due to the combined effects of the volcanic cover and the seismic acquisition technology available at the time (Hayward and Calvert, 2008). There is therefore a strong argument for acquiring extensive regional geophysical data across the basin. Seismic data are key, due to their greater resolution in depth and their ability to define subsurface structural boundaries that are required for the interpretation of data from other geophysical surveys (e.g., gravity or magnetotelluric). In the summer of 2008, Geoscience BC therefore acquired 330 line-kilometres of seismic data near Nazko along and across the north-northwesterly surface trend of Early Cretaceous rocks in the central Nechako Basin (Figure 1). The primary objectives of the survey were to

evaluate the effectiveness of modern seismic acquisition technology in this volcanic-covered area and optimize ties of the surface seismic to well-log data; and map the extension into the subsurface of the outcropping Early Cretaceous rocks and identify the primary structural controls on their distribution in the central part of the basin.

Survey Planning

An initial program for a vibroseis survey along existing roads was defined with input from the Geoscience BC Oil and Gas Technical Advisory Committee, and a Request for Proposals was issued by Geoscience BC on April 6, 2007, with submissions due on May 18. Four formal bids for the acquisition of the seismic survey were received, and the competitive nature of this process played an important role in maximizing the number of line-kilometres acquired within the fixed budget. The contract was awarded to CCGVeritas of Calgary, who undertook the preparatory work for permitting during the summer of 2007 through a subcontractor, Bighorn Land and Field Service. Information meetings with First Nations in the area began in late 2006. A formal application for a permit to conduct the survey was submitted to the BC Oil and Gas Commission (OGC) on September 17, 2007. A second permit application was submitted in November 2007 to add further seismic lines in the central part of the basin, which would also be coincident with a number of magnetotelluric survey lines acquired in the fall 2007 by the Geological Survey of Canada. This second permit was issued by the OGC on May 7, 2008, and the original permit was issued on June 17, 2008, after it was revised by the removal of several lines located in the southern part of the basin. Thus, the seismic survey, which had originally been conceived as a more regional study to investigate structures and well ties in the southern Nechako Basin and Nazko area, evolved into a study focused primarily on the north-northwesterly trend of

the Early Cretaceous rocks that are partly exposed in the central part of the basin and were the focus of Canadian Hunter's extensive exploration effort near Nazko.

Seismic Acquisition Parameters

The quality of the Canadian Hunter seismic data, which was shot in the early 1980s, is generally poor, likely due to the effects of the near-surface volcanic rocks, which can reach a thickness of 600 m (Hayward and Calvert, work in progress, 2008). In one or two areas, very few first arrivals can be observed in these data, suggesting that it may be difficult to generate a sufficiently strong source waveform. In areas with no surface volcanic rocks, the data quality is usually reasonable given the technology of the time. Therefore, much of the new survey design was directed towards maximizing the signal-to-noise ratio, and the main characteristics of the survey were

a large array of vibrators and long sweeps to maximize source effort;

a high stack fold through the use of a short source interval and large number of recording channels;

restriction of the sweep to lower frequencies to improve transmission through near-surface volcanic rocks;

long offsets to record deeper, subvolcanic reflections and first arrivals that can constrain the thickness of the volcanic layer, and perhaps the depth to the igneous basement; and

extended correlation of long sweeps to record mid-lower crustal reflections that will constrain the evolution of any sub-basins and provide data quality control in areas where shallower reflections may not be present.

Table 1 shows that the Geoscience BC survey employed approximately 3.5 times the source effort of one of the Canadian Hunter surveys, and that the stack fold is 10 times greater. Modern vibrator-drive control systems will also produce more accurate transmission of the sweep signal from the base plate into the ground.

Following further input from industry (C. Szelewski and B. Goodway of EnCana Corporation), source positions were also located on the half station between receivers to provide a more even offset distribution within CDP gathers, approximating the stack array response (Anstey, 1986) and resulting in less coherent noise (e.g., from the vibrator trucks or ground roll) leaking through into the stack section (Table 2).

Although the source interval was 40 m on all lines, a 22 m section of line 6 was acquired with a 20 m source interval to evaluate the effect of the closer shot spacing and increased source effort.

Table 1. Comparison of key parameters between the Canadian Hunter Ltd. seismic survey and the 2008 Geoscience BC survey.

Parameter	Geoscience BC (2008)	Canadian Hunter (1981)
Source interval (m)	40	100
Receiver interval (m)	20	50
No. of channels	960	96
Maximum offset (m)	14 390	2 550
Nominal fold	240	24
Fold at 0.5 s (estimated)	50	20
No. of vibrators x weight (kg)	4 x 24 000	5 x 7467
No. of sweeps per VP	4	16
Peak force (%)	80	60-75
Sweep duration (s)	28	15
Sweep bandwidth (Hz)	8–64	10–70
Source effort (kg-s/km)	215 x 10 ⁶	61 x 10 ⁶

Field Survey

The CGGVeritas crew began laying the recording spread on June 22, 2008 (Figure 2) and, after four hours of initial parameter testing, production recording began in the early morning of June 23 (Figure 3).

Initially, the daily production rate varied between 5 and 9 km, but this rate increased to 10–14 km per day when the crew began to operate three 12-hour shifts instead of two; individual shifts were spending up to four hours per day in transit from the crew base in Quesnel. Heavy logging traffic represented a significant source of noise, and was particularly heavy on parts of lines 6, 12 and 15. The recording crew shut down when large convoys of logging trucks travelled over the recording spread, and also when rain, strong winds and thunderstorms were present in the survey area. The survey was completed on August 4.



Figure 2. CGGVeritas equipment laid out in the initial staging area on June 22, 2008, prior to deployment on line 15.

Table 2. Acquisition parameters used in the 2008 Geoscience BC Nechako Basin seismic survey.

Source:	Vibroseis
Vibrator model	Mertz HD 18 Buggy 52,800 lbs
Source point interval	40 m on half station
No. of sweeps per source point	4
Static array	4 vibrators inline over 45 m
Total drag length	60 m with 5 m moveup after listen time
Drive level:	80%
Sweep length	28 s including 0.9 s tapers
Listen time	6 s
Sweep type	8 64 Hz linear upsweep
Receivers:	
Geophone model	Oyo GS32CT vertical
Receiver group interval	20 m
Receiver array	6 geophones over 16.7 m
Recording Spread	Asymmetric 240 720 split
Recording system:	
Instrument type	Sercel 428
No. of channels	960
Uncorrelated record length	34 s
Correlated record length	6 s
Sample interval	2 ms
Anti-aliasing filter	0.8 Nyquist linear phase
Recorded to tape	4 x 34 s sweeps, 1 x 6 s correlated diversity sum

Acknowledgments

The seismic project has been funded by Geoscience BC and through a \$500 000 grant from the Northern Development Initiative Trust. F. Ferri and J. Riddell of the Ministry of Mines, Energy and Petroleum Resources (MEMPR) helped to define the geological objectives. J. Harris, also of MEMPR, worked tirelessly to facilitate meetings with First Nations in the Nechako Basin area. T. Kunkel of the Nazko First Nation provide important guidance, and S. Alec was the representative from Nazko First Nation with the seismic crew. D. McIntosh co-ordinated the permitting for the sur-



Figure 3. CGGVeritas vibrators shaking on July 2, 2008 on line 5, with dust rising from the base plates.

vey and supported the pre-survey community workshops. M. Broughton of CGGVeritas cheerfully arranged the employment on the seismic crew of several members of Nazko First Nation. The successful completion of the survey would not have been possible without the efforts of CGGVeritas crew number 5.

References

- Anstey, N. (1986): Whatever happened to ground roll; *The Leading Edge*, p. 40–45.
- Ferri, F. and Riddell, J. (2006): The Nechako Basin project: new insights from the southern Nechako Basin; *in* Summary of Activities 2006, BC Ministry of Energy, Mines and Petroleum Resources, p. 89–124, URL <<http://www.empr.gov.bc.ca/OG/oilandgas/publications/TechnicalDataandReports/Pages/default.aspx>> [November 6, 2008].
- Hannigan, P., Lee, P.J., Osadetz, K.G., Dietrich, J.R. and Olsen-Heise, K. (1994): Oil and gas resource potential of the Nechako-Chilcotin area of British Columbia; BC Ministry of Energy, Mines and Petroleum Resources, GeoFile 2001-6, 37 p.
- Hayes, B. (2002): Petroleum exploration potential of the Nechako Basin, British Columbia; BC Ministry of Energy, Mines and Petroleum Resources, Petroleum Geology Special Paper 2002-3.
- Hayward, N. and Calvert, A.J. (2008): Structure of the south-eastern Nechako Basin, British Columbia: interpretation of the Canadian Hunter seismic reflection surveys and preliminary first-arrival tomographic inversion; Geoscience BC, unpublished report.
- Riddell, J., Ferri, F., Sweet, A. and O’Sullivan, P. (2007): New geoscience data from the Nechako Basin project; BC Ministry of Energy, Mines and Petroleum Resources, Petroleum Geology Open File 2007-1, URL <<http://www.empr.gov.bc.ca/OG/oilandgas/petroleumgeology/ConventionalOilAndGas/InteriorBasins/Pages/default.aspx>> [November 6, 2008].

Preliminary First-Arrival Modelling Constraints on the Character, Thickness and Distribution of Neogene and Eocene Volcanic Rocks in the Southeastern Nechako Basin, South-Central British Columbia (NTS 092N, O, 093B, C)

N. Hayward, Department of Earth Sciences, Simon Fraser University, Burnaby, BC, nhayward@sfu.ca

A.J. Calvert, Department of Earth Sciences, Simon Fraser University, Burnaby, BC

Hayward, N. and Calvert, A.J. (2009): Preliminary first-arrival modelling constraints on the character, thickness and distribution of Neogene and Eocene volcanic rocks in the southeastern Nechako Basin, south-central British Columbia (NTS 092N, O, 093B, C); in Geoscience BC Summary of Activities 2008, Geoscience BC, Report 2009-1, p. 151–156.

Introduction

The Nechako Basin is a primarily Mesozoic sedimentary basin located between the Rocky and Coast mountains of southern British Columbia (Figure 1). The basin formed over, and in part from, the accreted terranes of the western Canadian Cordillera. Transpressional tectonic processes were dominant until the Eocene (Best, 2004), when there was a shift to a dextral transtensional regime (Price, 1994). This episode of transtension was responsible for the formation of the Yalakom and Fraser faults, and was associated with widespread volcanism.

This volcanism resulted in a regionally extensive blanket of rocks of the Eocene Endako and Ootsa Lake groups. These rocks were later overlain by volcanic rocks of the Neogene Chilcotin Group and Quaternary drift and glacial deposits (e.g., Riddell, 2006). The Endako and Ootsa Lake groups consist, respectively, of basaltic to andesitic and intermediate to felsic flows, with tuff, breccia and sedimentary rocks (e.g., Riddell, 2006). The Chilcotin Group consists of a number of facies (Mathews, 1989; Farrell et al., 2007; Gordee et al., 2007), which are primarily dominated by basaltic lavas or tuffs.

Interpretation of the basin's near-surface stratigraphy and structure are precluded by Quaternary deposits, vegetation and the negative impact of the near-surface volcanic rocks on seismic reflection imaging. Seismic reflection data ac-

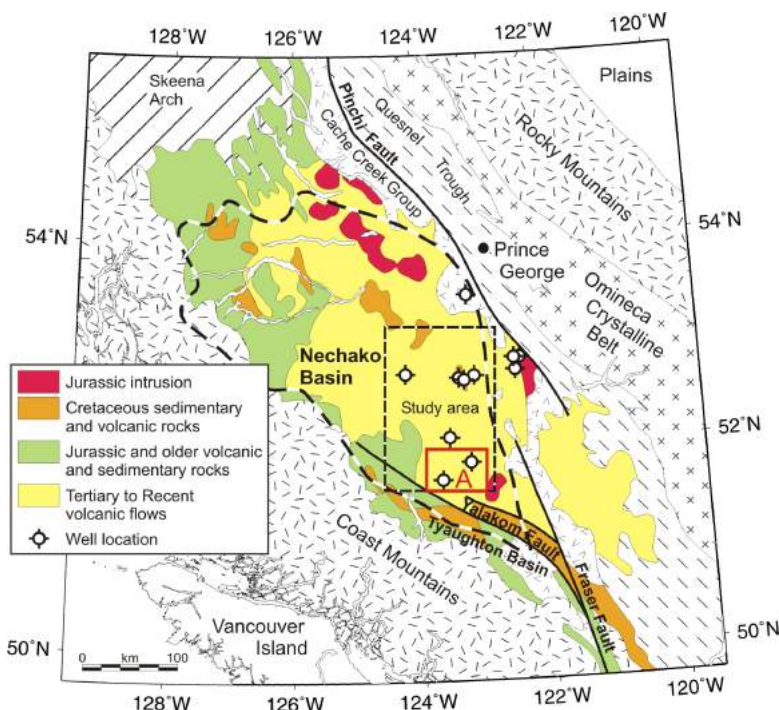


Figure 1. Location of the Nechako Basin and simplified geology of its western Canadian Cordillera setting. Black dashed box shows the broad study area. Red dashed box shows the focus region (block A) of this report.

quired by Canadian Hunter in the 1980s were reprocessed in 2006 by Arcis Corporation. Although seismic imaging is generally improved, near-surface resolution, especially in association with volcanic rocks, remains poor.

A component of this study investigates the velocity, thickness and distribution of the near-surface rocks in the southeastern Nechako Basin using tomographic models derived from first arrivals from the seismic reflection data. Interpretation of these models is aided by surface geological maps (e.g., Riddell, 2006) and seven wells (drilled by Canadian Hunter Exploration Limited, Esso, Honolulu Oil Corporation Limited and Hudson's Bay Oil and Gas Company Limited). Preliminary results from the block A area (Figure 1) are presented here.

Keywords: seismic reflection, structural geology, seismic stratigraphy, first-arrival tomography, velocity models

This publication is also available, free of charge, as colour digital files in Adobe Acrobat® PDF format from the Geoscience BC website: <http://www.geosciencebc.com/s/DataReleases.asp>.

First-Arrival Tomographic Velocity Modelling

An estimate of the seismic P-wave velocity was derived from the traveltimes of the first arrivals from the source to each receiver of a seismic reflection profile (Figure 2). Velocity variations can provide details of the character and structure of near-surface rocks, poorly imaged by seismic reflection profiles. The focusing of rays (ray density) in the model may reveal the thickness of the near-surface volcanic rocks or layers within them. First-arrival tomographic velocity models have been used effectively in a range of geological environments, including the Tofino Basin (Hayward and Calvert, 2007) and the Devil's Mountain fault (Hayward et al., 2006).

Method

First-arrival (the direct wave and subsurface refractions) tomographic-inversion velocity models were calculated (e.g., Calvert et al., 2003) for all straight seismic profiles. First arrivals picked during seismic reflection processing by Arcis were manually edited in the ProMAX™ software package (Landmark Graphics Corporation) in order to correct picking errors.

The Pronto software package (Aldridge and Oldenburg, 1993) was used to model the seismic velocity. First-arrival times to all locations in a subsurface velocity grid (25 m grid spacing) were derived from a finite-difference solution to the eikonal equation. Source-to-receiver ray paths along the steepest direction of descent were created through the traveltimes grid. A one-dimensional (1-D) starting model

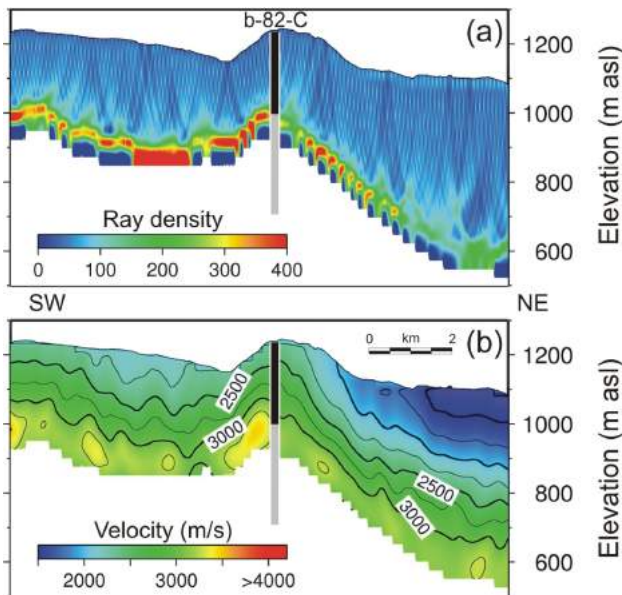


Figure 2. First-arrival tomographic ray density (a) and velocity model (b) derived from seismic reflection data in the vicinity of well b-82-C.

was estimated from the results of a few trial inversions. In order to obtain a realistic final model, the starting model was constrained by the sonic velocity logs (Figure 3). Setting the top of the starting model to 2000 m/s with a gradient of 1.25 (m/s)/m most effectively mimics the regionally variable well sonic velocities. A perturbation in the velocity model was calculated from the difference between the calculated and observed first-arrival traveltimes, for each of 15 iterations, to give a final velocity model.

Maximum ray penetration is controlled by the subsurface geology and maximum source-receiver offset (2550 m except for CH-159-02 and -02A at 1350 m). An estimate of P-wave velocity is well constrained for depths of up to ~400–500 m.

Thickness Constraint of the Near-Surface Volcanic Rocks in Block A

Volcanic rocks were intersected by four wells in the south-eastern Nechako Basin. In block A, well b-82-C sampled ~221 m (Ferri and Riddell, 2006) of Eocene Endako Group volcanic rocks (Figure 3). Rays in the models of two seismic lines, which tie with the well, converge at depths of ~255 m (Figure 2a) and ~288 m. These ray-density maxima are located immediately below the base of the Eocene volcanic rocks (~2400–3400 m/s) in higher velocity (~3900 m/s) Cretaceous sandstone of the Taylor Creek Group (Figure 3). Therefore, at well b-82-C, maximum ray density is an analogue for volcanic rock thickness. Else-

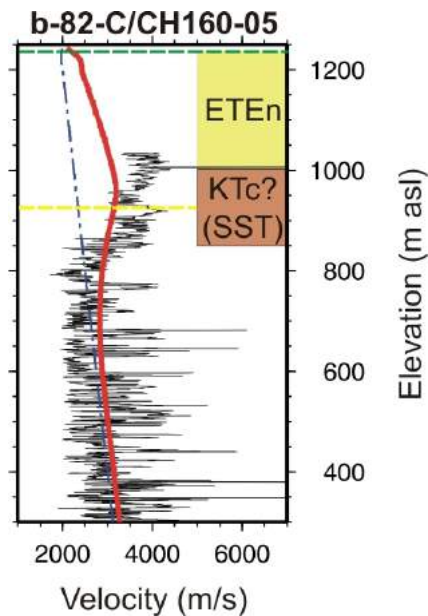


Figure 3. Comparison of tomographic velocity model (red line) with well sonic logs (black line) and stratigraphy (Ferri and Riddell, 2006). Blue dot-dashed line shows the starting velocity model. Yellow dashed line shows the base of the velocity model at well b-82-C. Green dashed line shows the ground surface at the well. Abbreviations: ETEen, Eocene Endako Group; KTc, Cretaceous Taylor Creek Group; SST, sandstone.

where, maximum ray density, primarily controlled by high-velocity layers, provides thickness constraint and information on the internal layering of near-surface volcanic and sedimentary rocks.

Points of maximum ray density (>100 ray paths), automatically picked every 5 m along each model profile, were manually edited to remove artifacts. The depth of the layer of maximum ray density (LMRD) in block A responds to changes in the local geology. The LMRD in the vicinity of well b-82-C (~270 m) can be traced over most of central block A (Figure 4). This interpretation suggests that rocks of the Endako Group cover this region below a thin veneer of outcropping younger volcanic rocks and/or drift deposits (Figure 5). The northwesterly continuation of the Eocene rocks is terminated by the outcrop of Cretaceous Spences Bridge Group volcanic rocks (Figure 5).

A striking feature of the LMRD in block A is the greatly increased depths of >500 m to the northeast (Figure 4). These anomalous depths may be the result of thicker Eocene Endako Group or Neogene Chilcotin Group rocks, which outcrop at this location (e.g., Riddell, 2006).

Seismic Interval Velocity of the Near-Surface Volcanic Rocks in Block A

The near-surface (0–175 m) interval velocity was extracted from each velocity model to investigate local and regional velocity variation. Comparison of the interval velocity with surface geology (e.g., Riddell, 2006) shows typical values of ~2500 m/s, with slightly lower velocities commonly in association with the outcrop of Chilcotin Group rocks and Quaternary deposits (Figure 5). High interval velocities (~3000 m/s) are coincident with the outcrop of Spences Bridge Group volcanic rocks towards the northwestern corner of block A. Rocks of the Eocene Endako and Ootsa Lake groups and Cretaceous Taylor Creek Group are shown to have typically higher interval velocities than the Neogene Chilcotin Group volcanic rocks and Quaternary drift deposits.

Interval velocities are anomalously low (down to ~1500 m/s) in northeastern block A (Figure 5). These velocity lows correspond to the deeper LMRD (Figure 4) and to the outcrop of Chilcotin Group volcanic rocks and Quaternary deposits (Figure 5).

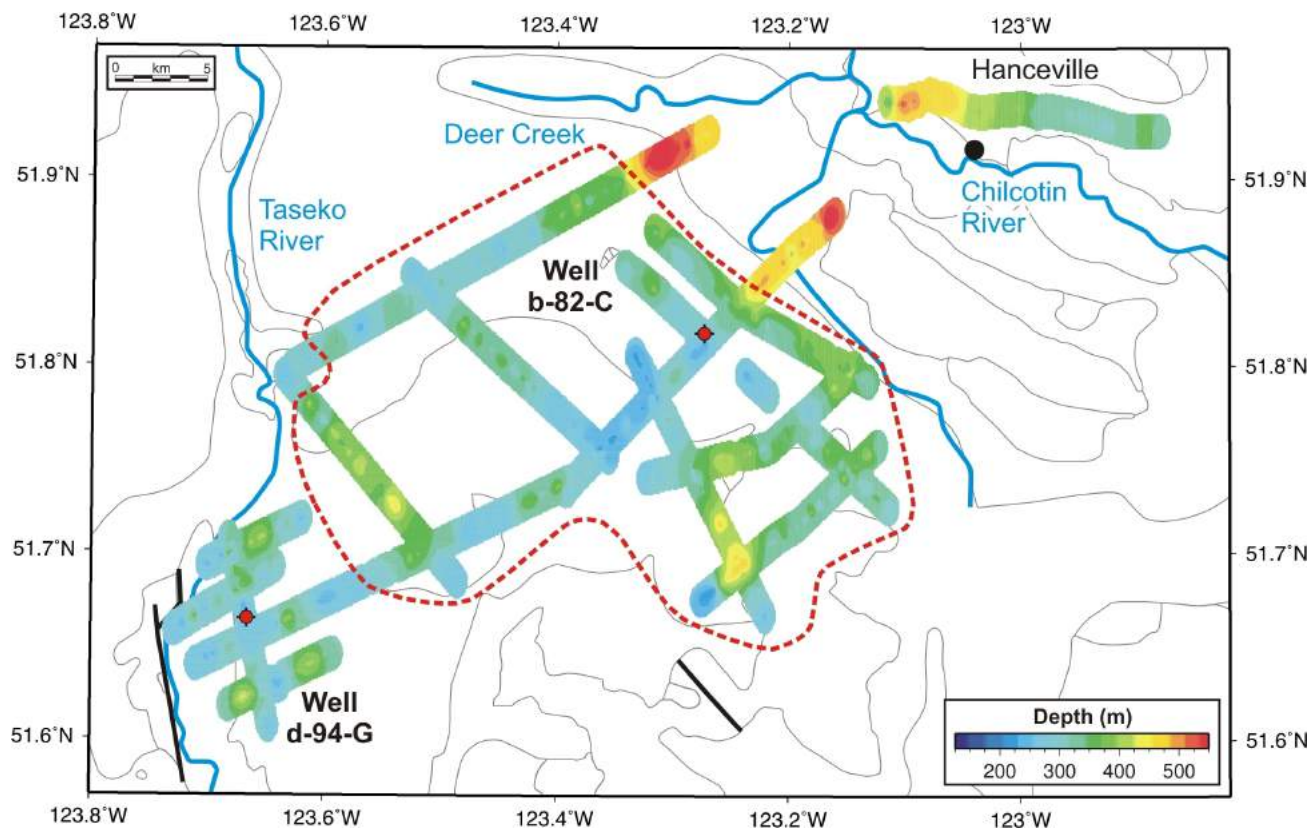


Figure 4. Depth (below ground) to the layer of maximum ray density (LMRD; density >100 ray paths) from first-arrival tomographic inversion. Thin grey lines show the surface geology (modified from Riddell, 2006). See Figure 5 for unit identification. Heavy red dashed line shows the probable presence of Eocene volcanic rocks. Blue lines are rivers.

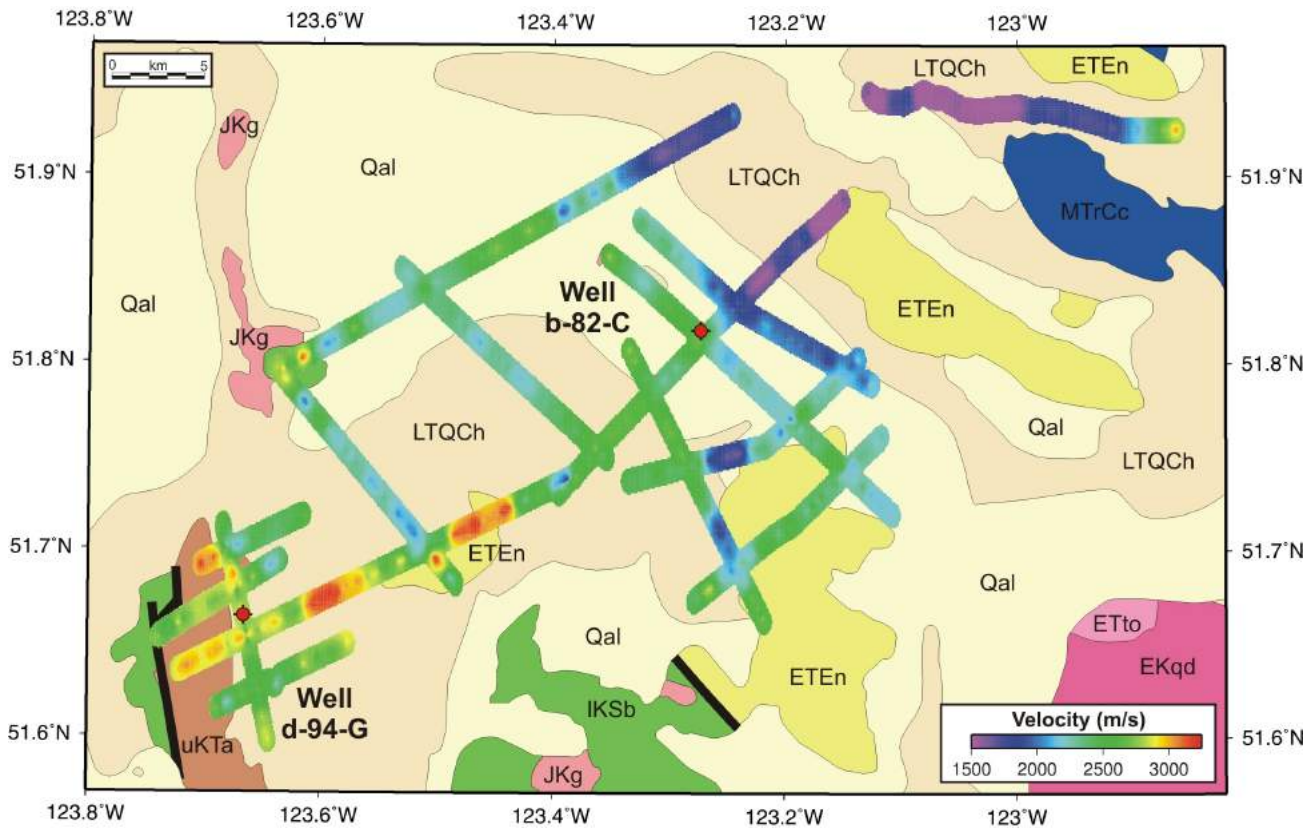


Figure 5. Interval velocity from the ground surface to a depth of 175 m, extracted from first-arrival tomographic models (underlying geology simplified from Riddell, 2006). Abbreviations: ETEn, Endako Group; IKSb, Spences Bridge Group; JKg, ETto, EKqd, various intrusive granitic rocks; LTQCh, Chilcotin Group; MTrCc, Cache Creek Group; Qal, drift.

Discussion

Geological mapping in the Chilcotin River area (Figure 4) has shown that, locally, the Chilcotin Group is of the Bull Canyon facies (Andrews and Russell, 2007). The Chilcotin Group is commonly lava rich, but the Bull Canyon facies is dominated by hyaloclastite, breccia and pillow lava.

Analysis of water well data and geological mapping (Andrews and Russell, 2008) have revealed that the Chilcotin Group is regionally thin (<50 m, probably <25 m). However, thicker accumulations have been attributed to local accumulation in paleo-drainage channels. The Chilcotin Group is interpreted to be ~100 m thick (Gordee et al., 2007) at Bull Canyon Provincial Park. Near Hanceville, along the Chilcotin River (Figure 4), the Chilcotin Group has a thickness of up to ~80 m (Andrews and Russell, 2007). Models of this region (Mihalynuk, 2007), based on mapped basal contacts of the Chilcotin Group and a digital elevation model, predict thicknesses of ~100–150 m on the Chilcotin River and to the south of Deer Creek (Figure 4).

Thicker accumulations of the Chilcotin Group in the Chilcotin River area (Figure 4) correspond to the regions of increased depth of the LMRD and a lower velocity. The breccia-dominated Bull Canyon facies rocks would likely have

a lower seismic velocity in comparison to the lava-rich facies of the Chilcotin and Endako groups observed elsewhere. A local increase in thickness of these rocks would account for the observed lows in interval velocity and supports the interpretation (Andrews and Russell, 2008) of an increased thickness of the Chilcotin Group in paleo-river valleys.

Conclusions

The layer of maximum ray density derived from first-arrival tomographic inversion models predicts that the Eocene Endako Group overlies most of the central area of block A. In this area, the models estimate the thickness of these rocks to be fairly uniform (~221 m at well b-82-C). In northeastern block A, low interval velocities are interpreted to be related to anomalously thicker deposits of Neogene Chilcotin Group rocks of the breccia-rich Bull Creek facies. The distribution of these lows in interval velocity supports the interpretation that the Chilcotin Group is thicker in paleo-river valleys.

Acknowledgments

The authors wish to thank Geoscience BC for funding this research.

References

- Aldridge, D.F. and Oldenburg, D.W. (1993): Two dimensional tomographic inversion with finite difference traveltimes; *Journal of Seismic Exploration*, v. 2, p. 257–274.
- Andrews, G.D.M. and Russell, J.K. (2007): Mineral exploration potential beneath the Chilcotin Group (NTS 092O, P; 093A, B, C, F, G, J, K), south-central British Columbia: preliminary insights from volcanic facies analysis; *in Geological Fieldwork 2006*, BC Ministry of Energy, Mines and Petroleum Resources, Paper 2007-1 and Geoscience BC, Report 2007-1, p. 229–238.
- Andrews, G.D.M. and Russell, J.K. (2008): Cover thickness across the southern Interior Plateau, British Columbia (NTS 092O, P; 093A, B, C, F): constraints from water-well records; *in Geoscience BC Summary of Activities 2007*, Geoscience BC, Report 2008-1, p. 11–20.
- Best, M.E. (2004): Qualitative interpretation of potential field profiles, southern Nechako Basin; *in Summary of Activities 2004*, BC Ministry of Energy, Mines and Petroleum Resources, p. 73–78.
- Calvert, A.J., Fisher, M.A., Johnson, S.Y. and SHIPS Working Group (2003): Along-strike variations in the shallow seismic velocity structure of the Seattle fault zone: evidence for fault segmentation beneath Puget Sound; *Journal of Geophysical Research*, v. 108, doi:10.1029/2001JB001703.
- Farrell, R.E., Andrews, G.D.M., Russell, J.K. and Anderson, R.G. (2007): Chasm and Dog Creek lithofacies, Chilcotin Group basalt, Bonaparte Lake map area, British Columbia; *Geological Survey of Canada, Current Research 2007-A5*, 11 p.
- Ferri, F. and Riddell, J. (2006): The Nechako Basin project: new insights from the southern Nechako Basin; *in Summary of Activities 2006*, BC Ministry of Energy and Mines and Petroleum Resources, p. 89–124.
- Gordee, S.M., Andrews, G.D.M., Simpson, K. and Russell, J.K. (2007): Subaqueous channel-confined volcanism within the Chilcotin Group, Bull Canyon Provincial Park (NTS 093B/03), south-central British Columbia; *in Geological Fieldwork 2006*, BC Ministry of Energy, Mines and Petroleum Resources, Paper 2007-1 and Geoscience BC, Report 2007-1, p. 285–290.
- Hayward, N. and Calvert, A.J. (2007): Seismic reflection and tomographic velocity model constraints on the evolution of the Tofino forearc basin, British Columbia; *Geophysical Journal International*, v. 168, p. 634–646.
- Hayward, N., Nedimoviæ, M.R., Cleary, M. and Calvert, A.J. (2006): Structural variation along the Devil’s Mountain fault zone, northwestern Washington; *Canadian Journal of Earth Sciences*, v. 43, p. 433–446.
- Mathews, W.H. (1989). Neogene Chilcotin basalts in south-central British Columbia: geology, ages, and geomorphic history; *Canadian Journal of Earth Sciences*, v. 26, p. 969–982.
- Mihalynuk, M.G. (2007): Neogene and Quaternary Chilcotin Group cover rocks in the Interior Plateau, south-central British Columbia: a preliminary 3-D thickness model; *in Geological Fieldwork*, BC Ministry of Energy, Mines and Petroleum Resources, Paper 2007-1, p. 143–147.
- Price, R.A. (1994): Cordilleran tectonics in the evolution of the Western Canada Sedimentary Basin; Chapter 2 *in Geological Atlas of the Western Canada Sedimentary Basin*, G. Mossop and I. Shetsin, (comp.), Canadian Society of Petroleum Geologists, Calgary, Alberta and Alberta Research Council, Edmonton, Alberta.
- Riddell, J.M., compiler (2006): Geology of the southern Nechako Basin, NTS 92N, 92O, 93B, 93C, 93F, 93G; BC Ministry of Energy and Mines and Petroleum Resources, Petroleum Geology Map 2006-1, 3 sheets at 1:400 000 scale.

Enhanced Velocity Structure from Waveform Tomography of Seismic First-Arrival Data: Application to the Nechako Basin, South-Central British Columbia (Parts of NTS 093B, C, F, G)

R.M. Clowes, Department of Earth and Ocean Sciences, University of British Columbia, Vancouver, BC, rclowes@eos.ubc.ca

B.R. Smithyman, Department of Earth and Ocean Sciences, University of British Columbia, Vancouver, BC

Clowes, R.M. and Smithyman, B.R. (2009): Enhanced velocity structure from waveform tomography of seismic first-arrival data: application to the Nechako Basin, south-central British Columbia (parts of NTS 093B, C, F, G); *in* Geoscience BC Summary of Activities 2008, Geoscience BC, Report 2009-1, p. 157–162.

Introduction

During the summer of 2008, Geoscience BC acquired approximately 330 km of vibroseis seismic reflection data in the Nechako Basin of interior British Columbia as part of an oil and gas exploration initiative in the region. The purpose of the survey was to 1) test the efficacy of modern seismic reflection methods in a region where near-surface volcanic rocks and related geological variations have made acquisition of quality data very difficult in the past; and 2) provide information about the sedimentary section and underlying basement of crystalline rocks to assist exploration efforts in the region through further seismic surveys and other geoscience studies. CGGVeritas acquired the data under contract to Geoscience BC and is currently processing the data to provide the subsurface images.

Since maximum offsets (source-to-receiver distances) for these data extend to 15 km, the first-arrival data, which are seismic refraction waves that travel subhorizontally, can be used to determine velocity-versus-depth information below the seismic line to depths of 2000–3000 m. Indeed, first-arrival traveltimes provide such velocity information to make near-surface corrections for the deeper reflection data in the standard processing procedures being applied by CGGVeritas of Calgary. However, the first-arrival data in the form of waveforms (i.e., traveltime, amplitude and frequency information) may be used to derive a much more highly resolved velocity structure than traveltimes alone through application of waveform tomography, a newly developed procedure. This velocity structure may be used to distinguish glacial deposits, sedimentary rocks and volcanic rocks, perhaps identifying shallow sub-basins within the Nechako Basin. As well, the enhanced velocity struc-

ture can also be used in a second stage of computer processing of the main reflection data to provide improved images where warranted.

This project first addresses the feasibility of the application of waveform tomography to vibroseis first-arrival data because no such study has yet been published. The technique will then be applied to some of the seismic lines recorded in 2008, to generate the enhanced velocity structure and its subsequent interpretation in terms of geological features.

Geological Background

The Nechako Basin in central BC is considered an area prospective for oil and gas resources. In the late 1970s and early 1980s, Canadian Hunter Exploration Ltd. carried out an exploration program that included a series of seismic reflection lines and a number of exploration wells (Figure 1). A general geological section for the basin was developed from these and surface geological studies. A summary is provided below.

The basal sedimentary unit, >1000 m of generally metamorphosed Jurassic rocks, is considered to have little or no hydrocarbon potential. Overlying it is several thousand metres of Early to mid-Cretaceous nonmarine sandstone and conglomerate, with lesser dark shale and siltstone, referred to as the Skeena Group by Hannigan et al. (1994). This sequence is considered to be the most prospective of the sedimentary units. Hannigan et al. (1994) estimated potential reserves of 8.7 trillion cubic feet of gas and 4.9 billion barrels of oil. The Skeena Group is overlain by up to 2500 m of mid- to Late Cretaceous, open and transitional marine to terrestrial sedimentary rocks. Their prospectivity is less than 1% of that of the underlying sedimentary rocks. In some parts of the basin, the upper part of this sequence includes sections of volcanic rocks. Overlying Tertiary rocks include some nonmarine sedimentary sequences but consist primarily of volcanic rocks that are interbedded with the sedimentary rocks. Estimated resource potential is

Keywords: *Nechako Basin, seismic reflection, waveform tomography, velocity structure, attenuation models, seismic processing, rock velocities*

This publication is also available, free of charge, as colour digital files in Adobe Acrobat® PDF format from the Geoscience BC website: <http://www.geosciencebc.com/s/DataReleases.asp>.

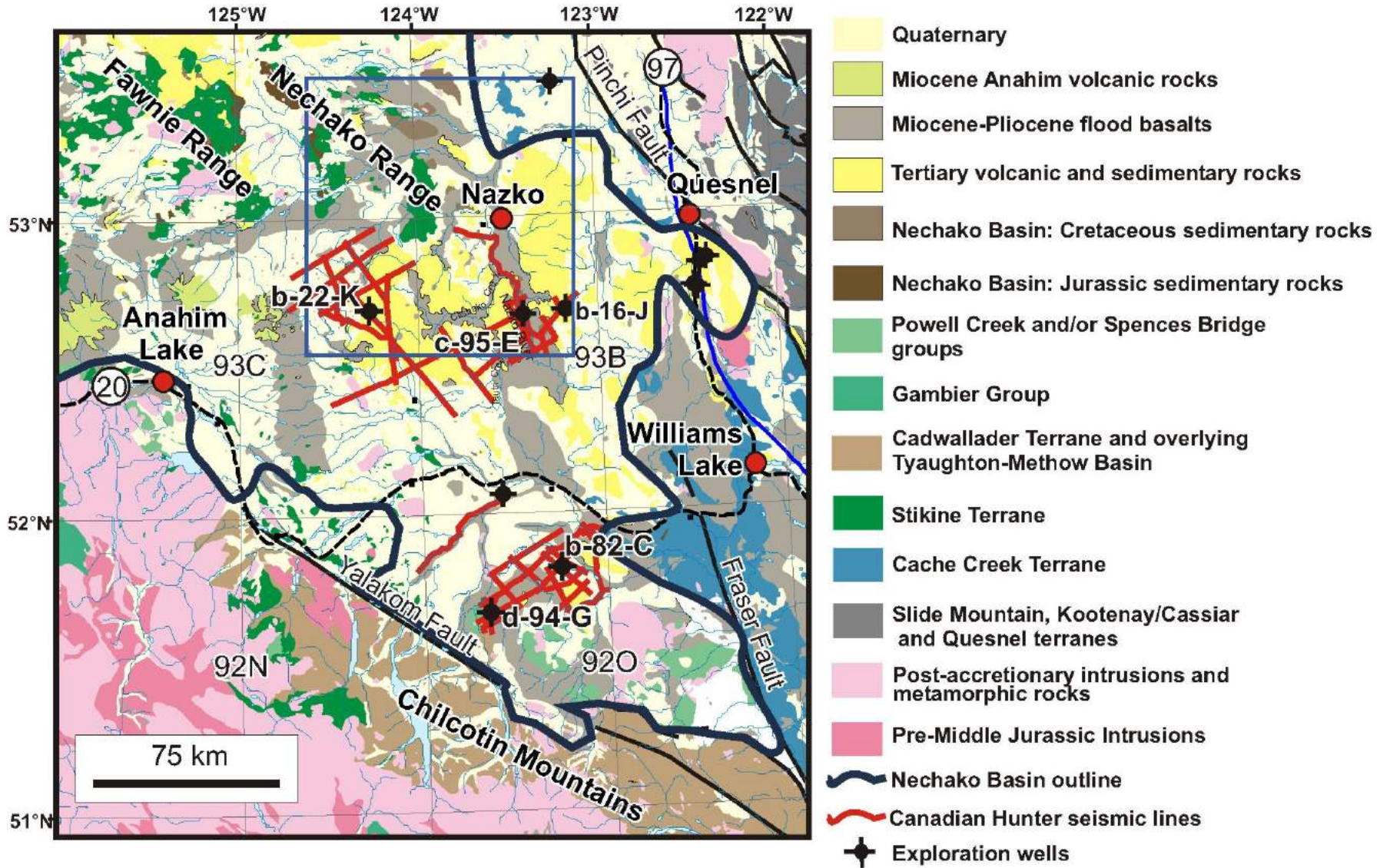


Figure 1. Geology of the southern Nechako Basin (outlined by thick purple line), showing locations of industry seismic reflection lines and exploratory drillholes. The blue rectangle identifies the area of the map in Figure 2. Numbers of 1:250 000 NTS map areas are indicated. Map provided by F. Ferri, BC Ministry of Energy, Mines and Petroleum Resources.

<5% of that in the Skeena Group (Hannigan et al., 1994). Recent volcanic rocks and thick glacial deposits cover much of the area.

Introduction — Seismic Background

Extensive volcanic rocks in the upper part of the stratigraphy can present problems in seismic reflection data because 1) they typically reflect upward much of the energy that is intended to penetrate to basement, and 2) the difference in physical properties between sedimentary and volcanic rocks can generate multiple reflections that obscure reflected energy from the depths of interest. The variable and thick glacial deposits can also degrade data quality. Modern acquisition and processing techniques may be able to overcome most of these problems. One aspect of the processing that is important in such situations is availability of good velocity models, particularly for the upper layers.

In the reflection method, near-surface velocity values are typically obtained from the traveltimes of the first-arrival refracted wave on individual shot gathers. Advantage is taken of the redundant information resulting from the acquisition procedure. Velocities are typically determined from generalized linear inversion (GLI; e.g., Hampson and Russell, 1984) and/or ray-based traveltime tomography (e.g., Zelt and Barton, 1998) of the first-arrival traveltime picks. The derived velocity models are used in determination of refraction statics, one of the seismic reflection processing steps that significantly improves the alignment of reflectors in the processed image. However, the variations in seismic velocities in the upper layers can also be interpreted in terms of variations in the near-surface rock types (e.g., Calvert et al., 2003; Feng and Calvert, 2006).

A relatively recent development that has applicability to the determination of enhanced velocity structure from the first-arrival data is waveform tomography, a combination of traveltime tomography and two-dimensional (2-D) waveform inversion that uses the full waveform of the data to resolve velocity and attenuation structure (e.g., Pratt and Gouly, 1991; Pratt, 1999). In a blind test of the method applied to a dataset derived from a complex crustal model, the waveform tomography result contained structure at wavelength-scale resolution that was not evident on the traveltime-only tomographic result (Brenders and Pratt, 2007). The derived velocity model was such that the waveforms calculated from the model matched the original data to a high degree of accuracy, indicating a high level of correspondence between the actual model and the derived one, a level that could not be achieved by traveltime methods alone. More recently, Smithyman and Pratt (work in progress, 2008) demonstrated the applicability of the approach to shallow seismic data (<100 m depth) to derive 2-D models of velocity and attenuation.

Project Objectives

The general objective of this project is to derive the seismic P-wave velocity structure of the uppermost crust through application of waveform tomography to the first-arrival data on vibroseis reflection profiles recorded in the Nechako Basin and use the results to distinguish layers or regions of glacial deposits and sedimentary and volcanic rocks in the subsurface. If the data are suitable, application of the procedure to also include models of seismic attenuation would represent a secondary objective, because such results could provide additional discrimination among rock types. Within this general objective, three sub-objectives are to

- 1) establish the efficacy of waveform tomography for data recorded using a vibroseis source. Prior applications of the method have involved data acquired from a point source (i.e., an explosive charge or weight drop). The vibroseis source involves a sweep of frequencies over a period of time. The recorded data are cross-correlated with the sweep signal to generate seismic data that emulate a point source. To date, waveform tomography has not been applied to vibroseis data, the type of data acquired in the Nechako Basin. The method needs to be tested for such data.
- 2) apply the waveform tomography method to first-arrival data recorded as part of the 2008 vibroseis acquisition survey to generate P-wave velocity structures for the upper 2000–3000 m of the crust and, if the data are suitable, information on seismic attenuation associated with the velocity structure.
- 3) interpret the derived velocity (and attenuation) structures in terms of rock types using information from geology, physical properties data (mainly from the literature) and the seismic reflection images generated from the 2008 survey. Glacial till and sedimentary and volcanic rocks should be distinguished by different velocity and attenuation characteristics.

Methodology

To address sub-objective 1, data with good-quality first-arrival waveforms from one reflection line of the 2008 survey will be selected. Since line 10 is relatively straight and lengthy, it will be considered first (Figure 2). Waveform tomography requires a good starting model for best results, so traveltime tomography is the first step in application of waveform tomography (Brenders and Pratt, 2007). Thus, first-arrival traveltimes for the selected dataset will be picked, or the values will be obtained from the processing contractor. Based on these data, initial velocity-depth models will be derived using both the GLI approach (Hampson and Russell, 1984) and traveltime tomography (Zelt and Barton, 1998). Then the applicability of waveform tomog-

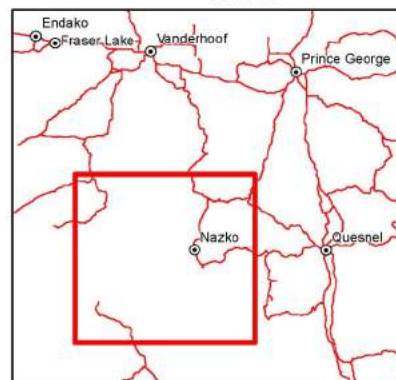
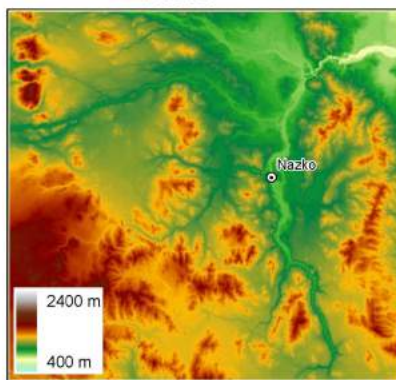
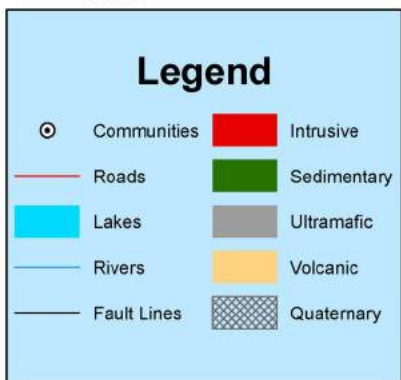
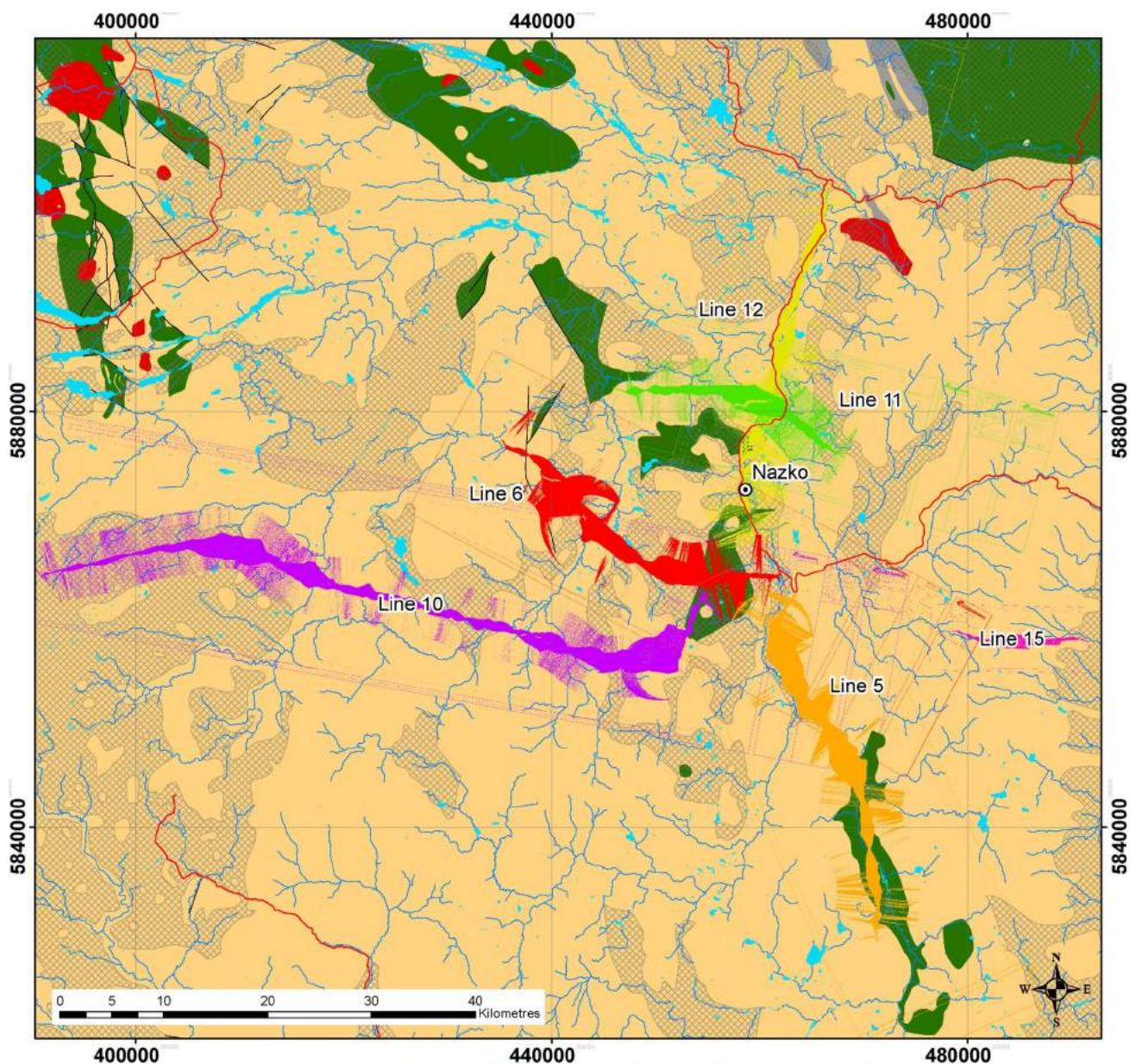


Figure 2. Locations of some of the vibroseis reflection lines recorded during the 2008 Nechako Basin seismic survey on a geological map of the region. The lines are shown in the form of binning maps from the processing contractor, these being a first stage in the computer processing of the acquired data. Each line is distinguished by a different colour. The location of the map is shown in the bottom right by the red rectangle and on Figure 1 by the blue rectangle. The bottom middle illustration shows topography for the same area as the main map.

raphy for the vibroseis first-arrival waveforms will be tested.

For sub-objective 2, first-arrival waveform data will be isolated from the remainder of the seismic shot gathers for the selected dataset. Data selection and waveform pre-processing are important for successful application of the procedure (Brenders and Pratt, 2007). Initially, waveform tomography will be applied to determine P-wave velocity structure. Dependent upon results and data characteristics, waveform tomography will then be carried out to determine both P-wave velocities and P-wave seismic attenuation. Assuming this approach is successful, data from other lines of the 2008 survey, selected in consultation with the other scientists working on the survey data, will be acquired and analyzed in a similar manner.

To address sub-objective 3, the P-wave velocity and attenuation models will be interpreted in terms of probable rock types, primarily glacial deposits, sedimentary rocks or volcanic rocks. This interpretation will be aided by information from the existing exploration drillholes (Figure 1) and knowledge of the physical properties of various rock types (e.g., Ji et al., 2002). One significant part of the interpretation will be to establish 1) the extent, if any, to which the Jurassic rocks exposed in the Fawnie and Nechako ranges (Figure 1) extend farther south, and 2) the thickness and nature of the rocks overlying them. For example, do Cretaceous sedimentary rocks overlie the Jurassic rocks and how thick are they? These interpretations will be done in collaboration with the seismologists involved in the acquisition and processing of the main seismic survey and geologists knowledgeable about the area.

Current Status

Vibroseis seismic reflection data were acquired along seven lines in the Nechako Basin from June to August of 2008 by CGGVeritas of Calgary and are currently being processed by the same company. During the acquisition in July, BS spent two weeks in the field as a quality-control monitor and to learn about the procedures involved in acquiring a major seismic reflection dataset. He is currently familiarizing himself with the seismic reflection processing software at the University of British Columbia (UBC) in anticipation of receiving part of the dataset to initiate the project. Line 10 (Figure 2) is the preferred initial choice because 1) it is relatively straight to accommodate waveform

tomography, which is based on a 2-D procedure; and 2) it crosses the basin immediately south of the exposed Jurassic rocks. Data from line 10 will be acquired from the contractor in an appropriate format for the UBC computer system in late November 2008, at which time the project research can begin.

Acknowledgments

Funding for this project is provided by Geoscience BC and the Natural Sciences and Engineering Research Council through grants to RMC.

References

- Brenders, A.J. and Pratt, R.G. (2007): Full waveform tomography for lithospheric imaging: results from a blind test in a realistic crustal model; *Geophysical Journal International*, v. 168, p. 133–151.
- Calvert, A.J., Fisher, M.A., Johnson, S.Y. and SHIPS Working Group (2003): Along-strike variations in the shallow seismic velocity structure of the Seattle fault zone: evidence for fault segmentation beneath Puget Sound; *Journal of Geophysical Research*, v. 103, 14 p., doi: 10.1029/2001JB001703.
- Feng, F. and Calvert, A.J. (2006): Imaging the upper part of the Red Lake greenstone belt, northwestern Ontario, with 3-D travelttime tomography; *Canadian Journal of Earth Sciences*, v. 43, p. 849–863.
- Hampson, D. and Russell, B. (1984): First-break interpretation using generalized linear inversion; *Journal of the Canadian Society of Exploration Geophysicists*, v. 20, p. 40–54.
- Hannigan, P., Lee, P.J., Osadetz, K.G., Dietrich, J.R. and Olsen-Heise, K. (1994): Oil and gas resource potential of the Nechako–Chilcotin area of British Columbia; unpublished report prepared by the Geological Survey of Canada for the Government of British Columbia, 37 p.
- Ji, S., Wang, Q. and Xia, B. (2002): *Handbook of Seismic Properties of Minerals, Rocks and Ores*; Polytechnic International Press, École Polytechnique de Montréal, 630 p.
- Pratt, R.G. (1999): Seismic waveform inversion in the frequency domain, part 1: theory and verification in a physical scale model; *Geophysics*, v. 64, p. 888–901.
- Pratt, R.G. and Gouly, N.R. (1991): Combining wave equation imaging with travelttime tomography to form high-resolution images from cross-hole data; *Geophysics*, v. 56, p. 208–224.
- Zelt, C.A. and Barton, P.J. (1998): 3D seismic refraction tomography: a comparison of two methods applied to data from the Faeroe Basin; *Journal of Geophysical Research*, v. 103, p. 7187–7210.

Mapping the Sedimentary Rocks and Crustal Structure of the Nechako Basin, British Columbia (NTS 092N, O, 093B, C, F, G), Using Teleseismic Receiver Functions

H.S. Kim, University of Victoria, School of Earth and Ocean Sciences, Victoria, BC; hkim@nrcan.gc.ca

J.F. Cassidy, Geological Survey of Canada, Sidney, BC; University of Victoria, School of Earth and Ocean Sciences, Victoria, BC

S.E. Dosso, University of Victoria, School of Earth and Ocean Sciences, Victoria, BC

H. Kao, Geological Survey of Canada, Sidney, BC

Kim, H.S., Cassidy, J.F., Dosso, S.E. and Kao, H. (2009): Mapping the sedimentary rocks and crustal structure of the Nechako Basin, British Columbia (NTS 092N, O, 093B, C, F, G), using teleseismic receiver functions; *in* Geoscience BC Summary of Activities 2008, Geoscience BC, Report 2009-1, p. 163–170.

Introduction

This paper describes a passive-source seismic mapping project in the Nechako Basin of central British Columbia, with the goal of assessing the hydrocarbon and mineral potential of the region. Over the last decade, an explosion of the mountain pine beetle population in central BC has devastated the lodgepole-pine forest industry on which many communities depend. Mineral or energy extraction may provide an alternative economic opportunity for the region. The Nechako Basin has been the focus of limited hydrocarbon exploration since the 1930s. Twelve exploratory wells were drilled, and oil stains on drill chip samples, as well as the evidence of gas in drill stem tests, attest to some hydrocarbon potential. Seismic data collected in the 1980s were of variable quality, mainly due to the effects of volcanic cover in this region. This study will utilize recordings of distant earthquakes to map sediment thickness, crustal thickness and overall geometry of the Nechako Basin. An array of seven seismic stations were deployed in September 2006 (Table 1, Figure 1) to sample a large area of the basin and two additional seismic stations were deployed in October and November 2007 (Table 1, Figure 1) due to unexpected local earthquake swarms (Cassidy et al., 2008b). This study will complement independent active-source seismic studies planned for the region by providing site-specific images and constraints on the shear-wave velocity structure. This research will also complement

Table 1. Locations of broadband seismic stations in the Nechako Basin. Stations ALRB, CLSB, FLLB, RAMB, SULB, TALB and THMB were deployed in September 2006; stations UBRB and FPLB were deployed in October and November 2007.

Seismic Station Location	Code	Latitude	Longitude	Elevation (km)
Anahim Lake, BC	ALRB	52.510	-125.084	1.237
Cack lake ¹ seismic station, BC	CLSB	52.759	-122.555	0.792
Fletcher Lake, BC	FLLB	51.739	-123.106	1.189
southwest Quesnel, BC	RAMB	52.632	-123.123	1.259
south of Vanderhoof, BC	SULB	53.279	-124.358	1.171
Tatla Lake, BC	TALB	52.015	-124.254	1.127
Thunder Mountain, BC	THMB	52.549	-124.132	1.126
upper Baezaeko River, BC	UBRB	52.890	-124.083	1.243
Fishpot Lake, BC	FPLB	52.954	-123.779	1.005

¹ unofficial place name

magnetotelluric (MT) measurements currently underway (Spratt and Craven, 2009), providing critical new information on porosity, fractures and fluids. This paper describes the methods that are being used, data collection, progress of calculation and inversion for receiver functions, some preliminary results and future work. In addition, there is an ambient noise study being conducted by the University of Manitoba (Idowu et al., 2009). It will complement the receiver function study, which provides site-specific information beneath the recording stations by generating models that average the velocity structure between pairs of stations using data from the same seismic stations as the receiver function study.

Methodologies

Receiver Function Analysis

The technique used in this study is receiver function analysis, in order to constrain the shear-wave velocity structure. In this method, locally generated P- to S-wave conversions in P waves from distant earthquakes (teleseisms; Figure 2; Cassidy, 1992, 1995; Eaton and Cassidy, 1996) are used to map major discontinuities beneath the nine three-component seismic stations deployed across the Nechako Basin

Keywords: geophysics, Nechako Basin, seismology, S-wave velocity

This publication is also available, free of charge, as colour digital files in Adobe Acrobat[®] PDF format from the Geoscience BC website: <http://www.geosciencebc.com/s/DataReleases.asp>.

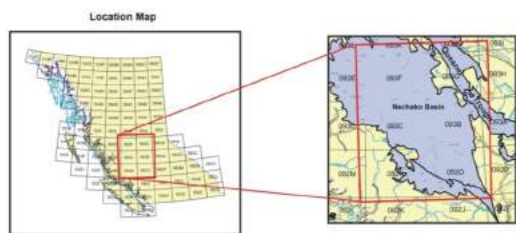
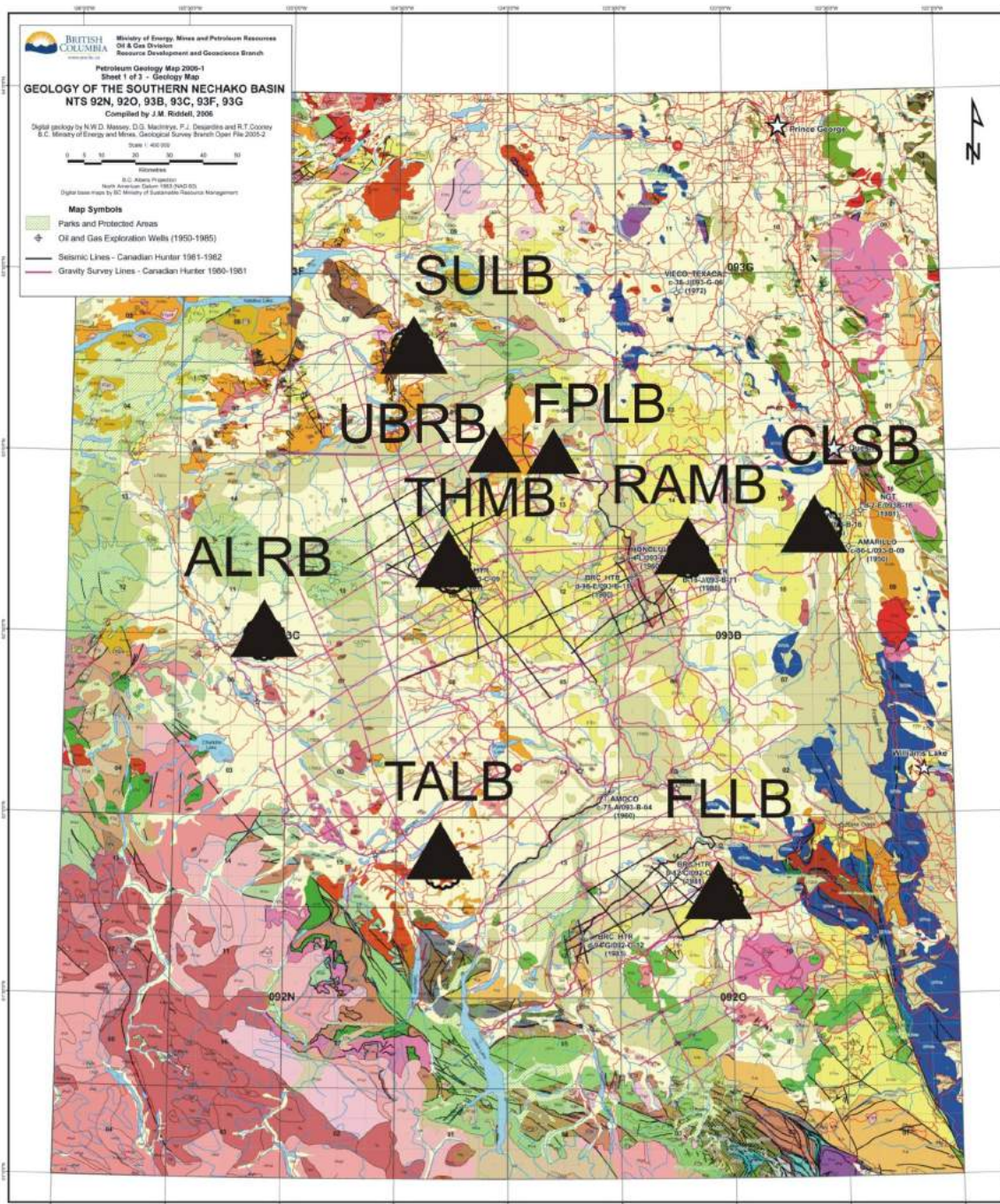


Figure 1. Location of study area. Filled triangles (and four-character station codes) indicate the locations of the nine broadband seismic stations. Base map from Riddell (2006).

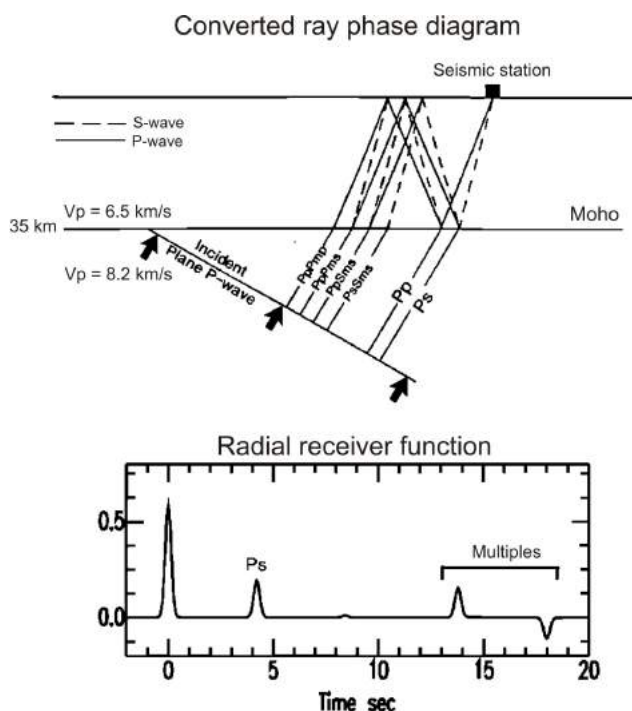


Figure 2. Schematic diagram of the receiver function method. When incident P waves from distant earthquakes encounter S-wave velocity boundaries beneath a seismic station (top), some of the energy is converted to an S wave (Ps). The amplitude and arrival time of the Ps phase, relative to the direct P wave, provides constraints on the velocity contrast and depth to the interface (Cassidy et al., 2008a).

(covering an area of approximately 33 000 km²). The receiver functions are calculated from the recorded teleseismic waveforms by deconvolving the radial components with the corresponding vertical components. This method typically requires recording for an approximately two-year period to collect enough events sampling a wide range of directions and distances.

The advantages of this method include site-specific information (mapping discontinuities directly beneath the recording site); S-velocity information (difficult to obtain from other studies); ability to determine interface geometry, including dip angle and direction; and images obtainable for structure beneath strong near-surface reflectors as the teleseismic energy is coming from below, thereby providing images of both near-surface and crustal-scale structure.

Receiver functions subsequently invert for S-wave velocity structure using the neighbourhood algorithm (Sambridge, 1999a, b). This inversion approach is one of the direct search methods that is suitable for complex nonlinear problems, such as receiver function analysis.

A similar study, conducted across the northern Coast Mountains of BC to image the coastal batholith, shows a



Figure 3. Photograph of Nechako seismic station RAMB, showing the typical station layout, with solar panels and a satellite dish (seismic vault is not visible).

pronounced change in crustal structure at the boundary between the batholith and the westernmost edge of the Nechako Basin (Calkins et al., 2006). This attests to the capacity of this imaging method to resolve the crustal structure in this region.

The receiver function method has been recently applied in studies of sedimentary basins around the world. In the Bohai Bay Basin (China), Zheng et al. (2005) used receiver functions to map sedimentary thicknesses (2–12 km) and velocities to better understand the petroleum potential of this region. In the Mississippi embayment, Julia et al. (2004) combined results from detailed geotechnical, seis-

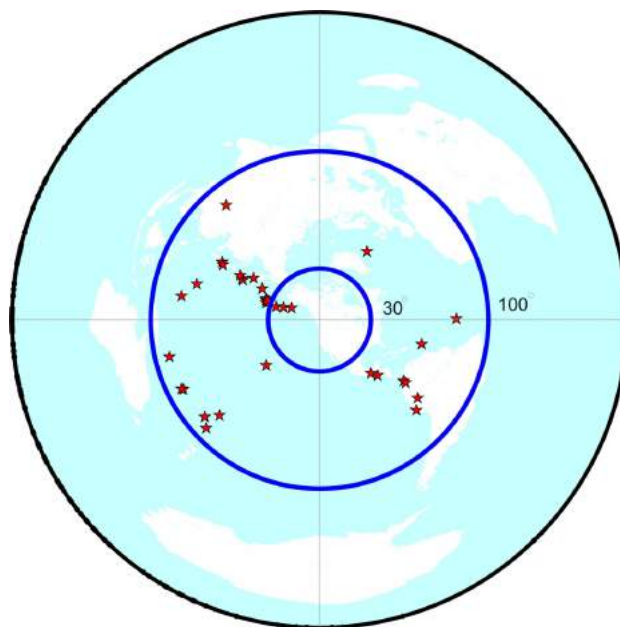


Figure 4. Distribution of distant earthquakes used in this study. Stars indicate large (magnitude >6), distant earthquakes. The map is centred on the Nechako Basin seismic array, with distances of 3360 km (30°) and 11200 km (100°) indicated. This is the useful distance range for receiver function studies.

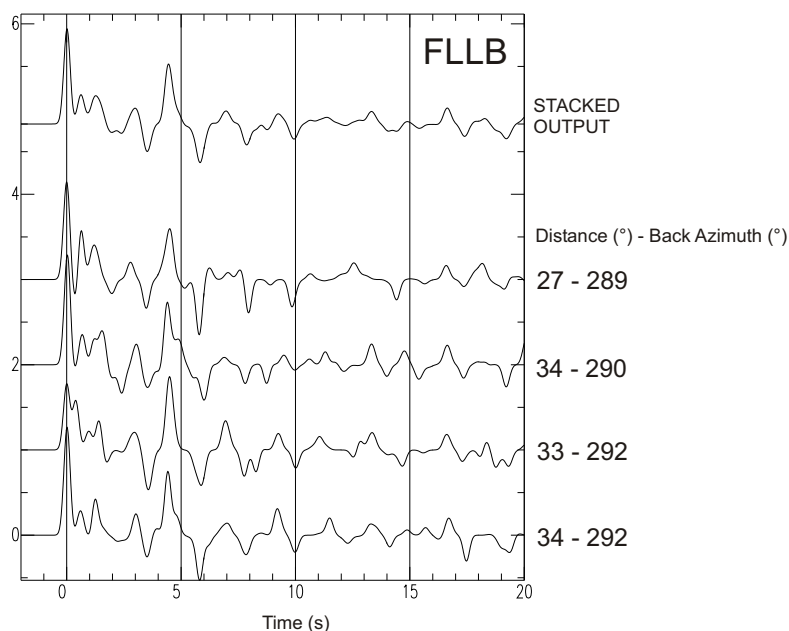


Figure 5. Weighted, stacked radial receiver function for station FLLB (top). Epicentral distances and back azimuths are indicated next to the receiver functions.

mic reflection and receiver function studies to determine the velocity structure and density profiles of the sedimentary column, as well as sedimentary thickness. In Chile, Lawrence and Wiens (2004) combined receiver function data with surface-wave data to map the sedimentary rocks in the Rocas Verdes Basin of Patagonia.

Data

In September 2006, seven three-component broadband seismic stations were deployed across the Nechako Basin area of central BC, and two additional stations were deployed in October and November 2007. The sites were chosen to sample a large portion of the basin and to be close to existing boreholes (Figure 1). These stations utilize solar power and satellite data transmission in order to continuously record ground shaking, transmit the data in real time and archive it at

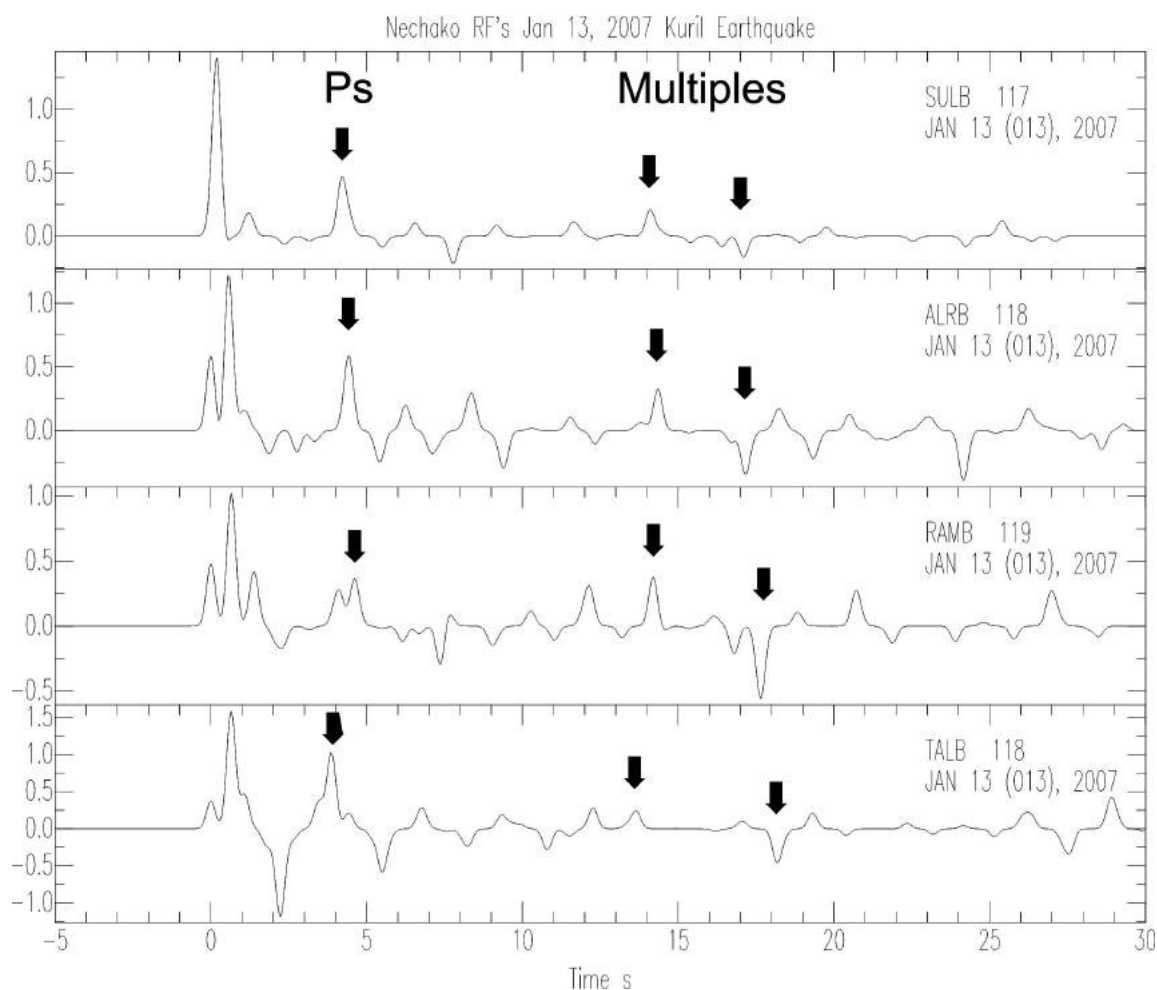


Figure 6. Sample receiver functions for select Nechako Basin stations. The large arrivals indicated by arrows are consistent with a Ps conversion from the continental Moho (near $T = 4$ s) and free-surface multiples of this phase near $T = 12-17$ s.

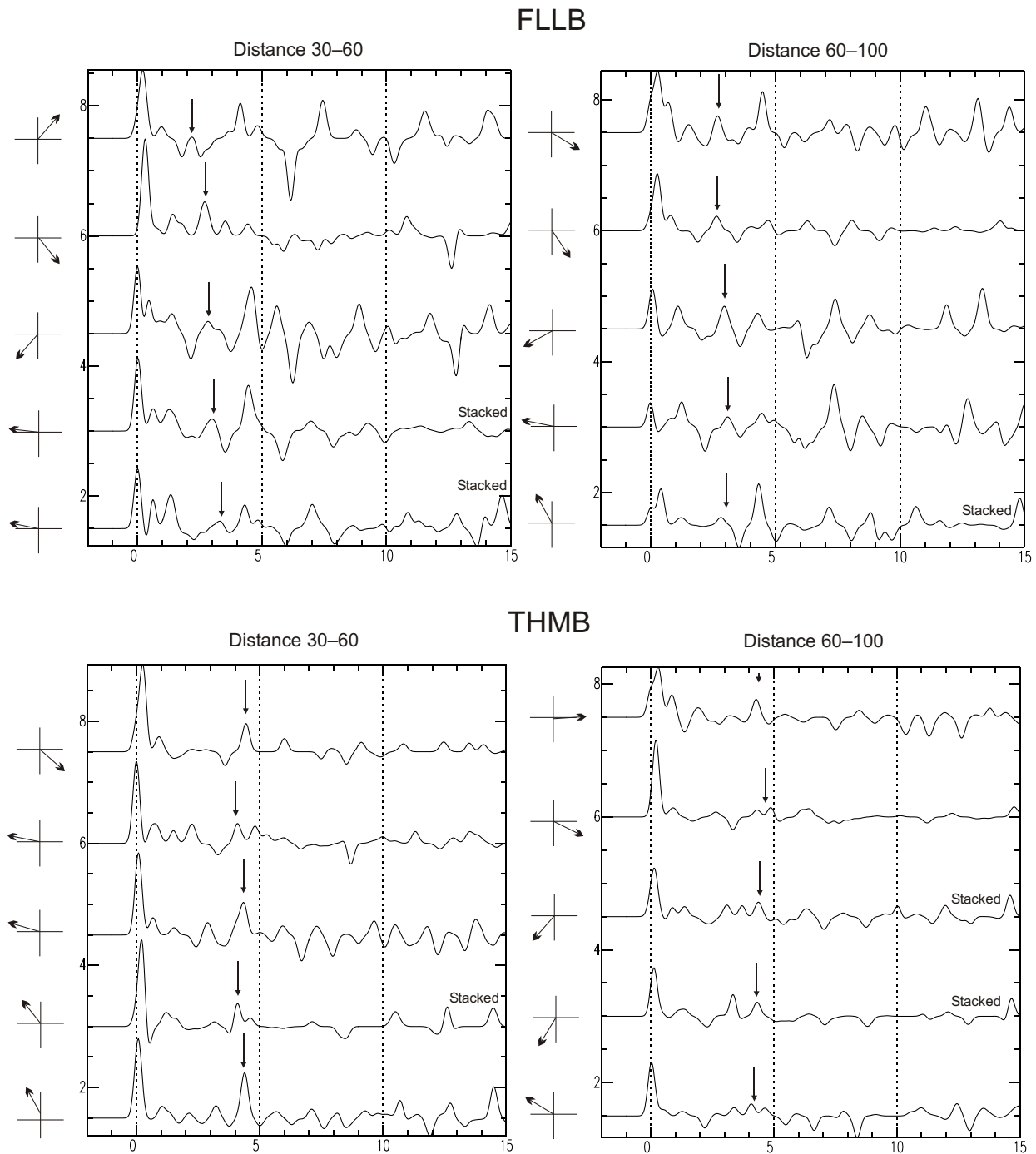


Figure 7. Receiver functions from station FLLB and THMB, ordered by back azimuths for two different distance ranges (30–60° and 60–100°). Thin arrows on the left show the back azimuth for each event. Thick arrows indicate the shifting of arrivals corresponding to the same phase. Stacked receiver functions are labelled.

data collection centres in Sidney, BC and Ottawa, ON. A typical station setup, consisting of solar panels, a seismic vault and a satellite dish with associated electronics, is shown in Figure 3.

During two years of operation (September 2006–August 2008), more than 1000 intermediate to large (magnitude >5.5), distant earthquakes (teleseisms) were recorded.

Among these events, 40 waveforms are the most appropriate for the receiver function analysis described above, and 25 additional waveforms may provide some information. The best 40 teleseisms for this study are shown in Figure 4. These events cover a wide range of azimuth and distance, providing a suitable dataset for examining geometry (dip angle and direction) of the structural boundaries beneath the seismic stations.

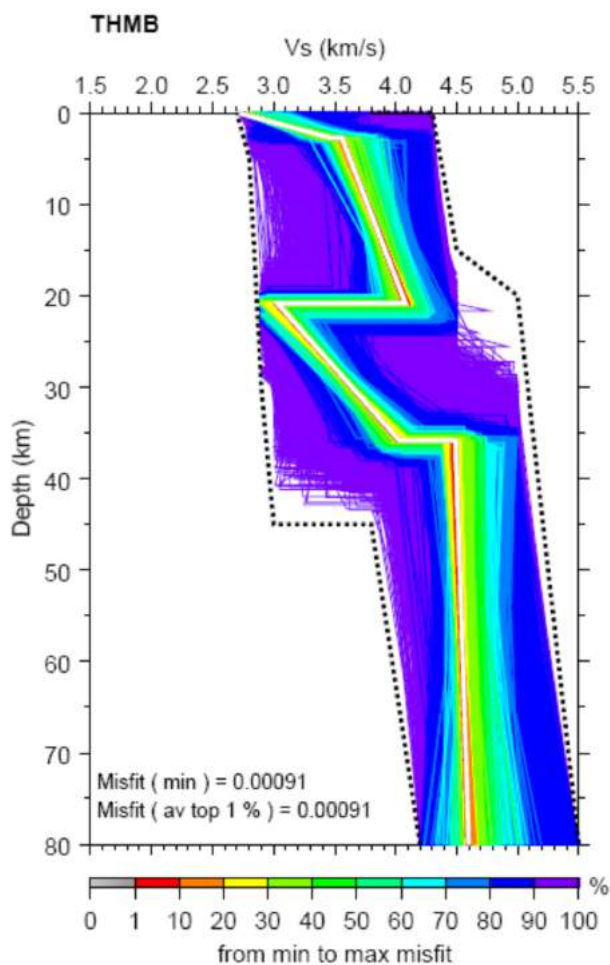


Figure 8. The S-wave velocity models for THMB. The best-fit model is in white. The black solid line shows the average of 1% models with the best data fits. Dotted lines show the minimum and maximum range of allowable models.

Receiver functions computed from the events that have similar distances and back azimuths are stacked together to identify the robust phases. By this process, the amplitude of significant arrivals associated with discontinuities add constructively and are enhanced, whereas noise is suppressed (Figure 5).

Preliminary Results

To date, receiver functions have been computed for waveforms collected over 2 years at three stations within the Nechako Basin: FLLB, THMB and SULB. These preliminary receiver functions are consistent and show arrivals indicative of sedimentary rocks in the basin and crustal thickness variations. For example, the receiver functions for the magnitude 8.1 Kuril Islands earthquake on January 13, 2007 is shown in Figure 6. The arrival at time '0' is the direct P wave; other arrivals are locally generated P- to S-wave converted phases and free-surface multiples. A small-amplitude arrival at $T = 0$, followed immediately by large-

amplitude arrivals, is indicative of near-surface low-velocity sedimentary rocks. The Ps-converted phase near 4 s is associated with the continental Moho (as are the multiples at 12–17 s). The earlier arrivals (i.e., the arrivals within the first 2 s) are associated with near-surface, low-velocity sedimentary rocks.

Although some arrivals indicate the same phase from the discontinuity, possibly the Moho, they may vary with the back azimuth. There is also a variation in arrival time with distance (Cassidy, 1992). Thick arrows in Figure 7 show the shifting of arrivals with the same phase.

The preliminary S-wave model indicates that the crustal thickness of the basin is about 37 km with an ~3 km thick sedimentary layer on the top and low-velocity zone at ~20–37 km depth (Figure 8). The discontinuity around 37 km depth in the model indicates the Moho.

Future Work

Receiver functions will be computed for all suitable events for remaining stations. These will be also stacked into distance and azimuth bins and modelled for S-wave velocity structures for all stations within the Nechako Basin. Amplitudes and arrival times will be used to constrain the S-wave velocity contrast and depth of the boundary, and azimuth variations in the receiver functions will help constrain the geometry of the interfaces. This research is a work in progress, being conducted by a University of Victoria M.Sc. student (H. Kim). The expected completion date of the study is August 2009.

Acknowledgments

The authors gratefully acknowledge the financial support of the BC Ministry of Energy, Mines, and Petroleum Resources, the Geological Survey of Canada and Geoscience BC in deploying and operating this seismic network. Thanks go to J. McCutcheon of the University of Manitoba, and S. Williams of the Geological Survey of Canada for their assistance in deploying this seismic array, and to I. Al-Khoubbi, I. Asudeh and the POLARIS team for maintaining these instruments. G. Rogers and R. Currie are thanked for providing a thorough review of this manuscript.

Geological Survey of Canada contribution 20080438.

References

- Calkins, J., Frassetto, A., Zandt, G. and Dueker, K. (2006): Nature of the crust and Moho in the Coast Mountains batholith near 52°N; *Eos, Transactions, American Geophysical Union*, v. 87, no. 52, Fall Meeting, abstr. S53B-1323.
- Cassidy, J.F. (1992): Numerical experiments in broadband receiver function analysis; *Bulletin of the Seismological Society of America*, v. 82, p. 1453–1474.
- Cassidy, J.F. (1995): A comparison of the receiver structure beneath stations of the Canadian National Seismograph Net-

- work; *Canadian Journal of Earth Sciences*, v. 32, p. 938–951.
- Cassidy, J.F., Al-Khoubbi, I. and Kim, H.S. (2008): Mapping the structure of the Nechako Basin using passive source seismology; *in* *Geoscience BC Summary of Activities 2007*, Geoscience BC, Report 2008-1, p. 115–120.
- Cassidy, J.F., Balfour, N., Hickson, C., Kao, H., Nazzotti, S., Rogers, G.C., Bird, A., Bentkowski, W., Al-Khoubbi, I., Esteban, L., White, R., Caplan-Auerbach, J. and Kelman, M. (2008): The upper Baezaeko River, British Columbia, earthquake sequence: unusual seismic activity in the Anahim volcanic belt (abstract); *Seismological Research Letters*, v. 79, p. 334.
- Eaton, D.W. and Cassidy, J.F. (1996): A relict subduction zone in western Canada: evidence from seismic reflection and receiver function data; *Geophysical Research Letters*, v. 23, p. 3791–3794.
- Idowu, O., Frederiksen, A. and Cassidy, J.F. (2009): Seismic tomography of the Nechako Basin, British Columbia (NTS 092N, O, 093B, C, F, G), using ambient seismic noise, *in* *Geoscience BC Summary of Activities 2008*, Geoscience BC, Report 2009-1, p. 169–172.
- Julia, J., Herrmann, R.B., Ammon, C.J. and Akinci, A. (2004): Evaluation of deep sediment velocity structure in the New Madrid seismic zone; *Bulletin of the Seismological Society of America*, v. 94, p. 334–340.
- Lawrence, J.F. and Wiens, D.A. (2004): Combined receiver-function and surface wave phase-velocity inversion using a niching genetic algorithm: application to Patagonia; *Bulletin of the Seismological Society of America*, v. 94, p. 977–987.
- Riddell, J.M. (2006): Geology of the southern Nechako Basin NTS 92N, 92O, 93B, 93C, 93F, 93F; BC Ministry of Energy, Mines and Petroleum Resources, Petroleum Geology Map 2006-1, 3 sheets at 1:400 000 scale.
- Sambridge, M. (1999a): Geophysical inversion with a neighbourhood algorithm – I. Searching a parameter space, *Geophysical Journal International*, v. 138, no. 2, p. 479–494.
- Sambridge, M. (1999b): Geophysical inversion with a neighbourhood algorithm – II. Appraising the ensemble, *Geophysical Journal International*, v. 138, no. 3, p. 727–746.
- Spratt, J.E. and Craven, J.A. (2009): Preliminary images of the conductivity structure of the Nechako Basin, south-central British Columbia (NTS 092N, O; 093B, C, F, G) from the magnetotelluric method; *in* *Geoscience BC Summary of Activities 2008*, Geoscience BC, Report 2009-1, p. 173–180.
- Zheng, T., Zhao, L. and Chen, L. (2005): A detailed receiver function image of the sedimentary structure of the Bohai Bay Basin; *Physics of the Earth and Planetary Interiors*, v. 152, p. 129–143.

Seismic Tomography of the Nechako Basin, South-Central British Columbia (NTS 092N, O, 093B, C, F, G) Using Ambient Seismic Noise

O. Idowu, University of Manitoba, Department of Geological Sciences, Winnipeg, MB, seyi_id@yahoo.ca

A. Frederiksen, University of Manitoba, Department of Geological Sciences, Winnipeg, MB

J.F. Cassidy, Geological Survey of Canada, Sidney, BC

Idowu, O., Frederiksen, A. and Cassidy, J.F. (2009): Seismic tomography of the Nechako Basin, British Columbia (NTS 092N, O, 093B, C, F, G) using ambient seismic noise; *in* Geoscience BC Summary of Activities 2008, Geoscience BC, Report 2009-1, p. 171–174.

Introduction

Ambient seismic noise is gaining popularity as an effective method for imaging large-scale crustal structure (e.g., see Bensen et al., 2007, 2008). Assuming that seismic noise contains waves propagating in all directions, cross-correlating sufficiently long noise records recorded simultaneously at two instruments will recover a Green's function—that is, a record equivalent to a seismogram recorded at one station from a source at another station. Given the frequency distribution of microseismic noise, this Green's function is typically dominated by high-frequency Rayleigh waves reflecting large-scale crustal structure, and is well suited to imaging sedimentary basins on a broad scale.

The authors are in the process of using ambient-noise surface-wave tomography to examine the Nechako Basin, British Columbia. The basin has been difficult to explore due to the presence of Tertiary volcanic outcrops. The volcanic rock that covers a major part of the basin has a strong velocity inversion at its base, making it difficult to use conventional seismic methods. Ambient-noise surface-wave tomography will help unravel the structural composition of the basin by estimating thicknesses of volcanic and sedimentary rocks, lateral velocity variations and crustal thicknesses within the basin area. These results will have applications to mineral and hydrocarbon exploration in the region by

Keywords: *Nechako Basin, seismic noise, shear-wave velocity, sedimentary rocks*

This publication is also available, free of charge, as colour digital files in Adobe Acrobat® PDF format from the Geoscience BC website: <http://www.geosciencebc.com/s/DataReleases.asp>.

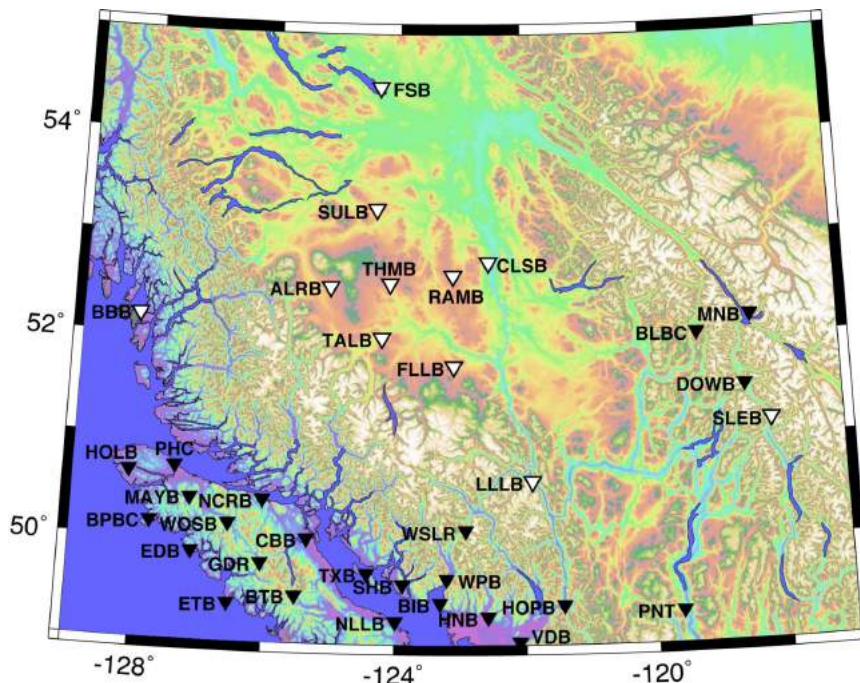


Figure 1. Location of seismic stations in the Nechako Basin and surrounding area. Stations used in this study are indicated by white triangles.

providing constraints on S-wave velocity, P-wave velocity, Poisson's ratio and layer thickness. In this study, the method, data and preliminary results as of October 2008 are described. In a related study (Kim et al., 2009), teleseismic receiver functions are providing site-specific constraints on S-wave velocity.

Data and Method

This study cross-correlated the vertical component of ambient seismic-noise data recorded by 12 POLARIS and Canadian National Seismograph Network CNSN seismic stations between September 2006 and November 2007. The stations used (white triangles on Figure 1) lie between latitudes 50.8–55.1 N and longitudes 122–128 W (Figure 1). A typical station layout is shown in Figure 2. The data processing procedure was based on that of Bensen et al.



Figure 2. Photograph of the seismic station THMB (see Figure 1 for location).

(2007). The time lengths of some data are shorter than 14 months as a result of station down-time.

Data were corrected for instrument response, normalized using a one-bit process to equalized amplitudes, and then spectrally whitened. Data for all possible station pairs were then cross-correlated in day-long blocks. Single-day cross-correlations (Figure 3) were quite noisy; stacking all available cross-correlations (Figure 4) greatly improved the results.

The stacked signal (Figure 4a) contains signal at both positive and negative lags, representing propagation in both directions between the two stations. For evenly distributed noise sources, the signal should be symmetric about zero-lag time; the presence of asymmetry in our results is indicative of a preferred noise direction. For further analysis, we summed the positive-lag and negative-lag signals together (Figure 4b).

The main signal in our reconstructed seismograms is a high-frequency Rayleigh wave. As Rayleigh waves are dispersive (i.e., they have frequency-dependent velocities), and the dispersion is controlled by velocity distribution with depth, frequency-time analysis was used to measure the group velocity dispersion relation for each station pair. The technique involves applying a sequence of Butterworth filters at selected frequency bands and measuring the group arrival times on the envelope of the filtered signals (Figure 5; Levshin et al., 1972). In order to estimate the error on these measurements, dispersion characteristics were measured on all sequential three-month stacks, so that for each Rayleigh waveform, that are approximately five dispersion curves instead of one from the 14-month stack. If at least three out of the five dispersion curves are repeated or nearly repeated measurements, their

standard error was computed at 95% certainty. Also, if the calculated standard error is >0.3 km/s, the measurement was rejected. Where the above requirements are satisfied, the authors are confident in the dispersion curve measurement from the 14-month stack, which will be used to generate dispersion maps and 1D velocity models.

Preliminary Results

Figure 6 is an example of some of the dispersion curves estimated from Rayleigh-wave velocity values after determining uncertainties in the dispersion curves. The dispersion curves tend to converge at frequency <0.30 Hz and >0.55 Hz. Significant variation in the dispersion curves was observed between 0.30 Hz and 0.55 Hz, probably resulting from crustal velocity variations between paths. Further processing of these curves will involve two forms of inversion: linear tomographic inversion of group velocities, which will produce a map of group velocity for each frequency range, and 1-D nonlinear inversion of individual dispersion curves, which will produce models of seismic velocity as a function of depth. From the tomography maps, relating the observed group-velocity variations to lateral changes in geology within and outside of the Nechako Basin can be expected. One-dimensional models will reference these changes to depth and define major crustal layers. Both modes of inversion are ongoing and are expected to be complete by May 2009.

Acknowledgments

The authors gratefully acknowledge the financial support of the BC Ministry of Energy, Mines and Petroleum Resources, the Geological Survey of Canada and Geoscience

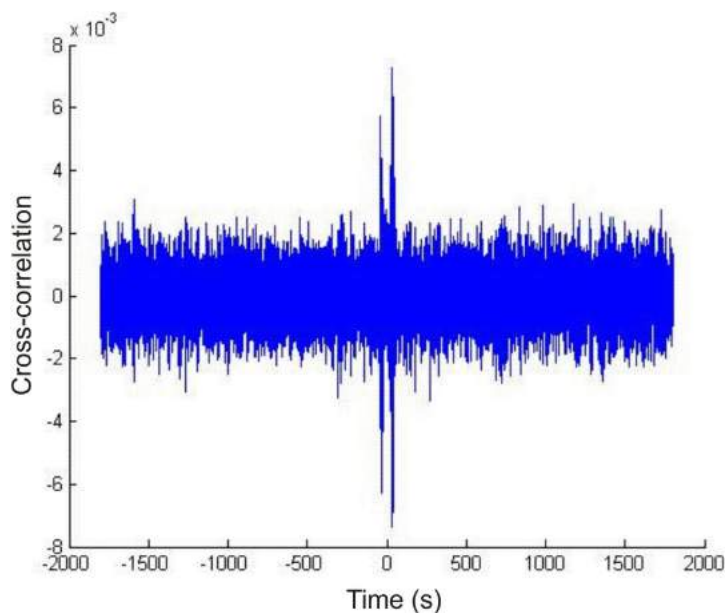


Figure 3. Example of a single-day cross-correlation for the travel path between SULB and ALRB.

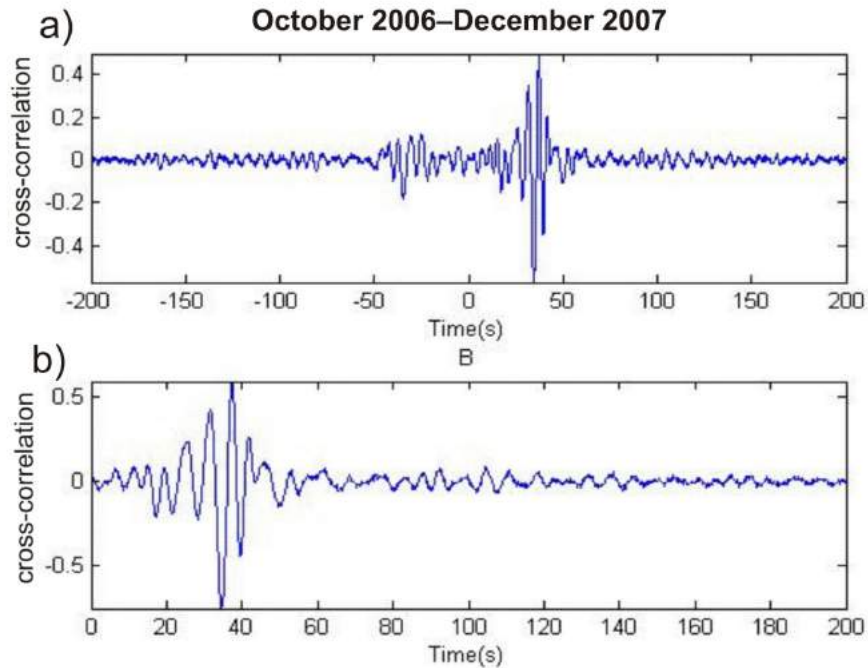


Figure 4. a) Asymmetric waveform, produced by stacking 14 months of cross-correlated signals. b) Symmetric waveform, produced by summing the causal and noncausal portions of the waveform in a).

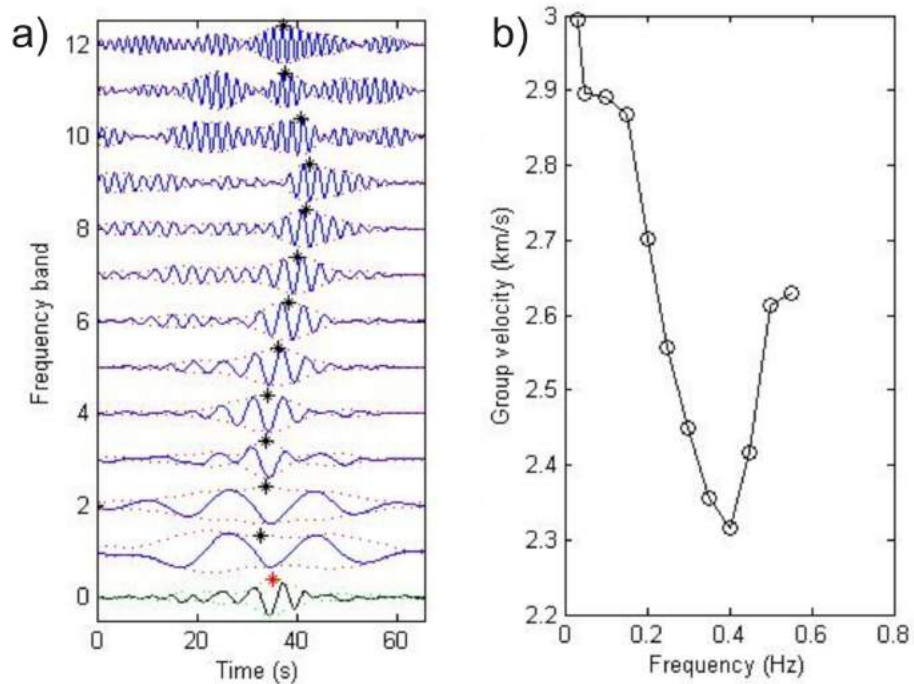


Figure 5. Graphs showing the estimation of dispersion characteristics: a) estimated Rayleigh waveform produced between station SULB and ALRB is filtered at selected frequency bands; the group arrival time corresponding to the peak of the envelope is measured in each band; the group velocity is the ratio of the distance between the two seismic stations and the group arrival time; b) the dispersion curve, made by plotting the group velocity (km/s) against the centre frequency of each band (Hz).

Group velocity curves

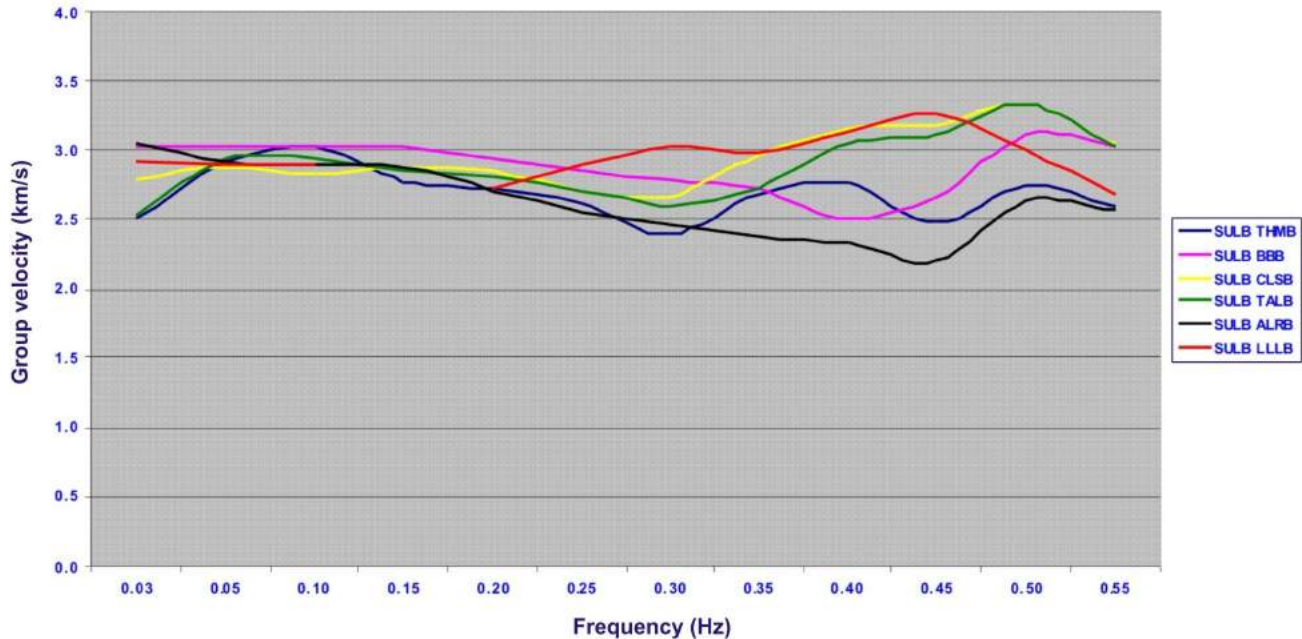


Figure 6. Dispersion curves between station SULB and six other stations: THMB, BBB, CLSB, TALB, ALRB and LLLB. Location of these seismic stations are shown in Figure 1.

BC in deploying and operating this seismic network. I. Al-Khoubi, I. Asudeh and the entire POLARIS team are thanked for maintaining these instruments. This research was funded by a National Sciences and Engineering Research Council of Canada (NSERC) grant and a University of Manitoba graduate fellowship.

Geological Survey of Canada contribution 20080444.

References

- Bensen, G.D., Ritzwoller, M.H. and Shapiro, N.M. (2008): Broad-band ambient noise surface wave tomography across the United States; *Journal of Geophysical Research*, v. 113, doi:10.1029/2007JB005248, p. 1–21.
- Bensen, G.D., Ritzwoller, M.H., Barmin, M.P., Levshin, A.L., Lin, F., Moschetti, M.P., Shapiro, N.M. and Yang, Y. (2007): Processing seismic ambient noise data to obtain reliable broadband surface wave dispersion measurements; *Geophysical Journal International*, v. 169, p. 1239–1260.
- Kim, H.S., Cassidy, J.F., Dosso, S.E. and Kao, H. (2009): Mapping the sedimentary rocks and crustal structure of the Nechako Basin, British Columbia (NTS 092N, O, 093B, C, F, G), using teleseismic receiver functions; *in* Geoscience BC Summary of Activities 2008, Geoscience BC, Report 2009-1, p. 163–168.
- Levshin, A.L., Pisarenko, V.F. and Pogrebinsky, G.A. (1972): On a frequency-time analysis of oscillations; *Annals of Geophysics*, v. 28, p. 211–218.

Preliminary Images of the Conductivity Structure of the Nechako Basin, South-Central British Columbia (NTS 092N, O, 093B, C, F, G) from the Magnetotelluric Method

J.E. Spratt, Geoscience BC, Vancouver, BC and Geological Survey of Canada, Ottawa, ON, jspratt@nrcan.gc.ca

J.A. Craven, Geological Survey of Canada, Ottawa, ON

Spratt, J.E. and Craven, J.A. (2009): Preliminary images of the conductivity structure of the Nechako Basin, south-central British Columbia (NTS 092N, O, 093B, C, F, G) from magnetotelluric methods; *in* Geoscience BC Summary of Activities 2008, Geoscience BC, Report 2009-1, p. 175–182.

Introduction

The rapid spread and destructive effects of the mountain pine beetle (MPB) in areas of British Columbia have prompted the need to develop economic diversification opportunities for the interior of the province. As a result, Geoscience BC has initiated a number of projects with the aim of assessing the mineral and petroleum potential of the affected region. Limited exploration to date has indicated some potential for oil and gas reservoirs within the interior basins of central BC, including the Nechako sedimentary basin (Hannigan et al., 1994; Hamblin, 2008). In order to gain a better understanding of the potential for hydrocarbon resources in the region, a magnetotelluric survey, designed to evaluate the usefulness of the method in oil and gas exploration and to characterize the conductivity structure of the Nechako Basin, was conducted in the fall of 2007 (Spratt et al., 2008; Spratt and Craven, 2008; Figure 1).

The Nechako Basin is an Upper Cretaceous to Oligocene sedimentary basin located in the Intermontane Belt of the Canadian Cordillera (Figure 1). The basin formed in response to terrane amalgamation to the western edge of ancestral North America, and consists of overlapping sedimentary sequences (Monger et al., 1972; Monger and Price, 1979; Monger et al., 1982; Gabrielse and Yorath, 1991). Underlying the Nechako sedimentary rocks are the Stikine and Quesnel volcanic arc terranes, separated by the oceanic Cache Creek Terrane (Struik and MacIntyre, 2001). Transpressional tectonic processes were dominant until the Eocene, with westward-directed thrusting between the Stikine and Cache Creek terranes prior to 165 Ma (Best, 2004). Regional transcurrent faulting and associated east-west extension, beginning in the Late Cretaceous, were accompanied by the extrusion of basaltic lava in Eocene and Miocene times.

Keywords: *Nechako Basin, hydrocarbon exploration, magnetotelluric, electromagnetic, conductivity structure*

This publication is also available, free of charge, as colour digital files in Adobe Acrobat® PDF format from the Geoscience BC website: <http://www.geosciencebc.com/s/DataReleases.asp>.

Basaltic flows of the Neogene Chilcotin Group, volcanic rocks of the Eocene Endako and Ootsa Lake groups, and Pleistocene glacial deposits cover a large portion of the Nechako Basin, complicating the interpretation of modern subsurface imaging methods. As a result, much of the stratigraphy and structure of the underlying sedimentary rocks remains uncertain. It has been suggested that the Chilcotin Group can reach a thickness of ~200 m and averages ~100 m (e.g., Mathews, 1989); however, new studies suggest that it is comparatively thin (<50 m) across most of its distribution and only thick (>100 m) in paleochannels (Andrews and Russell, 2008). The presence of the surface basaltic flows and Tertiary volcanic rocks covering most of the region has, to date, prevented uniform and consistent seismic-energy penetration and has complicated the magnetic interpretations. It has been shown that the magnetotelluric (MT) method can be useful in resolving geological structures that are less favourable for characterization by seismic methods (Unsworth, 2005; Spratt et al., 2007). As the method is sensitive to but not impeded by the surface volcanic rocks and can detect variations within the different units, it can be useful in locating the boundaries of the Nechako Basin and defining its internal structure.

Methodology

The magnetotelluric (MT) method measures the natural time-varying electrical and magnetic fields at the surface of the Earth to provide information on the electrical conductivity of its subsurface (Cagniard, 1953; Wait, 1962; Jones, 1992). Signal for MT is generated from interactions between solar winds and the ionosphere at low frequencies, and from distant lightning storms at higher frequencies. The MT response curves (phase lags and apparent resistivities) are calculated from the measured fields at various frequencies for each site recorded. As lower frequencies penetrate deeper through resistive materials, an estimate of conductivity variation with depth can be made from the response curves beneath each site.

Where the Earth is electrically two-dimensional (2-D), the conductivity varies laterally along a profile and with depth.

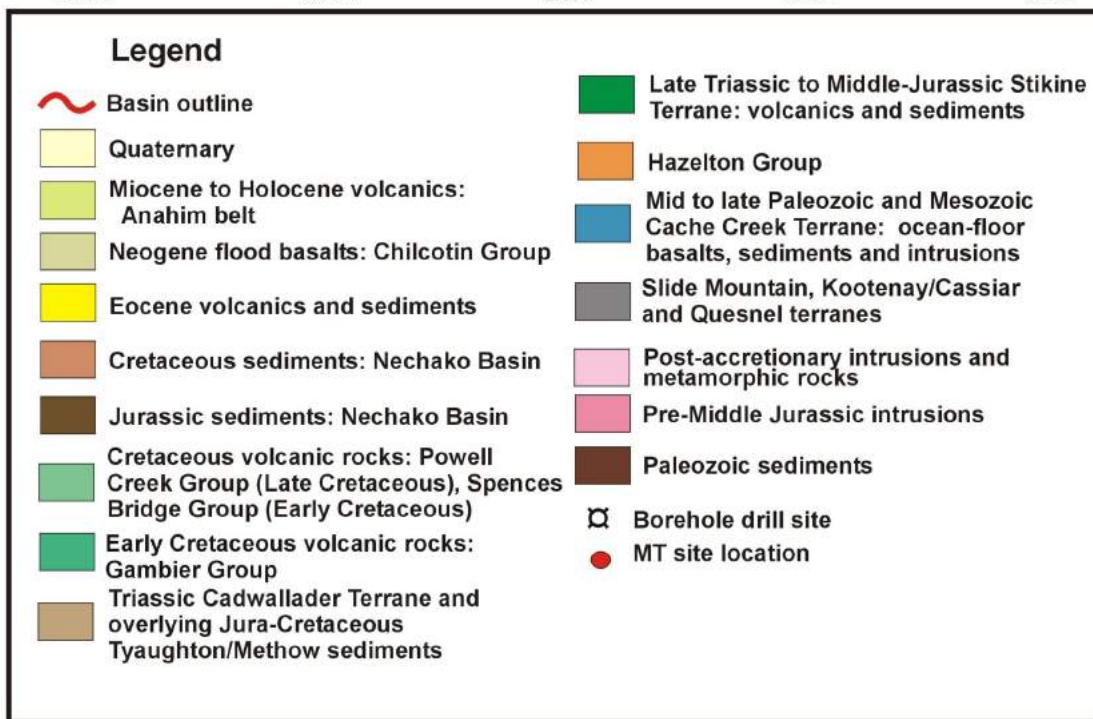
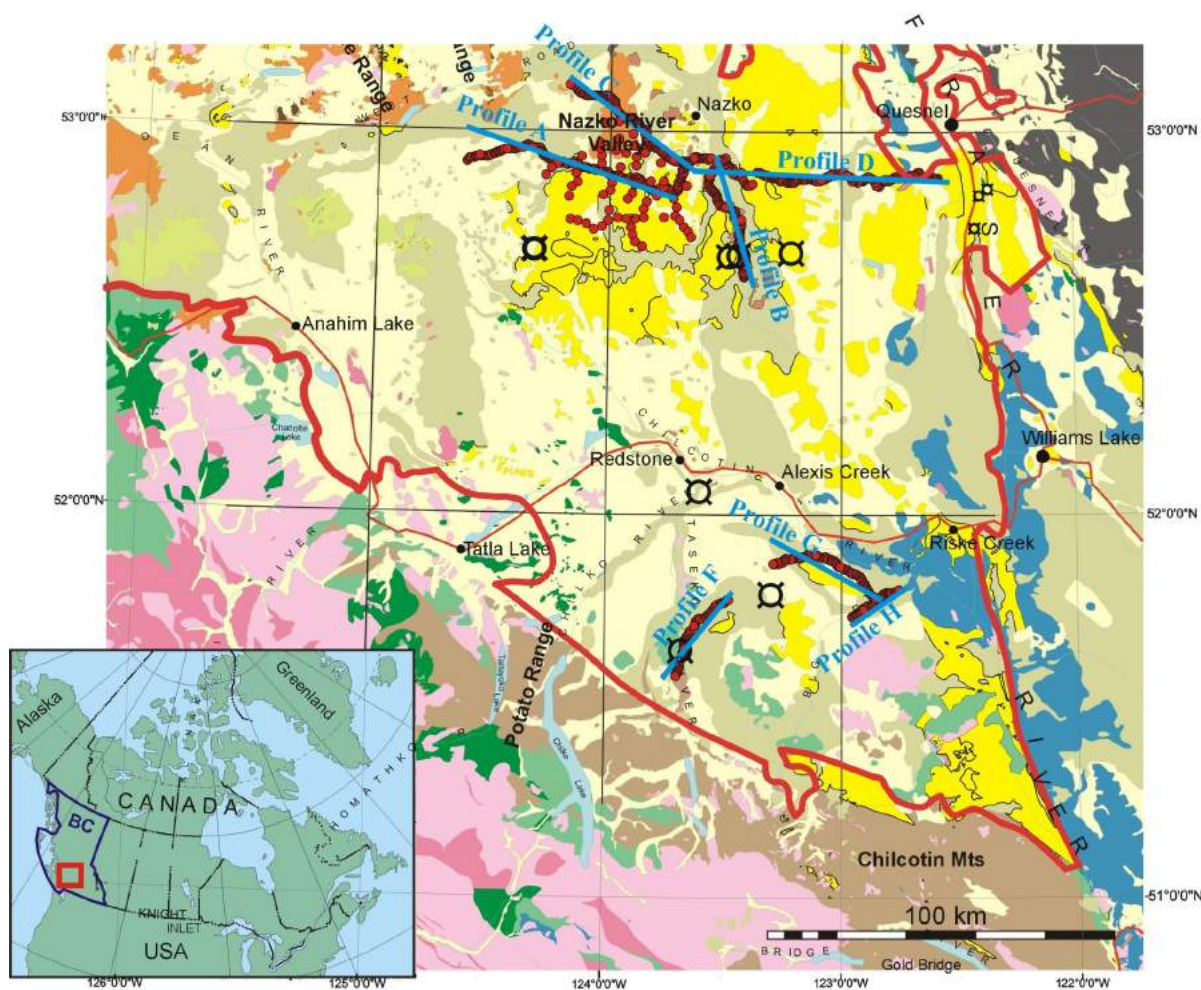


Figure 1. Regional geology of the study area (Riddell, 2006), showing the location of the magnetotelluric stations and the borehole wells.

In this case, apparent resistivities and phases differ along strike compared to those in the perpendicular direction, and some form of directionality analysis is required to determine the preferred geoelectric strike direction. The transverse-electric (TE) mode refers to the along-strike direction and the transverse-magnetic (TM) mode is perpendicular to strike.

The MT method is sensitive to contrasts in the resistivity of juxtaposed materials and can therefore distinguish between some lithological units. Basalt and igneous rocks, for example, commonly have electrical resistivity values >1000 ohm-m ($\dot{\text{U}}\text{-m}$), whereas sedimentary rocks are less resistive, with values ranging between 1 and 1000 $\dot{\text{U}}\text{-m}$. In the crust, other factors that can greatly influence the overall conductivity of a specific unit include the presence of saline fluids, changes in porosity and the presence of graphite films or interconnected metallic ores (Haak and Hutton, 1986; Jones, 1992). In addition to defining structure, the MT method may be able to provide some estimate of bulk properties, such as porosity and percent salinity, that may give direct evidence for the presence of hydrocarbons (Unsworth, 2005).

Data and Analysis

Combined high-frequency audio-magnetotelluric (AMT) and broadband (BBMT) data were collected at a total of 734 sites through the southern part of the Nechako Basin in the fall of 2007 (Figure 1). The data were acquired by Geosystem Canada using MTU-5A recording instruments manufactured by Phoenix Geophysics Ltd. of Toronto. The data were processed by Geosystem using robust remote reference techniques resulting, in general, in excellent data quality covering a period range of nearly seven decades (0.0001–1000 seconds). The dataset was divided into eight separate profiles for subsequent data analysis and 2-D modelling (Figure 1).

Single-site and multisite Groom-Bailey decompositions were applied to each of the MT sites along profiles A, B, C, D and F, in order to determine the most accurate geoelectric strike direction and to analyze the data for distortion effects (Groom and Bailey, 1989; McNeice and Jones, 2001). Figure 2 illustrates the results of single-site strike analysis for each decade period band recorded at each site along the profiles. Nearly all of the sites show a maximum phase difference between the two modes of less than 10° at periods below 0.1 second (s), indicating that the data are independent of the geoelectric strike angle and can be considered 1-D. The maximum phase splits are observed between 0.1 and 10 s, where small changes in the selected strike angle will most affect the data and associated errors.

Profiles A and C are similar, with strikes of 5° – 10° at the westernmost edge of the profiles changing to a strike of

$\sim 35^\circ$ towards the east. Profile B shows only moderate phase splits at only a few sites, suggesting that the majority of the data are 1-D. Profile D shows much stronger phase splits, with a preferred strike angle of $\sim 32^\circ$ for most sites to periods of 100 s; however, the misfit values for the decomposed data, even when no constraints were placed on the data, were significantly high. This is a strong indication of 3-D distortion effects, so 2-D models may not accurately represent the data. Results along profile F indicate strong phase differences at periods greater than 1 s with a fairly consistent strike angle of 22° – 28° . In general, there is a roughly northeast to southwest trend observed in the variations in the geoelectric strike angle. These changes may have resulted from different tectonic pulses, where the stress directions are preserved in the conductivity structure.

Data Modelling and Preliminary Results

One-Dimensional Models

One-dimensional models have been generated for all of the MT sites within the Nechako Basin. Layered Earth models were derived from Occam inversions using the WingLinkTM interpretation software package. Dimensionality and depth analysis indicate that, in general, the data can be considered 1-D up to periods between 0.1 and 1 s, corresponding to depths below 1000–2500 m. Figure 3 shows the results of the 1-D models for varying depth slices in the MT survey region. In general, among the northern set of sites, there appears to be a northeast to southwest trend in conductivity structure, consistent with the results from the decomposition analysis. However, more complex structure is revealed in the southern set of sites, and additional dimensionality analysis is necessary. At 50 m depth, the blue region at the westernmost extent of the survey area most likely represents the resistive volcanic cover. Consistent with the results from Andrews and Russell (2008), the limited lateral extent of this resistor suggests that the volcanic cover is either thinner than 50 m or not as widespread as initially presumed. There is a change in conductivity from ~ 200 to >700 $\dot{\text{U}}\text{-m}$ in the eastern half of the survey area between depths of 1000 and 2000 m. This likely represents the change from conductive sedimentary rocks to the underlying resistive basement units; however, this change is not observed through the entire region, indicating that the sedimentary packages are thicker towards the eastern edge of the Nechako Basin. An anomalously conductive zone (<15 $\dot{\text{U}}\text{-m}$) is observed in the centre of the MT survey region at a depth of 500 m, along profile D, within the sedimentary units and appears to dip towards the east. These dramatic changes may be related to salinity of groundwater or changes in porosity.

Two-Dimensional Modelling

Two-dimensional models have been generated along profiles A, B, C, D and F using the WingLink interpretation

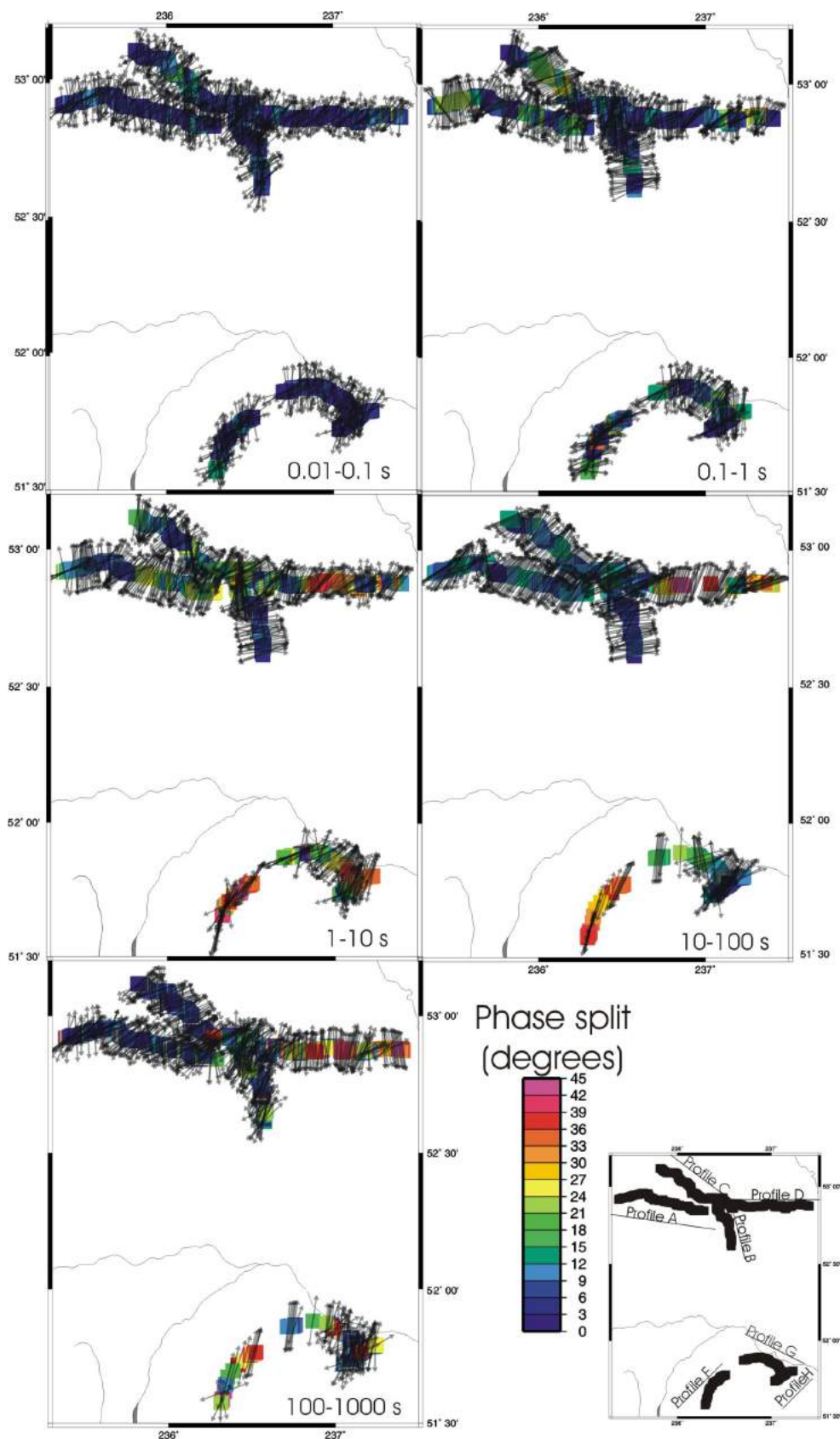


Figure 2. Preferred geoelectric strike angle at each decade period band recorded for each of the MT sites within in the Nechako Basin. The colours illustrate the maximum phase difference between the TM and TE modes, where the warmer colours represent a higher phase split.

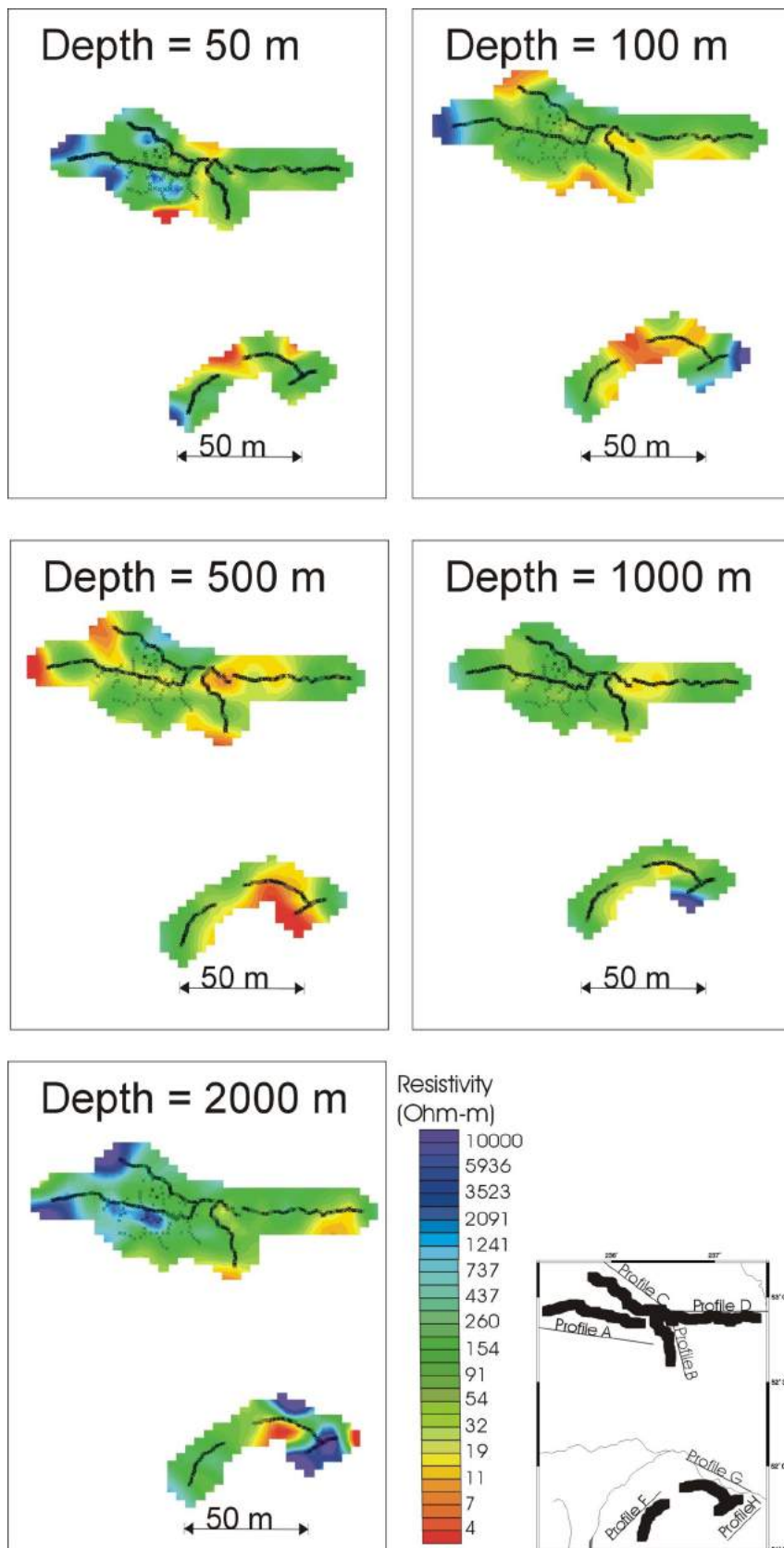


Figure 3. Results of one-dimensional modelling of all MT sites within the Nechako Basin at various depths within the Earth. The warm colours represent areas of high conductivity and the cooler colours represent resistive regions.

software package (Figure 4). More than 100 iterations were executed and included data from the TE mode, the TM mode and the vertical field transfer function, in the period between 0.0001 and 1000 s. All of the models reveal a decrease in conductivity at depths ranging from 1000 to 3000 m, corresponding to approximate depth estimates for the thickness of the Nechako sedimentary packages. This indicates that the MT data are sensitive to the base of the Nechako Basin and can delineate its structural boundaries.

In addition, along-profile variations in the conductivity structure are revealed. Feature A (Figure 4b, d) is an anomalously

conductive region ($>10 \text{ } \Omega\text{-m}$) that lies within the sedimentary units. This feature is observed at the northern end of profile B and along the west-central part of profile D, consistent with the northeast to southwest trend observed in the strike analysis. Causes for significantly high conductivity may include the presence of saline fluids, graphite sheets or sulphides, or may result from a significant increase in the relative porosity of the sedimentary rocks. Feature B is an anomalously resistive unit located at shallow depths along profile C (Figure 4c). This feature correlates spatially with the mapped exposure of the volcanic-arc assemblages of the Hazelton Group of the Stikine

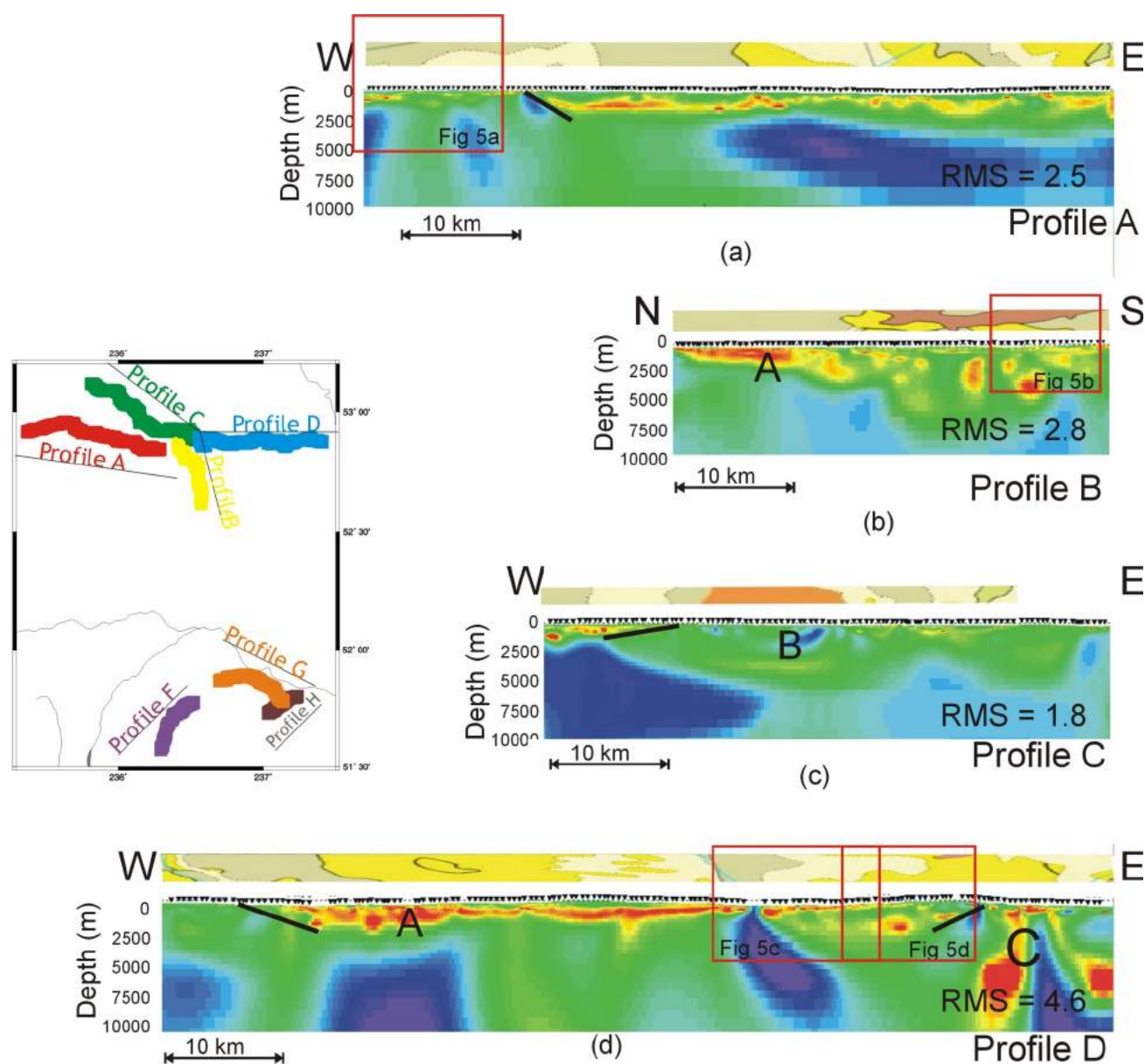


Figure 4. Cross-sections illustrating the two-dimensional models generated along profiles A, B, C and D. The local geology is shown above each profile and the different units are described in the legend for Figure 1. The red squares mark the sections where detailed focused inversions have been generated and shown in Figure 5. The black lines illustrate structural boundaries in the lateral continuity of the shallow conductive layer.

Terrane. Additional modelling is required to constrain the structural nature of this feature. The easternmost extent of profile D illustrates major structure at mid-crustal depths, labelled as feature C. These structures may be related to the lateral fault-bounded eastern extent of the Nechako Basin, and may be an indication for north-north-west-striking subvertical splays of the Fraser fault. Several breaks in the continuity of the upper conductor are observed along many of the profiles (Figure 4a, c, d). These may represent faulting that juxtaposes resistive material from deeper regions against the conductive sedimentary rocks.

Preliminary 2-D modelling has been initiated along profile F (not shown). Although additional testing is required to assess the validity of the model, there is a general deepening of the resistive lower layer from northeast to southwest. This is consistent with interpretation of the seismic data, which suggests a thickening of the Cretaceous sedimentary rocks towards the southwest (Hayward and Calvert, 2008).

Profiles A, B, and D were divided into shorter segments, and each segment was modelled separately to obtain higher resolution of the shallow structure beneath the profile and to generate a model that reasonably fits all the data. This is achieved by allowing a denser mesh and by reducing weighted averaging between sites by fitting the model to a smaller dataset. These focused inversions enable the resolution of enhanced detail, such as imaging the surficial volcanic rocks where they are thicker than ~50 m (Figure 5a), and reveal specific structure that imposes constraints on the lateral continuity of the conductive sedimentary rocks (Figure 5b, d). In addition, they allow for a comparison between the models and geological observations in the boreholes (Figure 5b). They also result in models that have a better fit to the data, reducing inaccurate modelling effects (Figure 5c).

Conclusions and Future Work

Continued analysis of magnetotelluric data collected throughout the Nechako Basin has, to date, yielded one-dimensional models for the entire dataset and two-dimensional conductivity models along four of the seven major profiles. A conductivity contrast between the surface volcanic rocks, the Nechako sedimentary rocks and the underlying basement rocks is observed, indicating that the method is capable of imaging the structure of the basin. The two-dimensional models image the surface volcanic rocks in isolated locations, suggest-

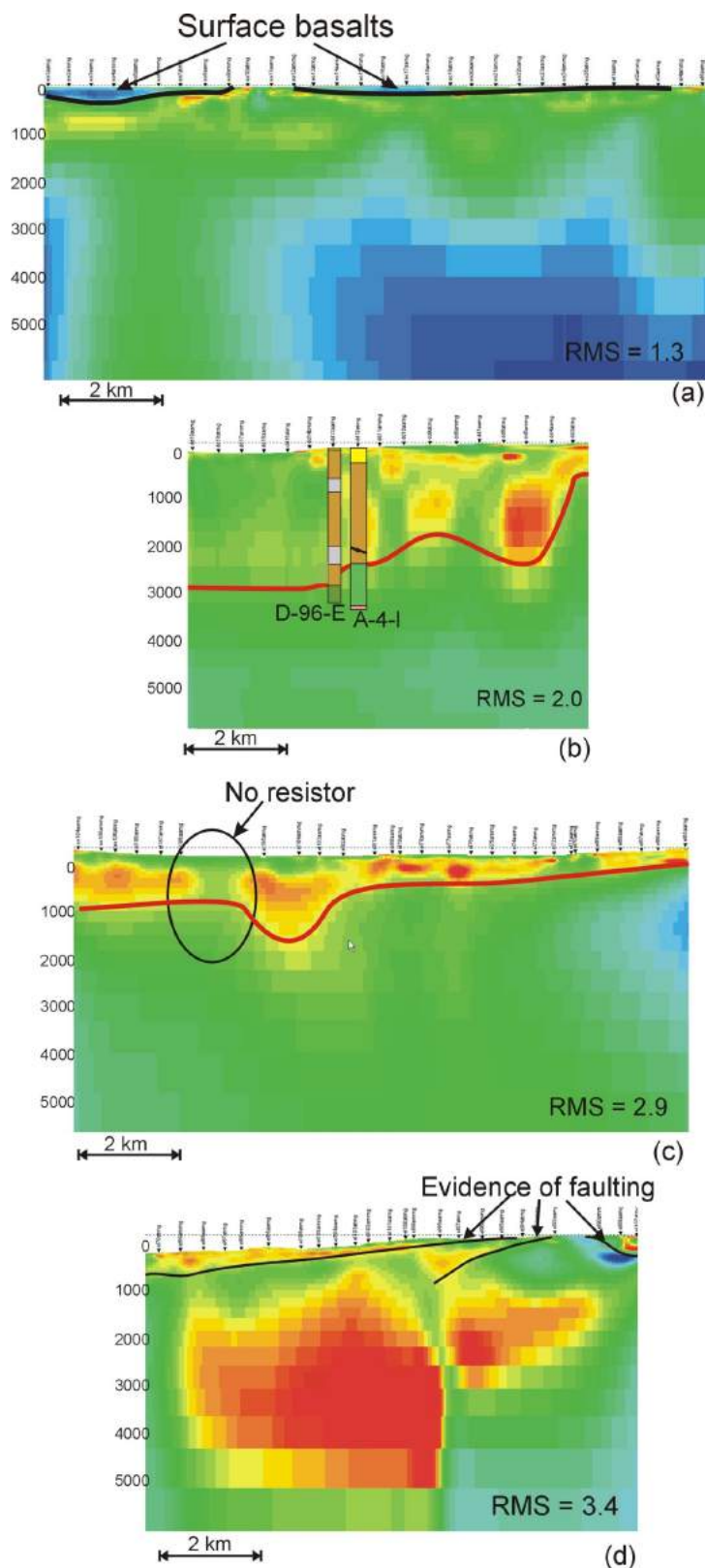


Figure 5. Examples of the detail obtained with focused two-dimensional inversions along sections of the main profiles. The red line marks the boundary between the conductive upper unit and a more resistive underlying layer, which is interpreted as the base of the Nechako sedimentary rocks. The black line indicates the base of the surface basalts. Wells d-96-A and a-4-L (from Ferri and Riddell, 2006) are shown in (b).

ing that they are either too thin to be detected using audio-magnetotelluric methods or they are not as widespread as initially thought. The thickness of the sedimentary packages varies greatly along the different profiles, and structural constraints are placed on the lateral continuity of the conductive sedimentary rocks. Along-strike variations in conductivity within the sedimentary packages are observed, suggesting changes in mineralogy, porosity or salinity. Characterizing these changes will be important in assessing the potential for oil and gas within the region.

Acknowledgments

The authors are grateful to the Geological Survey of Canada, Geoscience BC and the BC Ministry of Energy, Mines and Petroleum Resources for providing financial support for this research. They also thank M. Pilkington for providing insightful comments and a constructive review of this paper.

Geological Survey of Canada contribution 20080463.

References

- Andrews, G.D.M. and Russell, J.K. (2008): Cover thickness across the southern Interior Plateau, British Columbia (NTS 092O, P, 093A, B, C, F): constraints from water-well records; *in* Geoscience BC Summary of Activities 2007, Geoscience BC, Report 2008-1, p. 11–19.
- Best, M.E. (2004): Qualitative interpretation of potential field profiles, southern Nechako Basin; *in* Summary of Activities 2004, BC Ministry of Energy, Mines and Petroleum Resources, p. 73–78.
- Cagniard, L. (1953): Basic theory of the magnetotelluric method of geophysical prospecting; *Geophysics*, v. 18, p. 605–635.
- Ferri, F. and Riddell, J. (2006): The Nechako Basin project: new insights from the southern Nechako Basin; *in* Summary of Activities 2006, BC Ministry of Energy and Mines and Petroleum Resources, p. 89–124.
- Gabrielse, J. and Yorath, C.J., editors (1991): *Geology of the Cordilleran Orogen in Canada*; Geological Survey of Canada, *Geology of Canada*, no. 4 (*also* Geological Society of America, *Geology of North America*, v. G-2).
- Groom, R.W. and Bailey, R.C. (1989): Decomposition of magnetotelluric impedance tensors in the presence of local three dimensional galvanic distortion; *Journal of Geophysical Research*, v. 94, p. 1913–1925.
- Haak, V. and Hutton, V.R.S. (1986): Electrical resistivity in continental lower crust; *in* *The Nature of the Lower Continental Crust*, J.B. Dawson, D.A. Carswell, J. Hall and K.H. Wedepohl (ed.), Geological Society of London, Special Publication 24, p. 35–49.
- Hamblin, A.P., (2008): Hydrocarbon potential of the Tertiary successions of intermontane basins of the Cordillera: preliminary conceptual synthesis of background data; Geological Survey of Canada, Open File 5732, 10 p.
- Hannigan, P., Lee, P.J., Osadetz, K.J., Dietrich, J.R. and Olsen-Heise, K. (1994): Oil and gas resource potential of the Nechako-Chilcotin area of British Columbia; BC Ministry of Energy, Mines and Petroleum Resources, GeoFile 2001-6, 167 p. plus 5 maps at 1:1 000 000 scale.
- Hayward, N. and Calvert, A.J. (2008): Structure of the southeastern Nechako Basin, south-central British Columbia: preliminary results from seismic interpretation and first-arrival tomographic modelling; *in* Geoscience BC Summary of Activities 2007, Geoscience BC, Report 2008-1, p. 129–134.
- Jones, A.G. (1992): Electrical conductivity of the continental lower crust; *in* *Continental Lower Crust*, D.M. Fountain, R.J. Arculus and R.W. Kay (ed.), Elsevier, p. 81–143.
- Mathews, W.H. (1989): Neogene Chilcotin basalts in south-central British Columbia; *Canadian Journal of Earth Sciences*, v. 23, p. 1796–1803.
- McNeice, G.W. and Jones, A.G. (2001): Multisite, multifrequency tensor decomposition of magnetotelluric data; *Geophysics*, v. 66, p. 158–173.
- Monger, J.W.H. and Price R.A. (1979): Geodynamic evolution of the Canadian Cordillera—progress and problems; *Canadian Journal of Earth Sciences*, v. 16, p. 770–791.
- Monger, J.W.H., Price, R.A. and Tempelman-Kluit, D. (1982): Tectonic accretion of two major metamorphic and plutonic belts in the Canadian Cordillera; *Geology*, v. 10, p. 70–75.
- Monger, J.W.H., Souther, J.G. and Gabrielse, H. (1972): Evolution of the Canadian Cordillera—a plate tectonic model; *American Journal of Science*, v. 272, p. 557–602.
- Riddell, J.M., compiler (2006): *Geology of the southern Nechako Basin* (NTS 92N, 92O, 93B, 93C, 93F, 93G); BC Ministry of Energy and Mines and Petroleum Resources, Petroleum Geology Map 2006-1, 3 sheets at 1:4 000 000 scale.
- Spratt, J.E. and Craven, J. (2008): A first look at the electrical resistivity structure in the Nechako Basin from magnetotelluric studies west of Nazko, BC (NTS 092N, O, 093B, C, F, G); *in* Geoscience Reports 2008 [formerly Summary of Activities], BC Ministry of Energy, Mines and Petroleum Resources, p. 119–127.
- Spratt, J.E., Craven, J., Shareef, S., Ferri, F. and Riddell, J. (2008): Designing a test survey in the Nechako Basin, British Columbia (NTS 092N, O, 093B, C, F, G) to determine the usefulness of the magnetotelluric method in oil and gas exploration; *in* Geoscience BC Summary of Activities 2007, Geoscience BC, Report 2007-1, p. 145–150.
- Spratt, J.E., Craven, J., Jones, A.G., Ferri, F. and Riddell, J. (2007): Utility of magnetotelluric data in unravelling the stratigraphic-structural framework of the Nechako Basin (NTS 092N; 093C, B, G, H), south-central British Columbia, from a re-analysis of 20-year-old data; *in* Geological Fieldwork 2006, BC Ministry of Energy, Mines and Petroleum Resources, Paper 2007-1, p. 395–403.
- Struik, L.C. and MacIntyre, D.G. (2001): Introduction; *in* *The Nechako NATMAP Project of the Central Canadian Cordillera*; *Canadian Journal of Earth Sciences*, Special Issue, v. 38, p. 485–494.
- Unsworth, M.J. (2005): New developments in conventional hydrocarbon exploration with EM methods; *Canadian Society of Exploration Geophysicists Recorder*, p. 34–38.
- Wait, J.R. (1962): Theory of magnetotelluric fields; *Journal of Research of the National Bureau of Standards*, v. 66D, p. 509–541.

Regional Facies Patterns in the Northern Jackass Mountain Group, Northern Methow Basin, Southwestern British Columbia (NTS 0920)

J.B. Mahoney, Department of Geology, University of Wisconsin, Eau Claire, WI

J.W. Haggart, Geological Survey of Canada, Pacific Division, Vancouver, BC

C.I. MacLaurin, Department of Earth Sciences, Simon Fraser University, Burnaby, BC

M.M. Forgette, Department of Geology, University of Wisconsin, Eau Claire, WI

J.R. Goodin, Department of Earth Sciences, Simon Fraser University, Burnaby, BC

E.A. Balgord, Department of Geology, University of Wisconsin, Eau Claire, WI

P.S. Mustard, Department of Earth Sciences, Simon Fraser University, Burnaby, BC

Mahoney, J.B., Haggart, J.W., MacLaurin, C.I., Forgette, M.M., Goodin, J.R., Balgord, E.A. and Mustard, P.S. (2009): Regional facies patterns in the northern Jackass Mountain Group, northern Methow Basin, southwestern British Columbia (NTS 0920); *in* Geoscience BC Summary of Activities 2008, Geoscience BC, Report 2009-1, p. 183–192.

Introduction

The Jackass Mountain Group (JMG) is a thick accumulation (2–4 km) of clastic strata, which was deposited in the Methow Basin in late Early Cretaceous time. The Methow Basin is part of a complex Jurassic–Cretaceous depocentre that overlies a number of allochthonous terranes of the southern Canadian Cordillera (Figure 1a, b). The basin has been structurally imbricated and dismembered by Cretaceous contraction and Late Cretaceous to Tertiary transpression along the eastern edge of the Insular Belt and the western edge of the Intermontane Belt, and is currently exposed in a series of fault blocks strung out along the Yalakom, Fraser, Hozameen and Pasayten faults. Along the southern margin of the Nechako Plateau, two major exposures of the JMG of the Methow Basin on opposite sides of the Yalakom fault are spatially associated with the partly coeval Taylor Creek Group of the Tyaughton Basin. These strata extend northward under Neogene volcanic cover and potentially represent an important hydrocarbon reservoir within the Nechako Basin (Ferri and Riddell, 2006).

Accurate assessment of the petroleum potential of the Nechako Basin requires a comprehensive analysis of the basin architecture that developed within these Cretaceous strata, which represent the most prospective targets in the subsurface beneath the Nechako Plateau. However, regional facies patterns and basin architecture of the Cretaceous strata are poorly understood. The primary objective

of this investigation is to undertake a comprehensive regional analysis of temporal and spatial lithofacies variations in Lower Cretaceous strata along the southern margin of the Nechako Basin; this will assist in constraining basin evolution and depositional history. This analysis will provide first-order constraints on the nature of Lower Cretaceous strata in the subsurface, which are considered the most significant petroleum targets in the Nechako Basin (Hannigan et al., 1994); such an analysis is also a prerequisite for an accurate assessment of reservoir quality.

Regional Geological Setting

Regional mapping and stratigraphic studies demonstrate that Lower Cretaceous clastic strata of the Methow and Tyaughton basins represent an overlap assemblage linking several small allochthonous terranes (Methow, Bridge River, Cadwallader) with the eastern edge of the Insular Belt (Garver, 1992). The Hauterivian to Cenomanian–Turonian (?) JMG is a thick (2–4 km) succession of primarily feldspathic sandstone, siltstone and lesser conglomerate that unconformably overlies Middle to Upper Jurassic strata. The JMG has been interpreted by Kleinspehn (1982, 1985) as a coarsening-upward or progradational submarine-fan complex, although subsequent investigations suggest the system is a more complex assemblage of submarine-fan, deltaic and fluvial lithofacies (Schiarizza et al., 1997; Schiarizza and Riddell, 1997; Mustard et al., 2008). The Aptian to Cenomanian Taylor Creek Group is a thick succession of compositionally heterogeneous feldspathic to chert-lithic sandstone, chert-pebble conglomerate and siltstone that unconformably overlies Middle Jurassic and older strata of the Bridge River and Cadwallader terranes (Garver, 1992). The Taylor Creek Group is interpreted as having been deposited in a submarine-fan complex in a two-sided basin during major Albian–Cenomanian

Keywords: *sedimentology, stratigraphy, Jackass Mountain Group, Nechako, Methow, Tyaughton, Cretaceous*

This publication is also available, free of charge, as colour digital files in Adobe Acrobat® PDF format from the Geoscience BC website: <http://www.geosciencebc.com/s/DataReleases.asp>.

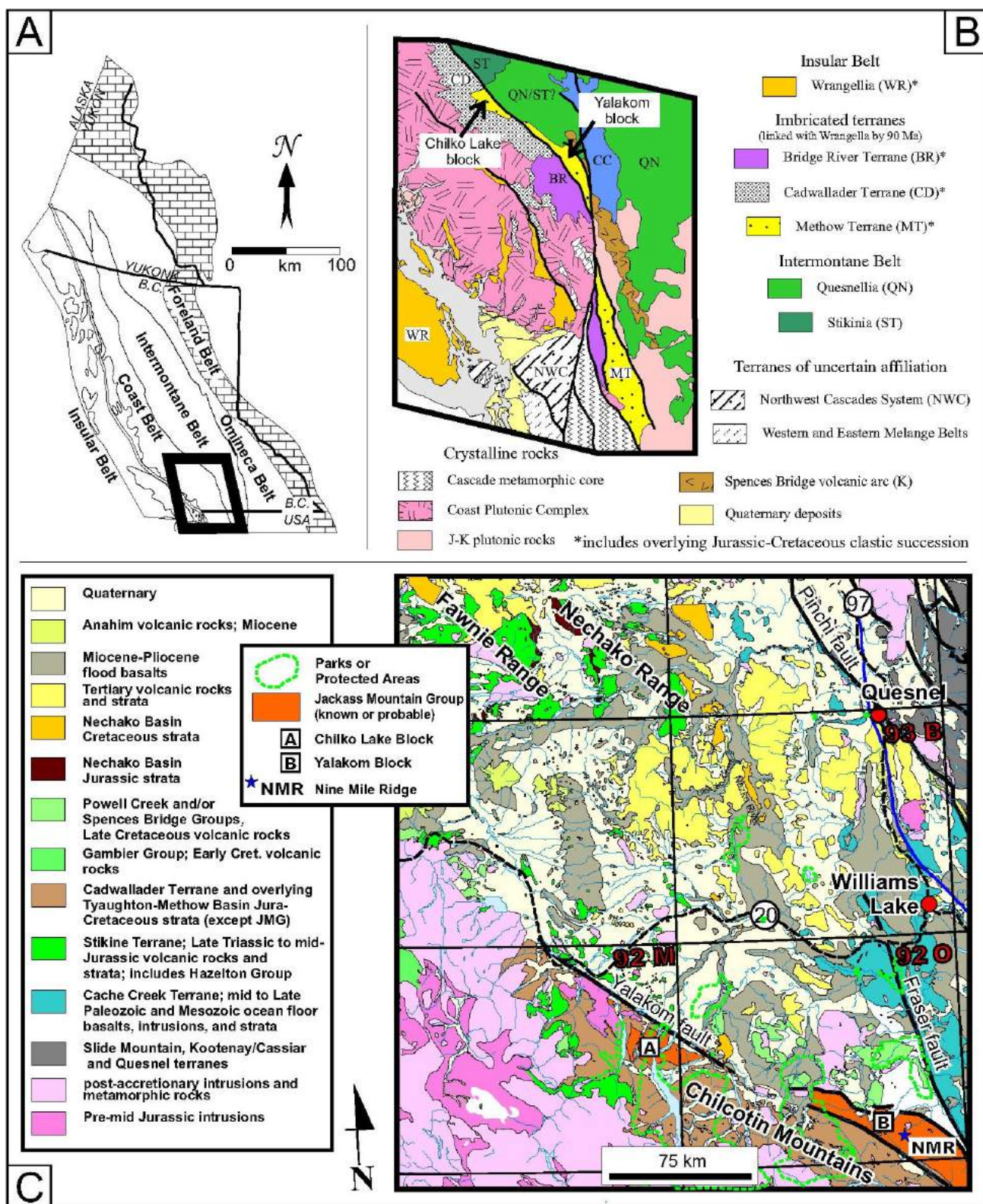


Figure 1. Regional geological framework and location of major areas of study discussed in this paper: a) morphogeological belts of the Canadian Cordillera; the boxed area indicates the location of (b); b) terrane map showing the regional geological framework of the Methow Terrane, including the Chilko Lake and the Yalakom blocks; c) smaller-scale terrane and geological map showing the location of the Chilko Lake and Yalakom blocks (JMG) in relation to physiogeographic and geographic landmarks (*modified with permission from Ferri and Riddell, 2006, and Riddell, 2006*).

contractual tectonism (Garver, 1992). Both the JMG and Taylor Creek Group are overlain by Albian–Santonian fluvial conglomeratic and volcanoclastic rocks of the Silverquick and Powell Creek formations, which were deposited in a complex series of northeast-vergent piggy-back basins (Schiarizza et al., 1997; Riesterer et al., 2001).

Cretaceous strata of the Methow and Tyaughton basins are bordered on the southwest by intrusive rocks of the Coast Plutonic Complex (CPC), on the north by Neogene volcanic rocks of the Nechako Plateau, and on the east by Triassic to Cretaceous arc volcanic and associated strata of the Quesnellia Terrane. Tertiary dextral transpression led to the development of several major northwest-trending high-angle strike-slip faults along the eastern margin of the CPC that effectively dismembered the Cretaceous outcrop belt into several structural panels (Figure 1). Dextral translation along the Tchaikazan, Yalakom and Fraser faults and associated structures is primarily Late Cretaceous–Oligocene, and is limited in its extension to several tens to more than one hundred kilometres per fault.

Facies Description and Distribution

The JMG is contained within two major outcrop belts, one on the northern side of the Yalakom fault, which is referred to as the Yalakom block, and one on the southwestern side of the Yalakom fault, referred to as the Chilko Lake block (Figure 1b, c). These two fault slices are offset by approximately 125 km of sinistral displacement on the Yalakom fault (Umhoefer and Miller, 1996). The most complete, structurally intact stratigraphic sections are exposed in a major northeast-trending synclinorium within the Chilko Lake block, where JMG strata unconformably overlie the Middle Jurassic Nemaia Formation and Middle to Upper Jurassic Relay Mountain Group (Figure 2). The upper Taylor Creek Group is exposed in a south-dipping monocline 10 km southeast of the JMG syncline, across the Konni Lake fault, where it unconformably overlies the Relay Mountain Group. In the Yalakom block, JMG strata are exposed in the central part of a ~150 km long, southward-tapering wedge of mainly medium- to coarse-grained sandstone, siltstone and polymictic conglomerate, which lies between the Yalakom and Fraser fault systems. The belt is cut by several high-angle faults (Schiarizza et al., 1997) and is part of a broad, asymmetric synclinorium with the base of the JMG exposed in steeply dipping beds on the western limb east of the Yalakom River, and the upper portion exposed in moderately west-dipping beds on the eastern limb (Mustard et al., 2008).

Jackass Mountain Group

One of the primary objectives of this investigation is to document the lateral and vertical variation in stratigraphic architecture and, from this data, reconstruct the history of basin evolution in the Cretaceous basin system. Stratigraphic

analysis of the JMG along the southern margin of the Nechako Plateau has identified distinct lithofacies associations that grade laterally and vertically into one another, and provide a record of basin evolution from Hauterivian to at least Cenomanian time.

A. Proximal Delta Front

The stratigraphically lowest unit in the Chilko Lake area is a ~400 m thick succession of sandstone, sandstone with pebbly stringers and lesser lenticular conglomerate. The unit is thickest on the eastern side of the northern limb of the synclinorium, and thins to the south and to the west, characterizing the area as presenting signs of a wedge-shaped geometry (Figure 3, left two columns). The sandstone displays abundant planar-parallel strata with lesser low-angle planar to planar cross-stratification. Rare bivalve fossils and sparse bioturbation are present. Lenticular, matrix-supported to rare clast-supported pebble conglomerate encased in sandstone sequences are interpreted as channel deposits. This unit coarsens then fines upward and the uppermost 100 m of the section contains siltstone intervals which display current- to wave-generated laminations, features which all suggest that an upward decrease in energy occurred.

The wedge-shaped geometry, presence of shallow-marine fossils, current-generated cross-stratified sands and lenticular conglomerate channels suggest deposition in a wave-dominated shoreface, perhaps a proximal delta front.

B. Distal Delta Front/Prodelta

In the Chilko Lake area, this 400–650 m thick, southward-thickening unit is composed of a dark brown to black mudstone to silty mudstone intercalated with varying amounts of thinly bedded siltstone and very thin- to thick-bedded fine- to medium-grained sandstone (Figure 3, 400–900 m in left section and 0–700 m in central section). This is the most fossiliferous facies association, containing articulated bivalves, gastropods and ammonites, suggesting accumulation in a low-energy marine environment. Fossilized wood fragments are abundant. Bioturbation is intense locally, but not diverse, and is often limited to diminutive *Chondrites*. The most dominant sedimentary structures are planar-parallel and microhummocky laminations, but current-generated and combined-flow ripples and lenticular bedding are also present. The relative abundance of siltstone suggests a fining- (~200 m) then coarsening-upward (~300 m) succession.

The laterally continuous geometry, presence of both current and oscillatory bedforms, abundance of intact marine fauna, and intense nondiverse bioturbation suggest deposition in a relatively quiet water environment in which mud and silt accumulation was periodically disturbed by intermittent currents, all of which suggest a lower shoreface or distal delta front environment.

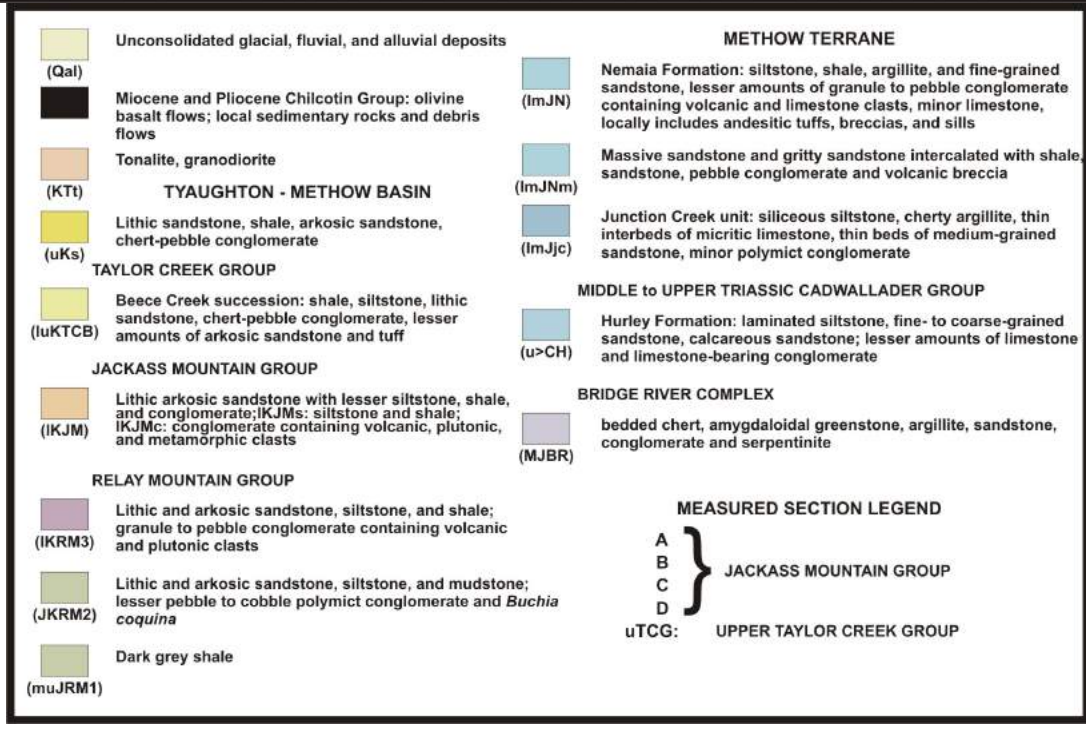
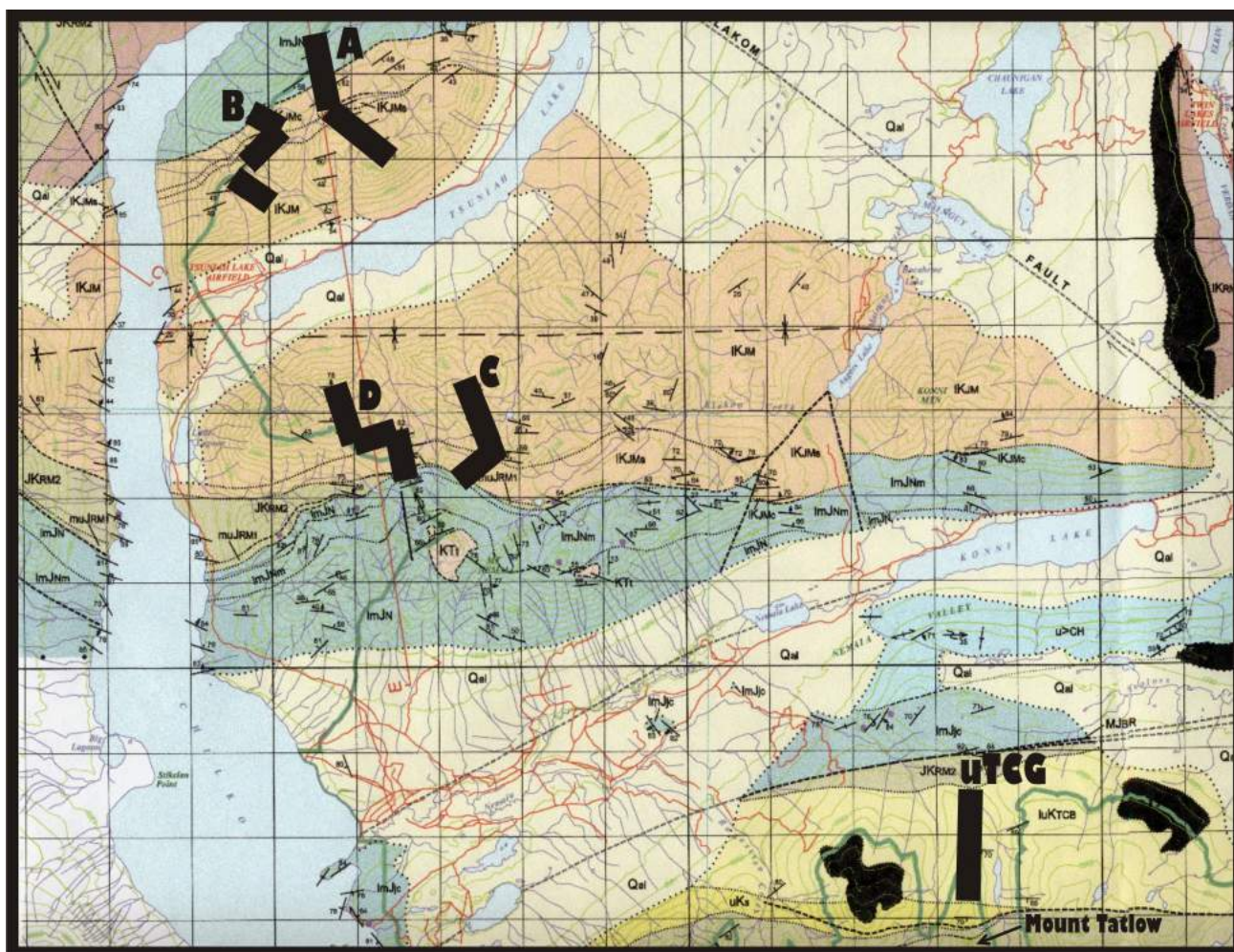


Figure 2. Geology of the area east of Chilko Lake, showing locations of measured sections (modified from Schiarizza et al., 1997).

C. Wave-Dominated Delta Front/Delta-Edge Turbidites

Approximately 50% of the sections in the Chilko Lake area are characterized by thick successions (700–1650 m on the middle section and 900–1700 m on the left section of Figure 3) of moderately well-sorted feldspathic arenite intercalated with lesser dark siltstone to mudstone intervals. The sandstone is well-stratified and represents both massive and nondescript, apparently structureless intervals, as well as successions containing abundant sedimentary structures; these include wavy lamination, swaley cross-stratification (SCS), loaded and erosional bases, and variably sized (<1–3 m long) rip-up clast horizons. Interbedded finer-grained intervals (on average 10 cm to a maximum of 15 m, 50 m in the south) display planar-parallel bedding, ripple cross-stratification, moderate bioturbation, water-escape structures, convolute bedding and soft-sediment deformation structures.

There is a distinct north to south transition in sedimentary structures within this lithofacies in the Chilko Lake area. Sedimentary structures in the northern limb vary from planar-parallel laminations to large-scale (<1.5 m) hummocky cross-stratification, progressively overlain by swaley cross-stratification followed by planar-parallel strata. Correlative strata on the southern limb are cyclic, grading from a thick (<1.5 m), massive, occasionally normally-graded to planar-parallel stratified sandstone; these strata are overlain by ~1 to 3 cm of planar-parallel-laminated sandy siltstone that grades into 1 to 3 cm of planar-laminated siltstone, which is in turn topped by mudstone of variable thickness. This siltstone often shows oscillatory to current-generated structures.

The presence of hummocky and swaley cross-stratification, basal erosive surfaces and abundant rip-up clast horizons suggests high rates of sedimentation prevailed in an environment characterized by periods of rapid, high-volume sediment influx and intermittent periods of wave reworking. Deposition was probably occurring in wave-dominated delta front to lower shoreface environments, with a transition to the south into a coarse-grained turbidite package, which accumulated at a depth above the storm wave base.

D. Mass Sediment Gravity Flows/Submarine Fan (?)

The Yalakom Mountain area contains a thick sequence (~1500 m) of northwest-trending, steeply dipping JMG strata dominated by massive, green, medium- to coarse-grained lithofeldspathic sandstone, minor pebble conglomerate and interbedded planar siltstone. The succession appears to gradationally overlie poorly exposed shallow marine JMG rocks, which themselves lie disconformably over Middle Jurassic strata adjacent to the Yalakom fault. The main JMG succession consists of thick sets of massive, medium- to thick-bedded, coarsening-upward sandstone in-

tercalated with thin- to medium-bedded sandstone and thin-bedded siltstone and mudstone. Bed sets tend to thicken upward, with thin-bedded siltstone and mudstone coarsening- and thickening-upward into coarse-grained, thick-bedded (~50 cm), massive sandstone. These cyclic sequences are generally greater than 10 m thick, and can reach up to 100 m. Beds are tabular and laterally continuous for hundreds of metres. Sedimentary structures include parallel laminations, graded bedding, mudstone rip-up clasts, flame structures, dish-and-pillar structures and rare soft-sediment folds. Partial Bouma sequences (AB, ABC) are locally evident. The succession becomes finer grained in the upper 500 m, gradually incorporating a higher percentage of sandstone-mudstone couplets with a decreasing percentage of massive sandstone intervals.

The tabular, laterally continuous nature of the stratigraphy, the cyclic coarsening- and thickening-upward nature of the bed sets and the presence of graded bedding, abundant rip-up clast horizons, flame structures, and partial Bouma sequences suggest that the succession represents a sequence of high-density sediment gravity flows. These turbidite deposits are classically interpreted as being deposited on fan lobes in a submarine-fan environment (Kliensphen, 1982, 1985), but the presence of rare trough cross-stratification and shallow-water bivalves suggests that the succession may instead represent sediment gravity flows deposited on a distal delta front on the lower shoreface at a depth above the storm wave base.

E. Distal Delta Front/Lower Shoreface

Both east and northeast of Yalakom Mountain, in the Dash Creek–Churn Creek area, massive sandstone intervals are gradationally overlain by, and laterally interfinger with, a distinct succession of tabular, laterally continuous, thin- to medium-bedded rhythmically interbedded sandstone and siltstone couplets. These striped, dark grey and pale olive green sandstone-siltstone couplets display parallel laminations, crosslaminations, graded bedding, well-developed partial Bouma sequences (BC, BCD) and soft-sediment deformation, including asymmetric folds up to 1.5 m in amplitude. These beds form intervals 15–125 m thick encased by massive, green, medium- to coarse-grained lithofeldspathic sandstone and lesser pebble conglomerate. Wood fragments are locally abundant and rip-up clast horizons are common at the base of sandy intervals. The thin-bedded sandstone-siltstone couplets appear to coarsen and thicken upward into the massive sandstone intervals, which are similar to the thick-bedded sandstone documented in the Yalakom Mountain section as they also display sharp, erosive bases, graded bedding, parallel laminations and top cut-out Bouma (AB) sequences. The sandstone-siltstone couplet succession gradationally overlies the lower part of the mass sediment gravity-flow succession, but the thickness of the couplet intervals and the ratio of couplet to mas-

sive sandstone beds varies across the map area, which suggests that an interfingering relationship may have existed between the couplet intervals and the upper part of the Yalakom Mountain succession of thick lithofeldspathic sandstone beds.

In many localities, the upper portions of the couplets contain oscillation ripples, combined flow ripples, unusual cross-stratification patterns (possibly SCS) and erosive scour surfaces. Lenticular bedding is evident within finer grained intervals. The upper portion of the massive sandstone beds are locally trough cross-stratified or display oscillation ripples.

The classic bottom cut-out Bouma sequences (BCD, CDE, DE) that are noted in the sandstone-siltstone couplets indicate that the couplets represent thin-bedded turbidite deposits, whereas rip-up clast horizons, graded bedding and sharp erosive bases of the interbedded massive sandstone bodies suggest that these strata were deposited by coarse-grained mass sediment gravity flows. The presence of trough cross-stratification, lenticular bedding and oscillation ripples indicates wave reworking, which suggests reworking of the original turbidites due to wave activity; thus, deposition occurred at depths at least partially above the storm wave base. These strata are interpreted as having accumulated as the result of abundant sediment supply and rapid deposition on a distal delta front to lower shoreface area, where mass sediment gravity flows deposited in relatively shallow water were subjected to intermittent reworking by wave activity. This area is further interpreted as transitional in nature to the deeper (sub-storm-wave-base depth) areas of the Yalakom Mountain submarine-fan

complexes, as well as the source of the sediment to those complexes.

F. Delta Plain/Fluvial

Northwest of Yalakom Mountain, strata on Nine Mile Ridge and on the western flank of Red Mountain consist of thick successions (10–100+ m) of olive green to black thin-bedded, parallel-laminated, organic-rich, sandy to silty shale and siltstone intercalated with thin-bedded, parallel-laminated to cross-stratified, fine- to coarse-grained lithic arenite to lithic wacke. These fine-grained intervals are dominantly recessive, concretionary in part, and contain organic-rich stringers, coal seams and *in situ* tree moulds. On Nine Mile Ridge, the fine-grained successions are separated by repeated intervals of 10–40 m thick medium- to coarse-grained trough cross-stratified sandstone and rare pebbly sandstone. To the north, the fine-grained successions are interbedded with a 10–30 m thick interval of clast- to matrix-supported, pebble to boulder, disorganized, volcanic plutonic conglomerate and associated coarse-grained sandstone. The conglomerate successions are lenticular, display channelized, erosive bases and tend to fine upward into lenticular beds of medium- to coarse-grained sandstone, pebbly sandstone and conglomeratic stringers.

The presence of fining-upward trough cross-stratified sandstone, lenticular conglomerate with erosive channelized bases, abundant organic material, and the dominance of recessive thin-bedded siltstone and shale indicates that deposition occurred in a fluvial environment, possibly on an emergent or near-emergent delta plain. The sandstone and conglomerate intervals represent fluvial channels, and the fine-grained intervals represent fluvial

Grain Size Legend		
mudst = mudstone	f = fine-grained sst	g = granule cong
siltst = siltstone	m = medium-grained sst	p = pebble cong
sst = sandstone	c = coarse-grained sst	c = cobble cong
cong = conglomerate		

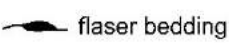
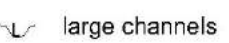
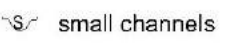
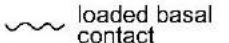
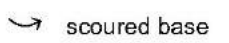
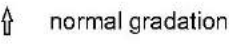
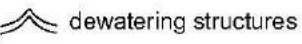
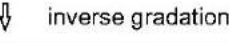
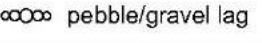
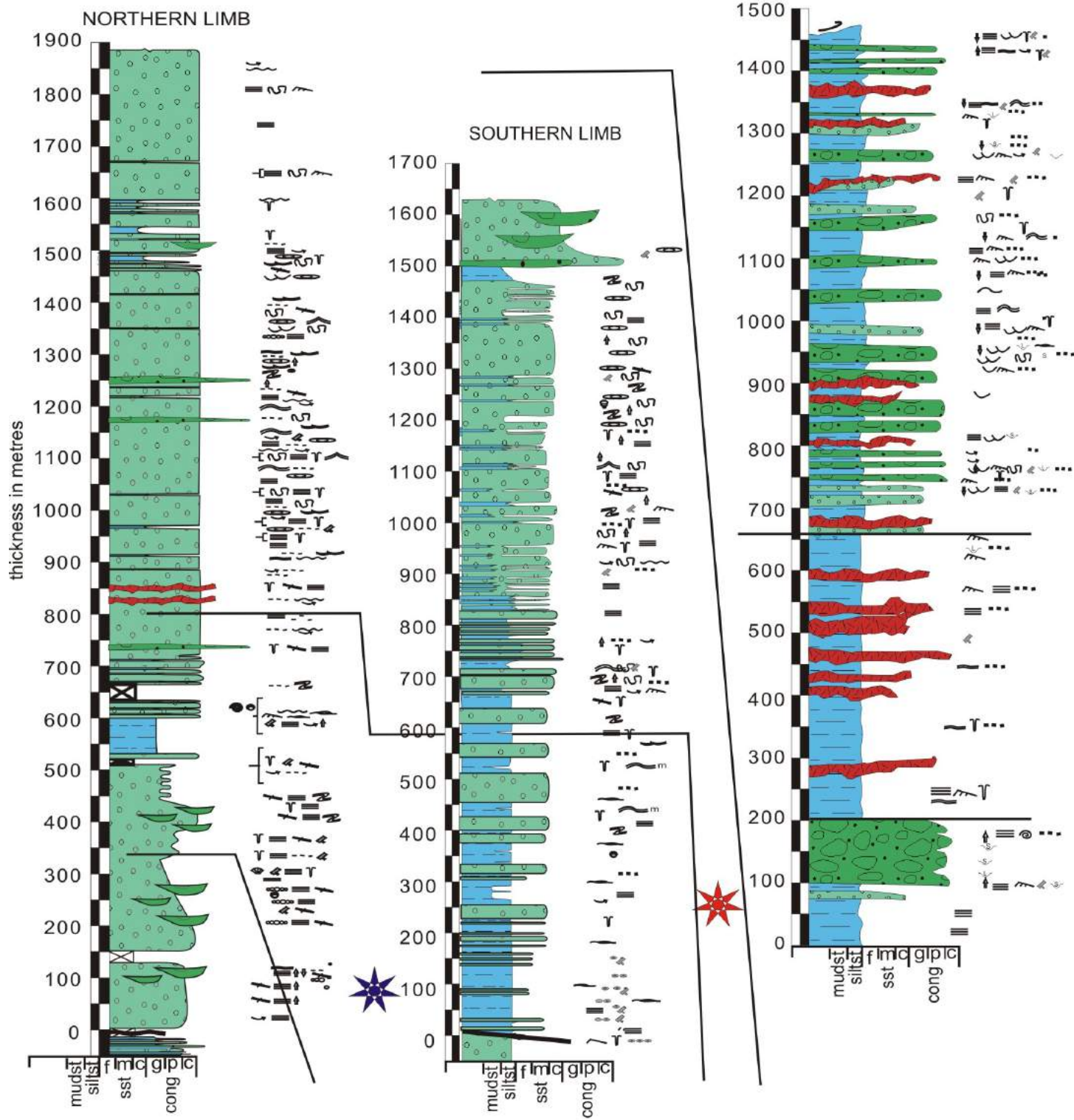
Measured Section Legend			
	horizontal planar parallel strata		ammonite
	low angle truncations		flaser bedding
	trough x-strata		large channels
	wavy lamination/bedding		small channels
	hummocky cross-strata		loaded basal contact
	swaley cross-strata		scoured base
	ripple x-lamination		normal gradation
			dewatering structures
			inverse gradation
			pebble/gravel lag
			concentric-ribbed bivalve
			radial-ribbed bivalve
			trace fossils
			concretion
			wood fragments
			ripup clast horizon

Figure 3. Stratigraphic sections of the JMG in the Chilko Lake area and of the upper Taylor Creek Group, north of Mt. Tatlow.

Jackass Mountain Group Chilko Lake area

U. Taylor Creek Group Mt. Tatlow



 Radiolarian age mid- Albian to Cenomanian

 Ammonite age upper to mid- Albian

overbank or possibly interdistributary deposits on the delta plain.

Taylor Creek Group

The Taylor Creek Group strata along the southern margin of the Nechako Plateau have been analyzed to constrain potential stratigraphic correlations between the Taylor Creek Group and coeval JMG strata. Stratigraphic analysis in the northern portion of the outcrop belt near Mt. Tatlow (Figure 2) documented the lithofacies shown on Figure 3 and discussed below.

A. Submarine Fan

The stratigraphically lowest unit (0–200 m on Figure 3, right column) in the Mt. Tatlow area consists of dark grey, thin-bedded, parallel-laminated siltstone and sandy shale intercalated with thinly-bedded, cross- to parallel-laminated, chert-lithic micaceous arenite. These strata are overlain by a thick sequence (~100 m) of organized, massively bedded, pebble to cobble, chert-rich conglomerate characterized by distinct nests of overlapping lenticular, crudely stratified channels. The conglomerate unit is interpreted as a channel fill in a submarine fan.

B. Prodelta

The middle portion of the section (200 to ~900 m on Figure 3, right column) consists of a thick package of dark grey, bioturbated shale to siltstone interbedded with minor calcareous lithic feldspathic arenite that locally displays parallel laminations to crosslaminations and thin-bedded, parallel-laminated, orange weathering micrite beds. Plant material is abundant, locally, on bedding planes. Rare ammonites and radiolarians indicate accumulation occurred in a marine setting.

The lateral continuity, monotonous fine-grained nature of the unit, rare cross-stratification and presence of marine fauna suggest deposition in a quiet-water marine environment that was periodically disturbed by wave or current activity, such as a distal prodelta setting.

C. Delta Plain

The upper portion of the Mt. Tatlow section (900+ m) consists of a coarsening-upward succession of chert-pebble conglomerate and chert-lithic micaceous feldspathic arenite intercalated with siltstone and shale. Coarse-grained intervals are lens-shaped, channellized and display trough cross-stratification, abundant rip-up clast horizons, and erosive bases. Within the conglomeratic intervals, bedding becomes distinctly thinner and grain size decreases upsection, while the relative abundance of conglomeratic intervals increases. The encasing intervals contain thinly-bedded, parallel- to cross-stratified sandy siltstone and silty shale with locally abundant plant debris, which, along with bioturbation, increases in abundance upsection. Hum-

mocky stratification is noted in the upper third of the succession.

The presence of multiple fining- and thinning-upward channellized sandstone and conglomerate packages encased in organic-rich, fine-grained siltstone and shale suggests that deposition took place in a channellized delta plain system. The presence of hummocky cross-stratification indicates that deposition occurred in a subaqueous environment characterized by intermittent storm wave activity. The overall coarsening-upward sequence suggests that deposition took place in a prograding upper to lower delta plain distributary system.

Facies Architecture

Regional stratigraphic analysis suggests that the lithofacies assemblages within the JMG grade laterally and vertically into one another. However, stratigraphic position, structural reconstructions, preliminary detrital zircon analysis and limited fossil control suggest the overall stratigraphic architecture presented in Table 1.

This generalized stratigraphic architecture is not strictly valid for each location within the outcrop belt, due to lateral stratigraphic variations. For example, the massive sandstone succession interpreted as mass sediment gravity flows is found primarily in the southeastern portion of the outcrop belt, whereas the wave-dominated delta front deposits are primarily restricted to the Chilko Lake block. On a regional basis, however, it is clear that the stratigraphic succession recorded in the JMG represents an overall shallowing-upward basinal succession.

The stratigraphic relationship between the JMG and the Taylor Creek Group is the subject of ongoing investigation. However, results of preliminary stratigraphic analysis, geochemistry and detrital zircon analyses suggest the Taylor Creek Group may interfinger with, and in part overlie, the JMG.

Summary and Regional Implications

Regional stratigraphic analysis of Cretaceous strata along the southern margin of the Nechako Plateau constrains the stratigraphic architecture and basin evolution represented

Table 1. Generalized stratigraphic architecture of the Jackass Mountain Group.

~~~~~ Top of section (modern erosive surface) ~~~~~
Delta front/Fluvial
Distal delta front/Lower shoreface
Wave-dominated delta front/Delta-edge turbidites
Mass sediment gravity flows/Submarine fan
Shallow marine/Proximal delta front
~~~~~ Unconformity ~~~~~
Jurassic strata

by the JMG, which contains extensive and, locally, extremely thick facies interpreted to represent shallow-marine, primarily deltaic, and nonmarine depositional environments. In the Yalakom block, sub-wave-base submarine-fan facies form a thick stratigraphic succession northeast of the Yalakom fault. These rocks interfinger laterally with, and are in part overlain by, a thick succession of shallow-marine deltaic and fluvial successions. Thick sequences of clastic strata in the Chilko Lake region, originally interpreted as submarine-fan facies (Kleinspehn, 1982, 1985), are documented herein as shallow-marine deltaic and shoreface facies. Taylor Creek Group rocks in the region also contain deltaic sequences that may stratigraphically overlie, and interfinger with, the JMG strata. Regionally, Cretaceous strata along the southern margin of the Nechako Plateau represent a shallow-marine to nonmarine transition between Barremian to Cenomanian time. Furthermore, the lithofacies assemblages are much more varied than originally thought, which has significant implications for hydrocarbon reservoir potential in the region.

Acknowledgments

Funding was provided primarily by Geoscience BC Grant 2006-014, with additional financial support from National Science and Engineering Research Council (NSERC) Grant 611258 to P. Mustard; Simon Fraser University to P. Mustard, J. Goodin and C. MacLaurin; the University of Wisconsin-Eau Claire to J. Mahoney; and the Geological Survey of Canada to J. Haggart. Special thanks to M. King of Whitesaddle Air Services for his continued outstanding helicopter support.

References

Ferri, F. and Riddell, J. (2006): The Nechako Basin project: new insights from the southern Nechako Basin; *in* Summary of Activities 2006, BC Ministry of Energy, Mines and Petroleum Resources, p. 89–124, URL <<http://www.empr.gov.bc.ca/OG/oilandgas/publications/TechnicalDataandReports/Pages/Summary2006.aspx>> [November 2006].

- Garver, J.I. (1992): Provenance of Albian-Cenomanian rocks of the Methow and Tyaughton basins, southern British Columbia: a mid-Cretaceous link between North America and the Insular terranes; *Canadian Journal of Earth Sciences*, v. 29, p. 1274–1295.
- Hannigan, P. Lee, P.J., Osadetz, K., Dietrich, J.R. and Olsen-Heise, K. (1994): Oil and gas resource potential of the Nechako-Chilcotin area of British Columbia; BC Ministry of Energy, Mines and Petroleum Resources, GeoFile 2001-6, 167 p., 5 maps at 1: 1 000 000 scale.
- Kleinspehn, K.L. (1982): Cretaceous sedimentation and tectonics, Tyaughton-Methow Basin, southwestern British Columbia; Ph.D. thesis, Princeton University, 184 p.
- Kleinspehn, K.L. (1985): Cretaceous sedimentation and tectonics, Tyaughton-Methow Basin, southwest British Columbia; *Canadian Journal of Earth Sciences*, v. 22, no. 2, p. 154–174.
- Mustard, P.S., Mahoney, J.B., Goodin, J.R., MacLaurin, C.I. and Haggart, J.W. (2008): New studies of the Lower Cretaceous Jackass Mountain Group on the southern margin of Nechako Basin—progress and preliminary observations; *in* Geoscience BC Summary of Activities 2007, Geoscience BC Report 2008-1, p. 135–144.
- Riddell, J.M., compiler (2006): Geology of the southern Nechako Basin (NTS 92N, 92O, 93B, 93C, 93F, 93G); BC Ministry of Energy, Mines and Petroleum Resources, Petroleum Geology Map 2006-1, scale 1:400 000.
- Riesterer, J.W., Mahoney, J.B. and Link, P.K. (2001): The conglomerate of Churn Creek: Late Cretaceous basin evolution along the Insular/Intermontane superterrane boundary, southern British Columbia; *Canadian Journal of Earth Sciences*, v. 38, no. 1, p. 59–73.
- Schiarizza, P. and Riddell, J. (1997): Geology of the Tatlayoko Lake–Beece Creek area; *in* Interior Plateau Geoscience Project: Summary of Geological, Geochemical and Geophysical Studies; BC Ministry of Energy, Mines and Petroleum Resources, Paper 1997-2 and Geological Survey of Canada Open File 3448, p. 63–101.
- Schiarizza, P., Gaba, R.G., Glover, J.K., Garver, J.I. and Umhoefer, P.J. (1997): Geology and mineral occurrences of the Taseko–Bridge River area; BC Ministry of Energy, Mines and Petroleum Resources, Bulletin 100, 291 p.
- Umhoefer, P.J. and Miller, R.B. (1996): Mid-Cretaceous thrusting faulting in the southern Coast Mountains, British Columbia and North Cascades, Washington as viewed after restoration of strike-slip faulting; *Tectonics*, v. 15, p. 545–565.

Sedimentation Patterns and Reservoir Distribution in a Siliciclastic, Tectonically Active Slope Environment, Bowser Basin, Northwestern British Columbia (NTS 104B/01)

Gagnon, J-F., Department of Earth and Atmospheric Sciences, University of Alberta, Edmonton, AB, jfgagnon@ualberta.ca

Waldron, J.W.F., Department of Earth and Atmospheric Sciences, University of Alberta, Edmonton, AB

Gagnon, J-F. and Waldron, J.W.F. (2009): Sedimentation patterns and reservoir distribution in a siliciclastic, tectonically active slope environment, Bowser Basin, northwestern British Columbia (NTS 104B/01); in Geoscience BC Summary of Activities 2008, Geoscience BC, Report 2009-1, p. 193–200.

Introduction

Deepwater submarine channels constitute important potential hydrocarbon reservoirs in offshore petroleum exploration. The spatial distribution and thickness of those sandstone bodies are highly unpredictable because they tend to be localized and interbedded with mass-transport complexes. Looking at well-preserved analogues in the rock record assists in understanding the behaviour of sedimentation processes in such environments. Sedimentary rocks mapped as Lower to Middle Jurassic Hazelton Group and exposed at Mount Dilworth, north of Stewart in British Columbia represent an excellent analogue of slope processes in deep-marine siliciclastic-dominated depositional systems (Figures 1, 2). Furthermore, the reservoir units associated with this stratigraphic interval are potentially charged with hydrocarbons in laterally equivalent units farther northeast in the Bowser Basin, where thermal maturation levels are favourable (Evenchick et al., 2002; Stasiuk et al., 2005). The relationships between the different sedimentary facies identified in a tectonically active slope environment described in this report assist in understanding the distribution of reservoir units and assessing the petroleum potential of this stratigraphic interval.

Geological Setting

Early to Middle Jurassic sedimentary rocks assigned to the upper Hazelton Group are widespread in northwestern BC. They mainly outcrop along the edge of the Bowser Basin and constitute the lowermost stratigraphic unit of the Bowser succession (Waldron et al., 2006). Siliciclastic sedimentary rocks of the upper Hazelton Group were deposited above the volcanic arc rocks of the Stikine Terrane during an episode of back-arc extension followed by thermal sub-

sidence (Thorkelson et al., 1995). In the study area north of Stewart, upper Hazelton Group sedimentary rocks were previously assigned to the Salmon River Formation by Grove (1986). Regionally, sedimentary rocks of the Salmon River Formation were deposited above the dacitic tuff breccia of the Mount Dilworth Formation (Anderson and Thorkelson, 1990). However, geological mapping conducted by the authors in the summer of 2008 suggests that these sedimentary rocks might be correlative with the Todagin assemblage of the Bowser Lake Group (Evenchick et al., 2006). Uranium-lead zircon work is currently being conducted at the University of Alberta and should provide new constraints on the minimum depositional age and provenance of these units. The current report uses the previous stratigraphic framework established by Grove (1986).

Description of Depositional Units

Fine-Grained Turbidity Flows

Normally graded siltstone-mudstone and sandstone-mudstone couplets are widely exposed in the sedimentary succession (Figure 3). They usually occur in thin to medium beds and form laterally extensive sheet-like units. The presence of partial Bouma (1962) sequences T_{a-e} is attributed to waning energy in turbidity flows. Abundant T_{cd} and T_{abd} sequences contain asymmetric current ripples and groove casts, which suggests that the predominant paleocurrent flowed towards the southwest. Loading features such as ball-and-pillow structures and flame structures are also common. These sedimentary structures are indicative of relatively high sedimentation rates, which led to density contrasts in water-saturated sediments shortly after deposition. In some cases, rapid deposition also produced pore pressure that exceeded the hydrostatic equilibrium and led to partial liquefaction of the sediments; this phenomenon is represented in the turbidite facies by abundant convolute laminations.

Keywords: submarine channels, turbidites, debris flows, Bowser Basin, petroleum exploration, Hazelton Group

This publication is also available, free of charge, as colour digital files in Adobe Acrobat® PDF format from the Geoscience BC website: <http://www.geosciencebc.com/s/DataReleases.asp>.

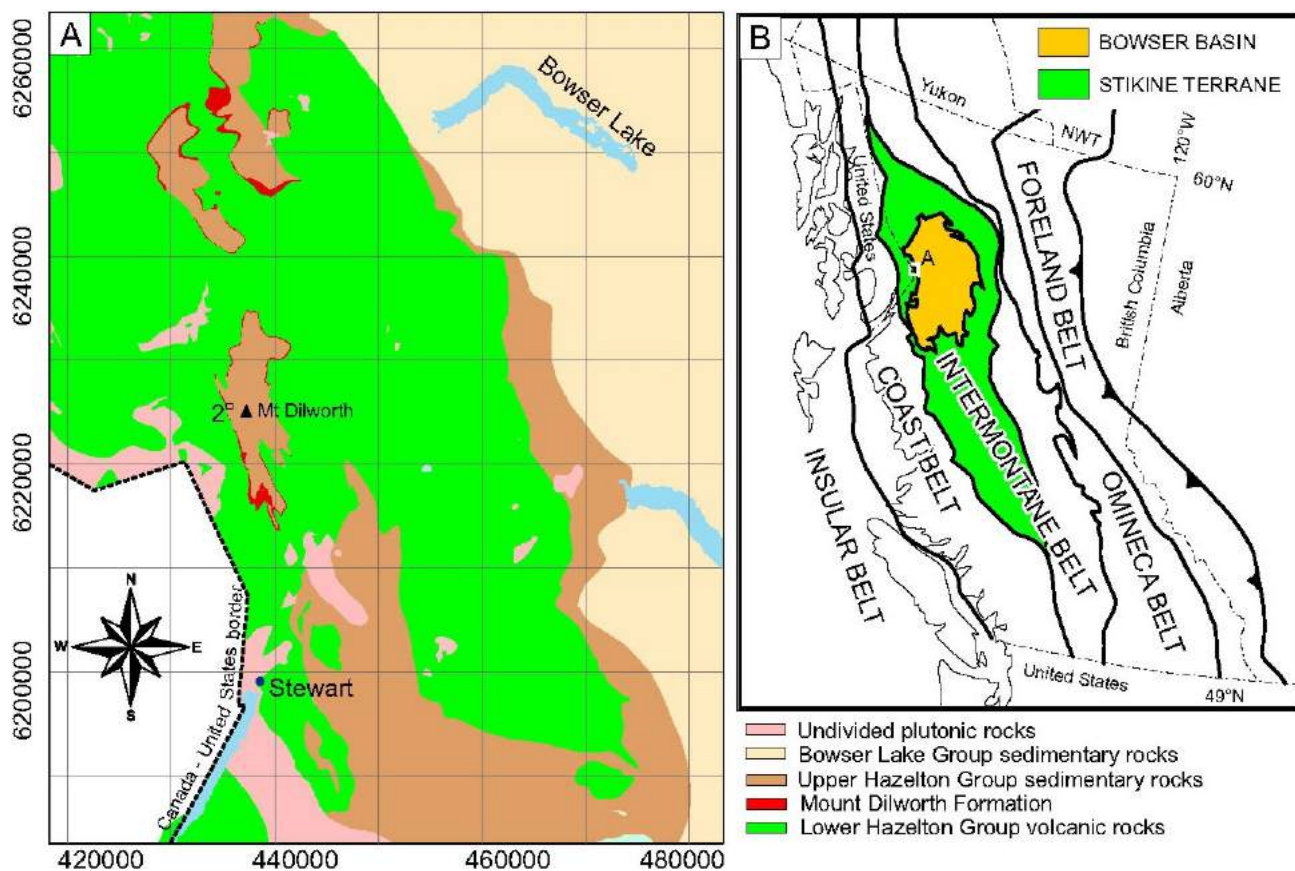


Figure 1. Simplified geology of the study area: **a)** location of the sedimentary succession presented in Figure 2 (projection in UTM NAD 83); **b)** location of the Bowser Basin in relation to principal tectonic belts of the Canadian Cordillera; white square delineates the extent of the geology described in (a). *Modified from Grove (1986), Evenchick and Thorkelson (2005).*

Some metre-thick intervals of thinly bedded fine-grained turbidites show evidence of biogenic reworking. The ichnological suite observed is dominated by two distinctive ichnogenera: *Phycosiphon* and *Helminthopsis*. These traces are horizontal to gently inclined, irregular, meandering burrows filled by organic-rich mud (Figure 4). Both these traces are generally interpreted as grazing trails of vermiform organisms (Pemberton et al., 2001) and typically occur near the sediment-water interface; this suggests that food resources were introduced mostly by suspension in a low-energy depositional environment, outside the principal sediment pathway. In terms of petroleum prospectivity, this unit has rather low reservoir potential due to its fine-grained nature. On the other hand, as it is situated above a thick sandstone package, it would constitute an excellent seal rock due to its impressive lateral extent and low permeability.

Submarine Channel Fills

The percentage of sandstone in turbidite deposits gradually increases upsection. The beds can consist of up to 90% of sand-dominated T_{abc} sequences, whereas the layers of laminated silt and hemipelagic mud T_{de} are centimetre-thick. This overall increase of sandstone is associated with a gen-

eral thickening- and coarsening-upward trend at the outcrop scale (Figure 2). The vertical pattern is interpreted as a change from an off-axis area characterized by bioturbated silt and very fine sand to an axial zone of sandstone deposition. Around 85 m above the base of the section, turbidites are truncated by a series of very thick sandstone bodies (Figure 2). The beds typically consist of coarse- to very coarse grained sandstone with occasional pebbly sandstone lenses and *in situ* calcareous concretions (Figure 5). They range in thickness from 10 to 50 m and extend laterally up to 500 m. Thin-section observations indicate that the framework grains are mainly composed of chert, monocrystalline quartz, plagioclase and mud clasts. The grains are well to moderately sorted, with less than 5 % clay matrix.

In some cases, distinct sandstone beds become amalgamated along strike and form channellized lobe geometries. Figure 6 shows the spatial distribution of a channel system cutting down into a debris flow unit. The base of the channel is marked by a scoured surface above which a drape of thinly laminated mud and silt accumulated. The absence of coarse material immediately above the scoured surface suggests that important sediment bypass occurred prior to accumulation of the fine-grained sediments. The mud-

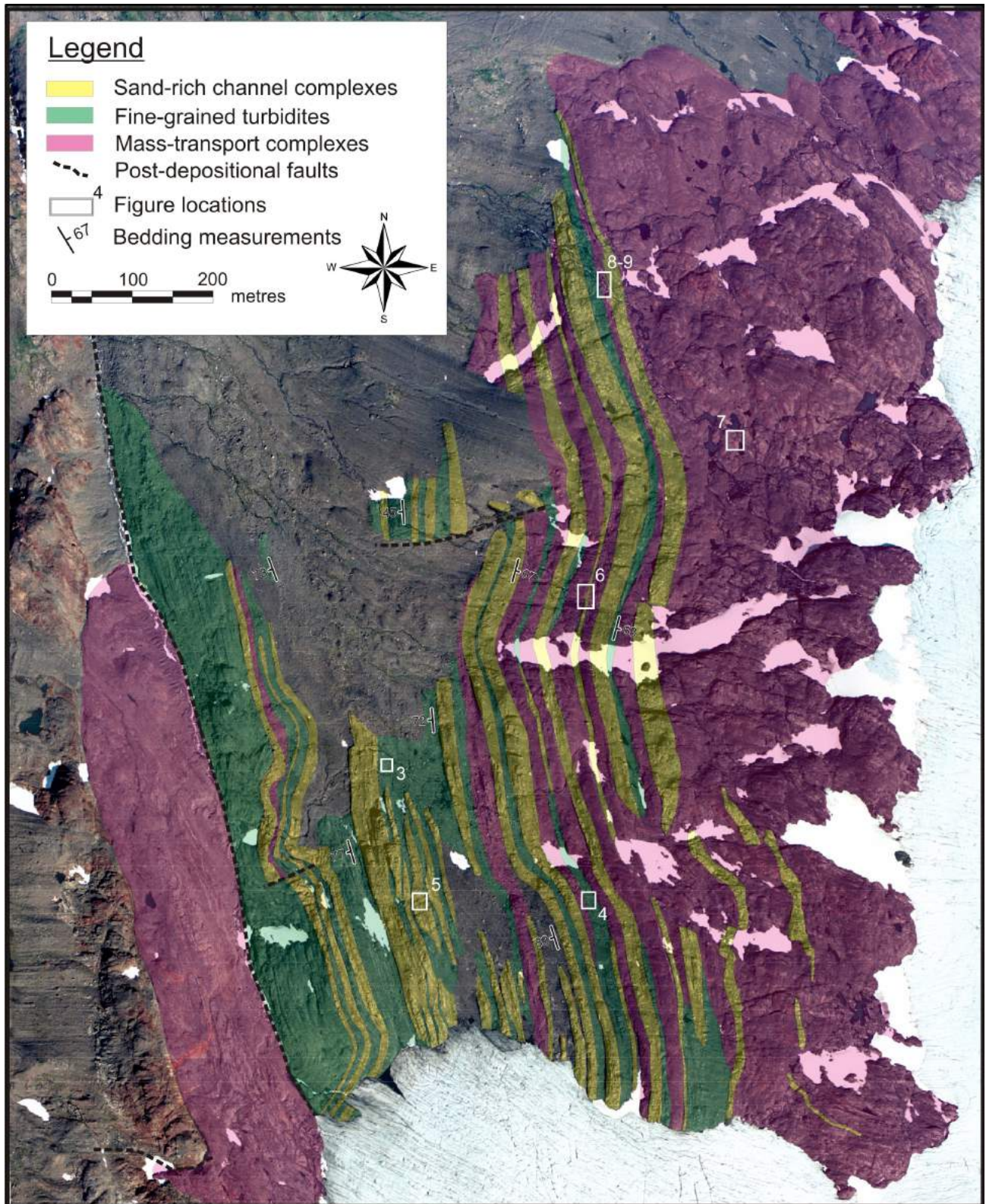


Figure 2. Annotated aerial photograph of the sedimentary succession, showing the main depositional units. Stratigraphic top is to the east.



Figure 3. Thinly bedded succession of fine-grained turbidites with abundant partial Bouma sequences T_{a-e}. Stratigraphic top to the right. Hammer for scale is 30 cm in length.



Figure 4. *Helminthopsis* trace fossil in fine-grained turbidites. These traces are interpreted as grazing trails of worm-like organisms in a low-energy depositional environment. Lens cap is 6.5 cm in diameter.



Figure 5. Thickly bedded, very coarse sandstone of amalgamated channel complexes. Note the fining- and thinning- upward character of the beds. Stratigraphic top is to the left.

filled channel is truncated by an irregular erosional surface above which a unit of normally graded, clast-supported conglomerate was deposited. Upsection, the conglomerate gradually passes into moderately sorted medium- to coarse-grained sandstone containing abundant current-generated sedimentary structures. In each measured stratigraphic section, the channel sand is interbedded with laminated silt and very fine grained sand. These relatively thin, finer grained intervals are interpreted to be levée deposits associated with lateral migration of the channel axis.

The sand-rich submarine channels possess very good reservoir characteristics: they consist of homogeneous sandstone arranged in laterally extensive (~500 m) and very thick (~10 to 50 m) units (Figure 2). The coarse-grained nature of the sediments, combined with the relatively good sorting, is favourable for development of high initial intergranular porosity. Under the proper thermal maturation levels, these sand-rich channels could be charged with hydrocarbons and would constitute significant resources.

Mass-Transport Complexes

Debris flows and slump units are the most abundant units within the succession. These gravitational features, organized in mass-transport complexes (MTCs), consist of large dismembered calcareous concretionary blocks and layered rafts of sandstone and siltstone supported in a very poorly sorted fine-grained matrix (Figure 7). Soft-sediment deformation features, such as syndepositional folds and extensional faults, are ubiquitous in those units. Detailed mapping of a debris flow unit provided better understanding of the deformation mechanisms prevalent during slope failure. Sliding of a cohesive mass of sediments was initiated over a detachment surface underneath which the parallel beds remained undisturbed (Figure 8). Immediately above the décollement, fine-grained layers were gently folded during compression but retained their original thickness, whereas the softer sand-rich units were subject to more thorough ductile deformation. Pull-apart boudins of mud in a sandy matrix also indicate rheology contrasts between units of different grain size (Figure 9), the finer grained units behaving more competently. The slump unit becomes progressively more deformed near its top where disharmonic folding predominates. Eventually, most of the primary features are lost and the initial layering of the sediments becomes indistinguishable. As the matrix incorporated more fluids during transport, the slump unit evolved into an incoherent debris flow.

The uppermost stratigraphic unit exposed above the submarine channels consists of a very thick MTC (Figure 2). Conservative estimates made from aerial photograph interpretations suggest a minimal thickness of 400 m and a lateral extent over 1.4 km. The basal contact of the MTC on sandstone is variable along strike. At the northern end, the

contact is erosional on granular sandstone; further south, the sandstone is cut by another debris flow, which shows that the MTC is a composite of several slumps. Internal deformation increases southward, where large blocks of the underlying sandstone become incorporated in the MTC. These rafts are organized in variable orientations and can reach up to 100 m in length. Even though no other mappable contacts were observed upsection, mostly due to extensive snow cover, the impressive thickness of the MTC

probably results from multiple amalgamated debris flows with similar facies. In terms of petroleum prospectivity, MTCs do not represent good reservoirs due to their dominant fine-grained composition.

Implication for Petroleum Exploration

The basal sedimentary rocks of the succession exposed on the western side of the fault (Figure 2) consist of debris

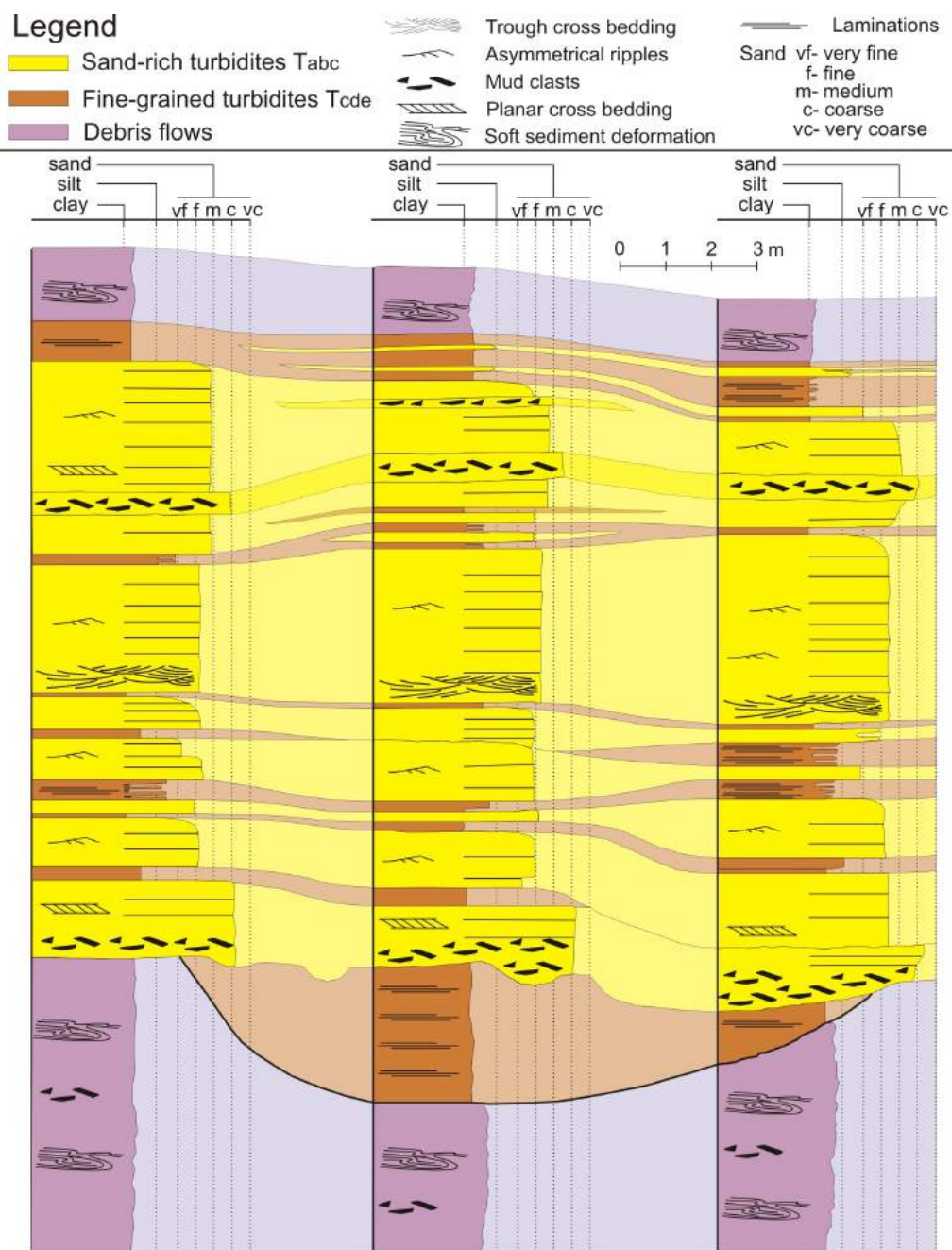


Figure 6. Stratigraphic cross-section of a mud-filled channel complex, showing the lateral variability of depositional units. No vertical exaggeration.

flows and slumps. Their fine-grained matrix and complexly folded laminated blocks suggest that they originally accumulated as fine-grained turbidites before being remobilized and deposited as cohesive gravity flows. Deposition probably took place in a slope environment, where gravitational collapses were more likely to occur. In contrast, younger sedimentary rocks located on the eastern side of the fault consist of unconfined thinly bedded turbidites and laterally extensive sandstone beds. Lobe geometry within those units suggests that repeated low- and high-density turbidity currents provided the bulk of the sediments to the submarine fan systems. The lack of MTCs in this interval suggests a return to more stable conditions. Upsection, scoured surfaces and mud-clast conglomerate found at the bases of the channel complexes are indicative of sediment bypass and incision (Figure 10). The sandstone beds are organized in channel-lobe geometries and show local incision into finer grained sedimentary rocks. These sand-filled channel complexes represent the best reservoirs of the succession. In addition to being relatively homogeneous and very thick, they are capped by intervening fine-grained deposits representing levée and overbank sediments, which

constitute an adequate seal to prevent vertical fluid flow. These channelled flows are in gradational contact above the underlying unconfined frontal splays and lobes, and probably constitute a progradation of the slope over the basin floor.

The proportion of MTCs gradually increases near the top of the succession. Incoherent debris flows are interbedded with amalgamated sandstone beds, whereas fine-grained turbiditic intervals are generally absent. Even though the sandstone beds are laterally extensive along strike, reservoirs tend to be compartmentalized due to the abundant reworking by debris flows. This could inhibit permeability within the reservoir and represent an additional risk for petroleum exploration. Confined mud-filled channels deposited above irregular scoured surfaces indicate that incision and sediment bypass were still dominant processes in the slope environment.



Figure 7. Folded calcareous concretionary block in a chaotic debris flow unit. Brunton compass for scale is 8 cm in width.



Figure 8. Deformed slump unit located above a detachment surface. During slope failure, the underlying thinly bedded turbidites remained undisturbed, while the mass-transport complex was subject to compressional and extensional deformation. The letter A indicates the location of Figure 9. Hammer for scale is 30 cm long.



Figure 9. Synsedimentary deformation features formed by flattening during deposition of the slump. The more competent mud layers pulled apart into boudins, whereas the surrounding sandy layers flowed to fill the remaining available space. Scale card is 8 cm long.



Figure 10. Poorly sorted mud-clast conglomerate located above a scouring surface. These intervals are common at the bases of channel fills and are indicative of sediment bypass and incision. Hammer for scale is 30 cm in length.

Depositional elements of deepwater clastic systems are highly variable and include a wide range of gravity flows with different reservoir properties. They consist of cohesive debris flows and slumps (MTCs), channel complexes and fine-grained turbidity flows. The occurrence of one specific gravity flow over another is mainly a function of sediment supply to the deep portion of the basin. Variations in sedimentation rates can be related to base-level fluctuations above the shelf edge and/or tectonic activity. Two different scenarios are explored (base-level changes vs. tectonic activity) to explain the succession of gravity flows observed in the area.

During development of a typical passive-margin sequence, an early stage of forced regression is likely to trigger instability at the shelf edge and deposition of cohesive debris flows on the slope (Catuneanu, 2006). This could correspond to the lowermost debris flow unit observed on the western side of the fault. During late forced regression, the shelf becomes subaerially exposed and accumulation of sand in the deep part of the basin is optimal. This is represented by the progradation of the incised channel complexes above the submarine fans. As base-level rises, increasing accommodation space is made available on the shelf, which reduces the amount of coarse sediment delivered to the deep marine basin.

In the case of a tectonically active basin, re-adjustment of the slope angle may have profound impacts on the distribution of the gravity flows, independently of shoreline shifts. In this model, MTCs observed in the area would be related to repeated slope failure initiated by tectonic activity. Paucity of tectonic activity is inferred during deposition of the submarine fan/channel complexes, when normal progradation of the slope environment would have occurred over the basin floor. In contrast, sudden steepening of the slope in response to fault movement is likely to have triggered rapid incision and sediment bypass, as represented by confined mud-filled channels (Figure 6) and abundant MTCs in the higher portion of the succession.

Even though it is difficult to clearly separate the effects associated with shoreline shifts from those driven by tectonic processes in the rock record, sedimentary rocks of the upper Hazelton Group at Mount Dilworth attest to the strong influence of tectonic input during deepwater sedimentation. The MTCs are unusually thick (up to 500 m) and constitute more than 50% of the entire sedimentary succession. This is significantly higher than most well-studied deepwater passive-margin analogues such as the Isaac Formation of Western Canada (Gammon et al., 2007; Laurin et al., 2007; Navarro et al., 2007; Schwarz and Arnott, 2007), the West Crocker Formation of Borneo (Crevello et al., 2007) and the San Vicente Formation of Spain (Arbues et al., 2007). In addition, sediment bypass facies and repeated incision of channel complexes are too abundant to solely be

driven by base-level fluctuations. Based on these observations, the authors conclude that synsedimentary faulting was a major component in determining the nature of the gravity flows. Thick MTCs were deposited during fault re-activation, which interrupted the overall regressive cycle responsible for progradation of the slope succession over the basin floor.

Acknowledgments

The authors would like to thank Geoscience BC for supporting this research. Additional field costs were supported by Natural Sciences and Engineering Research Council of Canada (NSERC) Discovery Grant A8508. Helicopter support was provided by Highland Helicopters and Pacific Western Helicopters. D. Dockman and M.-A. Bourgault assisted in the field. The authors also appreciate the support and discussion provided by C. Evenchick and J. Nelson, and thank M. Gingras, C. Anglin and C. Sluggett for their helpful comments on the manuscript.

References

- Anderson, R.G. and Thorkelson, D.J. (1990): Mesozoic stratigraphy and setting for some mineral deposits in Iskut River map area, northwestern British Columbia; *in* Current Research, Part E, Geological Survey of Canada, Paper 90-1A, p. 131–139.
- Arbues, P., Mellere, D., Puig, M. and Marzo, M. (2007): The effect of slumping on sandstone distribution in the Arro turbidites, Los Molinos road, Spain; *in* Atlas of Deep-Water Outcrops, T.H. Nilsen, R.D. Shew, G.S. Steffens and J.R.J. Studlick, J.R.J. (ed.), American Association of Petroleum Geologists, Studies in Geology 56, p. 333–335.
- Bouma, A.H. (1962): Sedimentology of Some Flysch Deposits: A Graphic Approach to Facies Interpretation (1st Edition); Elsevier, Amsterdam, 168 p.
- Catuneanu, O. (2006): Principles of Sequence Stratigraphy (1st Edition); Elsevier, Amsterdam, 375 p.
- Crevello, P.D., Johnson, H.D., Tongkul, F. and Wells, M.R. (2007): Channel-lobe and leveed-channel Complexes, Tman Bukit Sepanggar, Northwest Borneo; *in* Atlas of Deep-Water Outcrops, T.H. Nilsen, R.D. Shew, G.S. Steffens and J.R.J. Studlick, J.R.J. (ed.), American Association of Petroleum Geologists, Studies in Geology 56, p. 57–60.
- Evenchick, C.A. and Thorkelson, D.J. (2005): Geology of the Spatsizi River map area, north-central British Columbia; Geological Survey of Canada, Bulletin 577, 276 p.
- Evenchick, C.A., Hayes, M.C., Buddell, K.A. and Osadetz, K.G. (2002): Vitrinite and bitumen reflectance data and preliminary organic maturity model for the northern two thirds of the Bowser and Sustut basins, north-central British Columbia; Geological Survey of Canada, Open File 4343, 26 p.
- Evenchick, C.A., Mustard, P.S., McMechan, M.E., Ferri, F., Ritcey, D.H. and Smith, G.T. (2006): Compilation of geology of Bowser and Sustut basins draped on shaded relief map, north-central British Columbia; Geological Survey of Canada, Open File 5313.
- Gammon, P.R., Arnott, R.W.C. and Ross, G.M. (2007): Architectural relationships between channels, levees, and debris

- flows: Isaac Channel 6, Castle Creek south, Lower Isaac Formation, Windermere Supergroup, British Columbia, Canada; *in* Atlas of Deep-Water Outcrops, T.H. Nilsen, R.D. Shew, G.S. Steffens and J.R.J. Studlick, J.R.J. (ed.), American Association of Petroleum Geologists, Studies in Geology 56, p. 102–106.
- Grove, E.W. (1986): Geology and mineral deposits of the Unuk River–Salmon River–Anyox area, BC Ministry of Energy, Mines and Petroleum Resources, Bulletin 63, 474 p.
- Laurin, J., Wallace, K., Arnott, R.W.C. and Schwarz, E. (2007): Stratigraphic anatomy and depositional history of a mass-transport complex, Isaac Formation, Windermere Supergroup, British Columbia, Canada; *in* Atlas of Deep-Water Outcrops, T.H. Nilsen, R.D. Shew, G.S. Steffens and J.R.J. Studlick, J.R.J. (ed.), American Association of Petroleum Geologists, Studies in Geology 56, p. 119–122.
- Navarro, L., Khan, Z.A. and Arnott, R.W.C. (2007): Architecture of a deep-water channel-levee complex: Channel 3, Castle Creek south, Isaac Formation, Windermere Supergroup, British Columbia, Canada; *in* Atlas of Deep-Water Outcrops, T.H. Nilsen, R.D. Shew, G.S. Steffens and J.R.J. Studlick, J.R.J. (ed.), American Association of Petroleum Geologists, Studies in Geology 56, p. 93–96.
- Pemberton, S.G., Spila, M., Pulham, A.J., Saunders, T., MacEachern, J.A., Robbins, D. and Sinclair, I.K. (2001): Ichnology and sedimentology of shallow to marginal marine systems: Ben Nevis & Avalon reservoirs, Jeanne d'Arc Basin; Geological Association of Canada, Short Course Notes, v. 15, 343 p.
- Schwarz, E. and Arnott, R.W.C. (2007): Stratigraphic and depositional architecture of a slope channel system: Isaac Channel 5, Castle Creek south, Isaac Formation, Windermere Supergroup, British Columbia, Canada; *in* Atlas of Deep-Water Outcrops, T.H. Nilsen, R.D. Shew, G.S. Steffens and J.R.J. Studlick, J.R.J. (ed.), American Association of Petroleum Geologists, Studies in Geology 56, p. 97–101.
- Stasiuk, L.D., Evenchick, C.A., Osadetz, K.G., Ferri, F., Ritcey, P.S. and McMechan, M. (2005): Regional thermal maturation and petroleum stage assessment using vitrinite reflectance, Bowser and Sustut basins, north-central British Columbia; Geological Survey of Canada, Open File 4945, 16 p.
- Thorkelson, D.J., Mortensen, J.K., Marsden, H. and Taylor, D.C. (1995): Age and tectonic setting of Early Jurassic episodic volcanism along the northeastern margin of the Hazelton Trough, northern British Columbia; *in* Jurassic Magmatism and Tectonics of the North American Cordillera, D.M. Miller and C.J. Busby (ed.), Geological Society of America, Special Paper 299, p. 83–94.
- Waldron, J.W.F., Gagnon, J.-F., Loogman, W. and Evenchick, C.A. (2006): Initiation and deformation of the Jurassic-Cretaceous Bowser Basin: implications for hydrocarbon exploration; *in* Geological Fieldwork 2005, BC Ministry of Energy, Mines and Petroleum Resources, Paper 2006-1, and Geoscience BC, Report 2006-1, p. 349–360.